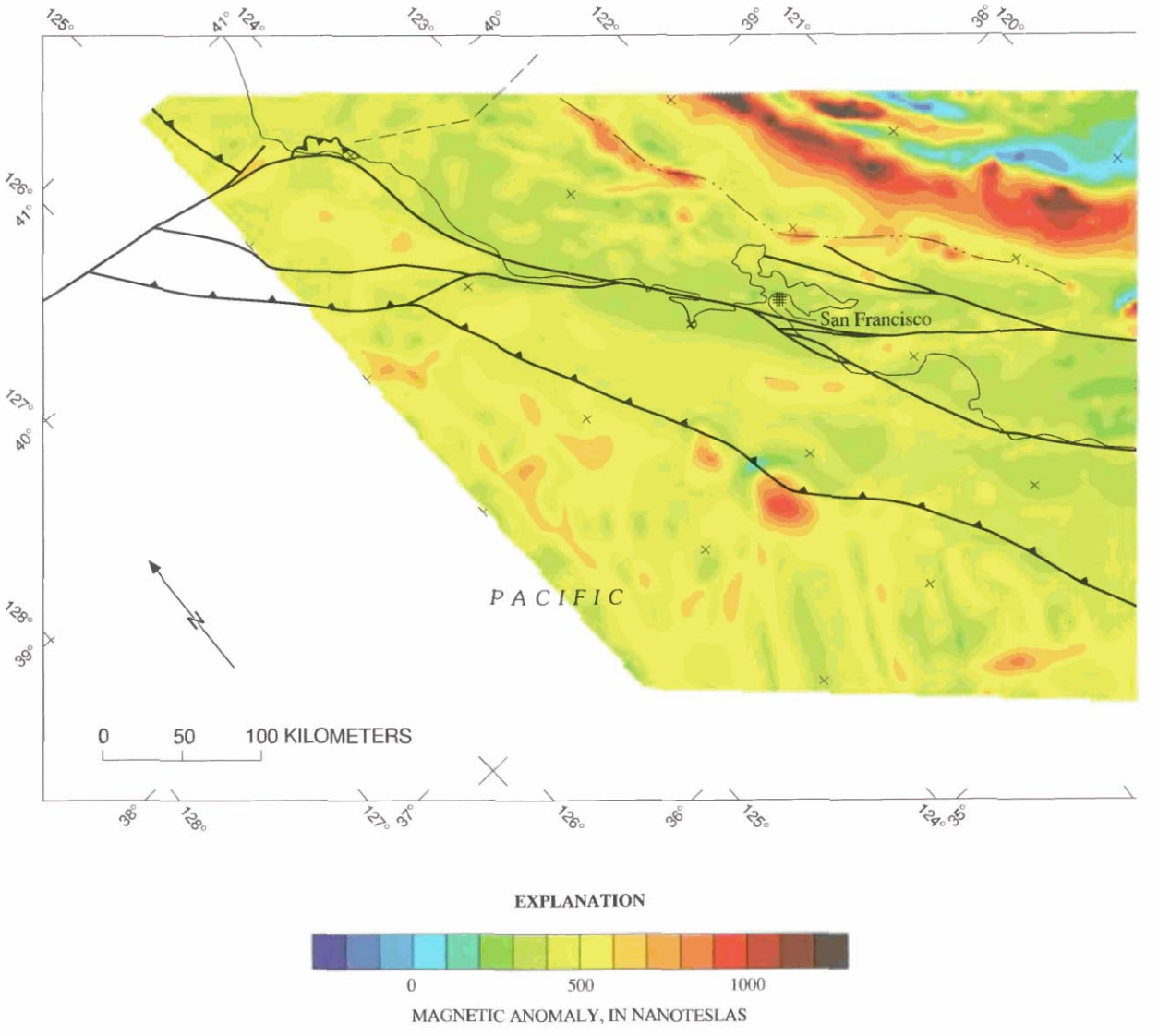

FIGURE 9.3.—Magnetic map of the San Andreas fault system (from Bond and Zietz, 1987). Contour interval, 100 nT. Faults simplified from Jennings and others (1977), McCulloch (1987), and Vedder (1987). Same symbols as in figure 9.4.

recent aeromagnetic map of this problematic area has, indeed, displayed a magnetic boundary trending close to and along the shore, thus representing the likely location of the San Andreas fault (Griscom, 1980a).

Aeromagnetic surveys over the Pacific Ocean at the entrance to the San Francisco Bay (Brabb and Hanna, 1981) show that the offshore extension of the Pilarcitos fault (an inactive fault branching westward from the San Andreas fault) is cut off by the offshore northward extension of the San Gregorio fault. The San Gregorio fault can be traced northward by using a detailed aeromagnetic map to the point where it intersects the San Andreas fault at Bolinas Lagoon, about 20 km northwest of the bay mouth (see McCulloch, 1987, fig. 15).

From San Francisco southward to lat 35°15′ N., the detailed gravity and magnetic data indicate that, in general, the westernmost strand of the main San Andreas fault zone is the major plate boundary. The layered Franciscan assemblage to the east may be less competent than the granitic basement of the Salinian block to the west, and new strands may be more likely to appear in the less competent rocks. An exception to this generalization is found at lat 36° N., where a thin fault sliver of

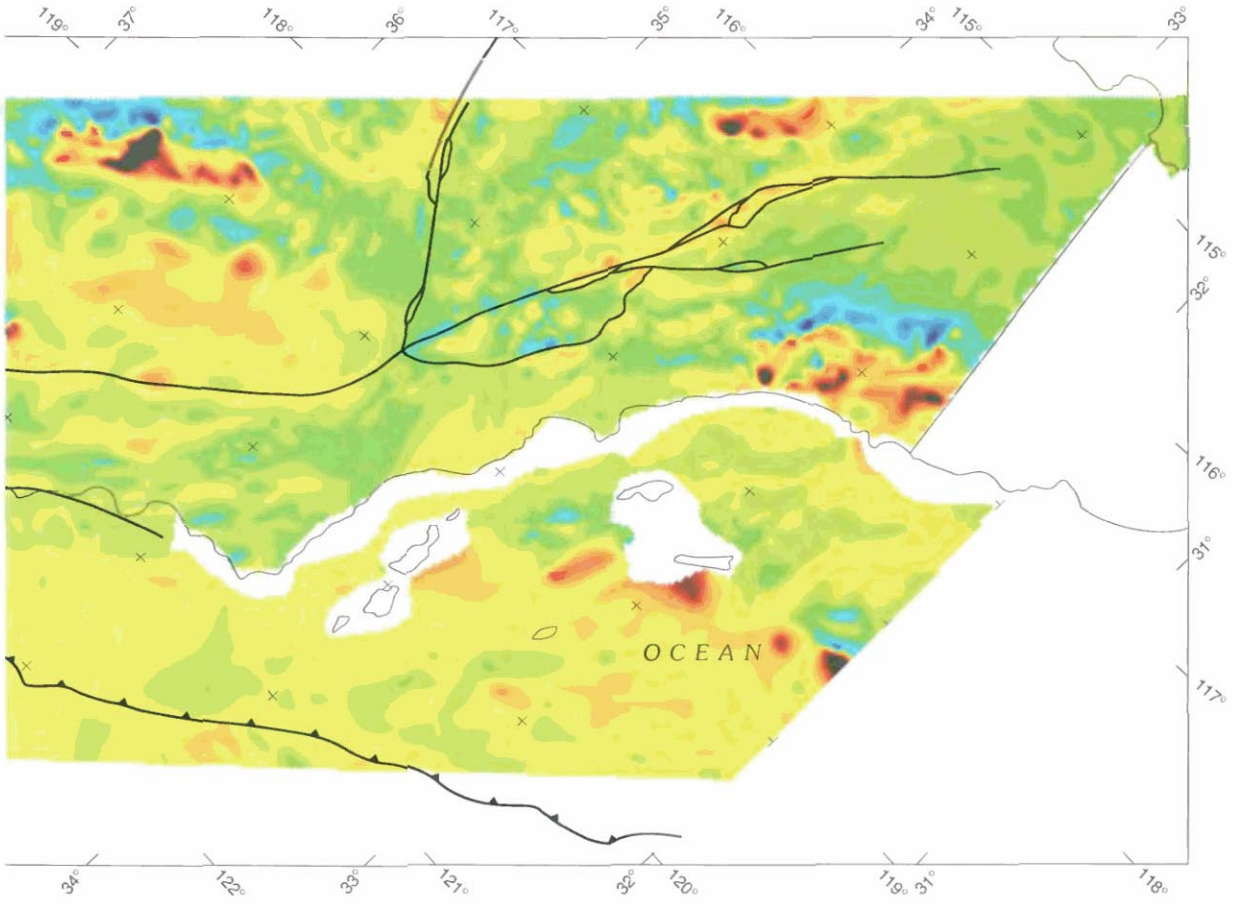

FIGURE 9.3.—Continued.

hornblende-quartz gabbro occurs at Gold Hill (Ross, 1970) that has been used to estimate offset on the San Andreas fault. The magnetic anomaly associated with this gabbro body indicates that it is at most 10 km long by 2 km wide (U.S. Geological Survey, 1987).

Farther south along the San Andreas fault, a linear magnetic high extends along the fault approximately between long 116° and 118° W. (fig. 9.3). On the basis of local model studies of this anomaly, Simpson and others (in press) show that this feature probably reflects the edge of an extensive block of magnetic rocks on the northeast side of the San Andreas fault, where the magnetic material is Precambrian igneous and metamorphic rocks, as well as Mesozoic plutonic rocks. Using detailed magnetic data (U.S. Geological Survey, 1979), the south border or magnetic boundary of this magnetic block (fig. 9.4) can be traced from west to east along a series of fault segments; from long 117°15′ W., the boundary follows the southern fault trace to long 116°15′ W., then crosses over to the northern trace along the short, east-west-trending fault segment, and finally continues eastward along the northern trace. These faults thus may represent the original fault boundary (now somewhat kinked) between the two plates. The geologic observation that rocks on the north side of these fault segments are native to the San Bernardino Mountains and contrast with compositionally different rocks on the south side (Matti and others, 1985) agrees with the magnetic interpretation. The magnetic boundary continues southeastward along the San Andreas fault in Coachella Valley to long 116°08′ W. A possible farther continuation of this linear magnetic high extends southeastward at a lower amplitude and diverges eastward from the present San Andreas fault, generally following and lying northeast of the Clemens Wells fault, a possible earlier strand of the San Andreas fault.

In Coachella Valley, the San Andreas fault (North Branch or Coachella segment) is situated along the northeast side of a substantial linear gravity low caused by at least 4.7 km of low-density sedimentary rocks

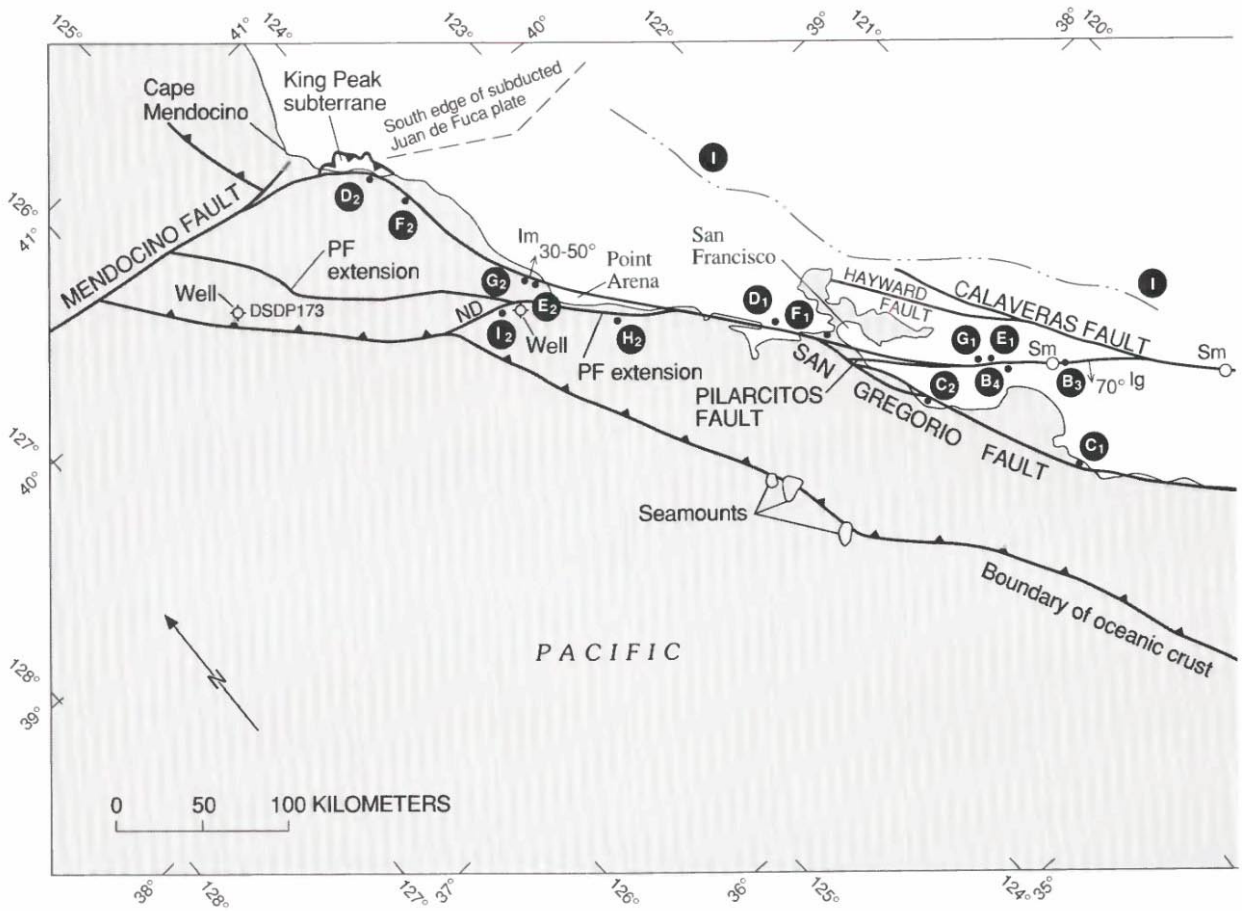

EXPLANATION

Sg
70°
Fault—Arrow indicates direction and amount of dip; circle, vertical dip. Capital letter, approximate depth to which dip is valid (S, shallow, about 2 km; I, intermediate, 2-5 km; D, deep, 5-10 km); lower case letter, geophysical data used for calculation of dip (m, magnetic; g, gravity)

Thrust fault—Sawteeth on upper plate

Crest of magnetic anomaly

Location of offset geophysical anomaly

Magnetic boundary (J_1 and J_2) discussed in text

Well

FIGURE 9.4.—San Andreas fault system, showing fault dips calculated from gravity and magnetic data, locations of offset geophysical anomalies, and south border of the subducted Juan de Fuca plate. Note wells at lat 39° and 40° N. ND, Navarro discontinuity; PF, Pilarcitos fault.

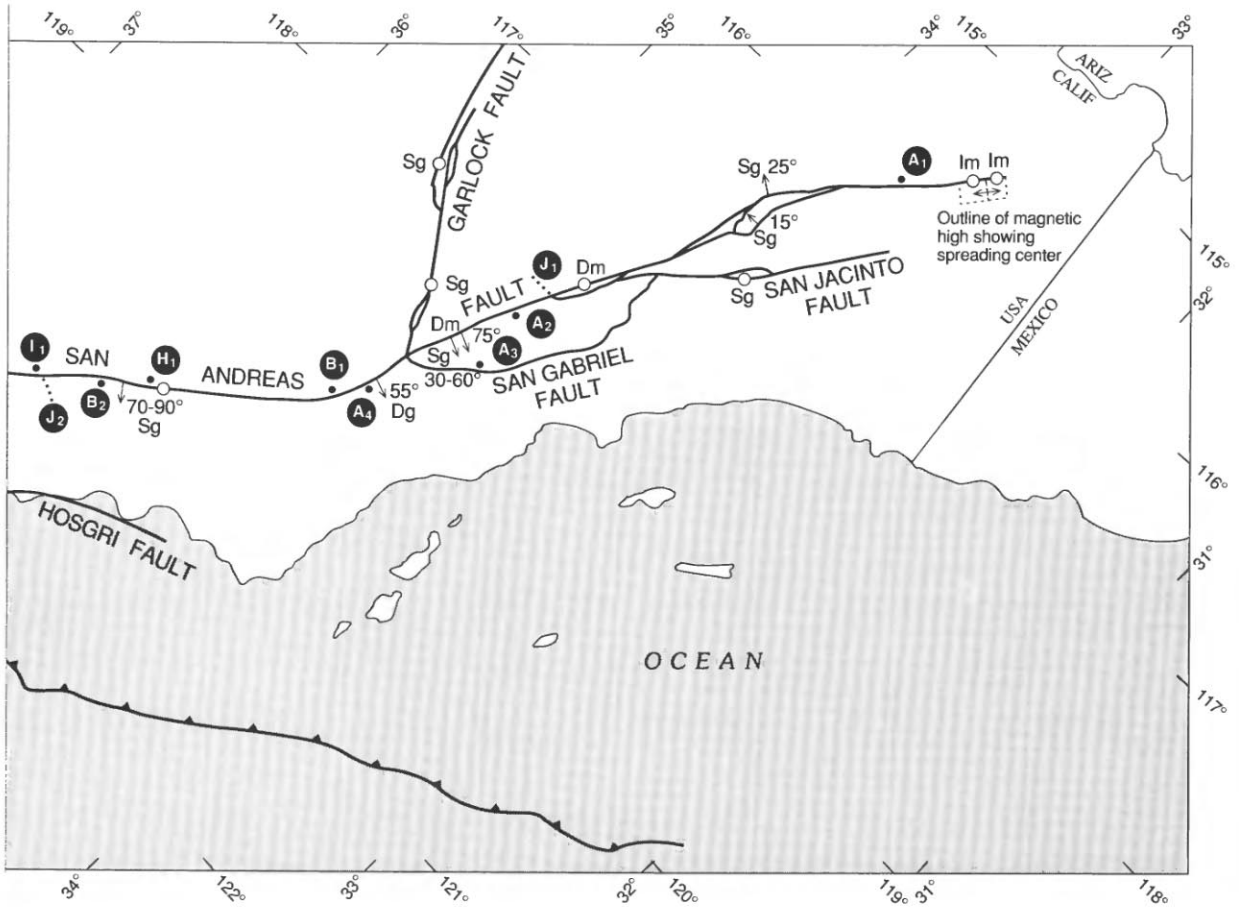

FIGURE 9.4.—Continued.

(Biehler, 1964) filling the valley. Gradient studies on the relatively detailed gravity data in this valley by one of us (Griscom) identify numerous fault strands, including the northern and southern branches of the San Andreas fault (the latter, the Banning fault), as well as several possible fault segments on the southwest side of the valley.

The Garlock fault at long 118° W. changes direction and forms a zone as much as 8 km wide. Models of both the magnetic and gravity fields calculated normal to the fault indicate that here the main lithologic boundary is the most northerly fault (fig. 9.4); the granitic rocks farther north are more magnetic and less dense than those to the south.

ATTITUDE

At several sites along the San Andreas fault, the juxtaposition of large masses with contrasting densities and (or) magnetizations causes characteristic potential-field anomalies that reflect the attitude of the fault. Information on the dip of the fault most commonly is obtained through quantitative modeling of these anomalies, but in some cases, the anomalies are so diagnostic that qualitative interpretations suffice to indicate the direction and approximate attitude of the fault plane.

The results of such interpretations at 16 sites primarily along the main trace of the San Andreas fault are shown in figure 9.4. The dip and depth-extent of the density or magnetization interfaces that are assumed to define the fault plane at these sites are somewhat uncertain because of the inherent ambiguity of gravity and magnetic interpretations, particularly those based on magnetic data, because rock magnetizations can have anomalous directions associated with their remanent components and because magnetic susceptibilities seldom are known with sufficient accuracy to serve as effective independent constraints. Thus, where the magnetic anomalies can be compatible with a vertical fault, we show the dip as vertical. The reader should be aware, however, that a

dipping interface extending to shallower depth would also be compatible with the data in some places.

Although major strike-slip faults probably are vertical over much of their reach, some have inferred dips of less than 90°, as indicated by many of the attitudes shown in figure 9.4. Just north of Point Arena, a buried magnetic body truncated on the east by the San Andreas fault has an east boundary that dips east beneath the trace of the fault (fig. 9.5*A*); its precise dip is uncertain but probably falls in the range 30°–50°. To the south, near the junction of the San Andreas and Calaveras faults, gravity modeling (Pavoni, 1973) suggests that the fault dips 70° SW. to a depth of about 6 km. A detailed study of seismicity along this section of the fault (Spieth, 1981) shows that hypocenters define a plane dipping 70° SW., thus strongly supporting the interpretation by Pavoni (1973). Robbins (1982) also found a southwest-dipping density interface at this site but argued that the fault plane was vertical, on the basis of a magnetic anomaly that he believed reflected a magnetic body, extending from 3- to 5-km depth, with a southwest edge directly beneath the surface trace of the fault. More recent, detailed magnetic measurements indicate that this magnetic body is much shallower (probably cropping out) than modeled by Robbins (1982) and thus weaken the argument for a vertical dip.

Near the intersection of the San Andreas and Garlock faults, gravity modeling by Andrew Griscom and K.G. Freeman (Griscom and Oliver, 1980) suggests that the fault dips 55° SW. to a depth of 6 km and thence vertically to a depth of at least 10 km (fig. 9.5*B*). About 60 km farther southeast, gravity data also indicate a southwesterly dip for the fault, but the angle of dip (30°–60°) is uncertain, owing to difficulty in interpreting the complex gravity field that results from large lateral density variations in the region southwest of the fault. Farther southeast, where the San Andreas fault splits into numerous branches (long 116°00′ W.), gravity data on two branches indicate that both faults dip northeast, with Precambrian crystalline rocks in the upper plate overlying young sedimentary rocks and alluvium. The gravity models suggest dips of 15°–25° NE. to depths of 1.5 to 2.5 km but do not resolve the fault attitude at greater depth (fig. 9.5*C*). Geologic mapping, which shows part of the southern branch of the San Andreas fault as a north-dipping thrust fault (Matti and others, 1985), and a study of recent earthquakes in this area, which yielded fault-plane solutions of predominantly oblique-slip motion and

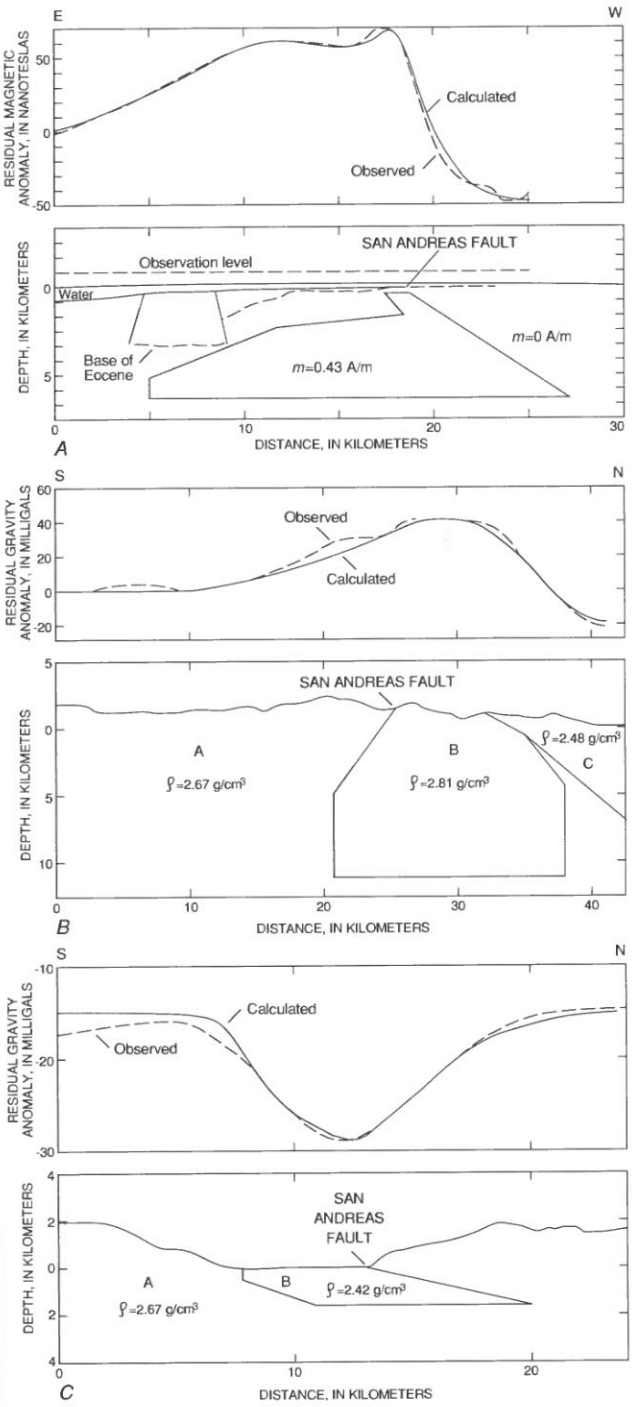

FIGURE 9.5.—Magnetic and gravity models across the San Andreas fault. m, magnetization; ρ, density. *A*, Magnetic model just north of Point Arena (long 123°40′ W.). *B*, Gravity model near junction of the San Andreas and Garlock faults (long 119°07′ N.). A, Mesozoic and Precambrian crystalline basement mantled by older Tertiary sedimentary rocks to south; B, mafic igneous rocks of the southern Sierra Nevada batholith; C, Tertiary and Quaternary sedimentary rocks of the Great Valley. *C*, Gravity model across southern branch at long 116°40′ W. A, Mesozoic and Precambrian crystalline basement; B, Tertiary and Quaternary sedimentary rocks of Coachella Valley.

including low-angle thrust solutions dipping 30° N. (Nicholson and others, 1986), both support the gravity interpretation of northeast-dipping faults in this area.

The inferred fault attitudes shown in figure 9.4 suggest a relation between attitude and plan-view geometry. Faults tend to be vertical except where they undergo abrupt changes of strike. The sinistral bends in the San Andreas fault near its junction with the Calaveras fault and in the Big Bend region southeast of its junction with the Garlock fault create regions likely to be subject to compression due to relative southward movement of the North American plate with respect to the Pacific plate. The dipping fault planes in these regions may reflect a thrust component of fault movement that accommodated the compression. Similarly, the region around the broad dextral bend in the San Andreas fault north of Point Arena may have a component of extension parallel to the direction of relative plate motion, and the low- angle eastward dip of fault plane there may reflect accommodation of the extension by low-angle normal faulting.

The number of examples on which the above speculations are based is quite limited, and further detailed investigations at critical sites along the San Andreas fault system are needed to test the relation between fault attitude, change of strike, and relative plate-motion direction.

FAULT-ZONE CHARACTERISTICS

Millions of years of strike-slip movement along faults of the San Andreas system have produced, in many places, a narrow fault zone in which physical properties differ from those in the surrounding rock masses. These differences are due to the presence within the fault zone of fractured or pulverized rock, exotic rock slivers that have been transported along the fault from other places, and such mobile materials as fluids and serpentinite that have migrated along the fault zone. A few investigators have used gravity and magnetic data to study the properties of this zone.

Although Stierman (1984) and Wang and others (1986) sought to explain gravity lows along the fault as the result of a substantial increase in porosity by fracturing, gravity lows not directly associated with basins filled by Cenozoic sedimentary rocks along the faults are very uncommon. These rare lows amount, with few exceptions (such as the 10–12-mGal low studied by Stierman, 1984), to amplitudes of only a few milligals. Feng and McEvilly (1983) and Trehu and Wheeler (1987) inferred from seismic data that zones of low seismic velocity 5 to 10 km wide and more than 10 km deep are associated with the San Andreas fault zone and, presumably, with fractured rocks. The low-velocity zone of Trehu and Wheeler (1987), however, has no associated gravity low, even though calculations by Andrew Griscom indicate that this zone might be expected to produce a gravity anomaly of about –25 mGal and more than 10 wide, using the standard velocity-density relations of Hill (1978). An explanation for this unexpected result can be found in the borehole gravity and seismic-velocity results (Schmoker, 1977; Stierman and Kovach, 1979) from a 600-m-deep borehole in diorite located 1.2 km from the San Andreas fault. For the lower half of this borehole, the seismic velocity averages only 3.1 km/s (although saturated core samples measured 6.6 km/s in the laboratory), and the average computed rock densities are as follows: bulk density from cores, 2.72 g/cm^3; borehole density from gravity measurements, 2.60 g/cm^3; and computed density from borehole velocities (density-velocity relations of Hill, 1978), 2.36 g/cm^3. Correcting for a nearby low-density sedimentary section that causes a gravity gradient along the hole raises the borehole density (from gravity measurements) closer to the bulk density. The results described above indicate that macrofractures can cause large decreases in seismic velocity but much smaller decreases in density than those predicted from standard velocity-density relations.

Allen (1968) pointed out a possible relation between the style of fault movement and the presence of serpentinite within fault zones of the San Andreas, Calaveras, and Hayward faults. He noted that serpentine is common within the fault zone along the creeping section of the San Andreas fault between Hollister and Cholame, whereas it is absent along the locked segments to the north and south. Irwin and Barnes (1975) noted the same relation between serpentinite and fault creep and discussed the possible role of metamorphic fluids on the seismic behavior of fault segments. Hanna and others (1972) studied aeromagnetic data along the San Andreas fault between San Francisco and San Bernardino and found that the creeping segment of the fault is characterized by broad aeromagnetic anomalies, which they interpreted as reflecting large concealed masses of serpentinite. Linear magnetic anomalies that most likely reflect serpentinite also are present along the creeping section of the Hayward fault east of the San Francisco Bay (fig. 9.3). These magnetic data support the speculation that appreciable amounts of serpentinite contained within a fault zone can influence the style of movement on the fault.

OFFSETS OF ANOMALIES

Strike-slip movement on the faults of the San Andreas system has produced offsets in formerly continuous geophysical anomalies. As might be expected, on those faults where the geologic offset is at most a few tens of kilometers, it is generally easy to identify corresponding magnetic or gravity features that are offset by similar

distances. Examples of such faults are the Elsinore fault and the rectilinear system of minor strike-slip faults in the Mojave Desert block northeast of the San Andreas fault. In figure 9.4, the two or more piercing points of an offset geophysical anomaly are labeled with the same letter, and the specific points being described are designated with subscripts, numbered consecutively from northeast to southwest across the fault system.

Offset along the San Andreas fault system in southern California is believed to be approximately 300 km in a right-lateral sense, based on offset of the Pelona-Orocopia schist belts, together with associated characteristic Precambrian and Triassic rock assemblages of the thrust plate overlying the schist belts (Crowell, 1962; Clarke and Nilsen, 1973; summarized in Hamilton, 1978). Isostatic gravity highs are associated with the Orocopia Schist (point A_1 at lat 33°35′ N., northeast side of fault), with the Pelona Schist of the Sierra Pelona/Soledad area (points A_2, A_3 at lat 34°35′ N., between the San Andreas and San Gabriel faults), and adjacent to the south side of the Pelona Schist of the Tejon/Garlock area (point A_4 at lat 34°50′ N., south of the San Andreas fault and west of the San Gabriel fault). Point A_4 is not well determined. The offsets of the gravity highs are, respectively, 240 km along the San Andreas between the first two highs (A_1 and A_2) and 60 km along the San Gabriel between the second two highs (A_3 and A_4), for a total of 300 km along the San Andreas fault system, in agreement with Crowell (1962). The source of the gravity highs is not obvious and may not be any of the rocks exposed at the surface (Griscom, 1980b), both because the density of the schist coring the antiforms is probably similar to or slightly lower than that of the surrounding Precambrian crystalline rocks and because other large areas of Pelona/Orocopia schist do not display associated gravity highs. The schist is marine in origin, predominantly metagraywacke of low metamorphic grade (Haxel and Dillon, 1978), and may be underlain by subducted oceanic crust. The gravity highs may indicate relatively uplifted oceanic crust beneath these specific antiformal exposures of the schist, or else the proportion of greenstone interbedded with schist may increase here with depth.

As mentioned above in the subsection entitled "Plan View," a linear magnetic high that extends along the San Andreas fault from long 116° to 118° W., a distance of about 200 km, indicates that a large area north of the fault in this region is composed of magnetic rocks, predominantly Mesozoic granitic plutons; the northwest limit of this magnetic area (J_1) is shown in figure 9.4. A similar large area of magnetic basement, also predominantly Mesozoic granitic rocks, that extends along the southwest side of the San Andreas fault is displaced from the former area right-laterally approximately 300 km; the northwest limit of this correlative area (J_2) is also shown in figure 9.4. This second area of magnetic rocks does not produce a significant magnetic high directly at the fault because the fault is on the northeast side of the magnetic mass and a magnetic low should occur for this geometry.

Several significant geophysical anomalies are found along the central section of the San Andreas fault north of its junction with the Garlock fault. A pronounced gravity high is located on the northeast side of the fault at lat 34°55′ N., where the southern "tail" of the Sierra Nevada is exposed. The associated rocks are hornblende-quartz gabbro and anorthositic gabbro (Ross, 1970, 1984) that also produce a substantial aeromagnetic high (point B_1, fig. 9.4). Similar rocks (Ross, 1970) are found within the San Andreas fault zone at Gold Hill (point B_2 at lat 35°50′ N., too small to show at this scale) and at Logan (point B_3 at lat 36°52′ N.), where magnetic anomalies (U.S. Department of Energy, 1981; U.S. Geological Survey, 1987) indicate that the gabbro bodies are thin slivers within the fault zone. The Logan outcrops are offset about 290 km from the gabbro of the Sierran "tail." A major northwest-trending magnetic anomaly extends northwestward of Logan near the coast (from point B_4 at lat 37°08′ N.). The source rocks for this magnetic anomaly are interpreted to be gabbro, similar to that exposed near Logan (Hanna and others, 1972a), because the anomaly requires a source body several kilometers thick. These corresponding offset geophysical anomalies support the geologic correlations implying about 300 to 320 km of offset.

The additional 100 km of granitic rocks extending northward from Logan to Montara Mountain (lat 37°35′ N.) along the southwest side of the San Andreas fault does not have any correlative rocks exposed on the northeast side of the fault north of the gabbro of Sierran "tail," but the concealed crystalline basement rocks beneath the sedimentary rocks of the Great Valley may be correlative. Indeed, recent work on the Tertiary sedimentary rocks that overlie this additional 100 km of granitic rocks on the San Francisco peninsula suggests a lithologic and paleogeographic correlation with similar sedimentary rocks of the Great Valley (San Joaquin Basin) that are relatively offset 320 to 330 km to the southeast (see fig. 3.4; Stanley, 1987).

Movement on the San Andreas fault north of San Francisco (Griscom and Jachens, 1989) is complicated by right-lateral displacement added by the presently active San Gregorio-Hosgri fault, which intersects the San Andreas fault at San Francisco and provides an additional 115 km (Graham and Dickinson, 1978) or 150 km (Clark and others, 1984; Ross, 1984) of offset. The total offset on the San Andreas fault system here is further complicated by movement on branch faults to the east (Calaveras and Hayward fault systems of unknown offset) and, more importantly, by past movement along the Pilarcitos fault,

the presently inactive fault strand branching westward from the San Andreas fault on the San Francisco peninsula. Probably most of the 300 to 320 km of displacement on the San Andreas fault has taken place along this strand because the presently active strand of the San Andreas fault that lies directly east of the Pilarcitos fault demonstrates only about 26 km of offset of a characteristic limestone belt within the Permanente terrane of the Franciscan assemblage (Bailey and others, 1964, p. 69; M.C. Blake, Jr., oral commun., 1987). The Pilarcitos fault (now truncated to the northwest by the San Gregorio fault) may have its former extension on the ocean side of the San Gregorio-San Andreas fault at about lat 38°30′ N. (see fig. 9.4), as proposed by Graham and Dickinson (1978). This proposed extension may have granitic rocks on the southwest side (more than the additional 100 km already discussed) that have no correlatives northeast of the San Andreas fault, unless the total offset on the San Andreas system substantially exceeds 300 km or unless granitic rocks underlie thrust blocks of Franciscan assemblage near the south end of the Great Valley (see preceding paragraph). There may be other, unidentified faults within the Salinian block that allow for this additional offset.

Offsets of geophysical anomalies along the San Gregorio-Hosgri fault support a total right-lateral movement of about 100 to 130 km that has been added to the total offset on the San Andreas fault system north of its junction with the San Gregorio fault. An offset gravity high (Silver, 1974) is located on the northeast side near Point Sur (point C_1 at lat 36°30′ N.) and on the southwest side at Año Nuevo (point C_2 at lat 37°15′ N.), with an offset of 105 to 130 km as remeasured by Graham and Dickinson (1978). We prefer an offset of 105 km (max 115 km) because any larger displacement will place the offset extension of the Pilarcitos fault on land north of lat 38°30′ N., where no such fault is known.

Displacements along the San Andreas fault north of lat 38°30′ N. have proved difficult to measure, both because the rocks exposed southwest of the fault near Point Arena have no obvious correlatives on the opposite side of the fault and because most of the fault trace is concealed beneath the Pacific Ocean (Griscom and Jachens, 1989). The rocks cropping out southwest of the fault near Point Arena are Upper Cretaceous and Tertiary marine sedimentary rocks, together with some older spilitic volcanic rocks that may be part of the Franciscan assemblage (Wentworth, 1968). Little basement information from rock samples is available in the shelf areas west of the San Andreas fault between Point Arena and the Mendocino fault. An important well 20 km west of Point Arena (fig. 9.4) recovered quartz-mica schist and slate basement cuttings (Hoskins and Griffiths, 1971) at a depth of about 1.43 km. This description resembles rocks either from the eastern metamorphosed Franciscan assemblage south of San Francisco or from roof pendants in the Salinian block, implying that a major strike-slip fault is located between the well and Point Arena. The proposed Pilarcitos fault extension is thus interpreted to lie here between the well and the coastline on a major fault shown by McCulloch (1987). Location of this proposed Pilarcitos fault extension farther northwest than Point Arena is uncertain, although the fault presumably continues to the former triple junction. McCulloch (1986; 1987, fig. 2b) described a boundary, termed the "Navarro discontinuity," trending east-west from the Point Arena area to the lower continental slope, on the basis of regional differences in magnetic pattern and physiography; this boundary may be the fault extension or an earlier strike-slip fault of this system. Griscom and Jachens (1989) also hypothesized a more northwestward extension, approximately colinear with the fault segment south of Point Arena, following a fault trace interpreted from seismic-reflection profiles (McCulloch, 1987, fig. 14).

Distinctive gravity and magnetic anomalies characterize the poorly known shelf area lying north of Point Arena and between the San Andreas fault and the proposed Pilarcitos extension (figs. 9.2, 9.3). The sources of these anomalies lie in the basement, with their upper surfaces at the basement interface below Tertiary sedimentary rocks, according to geophysical models and basement-depth calculations. A major gravity high (+20 mGal) is located near lat 40° N. (point D_2, fig. 9.4). We believe that the high-density basement rocks which cause this high extend southward along the west side of the San Andreas fault at least as far as at Point Arena (E_2, fig. 9.4), even though the gravity values on the map fall below 0 mGal along the southern part of this reach. The basement along the postulated southern part of the high is mantled by 1 to 3 km of Tertiary sedimentary rocks (Hoskins and Griffiths, 1971), which probably cause gravity lows (–15 to –30 mGal) that here mask the gravity high caused by the basement. Two magnetic anomalies on the shelf are truncated by the San Andreas fault at point F_2 and at a place a few kilometers south of point G_2 (fig. 9.4), which is located where the steepest gradient on the northeast side of the second anomaly is truncated by the fault (see McCulloch, 1987, fig. 17).

Our search for geophysical anomalies or features matching points D_2, E_2, F_2, and G_2 on the opposite (northeast) side of the San Andreas fault (see Griscom and Jachens, 1989) began with the observation that gravity highs are not characteristic of much of the Franciscan assemblage and are observed only extending along the San Andreas fault between approximately lat 37° and 38° N. (fig. 9.2). We have selected points D_1 and E_1 (fig. 9.4) as the approximate limits of the gravity highs

on the northeast side and propose to correlate these points and their connecting strip of high gravity with the corresponding points D_2 and E_2 and associated gravity high discussed in the previous paragraph. The positions of these points (D and E) along the fault vary in reliability but are probably no more accurate than ±20 km; point E_2 is the most uncertain. The total offset of the gravity high by the San Andreas fault is thus about 250±40 km. We have used the gravity results to explore our magnetic-anomaly map (fig. 9.3) for additional correlations. Only one correlation was found within an offset range of 200–300 km. We suggest that point F_1, marking the end of a truncated magnetic high passing through San Francisco, correlates with point F_2 and that point G_1, the truncated end of a magnetic gradient more than 50 km long, correlates with the other truncated gradient at point G_2. The locations of points F_1, F_2, and G_2 along the fault are accurate to within about ±5 km. Point G_1 is located a few kilometers too far to the southeast because a short northwestward extension of the feature was recently cut off by the young segment of the San Andreas fault in the San Francisco peninsula area and now lies between the San Andreas and Pilarcitos faults. The offset of points F_1 and F_2 is 250 km; the offset of points G_1 and G_2 is 263 km. The magnetic anomalies truncated at points F_1 and G_1 are associated with northwest-striking belts of mafic and ultramafic rocks within the Franciscan assemblage and are best shown on the more detailed maps by Brabb and Hanna (1981) and Griscom and Jachens (1989).

We conclude that the total offset of the pairs of corresponding magnetic features is approximately 250±10 km. Of this offset, about 105 km is attributable to the San Gregorio-Hosgri fault, leaving only 145 km for the San Andreas fault south of its junction with the San Gregorio fault. Because the total San Andreas offset south of the San Francisco peninsula is considered to be much larger, namely, about 300 km, we suggest that the missing 155 km is predominantly accounted for by former movement on the Pilarcitos fault and its proposed northwestward extension, which is thought to intersect the San Andreas at about lat 38°30′ N., as described above. This early Pilarcitos fault was thus formerly the main strand of an earlier San Andreas fault system that lay to the west of both magnetic features F and G (that is, before they were offset by faulting). Note that this interpreted fault-movement history and the subsequent plate-tectonic analysis all depend on the correctness of the correlation between the pairs of offset magnetic and gravity anomalies on the San Francisco peninsula and northwest of Point Arena. The magnetic and gravity anomalies northwest of Point Arena and west of the San Andreas fault are such conspicuous features and so obviously truncated by the San Andreas fault that we would expect to find their counterparts somewhere on the opposite side of the fault. Although we can find no alternative correlations for these anomalies other than those indicated in figure 9.4, we are aware that they may not correlate with any anomalies on the opposite side of the fault, although we consider this noncorrelation to be unlikely.

Additional information on offset along the proposed Pilarcitos fault extension is provided by interpretation of two strong magnetic anomalies on the northeast side of the San Andreas fault in central California (H_1 at lat 35°30′–35°40′ N. and lat 36°00′–36°15′ N., respectively). The source bodies for both anomalies appear to be truncated by the fault, and interpretations of the gravity and magnetic fields over both bodies suggest that they are composed of serpentinite (Hanna and others, 1972; Griscom and Jachens, in press). The most likely candidates for corresponding magnetic features on the southwest side of the fault system are the poorly defined anomalies at points H_2 and I_2 west of Point Arena. The magnetic field is poorly known in this area, and so anomaly locations and shapes may not be accurate, but the offset is approximately 435 km from points H_1 and I_1. This distance can be obtained by summing an assumed 320 km for offset on the San Andreas fault south of San Francisco plus 115 km offset on the San Gregorio-Hosgri fault. The location of point I_2 supports the Navarro discontinuity as a possible continuation of the proposed Pilarcitos fault extension, or some earlier continuation. We suggest that the large magnetic-high area bounded by the 500-nT contour and located 25 km south of point I_2 (fig. 9.3) may represent a southerly extension of anomaly I, which north of point I_1 extends for 400 km along the east side of the Coast Ranges. There appear to be no satisfactory alternative anomalies for correlation with points H_1 and I_1 along the southwest side of the present San Andreas fault near Point Arena.

IMPLICATIONS FOR PLATE TECTONICS

In the previous sections, we have discussed how potential-field data provide information on the three-dimensional configuration of the San Andreas fault and on the various offsets along member faults of the San Andreas system in relation to plate tectonics. Here, we interpret the potential-field expression of the two ends of the San Andreas fault system in relation to plate tectonics and lithospheric thickness.

MENDOCINO TRIPLE JUNCTION

At the north end of the San Andreas fault off Cape Mendocino, three lithospheric plates (the Juan de Fuca,

Pacific, and North American) meet at the Mendocino triple junction, where a trench meets two transform faults, the San Andreas and Mendocino faults. Along this trench to the north, the Juan de Fuca plate is subducting eastward beneath the North American plate. The geometry of this subducted plate has important implications (Jachens and Griscom, 1983) for an understanding of the Mendocino triple junction and its effects on the tectonics of California. During approximately the past 29 Ma, this triple junction has been migrating relatively northwestward along the coast of California from a latitude near Los Angeles (see fig. 3.11; Atwater, 1970; Atwater and Molnar, 1973). As this incipient San Andreas transform fault lengthened over time, eastward subduction continued to the north of the migrating triple junction.

During 29–23 Ma, the major fault of the San Andreas system was probably situated near the base of the continental slope, where an accreted wedge of Miocene(?) sedimentary rocks (McCulloch, 1987) accumulated between lat 35° and 40° N., presumably because of oblique subduction from transpressive forces between the plates. This now-inactive fault forms a contact between oceanic and continental crusts (fig. 9.4) that have major differences in magnetic properties (fig. 9.3). The oceanic crust displays the typical oceanic lineated or striped magnetic pattern striking north-south and northeast, with interruptions striking east-west or southeast that are caused by transform faults. The continental crust adjacent to this inactive fault is magnetically rather smooth and featureless. The magnetic boundary between oceanic and continental crust west of the San Andreas fault is very abrupt in comparison with active subduction zones (compare the magnetic expression of the Cascadia subduction zone off Oregon in Bond and Zietz, 1987); the oceanic stripes terminate at the base of the continental slope, even though reflection profiles show oceanic crust continuing farther east beneath the slope (McCulloch, 1987). The low convergence rate of oblique subduction and the time available since the fault became inactive may have allowed the concealed or subducted oceanic crust to heat up sufficiently beneath the continental margin to destroy the remanent magnetization that causes the stripes.

During early Miocene time (23 Ma), the motion along the transform must have been essentially strike slip and was substantially transferred to the present San Andreas fault system in central California. Without subduction east of the elongating transform, an ever-enlarging triangular hole or window (Dickinson and Snyder, 1979) developed in the slab of lithosphere subducted beneath the continent. This window model is also applicable to the time interval (29–23 Ma) but needs modification to include effects of transpression along the earlier San Andreas fault. The north boundary of this window is the subducted south edge of the Juan de Fuca plate, and hot upwelling asthenospheric material presumably occupies the window. The south edge of the Juan de Fuca plate lies beneath the North American plate at the shore about 20 km south of Cape Mendocino and can be identified by an east-west magnetic anomaly (Griscom, 1980a), as well as by the distribution of seismicity (Hutchings and others, 1981). This position coincides with a steep gravity gradient (here called the Cape Mendocino gravity anomaly) that slopes downward into a large gravity low (−50 mGal) to the north and east. The spatial coincidence between the position of the Cape Mendocino gravity anomaly at the coast and the place where the south edge of the Juan de Fuca plate passes beneath the coastline strongly suggests that this gravity anomaly reflects the south edge of the subducted plate (fig. 9.4). At least three other characteristics (Jachens and Griscom, 1983) of the anomaly support this interpretation. (1) The southeastward trend of the gravity anomaly and then its change to easterly are consistent with the directions of present and past relative motions between the Juan de Fuca and Pacific plates (Nishimura and others, 1981; Wilson, 1986). (2) The gravity anomaly broadens and is less steep toward the southeast, suggesting that its source progressively deepens in this direction; calculated depths along the anomaly to the end of the southeast-trending segment define a line plunging approximately 9° SE. with a depth of only 6 km at the coastline corresponding well to the 8-km depth estimated from aeromagnetic data (Griscom, 1980a). (3) A cross section across this anomaly, using the above depths together with reasonable densities and thicknesses for the subducted Juan de Fuca plate and the asthenospheric window fill to the southwest, produces a calculated gravity model (Jachens and Griscom, 1983) in good agreement with the observed gravity field. We draw the following conclusions from the gravity data (Jachens and Griscom, 1983).

1. Above the south edge of the Juan de Fuca plate, the North American plate must have the shape of a thin lip that gradually thickens eastward, attaining a thickness of possibly only about 30 km at the Coast Range fault; this fault marks the east limit of the Franciscan assemblage about 130 km inland from Cape Mendocino (see chap. 3). Just south of the Juan de Fuca plate, asthenospheric material that filled the slab window should lie beneath the North American plate at a depth comparable to that of the upper surface of the Juan de Fuca plate. Because the North American plate has been moving relatively southward across this boundary for many millions of years, the top of the asthenosphere probably is shallow beneath much of the Coast Ranges in central California, and the thin west lip of the North American plate may be decoupled from much of the mantle, although some underplating by mantle material is likely.

2. For reasons similar to conclusion 1, the lithosphere of southern California near the San Andreas fault system is thin and may be decoupled from much of the mantle.
3. Relatively thin, decoupled lithosphere may explain why deformation along the boundary between the Pacific and North American plates takes place over a zone 50 to 100 km wide rather than being restricted to the San Andreas fault, and why the plate boundary has been able to migrate eastward from the base of the continental slope to its present position at the San Andreas fault. It may also explain both why certain structural blocks southwest of the fault in southern California have been able to rotate clockwise by as much as 70°–90° during and after the Miocene (Luyendyk and others, 1985; Hornafius and others, 1986) and how extensional basins formed between these blocks. Furthermore, it can help explain why the seismicity of the San Andreas fault generally does not extend below 12-km depth.
4. Thin, relatively cool lithosphere of the southward-moving North American plate has been continuously placed on hot upwelling asthenosphere when crossing the Juan de Fuca plate boundary. As pointed out by Lachenbruch and Sass (1980), this process can explain the heat-flow anomaly in the North American plate that peaks in the Coast Ranges about 300 km south of the latitude of Cape Mendocino (Lachenbruch and Sass, 1973). Calculations by Lachenbruch and Sass (1980) show that, given a velocity of 5 cm/yr for movement of the Pacific plate relative to the North American plate, the heat flow should increase by a factor of 2 approximately 200 km south of the edge of the Juan de Fuca plate because 4 Ma is required for the heat anomaly to reach the surface from 20-km depth. These various parameters agree with the observed heat-flow anomaly. For a heat source as deep as 20 km, the model requires the hot asthenosphere to accrete to the bottom of the North American plate and to be conveyed off southward, so that a continuous supply of vertically moving, hot asthenosphere be supplied to the bottom near the Juan de Fuca plate boundary. This hypothesized coupling involves a rather thin layer of accreting upper mantle that, in turn, is probably decoupled from underlying asthenosphere. The gravitationally predicted depth to the base of the North American plate is within the limits required by Lachenbruch and Sass, (1980) model, at least within 70 km of the San Andreas fault.

Interpretation of geologic and geophysical data for the San Andreas fault system north of San Francisco (Griscom and Jachens, 1989) suggests that eastward migration of the plate boundary from its presumed original position at the base of the continental slope to its present position at the San Andreas transform fault may have occurred by means of a series of eastward jumps of the Mendocino triple junction covering a total distance of about 150 km during the past 29 Ma. Our general model for the history of this triple junction is one of successive eastward jumps, with sustained periods at each position while significant strike-slip motion occurred on the various transform fault systems, including the San Andreas fault. We are aware, however, that the picture in detail may have been far more complex. The present position of the San Andreas fault north of San Francisco is thus interpreted to be relatively youthful. The triple junction was initially situated near the base of the continental slope at the northwest end of the Miocene(?) accreted wedge (but far to the south of its present latitude); the basal fault (McCulloch, 1987) below the subduction complex is shown as a toothed line in figure 9.4 because of the thrust component in this transform fault. The triple junction is interpreted to have been subsequently situated at the north end of the proposed Pilarcitos fault extension and then to have jumped eastward a minimum of about 100 km to the present San Andreas fault trace at what is now approximately lat 38°20′ N. on the North American plate. When this jump occurred, the three faults that formed the junction all had to readjust; the simplest scenario is as follows: (1) The Mendocino fault was extended on strike farther eastward, for the distance of the jump, about 100 km; (2) a new segment of the San Andreas fault broke obliquely through the Franciscan assemblage to the northwest (severing the correlated geophysical anomalies described above) and extended from the new triple junction to the junction of the newly formed (or soon to be formed) San Gregorio fault with the Pilarcitos fault, a distance of about 250 km; and (3) the surface trace of the subduction zone north of the triple junction also jumped eastward 100 km, thus abruptly isolating a thin triangular slab of Franciscan assemblage (probably less than 15 km thick) from the North American plate. This postulated triangular slab of rocks is now gone, most likely subducted away. Further complexity is provided by the King Peak subterrane of the King Range terrane (McLaughlin and others, 1982), which is an elongate mass of turbidites, about 45 km long, just south of Cape Mendocino (fig. 9.4) that is believed to have been obductively accreted from the west during the early Pleistocene (McLaughlin and others, 1986). The King Peak subterrane may have been detached and transported northwestward from the San Francisco area (just south of lat 38°20′ N.) as part of the Pacific plate and then reattached to the North American plate by a very recent local jump of the triple junction westward less than 35 km (McLaughlin and others, 1982); this explanation may account for the anomalously higher thermal metamorphism of this subterrane relative to the terranes that are now adjacent to it. Recent work suggests that the triple

junction may be on shore at Cape Mendocino (Clarke, 1988; McLaughlin and others, 1988); if so, the King Peak subterrane may still be essentially part of the Pacific plate. The tectonic interpretation detailed above also requires that the San Gregorio-Hosgri fault first began moving and joined the present San Andreas fault at approximately the same time as or shortly after the eastward jump of the triple junction, and thus cut off the proposed northward extension of the Pilarcitos fault, after which the extension became inactive.

The proposed 150-km eastward movement of the triple junction can also explain the submarine topography near Cape Mendocino, where the Continental Shelf south of the Mendocino fault extends about 130 km farther west than that directly north of the fault.

The timing of the jump can be estimated from the horizontal offset of the paired geophysical anomalies, about 250 km, which translates to an age of about 5 Ma, assuming combined strike-slip rates of 4.8 cm/yr (DeMets and others, 1987; Minster and Jordan, 1978) for the San Andreas and San Gregorio faults. This age estimate is crude because it assumes that no other faults were absorbing the relative motion between the two plates. For example, simultaneous movement on the Hayward-Calaveras fault system will cause the computed age of offset to be too young. The eastward jump of the triple junction appears to be associated with a change in stress orientations in this region. The north end of the San Gregorio-Hosgri fault trends about 20° clockwise relative to the older fault traces. In addition, the northward-migrating triple junction subsequently traced out a major right-lateral bend, as shown by the present position of the San Andreas fault north of Point Arena. The central section of this bend is about 100 km long and trends 20° clockwise to the older trace. This change may correlate with the gradual change in absolute motion of the Pacific plate that occurred between 5 and 3.2 Ma (Cox and Engebretson, 1985; Pollitz, 1986), producing a change from strike slip to transpression in this region and a clockwise rotation of 20° (Harbert and Cox, 1986) in the relative-velocity vector for the plate pair, the same angle as the anomalous change in direction for both the San Gregorio fault and the right-lateral bend in the San Andreas fault north of Point Arena. This change in relative motion probably correlates with a change in strike direction of the subducting south edge of the Juan de Fuca plate, as deduced from gravity data (Jachens and Griscom, 1983). Before the jump, this strike was east-west, thus permitting eastward extension of the Mendocino transform fault without interference; after the jump, the strike of the subducting plate edge changed to S. 60° E., making later eastward fault extension more difficult.

Stratigraphic evidence for the postulated eastward jump of the triple junction about 5 Ma may be sought in the late Miocene and Pliocene stratigraphy of Deep Sea Drilling Project (DSDP) Site 173 (fig. 9.4). Depositional hiatuses occur at 5 and 4.3–3.2 Ma (Barron, 1989), whereas a study of both micropaleontology and tephra beds indicates a hiatus from about 4.4 to 2.8-Ma (Sarna-Wojcicki and others, 1987). McCulloch (1987, fig. 25) believed that the middle Pliocene deformation and minor erosion interpreted from reflection profiles correlate with this 4.4–2.8-Ma hiatus at Site 173. We suggest that the eastward jump of the triple junction about 5 Ma was shortly followed by the middle Pliocene deformation and by the hiatus at Site 173. These two correlative events were thus caused both by the jump and by the simultaneous change in the direction of relative plate motion.

SALTON BUTTES SPREADING CENTER

The San Andreas fault terminates to the southeast in a buried spreading center at the south end of the Salton Sea, where a row of five small siliceous volcanic domes ("buttes") protrude above recent sedimentary deposits of the Salton Trough. These domes, in addition to being associated with a local northeast-striking magnetic high, are situated on the crest of a larger, northwest-trending magnetic high (outlined on fig. 9.4) that is interpreted (Griscom and Muffler, 1971) to be caused by a magnetic mass, 30 km long, 3 to 12 km wide, and about 4 km thick, with its top buried more than 2 km below the surface. This magnetic high is associated with a similarly shaped gravity high (Biehler and Rotstein, 1979), the source of which may partly be the magnetic mass but may also be the relatively high density metamorphosed sedimentary rocks associated with the geothermal area (Elders and others, 1972). The Salton Buttes spreading center probably strikes northeast because the row of domes, the local aeromagnetic and gravity anomalies, and the geothermal area all coincide and strike northeast; (2) this proposed position for the center bisects the larger northwest-trending magnetic high into approximately equal parts interpreted to be new "oceanic" crust; and (3), ideally, a spreading center should trend approximately normal to an associated transform fault. In apparent contradiction, the Brawley seismic zone strikes S. 20° E. from the Salton Sea (Johnson and Hill, 1982) and consists of shallow earthquakes (Severson and McEvilly, 1987) located mostly within the valley fill; this seemingly anomalous direction may be due to accommodation of these overlying, partly decoupled materials to a series of short northeast-trending spreading centers between the Salton Sea and Cerro Prieto, Mexico (see fig. 3.6), on strike S. 20° E. and 100 km distant (Fuis and Kohler, 1984; Sibson, 1987). The large, northwest-trending magnetic mass is interpreted to reflect about 30 km of northwestward spreading along its long axis, in which the spreading was

associated with intrusive activity that built up a 30-km-long strip of magnetic mafic rocks and new crust in the lower section of and below the sedimentary fill. This magnetic feature may not be directly comparable to oceanic-crustal anomalies because slow cooling beneath the fill probably results in weak remanent magnetization, unlike the situation for oceanic crust. This anomaly thus may be predominantly caused by induced magnetization.

The gravity field of the Salton Trough, which is filled with great thicknesses of Cenozoic sedimentary rocks, varies systematically from north to south. An elongate gravity low of −30 to −40 mGal is associated with the sedimentary rocks northwest of the Salton Sea (beyond lat 33°20′ N.). Southward along the axis of the trough, the gravity field increases rapidly until the south end of the Salton Sea, where maximum values of 0 mGal are obtained over the presumed spreading center described above. Farther southeast, to the United States-Mexico border, gravity values range from only –10 to –20 mGal, an initially surprising observation because the 3.5 km or more of young, unmetamorphosed sedimentary deposits in this area might be expected to produce anomalies lower than –40 mGal (Biehler, 1964; Griscom, 1980c, p. 20), similar to the gravity expression northwest of the Salton Sea. Biehler (1964) offered two explanations for the missing low: thinner crust or local high-density basement beneath the trough. Seismic-refraction studies (Fuis and others, 1982, fig. 17A) confirm the second explanation and show a deep "subbasement" (density, 3.1 g/cm^3) in the trough that extends below about 12-km depth. Using this refraction model as a constraint, a gravity model (Fuis and others, 1982, fig. 20) indicates that the crust beneath the trough is no thinner than that of the bordering mountains a few kilometers to the northeast.

REFERENCES CITED

Allen, C.R., 1968, The tectonic environments of seismically active areas along the San Andreas fault system, *in* Dickinson, W.R., and Grantz, Arthur, eds., Proceedings of conference on geologic problems of San Andreas fault system: Stanford, Calif., Stanford University Publications in the Geological Sciences, v. 11, p. 70–82.

Atwater, Tanya, 1970, Implications of plate tectonics for the Cenozoic tectonic evolution of western North America: Geological Society of America Bulletin, v. 81, no. 12, p. 3513–3635.

Atwater, Tanya, and Molnar, Peter, 1973, Relative motion of the Pacific and North American plates deduced from sea-floor spreading in the Atlantic, Indian, and South Pacific Oceans, *in* Kovach, R.L., and Nur, Amos, eds., Proceedings of the conference on tectonic problems of the San Andreas fault system: Stanford, Calif., Stanford University Publications in the Geological Sciences, v. 13, p. 136–148.

Bailey, E.H., Irwin, W.P., and Jones, D.L., 1964, Franciscan and related rocks, and their significance in the geology of western California: California Division of Mines and Geology Bulletin 183, 177 p.

Barron, J.A., 1989, The late Cenozoic stratigraphic record and hiatuses of the northeast Pacific: Results from the Deep Sea Drilling Project, *in* Winterer, E.L., Hussong, D.M., and Decker, R.W., eds., The eastern Pacific Ocean and Hawaii (DNAG Associated Volume GSMV–N): Boulder, Colo., Geological Society of America.

Biehler, Shawn, 1964, Geophysical study of the Salton trough of southern California: Pasadena, Calif., California Institute of Technology, Ph.D. thesis, 139 p.

Biehler, Shawn, and Rotstein, Yair, compilers, 1979, Salton Sea sheet of Bouguer gravity map of California: Sacramento, California Division of Mines and Geology, scale 1:250,000.

Blakely, R.J., and Simpson, R.W., 1986, Approximating edges of source bodies from magnetic or gravity anomalies: Geophysics, v. 51, no. 7, p. 1494–1498.

Bond, K.R., and Zietz, Isadore, 1987, Composite magnetic-anomaly map of the conterminous United States west of 96° longitude: U.S. Geological Survey Geophysical Investigations Map GP–977, scale 1:2,500,000.

Brabb, E.E., and Hanna, W.F., 1981, Maps showing aeromagnetic anomalies, faults, earthquake epicenters, and igneous rocks in the southern San Francisco Bay region, California: U.S. Geological Survey Geophysical Investigations Map GP–932, scale 1:125,000.

Chapman, R.H., 1975, Geophysical study of the Clear Lake region, California; California Division of Mines and Geology Special Report 116, 23 p.

Chuchel, B.A., 1985, POLYGON—an interactive program for constructing and editing the geometries of polygons using a color graphics terminal: U.S. Geological Survey Open-File Report 85–233, 38 p.

Clark, J.C., Brabb, E.E., Greene, H.G., and Ross, D.C., 1984, Geology of Point Reyes peninsula and implications for San Gregorio fault history, *in* Crouch, J.K., and Bachman, S.B., eds., Tectonics and sedimentation along the California margin: Los Angeles, Society of Economic Paleontologists and Mineralogists, Pacific Section, p. 67–86.

Clarke, S.H., Jr., 1988, Late Cenozoic deformation of the California continental margin north of Cape Mendocino: Implications for Mendocino triple junction location [abs.]: Geological Society of America Abstracts with Programs, v. 20, no. 7, p. A382.

Clarke, S.H., Jr., and Nilsen, T.H., 1973, Displacement of Eocene strata and implications for the history of offset along the San Andreas fault, central and northern California, *in* Kovach, R.L., and Nur, Amos, eds., Proceedings of the conference on tectonic problems of the San Andreas fault system: Stanford, Calif., Stanford University Publications in the Geological Sciences, v. 13, p. 358–367.

Cox, Allan, and Engebretson, D.C., 1985, Change in motion of Pacific plate at 5 Myr Bp: Nature, v. 313, no. 6002, p. 472–474.

Crowell, J.C., 1962, Displacement along the San Andreas fault, California: Geological Society of America Special Paper 71, 61 p.

DeMets, Charles, Gordon, R.G., Stein, Seth, and Argus, D.F., 1987, A revised estimate of Pacific-North America motion and implications for western North America plate boundary zone tectonics: Geophysical Research Letters, v. 14, no. 9, p. 911–914.

Dickinson, W.R., and Snyder, W.S., 1979, Geometry of subducted slabs related to San Andreas transform: Journal of Geology, v. 87, no. 6, p. 609–627.

Elders, W.A., Rex, R.W., Meidav, Tsvi, Robinson, P.T., and Biehler, Shawn, 1972, Crustal spreading in southern California: The Imperial Valley and the Gulf of California formed by the rifting apart of a continental plate: Science, v. 178, no. 4056, p. 15–24.

Feng, Rui, and McEvilly, T.V., 1983, Interpretation of seismic reflection profiling data for the structure of the San Andreas fault zone: Seismological Society of America Bulletin, v. 73, no. 6, p. 1701–1720.

Fuis, G.S., and Kohler, W.M., 1984, Crustal structure and tectonics of the Imperial Valley region, California, *in* Rigsby, C.A., ed., The Imperial Basin—tectonics, sedimentation, and thermal aspects (Volume 40): Society of Economic Paleontologists and Mineralogists, Pacific Section Annual Convention, San Diego, Calif., 1984, Papers, p. 1–13.

Fuis, G.S., Mooney, W.D., Healey, J.H., McMechan, G.A., and Lutter, W.J., 1982, Crustal structure in the Imperial Valley region, *in* The Imperial Valley, California, earthquake of October 15, 1979: U.S. Geological Survey Professional Paper 1254, p. 25–49.

Geological Society of America, 1987, Magnetic anomaly map of North America: Boulder, Colo., scale 1:5,000,000, 4 sheets.

Godson, R.H., 1985, Preparation of a digital grid of gravity anomaly values of the conterminous United States, *in* Hinze, W.J., ed., The utility of regional gravity and magnetic anomaly maps: Tulsa, Okla., Society of Exploration Geophysicists, p. 38–45.

Graham, S.A., and Dickinson, W.R., 1978, Apparent offsets of on-land geologic features across the San Gregorio-Hosgri fault trend: California Division of Mines and Geology Special Report 137, p. 13–23.

Griscom, Andrew, 1980a, Aeromagnetic interpretation of the Mendocino triple junction, *in* Streitz, Robert, and Sherburne, R.W., eds., Studies of the San Andreas fault zone in northern California: California Division of Mines and Geology Special Report 140, p. 121–127.

—— 1980b, Aeromagnetic map and interpretation maps of the King Range and Chemise Mountain instant study areas, northern California: U.S. Geological Survey Miscellaneous Field Studies Map MF–1196–B, scale 1:62,500, 2 sheets.

—— 1980c, Salton Trough, *in* Oliver, H.W., ed., Interpretation of the gravity map of California and its continental margin: California Division of Mines and Geology Bulletin 205, p. 20–21.

Griscom, Andrew, and Jachens, R.C., 1989, Tectonic history of the north portion of the San Andreas fault system, California, inferred from gravity and magnetic anomalies: Journal of Geophysical Research, v. 93, no. B4, p. 3089–3099.

Griscom, Andrew, and Jachens, R.C., in press, Tectonic implications of gravity and magnetic models along east-west seismic profiles across the Great Valley near Coalinga, chap. 5 *of* Rymer, M.J., and Ellsworth, W.L., eds., The Coalinga, California, earthquake of May 2, 1983: U.S. Geological Survey Professional Paper 1487, p. 69–78.

Griscom, Andrew, and Muffler, L.J.P., 1971, Aeromagnetic map and interpretation of the Salton Sea geothermal area, California: U.S. Geological Survey Geophysical Investigations Map GP–754, scale 1:62,500.

Griscom, Andrew, and Oliver, H.W., 1980, Isostatic gravity highs along the west side of the Sierra Nevada and the Peninsular Ranges batholiths, California [abs.]: Eos (American Geophysical Union Transactions), v. 61, no. 46, p. 1126.

Hamilton, Warren, 1978, Mesozoic tectonics of the western United States, *in* Howell, D.G., and McDougall, K.A., eds., Mesozoic paleogeography of the western United States: Pacific Coast Paleogeography Symposium 2: Los Angeles, Society of Economic Paleontologists and Mineralogists, Pacific Section, p. 33–70.

Hanna, W.F., Brown, R.D., Ross, D.C., and Griscom, Andrew, 1972a, Aeromagnetic reconnaissance along the San Andreas fault between San Francisco and San Bernardino, California: U.S. Geological Survey Geophysical Investigations Map GP–815, scale 1:250,000.

Hanna, W.F., Burch, S.H., and Dibblee, T.W., Jr., 1972b, Gravity, magnetics, and geology of the San Andreas fault area near Cholame, California: U.S. Geological Survey Professional Paper 646–C, p. C1–C29.

Harbert, William, and Cox, Allan, 1986, Late Neogene motion of the Pacific plate [abs.]: Eos (American Geophysical Union Transactions), v. 67, no. 44, p. 1225.

Haxel, G.B., and Dillon, J.T., 1978, The Pelona-Orocopia schist and Vincent- Chocolate Mountain thrust system, southern California, *in* Howell, D.G., and McDougall, K.A., eds., Mesozoic paleogeography of the western United States: Pacific Coast Paleogeography Symposium 2: Los Angeles, Society of Economic Paleontologists and Mineralogists, Pacific Section, p. 453–469.

Heiskanen, W.A., and Moritz, Helmut, 1967, Physical geodesy: San Francisco, W.H. Freeman, 364 p.

Hill, D.P., 1978, Seismic evidence for the structure and Cenozoic tectonics of the Pacific Coast states, *in* Smith, R.B., and Eaton, G.P., eds., Cenozoic tectonics and regional geophysics of the western Cordillera: Geological Society of America Memoir 152, p. 145–174.

Hornafius, J.S., Luyendyk, B.P., Terres, R.R., and Kamerling, M.J., 1986, Timing and extent of Neogene tectonic rotation in the western Transverse Ranges, California: Geological Society of America Bulletin, v. 97, no. 12, p. 1476–1487.

Hoskins, E.G., and Griffiths, J.R., 1971, Hydrocarbon potential of northern and central California offshore, *in* Cram, I.H., ed., Future petroleum provinces of the United States—their geology and potential: American Association of Petroleum Geologists Memoir 15, v. 1, p. 212–228.

Hutchings, L.J., Turcotte, F.T., Schnapp, Madeleine, and McPherson, R.B., 1981, Seismicity of the Mendocino triple junction [abs.]: Earthquake Notes, v. 52, no. 1, p. 42–43.

Irwin, W.P., and Barnes, Ivan, 1975, Effect of geologic structure and metamorphic fluids on seismic behavior of the San Andreas fault system in central and northern California: Geology, v. 3, no. 12, p. 713–716.

Isherwood, W.F., 1976, Gravity and magnetic studies of the Geysers–Clear Lake geothermal region, California, U.S.A.: United Nations Symposium on the Development and Use of Geothermal Resources, 2d, San Francisco, 1975, Proceedings, v. 2, p. 1065–1074.

Jachens, R.C., and Griscom, Andrew, 1983, Three-dimensional geometry of the Gorda plate beneath northern California: Journal of Geophysical Research, v. 88, no. B11, p. 9375–9392.

—— 1985, An isostatic residual gravity map of California—a residual map for interpretation of anomalies from intracrustal sources, *in* Hinze, W.J., ed., The utility of regional gravity and magnetic anomaly maps: Tulsa, Okla., Society of Exploration Geophysicists, p. 347–360.

Jennings, C.W., Strand, R.G., and Rogers, T.H., compilers, 1977, Geologic map of California: Sacramento, California Division of Mines and Geology, scale 1:750,000.

Johnson, C.E., and Hill, D.P., 1982, Seismicity of the Imperial Valley, *in* The Imperial Valley, California, earthquake of October 15, 1979: U.S. Geological Survey Professional Paper 1254, p. 15–24.

Karki, Penti, Kivioja, Lassi, and Heiskanen, W.A., 1961, Topographic-isostatic reduction maps for the world for the Hayford Zones 18-l, Airy-Heiskanen system, T=30 km: International Association of Geodesy, Isostatic Institute Publication 35, 5 p.

King, P.B., compiler, 1969, Tectonic map of North America: Washington, U.S. Geological Survey, scale 1:5,000,000, 2 sheets.

Lachenbruch, A.H., and Sass, J.H., 1973, Thermo-mechanical aspects of the San Andreas fault system, *in* Kovach, R.L., and Nur, Amos, eds., Proceedings of the conference on tectonic problems of the San Andreas fault system: Stanford, Calif., Stanford University Publications in the Geological Sciences, v. 13, p. 190–205.

—— 1980, Heat flow and energetics of the San Andreas fault zone: Journal of Geophysical Research, v. 85, no. B11, p. 6185–6222.

Luyendyk, B.P., Kamerling, M.J., Terres, R.R., and Hornafius, J.S., 1985, Simple shear of southern California during Neogene time suggested by paleomagnetic declinations: Journal of Geophysical

Research, v. 90, no. B14, p. 12454–12466.
Matti, J.C., Morton, D.M., and Cox, B.F., 1985, Distribution and geologic relations of fault systems in the vicinity of the central Transverse Ranges, southern California: U.S. Geological Survey Open-File Report 85–365, 27 p., scale 1:250,000, 2 sheets.
McCulloch, D.S., 1986, The Vizcaino block south of the Mendocino triple junction [abs.]: Eos (American Geophysical Union Transactions), v. 67, no. 44, p. 1219–1220.
—— 1987, Regional geology and hydrocarbon potential of offshore central California, chap. 16 *of* Scholl, D.W., Grantz, Arthur, and Vedder, J.G., eds., Geology and resource potential of the continental margin of western North America and adjacent ocean basins--Beaufort Sea to Baja California (Earth Science Series, v. 6): Houston, Tex., Circum-Pacific Council for Energy and Mineral Resources, p. 353–401.
McLaughlin, R.J., Kling, S.A., Poore, R.Z., McDougall, Kristin, and Beutner, E.C., 1982, Post-middle Miocene accretion of Franciscan rocks, northwestern California: Geological Society of America Bulletin, v. 93, no. 7, p. 595–605.
McLaughlin, R.J., Sliter, W.V., Clarke, S.H., Jr., McCulloch, D.S., Frederiksen, N.O., and Engebretson, D.C., 1988, Implications of onshore and offshore structure for location and Cenozoic evolution of the Mendocino triple junction [abs.], Geological Society of America Abstracts with Programs, v. 20, no. 7, p. A382.
McLaughlin, R.J., Sliter, W.V., and Frederiksen, N.O., 1986, Plate motions recorded by tectonostratigraphic terranes adjacent to the Mendocino triple junction [abs.]: Eos (American Geophysical Union Transactions), v. 67, no. 44, p. 1219.
Minster, J.B., and Jordan, T.H., 1978, Present-day plate motions: Journal of Geophysical Research, v. 83, no. B11, p. 5331–5354.
Nicholson, Craig, Seeber, Leonardo, Williams, Patrick, and Sykes, L.R., 1986, Seismicity and fault kinematics through the eastern Transverse Ranges, California: Block rotation, strike-slip faulting, and low-angle thrusts: Journal of Geophysical Research, v. 91, no. B5, p. 4891–4908.
Nishimura, C., Wilson, D.S., and Hey, R.N., 1981, Present-day subduction of the Juan de Fuca plate [abs.]: Eos (American Geophysical Union Transactions), v. 62, no. 17, p. 404.
Oliver, H. W., ed., 1980, Interpretation of the gravity map of California and its continental margin: California Division of Mines and Geology Bulletin 205, 52 p.
Oliver, H.W., Chapman, R.H., Biehler, Shawn, Robbins, S.L., Hanna, W.F., Griscom, Andrew, Beyer, L.A., and Silver, E.A., 1980, Gravity map of California and its continental margin: California Division of Mines and Geology California Geologic Data Map 3, scale 1:750,000, 2 sheets.
Pavoni, Nazario, 1973, A structural model for the San Andreas fault zone along the northeast side of the Gabilan Range, *in* Kovach, R.L., and Nur, Amos, eds., Proceedings of the conference on tectonic problems of the San Andreas fault system: Stanford, Calif., Stanford University Publications in the Geological Sciences, v. 13, p. 259–267.
Pollitz, F.F., 1986, Pliocene change in Pacific plate motion: Nature, v. 320, no. 6064, p. 738–741.
Robbins, S.L., 1982, Complete Bouguer gravity, aeromagnetic, and generalized geologic map of the Hollister 15-minute quadrangle, California: U.S. Geological Survey Geophysical Investigations Map GP–945, scale 1:62,500, 2 sheets.
Roberts, C.W., Jachens, R.C., and Oliver, H.W., 1981, Preliminary isostatic residual gravity map of California: U.S. Geological Survey Open-File Report 81–573, scale 1:750,000, 5 sheets.
Ross, D.C., 1970, Quartz gabbro and anorthositic gabbro: Markers of offset along the San Andreas fault in the California Coast Ranges: Geological Society of America Bulletin, v. 81, no. 12, p. 3647–3661.
—— 1984, Possible correlations of basement rocks across the San Andreas, San Gregorio-Hosgri, and Rinconada-Reliz-King City faults, California: U.S. Geological Survey Professional Paper 1317, 37 p.
Saltus, R.W., and Blakely, R.J., 1983, Hypermag: An interactive, two-dimensional gravity and magnetic modeling program: U.S. Geological Survey Open-File Report 83–241, 91 p.
Sarna-Wojcicki, A.M., Morrison, S.D., Meyer, C.E., and Hillhouse, J.W., 1987, Correlation of upper Cenozoic tephra layers between sediments of the western United States and eastern Pacific Ocean and comparison with biostratigraphic and magnetostratigraphic age data: Geological Society of America Bulletin, v. 98, no. 2, p. 207–223.
Schmoker, J.W., 1977, Density variation in quartz diorite determined from borehole gravity measurements, San Benito County, California: Log Analyst, v. 18, no. 2, p. 32–38.
Severson, L.K., and McEvilly, T.V., 1987, Analysis of seismic reflection data from the Imperial Valley, California [abs.]: Geological Society of America Abstracts with Programs, v. 19, no. 6, p. 449–450.
Sibson, R.H., 1987, Earthquake rupturing as a mineralizing agent in hydrothermal systems: Geology, v. 15, no. 8, p. 701–703.
Silver, E.A., 1974, Structural interpretation from free-air gravity on the California continental margin, 35° to 40° N.: Geological Society of America Abstracts with Programs, v. 6, p. 253.
Simpson, R.W., Jachens, R.C., Blakely, R.J., and Saltus, R.W., 1986, A new isostatic residual gravity map of the conterminous United States with a discussion on the significance of isostatic residual anomalies: Journal of Geophysical Research, v. 91, no. B8, p. 8348–8372.
Simpson, R.W., Kelty, T.K., and Rodriguez, E.A., in press, Aeromagnetic map of the Cucamonga Roadless Areas, San Bernardino County, California: U.S. Geological Survey Miscellaneous Investigations Series Map I–1646–C, scale 1:62,500.
Snyder, D.B., Roberts, C.W., Saltus, R.W., and Sikora, R.F., 1982, A magnetic tape containing the principal facts of 64,026 gravity stations in California: U.S. National Technical Information Service Report PB 82–168287, 34 p.
Society of Exploration Geophysicists, 1982, Gravity anomaly map of the United States exclusive of Alaska and Hawaii: Tulsa, Okla., scale 1:2,500,000.
Spieth, M.A., 1981, Two detailed seismic studies in central California. Part I: Earthquake clustering and crustal structure studies of the San Andreas fault near San Juan Bautista. Part II: Seismic velocity structure along the Sierra foothills near Oroville, California: Stanford, Calif., Stanford University, Ph.D. thesis, 174 p.
Stanley, R.G., 1987, New estimates of displacement along the San Andreas fault in central California based on paleobathymetry and paleogeography: Geology, v. 15, no. 2, p. 171–174.
Stierman, D.J., 1984, Geophysical and geological evidence for fracturing, water circulation, and chemical alteration in granitic rocks adjacent to major strike-slip faults: Journal of Geophysical Research, v. 89, no. B7, p. 5849–5857.
Stierman, D.J., and Kovach, R.L., 1979, An *in situ* velocity study: The Stone Canyon well: Journal of Geophysical Research, v. 84, no. B2, p. 672–678.
Trehu, A.M., and Wheeler, W.H., IV, 1987, Possible evidence for subducted sedimentary materials beneath central California: Geology, v. 15, no. 3, p. 254–258.
U.S. Department of Energy, 1981, Airborne gamma-ray spectrometer and magnetometer survey, Santa Cruz quadrangle, California: Open-File Report GJBX 50(81), 2 v.
U.S. Geological Survey, 1979, Aeromagnetic map of the southern San Bernardino Mountains area, California: Open-File Report 79–1448, scale 1:62,500.
—— 1987, Aeromagnetic map of the Hernandez-Parkfield area, south-

western California: Open-File Report 87–092, scale 1:250,000.

Vedder, J.G., 1987, Regional geology and petroleum potential of the southern California borderland, *in* Scholl, D.W., Grantz, Arthur, and Vedder, J.G., eds., Geology and resource potential of the continental margin of western North America and adjacent ocean basins-Beaufort Sea to Baja California (Earth Science Series, v. 6): Houston, Tex., Circum-Pacific Council for Energy and Mineral Resources, p. 403–447.

Wang, C.-Y., Feng, Rui, Yao, Zhengsheng, and Shi, Xingjue, 1986, Gravity anomaly and density structure of the San Andreas fault zone: Pure and Applied Geophysics, v. 124, no. 1, p. 127–140.

Wentworth, C.M., 1968, Upper Cretaceous and lower Tertiary strata near Gualala, California, and inferred large right slip on the San Andreas fault, *in* Dickinson, W.R., and Grantz, Arthur, eds., Proceedings of conference on geologic problems of San Andreas fault system: Stanford, Calif., Stanford University Publications in Geological Sciences, v. 11, p. 130–148.

Wilson, D.S., 1986, A kinematic model for the Gorda deformation zone as a diffuse southern boundary of the Juan de Fuca plate: Journal of Geophysical Research, v. 91, no. B10, p. 10259–10269.

—— 1989, Deformation of the so-called Gorda plate: Journal of Geophysical Research, v. 94, no. B3, p. 3065–3075.

As the Pacific plate slides northward past the North American plate along the San Andreas fault, the frictional stress that resists plate motion there is overcome to cause earthquakes. However, the frictional heating predicted for the process has never been detected. Thus, in spite of its importance to an understanding of both plate motion and earthquakes, the size of this frictional stress is still uncertain, even in order of magnitude.

10. STRESS AND HEAT FLOW

By ARTHUR H. LACHENBRUCH and A. MCGARR

CONTENTS

INTRODUCTION

As one of the best exposed tectonic-plate boundaries in the world, the San Andreas fault provides an excellent opportunity to study the forces causing interplate motion and the associated great earthquakes. Thus, there is considerable motivation, scientific, social, and economic, to understand the thermomechanics of the San Andreas fault system, which has been the subject of intensive studies for the past several decades.

Although substantial progress has been made in unraveling the complex kinematics of the San Andreas fault system (Atwater, 1970; Minster and Jordan, 1984; Weldon and Humphries, 1986), efforts to determine the stresses that give rise to San Andreas fault slip, to date, have not led to anything resembling scientific consensus. The uncertainty results from widespread disagreement over the implications of different methods of assessing the stresses.

The question of how much shear stress acts on the San Andreas fault to cause dextral slip began to acquire definition in 1968, when the first heat-flow data adjacent to the fault zone (fig. 10.1) were gathered and analyzed by Henyey (1968). Because these data did not reveal any anomalous heat flow near the major active faults of the San Andreas system, upper bounds of about 10 to 20 MPa on the average frictional stress resisting fault motion could be calculated (Brune and others, 1969; Henyey and Wasserburg, 1971). These upper bounds were taken as evidence confirming speculation on the low strength of the crust based on earthquake stress drops, almost invariably in the range 0.1–10 MPa (for example, Chinnery, 1964; Brune and Allen, 1967). At the same time, however, laboratory experiments indicated typical frictional strengths for precut rock samples of about 100 MPa under pressure and temperature conditions thought to obtain in the upper crust (Byerlee and Brace, 1968, 1969; Byerlee, 1970).

◀ FIGURE 10.1.—Heat-flow and stress measurements are taken in wells such as this one being drilled by the U.S. Geological Survey at the Crystallaire site, 4 km northeast of the San Andreas fault in the western Mojave Desert. Photograph by M.D. Zoback.

Over the next several years, new heat-flow measurements supported the absence of any local heat-flow anomaly associated with the San Andreas fault (Lachenbruch and Sass, 1973) and thus augmented the position for low frictional fault strength. The recognition of a broad heat-flow high coincident with the Coast Ranges of California led Lachenbruch and Sass (1973) to suggest that partial decoupling at the base of the seismogenic part of the crust might account for both the weak fault (minimum in shear stress at the fault trace) and the broad thermal anomaly.

Additional laboratory experiments on different rock types, and in conditions of higher temperature and confining pressure than had been obtained previously, continued to support high frictional strength in the top 15 to 20 km of the fault zone (Stesky and Brace, 1973). The experimental results are most simply characterized in terms of a coefficient of friction that varies little with rock type (Byerlee, 1978), slip rate, or slip history (Dieterich, 1979; Ruina, 1983). As emphasized by Brace and Kohlstedt (1980) and Kirby (1980), these results still indicate a high-strength upper crust.

Beginning in the late 1970's, inplace stress measurements have provided another way to assess the stress acting on the San Andreas fault (Zoback and others, 1977), especially with the advent of stress measurements at depths approaching 1 km only a few kilometers distant from the fault (Zoback and others, 1980). If the observed depth gradient for the component of shear stress thought to act on the San Andreas fault could be extrapolated to the base of the seismogenic zone, as argued by McGarr and others (1982), then the corresponding frictional stress resisting fault motion is a factor of 3 greater than the upper bound from the heat-flow analyses, as presented most recently by Lachenbruch and Sass (1980).

The most recent developments, if accepted at face value, could be construed as additional evidence favoring a low-strength San Andreas fault. Specifically, stress-direction indicators on either side of the fault have been interpreted to mean that there is almost no shear stress resolved on the fault plane, thus implying a very weak fault zone (Mount and Suppe, 1987; Zoback and others, 1987). If so, then the question regarding the strength of the fault would be answered, and the outstanding problem would be the equally vexing one of understanding the nature of a remarkably weak fault zone.

This chapter is largely a review and commentary on the different approaches taken to estimate the tractions acting on the San Andreas fault. We restrict our attention to three main methods: (1) inferring stress from the fault's energy budget (thermal and kinetic), (2) inferring fault strength from laboratory measurements of the stresses needed to slide rocks past one another under pressure, and (3) inferring stress on the fault from observations of the crustal state of stress.

ESTIMATES OF AVERAGE STRESS FROM FAULT ENERGETICS

ENERGY BALANCE

In figure 10.2, an earthquake is viewed, according to Reid's (1910) rebound theory, as a strained patch of fault surface of area A that suddenly breaks, permitting points initially in contact to be displaced from one another by an average amount u. The breakage is like the sudden failure of an overloaded leaf spring. We are interested in the average shear stress acting parallel to the wall in the failed section of the fault surface. We denote its initial value by τ_1 and its final value by τ_2. The inclined line in figure 10.3 represents the elastic unloading of the medium as the earthquake displacement increases to its final value u. The area under this line, which represents the total elastic energy released by the earthquake per unit area of faulted surface, can be written as

$$\frac{E}{A} = \bar{\tau} u \,, \tag{1a}$$

where

$$\bar{\tau} = \tfrac{1}{2}(\tau_1 + \tau_2) \,. \tag{1b}$$

The energy E must supply the work E_a of generating seismic waves and the work E_r, converted to heat in overcoming frictional resisting forces. Thus,

$$E = E_a + E_r + ? \,, \tag{2}$$

where the question mark is a reminder (which we shall forget for the moment) that there may be other significant sinks of earthquake energy, such as the surface

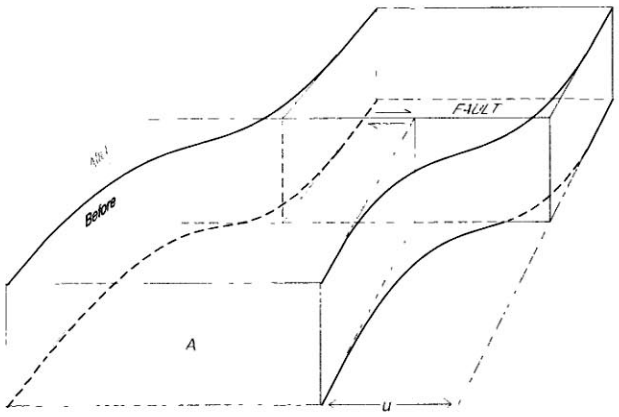

FIGURE 10.2.—Elastic-rebound theory (Reid, 1910), showing displacement near a strike-slip fault segment of area A before and after an earthquake with displacement u. Arrows along fault indicate direction of relative movement.

energy consumed in creating new fractures. We can now write

$$\frac{E_a}{A} = \tau_a u \tag{3}$$

$$\frac{E_r}{A} = \tau_r u , \tag{4}$$

where τ_a, the "apparent stress" of seismology, is the portion of the earthquake stress $\bar{\tau}$ allocated to the production of seismic waves, and τ_r is the average frictional resisting stress allocated to the production of heat. The individual areas represented by equations 3 and 4 are shown in figure 10.3 by contrasting patterns.

This interpretation of the areas in figure 10.3 is fairly general, as long as we define τ_1, τ_2, and τ_r, respectively, as the weighted averages of initial stress, final stress, and friction over the faulted surface, the weighting function being the local fault slip (see Savage and Wood, 1971; Lachenbruch and Sass, 1980). Combining equations 1 through 4 yields

$$\bar{\tau} = \tau_a + \tau_r + ? , \tag{5}$$

which states that unless the question mark represents something important that we've neglected, the average earthquake stress $\bar{\tau}$ is the sum of the apparent stress τ_a, to be estimated from seismic measurements of E_a (eq. 3), and the resisting stress τ_r, to be estimated from thermal measurements of frictional heat E_r (eq. 4).

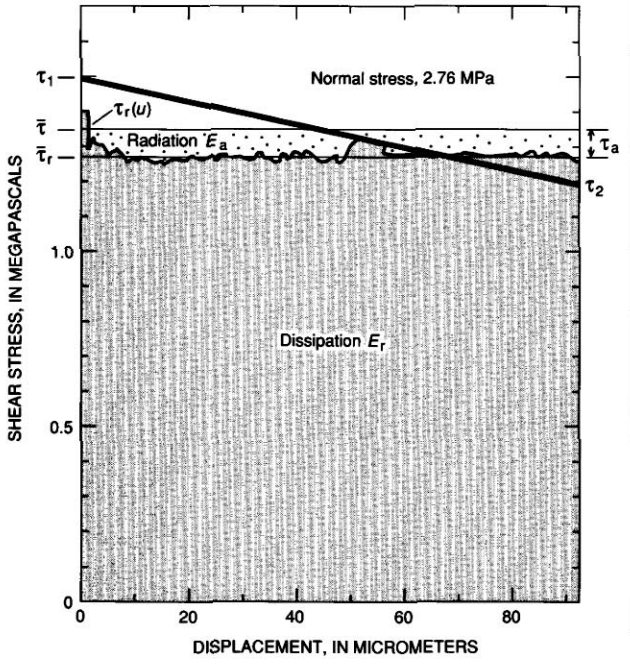

FIGURE 10.3.—Relation between resisting stress and displacement in the unloading elastic medium (inclined line) during an earthquake. As slip (u) increases, stress in the rock diminishes linearly from τ_1 to τ_2, with average value $\bar{\tau}$. Area under this line is total work expended per unit fault area; area (shaded) below curve of resisting stress ($\tau_r(u)$, with average value $\bar{\tau}_r$) is energy dissipated per unit fault area (E_r). Difference between total work expended and dissipated energy is work (done by apparent stress τ_a) that is available for seismic radiation (E_a, stippled area). Modified from a laboratory experiment on a large granite sample by Lockner and Okubo (1983).

APPARENT STRESS: SEISMIC ESTIMATE OF τ_a

Seismologists (for example, Wyss and Brune, 1968; Savage and Wood, 1971; Wyss and Molnar, 1972) have defined apparent stress as

$$\tau_a = \eta\bar{\tau} , \tag{6}$$

where η is the seismic efficiency, defined by

$$\eta = \frac{E_a}{E} \tag{7a}$$

$$= \frac{\tau_a}{\bar{\tau}} , \tag{7b}$$

where equation 7b follows from 7a according to equations 2 through 5; that is, η is simply the fraction of the total energy release, or the fraction of the average earthquake stress, allocated to seismic radiation.

To estimate τ_a, seismologists first determine the radiated energy E_a and the seismic moment M_0, defined as

$$M_0 = GAu , \tag{8}$$

where u is the average slip of an earthquake over a fault-surface area A, and G is the modulus of rigidity (Aki, 1966). Equations 1 and 6 through 8 then yield the simple relation

$$\tau_a = \frac{GE_a}{M_0} . \tag{9}$$

A numerical estimate of τ_a can be obtained from equation 9 with the following commonly used formulas relating earthquake magnitude M to E_a or M_0 (Gutenberg and Richter, 1956; Hanks and Kanamori, 1979),

$$\log M_0 = 16 + 1.5M \tag{10a}$$

$$\log E_a = 11.8 + 1.5M , \tag{10b}$$

where M_0 and E_a are in ergs. Substitution of equations 10 in 9 yields

$$\tau_a = 6.3\times10^{-5}G\ . \tag{11}$$

With $G=3\times10^4$ MPa, the value for τ_a is 2 MPa. Almost without exception, estimates of τ_a fall within the range 0–5 MPa, with no indication of any systematic dependence on either earthquake size or tectonic environment (Spottiswoode and McGarr, 1975; Fletcher and others, 1983; Boatwright and Choy, 1986). In short, 5 MPa appears to be a conservative upper bound to τ_a. Thus, the contribution of τ_a is small, and the average fault stress $\bar{\tau}$ can be large only if the frictional resistance τ_r is large (eq. 5).

If laboratory "earthquakes" are proper analogs of crustal earthquakes, which may or may not be the case, then data for such events, including those illustrated in figure 10.3, indicate that τ_a is indeed small, only a tiny fraction of τ_r. By inducing unstable frictional failure (earthquakes) across a 2-m-long fault between slabs of granite 40 cm thick (Dieterich, 1981), Lockner and Okubo (1983) measured seismic efficiencies η for numerous events to conclude that $\eta\approx0.05$. If this result were true also for natural earthquakes—a big "if"—then for a typical value τ_a of 2 MPa, the corresponding value of $\bar{\tau}$, from equation 6, would be 40 MPa, which, as will be seen, is nearly 3 times higher than the limit inferred from an analysis of heat-flow data (Lachenbruch and Sass, 1980).

FRICTION: THERMAL ESTIMATE OF τ_r

Unlike the energy of seismic waves, which permits an estimate of apparent stress τ_a for individual earthquakes from measurements at distant stations, the heat energy of individual earthquakes is not readily analyzable to estimate friction because it causes a measurable temperature rise only within a few meters of the earthquake source, a location inaccessible for measurement. Even for the largest earthquakes, these individual temperature pulses would be indistinguishable from background a few months after the event, and so timely attempts to detect them by drilling would be difficult (McKenzie and Brune, 1972; Lachenbruch, 1986). However, because the frictionally generated heat diffuses quite slowly, it should accumulate in the vicinity of the fault, eventually building up the local thermal gradient until the observable heat loss at the Earth's surface in the fault zone exceeds the normal background heat flow by the rate of heat generation on the fault. Thus, in principle, the measurement of a heat-flow anomaly in the fault zone should permit an estimate of the average frictional contribution τ_r to the earthquake fault stress $\bar{\tau}$ (eq. 5).

The heat-flow anomaly that we seek does not depend on the amount of heat E_r liberated by a single earthquake in a restricted fault area with a displacement u (eq. 4), but on the long-term average rate of heat generation (Q) and the long-term average slip rate (v) from the cumulative effect of successive events. Although most fault displacement probably occurs within a few tens of seconds during large earthquakes every century or so at slip velocities greater than the average ones by a factor of about 10^8, the long-term buildup of the heat-flow anomaly would be indistinguishable from that caused by uniform slip at an equivalent average velocity because the thermal time constant for the buildup (approx 10^6 yr) is large relative to the earthquake-recurrence interval (10^1-10^3 yr). Therefore, we view the slip as a uniform continuous process and introduce

$$Q = \frac{1}{A}\frac{dE_r}{dt} \tag{12a}$$

and

$$v = \frac{du}{dt}\ . \tag{12b}$$

Differentiation of equation 4 yields

$$Q = \tau_r v\ , \tag{13}$$

where v is the long-term average slip velocity, τ_r is the (displacement averaged) frictional resistance, and Q is the long-term average rate of frictional heat production per unit area on the fault surface.

Equation 13 refers to the entire seismogenic (brittle) layer (approx 10–15 km thick), not just a patch as in equation 5. Over this depth, it is reasonable to consider the long-term slip velocity v to be independent of depth, but generally the heat-production rate Q will not be. For example, if the friction τ_r increased linearly with depth (for example, because of increasing gravitational pressure on the fault, as discussed below), the heat production Q on the fault would also increase linearly, as shown in figure 10.4*B*. According to heat-conduction theory, the temperature in the fault plane would then build up over time, as shown in figure 10.4*C*, and a heat-flow anomaly would develop at the surface over the fault, as shown in figure 10.4*A*. For such a distribution, a sharp heat-flow anomaly is seen to build up over the fault in about 1 m.y.; after several million years, it approaches a maximum value somewhat greater than half the average frictional heat production Q on the fault surface (fig. 10.4*B*). This anomaly falls off over a distance from the fault of the same order as the depth of the seismic layer (assumed to be 14 km in fig. 10.4). Other reasonable distributions of

frictional sources give similar results (see Henyey, 1968; Brune and others, 1969; Henyey and Wasserburg, 1971; Lachenbruch and Sass, 1973, 1980).

The long-term slip rate v, which can be estimated from studies of offset (and dated) geologic features, generally ranges from 2 to 4 cm/yr for motion on the main trace of the San Andreas fault over the past several million years throughout California (see chap. 7; Grantz and Dickinson, 1968). As a useful rule of thumb, if the fault in figure 10.4 were slipping at an average rate (v) of 3 cm/yr and

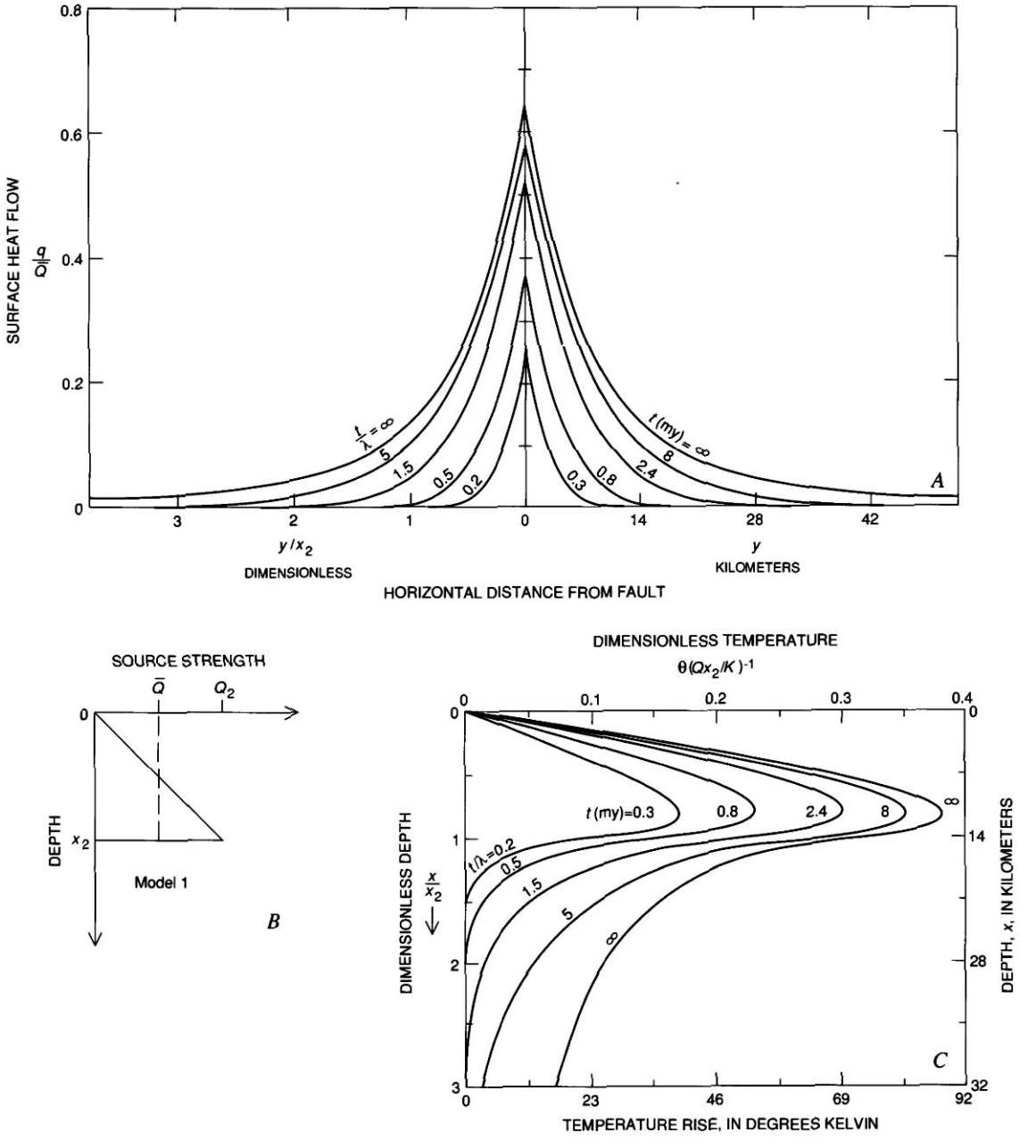

FIGURE 10.4.—Surface heat flow q (A) and fault-plane temperature Θ (C) for a linear increase in source strength from zero at the surface to Q_2 at depth x_2 (B). t, time since initiation of faulting; λ, dimensionless time; Q, average rate of frictional heat generation on fault; K, thermal conductivity. Dimensional results are for x_2=14 km, K=2.5 W/mK, and Q=42 mW/m^2 (equivalent to $2v$≈25 mm/yr, τ_r≈50 MPa) (Lachenbruch and Sass, 1980).

resisted by an average frictional stress τ_r of 100 MPa, then the average rate of frictional heat production Q (figure 10.4*B*) would be about 0.1 W/m^2; that is,

$$0.1 \text{ W/m}^2 = 100 \text{ MPa} \times 3 \text{ cm/yr}. \quad (14)$$

This quantity is about twice the stable continental heat flow, and so, according to figure 10.4*A*, the corresponding heat-flow anomaly over the fault would be about 100 percent of background after 2 or 3 m.y. of fault slip, whereas if the mean frictional resistance were only 10 MPa, the corresponding heat-flow anomaly would be only about 10 percent of background, close to the limit of detection. Accordingly, if no heat-flow anomaly could be detected over the fault, the mean frictional resistance would be no more than about 10 MPa; if the mean frictional resistance were about 100 MPa, a very conspicuous anomaly should be observed.

An example of heat-flow measurements near the San Andreas fault is shown in figure 10.5 for the Mojave Desert region of southern California (region 7, fig. 10.6). The pattern of anomaly curves from the model in figure 10.4 is scaled for the estimated local slip velocity (25 mm/yr; Weldon and Sieh, 1985) and for a mean frictional resistance of 50 MPa. Clearly, the data are incompatible with such an anomaly; in fact, the average heat flows near the fault and far from the fault ("within 10 km" and "beyond 10 km," figs. 10.7*C*, 10.7*D*) are statistically indistinguishable. Figures 10.7*A* and 10.7*B* show that the same condition prevails in the Coast Ranges of central California (regions 3–6, fig. 10.6). In fact, no local heat-flow anomaly has been confirmed anywhere on the main trace of the San Andreas fault (for possible exceptions, see Lee, 1983; Lachenbruch and Sass, 1988), and so, according to the foregoing simple considerations, the average friction on the fault, τ_r, probably does not exceed 10 MPa.

SUMMARY

In summary, we note that analysis of the kinetic energy of seismic waves suggests that the associated apparent stresses (τ_a) do not exceed 5 MPa. Similarly, analysis of long-term frictional heating and the predicted and observed effects on heat flow from conduction theory

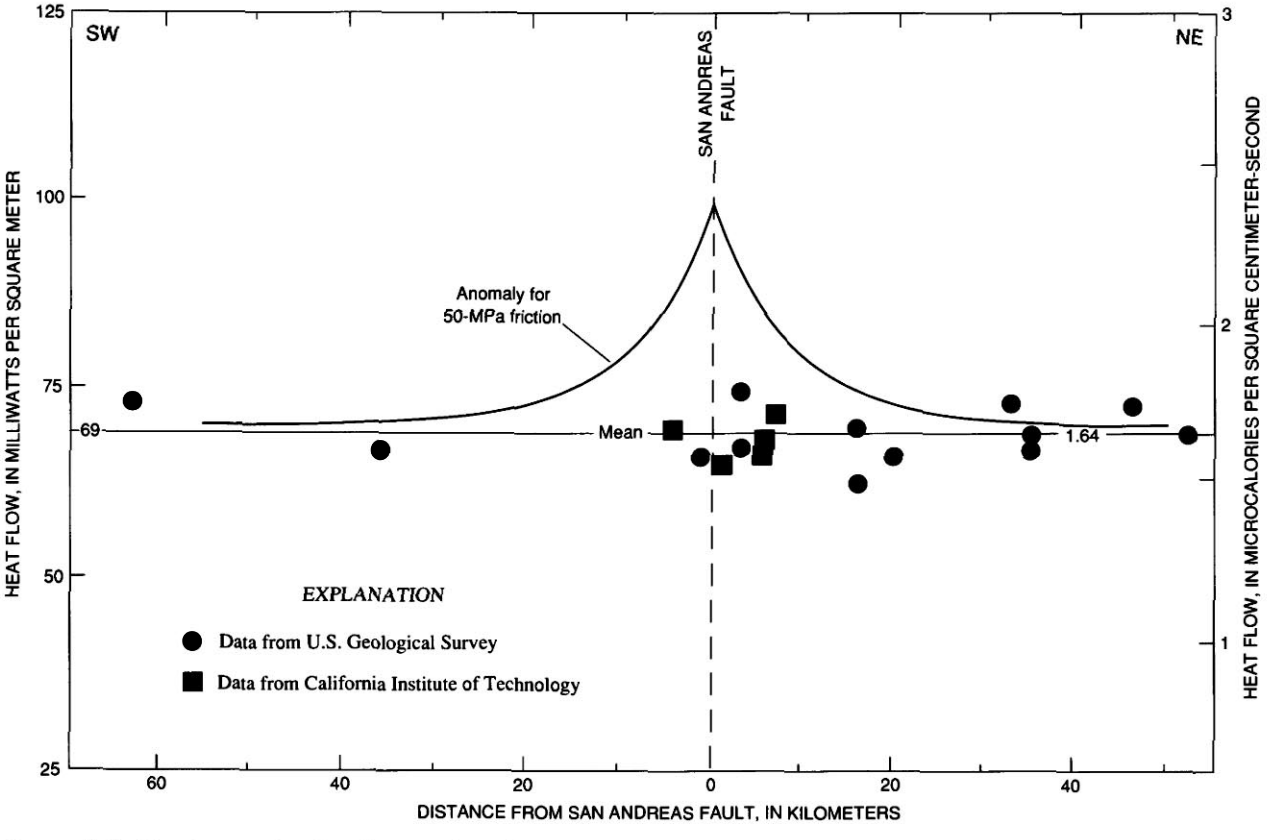

FIGURE 10.5.—Heat flow as a function of distance from the San Andreas fault in the Mojave segment (region 7, fig. 10.6). Theoretical anomaly is for a slip velocity of 25 mm/yr and average friction of 50 MPa (Lachenbruch and Sass, 1988).

suggest that the average frictional resistance τ_r does not exceed about 10 MPa. Thus, according to equation 5, the long-term average combined earthquake stress $\bar{\tau}$ probably does not exceed about 15 MPa, and, of course, it could be much less. The initial stress τ_1, or "fault strength," would be greater by half the stress drop (fig. 10.2; Lachenbruch and Sass, 1980, eq. 41a), no more than another 5 MPa, for an upper limit of 20 MPa. The major assumptions in this analysis are (1) that heat transfer is exclusively by conduction—that is, no significant heat is transferred by moving ground water; (2) that the fault geometry can be represented by the usual simple conventions (see figs. 10.2, 10.3, and 10.4); and (3) that an earthquake's energy is converted exclusively to seismic waves and heat—that is, no appreciable energy is consumed by creating new surfaces, phases, or chemical combinations (Lachenbruch and Sass, 1973, 1980). We shall discuss these points later.

ESTIMATES OF AVERAGE STRESS FROM LABORATORY MEASUREMENTS OF FRICTION

ROCK FRICTION AND THE STRENGTH OF THE FAULT

We have seen that the average shear stress $\bar{\tau}$ on an earthquake fault can be viewed as the sum of a dynamic part τ_a and a frictional part τ_r. The dynamic part is shown to be small from seismic evidence, and so the earthquake stress must be large or small according to the size of τ_r. We have also seen that τ_r is small according to geothermal evidence. We now consider a second line of evidence from laboratory measurement of friction which suggests to many that, contrary to the geothermal evidence, τ_r must be large.

According to these results, rock surfaces will slide when the shear stress on their surface of contact exceeds the static frictional strength τ_f, given by

$$\tau_f = \mu\sigma_n' , \tag{15a}$$

where

$$\sigma_n' = \sigma_n - P \tag{15b}$$

σ_n is the normal pressure pushing the surfaces together, and P is the fluid pressure in the pores and cracks tending to hold the surfaces apart; σ_n' is called the "effective" normal stress (we generally denote such effective stresses by a prime, " ′ "). The proportionality constant μ in equation 15a is the coefficient of static friction; extensive laboratory experiments show that its value is generally in the range 0.6–0.9 for a remarkably large variety of rock types and surface conditions (Byerlee, 1978), although some studies (for example, Wang and others, 1980), reported substantially lower friction coefficients for some geologic materials, including certain types of fault gouge.

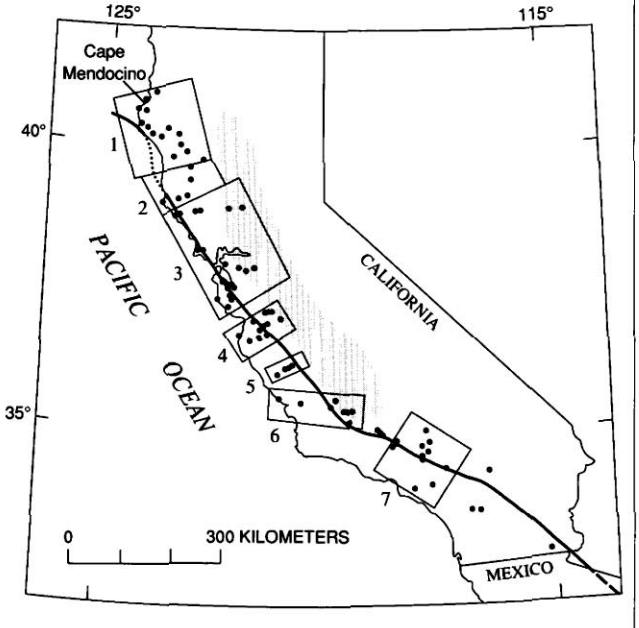

FIGURE 10.6.—Locations of heat-flow measurements near the San Andreas fault and of numbered regions referred to in figure 10.7 (Lachenbruch and Sass, 1980). Heavy line, San Andreas fault, dashed where approximately located, dotted where concealed; stippled area, Great Valley.

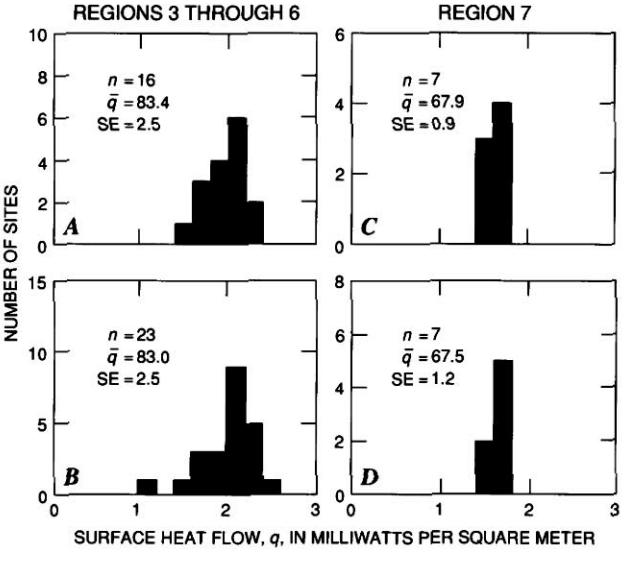

FIGURE 10.7.—Comparison of heat flow within 10 km of main trace of the San Andreas fault (*A*, *C*) and beyond 10 km (*B*, *D*) for regions 3–6 (*A*, *B*) and region 7 (*C*, *D*) (see fig. 10.6 for locations); transitional regions 1 and 2 are not represented. Modified from Lachenbruch and Sass (1980). n, number of samples; $\bar{q}$, mean heat flow; SE, standard error.

We presume that a fault is a fracture with little cohesive strength that remains inactive until the natural shear stress τ resolved along it exceeds its frictional strength τ_f given by equation 15. This shear stress, which depends on the magnitudes of the principal stresses and on the angular relation between the fault plane and the principal stress directions (fig. 10.8), is given by (Jaeger, 1956, p. 8)

$$\tau = \tfrac{1}{2}(\sigma_1 - \sigma_3)\sin 2\Theta\ , \qquad (16)$$

where it is assumed for convenience that the intermediate-principal-stress direction (σ_2) lies in the fault plane (true if μ is independent of the orientation of this plane). In figure 10.8, σ_2 is vertical, and σ_1 and σ_3 are the maximum and minimum horizontal principal stresses. Θ is the angle formed by the fault normal and the direction of least compression (σ_3); it is also the angle between the fault trace and the direction of greatest compression (σ_1). To express the failure criterion (eq. 15) in terms of the stress field and fault orientation, we note that the effective normal stress, σ_n', in equation 15 can be written as (Jaeger, 1956, p. 8)

$$\sigma_n' = \tfrac{1}{2}(\sigma_1' + \sigma_3') - \tfrac{1}{2}(\sigma_1' - \sigma_3')\cos 2\Theta\ . \qquad (17)$$

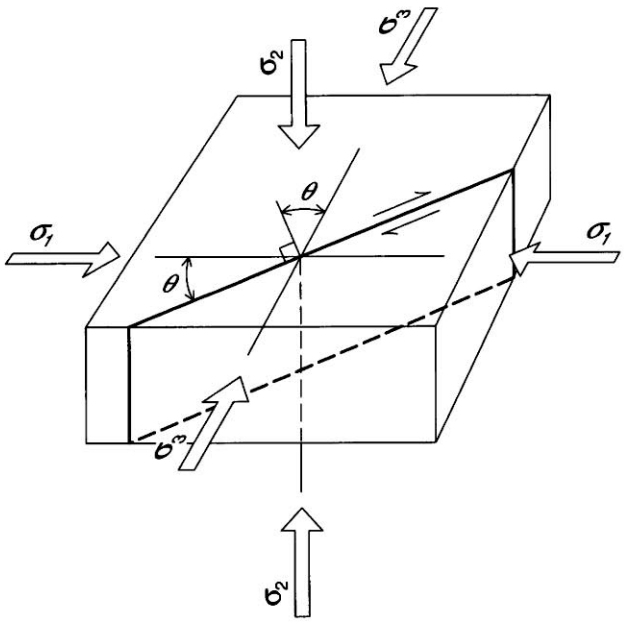

FIGURE 10.8.—Conventions for discussing orientation of fault relative to direction of principal stresses: $\sigma_1 > \sigma_2 > \sigma_3$. Arrows indicate direction of relative movement along fault.

With equations 15 through 17, the friction stress τ_f that must be exceeded on a fault for it to slip can be determined if we know (1) the maximum and minimum principal stresses σ_1 and σ_3, (2) the fluid pressure P, (3) the coefficient of friction μ, and (4) the angle Θ describing the orientation of the fault relative to the principal-stress axes.

As we increase the stress difference, in what direction (Θ) will the Earth ultimately break, and what will be the stress on the failure plane? Clearly, the answer could be influenced by the existence of planes of weakness (McKenzie, 1969); for example, major preexisting faults or foliated country rock might result in directions with anomalously low μ.

THE CASE OF EQUAL STRENGTH IN ALL DIRECTIONS

We first assume that no such directional strength variation exists, that the rock is fractured in all directions, and that all potential shear surfaces have the same coefficient of friction μ. In this case, the foregoing equations show that the trace of the favored fault plane will depart from the direction of maximum compression by an angle Θ_0, dependent only on the coefficient of friction, as follows:

$$\Theta_0 = 45° - \tfrac{1}{2}\tan^{-1}\mu\ . \qquad (18)$$

Note that generally $\Theta_0 < 45°$ (the direction of the surface of maximum resolved elastic shear stress, eq. 16) because of the effects of normal stress on friction (Jaeger, 1956). With this additional relation (eq. 18), we can express the frictional strength τ_f of a plane of orientation Θ in terms of the coefficient of friction and the effective-principal-stress components as follows:

$$\frac{\tau_f}{\sigma_1'} = \frac{\mu}{1 + \mu\cot\Theta} = \frac{\mu}{1+\mu^2}\left(1 + \frac{\mu}{\sqrt{1+\mu^2}}\right)^{-1}, \qquad \Theta = \Theta_0 \qquad (19a)$$

$$\frac{\tau_f}{\sigma_3'} = \frac{\mu}{1 - \mu\tan\Theta} = \frac{\mu}{1+\mu^2}\left(1 + \frac{\mu}{\sqrt{1+\mu^2}}\right)^{-1}, \qquad \Theta = \Theta_0 \qquad (19b)$$

$$\frac{\tau_f}{\frac{1}{2}(\sigma_1' + \sigma_3')} = \frac{\mu}{1 + \mu \cot 2\Theta}$$

$$= \frac{\mu}{1 + \mu^2}, \qquad \Theta = \Theta_0 \qquad (19c)$$

To evaluate the frictional strength, the vertical stress is generally assumed to be a principal stress (reasonable because the Earth's surface supports no traction) equal to the rock column's weight, ρgz, an assumption supported by inplace stress measurements (McGarr and Gay, 1978). In this case, the vertical effective stress σ_v' will be

$$\sigma_v' = \rho gz - P, \qquad (20a)$$

where ρ is the rock density, and the fluid pressure P is given by

$$P = \lambda \rho gz\,. \qquad (20b)$$

The value $\lambda=0$ represents conditions in dry rock. For a typical open ("hydrostatic") hydrologic system, we have $\lambda \sim 0.37$ ($= \rho_w/\rho_{rock}$, where ρ_w is the density of water). As $\lambda \to 1$, the fluid pressure approaches the weight of overburden, and the vertical effective stress σ_v' vanishes (as discussed below, this limit probably occurs only in the thrusting regime, where σ_3 is vertical).

The curves in figure 10.9 (referred to ordinate scale at left margin) give the frictional strength normalized by the effective vertical principal stress for those cases in which the vertical stress is the maximum (dashed curve), average (solid curve), or minimum (dotted curve) principal stress, respectively. The first right-hand ordinate scale gives the increase in frictional strength with depth (τ_f/z) for the usual assumption of hydrostatic fluid pressure ($P=\rho_w gz$). For typical values of μ from Byerlee's results (for example, 0.6–0.9), the frictional strength for normal and thrust faults increases with depth at rates of about 5 and 20 MPa/km, respectively (fig. 10.9). The rate of increase for strike-slip faults lies between these limits; a commonly used value, 8 MPa/km, is shown by the solid curve in figure 10.9. For an upper-crustal fault extending to 14 km depth, these increases would result in average friction (the value at a 7-km depth) of 35, 56, and 140 MPa for normal, strike-slip, and thrust faults, respectively (see second ordinate scale on right, fig. 10.9). Such calculations provide the basis for the expectation of high fault stress from the analysis of laboratory results: These values are substantially greater than the 20 MPa upper limit for initial stress suggested from the analysis of heat-flow data in strike-slip tectonic regimes (horizontal dashed line, fig. 10.9). Note that the heat-flow limit would require $\mu \lesssim 0.2$ for the assumed conditions.

THE CASE OF A WEAK DIRECTION

The estimates of large friction from the fault model of figure 10.9 depend on three principal assumptions: (1) that the average coefficient of friction on real faults is comparable to typical laboratory values ($\mu \sim 0.6$–0.9), (2) that the average fluid pressure throughout the depth of the fault is comparable to the weight of the overlying column of water ($\lambda \sim 0.37$, eq. 20), and (3) that the coefficient of friction (μ) is the same in all directions, so that the fault direction (Θ_0) is determined by the applied stress (eq. 18) and not by the orientation of a special plane of weakness. Partly in response to recent reports that the maximum horizontal principal stress is oriented nearly perpendicular to the San Andreas fault (Mount and Suppe, 1987; Zoback and others, 1987), we drop the last assumption and suppose that the fault occupies a very weak plane (which is assumed to contain the intermediate principal stress). Because of the anomalous weakness of this plane, the friction along it could be very low, consistent with the heat-flow data, and faulting could persist there irrespective of the ambient stress field.

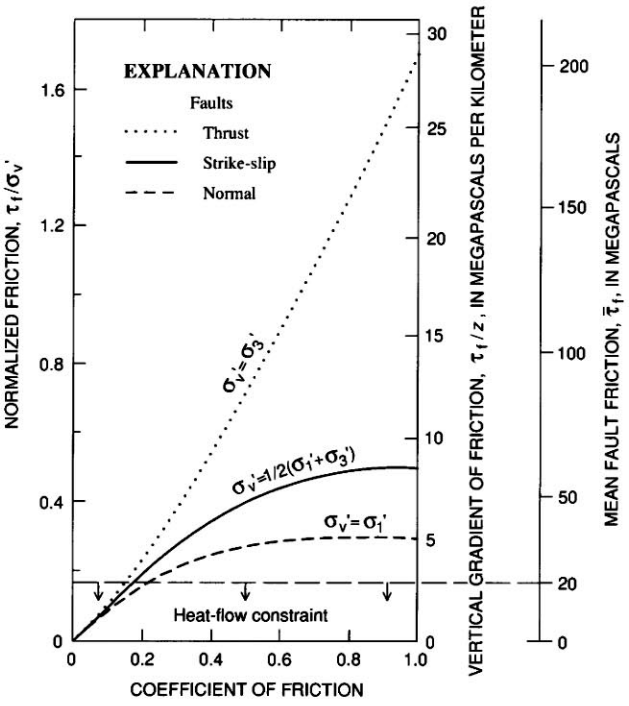

FIGURE 10.9.—Variation of normalized fault friction (left-hand ordinate scale) with coefficient of friction under three conditions for vertical effective stress (σ_v') for failure at optimum angle Θ_0. Increase in fault friction τ_f with depth z under hydrostatic fluid pressure is given by right-hand ordinate scale, and mean friction $\bar{\tau}_f$ on a fault 14 km deep by scale on far right. Horizontal dashed line is upper limit of mean friction suggested by heat-flow constraint. σ_1' and σ_3', maximum and minimum horizontal effective principal stress, respectively.

According to the friction model (eq. 15), the two factors that might weaken the plane are either an abnormally low coefficient of friction or unusually high pore pressure. For now, we assume that each of these conditions can exist regardless of laboratory or hydrologic evidence.

The first question we consider is whether a very weak fault can coexist with stronger faults such that both types are active, as may be the case along the San Andreas fault (for a closely related discussion, see Sibson, 1985). To address this question, it is convenient to express the crustal strength in terms of the ratio σ_1'/σ_3' (Brace and Kohlstedt, 1980). From equations 19a and 19b, the condition at failure (eq. 15a) for a weak plane oriented at an angle Θ to the direction of σ_1 (fig. 10.8) is

$$\frac{\sigma_1'}{\sigma_3'} = \frac{1 + \mu \cot \Theta}{1 - \mu \tan \Theta}. \qquad (21a)$$

For isotropic strength, failure occurs at Θ_0 (eq. 18), the direction in which σ_1'/σ_3' is a minimum for a given μ:

$$\frac{\sigma_1'}{\sigma_3'} = (\sqrt{1 + \mu^2} + \mu)^2, \qquad \Theta = \Theta_0. \qquad (21b)$$

Faults at angles other than Θ_0 support greater deviatoric stresses and the higher values of σ_1'/σ_3' given by equation 21a.

The conditions necessary for the coexistence of active faults with different coefficients of friction are illustrated in figure 10.10, where the ratio of effective principal stresses at the point of failure is plotted as a function of the fault angle for various values of the coefficient of friction (eq. 21a). Suppose, for example, that the coefficient of friction is only 0.1 in the direction of the San Andreas fault, whereas in all other directions it is 0.6. Because σ_1'/σ_3' must be at least 3.1 to cause faulting in the crustal environs, the low-strength San Andreas fault must be oriented at $\Theta \leq 3.5°$ or $\Theta \geq 81.5°$ (fig. 10.10); otherwise, σ_1'/σ_3' would be too low to cause slip in the stronger directions. In this example, then, the weak fault must be oriented either nearly parallel or nearly perpendicular to the direction of σ_1.

In the context of the notion that the San Andreas fault is nearly perpendicular to the direction of σ_1', or at $\Theta \sim 90°$ in figure 10.10, we note that a very low coefficient of fault friction is required. The strength curves for each value of μ have two asymptotes where $\sigma_1'/\sigma_3' \to \infty$. These asymptotes occur where the denominator of equation 21a vanishes; one asymptote is at $\Theta = 0$, or σ_1 parallel to the fault, for any value of μ, and the other is at $\Theta = 2\Theta_0$ (eq. 8), or $\Theta = 90 - \tan^{-1} \mu$. Thus, the normal to any fault that fails in shear must be oriented at an angle of at least $\tan_{-1}$ μ from the direction of σ_1. For the four curves in figure 10.10, the right-hand asymptotes are at $\Theta = 84.3$, 73.3, 59.0, and 48.0, respectively, for $\mu = 0.1$, 0.3, 0.6, and 0.9. Thus, if the fault trace makes an angle greater than 59°, then μ must be less than 0.6 as long as the fluid pressure is less than the least principal stress.

More generally, enhanced pore pressure alone cannot lead to active faults nearly normal to σ_1 unless $P > \sigma_3$, in which case $\sigma_3' < 0$ and failure is likely to manifest itself as hydraulic fracturing rather than fault slip.

SUMMARY

To recapitulate, the simplest interpretation of earthquakes in terms of the frictional fault model and laboratory measurements of rock friction leads to fault stresses many times larger than the limits suggested from heat-flow and fault energetics. This interpretation depends on three assumptions: (1) that the average coefficient of friction on real faults is comparable to typical laboratory values ($\mu \sim 0.6$–0.9), (2) that the pore-fluid pressure throughout the depth of faulting is comparable to the weight of the overlying column of water, and (3) that the intrinsic resistance of the Earth to sliding is isotropic—that is, no weak directions exist. To reduce the high estimates of friction obtained from rock mechanics to the low ones obtained from heat flow, we must assume either smaller values of the coefficient of friction μ or larger

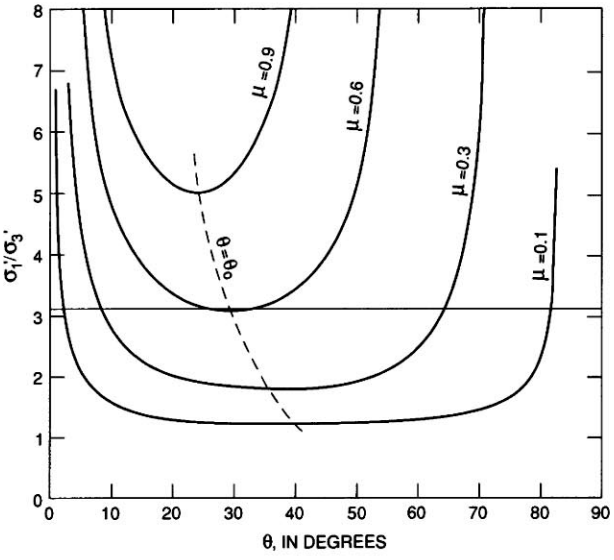

FIGURE 10.10.—Failure criteria for various coefficients of friction as functions of fault angle Θ. For fixed σ_1', σ_3', and μ, slip will occur for all Θ between points where horizontal line defined by σ_1'/σ_3' intersects curve defined by μ. For example shown, if $\sigma_1'/\sigma_3' = 3.1$, then for $\mu = 0.1$, slip can occur at all angles between 3° and 82° but only at optimum angle 29.5° if $\mu = 0.6$. Dashed curve, optimal failure angle $\Theta_0(\mu)$ (eq. 18). σ_1' and σ_3', maximum and minimum horizontal effective principal stress, respectively.

values of fluid pressure P (see eq. 15). Of particular interest in this connection is reported evidence that the trend of the San Andreas fault in California might occupy an anomalous weak direction. According to Mount and Suppe (1987) and Zoback and others (1987), the fault plane is nearly perpendicular to the direction of maximum compression ($\Theta \sim \pi/2$, fig. 10.10), a direction in which the resolved shear stress is very small. Such a condition could be consistent with the low friction required by heat flow, while permitting high stresses to accommodate the subsidiary faulting observed on more favorably situated planes. This model, however, raises some basic questions regarding the mechanics of faulting; for the fault to slip, it must have a low shear strength, as well as the low shear stress suggested by its orientation. If conventional friction theory applies, anomalously high fluid pressure along the fault cannot readily account for the required low friction because, unless μ is unusually low, the fault becomes exceedingly resistant to shear failure as Θ begins to approach $\pi/2$ (fig. 10.10).

ESTIMATION OF FAULT STRENGTH FROM INPLACE STRESS MEASUREMENTS

In principle, measurements of the magnitude and orientation of crustal stress in the vicinity of the San Andreas fault should provide the most direct evidence of the forces acting to cause interplate motion there. However, some essential problems exist with this approach. Because we have little understanding of the mechanics of the system, it is difficult to interpret the data. We are not dealing with a laboratory experiment in which a sample is loaded in a testing machine whose characteristics are well known; in such a situation, it is straightforward to use gages to estimate the magnitude of the load. In contrast to the well-controlled laboratory situation, we have little idea of the nature of the forces applied to the Earth's crust to cause a deviatoric state of stress and, in the case of tectonically active areas, slip across major throughgoing faults. We know neither where the forces are applied nor what is applying them; moreover, there is even debate about what the state of stress would be if only gravity were acting (McGarr, 1988).

In addition to the absence of a conceptual framework, there are numerous experimental difficulties in determining the state of stress, that is, the magnitudes and orientations of the three principal stresses as functions of position within the crust. Data must be obtained from depths below the zone of weathering, in rock that is sufficiently strong to support deviatoric stresses. In granitic rocks, this requirement, in effect, necessitates stress measurements at depths of about 50 m or more, thus limiting the measurement technique to hydraulic fracturing, the only common procedure that can be used at such depths (Haimson and Fairhurst, 1970).

The hydraulic-fracturing, or "hydrofrac," method involves isolating a section of a borehole and then pressurizing this cylinder by pumping in fluid until a tensile crack forms and propagates into the previously unfractured rock. By monitoring the pressure-time history of the fluid in the isolated section, both the maximum and minimum horizontal stresses can be estimated (Hubbert and Willis, 1957; Zoback and Haimson, 1983). This approach assumes that one of the principal stresses σ_v is oriented vertically and can be calculated from the weight of overburden (eq. 20). The other two principal stresses are the maximum, σ_H, and minimum, σ_h, horizontal stresses. In contrast to engineering usage, the convention adopted here is for compressional stresses to be positive because, in the Earth's crust, tensional stresses are rarely encountered, even at the surface.

Although the uppermost crust near the San Andreas fault system has not been sampled as much for stress as for heat flow, enough inplace stresses have been measured to provide an indication of the state of stress there and how it compares with crustal stresses in other tectonic settings. To date, 41 successful hydrofrac measurements have been made in the 12 wells shown in figure 10.11 at depths of as much as 850 m. A total of 29 of these data, in wells along the Mojave reach of the fault (fig. 10.11*C*), were analyzed by McGarr and others (1982). Since that study, four stress measurements have been made at Black Butte (BB, fig. 10.11*C*) in the Mojave Desert (Stock and Healy, 1988), the data from the Hi Vista well have been reanalyzed by Hickman and others (1988), and additional measurements have been made in central California (Zoback and others, 1980). Currently, stress measurements are being made at the Cajon Pass well near the southeast end of the Mojave reach of the San Andreas fault, with some observations at depths below 3 km. Because no clear picture has yet emerged (see Healy and Zoback, 1988), we have not incorporated the Cajon Pass results into this review.

The state of horizontal deviatoric stress can be characterized in terms of two parameters: the maximum horizontal shear stress τ_m given by

$$\tau_m = \tfrac{1}{2}(\sigma_H - \sigma_h) , \qquad (22)$$

and the angle Θ between the trace of the fault and the direction of maximum horizontal compressive stress σ_H. Under favorable conditions, both parameters can be determined by the hydrofrac technique. We have shown that if $\Theta \sim 45°$, then τ_m is entirely resolved onto the plane of the fault to produce its slip; as Θ approaches 0° or 90°,

the resolved stress on the fault becomes arbitrarily small irrespective of the magnitude of τ_m (eq. 16).

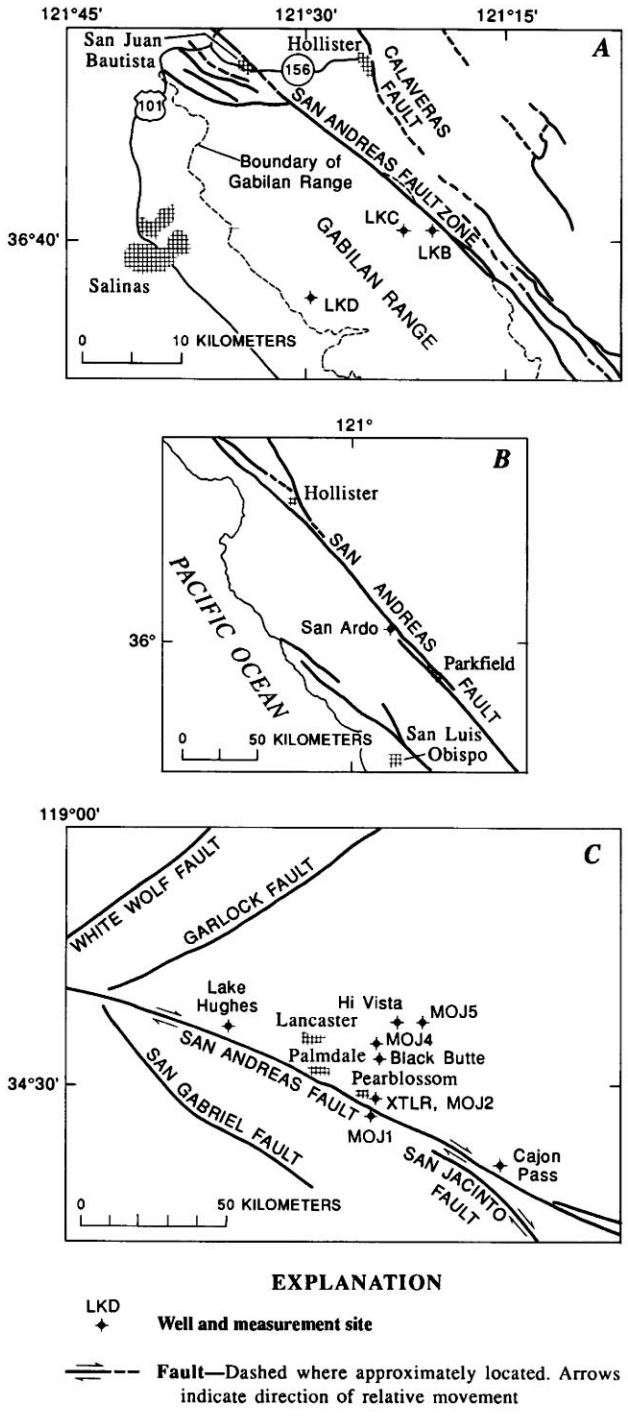

FIGURE 10.11.—Sketch maps of the Gabilan Range (*A*), central California coast (*B*), and western Mojave Desert (*C*), showing locations of wells where stress measurements have been taken along the San Andreas fault using the hydrofracturing technique.

Evidence regarding the actual orientation of σ_H relative to the strike of the San Andreas fault is contradictory. Observations favoring Θ distributed about 45°, so as to cause dextral fault slip, were presented by McNalley and others (1978), Zoback and others (1980), Zoback and Zoback (1980), and Hickman and others (1988); however, these data, from the Mojave Desert, show considerable scatter. In contrast, Mount and Suppe (1987) and Zoback and others (1987) reviewed a broad set of data, including many borehole breakout orientations, that suggest $\Theta \approx 90°$; Oppenheimer and others (1988) came to a similar conclusion. An intermediate result was obtained by Jones (1988), who stated that σ_H is oriented at 65° to the local strike of the San Andreas fault in southern California. Thus, currently, we know neither the preferred value of Θ nor whether such a value even exists. For the foregoing values of Θ (45°, 65°, or 90°), the shear stress resolved on the fault (eq. 16) would be τ_m, $0.77\tau_m$, or 0, respectively. In view of this uncertainty, we leave Θ unspecified and describe what is known of τ_m the upper limit to the shear stress that can be resolved on the fault.

The first-order feature seen in data from the San Andreas fault zone (fig. 10.12) is a marked tendency for τ_m to increase with depth. The solid line, a regression fit to all of the data, indicates a depth gradient of 8.3 MPa/km, not significantly greater than the gradient of 7.9 MPa/km reported by McGarr and others (1982) on the basis of 29 of the 41 data plotted in figure 10.12. We note that the observed depth gradient of τ_m also agrees well with the curves for strike-slip faults (solid curves, fig. 10.9) for a coefficient of friction of 0.6 or greater. In addition to the general increase in τ_m with depth, considerable variation from one well to another and within individual wells is suggested by figure 10.12.

Figure 10.13 shows that the departure of the measured values of τ_m from the regression line in figure 10.12 does not vary systematically with distance from the San Andreas fault. The principal conclusion to be drawn from figure 10.13 seems to be that the magnitude of deviatoric stress is not measurably affected by proximity to the San Andreas fault. Thus, whatever effect the fault may have on the magnitude of the shear stress, it is either too subtle, too localized, or too deep to be recognized in the current data set.

We note that there is no detectable difference between the Mojave Desert residuals, measured near a locked section of the San Andreas fault, and those in central California (fig. 10.11*A*), where the fault is creeping and presumably does not produce great earthquakes. If measurements were made to greater depths, some differences might appear, but at least in the topmost several hundred meters, the magnitude of shear stress seems to be largely independent of position along the strike of the San Andreas fault.

Having failed to discover any spatial relation between the San Andreas fault and deviatoric-stress magnitudes, we now consider the question of whether or not any detectable differences exist between the stress states measured near the San Andreas fault (fig. 10.12) and those measured elsewhere in different tectonic settings. A review of crustal shear stress by McGarr (1980) considered a large suite of stress data in "hard" rocks measured at depths extending to 3.6 km. The resulting regression line of

$$\tau_m \text{ (MPa)} = 5.0 + 6.59z \text{ (km)} \quad (23)$$

has a greater surface intercept but a similar depth gradient to the San Andreas regression

$$\tau_m \text{ (MPa)} = 1.58 + 7.51z \text{ (km)} \quad (24)$$

fitted to the crystalline-rock data in figure 10.12. The comparison between equations 23 and 24 is not entirely appropriate because the data used to develop equation 23 represent all three stress states; stresses measured in regions of strike-slip tectonics were not considered separately by McGarr (1980) (see fig. 10.9). More recently, however, data measured in a 2,000-m-deep well in Cornwall, U.K. (Pine and others, 1983), permit quite an interesting comparison. For both the San Andreas and the Cornwall data sets, most of the stress observations are compatible with strike-slip tectonics; that is, σ_v is the intermediate principal stress. For most of the San Andreas and all of the Cornwall measurements, the rock is granitic. In contrast to the San Andreas system, however, the tectonic setting in Cornwall is presently inactive. The deviatoric stresses at Cornwall are believed to be a consequence of the Alpine orogeny, which apparently has caused the maximum horizontal stress to be oriented northwestward throughout much of Europe (for example, McGarr and Gay, 1978).

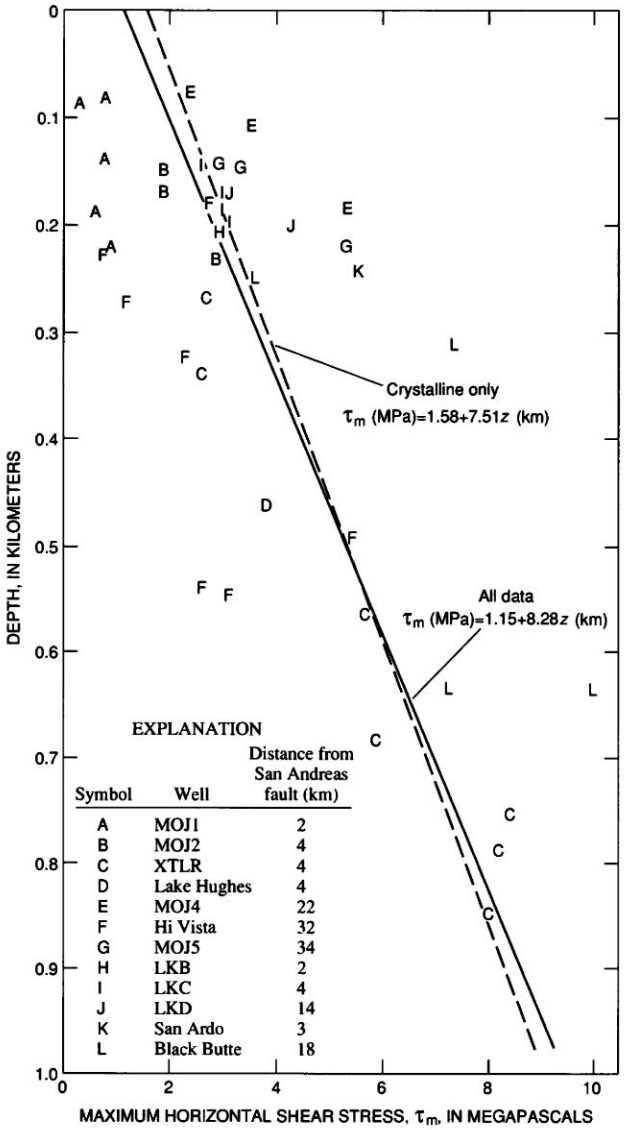

FIGURE 10.12.—Maximum horizontal shear stress as a function of depth z. Solid regression line has been fitted to all data, and dashed line to measurements in crystalline rock only. See figure 10.11 for locations of wells.

The 12 data sets obtained by Pine and others (1983) indicate a stress state (fig. 10.14) surprisingly similar to that of the San Andreas fault (fig. 10.12). For the maximum shear stress, the depth gradient of 7.52 MPa/km is indistinguishable from its counterpart in the crystalline San Andreas crust of 7.46 MPa/km; however, the surface intercept at Cornwall is larger. If the state of deviatoric stress is much the same in Cornwall as along the San Andreas system, then we must conclude that the plate-tectonic motion in California along the San Andreas fault has no expression in the shallow (1–2 km deep) stress field. Accordingly, much of what has been discovered about continental-crustal stress in general may apply to the crust adjacent to the San Andreas fault.

This generalization implies that the applied forces which give rise to τ_m in the vicinity of the San Andreas fault are not specific to the Pacific-North American plate boundary. In terms of observed shear stress, a major active plate-boundary fault would be at least as likely in Cornwall, U.K., as in California from what we currently know of stress magnitudes, at depths down to a few kilometers.

DISCUSSION

From what we currently know of crustal stress and heat flow, neither is influenced by proximity to the San Andreas fault, the most conspicuous and best studied

plate-boundary fault on the continents. The measured horizontal shear stress increases rapidly with depth (approx 8 MPa/km), essentially as would be predicted from laboratory measurements of friction and the assumption that crustal stress is limited by the frictional resistance of fractures forced together by the weight of overlying rocks. From this consistency of independent observations, two large "if's" lead to what seems to be a physical contradiction: (1) if these vertical stress gradients persist throughout the depth of the seismogenic faulting layer (approx 12–15 km), then the average of the maximum horizontal shear stresses throughout the layer is quite large (approx 50 MPa); and (2) if the direction of the San Andreas fault is aligned with this maximum-horizontal-shear-stress direction, then the frictional heat generated by such stress during the documented fault motion (tens of kilometers per million years) should cause the background heat flow to double as the fault is approached. In 100 heat-flow measurements over a 1,000-km span of the San Andreas fault, no such heat-flow anomaly has been observed.

The contradiction stems from two separate lines of argument: (1) inplace and laboratory measurements of rock stress imply average fault stresses of about 50 MPa or more, and (2) the absence of a local heat-flow anomaly and the energy balance of the fault imply an average fault stress of about 15 MPa or less. At least one of these arguments must be wrong. We have outlined the major factors in each argument, and we shall now point out some possible loopholes and areas for further study.

The energy-balance argument leading to the heat-flow constraint on fault stress could be invalidated if the neglected energy sinks turn out to be important, or if the heat-conduction model is unrealistic or inappropriate. The general energy argument assumes that fault slip produces only seismic radiation and heat. It supposes that the energy consumed by the grinding of rocks into fault gouge (Lachenbruch and Sass, 1980) or the heat absorbed by possible phase changes or chemical reactions is negligible, and that the energy of seismic radiation does not grossly differ from the estimates made by seismologists. The heat-conduction model assumes that the frictional heat production occurs in a near-vertical fault zone (whose width is small relative to its depth) extending throughout the seismogenic layer. Systematic nonconductive removal of frictional heat by circulating ground water could invalidate this model (see O'Neill and Hanks, 1980; Williams and Narasimhan, 1989), as could a grossly different fault geometry—for example, a fault whose lower half was continually being rejuvenated because of migration of the upper half away from it along an upper-crustal detachment surface (Namson and Davis, 1988). All of these effects probably deserve further study.

The mechanical argument leading to large fault stress is based on observations of inplace stress (to maximum depths of approx 1 km in the San Andreas fault zone and of approx 4 km elsewhere on the continents), on laboratory measurements of rock friction and the efficiency of simulated earthquakes, and on downward extrapolation of these results through the seismic layer, on the assumption that fluid pressure is normal and frictional properties are uniform and isotropic. The consistency between the most frequently measured friction coefficients and the inplace determinations of the vertical gradient of maximum shear stress is reassuring (solid curves, fig. 10.9; fig. 10.12); however, the downward extrapolation of these results to depths of 10 or 15 km is an uncertain step, with loopholes that could invalidate the high-fault-stress conclusion.

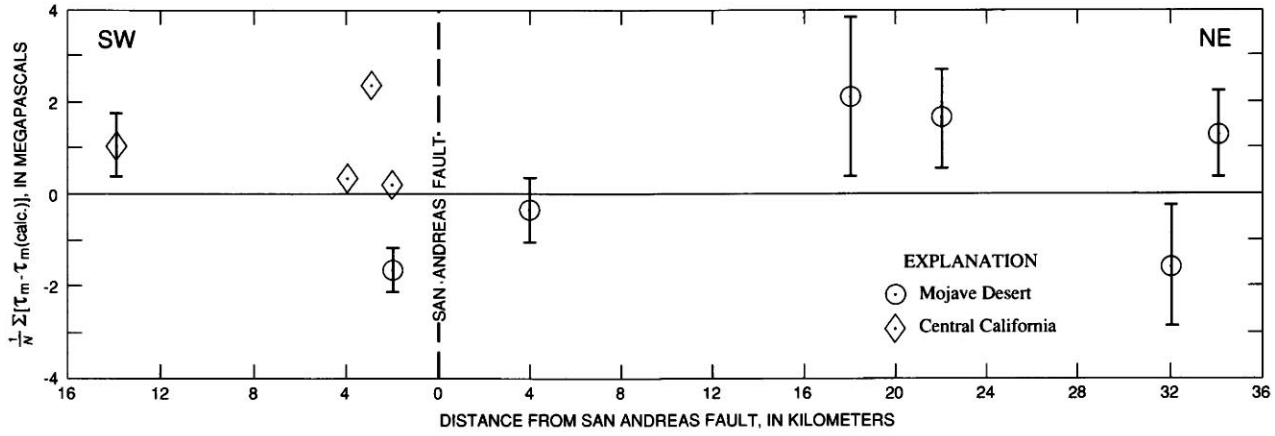

FIGURE 10.13.—Averages of N maximum-shear-stress (τ_m) residuals as functions of distance from the San Andreas fault. In calculating residual at a particular distance, effect of depth z is removed by using solid-line regression fit to data of figure 10.12 [τ_m (MPa)=1.15+8.28z (km)]. Error bars, 1σ.

There are at least three such loopholes. First, the fluid pressure might increase with depth, as it is known to do in some sedimentary basins, approaching the minimum principal stress (Berry, 1973). Second, the friction coefficient at depth might be lower than average laboratory values; such lower values have been reported in some studies of gouge and other clay-size aggregates (Wang and others, 1980). Each of these effects could substantially lower the maximum stress at depth. Third, the frictional strength properties might be anisotropic, with the main trace of the fault occupying a weak direction. If so, the maximum stress at depth might be high, as maintained in the mechanical argument, but the shear stress resolved on the fault might be very low, as maintained in the thermal argument. Under these circumstances, the fault must be nearly parallel to a principal axis, as suggested by Mount and Suppe (1987) and Zoback and others (1987). Such a condition could be consistent with the low friction on the main fault required by heat flow, while permitting high stresses to accommodate subsidiary faulting on more favorably situated planes with normal frictional properties.

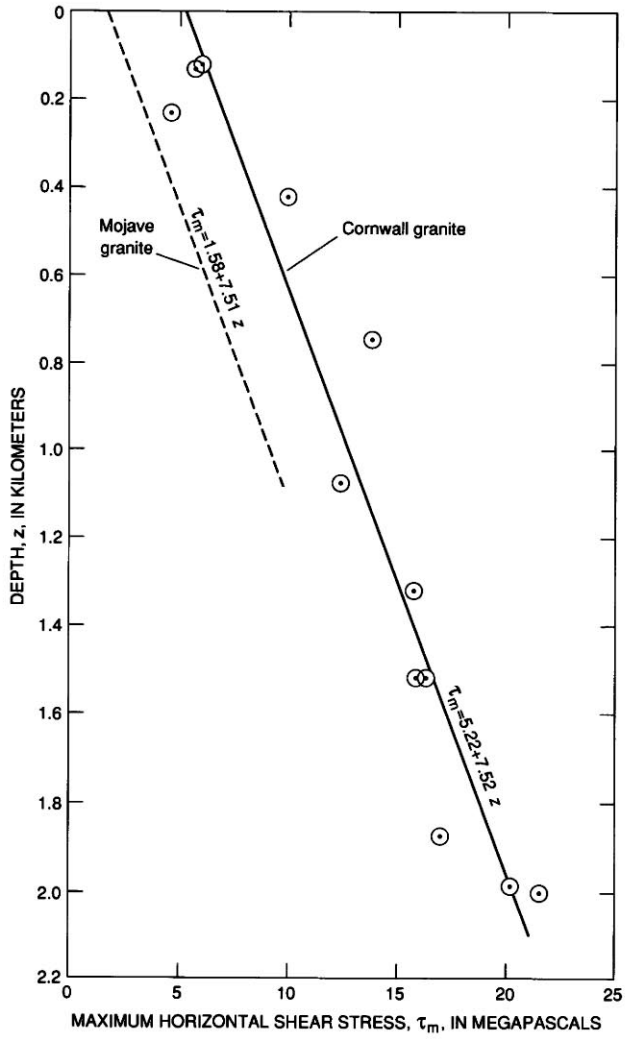

FIGURE 10.14.—Maximum horizontal shear stress τ_m as a function of depth z in granite near Cornwall, U.K. Data from Pine and others (1983).

As mentioned above in the section entitled "Introduction," geothermal studies of the San Andreas fault have provided evidence for a very weak fault for two decades; the meaning of this result depends heavily on the direction of principal stresses in the fault zone and the magnitude of the stress differences there. As we have shown, existing evidence is contradictory, especially in the Mojave Desert region. Many measurements of stress near the San Andreas fault suggest that the fault trace is inclined at an intermediate azimuth (approx 45°) to the principal-stress directions, and thereby imply that the fault coincides approximately with the direction of maximum shear stress and that the heat-flow constraint could not be satisfied unless horizontal shear stress (and stress differences) were low everywhere. In this case, both the San Andreas fault and active subsidiary faults with other orientations would have to be weak. If, however, the horizontal-stress differences are large, the weak fault required by heat flow is a "zero shear stress" boundary condition on the adjacent fault blocks that requires the fault to be almost normal to a principal-stress direction. In this case, the heat-flow constraint could be honored on an anomalously weak main trace, whereas subsidiary faults with other orientations and normal strength could also be active.

Thus, the occurrence of a weak direction may reconcile observations of rock mechanics with the longstanding implications of thermomechanical studies. It does, however, raise several questions:

1. Does the maximum-horizontal-principal-stress direction form an intermediate angle with the trace of the San Andreas fault (as was formerly accepted and as is required by isotropic frictional properties), or is the maximum compression nearly fault normal, as suggested by more recent observations (Mount and Suppe, 1987; Zoback and others, 1987)? As we have pointed out, there is conflicting observational evidence on this issue.
2. If the horizontal compressive stress is nearly fault-normal, what is the physical mechanism that permits the fault to slip under the small shear stress resolved on its direction? We have shown that the mechanism commonly invoked to explain a weak fault—namely, locally elevated fluid pressure—is not likely; however, anomalously low coefficients of friction could

account for slip under near fault-normal compression if the frictional fault model is valid.

3. How would such a weak plate-boundary fault evolve, and would its existence imply that the resistance to relative motion between the Pacific and North American plates is negligible? What is the role of decoupling and basal resistance? Lachenbruch and Sass (1973) pointed out that strong shear stresses in the far field which might drive dextral slip between the plates cannot be balanced by a weak fault without invoking unexpected strength in the lower crust and drag (and possible decoupling or "detachment") beneath the horizontal base of the faulting layers. If the faulted plate boundary should weaken as it evolves, then either such basal drag must develop near the fault, or the far-field stress must diminish to maintain the equilibrium condition. The best way to learn whether such basal tractions exist is to determine whether the shear stress resolved parallel to the fault diminishes as the fault is approached (Lachenbruch and Sass, 1973; McGarr and others, 1982). We have shown here that a transect normal to the San Andreas fault shows no such diminution, although the observations were much shallower (approx 1 km deep or above) than the depth of earthquakes; direct stress measurements at seismogenic depths (below 5 km) are needed. Whether or not such basal decoupling and drag exist near the San Andreas fault is fundamental to our understanding of its earthquakes and of the nature of continental transform plate boundaries and their resistance to plate motion.

REFERENCES CITED

Aki, Keiiti, 1966, Generation and propagation of *G* waves from the Niigata earthquake of June 16,1964. Part 2, Estimation of earthquake moment, released energy, and stress-strain drop from the *G* wave spectrum: University of Tokyo, Earthquake Research Institute Bulletin, v. 44, pt. 1, p. 73–88.

Atwater, Tanya, 1970, Implications of plate tectonics for the Cenozoic tectonic evolution of western North America: Geological Society of America Bulletin, v. 81, no. 12, p. 3513–3536.

Berry, F.A.F., 1973, High fluid potentials in California Coast Ranges and their tectonic significance: American Association of Petroleum Geologists Bulletin, v. 57 no. 7, p. 1219–1248.

Boatwright, John, and Choy, G.L., 1986, Teleseismic estimates of the energy radiated by shallow earthquakes: Journal of Geophysical Research, v. 91, no. B2, p. 2095–2112.

Brace, W.F., and Kohlstedt, D.L., 1980, Limits on lithospheric stress imposed by laboratory experiments: Journal of Geophysical Research, v. 85, no. B11, p. 6248–6252.

Brune, J.N., and Allen, C.R., 1967, A low-stress-drop, low-magnitude earthquake with surface faulting: The Imperial, California, earthquake of March 4, 1966: Seismological Society of America Bulletin, v. 57, no. 3, p. 501–514.

Brune, J.N., Henyey, T.L., and Roy, R.F., 1969, Heat flow, stress, and rate of slip along the San Andreas fault, California: Journal of Geophysical Research, v. 74, no. 15, p. 3821–3827.

Byerlee, J.D., 1970, Static and kinetic friction of granite at high normal stress: International Journal of Rock Mechanics and Mining Sciences, v. 7, no. 6, p. 577–582.

—— 1978, Friction of rocks: Pure and Applied Geophysics, v. 116, no. 4–5, p. 615–626.

Byerlee, J.D., and Brace, W.F., 1968, Stick-slip, stable sliding, and earthquakes—effect of rock type, pressure, strain rate, and stiffness: Journal of Geophysical Research, v. 73, no. 18, p. 6031–6037.

—— 1969, High-pressure mechanical instability in rocks: Science, v. 164, no. 3880, p. 713–715.

Chinnery, M.A., 1964, The strength of the earth's crust under horizontal shear stress: Journal of Geophysical Research, v. 69, no. 10, p. 2085–2089.

Dieterich, J.H., 1979, Modelling of rock friction, 1. Experimental results and constitutive equations: Journal of Geophysical Research, v. 84, no. B5, p. 2161–2168.

—— 1981, Potential for geophysical experiments in large scale tests: Geophysical Research Letters, v. 8, no. 7, p. 653–656.

Fletcher, J.B., Boatwright, John, and Joyner, W.B., 1983, Depth dependence of source parameters at Monticello, South Carolina: Seismological Society of America Bulletin, v. 73, no. 6, pt. A, p. 1735–1751.

Grantz, Arthur, and Dickinson, W.R., 1968, Indicated cumulative offsets along the San Andreas fault in the California Coast Ranges, *in* Dickinson, W.R., and Grantz, Arthur, eds., Proceedings of conference on geologic problems of San Andreas fault system: Stanford, Calif., Stanford University Publications in the Geological Sciences, v. 11, p. 117–120.

Gutenberg, Beno, and Richter, C.F., 1956, Magnitude and energy of earthquakes: Annali di Geofisica, Rome, v. 9, no. 1, p. 1–15.

Haimson, B.C., and Fairhurst, Charles, 1970, In situ stress determination at great depth by means of hydraulic fracturing, chap. 28 *of* Somerton, W.H., ed., Rock mechanics, theory and practice: Symposium on Rock Mechanics, 11th, Berkeley, Calif., 1969, Proceedings, p. 559–584.

Hanks, T.C., and Kanamori, Hiroo, 1979, A moment magnitude scale: Journal of Geophysical Research, v. 84, no. B5, 2348–2350.

Healy, J.H., and Zoback, M.D., 1988, Hydraulic fracturing in situ stress measurements to 2.1 km depth at Cajon Pass, California: Geophysical Research Letters, v. 15, no. 9, p. 1005–1008.

Henyey, T.L., 1968, Heat flow near major strike-slip faults in central and southern California: Pasadena, California Institute of Technology, Ph.D. thesis, 421 p.

Henyey, T.L., and Wasserburg, G.J., 1971, Heat flow near major strike-slip faults in California: Journal of Geophysical Research, v. 76, no. 32, p. 7924–7946.

Hickman, S.H., Zoback, M.D., and Healy, J.H., 1988, Continuation of a deep borehole stress measurement profile near the San Andreas fault, 1, Hydraulic fracturing stress measurements at Hi Vista, Mojave Desert, California: Journal of Geophysical Research, v. 93, no. B12, p. 15183–15195.

Hubbert, M.K., and Willis, D.G., 1957, Mechanics of hydraulic fracturing: Journal of Petroleum Technology, v. 9, no. 6, p. 153–168.

Jaeger, J.C., 1956, Elasticity, fracture, and flow: New York, John Wiley and Sons, 152 p.

Jones, L.M., 1988, Focal mechanisms and the state of stress on the San Andreas fault in southern California: Journal of Geophysical Research, v. 93, no. B8, p. 8869–8891.

Kirby, S.H., 1980, Tectonic stresses in the lithosphere: Constraints provided by the experimental deformation of rocks: Journal of Geophysical Research, v. 85, no. B11, p. 6353–6363.

Lachenbruch, A.H., 1986, Simple models for the estimation and measurement of frictional heating by an earthquake: U.S. Geological Survey Open-File Report 86–508, 13 p.

Lachenbruch, A.H., and Sass, J.H., 1973, Thermomechanical aspects of the San Andreas fault system, *in* Kovach, R.L., and Nur, Amos, eds., Proceedings of the conference on tectonic problems of the San Andreas fault system: Stanford, Calif., Stanford University Publications in the Geological Sciences, v. 13, p. 192–205.

—— 1980, Heat flow and energetics of the San Andreas fault zone: Journal of Geophysical Research, v. 85, no. B11, p. 6185–6222.

—— 1988, The stress heat-flow paradox and thermal results from Cajon Pass: Geophysical Research Letters, v. 15, no. 9, p. 981–984.

Lee, T.C., 1983, Heat flow through the San Jacinto fault zone, southern California: Royal Astronomical Society Geophysical Journal, v. 72, no. 3, p. 721–731.

Lockner, D.A., and Okubo, P.G., 1983, Measurements of frictional heating in granite: Journal of Geophysical Research, v. 88, no. B5, p. 4313–4320.

McGarr, Arthur, 1980, Some constraints on levels of shear stress in the crust from observations and theory: Journal of Geophysical Research, v. 85, no. B11, p. 6231–6238.

—— 1988, On the state of lithospheric stress in the absence of applied tectonic forces: Journal of Geophysical Research, v. 93, no. B11, p. 13609–13617.

McGarr, Arthur, and Gay, N.C., 1978, State of stress in the earth's crust: Annual Review of Earth and Planetary Sciences, v. 6, p. 405–436.

McGarr, Arthur, Zoback, M.D., and Hanks, T.C., 1982, Implications of an elastic analysis of in situ stress measurements near the San Andreas fault: Journal of Geophysical Research, v. 87, no. B9, p. 7797–7806.

McKenzie, D.P., 1969, The relation between fault plane solutions for earthquakes and the directions of the principal stresses: Seismological Society of America Bulletin, v. 59, no. 2, p. 591–601 .

McKenzie, D.P. and Brune, J.N., 1972, Melting on fault planes during large earthquakes: Royal Astronomical Society Geophysical Journal, v. 29, no. 1, p. 65–78.

McNally, K.C., Kanamori, Hiroo, Pechmann, J.C., and Fuis, G.S., 1978, Earthquake swarm along the San Andreas fault near Palmdale, southern California, 1976 to 1977: Science, v. 201, no. 4358, p. 814–817.

Minster, J.B., and Jordan, T.H., 1984, Vector constraints on Quaternary deformation of the western United States east and west of the San Andreas fault, *in* Crouch, J.K., and Bachman, S.B., eds., Tectonics and sedimentation along the California margin: Society of Economic Paleontologists and Mineralogists, Pacific Section field trip guide, v. 38, p. 1–16.

Mount, V.S., and Suppe, John, 1987, State of stress near the San Andreas fault: Implications for wrench tectonics: Geology, v. 15, no. 12, p. 1143–1146.

Namson, J.S., and Davis, T.L., 1988, Seismically active fold and thrust belt in the San Joaquin Valley, central California: Geological Society of America Bulletin, v. 100, no. 2, p. 257–273.

O'Neill, J.R., and Hanks, Thomas, 1980, Geochemical evidence for water-rock interaction along the San Andreas and Garlock faults of California: Journal of Geophysical Research, v. 85, no. B11, p. 6286–6292.

Oppenheimer, D.H., Reasenberg, P.A., and Simpson, R.W., 1988, Fault-plane solutions for the 1984 Morgan Hill, California, earthquake sequence: Evidence for the state of stress on the Calaveras fault: Journal of Geophysical Research, v. 93, no. B8, p. 9007–9026.

Pine, R.J., Ledingham, Peter, and Merrifield, C.M., 1983, In-situ stress measurement in the Carnmenellis granite—II. Hydrofracture tests at Rosemanowes Quarry to depths of 2000 m: International Journal of Rock Mechanics and Mining Sciences & Geomechanical Abstracts, v. 20, no. 2, p. 63–72.

Reid, H.F., 1910, The mechanics of the earthquake, v. 2 of The California earthquake of April 18, 1906: Report of the State Earthquake Investigation Commission: Carnegie Institution of Washington Publication 87, 192 p.

Ruina, A.L., 1983, Slip instability and state variable friction laws: Journal of Geophysical Research, v. 88, no. B12, p. 10359–10370.

Savage, J.C., and Wood, M.D., 1971, The relationship between apparent stress and stress drop: Seismological Society of America Bulletin, v. 61, no. 5, p. 1381–1388.

Sibson, R.H., 1985, A note on fault reactivation: Journal of Structural Geology, v. 7, no. 6, p.751–754.

Spottiswoode, S.M., and McGarr, Arthur, 1975, Source parameters of tremors in a deep-level gold mine: Seismological Society of America Bulletin, v. 65, no. 1, p. 93–112.

Stesky, R.M., and Brace, W.F., 1973, Estimation of frictional stress on the San Andreas fault from laboratory measurements, *in* Kovach, R.L., and Nur, Amos, eds., Proceedings of the conference on tectonic problems of the San Andreas fault system: Stanford, Calif., Stanford University Publications in the Geological Sciences, v. 13, p. 206–214.

Stock, J.M., and Healy, J.H., 1988, Continuation of a deep borehole stress measurement profile near the San Andreas fault zone, 2, Hydraulic fracturing stress measurements at Black Butte, Mojave Desert, California: Journal of Geophysical Research, v. 93, no. B12, p. 15196–15206.

Wang, C.-Y., Mao, N.-H., and Wu, F.T., 1980, Mechanical properties of clays at high pressure: Journal of Geophysical Research, v. 85, no. B3, p. 1462–1468.

Weldon, R.J., and Humphries, E.D., 1986, A kinematic model of southern California: Tectonics, v. 5, no. 1, p. 33–48.

Weldon, R.J., and Sieh, K.E., 1985, Holocene rate of slip and tentative recurrence interval for large earthquakes on the San Andreas fault in Cajon Pass, southern California: Geological Society of America Bulletin, v. 96, no. 6, p. 793–812.

Williams, C.F., and Narasimhan, T.N., 1989, Hydrogeologic constraints on heat flow along the San Andreas fault—a testing of hypotheses: Earth and Planetary Science Letters, v. 92, p. 131–143.

Wyss, Max, and Brune, J.N., 1968, Seismic moment, stress, and source dimensions for earthquakes in the California-Nevada region: Journal of Geophysical Research, v. 73, no. 14, p. 4681–4694.

Wyss, Max, and Molnar, Peter, 1972, Efficiency, stress drop, apparent stress, effective stress, and frictional stress of Denver, Colorado, earthquakes: Journal of Geophysical Research, v. 77, no. 8, p. 1433–1438.

Zoback, M.D., and Haimson, B.C., eds., 1983, Hydraulic fracturing stress measurements: Washington, D.C., National Academy Press, 270 p.

Zoback, M.D., Healy, J.H., and Roller, J.C., 1977, Preliminary stress measurements in central California using the hydraulic fracturing technique: Pure and Applied Geophysics, v. 115, p. 135–152

Zoback, M.D., Tsukahara, Hiroaki, and Hickman, S.H., 1980, Stress measurements at depth in the vicinity of the San Andreas fault: Implications for the magnitude of shear stress at depth: Journal of Geophysical Research, v. 85, no. B11, p. 6157–6173.

Zoback, M.D., Zoback, M.L., Mount, V.S., Suppe, John, Eaton, J.P., Healy, J.H., Oppenheimer, D.H., Reasenberg, P.A., Jones, L.M., Raleigh, C.B., Wong, I.G., Scotti, Oona, and Wentworth, C.M., 1987, New evidence on the state of stress of the San Andreas fault system: Science, v. 238, no. 4830, p. 1105–1111.

Zoback, M.L., and Zoback, M.D., 1980, State of stress in the conterminous United States: Journal of Geophysical Research, v. 85, no B11, p. 6113–6156.

SUPPLEMENT: ADDITIONAL READING AND SOURCE MATERIAL

ROBERT E. WALLACE, Compiler

To help the reader find avenues into the voluminous literature about the San Andreas fault system, the following selected references are grouped into four sets: (1) maps, (2) review and reference publications, (3) publications of historical interest, and (4) publications of general interest. Many of these selected references have been included because they themselves have extensive bibliographies. The references in section 3 are limited to those pre-1965, except for Hill's review (1981) on the history of concepts. The references in section 4 are directed especially toward the layman or specialists in disciplines other than earth science. These suggested additional readings should be available in most earth-science libraries or from the publisher; many can also be found in larger public libraries.

MAPS

Bond, K.R., and Zietz, Isidore, 1987, Composite magnetic anomaly map of the conterminous United States: U.S. Geological Survey Geophysical Investigations Map GP–977, scale 1:2,500,000.

Dibblee, T.W., Jr., 1973, Regional geologic map of San Andreas and related faults in Carrizo Plain, Temblor, Caliente, and La Panza Ranges and vicinity, California: U.S. Geological Survey Miscellaneous Geologic Investigations Map I–757, 9 p., scale 1:125,000.

Drummond, K.J., chairman, 1981, Pacific Basin sheet *of* Plate-tectonic map of the circum-Pacific region: Tulsa, Okla., American Association of Petroleum Geologists, scale 1:10,000,000.

Engdahl, E.R., and Rinehart, W.A., 1988, Seismicity map of North America: Boulder, Colo., Geological Society of America: scale 1:5,000,000, 4 sheets.

Geological Society of America, 1987, Gravity anomaly map of North America: Boulder, Colo., scale 1:5,000,000, 4 sheets.

—— 1987, Magnetic anomaly map of North America: Boulder, Colo., scale 1:5,000,000, 4 sheets.

Goter, S.K., 1988, Seismicity of California 1808–1987: U.S. Geological Survey Open-File Report 88–286, scale 1:1,000,000.

Shaded relief map in color with earthquake epicenters in red.

Jennings, C.W., compiler, 1958–66, Geologic atlas of California: Sacramento, California Division of Mines and Geology, scale 1:250,000, 27 sheets.

This atlas contains 27 geologic map sheets that together constitute the "Geologic Map of California" at a scale of 1:250,000. Information sheets accompany each geologic map. As of 1989, the map series is being brought up to date, and the Santa Rosa Regional Geologic map series 2A (1982, 5 sheets) and San Bernardino Regional Geologic map series 3A (1987, 5 sheets) have been completed.

—— compiler, 1975, Fault map of California with locations of volcanoes, thermal springs, and thermal wells: California Division of Mines and Geology Geologic Data Map 1, scale 1:750,000.

This is the principal map representation of faults in California on a single map sheet. It contains a wealth of information and is indispensable to anyone interested in the San Andreas fault. An updated edition is in preparation.

—— compiler, 1977, Geologic map of California: California Division of Mines and Geology Geologic Data Map 2, scale 1:750,000.

—— 1985, An explanatory text to accompany the 1:750,000 scale fault and geologic maps of California: California Division of Mines and Geology Bulletin 201, 197 p.

A significant review of data. For example, plate 2 includes four maps: (1) structural provinces of California, (2) parallelism between major Quaternary faults, (3) relation of earthquake epicenters to faults, and (4) earthquake epicenters.

King, P.B., compiler, 1969, Tectonic map of North America: Washington, U.S. Geological Survey, scale 1:5,000,000, 2 sheets.

King, P.B., and Beikman, H.M., compilers, 1974, Geologic map of the United States (exclusive of Alaska and Hawaii): Washington, U.S. Geological Survey, scale 1:2,500,000, 3 sheets.

Real, C.R., Toppozada, T.R., and Parke, D.L., 1978, Earthquake epicenter map of California: California Division of Mines and Geology Map sheet 39, scale 1:1,000,000. A map and tabulation of earthquakes of

magnitude 5 and greater, 1900–74.

Simpson, R.W., Hildenbrand, T.G., Godson, R.H., and Kane, M.F., 1987, Digital colored Bouguer gravity, free-air gravity, station location, and terrain maps for the conterminous United States: U.S. Geological Survey Geophysical Investigations Map GP–953-B, scale 1:7,500,000, 2 sheets.

Simpson, R.W., Jachens, R.C., Saltus, R.W., and Blakely, R.J., 1986, Isostatic residual gravity, topographic, and first-vertical-derivative gravity maps of the conterminous United States: U.S. Geological Survey Geophysical Investigations Map GP–975, scale 1:7,500,000, 2 sheets.

Stover, C.W., 1986, Seismicity map of the conterminous United States and adjacent areas, 1975–1984: U.S. Geological Survey Geophysical Investigations Map GP–984, scale 1:5,000,000.

A standard reference depicting seismicity in the United States.

REVIEW AND REFERENCE PUBLICATIONS

Atwater, Tanya, 1970, Implications of plate tectonics for the Cenozoic tectonic evolution of western North America: Geological Society of America Bulletin, v. 81, no. 12, p. 3513–3536.

Develops the concept of the Pacific system of plates converging with and underriding the North American plate.

Crowell, J.C., ed., 1975, San Andreas fault in southern California: California Division of Mines and Geology Special Report 118, 272 p.

A guidebook containing 29 papers and a useful preliminary fault and geologic map of southern California at a scale of 1:750,000.

Dibblee, T.W., 1967, Areal geology of the western Mojave Desert, California: U.S. Geological Survey Professional Paper 522, 153 p.

Documents many of the bedrock features that characterize the San Andreas fault system.

Dickinson, W.R., and Grantz, Arthur, eds., 1968, Proceedings of conference on geologic problems of San Andreas fault system: Stanford, Calif., Stanford University Publications in the Geological Sciences, v. 11, 374 p.

An important collection of 47 papers, representing the prevailing state of knowledge about the San Andreas fault system at the time of its publication.

Eaton, J.P., O'Neill, M.E., and Murdock, J.N., 1970, Aftershocks of the 1966 Parkfield-Cholame, California, earthquake: A detailed study: Seismological Society of America Bulletin, v. 60, no. 4, p. 1151–1197.

Ernst, W.G., ed., 1981, The geotectonic development of California (Rubey volume 1): Englewood Cliffs, N.J., Prentice-Hall, 706 p.

Possibly the best general review in one volume of the geologic and tectonics relations pertinent to the San Andreas fault system. More than 1,300 references listed in the back of the volume provide an invaluable source for further study.

Hart, E.W., Hirschfeld, S.E., and Schulz, S.S., eds., 1982, Conference on Earthquake Hazards in the Eastern San Francisco Bay Area, Hayward, Calif., 1982, Proceedings: California Division of Mines and Geology Special Publication 62, 447 p.

A collection of 61 papers in which the Hayward and Calaveras faults, and other smaller branches of the San Andreas fault system, receive considerable attention.

Hinze, W.J., Kane, M.F., O'Hara, N.W., Redford, M.S., Tanner, James, and Weber, Christian, eds., 1985, The utility of regional gravity and magnetic anomaly maps: Tulsa, Okla., Society of Exploration Geophysicists, 454 p.

A set of 34 papers providing information and guidance on the use and interpretation of gravity and magnetic-anomaly data, as well as regional maps.

Kovach, R.L., and Nur, Amos, eds., 1973, Proceedings of the conference on tectonic problems of the San Andreas fault system: Stanford, Calif., Stanford University Publications in the Geological Sciences, v. 13, 494 p.

An important collection of 53 papers, representing the prevailing state of knowledge about the San Andreas fault system at the time of its publication.

Oliver, H.W., 1980, Interpretation of the gravity map of California and its continental margin: California Division of Mines and Geology Bulletin 205, 52 p.

A general reference and bibliographic source of gravity data.

Pakiser, L.C., Jr., and Mooney, W.D., eds., in press, Geophysical framework of the continental United States: Geological Society of America Memoir 172.

A collection of 34 papers covering a broad range of subjects, including stress, tectonics, regional summaries, and methods.

Ross, D.C., 1984, Possible correlations of basement rocks across the San Andreas, San Gregorio-Hosgri and Rinconada-Reliz-King City faults, California: U.S. Geological Survey Professional Paper 1317, 37 p.

An insight into the longer term history of the San Andreas fault system as indicated by the disruption of older rocks.

Scholl, D.W., Grantz, Arthur, and Vedder, J.G., eds.

1987, Geology and resource potential of the continental margin of western North America and adjacent ocean basins—Beaufort Sea to Baja California (Earth Science Series, v. 6): Houston, Tex., Circum-Pacific Council for Energy and Mineral Resources.

A major source volume about the continental margin of North America. Includes 33 chapters concerned with topics ranging from tectonic and basin evolution to hydrocarbon and metallic-mineral occurrence and potential.

Sharp, R.V., 1967, San Jacinto fault zone in the Peninsular Ranges of southern California: Geological Society of America Bulletin, v. 78, no. 6, p. 705–729.

Stewart, J.H., and Crowell, J.C., in press, Strike-slip tectonics in the Cordilleran region, western United States in Burchfiel, B.C., Libman, P.W., and Zoback, M.L., eds., The Cordilleran orogen: Boulder, Colo., Geological Society of America.

A review of strike-slip faults, including the San Andreas fault, in the Western United States.

Streitz, Robert, and Sherburne, R.W., eds., 1980, Studies of the San Andreas fault zone in northern California: California Division of Mines and Geology Special Report 140, 187 p.

A valuable set of 16 papers on subjects including geology, geophysics, seismology, and engineering.

Sylvester, A.G., 1988, Strike-slip faults: Geological Society of America Bulletin, v. 100, no. 11, p. 1666–1703.

An excellent review of the concept, recognition, mechanics, and behavior of strike-slip faults, with numerous references to the San Andreas fault. Includes an extensive bibliography.

Ziony, J.I., ed., 1985, Evaluating earthquake hazards in the Los Angeles region—an earth-science perspective: U.S. Geological Survey Professional Paper 1360, 505 p.

A valuable collection of 16 papers that review the state of the art about geologic hazards, ranging from predicting earthquake faulting and ground motion to landslides, tsunamis, and the use of earth-science information.

PUBLICATIONS OF HISTORICAL INTEREST

Allen, C.R., 1957, San Andreas fault in San Gorgonio Pass, southern California: Geological Society of America Bulletin, v. 68, no. 3, p. 315–349.

Anderson, F.M., 1899, The Geology of Point Reyes peninsula: Berkeley, University of California Publications, Department of Geology Bulletin, v. 2, no. 5, p. 119–153.

Bailey, E.H., Irwin, W.P., and Jones, D.L., 1964, Franciscan and related rocks, and their significance in the geology of western California: California Division of Mines and Geology Bulletin 183, 177 p.

A classic paper in which the San Andreas fault receives considerable attention and early tectonic models are presented.

Branner, J.C., 1906, An authoritative opinion: Mining and Scientific Press, v. 92, p. 347.

Crowell, J.C., 1952, Probable large lateral displacement on the San Gabriel fault, southern California: American Association of Petroleum Geologists Bulletin, v. 36, no. 10, p. 2026–2035.

—— 1962, Displacement along the San Andreas fault, California: Geological Society of America Special Paper 71, 59 p.

Documents large-scale strike slip on the San Andreas fault system.

Eaton, J.E., 1939, Geology and oil possibilities of Caliente Range, Cuyama Valley and Carrizo Plain, California: California Journal of Mines and Geology, v. 35, no. 3, p. 255–274.

Suggests 25 miles of strike slip on the San Andreas fault.

Gilbert, G.K., 1907, The earthquake as a natural phenomenon, *in* The San Francisco earthquake and fire of April 18, 1906, and their effects on structures and structural materials: U.S. Geological Survey Bulletin 324, p. 1–13.

This paper provided the first overview of the San Andreas fault in northern California. From Gilbert's field notes, he appears to have been the first to appreciate the true significance of the fault.

Hill, M.L., 1981, San Andreas fault: History of concepts: Geological Society of America Bulletin, pt. 1, v. 92, no. 3, p. 112–131.

A review of the early development of concepts about the significance of the San Andreas fault, especially the amount of strike slip.

Hill, M.L., and Dibblee, T.W., Jr., 1953, San Andreas, Garlock, and Big Pine faults, California: A study of the character, history, and tectonic significance of their displacements: Geological Society of America Bulletin, v. 64, no. 4, p. 443–458.

This classic paper was the first to provide data indicative of hundreds of miles of strike slip on the San Andreas fault.

Hill, R.T., 1928, Southern California geology and Los Angeles earthquakes: Los Angeles, Southern California Academy of Sciences, 232 p.

Lawson, A.C., 1895, Sketch of the geology of the San Francisco peninsula: U. S. Geological Survey Annual Report 15, p. 439–473.

First use of the name "San Andreas fault."

—— chairman, 1908, The California earthquake of April 18, 1906: Report of the State Earthquake Investigation Commission: Carnegie Institution of Washington Publication 87, 2 v.
This treatise on the 1906 earthquake contains an abundance of important data about the San Andreas fault.

Noble, L.F., 1926, The San Andreas rift and some other active faults in the desert region of southeastern California: Carnegie Institution of Washington Year Book 25, p. 415–422..

—— 1933, Excursion to the San Andreas fault and Cajon Pass: International Geological Congress, 16th, Washington, 1933, Guidebook 15, p. 10–21.

—— 1954, The San Andreas fault zone from Soledad Pass to Cajon Pass, California, [pt] 5 *off* Structural features, chap. 4 *of* Jahns, R.H., ed., Geology of southern California: California Division of Mines Bulletin 170, v. 1, p. 37–48.

Oakeshott, G.B., 1959, The San Andreas fault in Marin and San Mateo Counties, *in* Oakeshott, G.B., ed., San Francisco earthquakes of March 1957: California Division of Mines Special Report 57, 127 p.

Pack, R.W., 1920, The Sunset-Midway oil field, California, part 1, Geology and oil resources: U.S. Geological Survey Professional Paper 116, 179 p.

Pack, R.W., and English, W.A., 1915, Geology and oil prospects of Waltham, Priest, Bitterwater, and Peachtree Valleys, California: U.S. Geological Survey Bulletin 581, p. 119–160.

Reed, R.D., 1933, Geology of California: Tulsa, Okla., American Association of Petroleum Geologists, 355 p.

—— 1943, California's record in the geologic history of the world, *in* Geologic formations and economic development of the oil and gas fields of California: California Division of Mines Bulletin 118, p. 99–118.
Does not mention strike slip on the San Andreas fault.

Reed, R.D., and Hollister, J.S., 1936, Structural evolution of southern California: American Association of Petroleum Geologists Bulletin, v. 20, no. 12, p. 1529–1704.

Reid, H.F., 1910, The mechanics of the earthquake, v. 2 of The California earthquake of April 18, 1906: Report of the State Earthquake Investigation Commission: Carnegie Institution of Washington Publication 87, 192 p.
Develops elastic-rebound theory.

Schuyler, J.D., 1896, Reservoirs for irrigation: U.S. Geological Survey Annual Report 18, p. 617–740.

Steinbrugge, K.V., Zacher, E.G., Tocher, Don, Whitten, C.A., and Claire, C.N., 1960, Creep on the San Andreas fault: Seismological Society of America Bulletin, v. 50, no. 3, p. 389–415.
This paper was the first to report slow, continuous slip (creep) on the San Andreas fault.

Taliaferro, N.L., 1938, San Andreas fault in central California [abs.]: Geological Society of America Proceedings, 1937, p. 254–255.
Concludes that horizontal slip on the San Andreas fault is less than a mile.

Vaughan, F.E., 1922, Geology of San Bernardino Mountains north of San Gorgonio Pass: Berkeley, University of California Publications, Department of Geological Sciences Bulletin, v. 13, no. 9, p. 319–411.

Vickery, F.P., 1925, The structural dynamics of the Livermore [California] region: Journal of Geology, v. 33, no. 6, p. 608–628.

Wallace, R.E., 1949, Structure of a portion of the San Andreas rift in southern California: Geological Society of America Bulletin, v. 60, no. 4, p. 781–806.

Wilson, J.T., 1965, A new class of faults and their bearing on continental drift: Nature, v. 207, no. 4995, p. 343–347.
Develops the concept of a transform fault.

Wood, H.O., and Buwalda, J.P., 1930, Horizontal displacement along the San Andreas fault in Carrizo Plain, California [abs.] : Pan-American Geologist, v. 54, no. 1, p. 75.

PUBLICATIONS OF GENERAL INTEREST

Dewey, J.F., 1972, Plate tectonics: Scientific American, v. 226, no. 5, p. 56–68.
A brief introduction to the concepts of plate tectonics, including excellent diagrams of the geometry of the global plates.

Iacopi, Robert, 1971, Earthquake country: Menio Park, Calif., Lane, 160 p.
A review and guidebook about the San Andreas fault, written for the layman, but includes useful maps and photographs of interest

to the scientist and layman alike.

Jones, D.L., Cox, Allan, Coney, Peter, and Beck, Myrl, 1982, The growth of western North America: Scientific American, v. 247, no. 5, p. 70–84.

Refines the concept of plate tectonics has been refined to include the accretion of smaller blocks to the main continental masses. The San Andreas fault system is involved with the motions of both larger and smaller plates.

Jordan, T.H., and Minster, J.B., 1988, Measuring crustal deformation in the American West: Scientific American, v. 259, no. 2, p. 48–58.

Provides some ideas and data about how western North America is being deformed.

Schulz, S.S., and Wallace, R.E., 1987, The San Andreas fault: Washington, U.S. Geological Survey, 17 p.

Pamphlet providing a brief review for the layman.

Wesson, R.L., and Wallace, R.E., 1985, Predicting the next great earthquake in California: Scientific American, v. 252, no. 2, p. 35–43.

The science of earthquake prediction has been evolving, and the San Andreas fault system has been a target of major interest. This paper reviews some progress that has been made.

☆ U. S. GOVERNMENT PRINTING OFFICE: 1991-586-938

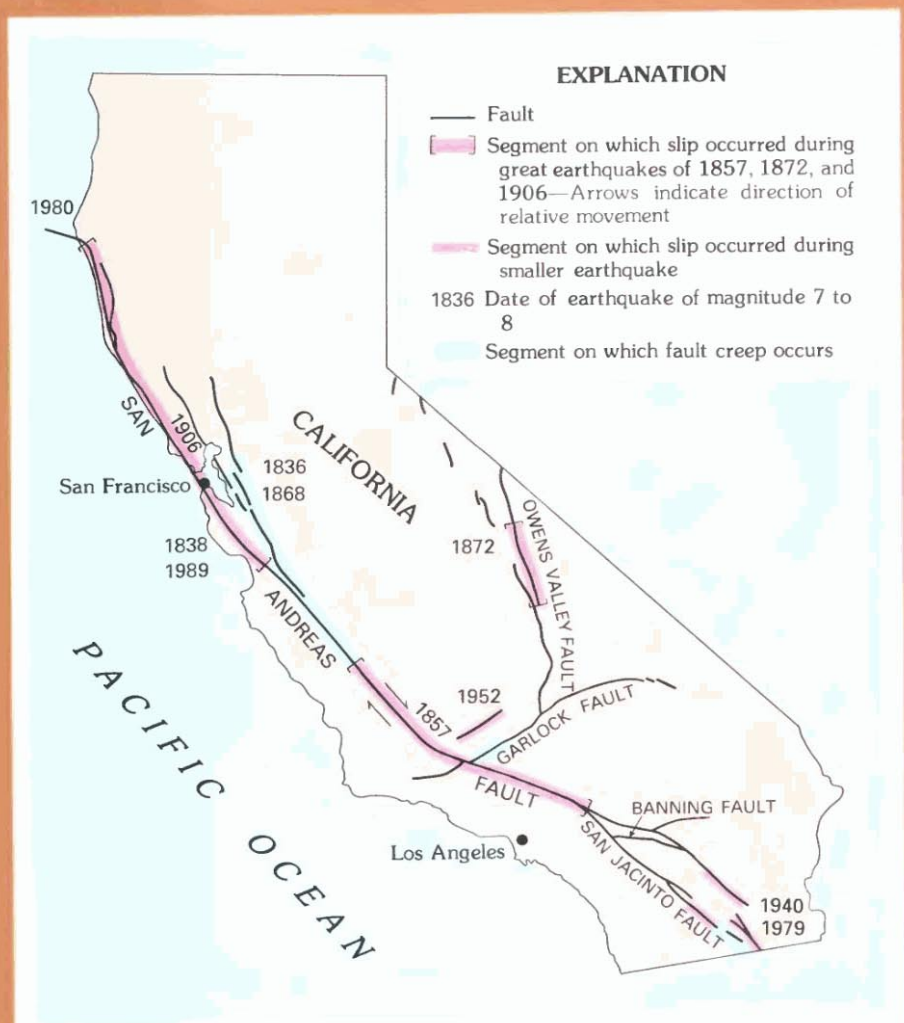

SAN ANDREAS FAULT SYSTEM AND OTHER LARGE FAULTS IN CALIFORNIA

Different segments of fault display different behavior.

Memorandum

Date:	July 6, 2020
From:	Catalyst Environmental Solutions Inc.
RE:	Heber 2 Project Description Information

This information was copied directly from the Conditional Use Permit Amendment Application. None of the information provided in this memorandum is new or revised.

Construction Schedule

The proposed Project facilities are anticipated to take up to eight months to install, test, and become fully integrated with the existing system. Construction will begin immediately after all permits are secured.

Construction Equipment

Heavy construction equipment, including semi-truck trailers, flatbed trucks, excavators/bulldozers, forklifts, roller, and cranes would be used to deliver and place the proposed facilities on the Heber 2 Project Site. Smaller powered hand tools, such as drills, compressors, and welding equipment would also be used. Employee vehicles would be used to transport workers to the Project Site and parked at the designated parking locations.

Workforce

The Project would require a temporary increase in labor force (15 workers) during the short-term construction period (approximately eight months). The workforce is assumed to be from southern California and would likely not require accommodations.

Site Preparation

The Project Site was developed and graded during the original construction of the Heber 2 Complex in 1992, and its current condition is exposed soil and gravel. To ensure the proposed facilities are situated on safe and stable surfaces, minor excavation and compaction activities would be performed. The top 18 inches of the Project Site's exposed soil would be removed, extending approximately 5 feet beyond the proposed facilities. A minimum of 18 inches of CalTrans Class 2 aggregate based will be placed and compacted to the appropriate density (ASTM D1557). On-site soil that has been piled during excavation will be used as backfill material, as necessary. Only those soils free of debris and deleterious matter would be used as backfill material. The proposed facilities would be placed on shallow-spread footers and wall footers to support the structures. All site preparation and fill placement activities will be monitored by a qualified geotechnical engineer to detect undesirable materials and/or site conditions that may arise during site preparation.

Demolition and Disposal

As provided in the CUP application, the Application would apply the following demolition and disposal measures:

- Workers would be required to properly dispose of all refuse and trash to prevent any litter on the site.

- During construction, portable chemical sanitary facilities would be used by all construction personnel. These facilities would be serviced by a local contractor.
- All construction wastes, liquid or solid, would be disposed of in compliance with all appropriate local, state, and federal disposal regulations.
- Solid wastes would be disposed of in an approved solid waste disposal site in accordance with Imperial County Environmental Health Department requirements. Waste would be routinely collected and disposed of at an authorized landfill by a licensed disposal contractor.
- All hazardous materials would be used, transported, and disposed of in accordance with applicable safe handling and disposal regulations.

Records Index

Date:	July 8, 2020
From:	Catalyst Environmental Solutions Inc.
RE:	Requested Documents for Heber 2 Repower Project Initial Study & Negative Declaration

The index below provides an identification number for each document requested in support of the Heber 2 Repower Project Initial Study and Negative Declaration (IS/ND). The document number provided in the index table correlates to the file name for each requested document.

Requested Document	Document No.
Conditional Use Permit (CUP No. 06-0006) under which the Project must obtain an amendment.	H2RP-1
The Permit to Operate, issued to the Heber 2 Complex by the Imperial County Air Pollution Control District ("ICAPCD").	H2RP-2
The California Historical Resources Information System (CHRIS), managed by the California Office of Historic Preservation.	H2RP-3 (CONFIDENTIAL – NOT FOR PUBLIC RELEASE)
Bryant, William A. and Earl W. Hart. 2007. Fault-Rupture Hazard Zones in California, Alquist-Priolo Earthquake Studies Zoning Act with Index to Earthquake Fault Zones Maps, Department of Conservation, California Geological Survey, Special Publication 42.	H2RP-4
Olive, WW., et al. 1989. Swelling Clays Map of the Conterminous United States	H2RP-5
Existing Water Permit	H2RP-6
Imperial County 2018 PM10 Plan and Imperial County 2018 PM2.5 Plan.	H2RP-7
ASTM International. 2019. Standard Test Methods for Laboratory Compaction Characteristics of Soil Using Modified Effort (DM1557).	H2RP-8
California Air Resources Board (CARB). 2017. Ambient Air Quality Standards.	H2RP-9
California Department of Fish and Wildlife. 2019. CNDDB Maps and Data	H2RP-10 (1 PDF, 2 Excel files)
California Department of Industrial Relations (DIR). 2016. Safety and Health Protocol on the Job	H2RP-11
California Department of Resources Recycling and Recovery (CalRecycle). 2017. Integrated Waste Management Plans	H2RP-12
California Department of Toxic Substances Control (DTSC). 2010. Certified Union Program Agencies (CUPA).	H2RP-13
California Department of Transportation (Caltrans). 2013. Technical Noise Supplement to the Traffic Noise Analysis Protocol.	H2RP-14
California Department of Transportation. 2017. California Scenic Highway Mapping System.	H2RP-15
California Department of Water Resources. 2003. California's Groundwater.	H2RP-16
California Office of Planning and Research. 2003. General Plan	H2RP-17

Guidelines.	
United States Environmental Protection Agency (EPA). 2015. National Ambient Air Quality Standards.	H2RP-18
United States Geological Survey (USGS). 1990. The San Andreas Fault System, California, Robert E. Wallace, editor, U.S. Geological Survey Professional Paper 1515.	H2RP-19
Detailed construction schedule.	H2RP-20
List of all construction equipment.	H2RP-20
Description of construction equipment: hp, engine tier, hours of operation per day over the duration of construction.	H2RP-20
Number of workers and commute distance.	H2RP-20
Amount of demolition debris and its disposal location	H2RP-20
Amount of imported fill.	H2RP-20
Acres of grading	H2RP-20

HEBER 2

UPDATED PROJECT DESCRIPTION

(AND RESPONSES TO COMMENTS)

APPENDIX A

Site Photographs

(Collected on June 1, 2019 and June 13, 2019)

Photo 1 – western portion of development site.

Photo 2 – southwest portion of development site.

Photo 3 – northwestern portion of development site.

Photo 4 – northern portion of development site.

Photo 5 – central portion of development site.

Photo 6 – central portion of development site.

Photo 7 – northern portion of development site.

Biological Resources Clearance Memorandum

Date:	June 3, 2019
From:	Catalyst Environmental Solutions
RE:	**Biological Resources Clearance Survey for the Heber 2 Geothermal Repower Project**

INTRODUCTION

The Second Imperial Geothermal Company (SIGC), a wholly owned subsidiary of ORMAT Nevada, Inc (ORMAT), owns and operates the Heber 2 Geothermal Energy Complex, which was originally constructed in 1992 and expanded in 2006. SIGC proposes to amend the existing Conditional Use Permit (CUP; No. 06-0006) to install two water-cooled ORMAT Energy Converters (OECs) to replace six old units from 1992; three 10,000 gallon isopentane above ground storage tanks; and, additional pipeline to connect the proposed facilities with the existing Heber 2 Complex (hereinafter, "Project"). All proposed facilities would be developed within the existing Heber 2 Complex and fence line. The proposed action also includes the extension of the permitted life of the entire Heber 2 facility (including the Goulds 2 and Heber South geothermal energy facilities) to 30 years (2019-2049). The objective of the Project is to improve the efficiency of geothermal energy generation and refurbish the Heber 2 Complex to the original net generation of 33 megawatts (MW) gross. The total project footprint from developing the proposed facilities is approximately 4 acres, with all disturbances occurring within the existing power plant fence line.

Th purpose of this technical memorandum is to verify the absence of any sensitive biological resources occurring on/near the proposed development site at the Heber 2 Complex in Imperial County and to demonstrate the proposed project's compliance with applicable federal and state regulations.

Project Location

The Heber 2 Complex is located on private lands owned by ORMAT in southern Imperial County (**Figure 1)**. The proposed development would occur entirely on Assessor's Parcel Number (APN) 054-250-031, which is a 39.99-acre property. The address for Heber 2 is 855 Dogwood Road, Heber, CA 92249.

Project Description

Existing Facilities

The existing Heber 2 Geothermal Energy Power Plant (Heber 2) was permitted for development under CUP No. 06-0006 in 1996 and consists of the following facilities:

- The Heber 2 Complex currently generates less than the 33 MW net generation capacity, the proposed improvements will restore the facility's generation capacity to 33 MW of renewable energy.

- The Heber 2 Complex currently includes two injection wells, two six-cell cooling towers, an electrical substation, emergency fire water pump, evacuation skid system-vapor recovery maintenance unit, control room, office space, maintenance facilities, two 10,000 gallons isopentane storage tanks, piping, and ancillary equipment/facilities.
- The parcel where the Heber 2 Complex site is located is approximately 40 acres and is enclosed by security fencing.
- Operations personnel are present at the Heber 2 Complex during routine working hours (8am-5pm), and the facility is monitored 24 hours per day from the control room at the Heber 1 geothermal power plant, approximately 1 mile to the east.

Proposed Facilities

SIGC proposes to install two new water-cooled ORMAT Energy Converters (OECs); three 10,000 gallon above ground storage tanks; and, additional pipeline to connect the proposed facilities with the existing Heber 2 Complex (hereinafter, "Project"). This application also proposes to extend the permitted life of the entire Heber 2 Complex (including the related Goulds 2 and Heber South geothermal energy facilities) to 30 years (2019-2049). The objective of the Project is to improve the efficiency of geothermal energy generation and refurbish the Heber 2 Complex to the original nameplate generation of 33 megawatts (MW). The total project disturbance from developing the new OECs is approximately 4 acres, all within the existing power plant footprint and fencing. Figure 2 provides a site plan of the proposed and existing facilities.

The existing OEC units would be shut down, disassembled, and removed from the Heber 2 site likely immediately after the completion of the development of the proposed facilities, and no later than 5 years after issuance of the CUP.

The development site is completely devoid of any vegetation and is actively disturbed as part of ongoing energy generation operations at Heber 2. Appendix A provides photographs of the development site. Considering its current condition, site preparation for the installation of the proposed facilities would be limited to minor excavation and soil/gravel compaction.

ORMAT Energy Converter-1 (OEC-1)

The proposed OEC-1 unit is a two-turbine combined cycle binary unit, operating on a subcritical Rankine cycle, with isopentane as the motive fluid for the system. This system also consists of a generator, turbines, vaporizer, water cooled condensers, preheaters and recuperators, with the OEC served by the existing evacuation skid/vapor recovery maintenance unit (VRMU) for purging and maintenance events. The design capacity for the unit is 25.43 MW Gross.

ORMAT Energy Converter-2 (OEC-2)

The proposed OEC-2 unit is a two-cycle binary unit, operating on a subcritical Rankine cycle, with isopentane as the motive fluid for the system. This system also consists of a generator, turbines, vaporizers, water cooled condensers and preheaters, with the OEC served by the existing portable evacuation skid/vapor recovery maintenance unit (VRMU) for purging and maintenance events. The design capacity for the unit is 14.01 MW Gross.

Three Additional Isopentane Above Ground Storage Tanks

To support the new OEC units, three new ABSTs for additional isopentane supply would be installed. There are two existing ABSTs, and the new ABSTs would be sited adjacent to the existing tanks. Each ABST has a capacity of 10,000 gallons.

Construction Schedule

The proposed developments are anticipated to take up to eight months to install, test, and become fully integrated with the existing system. Construction will initiate immediately after all permits are secured.

REGULATORY FRAMEWORK

Federal

Endangered Species Act (ESA) of 1973 (16 U.S.C. 1531-1544) protects federal listed threatened and endangered species from unlawful take (harass, harm, pursue, hunt, shoot, kill ,wound, collect, capture, trap or attempt to do so) or significantly modify habitat. If a proposed project would jeopardize a threatened or endangered species, then a Section 7 consultation with a federal agency could be required.

Migratory Bird Treaty Act (50 Code Federal Regulations (CFR) 10.13) is a federal statute with several foreign countries to protect species that migrate between countries. Over 1000 species are listed and may not be disrupted during nesting activities. It is illegal to collect any part (nest, feather, eggs, etc.) of a listed species, disturb species while nesting or offer for trade or barter any listed species or parts thereof.

Bald and Golden Eagle Protection Act (16 U.S.C. 668-668c) protects bald and golden eagles from take (harass, harm, pursue, hunt, shoot, kill, wound, collect, capture, trap or attempt to do so) or interference with breeding, feeding or sheltering activities.

Clean Water Act, 1972 (CWA 33 U.S.C. 1251 et seq.) regulates discharges into waters of the U.S. EPA is given the responsibility to implement programs to prevent pollution.

State of California

California Environmental Quality Act (CEQA) Title 14 CA Code of Regulations 15380 requires that endangered, rare or threatened species or subspecies of animals or plants be identified within the influence of the project. If any such species are found, appropriate measures should be identified to avoid, minimize or mitigate to the extent possible the effects of the project.

Native Plant Protection Act CDFG Code Section 1900-1913 prohibits the taking, possessing, or sale within the stare of any plant listed by CDFG as rare, threatened or endangered. Landowners may be allowed to take these species if CDFW is notified at least 10 days prior to plant removal or if these plants are found within public right of ways.

California Fish and Game Codes 3503, 3503.5. 3513 protect migratory birds, bird nests, and eggs including raptors (birds of prey) and raptor nests from take unless authorized by CDFW.

California Fish and Game Code Section 1600 (as amended) regulates activities that substantially diverts or obstructs the natural flow of any river, stream or lake or uses materials from a streambed. This can include riparian habitat associated with watercourses.

State of CA Fully Protected Species identifies and provides additional protection to species that are rare or face possible extinction. These species may not be taken or possessed at any time except for scientific research or relocation for protection of livestock.

Porter-Cologne Water Quality Control Act (as amended) is administered by the State Water Resource Control Board (SWRCB) to protect water quality and is an avenue to implement California

responsibilities under the federal Clean Water Act. This act regulates discharge of waste into a water resource.

EXISTING CONDITIONS

Topography and Soils

The entire Heber 2 project site contains Holtville silty clay, wet (63.2%) and Imperial-Glenbar silty clay loams, wet, 0-2 percent slopes (36.8%) (NRCS 2019). The proposed 4 acres of disturbance contains Imperial-Glenbar silty clay loams, wet, 0-2 percent slopes. The project site is relatively flat and located at approximately -5 below sea level.

Vegetation

No vegetation is present on the project site. The site is classified as "Agricultural and Developed Vegetation" and "Developed and Other Human Use" (USGS 2011). The project site is surrounded on all sides by farmland (Agricultural and Developed Vegetation).

Jurisdictional Waters

No wetlands or jurisdictional waters are located on the project site. Man-made channels are located along the southern (Central Main Canal - classified as R2UBHx), northern and eastern (both classified as R4SBCx) property line of the project site (USFWS 2019c).

Wildlife

The project site is developed with an active geothermal plant. Due to lack of vegetation and water, no amphibians, fish, or reptiles are expected to occur onsite. Due to the developed and active nature of the site, no mammals or birds are expected to inhabit the site. Mammals including coyote (*Canis latrans*) and pocket gopher (*Thomomys* spp.) have been observed in the vicinity of the project but are not likely to occur onsite due to security fencing. Common bird species including red tailed hawk (*Buteo jamaicensis*), crow (*Corvus* spp.) pigeon (*Columbia livia*) have been observed in the vicinity of the project and could be transient visitors to the site.

SENSITIVE AND SPECIAL STATUS SPECIES

The potential for sensitive species to occur in the vicinity of the project site was evaluated using information from the U.S. Fish and Wildlife (USFWS) Information, Planning, and Consultation System (IPaC System); California Natural Diversity Database (CNDDB); and California Native Plant Society (CNPS) Rare Plant Program.

Special Status Plants

No federally listed threatened or endangered plant species have the potential to occur on or near the project site (USFWS 2019a).

Five plant species listed by the CNPS have the potential to occur in the Heber quandrangle in which Heber 2 Complex is located (CNPS 2019):

- Watson's amaranth (*Amaranthus watsonii*)
- Abrams' spurge (*Euphorbia abramsiana)*
- California satintail (*Imperata brevifolia*)
- ribbed cryptantha (*Johnstonella costata*)

- winged cryptantha (*Johnstonella holoptera*)

Special Status Wildlife Species

No federally listed threatened or endangered wildlife species have the potential to occur on the project site and no critical habitat exists on or near the project site (USFWS 2019a, b). The following six migratory bird species are listed by IPaC as having the potential to occur on or near the project site:

- Burrowing owl (*Athene cunicularia*)
- Costa's hummingbird (*Calypte costae*)
- Gila woodpecker (*Melanerpes uropygialis*)
- Long-billed curlew (*Numenius americanus*)
- Rufous hummingbird (*Selasphorus rufus*)
- Whimbrel (*Numenius phaeopus*)

No California special status species are known to occur on the project site (CDFW 2019).

BIOLOGICAL RESOURCES CLEARANCE SURVEY

Methodology

On Saturday, June 1, 2019, biologist Amy Plesetz conducted a biological compliance clearance survey of the ORMAT Heber Site 2 via pedestrian survey.

Findings

The area to be disturbed for the Heber 2 project is completely void of any vegetation. There is no suitable habitat for special-status plant species. There are no tall trees that would encourage raptor nesting, no suitable habitat for burrowing owl, and no food source for hummingbirds. No wildlife or traces of wildlife, including nesting birds, were observed.

The area immediately to the west of the proposed disturbed area is developed with solar panels with scarce disturbed-like vegetation that does not provide suitable habitat for any special-status or common species. Areas north and south of the proposed disturbed area contain geothermal plant facilities. Active farmland surrounds the entire project site.

There may be suitable habitat for burrowing owl in the project vicinity, but this habitat is off-site and more than 500 feet away.

POTENTIAL PROJECTS IMPACTS

No impacts to biological resources from the proposed project are expected due to the developed nature of the site, small project footprint, lack of vegetation and suitable habitat for wildlife, and lack of wildlife traces observed during the biological site visit (June 1, 2019).

No canals or drain structures will be removed or impacted; therefore, there will be no impacts to jurisdictional waters.

RECOMMENDED AVOIDANCE, MINIMIZATION, AND MITIGATION MEASURES

- Speed limits of 10 mph would be observed on the project site in order to minimize dust and avoid collision and incidental mortality of transient wildlife.
- The site is void of vegetation; however, vegetation control, including invasive species eradication, will be controlled to prevent growth under/near the proposed facilities.

BIBLIOGRAPHY

California Department of Fish and Wildlife (CDFW). 2019. California Natural Diversity Database. Accessed 13 June 2019.

California Native Plant Society (CNPS). 2019. Inventory of Rare and Endangered Plants of California (online edition, v8-03 0.39). Website http://www.rareplants.cnps.org. Accessed 12 June 2019.

Natural Resource Conservation Service (NRCS). 2019. SUGGO Database.

U.S. Geological Survey (USGS). 2011. GAP/LANDFIRE National Terrestrial Ecosystems 2011. Website: https://maps.usgs.gov/terrestrial-ecosystems-2011/. Accessed 13 June 2019.

U.S. Fish and Wildlife Service (USFWS). 2019a. IPac Resource List.

USFWS 2019b. Critical Habitat for Threatened & Endangered Species Website. Website: https://fws.maps.arcgis.com/home/webmap/viewer.html. Accessed 12 June 1029.

USFWS. 2019c. National Wetlands Inventory, Wetlands Mapper. Website: https://www.fws.gov/wetlands/data/Mapper.html. Accessed 12 June 2019.

Legend

- United States/Mexico Border
- County Line
- Project Site
- 1-Mile Radius

PROPOSED PROJECT SITE - HEBER 2

Catalyst ENVIRONMENTAL SOLUTIONS

Figure 1

ORMAT

Date: July 2019

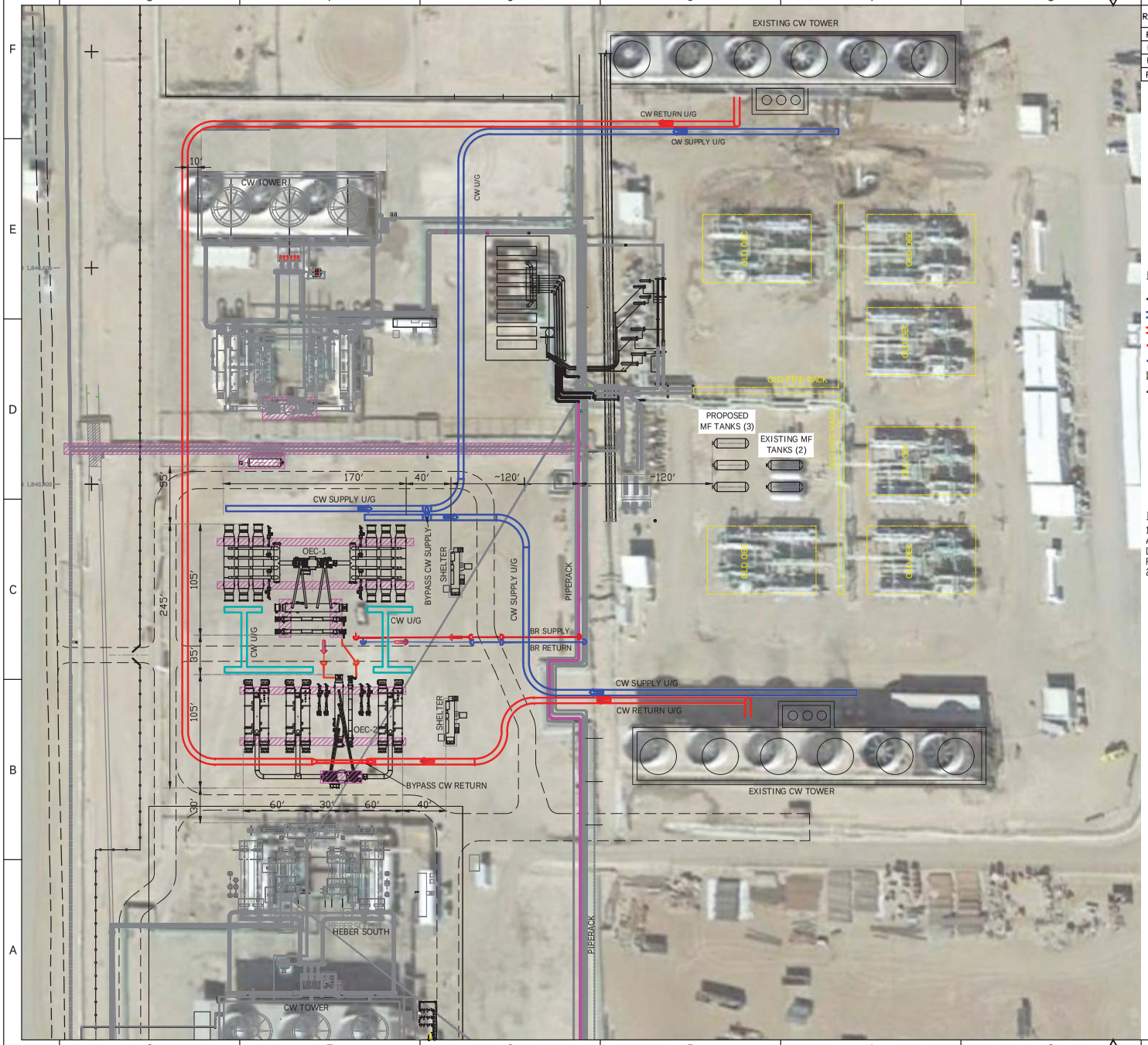

REV	DESCRIPTION	DATE	BY	CHK	ENG	PRJ
P6	UPDATE MODELS OES-1 & OEC-2	5.APR.2019	A.S.	A.N.		S.H.
P7	UPDATE MODELS OES-1	17.APR.2019	A.S.	A.N.		S.H.
P8	UPDATE OEC-1 & OEC-2	27.MAY.2019	A.S.	A.N.		S.H.
P9	UPDATE LOCATION OEC-1	18.JULY.2019	A.S.	A.N.		S.H.

KEY:

- EXISTING FENCE LINE
- PROPOSED UNDERGROUND CW SUPPLY LINE
- PROPOSED UNDERGROUND CW RETURN LINE
- PROPOSED BR SUPPLY LINE
- PROPOSED BR RETURN LINE
- EQUIPMENT TO BE DECOMMISSIONED
- EXISTING EQUIPMENT TO REMAIN

CW	COOLING WATER
U/G	UNDERGROUND
BR	GEOTHERMAL BRINE
OEC	ORMAT ENERGY CONVERTOR
MF	MOTIVE FLUID

NOTE:

1. THE ARRANGEMENT AND SIZES PRESENTED ARE PRELIMINARY AND INDICATIVE ONLY AND SUBJECT TO CHANGED ON DESIGN OPTIMIZATION , DETAILED DESIGN AND ACTUAL EQUIPMENT PURCHASED (MANUFACTURED).
2. DIMENSIONS ARE IN MM [FEET], ELEVATIONS ARE IN MM FEET]

0 20' 100' 200'

GRAPHIC SCALE (FEET)

PREPARED BY:

Stantec

PHONE: FAX:

FOR:

Second Imperial Geothermal Company
855 B Dogwood Road
Heber CA 92249

TITLE:

HEBER2 REPOWER
GENERAL ARRANGEMENT
POWER PLANT ON MAP

DRAWN BY: KAM	DESIGNED BY:
CHECKED BY:	APPROVED BY:
PROJECT NUMBER: 01OT.01234.01.0123	SCALE: AS SHOWN
DATE: 04/01/04	FILE PATH: K:\(CLIENT) OR JOB #

SHEET:

1 OF 1

APPENDIX A

Site Photographs

(Collected on June 1, 2019 and June 13, 2019)

Photo 1 – western portion of development site.

Photo 2 – southwest portion of development site.

Photo 3 – northwestern portion of development site.

Photo 4 – northern portion of development site.

Photo 5 – central portion of development site.

Photo 6 – central portion of development site.

Photo 7 – northern portion of development site.

Technical Memorandum

Cardno

801 Second Avenue
Suite 1150
Seattle, WA 98104
USA

Phone (206) 269-0104
Fax (206) 269-0098

www.cardno.com

Date June 28, 2019

To: Ben Pogue, PMP, AICP
Director of Environmental Planning & Natural Resource Management
Catalyst Environmental Solutions
315 Montana Avenue, Suite 311
Santa Monica, California 90403

From: Jennifer M. Ferris, MA, RPA

RE **Cultural Resources Records Review for the Heber 2 Geothermal Optimization Project**
Confidential – Not for Public Disclosure

Dear Mr. Pogue:

This technical memorandum describes the results of the cultural resources records review completed in June 2019 for the Heber 2 Geothermal Optimization Project. The project is located at 855 Dogwood Road, Heber, Imperial County, California. The project is in Section 33 of Township 16 South, Range 14 East of the San Bernardino Base & Meridian.

The cultural resources records review was completed by Cardno, who requested a records search at the South Central Coastal Information Center (SCCIC) of the California Historical Resources Information System (CHRIS). The SCCIC records search included a review of archives containing archaeological site records and reports of cultural resource studies previously conducted near the project area. Other resources reviewed include the National Register of Historic Places (NRHP), the California Register of Historical Resources (CRHR), the California Inventory of Historic Resources, California Historical Landmarks, California Points of Historical Interest, and the Historic Property Data File.

1.0 Review Results

There are no previously recorded cultural resources (archaeological or historic) within the project area. One previously recorded cultural resource (CA-IMP-008166, Niland to Calexico Railroad) lies within 1.0 mile of the project area (Figure 1). The railroad, which is still in use today, was constructed between 1902 and 1904 by the Southern Pacific Company and runs 65 miles from Niland to Calexico. The railroad has not been evaluated for listing in the NRHP.

There have been 23 surveys, records searches, and environmental impact reports completed within 1.0 mile of the project area. These are shown in Table 1 and Figure 2. Two of the studies

(SCCIC report numbers IM-00115 and IM-00235) partially covered the current project area. None of these studies resulted in the discovery of cultural resources.

Table 1. Previously Conducted Studies within 1.0 mile of the Project Area.

SCCIC Report Number	Authors/ Association	Year	Title	Associated Cultural Resources
IM-00063	Von Werlhof, Jay, and Shrilee Von Werlhof/ Imperial Valley College Museum	1976	Archaeological Examination of a Proposed Geothermal Testing Site near Heber, California	None
IM-00066	Von Werlhof, Jay, and Sherilee Von Werlhof/ Imperial Valley College Museum	1976	Archaeological Record Search of the Heber, California, Region	None
IM-00075	Von Werlhof, Jay, and Sherilee Von Werlhof/ Imperial Valley College Museum	1976	Archaeological Examinations of Certain Geothermal Well Test-Site Areas in the Heber, California, District	None
IM-00115	Von Werlhof, Jay, and Sherilee Von Werlhof/ Imperial Valley College Museum	1977	Archaeological Examination of the Heber Anomaly Report Prepared For VTN Consolidated, Inc.	None
IM-00123	VTN Consolidated, Inc.	1977	Draft Environmental Impact Report for the Heber Geothermal Demonstration Project	None
IM-00185	Von Werlhof, Jay, and George E. Collins/ Imperial Valley College Museum	1979	Archaeological Examinations of Proposed Geothermal Facilities near Heber, CA	None
IM-00192	VTN Consolidated, Inc.	1979	Draft Master Environmental Impact Report for a 500-Megawatt Geothermal Development at Heber, Imperial County, California	None
IM-00199	Walker, Carol, Charles Bull, and Jay Von Werlhof/ Recon	1979	Cultural Resource Study of a Proposed Electric Transmission Line From Jade to the Sand Hills, Imperial County, California	None
IM-00233	Walker, Carol, Charles Bull, and Jay Von Werlhof/ Recon	1981	Cultural Resource Study of a Proposed Electric Transmission Line From Jade to the Sand Hills, Imperial County, California	None
IM-00235	Bureau of Land Management	1981	APS/SDG&E Interconnection Project - Supplement to the Draft Environmental Document	None
IM-00272	Sanchez, Miguel/ PBS & Associates	1982	Draft Environmental Impact Report - Current Land Use Plan, Heber Planning Unit	None
IM-00301	Welch, Patrick/ Bureau of Land Management	1983	Cultural Resource Inventory for Thirty Proposed Asset Management Parcels in Imperial County, California	None
IM-00368	Imperial County Planning Department	1987	Chevron Geothermal Company Of California Supplemental Project Information for the Auxiliary Production Facility Heber Geothermal Unit, Imperial County	None

SCCIC Report Number	Authors/ Association	Year	Title	Associated Cultural Resources
IM-00441	ENSR Consulting and Engineering	1990	Environmental Assessment/Initial Study for the Placement of Fiber Optic Facilities Between Salton Microwave Station And Calexico California	None
IM-00536	Burkenroad, David	1979	Phase One Regional Studies APS/SDG&E Interconnection Project Transmission System Environmental Study Cultural Resources: History	None
IM-00537	Wirth Associates, Inc.	1979	Phase One Regional Studies APS/SDG&E Interconnection Project Transmission System Environmental Study Cultural Resources: Archaeology	None
IM-00538	Imperial County	1979	Proposed Workscope Phase II Cultural Resources Studies APS-SDG&E Transmission Interconnect Project, Miguel to Sand Hills, Sand Hills to Pvngs	None
IM-00547	Cultural Systems Research, Inc.	1982	Draft Archaeological Research Design and Data Recovery Program for Cultural Resources Within the Mountain Springs (Jade) to Sand Hills Portion of the APS/SDG&E Interconnection Project 500kv Transmission Line	None
IM-00595	Cultural Systems Research, Inc.	1982	Mountain Springs (Jade) to Sand Hills Data Recovery Preliminary Report	None
IM-01080	Von Werlhof, Jay/ Imperial Valley College Desert Museum	1999	Archaeological Examinations Of The Heber Facilities Sewer And Water Improvements Project	None
IM-01095	Garnsey, Michael/ ASM Affiliates	2007	Cultural Resources Study For The Proposed Mosaic Project, Imperial County, California	None
IM-01306	Wirth Associates, Inc.	1980	APS/SDG&E Interconnection Project Environmental Study Phase Ii Corridor Studies - Native American Cultural Resources Appendices	None
IM-01313	Wirth Associates, Inc.	1980	APS/SDG&E Interconnection Project (Phase II Corridor Studies) - Cultural Resources: Archaeology	None

Attachment A
Figures

South Coastal Information Center
San Diego State University
5500 Campanile Drive
San Diego, CA 92182-5320
(619) 594-5682
nick@scic.org

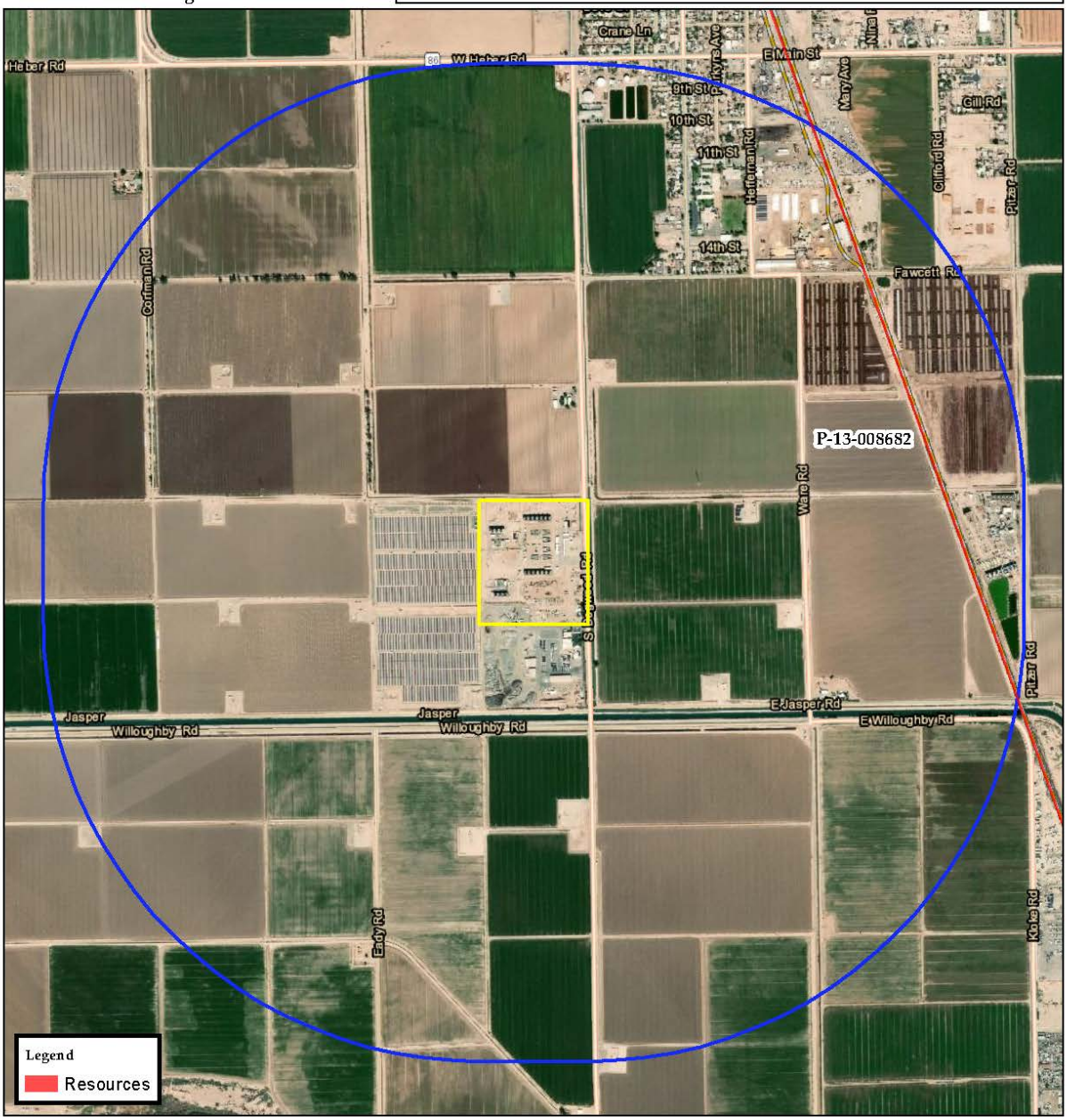

1:19,000

Historical Resources with Primary and Trinomial Designations

0 250 500 1,000
Meters

Nick Doose, Jun 23, 2019

Aerial © ESRI 2017

Figure 1 Cultural resources located within search radius.

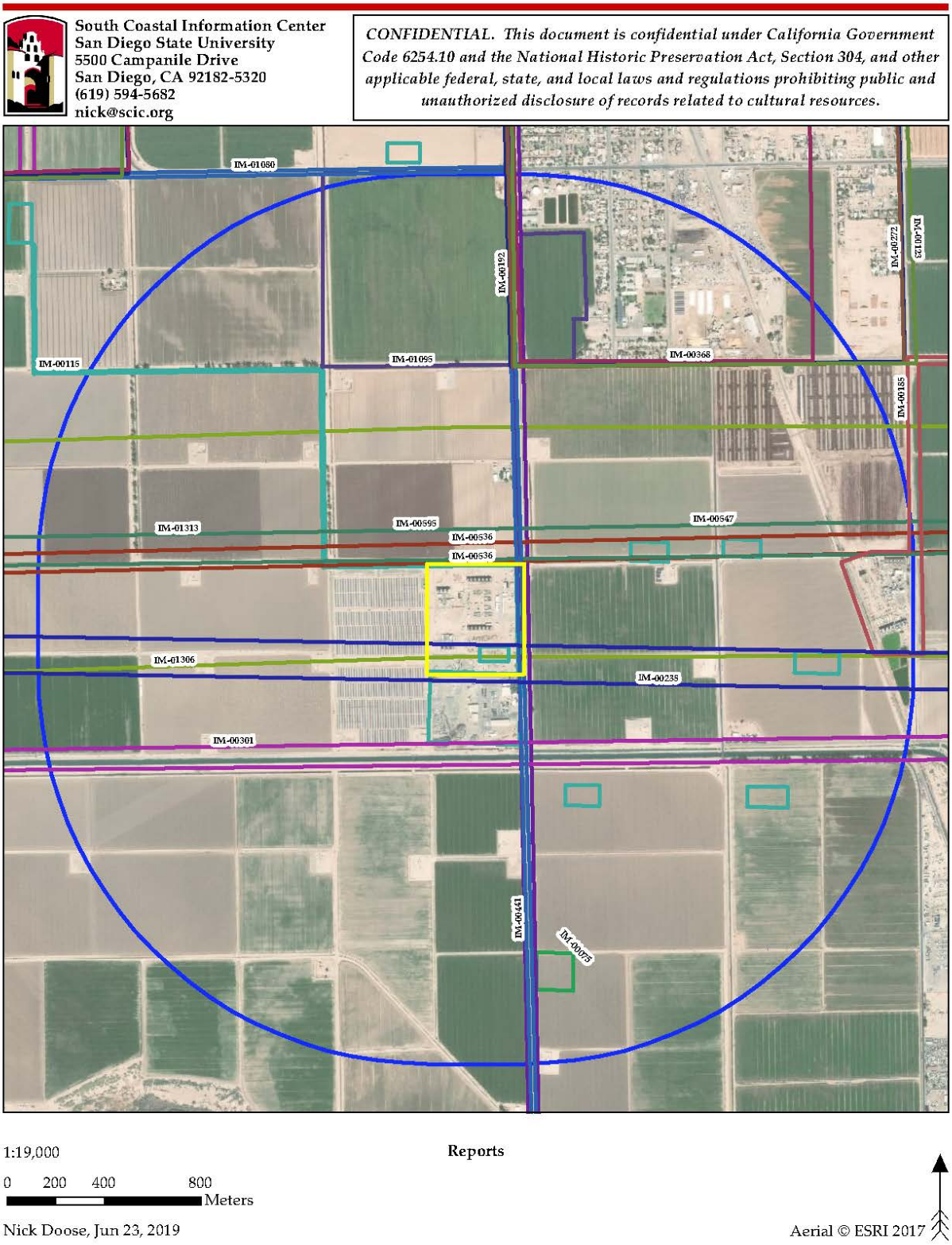

Figure 2 Previously conducted cultural resources studies within search radius.

Water Quality Management Plan
Heber 2 Geothermal Repower Project

(855 Dogwood Road, Heber, California)

July 2019

Prepared By:

Catalyst Environnemental Solutions
315 Montana Avenue, Suite 311
Santa Monica, CA 90403

Prepared For:

Second Imperial Geothermal Company (ORMAT Nevada Inc.)
947 Dogwood Road
Heber, CA 92249

This Page is Intentionally Blank

Document Information

Prepared for	Second Imperial Geothermal Company (ORMAT Nevada Inc.)
Project Name	Heber 2 Geothermal Repower Project 855 Dogwood Road, Heber, California
Address	Second Imperial Geothermal Company 947 Dogwood Road Heber, CA 92249
Project Manager	Ben Pogue bpogue@ce.solutions
Project Engineer	Paden Voget, P.E. pvoget@ce.solutions State of California Professional Engineer #69238
Date	July 19, 2019

This Page is Intentionally Blank

Professional Certification

Water Quality Management Plan

Heber 2 Geothermal Repower Project

This report has been prepared by Catalyst Environmental Solutions Corporation under the professional supervision of the Principal(s) and/or staff whose signature(s) appear hereon.

The scope of work and specifications are presented in accordance with generally accepted professional engineering practice and those of the California State Water Resources Control Board Order No. 20013-001-DWQ. There is no other warranty either expressed or implied.

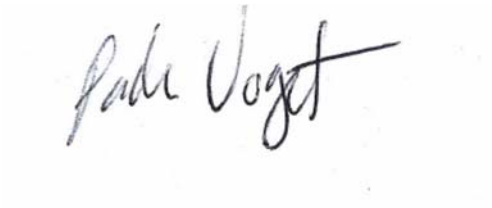

Paden Voget, PE
State of California Professional Engineer #69238

This Page is Intentionally Blank

Project Owner's Certification

This Water Quality Management Plan (WQMP) has been prepared for Second Imperial Geothermal Company (ORMAT Nevada Inc.) by Catalyst Environmental solutions. The WQMP is intended to comply with the requirements of the County of Imperial and the Phase II Small MS4 General Permit Imperial Valley Watershed. The undersigned, while it owns the subject property, is responsible for the implementation of the provisions of the site consistent with the Phase II Small MS4 Permit and the intent of the County of Imperial and the unincorporated community of Heber. Once the undersigned transfers its interest in the property, its successors in interest and the city/county/town shall be notified of the transfer. The new owner will be informed of its responsibility under this WQMP. A copy of the approved WQMP shall be available on the subject site in perpetuity.

"I certify under a penalty of law that the provisions (implementation, operation, maintenance, and funding) of the WQMP have been accepted and that the plan will be transferred to future successors."

Project Data			
Permit/Application Number(s):	CUP No. 06-0006	Grading Permit Number(s)	N/A
Tract/Parcel Map Number(s):	APN 054-250-031	Building Permit Number(s)	N/A
CUP, SUP, and/or APN:			06-0006
Owner's Signature			
Owner Name:	Connie Stechman		
Title:	VP, Finance		
Company:	Ormat Nevada Inc.		
Address:	6140 Plumas Street, Reno, NV 89519		
Email:	cstechman@ormat.com		
Telephone:	775-356-9029		
Signature:	Connie Stechman	Date:	8/12/19

Table of Contents

Tables

Figures

SECTION 1 Project Description

The Second Imperial Geothermal Company, a wholly owned subsidiary of ORMAT Nevada Inc (ORMAT), owns and operates the Heber 2 Geothermal Energy Complex. The proposed Heber 2 Geothermal Repower Project (Project) is located at 855 Dogwood Road, Heber, California within unincorporated Imperial County. The Project includes the installation of two water-cooled ORMAT Energy Converters (OECs) to replace six old units from 1992; three 10,000 gallon isopentane above ground storage tanks; and, additional pipeline to connect the proposed facilities with the existing Heber 2 Complex (Site). The total project disturbance from developing the new OECs is approximately 4 acres, all within the existing power plant complex and fence line. A vicinity map of the Project Site is included in **Figure 1**.

The Project includes the replacement of six air-cooled OECs with two water-cooled OECs. The pre-Project pervious area is roughly 4 acres. The Project will result in less than 200 square feet of area converted in impervious surface area resulting from installation of equipment footings/foundations. In addition, no grading is proposed for the Project. Accordingly, the Project will not result in a change to the existing grade and stormwater flows and drainage will not be altered from existing conditions. **Figure 2** illustrates the existing drainage facilities in the vicinity of the Project. **Figure 3** provides a site plan of the proposed facilities.

1.1 SITE LOCATION

The Site includes approximately 4 acres within the Heber quadrangle of the U.S. Geological Survey (USGS) 7.5" topographic map, and sits within Township 16 South, Range 14 East of the San Bernardino Base and Meridian in Imperial County, California.

1.2 LAND USE AND TOPOGRAPHY

The Project is located on private lands owned by ORMAT in southern Imperial County as shown in **Figure 1**. The Project site includes approximately 4 acres entirely within the Assessor's Parcel Number (APN) 054-250-031, which is a 39.99-acre property. APN 054-250-031 is zoned as A-2-G SPA, for General Agriculture (A-2), Geothermal Overlay Zone (G), and in the Heber Specific Plan Area (SPA). The Project Site lies at an elevation approximately 15 feet below mean sea level (msl) in the Imperial Valley region of the California low desert. The surrounding properties lie on terrain which is flat, part of a large agricultural valley.is The Site is currently vacant and unimproved. The Site is also devoid of vegetation and is actively disturbed as part of ongoing energy generation operations at Heber 2. Adjacent properties outside of the fenced operations yard consists of agricultural land to the north and a solar farm to the west.

1.3 SITE GEOLOGY, HYDROGEOLOGY, AND SOILS

The part of Imperial County containing Heber lies within the Pliocene to Holocene, Q Geologic Unit (McCrink et al. 2011). Three natural geomorphic provinces underlay Imperial County, including the Peninsular Ranges, the Colorado Desert, and the Mojave Desert. The Colorado Desert geomorphic province spans central Imperial County and contains the Salton Sea and the Imperial valley. This Basin and Range province, sometimes referred to as the Salton Trough, is composed of a low-lying barren

desert basin located between alluvium-covered, active branches of the San Andreas Fault containing Cenozoic sedimentary rocks and alluvial, lacustrine, and eolian deposits. The surface of sediments in the middle of the trough are about 275 feet below sea-level (bsl) (Digital Desert, 2019).

Surface water in the area of the Site consists of canals and agricultural drains operated and maintained by the Imperial Irrigation District. Canals adjacent to the Project Site include Date Drain No. 3, Date Drain No. 3a, Date Drain No. 3b, and Date Drain No. 3c as illustrated in **Figure 2**. These canals ultimately drain to the Alamo River, a tributary to the Salton Sea. Surface runoff within the Project Site occurs primarily as sheetflow across the lot generally to the north, eventually flowing into the adjoining ditches.

The regional groundwater flow direction within the Imperial Valley is toward the Salton Sea, a closed basin with a surface elevation of approximately 225 feet below sea level. Groundwater flow in the Project area flows in a general northwest direction.

Dry lean silty clays dominate the project site surface extending to approximately 4 to 5 feet below ground surface (bgs). These silty clays are underlain by moist stiff clays from approximately 6 ft to 38-40 ft bgs. Silty clay to clayey silt dominate 40-50 ft bgs to the extent of geotechnical exploration (Landmark 2019).

1.4 HYDROMODIFICAITON APPLICABILITY

As discussed above, the Project would result in less than 50 square feet of impervious area from pre-Project conditions. In addition, no grading is proposed for the Project or changes to the permeability of the Site. As such, the post-development runoff volume, time of concentration, and peak flow velocity would not be altered from that of the pre-development condition.

1.5 POTENTIAL STORMWATER POLLUTANTS

Table 1 summarizes expected stormwater pollutants of concern based on land use and site activities.

Table 1. Pollutants of Concern

Pollutant	Potential to Impact Stormwater (Y/N)	Additional Information and Comments
Pathogens (Bacterial/Virus)	N	--
Nutrients – Phosphorous	N	--
Nutrients - Nitrogen	N	--
Noxious Aquatic Plants	N	--
Sediment	Y	Overland flows over unpaved surface may result in sediment in stormwater runoff
Metals	Y	Leaks/spills in Project area may result in metals in stormwater runoff
Oil and Grease	Y	Leaks/spills in Project area may result in oil and grease in stormwater runoff

Trash/Debris	Y	Improperly disposed of trash/debris may result in trash in stormwater runoff
Pesticides/Herbicides	N	--
Other	N	--

SECTION 2 Best Management Practices

This section describes the Best Management Practices (BMPs) that will be implemented and maintained throughout the life of the project. The BMPs will be used to prevent and minimize water pollution that can be caused by stormwater runoff. **Table 2** details the BMPs selected to be implemented at the Site based on the potential pollutants. Note that the Site is within the existing operational footprint and is subject to the existing policies and programs implemented by ORMAT for the facility. Because the Project does not propose any changes to the existing stormwater volume, peak flow velocity, time of concentration or drainage patterns, no structural BMPs are proposed.

Table 2. Non-Structural Source Control BMPs

Pollutant Source	Pollutant	BMP	Existing?	New/Revised?
Stormwater run-on and runoff	Erosion, sediment, contaminated stormwater	• Stabilize drainage with rocks, gravel, vegetation, or riprap • Provide perimeter control to isolate sediment (loose dirt). Includes earthen berms, fiber rolls, silt fence, etc.	X	
Vehicle Track Out	Sediment, Dust	• Provide tracking control devise • Conduct street sweeping	X	
Work Areas	Trash	• Regularly monitor and clean trash • Provide employee training for good housekeeping	X	
Equipment Areas (OECs, ITLUs, pipes)	Isopentane, sediment	• Control drainage patterns with berms • Use water truck for dust control • Conduct routine inspections	X	X
Stored materials and equipment maintenance	Oil, grease, hydraulic fluid, anti-freeze, metals	• Provide good housekeeping training • Store materials in secondary containment • Spill kit and response training	X	

In addition to the activities listed above, ORMAT follows all approved operational guidelines that are currently in place. Temporary and permanent soil erosion control BMPs will be implemented in conformance with the BMP Fact Sheets provided in the CASQA Stormwater Best Management Practice Handbook – Industrial and Commercial (2014).

2.1 NON-STRUCTURAL BMPS

The following are prevention practices utilized to minimize the probability of pollution of stormwater discharge.

2.1.1 Good Housekeeping

As a component of this program, good housekeeping practices are performed so that facility is kept in a clean and orderly condition. Proper housekeeping practices include:

- Periodic cleanup of equipment, as needed, based upon facility inspections,
- Sweeping impervious surfaces, as needed, based upon facility inspections,
- Proper waste disposal practices and covering of waste storage areas at all times,
- Proper storage and covering of materials at all times,
- Removal of any oil-stained soil/gravel, especially around equipment locations and loading areas,
- Cleaning of significant oil and grease stains on surfaces that drain to the stormwater drainage areas, and
- Cleaning the exterior of oil containers on hydraulic machinery upon discovery of an accumulation of hydraulic fluid.

2.1.2 Preventative Maintenance

As a component of this program, operations and maintenance staff perform preventative maintenance of stormwater management devices to assure their proper operation. Preventative maintenance of stormwater management devices includes the following:

- Cleaning of accumulated sediment, potential contaminants, and debris from the Site;
- Inspection of secondary containment structures as part of the regular daily visual inspections;
- Maintenance and inspection of secondary containment structures, as needed, based upon inspections;
- Daily inspection and maintenance of equipment and associated piping and valves as required by preventive maintenance procedures;
- Inspection and maintenance of rainfall protection coverings for waste storage bins and receptacles on a periodic basis; and
- A comprehensive preventive maintenance schedule is performed on all facility operations equipment as part of routine procedures.

2.1.3 Spill Response

Spill prevention and response is performed according to the facility's SPCC Plan . Copies of this plan are located in the on-site ORMAT office.

A limited amount of spill cleanup equipment is stored onsite. This equipment is found within hazardous material storage areas. Detailed information concerning spill cleanup equipment and resources is included in the SPCC Plan.

The volume of containment areas surrounding each potential source is designed to hold the contents of a spill from the largest vessel / container. The SPCC Plan summarizes the capacity of potential sources and volume of the respective secondary containment areas.

2.1.4 Material Handling and Storage

The primary hazardous material to be stored on-site is isopentane. The additional isopentane will be stored in the appropriately designed (3x) 10,000 gallon above ground storage tanks, as well as the existing (2x) 10,000 gallon tanks. The isopentane is used as a motive fluid for geothermal energy generation and is not directly discharged, rather is released as an air emission. Therefore, the isopentane would not be directly exposed to stormwater. All other hazardous waste would be stored in 55-gallon drums and other Department of Transportation (DOT) approved packaging within a contained area located on the Site. Stormwater that accumulates within the hazardous material and hazardous waste containment area is collected via vacuum truck and disposed of off-site or recycled back into the production system. A bill of lading, non-hazardous waste manifest or uniform hazardous waste manifest is used to document all such shipments.

2.1.5 Employee Training

A combined annual Storm Water Compliance / SPCC Plan training program is conducted for the Pollution Prevention Team members and operations personnel. Participants undergo stormwater management training for all areas and operations at this facility, as well as reviewing the spill response, control and countermeasure procedures. Other stormwater training is done on an as-needed basis.

2.1.6 Waste Handling/Recycling

At times, product or oily waste streams are transferred from the facility in 55-gallon drums. A bill of lading, non-hazardous waste manifest or uniform hazardous waste manifest is used to document all such shipments. Operations or contractor personnel closely monitor loading of transport vehicles. Collection and satellite accumulation containers for hazardous and non-hazardous waste are kept covered to prevent contact with stormwater. Appropriate spill control equipment and supplies are kept readily available in case of a spill.

2.1.7 Record Keeping and Internal Reporting

All inspection, sampling, maintenance, corrective action records, and any other information that is a part of this plan are maintained at the facility office. All records are maintained for a period of at least three (3) years.

2.1.8 Erosion Control and Site Stabilization

Permanent BMPs used at the facility to prevent soil erosion include routing runoff along earthen swales or drainage areas, and preventing run-off with berms along certain sections of the property line. Temporary BMPs used at the Site to prevent soil erosion include the use of sandbags, crushed rock, and silt fence. These BMPs are used as and where needed, especially in areas that are undeveloped or in the process of being developed.

SECTION 3 Operation and Maintenance Plan

The Heber 2 Geothermal Repower Project is located at 855 Dogwood Road, Heber, California. The following non-structural water quality best management practices (BMPs) are proposed for the Project:

- Good Housekeeping
- Preventative Maintenance
- Spill Response
- Material Handling and Storage
- Employee Training
- Waste Handling/Recycling
- Record Keeping and Internal Reporting
- Erosion Control and Site Stabilization

3.1 MAINTENANCE RESPONSIBILITY

The Second Imperial Geothermal Company, a wholly owned subsidiary of ORMAT Nevada Inc (ORMAT) is the property owner and is responsible for BMP maintenance. Since ORMAT is the owner, no access agreement or easement is necessary to maintain the BMPs. ORMAT funds will be used to support Operation and Maintenance (O&M) activities to maintain BMP functionality. ORMAT maintenance staff are expected to perform the maintenance.

3.2 MAINTENANCE ACTIONS AND FREQUENCY

Maintenance actions are generally grouped into two categories: routine and intermittent.

Routine Maintenance

Routine inspections of the Project facilities and grounds will be performed annually. During these inspections staff evaluate if there is significant accumulation of trash, debris, or sediment that would need to be removed. Cleaning is done as needed based on the results of the inspections. The inspection frequency may be adjusted based on experience at the site (e.g., if inspections rarely find any material that needs to be cleaned out, then the inspection frequency can be reduced).

Intermittent Maintenance

Intermittent maintenance activities include more substantial maintenance that is not required as frequently as routine maintenance. The most likely form of intermediate maintenance is removal of sediment from existing drainage infrastructure and detention basins where necessary to maintain the capacity of the basins. Given that the Project Site is pervious and will not be graded or significantly altered and that rain is infrequent in Heber, this type of maintenance is expected to be required approximately once every year.

3.3 MAINTENANCE PROCEDURES

During each maintenance visit, the maintenance crew will evaluate existing drainage paths and infrastructure by inspecting for the maintenance indicators in **Table 3**. When a maintenance indicator is observed, the action described in the "Maintenance Actions" column will be taken.

Note that regardless of the projected maintenance type (routine or intermittent) described in the previous section, when a maintenance indicator is observed, the required maintenance action will be taken. For example, if significant sediment accumulation is observed in year three instead, then the accumulated sediment will still be cleaned out, even though the estimated frequency was once every year.

Table 3-1. Maintenance Indicators and Actions for BMPs

Typical Maintenance Indicator	Maintenance Action
Erosion due to concentrated stormwater runoff flow	Repair eroded areas and make appropriate corrective measures such as adding berm or stone at flow entry points, or re-grading as necessary.
Accumulated sediment, litter, or debris	Remove and properly dispose of accumulated materials, without damage to stormwater drainage structures.
Standing water	Remove any obstructions or debris or invasive vegetation, loosing or replace top-soil to allow for better infiltration, or minor re-grading for proper drainage.
Obstructed inlet or outlet structures	Clear obstructions.
Damage to structural components such as inlet or outlet structures	Repair or replace as applicable.

SECTION 4 References

Digital Desert. 2019. Ecological Sections: Mojave Desert. Available online at: http://digital-desert.com/ecosections/322c.htm).

Landmark Consultants, Inc. (Landmark). 2019. Geotechnical Report Update, Heber 2 Repower Project, Heber, California. Prepared for Ormat Nevada. April 2019.

McCrink, T.P., Pridmore, C.L., Tinsley, J.C., Sickler, R.R., Brandenberg, S.J., and J.P. Stewart. 2011. Liquefaction and other ground failures in Imperial County, California, from the April 4, 2010, El Mayor–Cucapah earthquake: U.S. Geological Survey Open-File Report 2011–1071 and California Geological Survey Special Report 220, 94 p. pamphlet, 1 pl., scale 1:51,440. Available at http://pubs.usgs.gov/of/2011/1071.

Figures

Legend

- United States/Mexico Border
- County Line
- Project Site
- 1-Mile Radius

PROPOSED PROJECT SITE - HEBER 2

Catalyst ENVIRONMENTAL SOLUTIONS

Figure 1

ORMAT

Date: July 2019

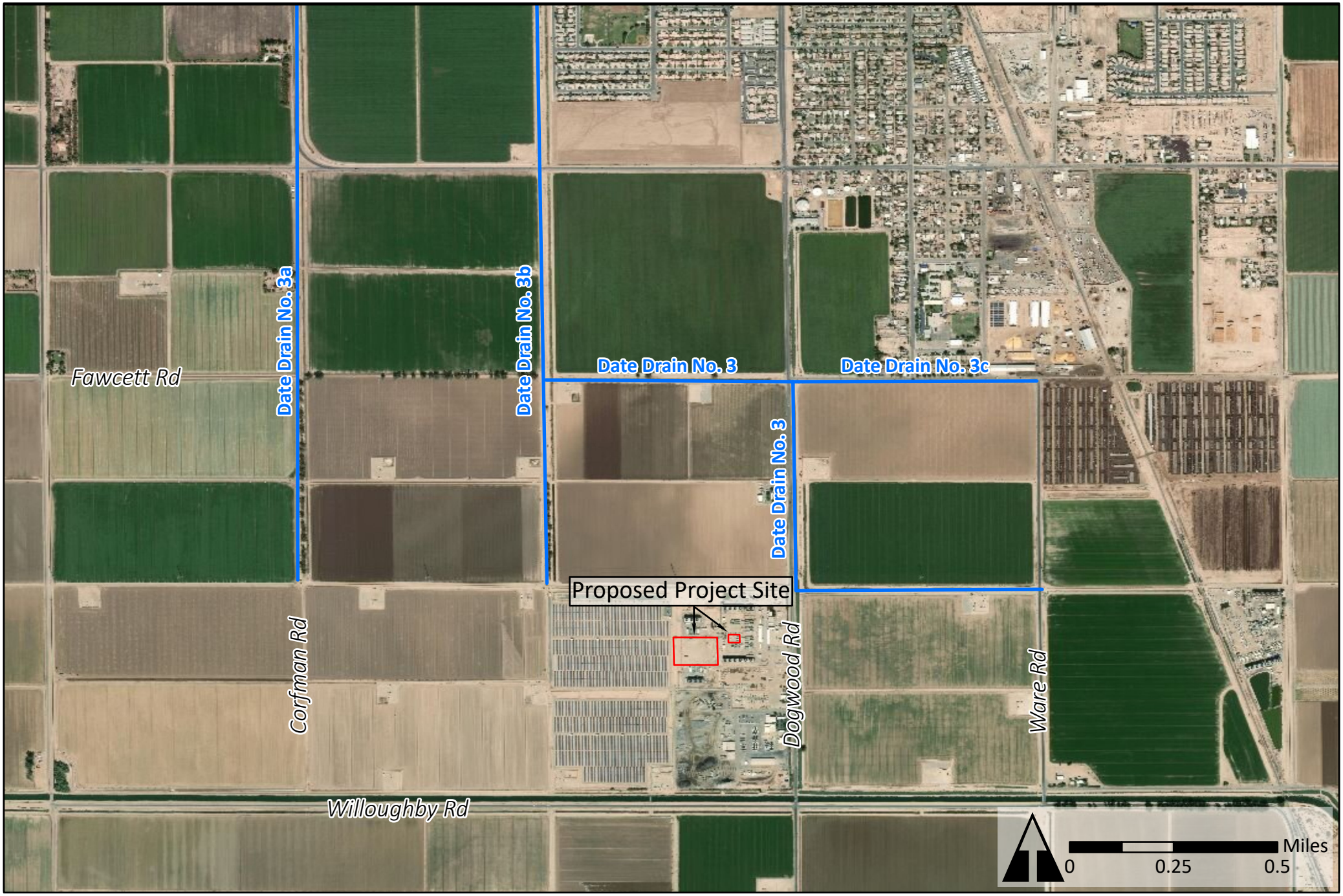

Legend

- Drainage Canal
- Project Site

DRAINAGE CANALS

Figure 2

ORMAT

Date: July 2019

Catalyst ENVIRONMENTAL SOLUTIONS

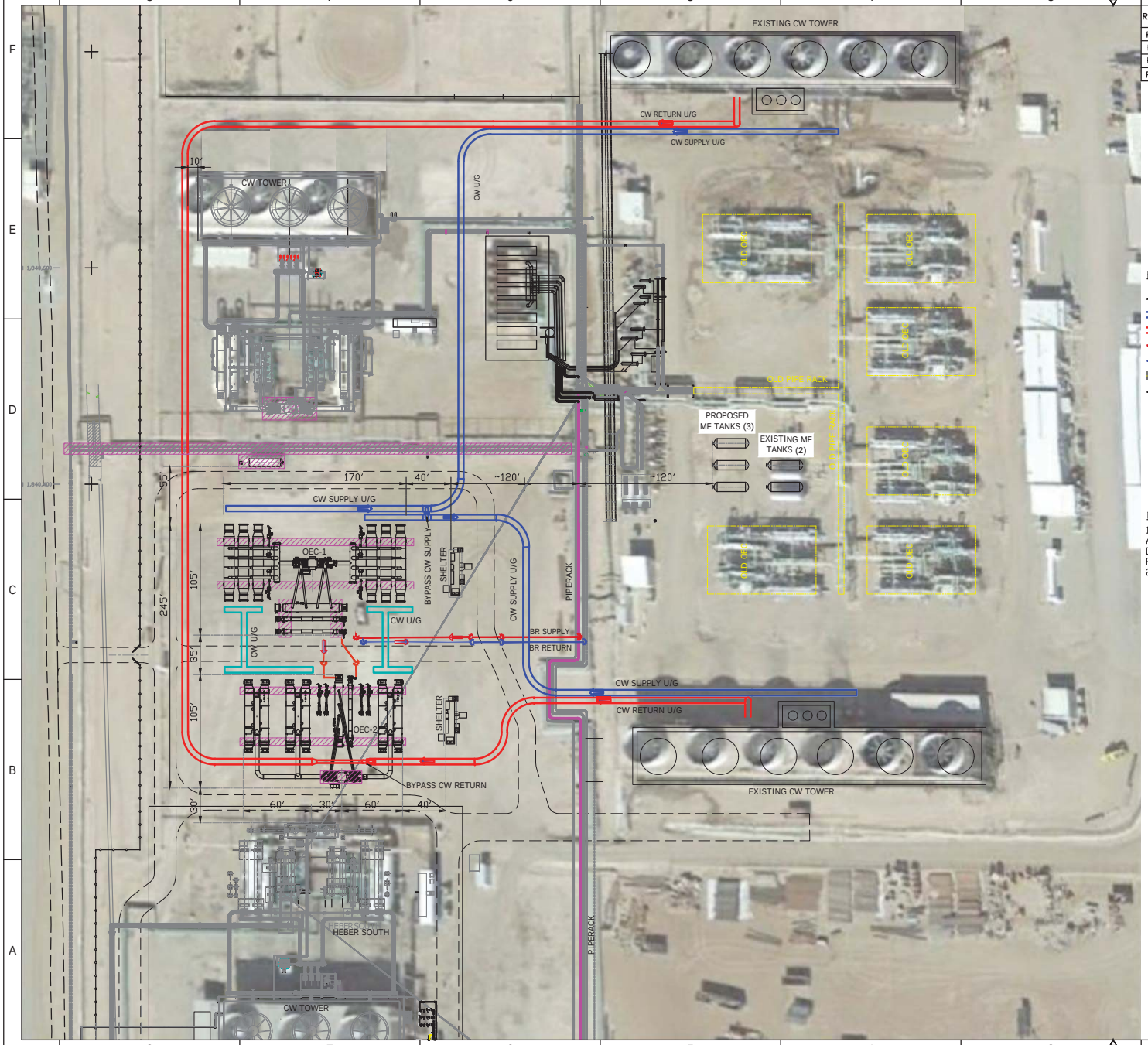

REV	DESCRIPTION	DATE	BY	CHK	ENG	PRJ
P6	UPDATE MODELS OES-1 & OEC-2	5.APR.2019	A.S.	A.N.		S.H.
P7	UPDATE MODELS OES-1	17.APR.2019	A.S.	A.N.		S.H.
P8	UPDATE OEC-1 & OEC-2	27.MAY.2019	A.S.	A.N.		S.H.
P9	UPDATE LOCATION OEC-1	18.JULY.2019	A.S.	A.N.		S.H.

N

KEY:

- EXISTING FENCE LINE
- PROPOSED UNDERGROUND CW SUPPLY LINE
- PROPOSED UNDERGROUND CW RETURN LINE
- PROPOSED BR SUPPLY LINE
- PROPOSED BR RETURN LINE
- EQUIPMENT TO BE DECOMMISSIONED
- EXISTING EQUIPMENT TO REMAIN

CW	COOLING WATER
U/G	UNDERGROUND
BR	GEOTHERMAL BRINE
OEC	ORMAT ENERGY CONVERTOR
MF	MOTIVE FLUID

NOTE:

1. THE ARRANGEMENT AND SIZES PRESENTED ARE PRELIMINARY AND INDICATIVE ONLY AND SUBJECT TO CHANGED ON DESIGN OPTIMIZATION , DETAILED DESIGN AND ACTUAL EQUIPMENT PURCHASED (MANUFACTURED).
2. DIMENSIONS ARE IN MM [FEET], ELEVATIONS ARE IN MM FEET]

0 20' 100' 200'

GRAPHIC SCALE (FEET)

PREPARED BY:

Stantec

PHONE: FAX:

FOR:

Second Imperial Geothermal Company
855 B Dogwood Road
Heber CA 92249

TITLE:

HEBER2 REPOWER
GENERAL ARRANGEMENT
POWER PLANT ON MAP

DRAWN BY: KAM	DESIGNED BY:
CHECKED BY:	APPROVED BY:
PROJECT NUMBER: 01OT.01234.01.0123	SCALE: AS SHOWN
DATE: 04/01/04	FILE PATH: K:/[CLIENT] OR JOB #

SHEET:

1 OF 1

Geotechnical Site Summary Memorandum

Date: July 2019

From: Catalyst Environmental Solutions - Dan Tormey, P.G., Ph.D; Ben Pogue, M.P.A., P.M.P., A.I.C.P.

RE: Heber 2 Geothermal Repower Project – Geotechnical Site Assessment

---

This technical memorandum provides a summary of the geotechnical conditions for the Heber 2 project site, located at the Second Imperial Geothermal Company's (a wholly owned subsidiary of ORMAT Nevada, Inc.) existing Heber 2 Geothermal Energy Complex at 855 Dogwood Road, Heber, California, in Imperial County. Site-specific information was gathered from available online resources and extrapolated from the *Geotechnical Report Update* prepared by Landmark Consultants (Landmark, 2019). Landmark's report provides an update to previous geotechnical reports conducted at the site (Landmark 2005, 2007) and reflects the adoption of the 2016 California Building Code (CBC) and Imperial County's geotechnical engineering standard of practice.

Desktop reconnaissance was conducted to gather information on the geological-geotechnical site conditions, soil conditions, seismic conditions, liquefaction potential, site stability, and stormwater infiltration potential. Collectively, this memorandum provides a comprehensive review of the project site's geotechnical conditions to support the development of a California Environmental Quality Act (CEQA) Initial Study/Negative Declaration (IS/ND), as opposed to an as-graded, or as-built geotechnical report.

1.0 Geological/Geotechnical Site Conditions

The part of Imperial County containing Heber lies within the Pliocene to Holocene, Q Geologic Unit (McCrink et al. 2011). Three natural geomorphic provinces underlay Imperial County, including the Peninsular Ranges, the Colorado Desert, and the Mojave Desert. The Colorado Desert geomorphic province spans central Imperial County and contains the Salton Sea and the Imperial valley. This Basin and Range province, sometimes referred to as the Salton Trough, is composed of a low-lying barren desert basin located between alluvium-covered, active branches of the San Andreas Fault containing Cenozoic sedimentary rocks and alluvial, lacustrine, and eolian deposits. The surface of sediments in the middle of the trough are about 275 feet below sea-level (bsl) (Digital Desert, 2019).

2.0 Soil Conditions

There are approximately 28 soil types found in the region of the project area (Aco, Antho, Carrizo, Carsitas, Chuckwalla, Cibola, Coachella, Fluvaquents, Gadsden, Gilman, Glenbar, Holtville, Imperial, Indio, Kofa, Lagunita, Laposa, Laveen, Mecca, Meloland, Niland, Orita, Ripley, Rositas, Salorthids, Superstition, Torriorthents, and Vint). Glenbar, Holtville, and Imperial parent

spoils are formed from fine-textured, stratified alluvial basin deposits (ICPDS 2015). The clay material deposited during the formation of the Colorado River delta terrace is the original source of Holtville and Imperial parent soils. Many of the other soils were formed from fan sediment originating from large gullies created by runoff into the Salton Sea. Imperial County soils are characterized by hyperthermic soil temperature and aridic soil moisture regimes (Digital Desert, 2019).

Dry lean silty clays dominate the project site surface extending to approximately 4 to 5 feet below ground surface (bgs). These silty clays are underlain by moist stiff clays from approximately 6 ft to 38-40 ft bgs. Silty clay to clayey silt dominate 40-50 ft bgs to the extent of geotechnical exploration (Landmark 2019).

3.0 Seismic Conditions/Liquefaction Potential

There are several active faults in the Imperial Valley, including the Brawley Fault Zone, San Jacinto Fault Zone (contains the Coyote Creek Fault, the Elmore Ranch Fault, and the Wienert Fault), the Elsinore Fault (contains the Laguna Salada Fault), the Imperial Fault, the San Andreas Fault Zone, and the Superstitions Hills Fault (ICPDS 2015). There are several mapped faults of the San Andreas Fault System across the valley, which is comprised of the San Andreas, San Jacinto, and Elsinore Fault Zones. Landmark (2019) employed a computer-aided search approach to assess known faults and seismic zones within 36 miles of the project site. The Imperial Fault located 9.4 miles southwest of the project site was the closest mapped Earthquake Fault Zone.

Earthquake hazard zones are characterized by areas susceptible to fault ruptures (ground surface breaks/cracks along a fault), liquefaction, and landslides. Ground shaking can occur during an earthquake, and its intensity is related to the proximity of the area to the fault, the focal depth, soil types, the location of the epicenter, and the size (magnitude) of the earthquake. Soils formed from alluvial deposits are more prone to ground shaking than dense materials such as bedrock. Moderate to strong ground motion could be expected in the project area; however, ground motions could vary considerably due to potential attenuation by rock and soil deposits, as well as the type of fault and direction of rupture (Landmark 2019). Soils in the project area were classified as Site Class D, which is characterized by a stiff soil profile. Further, Landmark determined a Seismic Design Category of D based on a Risk Category III.

Liquefaction occurs when loosely packed, saturated soil or sediment at or near the ground surface loses its strength, which can lead to excessive settlement, ground rupture, lateral spreading, or failure of shallow bearing foundations (Imperial County 2015). Landslide and liquefaction zones have not been mapped in this area (ICPDS 2015); however, the Colorado River Delta region of southern Imperial County (including Heber) is a seismically active area. Landmark (2019) evaluated liquefaction potential at the project site using the 1997 NCEER Liquefaction Workshop methods. Due to the cohesive nature of the subsurface soils, liquefaction is not anticipated at the project site, and mitigation is not recommended.

Several significant earthquakes have occurred in the vicinity with corresponding surface fault ruptures and liquefaction events (McCrink et al. 2011). Four earthquakes greater than

magnitude 5 were recorded near Heber, between 1915 and 1979. The El Mayor-Cucapah earthquake (magnitude 7.2) that occurred throughout southern Imperial valley in 2010 caused widespread liquefaction near the towns of Calexico (immediately south of Heber) and El Centro (immediately north of Heber).

4.0 Stormwater Infiltration Potential

Encouraging stormwater infiltration by means of a stormwater management plan (SWMP) can improve water conservation by reducing evaporation and increasing groundwater recharge, as well avoiding erosion and potential damage to concrete foundations and slabs. Beneficial water quality of streams and rivers can also be maintained by preventing discharge of stormwater containing sediments and other materials. The City of El Centro and City of Imperial SMP provide best management practices (BMPs) for stormwater management by commercial businesses and industrial operations (City of El Centro and Imperial County 2013).

Heber also has a Master Drainage Plan (established in 2006), although the town's management of stormwater defers to the Imperial County Planning and Development guidelines and the county Public Works Department. The Imperial Irrigation District board adopted the Imperial Integrated Regional Water Management Plan (IRWMP) in 2012 (GEI 2012). The plan was developed to support the efforts to meet the County's future water resource demands while conforming to California Department of Water Resources guidelines.

Groundwater is encountered approximately 8 to 10 feet bgs at the project site (Landmark 2019). Onsite infiltration potential (capacity of the most limiting layer to transmit water [Ksat]) ranges from very low to moderately low (0.00 to 0.06 inches per hour) (Holtville silty clay, wet; approximately 71% of the project site) to moderately high (0.20 to 0.57 inches per hour) (Imperial-Glenbar silty clay loams, wet; approximately 29% of the project site). These soil types are also considered to be moderately well drained (NRCS 2019). Evaporation potential is considered poor at the project site.

5.0 Site Stability

The project site is located within the seismically active Imperial Valley and has the potential for ground disturbance based on soil and subsurface characteristics. Recommendations for the expansion project, including engineered design and earthquake-resistant construction complying with the latest edition of the CBC for Site Class D are provided in Landmark's updated geotechnical report (2019).

6.0 References

City of El Centro and City of Imperial. 2013. Stormwater Management Plan. August 15, 2013.

City of San Diego. 2018. Guidelines for Geotechnical Reports. Available at https://www.sandiego.gov/sites/default/files/legacy/development-services/pdf/industry/geoguidelines.pdf.

Digital Desert. 2019. Ecological Sections: Mojave Desert. Available online at: http://digital-desert.com/ecosections/322c.htm).

GEI Consultants, Inc. (GEI). 2012. Imperial Integrated Regional Water Management Plan. Appendix C - Disadvantaged Community Needs Assessment Technical Memorandum (Working Group Draft). Prepared for the Imperial Water Forum. October 2012. Available at http://imperialirwmp.org/2013%20Updates/finalirwmp.html.

Imperial County. 2015. Final EIR. SEPV Dixieland East and West Solar Farm Projects. SCH No. 2015051043. December 2015.

Imperial County Planning and Development Services (ICPDS). 2015. Baseline Environmental Inventory Report, Imperial County Conservation and Open Space Element Update. June 2015.

Landmark Consultants, Inc. (Landmark). 2019. Geotechnical Report Update, Heber 2 Repower Project, Heber, California. Prepared for SIGC/ORMAT Nevada. April 2019.

Landmark. 2007. Geotechnical Investigation, Proposed Heber South Geothermal Plant, Dogwood Road, Heber, California. Prepared for SIGC/ORMAT. May 2007.

Landmark. 2005. Geotechnical Report, New Turbine Generator and Cooling Tower, Heber 2 Geothermal Plant, Heber, California. Prepared for SIGC/ORMAT. January 2005.

McCrink, T.P., Pridmore, C.L., Tinsley, J.C., Sickler, R.R., Brandenberg, S.J., and J.P. Stewart. 2011. Liquefaction and other ground failures in Imperial County, California, from the April 4, 2010, El Mayor–Cucapah earthquake: U.S. Geological Survey Open-File Report 2011–1071 and California Geological Survey Special Report 220, 94 p. pamphlet, 1 pl., scale 1:51,440. Available at http://pubs.usgs.gov/of/2011/1071.

Natural Resources Conservation Service (NRCS). 2019. Web Soil Survey, National Cooperative Soil Survey. Report generated on June 5, 2019.

Geotechnical Report Update

Heber 2 Repower Project
Heber, CA

Prepared for:

Ormat Nevada
1010 Power Plant Road
Reno, NV 89521

LANDMARK
Geo-Engineers and Geologists

Prepared by:

Landmark Consultants, Inc.
780 N. 4th Street
El Centro, CA 92243
(760) 370-3000

April 2019

LANDMARK
Geo-Engineers and Geologists

780 N. 4th Street
El Centro, CA 92243
(760) 370-3000
(760) 337-8900 fax

77-948 Wildcat Drive
Palm Desert, CA 92211
(760) 360-0665
(760) 360-0521 fax

April 30, 2019

Mr. Shlomi Huberman
Ormat Nevada
1010 Power Plant Road
Reno, NV 89521

Geotechnical Report Update
Proposed Heber 2 Repower Project
855 Dogwood Road
Heber, California
LCI Report No. LE19075

Dear Mr. Huberman:

Landmark Consultants, Inc. is providing this geotechnical report for the project at the Heber 2 Repower geothermal power plant. This report updates Landmark's 2004 and 2007 Geotechnical Reports for the power plant located at 855 Dogwood Road southwest of Heber, California. The update addresses changes made due to the adoption of the 2016 California Building Code (CBC) and geotechnical engineering standard of practice in Imperial County. The original reports (LCI Report No. LE04354, dated January 10, 2005 and LCI Report No. LE07178, dated May 9, 2007) are provided in Appendix D and Appendix E, respectively.

This update report presents selected elements of our findings and professional opinions only. It does not present all details that may be needed for the proper application of our findings and professional opinions. Our findings, professional opinions, and application options are best related through reading the full Geotechnical Report Update, and with the active participation of the engineer of record who developed them during design and construction of the project.

Seismic Parameters

Seismic Risk: The project site is located in the seismically active Imperial Valley of southern California with numerous mapped faults of the San Andreas Fault System traversing the region. The San Andreas Fault System is comprised of the San Andreas, San Jacinto, and Elsinore Fault Zones in southern California. The Imperial fault represents a transition from the more continuous San Andreas fault to a more nearly echelon pattern characteristic of the faults under the Gulf of California (USGS 1990). We have performed a computer-aided search of known faults or seismic zones that lie within a 36 mile (57 kilometer) radius of the project site as provided in Table 1.

A fault map illustrating known active faults relative to the site is presented on Figure 1, *Regional Fault Map*. A legend for the regional fault map is presented on Figure 2. The criterion for fault classification adopted by the California Geological Survey defines Earthquake Fault Zones along active or potentially active faults. An active fault is one that has ruptured during Holocene time (roughly within the last 11,000 years). A fault that has ruptured during the last 1.8 million years (Quaternary time), but has not been proven by direct evidence to have not moved within Holocene time is considered to be potentially active. A fault that has not moved during both Pleistocene and Holocene time (that is no movement within the last 1.8 million years) is considered to be inactive. Review of the current Alquist-Priolo Earthquake Fault Zone maps (CGS, 2000a) indicates that the nearest mapped Earthquake Fault Zones are the Imperial fault located approximately 9.4 miles southwest of the project site.

Site Acceleration: The project site is considered likely to be subjected to moderate to strong ground motion from earthquakes in the region. Ground motions are dependent primarily on the earthquake magnitude and distance to the seismogenic (rupture) zone. Accelerations also are dependent upon attenuation by rock and soil deposits, direction of rupture and type of fault; therefore, ground motions may vary considerably in the same general area.

CBC General Ground Motion Parameters: The 2016 CBC general ground motion parameters are based on the Risk-Targeted Maximum Considered Earthquake (MCE_R). The Structural Engineers Association of California (SEAOC) and Office of Statewide Health Planning and Development (OSHPD) Seismic Design Maps Web Application (SEAOC, 2019) was used to obtain the site coefficients and adjusted maximum considered earthquake spectral response acceleration parameters. **The site soils have been classified as Site Class D (stiff soil profile).**

Design spectral response acceleration parameters are defined as the earthquake ground motions that are two-thirds (2/3) of the corresponding MCE_R ground motions. Design earthquake ground motion parameters are provided in Table 2. **A Risk Category III was determined using Table 1604.5 and the Seismic Design Category is D since S_1 is less than 0.75**.

The Maximum Considered Earthquake Geometric Mean (MCE_G) peak ground acceleration (PGA_M) value was determined from the "U.S. Seismic Design Maps Web Application" (SEAOC, 2019) for liquefaction and seismic settlement analysis in accordance with 2016 CBC Section 1803.5.12 and CGS Note 48 ($PGA_M = F_{PGA}*PGA$). **A PGA_M value of 0.50g is used for liquefaction settlement analysis.**

Subsurface Soil and Groundwater

Subsurface soils encountered during Landmark's 2004 and 2007 geotechnical studies consist of surficial dry very stiff lean silty clays to a depth of 4 to 5 feet. Stiff clays extend from about 6 feet to a depth of 38 to 40 feet. Silty clay to clayey silt was encountered from 40 to 50 feet, the maximum depth of exploration. The subsurface logs (Plates B-1 through B-5 in Appendix B) depict the stratigraphic relationships of the various soil types. Groundwater was not noted in the CPT soundings, but is typically encountered at a depth of about 8 to 10 feet below ground surface at the plant site.

Liquefaction Potential

Liquefaction potential at the project site was evaluated using the 1997 NCEER Liquefaction Workshop methods. The 1997 NCEER methods utilize direct SPT blow counts or CPT cone readings from site exploration and earthquake magnitude/PGA estimates from the seismic hazard analysis. The resistance to liquefaction is plotted on a chart of cyclic shear stress ratio (CSR) versus a corrected blow count $N_{1(60)}$ or Qc_{1N}. A PGA_M value of 0.50g was used in the analysis with a 15-foot groundwater depth and a threshold factor of safety (FS) of 1.3.

The computer program CLiq (Version 2.2.0.32, Geologismiki, 2017) was utilized for liquefaction assessment at the project site. The estimated settlements have been adjusted for transition zones between layers and the post liquefaction volumetric strain has been weighed with depth (Robertson, 2014 and Cetin et al., 2009). Computer printouts of the liquefaction analyses are provided in Appendix C.

Liquefaction is not expected occur at the project site due to the cohesive nature of the subsurface soils. No mitigation is required for liquefaction induced settlements at this project site.

Site Preparation

Structure Subgrade Preparation: The exposed surface soil within foundation areas should be removed to 18 inches below the foundation elevation or existing grade (whichever is lower) extending five feet beyond all foundation lines. Exposed subgrade should be neat cut (flat blade on bucket).

A minimum of 18 inches of Caltrans Class 2 aggregate base shall be placed and compacted in 6 inch maximum lifts to 95% of ASTM D1557 maximum dry density below each foundation or mat slab.

Imported fill soil (if required) should have a Plasticity Index less than 15 and sulfates (SO_4) less than 1,000 ppm or non-expansive, granular soil meeting the USCS classifications of SM, SP-SM, or SW-SM with a maximum rock size of 3 inches and 5 to 35% passing the No. 200 sieve. The geotechnical engineer should approve imported fill soil sources before hauling material to the site. Imported granular fill should be placed in lifts no greater than 8 inches in loose thickness and compacted to at least 95% of ASTM D1557 maximum dry density at optimum moisture ±2%.

Trench Backfill: On-site soil free of debris, vegetation, and other deleterious matter may be suitable for use as utility trench backfill. Backfill soil within paved areas should be placed in layers not more than 6 inches in thickness and mechanically compacted to a minimum of 90% of the ASTM D1557 maximum dry density except for the top 12 inches of the trench which shall be compacted to at least 95%. Native backfill should only be placed and compacted after encapsulating buried pipes with suitable bedding and pipe envelope material. Pipe envelope/bedding should either be clean sand (Sand Equivalent SE>30). Precautions should be taken in the compaction of the backfill to avoid damage to the pipes and structures.

Observation and Density Testing: All site preparation and fill placement should be continuously observed and tested by a representative of a qualified geotechnical engineering firm. Full-time observation services during the excavation and scarification process is necessary to detect undesirable materials or conditions and soft areas that may be encountered in the construction area. The geotechnical firm that provides observation and testing during construction shall assume the responsibility of "*geotechnical engineer of record*" and, as such, shall perform additional tests and investigation as necessary to satisfy themselves as to the site conditions and the geotechnical parameters for site development.

Auxiliary Structures Foundation Preparation: Auxiliary structures such as free standing or retaining walls should have footings extended to a minimum of 24 inches below grade. The existing soil beneath the structure foundation prepared in the manner described for foundations except the preparation needed only to extend 12 inches below and beyond the footing.

Foundations and Settlements

Shallow spread footings and continuous wall footings are suitable to support the structures associated with the plant upgrades. Footings shall be founded on a layer of properly prepared and compacted soil as described in Section 4.1. The foundations may be designed using an allowable soil bearing pressure of 2,000 psf at 18-inch embedment depth when foundations are supported on compacted Caltrans Class 2 aggregate base (extending a minimum of 1.5 feet below footings).

The allowable soil pressure may be increased by 20% for each foot of embedment depth in excess of 18 inches and by one-third for short term loads induced by winds or seismic events. The maximum allowable soil pressure at increased embedment depths shall not exceed 4,000 psf.

Flat Plate Structural Mats: Structural mats may be designed for a modulus of subgrade reaction (Ks) of 100 pci when placed on compacted clay or a subgrade modulus of 250 pci when placed on 2.5 feet of granular fill. Mats shall overlay 2 inches of sand and a 10-mil polyethylene vapor retarder. The structure support pad shall be moisture conditioned and recompacted as specified in Section 4.1 of this report.

Resistance to horizontal loads will be developed by passive earth pressure on the sides of footings and frictional resistance developed along the bases of footings and concrete slabs. Passive resistance to lateral earth pressure may be calculated using an equivalent fluid pressure of 300 pcf to resist lateral loadings. The top one foot of embedment should not be considered in computing passive resistance unless the adjacent area is confined by a slab or pavement. An allowable friction coefficient of 0.35 may also be used at the base of the footings to resist lateral loading. Foundation movement under the estimated loadings are estimated to not exceed ½ inch with differential movement of about two-thirds of total movement for the loading assumptions stated above when the subgrade preparation guidelines given above are followed.

Note: The entire plant area overlays a geothermal fluids reservoir that geothermal fluids extraction and reinjection is causing annual ground surface settlement of 1 to 2 inches per year. The settlement is not uniform.

Drilled Piers: New foundations may be supported on cast-in-place, drilled piers. Design criteria are provided below.

Vertical Capacity: Vertical capacity for 24 and 36-inch diameter shafts are presented in Figure 3. Capacities for other shaft sizes can be determined in direct proportion to shaft diameters. Point bearing and skin friction parameters have been used to determine the allowable shaft capacity. The allowable capacities include a factor of safety of 2.5. The allowable vertical compression capacities may be increased by 33 percent to accommodate temporary loads such as from wind or seismic forces. The allowable vertical shaft capacities are based on the supporting capacity of the soil.

Lateral Capacity: The allowable lateral capacities for 24 and 36-inch diameter shafts are given in the table shown below. The allowable horizontal deflection has been assumed to be one-half inch (0.50 inch).

Table 3 – Lateral Capacities

Shaft Diameter (in.)	24		36	
Head Condition	Free	(*) Fixed	Free	(*) Fixed
Allowable Head Deflection (in.)	0.5	0.5	0.5	0.5
Minimum Length (ft.)	10	10	10	10
Lateral Capacity (kips)	15.6	50.8	20.0	65.0
Maximum Moment (foot-kips)	42.2	-293.3	53.7	-362.4
@Depth from Pier Head (ft.)	4.2	0	4.2	0
Minimum Length (ft.)	20	20	20	20
Lateral Capacity (kips)	32.0	70.5	52.0	124.0
Maximum Moment (foot-kips)	142.5	-393.3	266.7	-1025.0
@Depth from Pier Head (ft.)	9.0	0	9.8	0
Minimum Length (ft.)	30	30	30	30
Lateral Capacity (kips)	32.5	73.5	65.8	152.0
Maximum Moment (foot-kips)	145.0	-407.5	413.3	-1141.7
@Depth from Pier Head (ft.)	9.0	0	11.6	0

(*) Fixed head is defined as there is no rotation in the pier head (concrete foundation surrounding the pier heads).

Uplift Capacity: Pier capacity in tension may be assumed to be 50% of the compression capacity.

Settlement: Total settlements (non-seismic) of less than ¼ inch, and differential movement of about two-thirds of total movement for single pier designed according to the preceding recommendations. If pier spacing is at least 2.5 pier diameters center-to-center, no reduction in axial load capacity is considered necessary for group effect.

Note: The entire plant area overlays a geothermal fluids reservoir that geothermal fluids extraction and reinjection is causing annual ground surface settlement of 1 to 2 inches per year. The settlement is not uniform.

Note: Soil strength parameters obtained from field data and laboratory testing were modified based on our engineering judgment and our previous experience in the general site vicinity.

Soil Parameters: Interpretive engineering soil parameters of the subsurface soil for use in the Allpile Computer Program are presented in the table below.

Table 4 – Soil Strength Parameters

Layer Type	Depth (ft)	Unit Weight (pcf)	Friction Angle (deg)	Cohesion (ksf)	Lateral Soil Modulus, k (pci)	ϵ_{50} or Dr	Strength Reduction Factor
SM	0 to 5	115	34°	0	80	45.0	1.0
CL-CH	5 to 12	125	---	1.25	315	0.85	1.0
CL-CH	12 to 40	125	---	1.75	550	0.70	1.0
ML	40 to 50	120	24°	0.50	225	1.00	1.0

Installation: The drilled piers shall be placed in conformance to ACI 336 guidelines. Excavation for piers should be inspected by the geotechnical consultant. A tremie pipe should be used to pour concrete from the bottom up and to ensure less than five feet of free fall. All drilled piers extending below groundwater shall be cased to prevent caving or lateral deformation. Groundwater is expected to be encountered at approximately 8 feet below ground surface.

The structural steel and concrete should be placed immediately after drilling. Prior to placing any structural steel or concrete, loose soil or slough material should be removed from the bottom of the drilled pier excavation.

Slabs-On-Grade

Structural Concrete: Structural concrete slabs are those slabs (foundations) that underlie structures or covered housekeeping slabs (shades). Concrete slabs and flatwork shall be a minimum of 6 inches thick due to equipment loads. Concrete slab and flatwork reinforcement should consist of chaired rebar slab reinforcement (minimum of No. 3 bars at 18-inch centers, both horizontal directions) placed at slab mid-height to resist drying shrinkage cracking. Slab thickness and steel reinforcement are minimums only and should be verified by the structural engineer/designer knowing the actual project loadings.

All steel components of the foundation system should be protected from corrosion by maintaining a 3-inch minimum concrete cover of densely consolidated concrete at footings (by use of a vibrator).

Control joints should be provided in all concrete slabs-on-grade at a maximum spacing (in feet) of 2 to 3 times the slab thickness (in inches) as recommended by American Concrete Institute (ACI) guidelines. All joints should form approximately square patterns to reduce randomly oriented contraction cracks. Contraction joints in the slabs should be tooled at the time of the pour or sawcut (¼ of slab depth) within 6 to 8 hours of concrete placement. Construction (cold) joints in foundations and area flatwork should either be thickened butt-joints with dowels or a thickened keyed-joint designed to resist vertical deflection at the joint.

All joints in flatwork should be sealed to prevent moisture, vermin, or foreign material intrusion. Precautions should be taken to prevent curling of slabs in this arid desert region (refer to ACI guidelines).

Concrete Mixes and Corrosivity

Selected chemical analyses for corrosivity were conducted on bulk samples of the near surface soil from the project site. The native soils were found to have S1 to S2 (moderate to severe) levels of sulfate ion concentration (1,052 to 3,006 ppm). Sulfate ions in high concentrations can attack the cementitious material in concrete, causing weakening of the cement matrix and eventual deterioration by raveling. The following table provides American Concrete Institute (ACI) recommended cement types, water-cement ratio and minimum compressive strengths for concrete in contact with soils:

Table 5. Concrete Mix Design Criteria due to Soluble Sulfate Exposure

Sulfate Exposure Class	Water-soluble Sulfate (SO_4) in soil, ppm	Cement Type	Maximum Water-Cement Ratio by weight	Minimum Strength f'c (psi)
S0	0-1,000	–	–	–
S1	1,000-2,000	II	0.50	4,000
S2	2,000-20,000	V	0.45	4,500
S3	Over 20,000	V (plus Pozzolon)	0.45	4,500

Note: From ACI 318-14 Table 19.3.1.1 and Table 19.3.2.1

A minimum of 6.0 sacks per cubic yard of concrete (4,500 psi) of Type V Portland Cement with a maximum water/cement ratio of 0.45 (by weight) should be used for concrete placed in contact with native soil on this project (sitework including foundations and housekeeping slabs). Admixtures may be required to allow placement of this low water/cement ratio concrete.

The native soil has moderate to very severe level of chloride ion concentration (210 to 3,040 ppm). Chloride ions can cause corrosion of reinforcing steel, anchor bolts and other buried metallic conduits. Resistivity determinations on the soil indicate very severe potential for metal loss because of electrochemical corrosion processes. Mitigation of the corrosion of steel can be achieved by using steel pipes coated with epoxy corrosion inhibitors, asphaltic and epoxy coatings, cathodic protection or by encapsulating the portion of the pipe lying above groundwater with a minimum of 3 inches of densely consolidated concrete. ***No metallic water pipes or conduits should be placed below foundations.***

Foundation designs shall provide a minimum concrete cover of three (3) inches around steel reinforcing or embedded components (anchor bolts, etc.) exposed to native soil. If the 3-inch concrete edge distance cannot be achieved, all embedded steel components (anchor bolts, etc.) shall be epoxy coated for corrosion protection (in accordance with ASTM D3963/A934) or a corrosion inhibitor and a permanent waterproofing membrane shall be placed along the exterior face of the exterior footings.

Additionally, the concrete should be thoroughly vibrated at footings during placement to decrease the permeability of the concrete.

Excavations

All site excavations should conform to CalOSHA requirements for Type C soil. The contractor is solely responsible for the safety of workers entering trenches. Temporary excavations with depths of 4 feet or less may cut nearly vertical for short duration. Sandy soil slopes should be kept moist, but not saturated, to reduce the potential of raveling or sloughing. Excavations below 4 feet will require shoring or slope inclinations in conformance to CAL/OSHA regulations for Type C soil.

Surcharge loads of stockpiled soil or construction materials should be set back from the top of the slope a minimum distance equal to the height of the slope. All permanent slopes should not be steeper than 3:1 to reduce wind and rain erosion. Protected slopes with ground cover may be as steep as 2:1. However, maintenance with motorized equipment may not be possible at this inclination.

Seismic Design

This site is located in the seismically active southern California area and the site structures are subject to strong ground shaking due to potential fault movements along the Imperial and Cerro Prieto faults. Engineered design and earthquake-resistant construction are the common solutions to increase safety and development of seismic areas. Designs should comply with the latest edition of the CBC for Site Class D using the seismic coefficients given in Table 2 of this report.

Closure

We did not encounter soil conditions that would preclude implementation of the proposed project provided the recommendations contained in this report are implemented in the design and construction of this project. We appreciate the opportunity to provide our findings and professional opinions regarding geotechnical conditions at the site. If you have any questions or comments regarding our findings, please call our office at (760) 370-3000.

Respectfully Submitted,
Landmark Consultants, Inc.

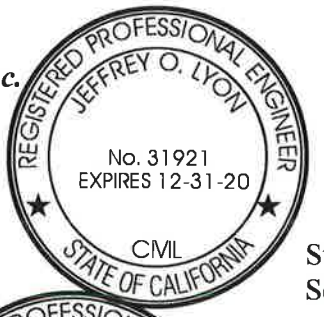

Jeffrey O. Lyon, PE
President

Steven K. Williams, PG, EG
Senior Engineering Geologist

Julian R. Avalos, PE
Senior Engineer

TABLES

Table 1
Summary of Characteristics of Closest Known Active Faults

Fault Name	Approximate Distance (miles)	Approximate Distance (km)	Maximum Moment Magnitude (Mw)	Fault Length (km)	Slip Rate (mm/yr)
Imperial	7.0	11.2	7	62 ± 6	20 ± 5
Superstition Hills	8.4	13.5	6.6	23 ± 2	4 ± 2
Unnamed 2*	8.5	13.6			
Brawley *	8.8	14.1			
Rico *	9.9	15.9			
Unnamed 1*	12.0	19.2			
Borrego (Mexico)*	13.0	20.7			
Yuha*	13.3	21.2			
Superstition Mountain	14.7	23.5	6.6	24 ± 2	5 ± 3
Laguna Salada	14.8	23.6	7	67 ± 7	3.5 ± 1.5
Cerro Prieto *	15.2	24.3			
Pescadores (Mexico)*	17.2	27.5			
Shell Beds	17.3	27.6			
Yuha Well *	17.8	28.5			
Cucapah (Mexico)*	18.4	29.4			
Vista de Anza*	20.4	32.7			
Painted Gorge Wash*	24.0	38.4			
Ocotillo*	25.4	40.6			
Elmore Ranch	28.3	45.3	6.6	29 ± 3	1 ± 0.5
Elsinore - Coyote Mountain	29.1	46.6	6.8	39 ± 4	4 ± 2
San Jacinto - Borrego	33.6	53.8	6.6	29 ± 3	4 ± 2
Algodones *	35.6	57.0			

* Note: Faults not included in CGS database.

Table 2
2016 California Building Code (CBC) and ASCE 7-10 Seismic Parameters

		ASCE 7-10 Reference
Soil Site Class:	**D**	Table 20.3-1
Latitude:	32.7139 N	
Longitude:	-115.5375 W	
Risk Category:	III	
Seismic Design Category:	D	

Maximum Considered Earthquake (MCE) Ground Motion

Mapped MCE_R Short Period Spectral Response	S_s	1.500 g	CBC Figure 1613.3.1(1)	
Mapped MCE_R 1 second Spectral Response	S_1	0.600 g	CBC Figure 1613.3.1(2)	
Short Period (0.2 s) Site Coefficient	F_a	1.00	CBC Table 1613.3.3(1)	
Long Period (1.0 s) Site Coefficient	F_v	1.50	CBC Table 1613.3.3(2)	
MCE_R Spectral Response Acceleration Parameter (0.2 s)	S_{MS}	1.500 g	$= F_a * S_s$	CBC Equation 16-37
MCE_R Spectral Response Acceleration Parameter (1.0 s)	S_{M1}	0.900 g	$= F_v * S_1$	CBC Equation 16-38

Design Earthquake Ground Motion

Design Spectral Response Acceleration Parameter (0.2 s)	S_{DS}	1.000 g	$= 2/3*S_{MS}$	CBC Equation 16-39
Design Spectral Response Acceleration Parameter (1.0 s)	S_{D1}	0.600 g	$= 2/3*S_{M1}$	CBC Equation 16-40
Risk Coefficient at Short Periods (less than 0.2 s)	C_{RS}	1.106		ASCE Figure 22-17
Risk Coefficient at Long Periods (greater than 1.0 s)	C_{R1}	1.073		ASCE Figure 22-18
	T_L	8.00 sec		ASCE Figure 22-12
	T_O	0.12 sec	$=0.2*S_{D1}/S_{DS}$	
	T_S	0.60 sec	$=S_{D1}/S_{DS}$	
Peak Ground Acceleration	PGA_M	0.50 g		ASCE Equation 11.8-1

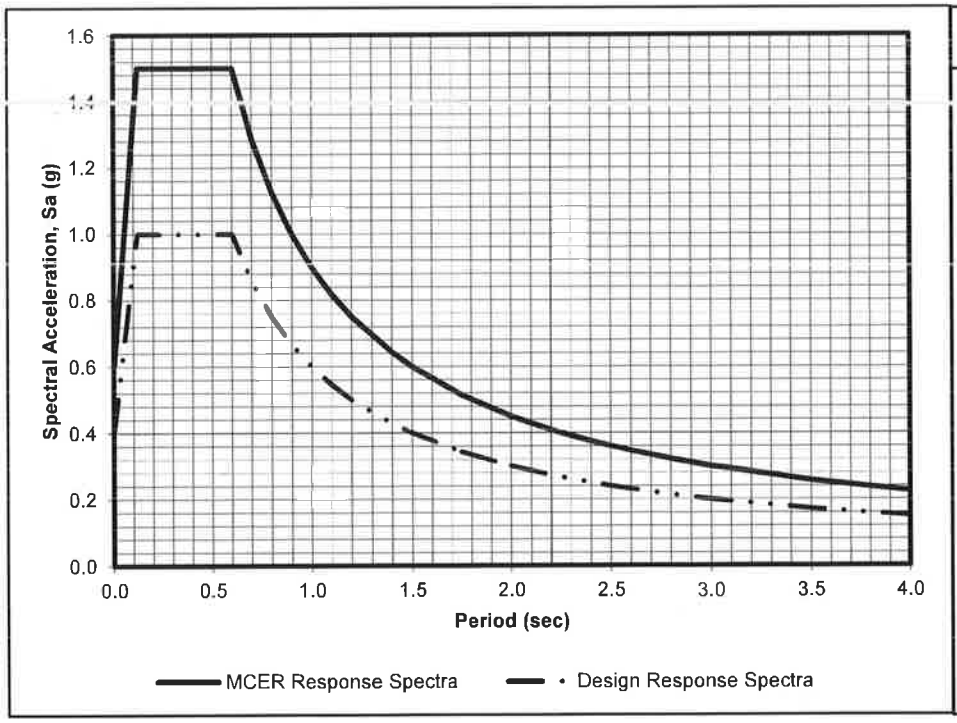

Period T (sec)	Sa (g)	MCE_R Sa (g)
0.00	0.40	0.60
0.12	1.00	1.50
0.60	1.00	1.50
0.70	0.86	1.29
0.80	0.75	1.13
0.90	0.67	1.00
1.00	0.60	0.90
1.10	0.55	0.82
1.20	0.50	0.75
1.20	0.50	0.75
1.40	0.43	0.64
1.50	0.40	0.60
1.75	0.34	0.51
2.00	0.30	0.45
2.20	0.27	0.41
2.40	0.25	0.38
2.60	0.23	0.35
2.80	0.21	0.32
3.00	0.20	0.30
3.50	0.17	0.26
4.00	0.15	0.23

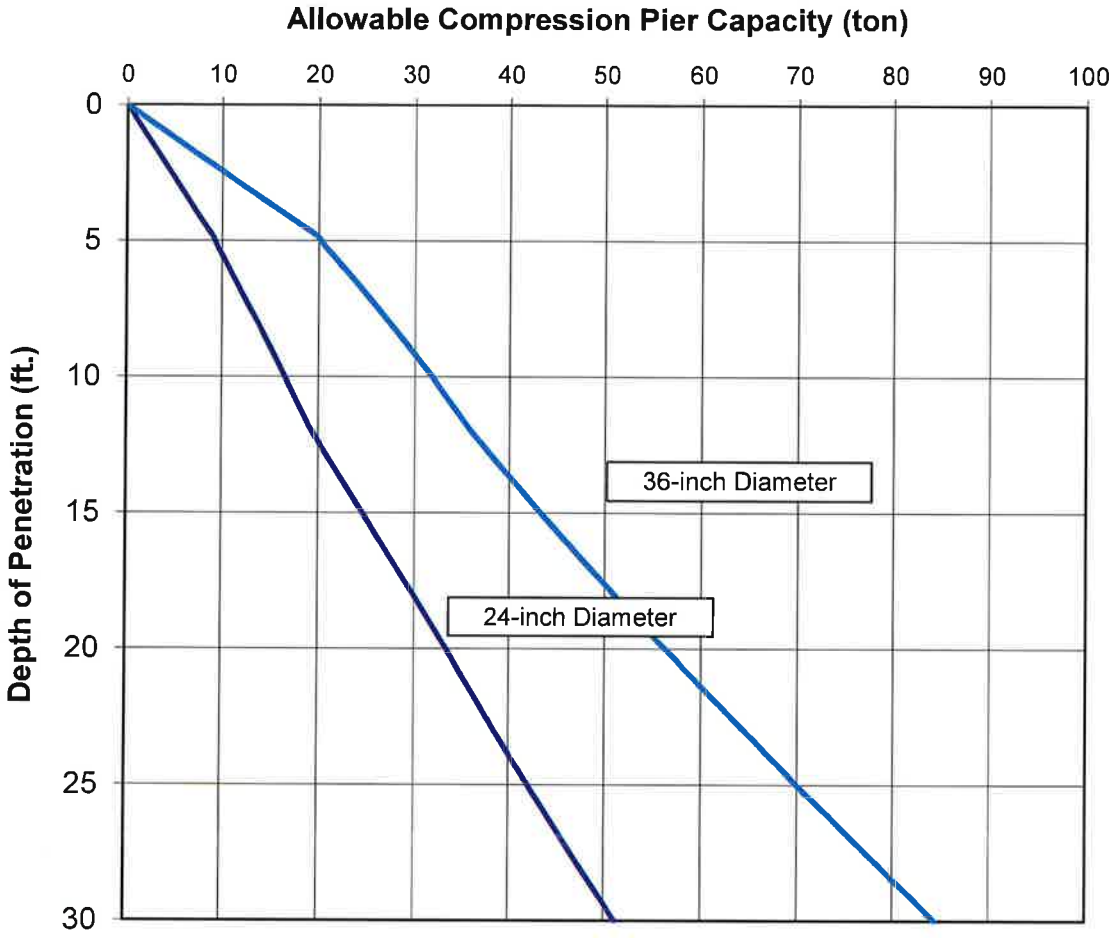

Notes:

1. Compression load capacity are based on skin friction and end-bearing capacity. The structural capacity of the piers should be checked.
2. The indicated capacities are for sustained (dead plus live) vertical compression load, and include a factor of safety of at least 2.5
3. For temporary wind or seismic load, the above values may be increased by one-third.
4. Capacities of other pier sizes are in direct proportion to the pile diameter.

LANDMARK Geo-Engineers and Geologists a DBE/MBE/SBE Company Project No.: LE19075	**Drilled Pier Compression Capacity Chart** **Ormat's Heber #2 Plant Expansion** **Heber, California**	**Figure 3**

FIGURES

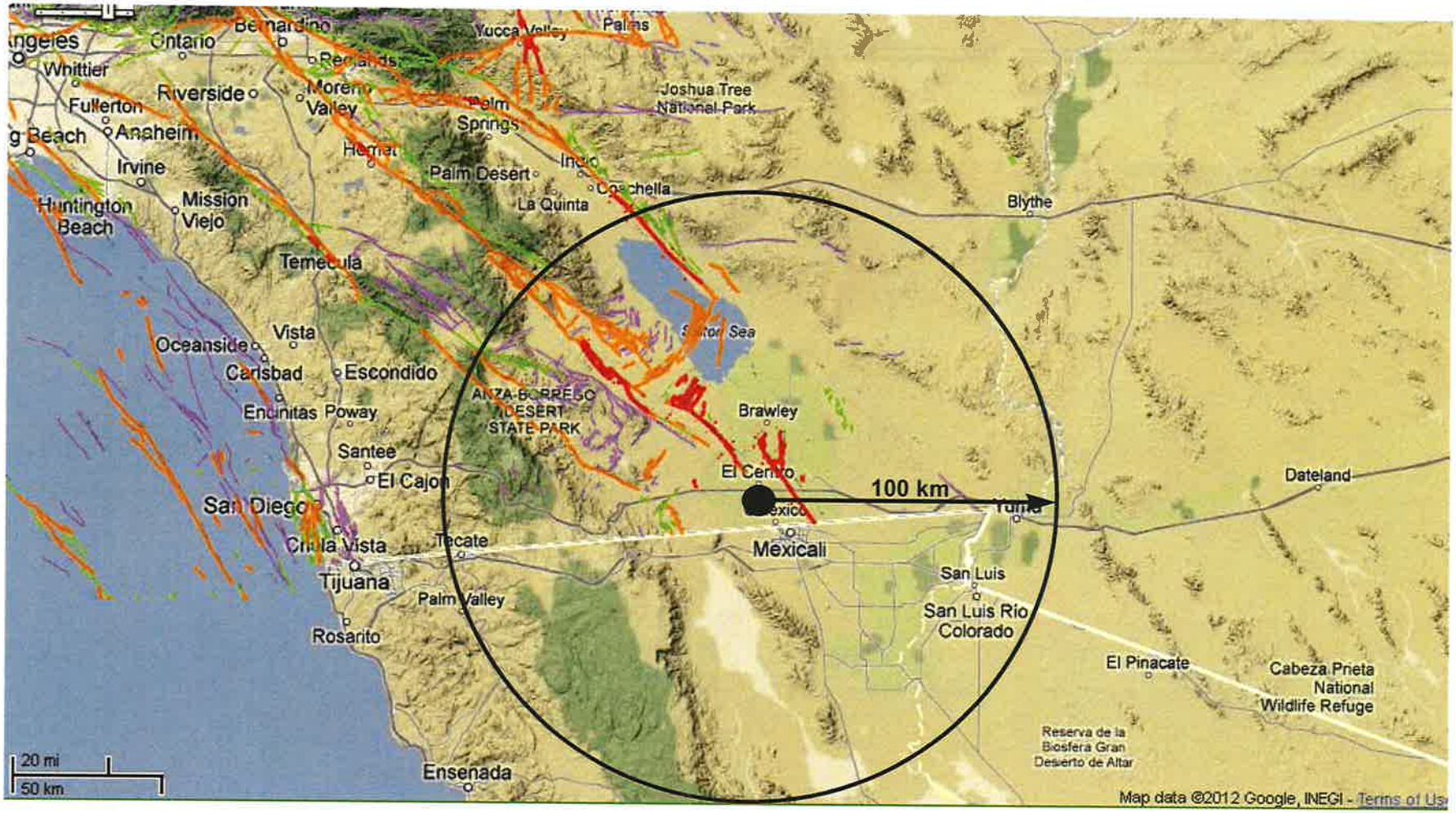

Source: California Geological Survey 2010 Fault Activity Map of California
http://www.quake.ca.gov/gmaps/FAM/faultactivitymap.html#

LANDMARK Geo-Engineers and Geologists **Project No.: LE19075**	**Regional Fault Map**	**Figure 1**

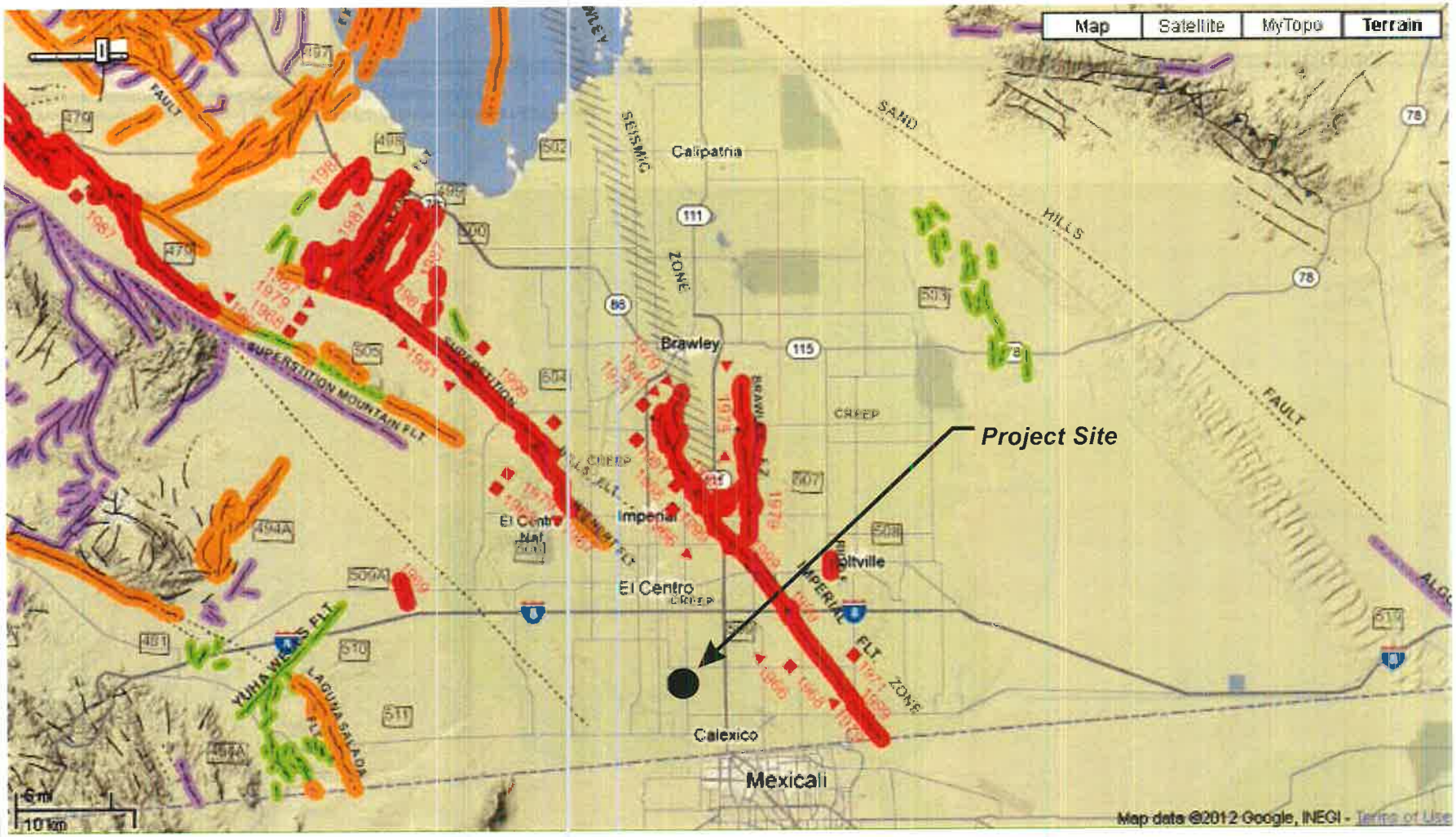

Source: California Geological Survey 2010 Fault Activity Map of California
http://www.quake.ca.gov/gmaps/FAM/faultactivitymap.html#

LANDMARK
Geo-Engineers and Geologists

Project No.: LE19075

Map of Local Faults

Figure 2

APPENDIX A

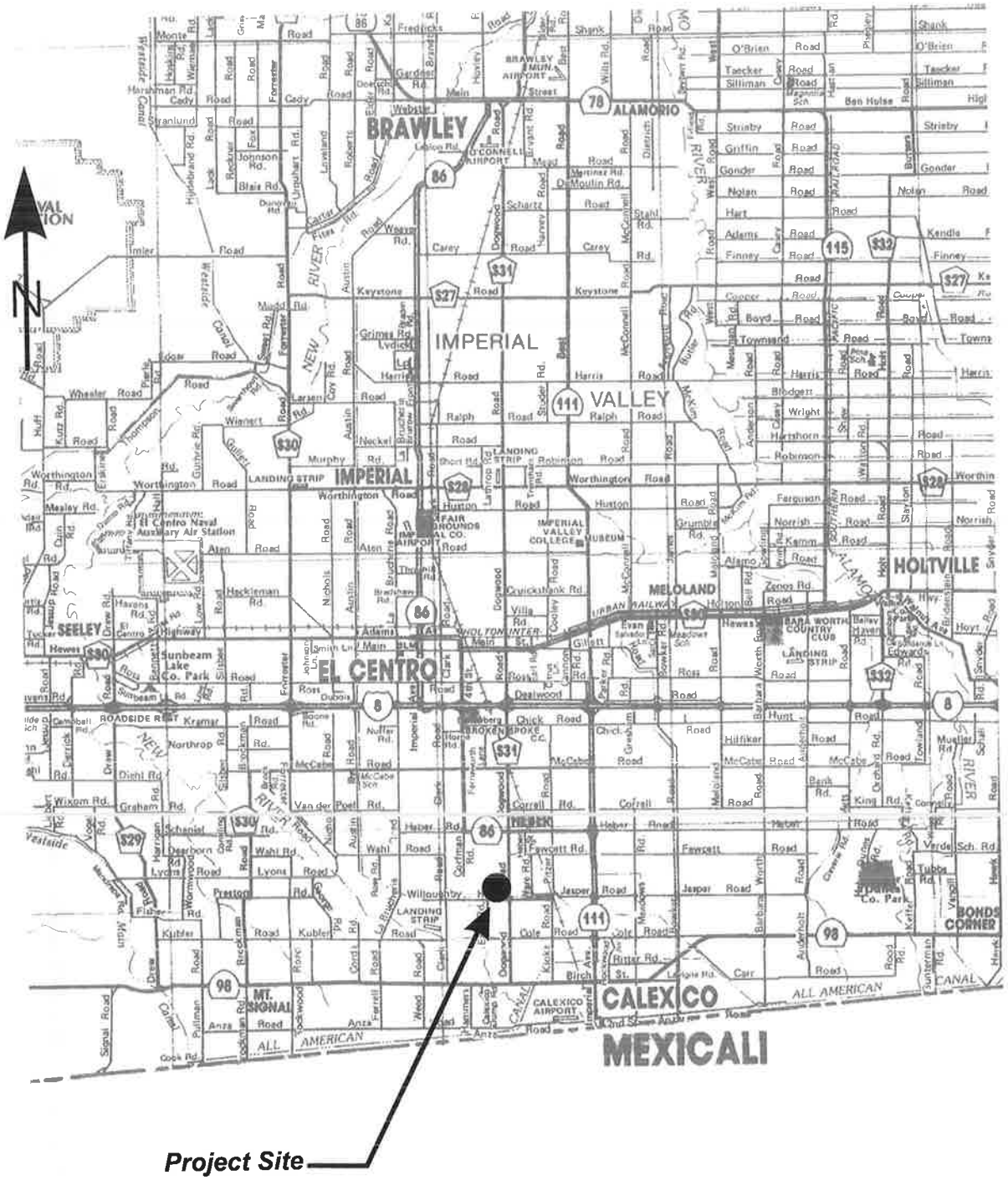

LANDMARK
Geo-Engineers and Geologists

Project No.: LE19075

Vicinity Map

Plate
A-1

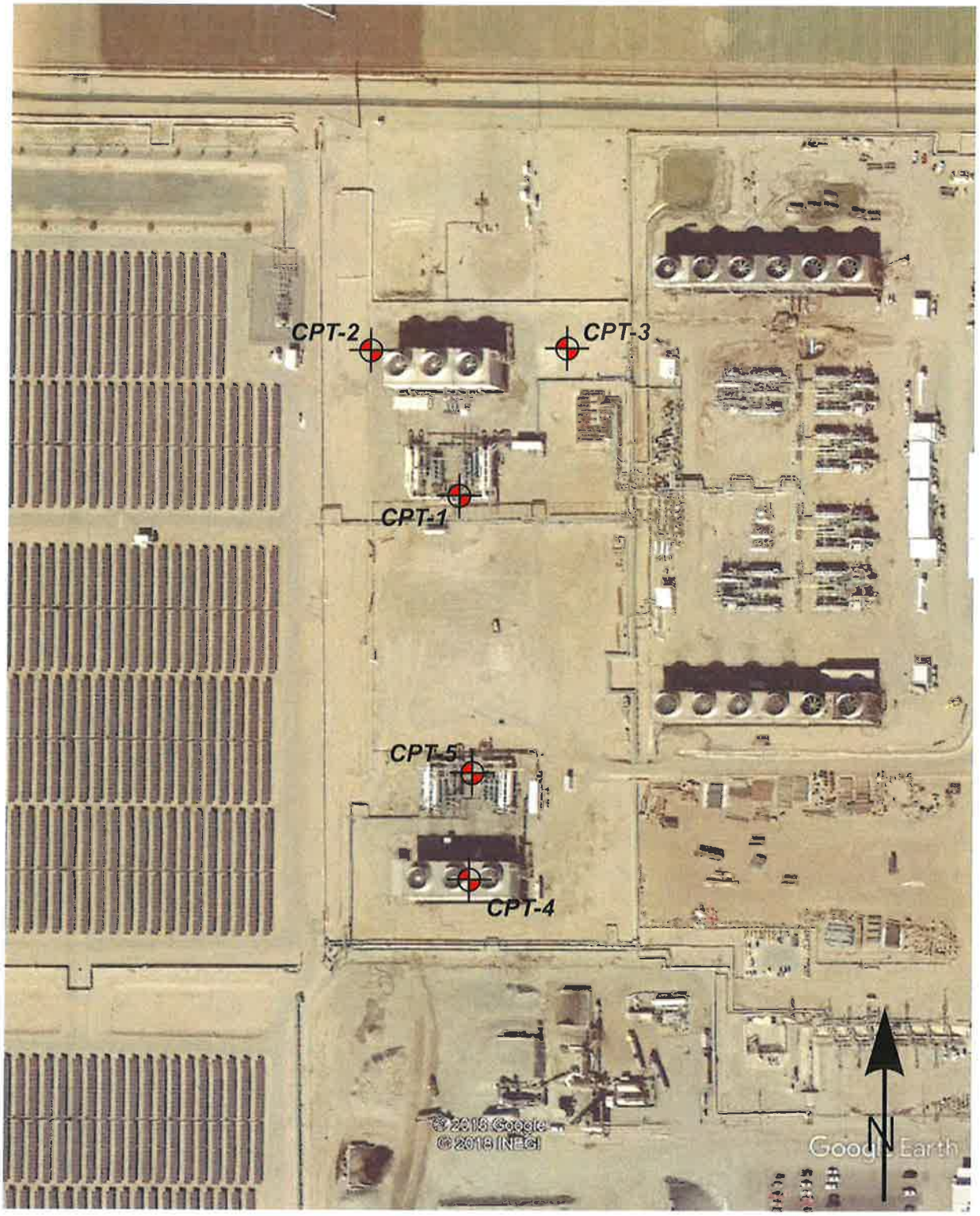

LANDMARK
Geo-Engineers and Geologists

Project No.: LE19075

Site and Exploration Map

Plate
A-2

APPENDIX B

CLIENT: Ormat Nevada Inc
PROJECT: Heber 2 Repower Project - Heber, CA

CONE PENETROMETER: Middle Earth Geotesting Truck Mounted Electric Cone with 23 ton reaction weight

LOCATION: See Site and Boring Location Plan

DATE: 12/20/2004

CONE SOUNDING DATA CPT-1

INTERPRETED SOIL PROFILE
From Robertson and Campanella (1989

GROUND ELEVATION +/-

DEPTH			
	Clayey Silt to Silty Clay	ML/CL	hard
	Sandy Silt to Clayey Silt	ML	very dense
	Silty Sand to Sandy Silt	SM/ML	very dense
	Silty Sand to Sandy Silt	" "	very dense
5	Silty Clay to Clay	CL	stiff
	Silty Clay to Clay	" "	stiff
	Clay	CL/CH	stiff
	Clay	" "	stiff
	Clay	" "	stiff
10	Clay	" "	very stiff
	Clay	" "	very stiff
	Silty Clay to Clay	CL	very stiff
	Clay	CL/CH	stiff
	Clay	" "	stiff
15	Clay	" "	very stiff
	Clay	" "	very stiff
	Clay	" "	very stiff
	Clay	" "	very stiff
	Clay	" "	very stiff
20	Clay	" "	very stiff
	Clay	" "	stiff
	Clay	" "	very stiff
	Clay	" "	very stiff
	Clay	" "	very stiff
25	Clay	" "	very stiff
	Clay	" "	very stiff
	Clay	" "	very stiff
	Clay	" "	very stiff
	Clay	" "	very stiff
30	Clay	" "	very stiff
	Clay	" "	very stiff
	Clay	" "	very stiff
	Clay	" "	very stiff
	Clay	" "	stiff
35	Clay	" "	stiff
	Clay	" "	very stiff
	Clay	" "	very stiff
	Clayey Silt to Silty Clay	ML/CL	very stiff
	Silty Clay to Clay	CL	stiff
40	Clayey Silt to Silty Clay	ML/CL	stiff
	Clayey Silt to Silty Clay	" "	stiff
	Clayey Silt to Silty Clay	" "	stiff
	Clayey Silt to Silty Clay	" "	very stiff
	Clayey Silt to Silty Clay	" "	very stiff
45	Clayey Silt to Silty Clay	" "	very stiff
	Clayey Silt to Silty Clay	" "	stiff
	Sandy Silt to Clayey Silt	ML	very loose
	Sandy Silt to Clayey Silt	" "	very loose
	Clayey Silt to Silty Clay	ML/CL	stiff
50	Sandy Silt to Clayey Silt	ML	very loose
55			

END OF SOUNDING AT 50 ft.

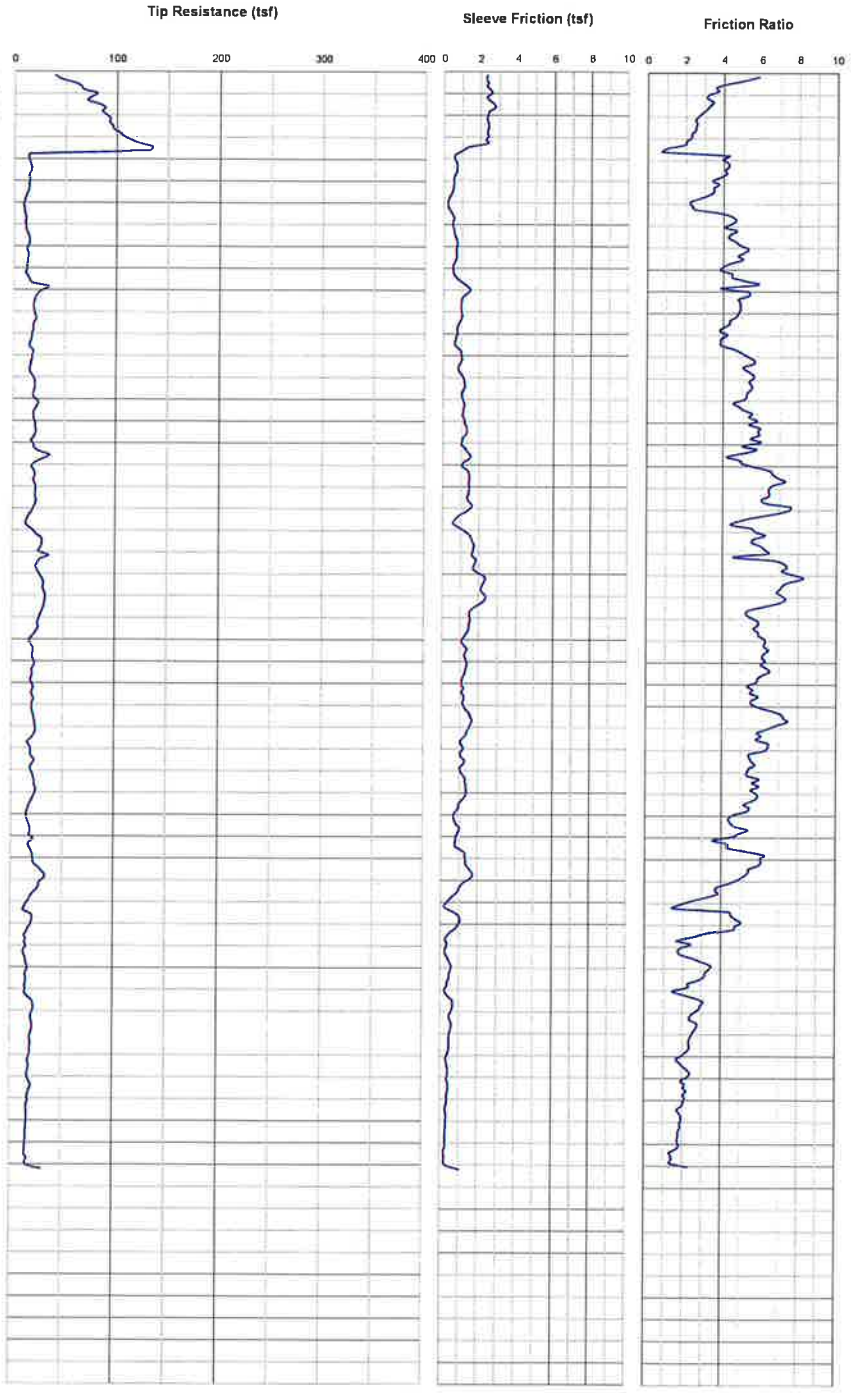

Project No.		PLATE
LE19075	LANDMARK Geo-Engineers and Geologists	B-1

LANDMARK CONSULTANTS, INC.

CONE PENETROMETER INTERPRETATION (based on Robertson & Campanella, 1989, refer to Key to CPT logs)

Project: Heber 2 Repower Project - Heber, CA **Project No:** LE19075 **Date:** 12/20/2004

CONE SOUNDING: CPT-1
Est. GWT (ft): 8
Phi Correlation: 0 0-Schm(78),1-R&C(83),2-PHT(74)

Base Depth (m)	Base Depth (ft)	Avg Tip Qc, tsf	Avg Friction Ratio, %	Soil Classification	USCS	Density or Consistency	Est. Density (pcf)	SPT N(60)	Norm. Qc1n	Est. % Fines	Rel. Dens. Dr (%)	Nk: Phi (deg.)	17 Su (tsf)	OCR
0.15	0.5	47.46	5.04	Silty Clay to Clay	CL	hard	125	27		60			2.79	>10
0.30	1.0	71.19	3.50	Sandy Silt to Clayey Silt	ML	very dense	115	20	134.6	45	107	43		
0.45	1.5	76.38	3.27	Sandy Silt to Clayey Silt	ML	very dense	115	22	144.4	40	102	42		
0.60	2.0	88.21	2.88	Sandy Silt to Clayey Silt	ML	very dense	115	25	166.8	35	101	42		
0.75	2.5	94.19	2.53	Silty Sand to Sandy Silt	SM/ML	very dense	115	21	178.0	30	100	42		
0.93	3.0	101.94	2.35	Silty Sand to Sandy Silt	SM/ML	very dense	115	23	192.7	30	99	42		
1.08	3.5	123.24	1.66	Sand to Silty Sand	SP/SM	very dense	115	22	233.0	20	102	42		
1.23	4.0	53.93	2.99	Sandy Silt to Clayey Silt	ML	dense	115	15	101.9	45	76	39		
1.38	4.5	16.43	4.19	Clay	CL/CH	stiff	125	13		85			0.95	>10
1.53	5.0	15.53	3.80	Silty Clay to Clay	CL	stiff	125	9		85			0.90	>10
1.68	5.5	13.99	3.48	Silty Clay to Clay	CL	stiff	125	8		85			0.80	>10
1.83	6.0	10.16	2.42	Clayey Silt to Silty Clay	ML/CL	stiff	120	4		85			0.58	>10
1.98	6.5	10.41	3.55	Silty Clay to Clay	CL	stiff	125	6		95			0.59	>10
2.13	7.0	11.62	4.38	Clay	CL/CH	stiff	125	9		100			0.66	>10
2.28	7.5	13.29	4.44	Clay	CL/CH	stiff	125	11		95			0.76	>10
2.45	8.0	14.55	4.93	Clay	CL/CH	stiff	125	12		95			0.83	>10
2.60	8.5	13.90	4.96	Clay	CL/CH	stiff	125	11		95			0.79	>10
2.75	9.0	13.23	4.08	Clay	CL/CH	stiff	125	11		95			0.75	>10
2.90	9.5	13.66	4.68	Clay	CL/CH	stiff	125	11		100			0.77	>10
3.05	10.0	26.88	5.00	Clay	CL/CH	very stiff	125	22		80			1.55	>10
3.20	10.5	21.69	5.01	Clay	CL/CH	very stiff	125	17		85			1.24	>10
3.35	11.0	19.84	4.85	Clay	CL/CH	very stiff	125	16		90			1.13	>10
3.50	11.5	21.31	4.45	Silty Clay to Clay	CL	very stiff	125	12		85			1.22	>10
3.65	12.0	18.97	4.00	Silty Clay to Clay	CL	very stiff	125	11		85			1.08	>10
3.80	12.5	16.82	3.88	Silty Clay to Clay	CL	stiff	125	10		90			0.95	>10
3.95	13.0	18.18	4.91	Clay	CL/CH	very stiff	125	15		95			1.03	>10
4.13	13.5	17.33	5.43	Clay	CL/CH	stiff	125	14		100			0.98	>10
4.28	14.0	17.04	5.46	Clay	CL/CH	stiff	125	14		100			0.96	>10
4.43	14.5	21.21	5.45	Clay	CL/CH	very stiff	125	17		100			1.21	>10
4.58	15.0	19.96	5.21	Clay	CL/CH	very stiff	125	16		100			1.13	>10
4.73	15.5	23.41	4.80	Clay	CL/CH	very stiff	125	19		90			1.34	>10
4.88	16.0	20.50	5.51	Clay	CL/CH	very stiff	125	16		100			1.16	>10
5.03	16.5	21.94	5.88	Clay	CL/CH	very stiff	125	18		100			1.25	>10
5.18	17.0	19.22	5.48	Clay	CL/CH	very stiff	125	15		100			1.09	>10
5.33	17.5	27.57	5.03	Clay	CL/CH	very stiff	125	22		90			1.58	>10
5.48	18.0	23.29	5.22	Clay	CL/CH	very stiff	125	19		100			1.32	>10
5.65	18.5	20.85	6.67	Clay	CL/CH	very stiff	125	17		100			1.18	>10
5.80	19.0	21.33	6.77	Clay	CL/CH	very stiff	125	17		100			1.21	>10
5.95	19.5	21.97	6.29	Clay	CL/CH	very stiff	125	18		100			1.24	>10
6.10	20.0	21.34	7.09	Clay	CL/CH	very stiff	125	17		100			1.21	>10
6.25	20.5	15.48	5.72	Clay	CL/CH	stiff	125	12		100			0.86	6.21
6.40	21.0	15.87	5.20	Clay	CL/CH	stiff	125	13		100			0.88	6.32
6.55	21.5	26.53	5.79	Clay	CL/CH	very stiff	125	21		100			1.51	>10
6.70	22.0	27.19	6.21	Clay	CL/CH	very stiff	125	22		100			1.55	>10
6.85	22.5	29.12	6.18	Clay	CL/CH	very stiff	125	23		100			1.66	>10
7.00	23.0	24.40	7.41	Clay	CL/CH	very stiff	125	20		100			1.38	>10
7.18	23.5	29.74	7.65	Clay	CL/CH	very stiff	125	24		100			1.69	>10
7.33	24.0	31.24	7.01	Clay	CL/CH	very stiff	125	25		100			1.78	>10
7.48	24.5	31.71	6.74	Clay	CL/CH	very stiff	125	25		100			1.81	>10
7.63	25.0	28.38	5.36	Clay	CL/CH	very stiff	125	23		100			1.61	>10
7.78	25.5	25.50	5.79	Clay	CL/CH	very stiff	125	20		100			1.44	>10
7.93	26.0	21.23	6.01	Clay	CL/CH	very stiff	125	17		100			1.19	7.85
8.08	26.5	19.41	6.26	Clay	CL/CH	very stiff	125	16		100			1.08	6.54
8.23	27.0	21.10	6.12	Clay	CL/CH	very stiff	125	17		100			1.18	7.27
8.38	27.5	20.13	6.30	Clay	CL/CH	very stiff	125	16		100			1.12	6.54
8.53	28.0	19.23	5.66	Clay	CL/CH	very stiff	125	15		100			1.07	6.00
8.68	28.5	20.08	5.65	Clay	CL/CH	very stiff	125	16		100			1.12	6.32
8.85	29.0	20.55	5.67	Clay	CL/CH	very stiff	125	16		100			1.14	6.32
9.00	29.5	20.76	7.00	Clay	CL/CH	very stiff	125	17		100			1.15	6.32
9.15	30.0	22.80	6.88	Clay	CL/CH	very stiff	125	18		100			1.27	7.27
9.30	30.5	21.60	5.89	Clay	CL/CH	very stiff	125	17		100			1.20	6.43
9.45	31.0	17.19	6.36	Clay	CL/CH	stiff	125	14		100			0.94	4.37
9.60	31.5	20.05	5.47	Clay	CL/CH	very stiff	125	16		100			1.11	5.53
9.75	32.0	19.47	5.50	Clay	CL/CH	very stiff	125	16		100			1.07	5.10
9.90	32.5	21.74	5.63	Clay	CL/CH	very stiff	125	17		100			1.21	6.00
10.05	33.0	23.37	5.76	Clay	CL/CH	very stiff	125	19		100			1.30	6.65
10.20	33.5	20.39	5.56	Clay	CL/CH	very stiff	125	16		100			1.13	5.21
10.38	34.0	15.97	5.12	Clay	CL/CH	stiff	125	13		100			0.86	3.50
10.53	34.5	16.45	4.48	Clay	CL/CH	stiff	125	13		100			0.89	3.58
10.68	35.0	18.50	4.96	Clay	CL/CH	very stiff	125	15		100			1.01	4.18
10.83	35.5	19.11	4.05	Silty Clay to Clay	CL	very stiff	125	11		100			1.05	5.53
10.98	36.0	20.64	5.86	Clay	CL/CH	very stiff	125	17		100			1.13	4.78
11.13	36.5	25.44	5.72	Clay	CL/CH	very stiff	125	20		100			1.42	6.65
11.28	37.0	31.72	4.84	Silty Clay to Clay	CL	very stiff	125	18		100			1.79	>10
11.43	37.5	25.49	3.77	Clayey Silt to Silty Clay	ML/CL	very stiff	120	10		100			1.42	>10
11.58	38.0	17.68	2.48	Clayey Silt to Silty Clay	ML/CL	stiff	120	7		100			0.96	6.10
11.73	38.5	15.25	3.47	Silty Clay to Clay	CL	stiff	125	9		100			0.81	3.50

LANDMARK CONSULTANTS, INC.

CONE PENETROMETER INTERPRETATION (based on Robertson & Campanella, 1989, refer to Key to CPT logs)

Project: Heber 2 Repower Project - Heber, CA **Project No:** LE19075 **Date:** 12/20/2004

CONE SOUNDING: CPT-1

Est. GWT (ft): 8

Phi Correlation: 0 0-Schm(78),1-R&C(83),2-PHT(74)

Base Depth (m)	Base Depth (ft)	Avg Tip Qc, tsf	Avg Friction Ratio, %	Soil Classification	USCS	Density or Consistency	Est. Density (pcf)	SPT N(60)	Norm. Qc1n	Est. % Fines	Rel. Dens. Dr (%)	Nk: Phi (deg.)	17 Su (tsf)	OCR
11.88	39.0	20.64	4.84	Clay	CL/CH	very stiff	125	17		100			1.13	4.28
12.05	39.5	15.50	3.51	Silty Clay to Clay	CL	stiff	125	9		100			0.83	3.50
12.20	40.0	14.77	2.00	Clayey Silt to Silty Clay	ML/CL	stiff	120	6		100			0.78	4.18
12.35	40.5	13.50	2.07	Clayey Silt to Silty Clay	ML/CL	stiff	120	5		100			0.71	3.58
12.50	41.0	15.96	3.29	Silty Clay to Clay	CL	stiff	125	9		100			0.85	3.50
12.65	41.5	15.32	3.05	Clayey Silt to Silty Clay	ML/CL	stiff	120	6		100			0.81	4.28
12.80	42.0	14.74	2.01	Clayey Silt to Silty Clay	ML/CL	stiff	120	6		100			0.78	3.91
12.95	42.5	17.48	2.54	Clayey Silt to Silty Clay	ML/CL	stiff	120	7		100			0.94	5.10
13.10	43.0	22.47	2.80	Clayey Silt to Silty Clay	ML/CL	very stiff	120	9		100			1.23	7.70
13.25	43.5	20.78	2.49	Clayey Silt to Silty Clay	ML/CL	very stiff	120	8		100			1.13	6.65
13.40	44.0	21.29	2.62	Clayey Silt to Silty Clay	ML/CL	very stiff	120	9		100			1.16	6.76
13.58	44.5	19.71	2.35	Clayey Silt to Silty Clay	ML/CL	very stiff	120	8		100			1.07	5.88
13.73	45.0	19.60	2.17	Clayey Silt to Silty Clay	ML/CL	very stiff	120	8		100			1.06	5.76
13.88	45.5	18.05	1.84	Sandy Silt to Clayey Silt	ML	very loose	115	5	13.8	100	14	30		
14.03	46.0	17.42	2.29	Clayey Silt to Silty Clay	ML/CL	stiff	120	7		100			0.93	4.57
14.18	46.5	19.49	2.03	Sandy Silt to Clayey Silt	ML	very loose	115	6	14.7	100	16	30		
14.33	47.0	17.99	2.10	Clayey Silt to Silty Clay	ML/CL	stiff	120	7		100			0.96	4.68
14.48	47.5	16.62	1.85	Clayey Silt to Silty Clay	ML/CL	stiff	120	7		100			0.88	4.09
14.63	48.0	16.66	1.91	Clayey Silt to Silty Clay	ML/CL	stiff	120	7		100			0.88	4.00
14.78	48.5	15.96	1.83	Clayey Silt to Silty Clay	ML/CL	stiff	120	6		100			0.84	3.74
14.93	49.0	15.56	1.78	Clayey Silt to Silty Clay	ML/CL	stiff	120	6		100			0.81	3.58
15.10	49.5	14.89	1.48	Sandy Silt to Clayey Silt	ML	very loose	115	4	11.0	100	7	29		
15.25	50.0	16.44	1.69	Sandy Silt to Clayey Silt	ML	very loose	115	5	12.1	100	10	29		

CLIENT: Ormat Nevada Inc
PROJECT: Heber 2 Repower Project - Heber, CA

CONE PENETROMETER: Middle Earth Geotesting Truck Mounted Electric Cone with 23 ton reaction weight

LOCATION: See Site and Boring Location Plan

DATE: 12/20/2004

CONE SOUNDING DATA CPT-2

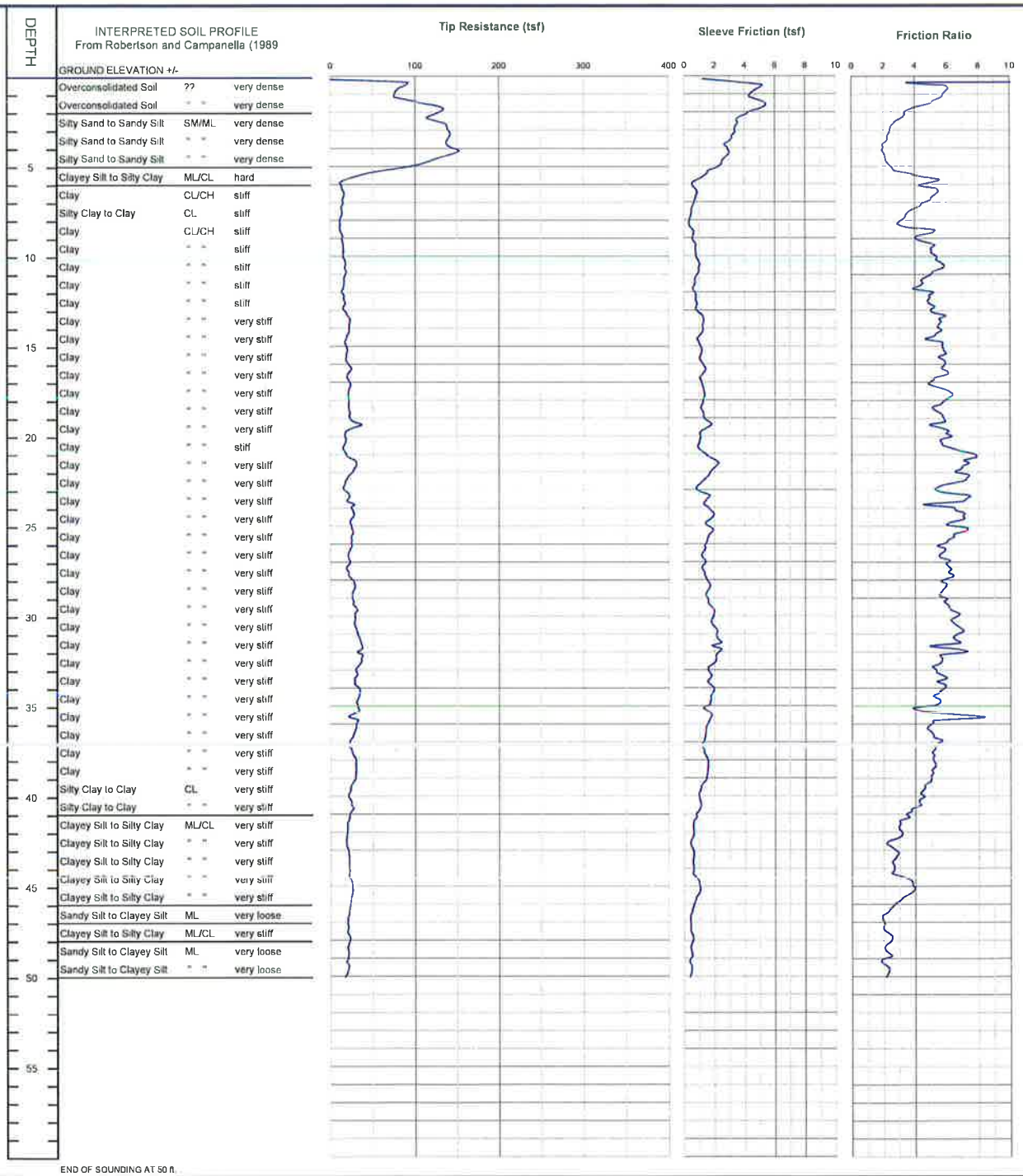

END OF SOUNDING AT 50 ft.

Project No.		PLATE
LE19075	LANDMARK Geo-Engineers and Geologists	B-2

LANDMARK CONSULTANTS, INC.

CONE PENETROMETER INTERPRETATION (based on Robertson & Campanella, 1989, refer to Key to CPT logs)

Project: Heber 2 Repower Project - Heber, CA **Project No:** LE19075 **Date:** 12/20/2004

CONE SOUNDING: CPT-2
Est. GWT (ft): 8
Phi Correlation: 0 0-Schm(78),1-R&C(83),2-PHT(74)

Base Depth (m)	Base Depth (ft)	Avg Tip Qc, tsf	Avg Friction Ratio, %	Soil Classification	USCS	Density or Consistency	Est. Density (pcf)	SPT N(60)	Norm. Qc1n	Est. % Fines	Rel. Dens. Dr (%)	Nk: Phi (deg.)	17 Su (tsf)	OCR
0.15	0.5	60.03	169.32	Overconsolidated Soil	??	very dense	120	60	113.5	100	119	45		
0.30	1.0	77.82	5.97	Overconsolidated Soil	??	very dense	120	78	147.1	55	110	43		
0.45	1.5	91.98	5.31	Overconsolidated Soil	??	very dense	120	92	173.9	50	107	43		
0.60	2.0	129.94	3.78	Sandy Silt to Clayey Silt	ML	very dense	115	37	245.6	35	113	44		
0.75	2.5	119.62	3.11	Sandy Silt to Clayey Silt	ML	very dense	115	34	226.1	30	107	43		
0.93	3.0	137.68	2.51	Silty Sand to Sandy Silt	SM/ML	very dense	115	31	260.3	25	108	43		
1.08	3.5	140.87	2.30	Silty Sand to Sandy Silt	SM/ML	very dense	115	31	266.3	25	106	43		
1.23	4.0	139.35	2.04	Silty Sand to Sandy Silt	SM/ML	very dense	115	31	263.4	20	104	43		
1.38	4.5	144.85	2.01	Silty Sand to Sandy Silt	SM/ML	very dense	115	32	273.8	20	103	42		
1.53	5.0	113.08	2.24	Silty Sand to Sandy Silt	SM/ML	very dense	115	25	208.9	25	94	41		
1.68	5.5	52.70	3.38	Clayey Silt to Silty Clay	ML/CL	hard	120	21		50			3.08	>10
1.83	6.0	13.87	4.91	Clay	CL/CH	stiff	125	11		95			0.80	>10
1.98	6.5	15.08	5.36	Clay	CL/CH	stiff	125	12		95			0.87	>10
2.13	7.0	14.77	4.81	Clay	CL/CH	stiff	125	12		95			0.85	>10
2.28	7.5	13.38	3.90	Clay	CL/CH	stiff	125	11		90			0.76	>10
2.45	8.0	12.25	3.27	Silty Clay to Clay	CL	stiff	125	7		90			0.69	>10
2.60	8.5	11.34	3.86	Clay	CL/CH	stiff	125	9		95			0.64	>10
2.75	9.0	13.62	4.43	Clay	CL/CH	stiff	125	11		95			0.77	>10
2.90	9.5	14.76	4.97	Clay	CL/CH	stiff	125	12		95			0.84	>10
3.05	10.0	15.04	5.19	Clay	CL/CH	stiff	125	12		100			0.85	>10
3.20	10.5	17.24	5.61	Clay	CL/CH	stiff	125	14		100			0.98	>10
3.35	11.0	17.82	5.31	Clay	CL/CH	very stiff	125	14		95			1.02	>10
3.50	11.5	16.22	4.53	Clay	CL/CH	stiff	125	13		95			0.92	>10
3.65	12.0	14.59	4.45	Clay	CL/CH	stiff	125	12		100			0.82	>10
3.80	12.5	15.95	4.89	Clay	CL/CH	stiff	125	13		100			0.90	>10
3.95	13.0	16.10	5.07	Clay	CL/CH	stiff	125	13		100			0.91	>10
4.13	13.5	20.52	5.55	Clay	CL/CH	very stiff	125	16		95			1.17	>10
4.28	14.0	22.48	5.55	Clay	CL/CH	very stiff	125	18		95			1.28	>10
4.43	14.5	20.89	5.42	Clay	CL/CH	very stiff	125	17		100			1.19	>10
4.58	15.0	17.79	5.37	Clay	CL/CH	very stiff	125	14		100			1.01	>10
4.73	15.5	19.47	5.86	Clay	CL/CH	very stiff	125	16		100			1.10	>10
4.88	16.0	19.76	5.77	Clay	CL/CH	very stiff	125	16		100			1.12	>10
5.03	16.5	22.53	5.91	Clay	CL/CH	very stiff	125	18		100			1.28	>10
5.18	17.0	21.67	5.09	Clay	CL/CH	very stiff	125	17		100			1.23	>10
5.33	17.5	22.15	5.77	Clay	CL/CH	very stiff	125	18		100			1.26	>10
5.48	18.0	21.43	6.10	Clay	CL/CH	very stiff	125	17		100			1.21	>10
5.65	18.5	21.56	5.34	Clay	CL/CH	very stiff	125	17		100			1.22	>10
5.80	19.0	22.73	5.72	Clay	CL/CH	very stiff	125	18		100			1.29	>10
5.95	19.5	30.63	5.48	Clay	CL/CH	very stiff	125	25		90			1.75	>10
6.10	20.0	17.95	6.14	Clay	CL/CH	very stiff	125	14		100			1.01	8.41
6.25	20.5	17.30	5.70	Clay	CL/CH	stiff	125	14		100			0.97	7.56
6.40	21.0	16.60	6.99	Clay	CL/CH	stiff	125	13		100			0.93	6.76
6.55	21.5	26.75	7.44	Clay	CL/CH	very stiff	125	21		100			1.52	>10
6.70	22.0	28.17	6.81	Clay	CL/CH	very stiff	125	23		100			1.60	>10
6.85	22.5	20.17	7.24	Clay	CL/CH	very stiff	125	16		100			1.13	8.85
7.00	23.0	16.15	5.62	Clay	CL/CH	stiff	125	13		100			0.90	5.88
7.18	23.5	21.37	6.84	Clay	CL/CH	very stiff	125	17		100			1.20	9.19
7.33	24.0	24.23	5.98	Clay	CL/CH	very stiff	125	19		100			1.37	>10
7.48	24.5	27.09	6.88	Clay	CL/CH	very stiff	125	22		100			1.54	>10
7.63	25.0	23.97	6.46	Clay	CL/CH	very stiff	125	19		100			1.35	>10
7.78	25.5	25.90	6.98	Clay	CL/CH	very stiff	125	21		100			1.46	>10
7.93	26.0	24.80	6.17	Clay	CL/CH	very stiff	125	20		100			1.40	>10
8.08	26.5	22.94	5.66	Clay	CL/CH	very stiff	125	18		100			1.29	8.85
8.23	27.0	22.28	5.92	Clay	CL/CH	very stiff	125	18		100			1.25	8.14
8.38	27.5	20.15	6.14	Clay	CL/CH	very stiff	125	16		100			1.12	6.65
8.53	28.0	24.13	6.05	Clay	CL/CH	very stiff	125	19		100			1.36	9.00
8.68	28.5	28.28	5.86	Clay	CL/CH	very stiff	125	23		100			1.60	>10
8.85	29.0	26.02	5.73	Clay	CL/CH	very stiff	125	21		100			1.46	>10
9.00	29.5	28.06	6.01	Clay	CL/CH	very stiff	125	22		100			1.58	>10
9.15	30.0	29.72	6.57	Clay	CL/CH	very stiff	125	24		100			1.68	>10
9.30	30.5	28.55	6.41	Clay	CL/CH	very stiff	125	23		100			1.61	>10
9.45	31.0	31.07	6.84	Clay	CL/CH	very stiff	125	25		100			1.76	>10
9.60	31.5	34.71	6.59	Clay	CL/CH	very stiff	125	28		100			1.97	>10
9.75	32.0	35.27	6.25	Clay	CL/CH	hard	125	28		100			2.00	>10
9.90	32.5	37.01	5.65	Clay	CL/CH	hard	125	30		100			2.10	>10
10.05	33.0	32.37	5.31	Clay	CL/CH	very stiff	125	26		100			1.83	>10
10.20	33.5	30.28	5.70	Clay	CL/CH	very stiff	125	24		100			1.71	>10
10.38	34.0	29.97	5.71	Clay	CL/CH	very stiff	125	24		100			1.69	>10
10.53	34.5	34.16	5.42	Clay	CL/CH	very stiff	125	27		100			1.93	>10
10.68	35.0	31.53	5.44	Clay	CL/CH	very stiff	125	25		100			1.78	>10
10.83	35.5	31.18	4.96	Clay	CL/CH	very stiff	125	25		100			1.76	>10
10.98	36.0	28.08	6.21	Clay	CL/CH	very stiff	125	22		100			1.57	8.14
11.13	36.5	28.95	4.94	Clay	CL/CH	very stiff	125	23		100			1.62	8.41
11.28	37.0	23.74	5.43	Clay	CL/CH	very stiff	125	19		100			1.32	5.88
11.43	37.5	24.03	5.19	Clay	CL/CH	very stiff	125	19		100			1.33	5.88
11.58	38.0	28.73	5.16	Clay	CL/CH	very stiff	125	23		100			1.61	7.70
11.73	38.5	29.89	5.19	Clay	CL/CH	very stiff	125	24		100			1.68	8.14

LANDMARK CONSULTANTS, INC.

CONE PENETROMETER INTERPRETATION (based on Robertson & Campanella, 1989, refer to Key to CPT logs)

Project: Heber 2 Repower Project - Heber, CA **Project No:** LE19075 **Date:** 12/20/2004

CONE SOUNDING: CPT-2 Phi Correlation: 0 0-Schm(78),1-R&C(83),2-PHT(74)

Est. GWT (ft): 8

Base Depth (m)	Base Depth (ft)	Avg Tip Qc, tsf	Avg Friction Ratio, %	Soil Classification	USCS	Density or Consistency	Est. Density (pcf)	SPT N(60)	Norm. Qc1n	Est. % Fines	Rel. Dens. Dr (%)	Nk: Phi (deg.)	17 Su (tsf)	OCR
11.88	39.0	29.55	5.05	Clay	CL/CH	very stiff	125	24		100			1.65	7.85
12.05	39.5	25.32	4.72	Clay	CL/CH	very stiff	125	20		100			1.40	5.88
12.20	40.0	22.19	4.46	Clay	CL/CH	very stiff	125	18		100			1.22	4.68
12.35	40.5	24.43	4.30	Silty Clay to Clay	CL	very stiff	125	14		100			1.35	7.00
12.50	41.0	24.85	3.66	Clayey Silt to Silty Clay	ML/CL	very stiff	120	10		100			1.37	>10
12.65	41.5	21.29	3.25	Clayey Silt to Silty Clay	ML/CL	very stiff	120	9		100			1.16	7.41
12.80	42.0	19.81	3.04	Clayey Silt to Silty Clay	ML/CL	very stiff	120	8		100			1.08	6.43
12.95	42.5	18.87	2.79	Clayey Silt to Silty Clay	ML/CL	very stiff	120	8		100			1.02	5.88
13.10	43.0	19.60	2.48	Clayey Silt to Silty Clay	ML/CL	very stiff	120	8		100			1.06	6.10
13.25	43.5	21.70	2.84	Clayey Silt to Silty Clay	ML/CL	very stiff	120	9		100			1.18	7.13
13.40	44.0	22.24	2.62	Clayey Silt to Silty Clay	ML/CL	very stiff	120	9		100			1.22	7.27
13.58	44.5	22.52	2.78	Clayey Silt to Silty Clay	ML/CL	very stiff	120	9		100			1.23	7.41
13.73	45.0	25.15	3.77	Clayey Silt to Silty Clay	ML/CL	very stiff	120	10		100			1.38	8.85
13.88	45.5	26.20	3.80	Clayey Silt to Silty Clay	ML/CL	very stiff	120	10		100			1.45	9.59
14.03	46.0	24.44	3.02	Clayey Silt to Silty Clay	ML/CL	very stiff	120	10		100			1.34	8.14
14.18	46.5	22.65	2.43	Clayey Silt to Silty Clay	ML/CL	very stiff	120	9		100			1.24	7.00
14.33	47.0	20.81	1.98	Sandy Silt to Clayey Silt	ML	very loose	115	6	15.7	100	18	30		
14.48	47.5	20.51	2.12	Sandy Silt to Clayey Silt	ML	very loose	115	6	15.4	100	17	30		
14.63	48.0	22.61	2.50	Clayey Silt to Silty Clay	ML/CL	very stiff	120	9		100			1.23	6.65
14.78	48.5	20.83	2.13	Sandy Silt to Clayey Silt	ML	very loose	115	6	15.5	100	17	30		
14.93	49.0	20.93	2.27	Clayey Silt to Silty Clay	ML/CL	very stiff	120	8		100			1.13	5.76
15.10	49.5	20.67	2.11	Sandy Silt to Clayey Silt	ML	very loose	115	6	15.3	100	17	30		
15.25	50.0	19.06	2.25	Clayey Silt to Silty Clay	ML/CL	very stiff	120	8		100			1.02	4.78

CLIENT: Ormat Nevada Inc
PROJECT: Heber 2 Repower Project - Heber, CA

CONE PENETROMETER: Middle Earth Geotesting Truck Mounted Electric Cone with 23 ton reaction weight

LOCATION: See Site and Boring Location Plan

DATE: 12/20/2004

CONE SOUNDING DATA CPT-3

INTERPRETED SOIL PROFILE
From Robertson and Campanella (1989

GROUND ELEVATION +/-

DEPTH			
	Clay	CL/CH	hard
	Clay	" "	hard
	Sandy Silt to Clayey Silt	ML	very dense
	Silty Sand to Sandy Silt	SM/ML	very dense
	Silty Sand to Sandy Silt	" "	very dense
5	Sandy Silt to Clayey Silt	ML	dense
	Clay	CL/CH	stiff
	Clay	" "	stiff
	Clay	" "	stiff
	Clay	" "	stiff
10	Clay	" "	stiff
	Clay	" "	stiff
	Clay	" "	very stiff
	Clay	" "	very stiff
	Clay	" "	very stiff
15	Clay	" "	stiff
	Clay	" "	stiff
	Clay	" "	stiff
	Clay	" "	stiff
	Clay	" "	stiff
20	Clay	" "	stiff
	Clay	" "	stiff
	Clay	" "	very stiff
	Clay	" "	hard
	Clay	" "	very stiff
25	Clay	" "	very stiff
	Clay	" "	very stiff
	Clay	" "	very stiff
	Clay	" "	very stiff
	Clay	" "	very stiff
30	Clay	" "	very stiff
	Clay	" "	very stiff
	Clay	" "	very stiff
	Clay	" "	very stiff
	Clay	" "	very stiff
35	Clay	" "	very stiff
	Clay	" "	very stiff
	Clay	" "	stiff
	Clay	" "	stiff
	Clay	" "	very stiff
40	Clayey Silt to Silty Clay	ML/CL	very stiff
	Silty Clay to Clay	CL	very stiff
	Silty Clay to Clay	" "	very stiff
	Clayey Silt to Silty Clay	ML/CL	very stiff
	Clayey Silt to Silty Clay	" "	very stiff
45	Silty Clay to Clay	CL	very stiff
	Clayey Silt to Silty Clay	ML/CL	stiff
	Clayey Silt to Silty Clay	" "	stiff
	Clayey Silt to Silty Clay	" "	very stiff
	Clayey Silt to Silty Clay	" "	very stiff
50	Clayey Silt to Silty Clay	" "	stiff
55			

END OF SOUNDING AT 50 ft.

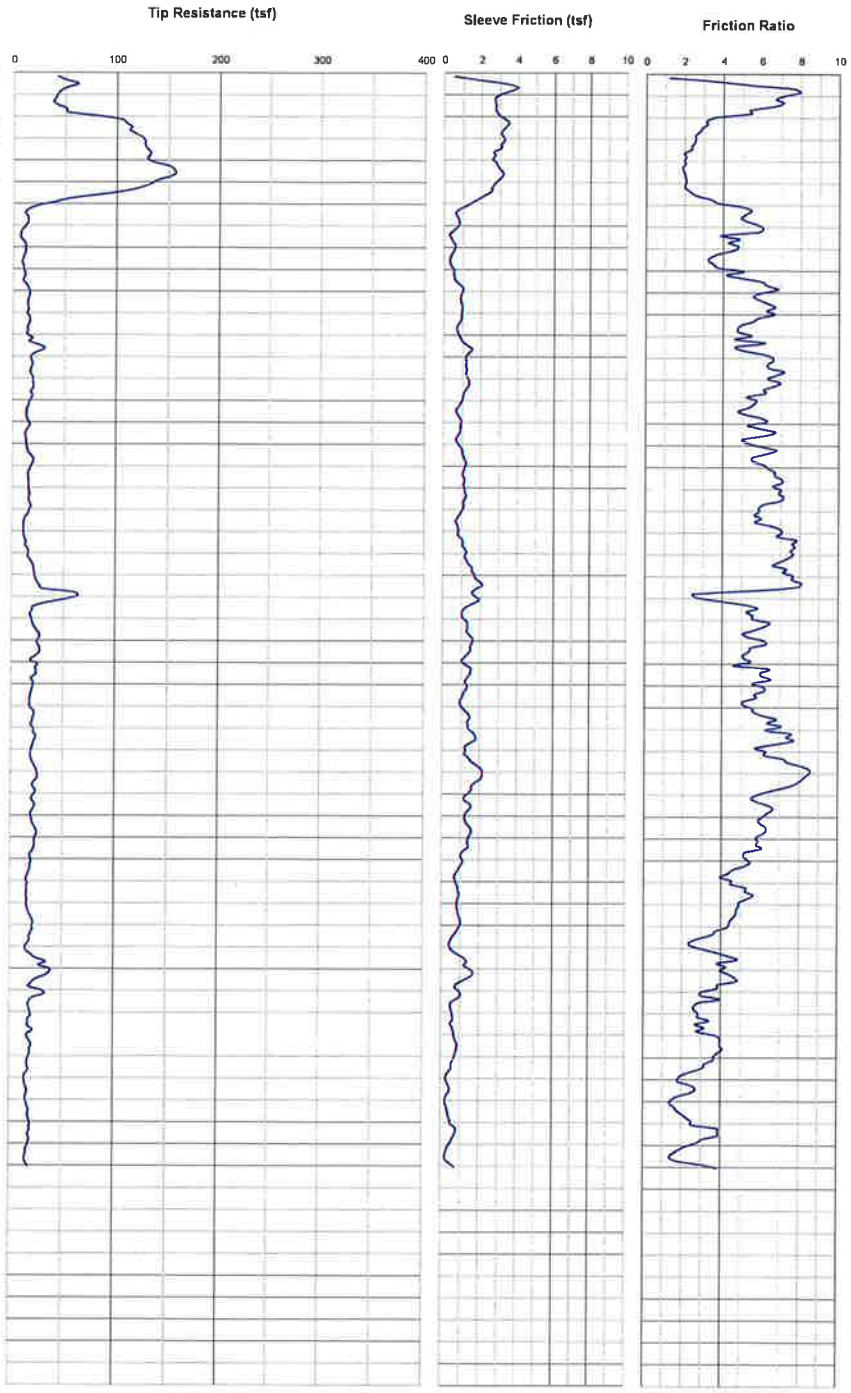

Project No.		PLATE
LE19075	LANDMARK Geo-Engineers and Geologists	B-3

LANDMARK CONSULTANTS, INC.

CONE PENETROMETER INTERPRETATION (based on Robertson & Campanella, 1989, refer to Key to CPT logs)

Project: Heber 2 Repower Project - Heber, CA **Project No:** LE19075 **Date:** 12/20/2004

CONE SOUNDING: CPT-3
Est. GWT (ft): 8
Phi Correlation: 0 0-Schm(78),1-R&C(83),2-PHT(74)

Base Depth (m)	Base Depth (ft)	Avg Tip Qc, tsf	Avg Friction Ratio, %	Soil Classification	USCS	Density or Consistency	Est. Density (pcf)	SPT N(60)	Norm. Qc1n	Est. % Fines	Rel. Dens. Dr (%)	Nk: Phi (deg.)	17 Su (tsf)	OCR
0.15	0.5	51.76	3.36	Clayey Silt to Silty Clay	ML/CL	hard	120	21		50			3.04	>10
0.30	1.0	46.42	7.56	Clay	CL/CH	hard	125	37		75			2.73	>10
0.45	1.5	40.35	6.79	Clay	CL/CH	hard	125	32		75			2.37	>10
0.60	2.0	61.72	4.80	Silty Clay to Clay	CL	hard	125	35		55			3.62	>10
0.75	2.5	109.67	3.07	Sandy Silt to Clayey Silt	ML	very dense	115	31	207.3	35	104	43		
0.93	3.0	118.60	2.64	Silty Sand to Sandy Silt	SM/ML	very dense	115	26	224.2	30	103	42		
1.08	3.5	127.70	2.43	Silty Sand to Sandy Silt	SM/ML	very dense	115	28	241.4	25	103	42		
1.23	4.0	131.15	2.02	Silty Sand to Sandy Silt	SM/ML	very dense	115	29	247.9	25	102	42		
1.38	4.5	147.55	1.96	Silty Sand to Sandy Silt	SM/ML	very dense	115	33	278.9	20	103	42		
1.53	5.0	148.38	2.05	Silty Sand to Sandy Silt	SM/ML	very dense	115	33	271.7	20	102	42		
1.68	5.5	111.44	2.28	Silty Sand to Sandy Silt	SM/ML	very dense	115	25	194.4	25	92	41		
1.83	6.0	40.17	4.02	Clayey Silt to Silty Clay	ML/CL	hard	120	16		60			2.34	>10
1.98	6.5	13.36	5.18	Clay	CL/CH	stiff	125	11		100			0.76	>10
2.13	7.0	13.22	5.65	Clay	CL/CH	stiff	125	11		100			0.75	>10
2.28	7.5	7.68	4.85	Clay	CL/CH	firm	125	6		100			0.43	6.10
2.45	8.0	11.50	4.55	Clay	CL/CH	stiff	125	9		100			0.65	>10
2.60	8.5	10.61	3.49	Silty Clay to Clay	CL	stiff	125	6		95			0.60	>10
2.75	9.0	9.81	4.10	Clay	CL/CH	stiff	125	8		100			0.55	7.27
2.90	9.5	10.85	5.09	Clay	CL/CH	stiff	125	9		100			0.61	8.27
3.05	10.0	14.61	6.36	Clay	CL/CH	stiff	125	12		100			0.83	>10
3.20	10.5	14.97	5.91	Clay	CL/CH	stiff	125	12		100			0.85	>10
3.35	11.0	14.49	6.53	Clay	CL/CH	stiff	125	12		100			0.82	>10
3.50	11.5	15.94	5.42	Clay	CL/CH	stiff	125	13		100			0.90	>10
3.65	12.0	14.15	5.01	Clay	CL/CH	stiff	125	11		100			0.80	>10
3.80	12.5	20.31	5.15	Clay	CL/CH	very stiff	125	16		95			1.16	>10
3.95	13.0	23.81	5.79	Clay	CL/CH	very stiff	125	19		95			1.36	>10
4.13	13.5	18.35	6.42	Clay	CL/CH	very stiff	125	15		100			1.04	>10
4.28	14.0	18.13	6.73	Clay	CL/CH	very stiff	125	15		100			1.03	>10
4.43	14.5	19.70	6.56	Clay	CL/CH	very stiff	125	16		100			1.12	>10
4.58	15.0	18.07	5.71	Clay	CL/CH	very stiff	125	14		100			1.02	>10
4.73	15.5	14.86	5.24	Clay	CL/CH	stiff	125	12		100			0.83	8.27
4.88	16.0	14.60	5.69	Clay	CL/CH	stiff	125	12		100			0.82	7.70
5.03	16.5	13.49	6.25	Clay	CL/CH	stiff	125	11		100			0.75	6.43
5.18	17.0	13.31	5.44	Clay	CL/CH	stiff	125	11		100			0.74	6.10
5.33	17.5	16.20	6.21	Clay	CL/CH	stiff	125	13		100			0.91	8.27
5.48	18.0	19.16	5.98	Clay	CL/CH	very stiff	125	15		100			1.08	>10
5.65	18.5	15.49	6.80	Clay	CL/CH	stiff	125	12		100			0.86	7.13
5.80	19.0	15.81	6.89	Clay	CL/CH	stiff	125	13		100			0.88	7.13
5.95	19.5	16.32	7.00	Clay	CL/CH	stiff	125	13		100			0.91	7.27
6.10	20.0	17.26	5.95	Clay	CL/CH	stiff	125	14		100			0.97	7.85
6.25	20.5	13.28	5.76	Clay	CL/CH	stiff	125	11		100			0.73	4.89
6.40	21.0	11.14	6.84	Clay	CL/CH	stiff	125	9		100			0.60	3.58
6.55	21.5	12.48	7.40	Clay	CL/CH	stiff	125	10		100			0.68	4.18
6.70	22.0	14.92	7.62	Clay	CL/CH	stiff	125	12		100			0.82	5.42
6.85	22.5	17.77	6.98	Clay	CL/CH	stiff	125	14		100			0.99	7.00
7.00	23.0	21.45	7.34	Clay	CL/CH	very stiff	125	17		100			1.21	9.59
7.18	23.5	24.58	7.84	Clay	CL/CH	very stiff	125	20		100			1.39	>10
7.33	24.0	51.65	3.68	Clayey Silt to Silty Clay	ML/CL	hard	120	21		70			2.98	>10
7.48	24.5	34.37	4.91	Clay	CL/CH	very stiff	125	27		90			1.96	>10
7.63	25.0	18.84	5.44	Clay	CL/CH	very stiff	125	15		100			1.05	6.76
7.78	25.5	21.09	6.11	Clay	CL/CH	very stiff	125	17		100			1.18	8.00
7.93	26.0	26.12	5.49	Clay	CL/CH	very stiff	125	21		100			1.48	>10
8.08	26.5	26.28	5.55	Clay	CL/CH	very stiff	125	21		100			1.48	>10
8.23	27.0	21.92	5.06	Clay	CL/CH	very stiff	125	18		100			1.23	7.85
8.38	27.5	23.63	6.15	Clay	CL/CH	very stiff	125	19		100			1.33	8.85
8.53	28.0	20.49	6.07	Clay	CL/CH	very stiff	125	16		100			1.14	6.65
8.68	28.5	19.11	5.87	Clay	CL/CH	very stiff	125	15		100			1.06	5.88
8.85	29.0	18.15	5.24	Clay	CL/CH	very stiff	125	15		100			1.00	5.21
9.00	29.5	21.72	6.18	Clay	CL/CH	very stiff	125	17		100			1.21	6.88
9.15	30.0	20.63	6.55	Clay	CL/CH	very stiff	125	17		100			1.15	6.21
9.30	30.5	22.90	7.51	Clay	CL/CH	very stiff	125	18		100			1.28	7.13
9.45	31.0	20.57	6.23	Clay	CL/CH	very stiff	125	16		100			1.14	5.88
9.60	31.5	19.55	6.90	Clay	CL/CH	very stiff	125	16		100			1.08	5.31
9.75	32.0	23.76	8.37	Clay	CL/CH	very stiff	125	19		100			1.33	7.13
9.90	32.5	24.30	8.05	Clay	CL/CH	very stiff	125	19		100			1.36	7.27
10.05	33.0	22.78	6.54	Clay	CL/CH	very stiff	125	18		100			1.27	6.32
10.20	33.5	21.56	5.91	Clay	CL/CH	very stiff	125	17		100			1.19	5.76
10.38	34.0	20.82	6.40	Clay	CL/CH	very stiff	125	17		100			1.15	5.31
10.53	34.5	21.17	6.04	Clay	CL/CH	very stiff	125	17		100			1.17	5.31
10.68	35.0	24.71	6.05	Clay	CL/CH	very stiff	125	20		100			1.38	6.65
10.83	35.5	23.14	5.91	Clay	CL/CH	very stiff	125	19		100			1.28	5.88
10.98	36.0	19.96	5.21	Clay	CL/CH	very stiff	125	16		100			1.10	4.57
11.13	36.5	19.03	4.88	Clay	CL/CH	very stiff	125	15		100			1.04	4.18
11.28	37.0	16.19	4.33	Clay	CL/CH	stiff	125	13		100			0.87	3.28
11.43	37.5	16.02	5.36	Clay	CL/CH	stiff	125	13		100			0.86	3.14
11.58	38.0	16.15	5.06	Clay	CL/CH	stiff	125	13		100			0.87	3.14
11.73	38.5	17.81	4.75	Clay	CL/CH	stiff	125	14		100			0.96	3.50

LANDMARK CONSULTANTS, INC.

CONE PENETROMETER INTERPRETATION (based on Robertson & Campanella, 1989, refer to Key to CPT logs)

Project: Heber 2 Repower Project - Heber, CA **Project No:** LE19075 **Date:** 12/20/2004

CONE SOUNDING: CPT-3
Est. GWT (ft): 8
Phi Correlation: 0 0-Schm(78),1-R&C(83),2-PHT(74)

Base Depth (m)	Base Depth (ft)	Avg Tip Qc, tsf	Avg Friction Ratio, %	Soil Classification	USCS	Density or Consistency	Est. Density (pcf)	SPT N(60)	Norm. Qc1n	Est. % Fines	Rel. Dens. Dr (%)	Nk: Phi (deg.)	17 Su (tsf)	OCR
11.88	39.0	21.66	4.41	Silty Clay to Clay	CL	very stiff	125	12		100			1.19	6.00
12.05	39.5	20.18	3.42	Clayey Silt to Silty Clay	ML/CL	very stiff	120	8		100			1.10	7.13
12.20	40.0	17.00	2.62	Clayey Silt to Silty Clay	ML/CL	stiff	120	7		100			0.91	5.31
12.35	40.5	20.64	4.32	Silty Clay to Clay	CL	very stiff	125	12		100			1.13	5.31
12.50	41.0	33.91	4.01	Clayey Silt to Silty Clay	ML/CL	very stiff	120	14		100			1.91	>10
12.65	41.5	31.64	4.64	Silty Clay to Clay	CL	very stiff	125	18		100			1.77	>10
12.80	42.0	23.58	3.56	Clayey Silt to Silty Clay	ML/CL	very stiff	120	9		100			1.30	8.70
12.95	42.5	24.97	3.28	Clayey Silt to Silty Clay	ML/CL	very stiff	120	10		100			1.38	9.79
13.10	43.0	19.07	2.71	Clayey Silt to Silty Clay	ML/CL	very stiff	120	8		100			1.03	5.88
13.25	43.5	18.86	2.98	Clayey Silt to Silty Clay	ML/CL	very stiff	120	8		100			1.02	5.65
13.40	44.0	19.54	3.20	Clayey Silt to Silty Clay	ML/CL	very stiff	120	8		100			1.06	5.88
13.58	44.5	19.29	3.97	Silty Clay to Clay	CL	very stiff	125	11		100			1.04	4.18
13.73	45.0	19.79	3.86	Silty Clay to Clay	CL	very stiff	125	11		100			1.07	4.28
13.88	45.5	17.66	3.31	Clayey Silt to Silty Clay	ML/CL	stiff	120	7		100			0.94	4.76
14.03	46.0	16.42	2.18	Clayey Silt to Silty Clay	ML/CL	stiff	120	7		100			0.87	4.18
14.18	46.5	15.61	2.35	Clayey Silt to Silty Clay	ML/CL	stiff	120	6		100			0.82	3.74
14.33	47.0	16.68	1.80	Sandy Silt to Clayey Silt	ML	very loose	115	5	12.5	100	11	30		
14.48	47.5	18.25	1.80	Sandy Silt to Clayey Silt	ML	very loose	115	5	13.7	100	14	30		
14.63	48.0	19.39	2.43	Clayey Silt to Silty Clay	ML/CL	very stiff	120	8		100			1.04	5.21
14.78	48.5	19.39	3.87	Silty Clay to Clay	CL	very stiff	125	11		100			1.04	3.83
14.93	49.0	19.13	2.69	Clayey Silt to Silty Clay	ML/CL	very stiff	120	8		100			1.02	4.89
15.10	49.5	16.46	1.59	Sandy Silt to Clayey Silt	ML	very loose	115	5	12.1	100	10	29		
15.25	50.0	16.91	2.83	Clayey Silt to Silty Clay	ML/CL	stiff	120	7		100			0.89	3.91

CLIENT: Ormat Nevada Inc
PROJECT: Heber 2 Repower Project - Heber, CA

CONE PENETROMETER: Middle Earth Geotesting Truck Mounted Electric Cone with 23 ton reaction weight

LOCATION: See Site and Boring Location Plan

DATE: 5/2/2007

CONE SOUNDING DATA CPT-4

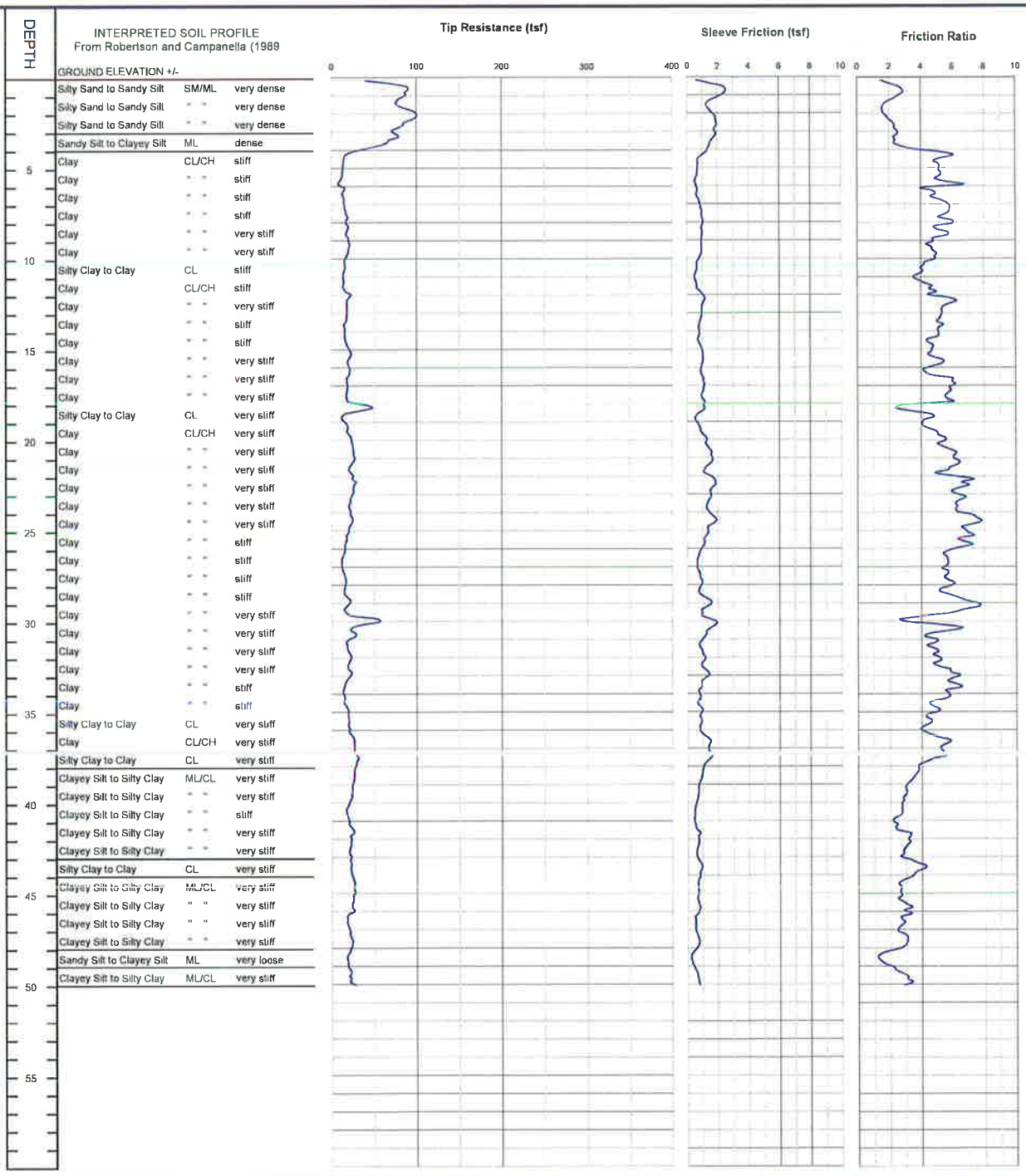

Project No.		PLATE
LE19075	LANDMARK Geo-Engineers and Geologists	B-4

LANDMARK CONSULTANTS, INC.

CONE PENETROMETER INTERPRETATION (based on Robertson & Campanella, 1989, refer to Key to CPT logs)

Project: Heber 2 Repower Project - Heber, CA **Project No:** LE19075 **Date:** 5/2/2007

CONE SOUNDING: CPT-4
Est. GWT (ft): 8
Phi Correlation: 0 0-Schm(78),1-R&C(83),2-PHT(74)

Base Depth (m)	Base Depth (ft)	Avg Tip Qc, tsf	Avg Friction Ratio, %	Soil Classification	USCS	Density or Consistency	Est. Density (pcf)	SPT N(60)	Norm. Qc1n	Est. % Fines	Rel. Dens. Dr (%)	Nk: Phi (deg.)	17 Su (tsf)	OCR
0.15	0.5	66.25	2.04	Silty Sand to Sandy Silt	SM/ML	very dense	115	15	125.2	35	122	45		
0.30	1.0	88.18	2.75	Sandy Silt to Clayey Silt	ML	very dense	115	25	166.7	35	114	44		
0.45	1.5	77.73	1.95	Silty Sand to Sandy Silt	SM/ML	very dense	115	17	146.9	30	103	42		
0.60	2.0	92.53	1.60	Silty Sand to Sandy Silt	SM/ML	very dense	115	21	174.9	25	103	42		
0.75	2.5	93.95	2.02	Silty Sand to Sandy Silt	SM/ML	very dense	115	21	177.6	25	100	42		
0.93	3.0	77.68	2.40	Silty Sand to Sandy Silt	SM/ML	very dense	115	17	146.8	35	91	41		
1.08	3.5	74.47	2.39	Sandy Silt to Clayey Silt	ML	dense	115	21	140.8	35	88	40		
1.23	4.0	52.73	2.83	Sandy Silt to Clayey Silt	ML	dense	115	15	99.7	45	75	39		
1.38	4.5	18.49	5.55	Clay	CL/CH	very stiff	125	15		90			1.07	>10
1.53	5.0	13.75	5.02	Clay	CL/CH	stiff	125	11		100			0.79	>10
1.68	5.5	12.39	5.11	Clay	CL/CH	stiff	125	10		100			0.71	>10
1.83	6.0	10.98	5.45	Clay	CL/CH	stiff	125	9		100			0.63	>10
1.98	6.5	13.51	4.77	Clay	CL/CH	stiff	125	11		95			0.77	>10
2.13	7.0	14.72	5.56	Clay	CL/CH	stiff	125	12		100			0.84	>10
2.28	7.5	16.58	5.71	Clay	CL/CH	stiff	125	13		95			0.95	>10
2.45	8.0	17.99	5.72	Clay	CL/CH	very stiff	125	14		95			1.03	>10
2.60	8.5	18.67	5.21	Clay	CL/CH	very stiff	125	15		90			1.07	>10
2.75	9.0	19.02	5.07	Clay	CL/CH	very stiff	125	15		90			1.09	>10
2.90	9.5	20.56	4.59	Clay	CL/CH	very stiff	125	16		85			1.18	>10
3.05	10.0	17.46	4.91	Clay	CL/CH	stiff	125	14		90			1.00	>10
3.20	10.5	15.45	4.14	Clay	CL/CH	stiff	125	12		90			0.88	>10
3.35	11.0	13.93	3.83	Silty Clay to Clay	CL	stiff	125	8		95			0.79	>10
3.50	11.5	13.83	4.23	Clay	CL/CH	stiff	125	11		100			0.78	>10
3.65	12.0	18.01	4.65	Clay	CL/CH	very stiff	125	14		95			1.02	>10
3.80	12.5	18.70	5.93	Clay	CL/CH	very stiff	125	15		100			1.06	>10
3.95	13.0	18.01	5.35	Clay	CL/CH	very stiff	125	14		100			1.02	>10
4.13	13.5	17.39	5.15	Clay	CL/CH	stiff	125	14		100			0.99	>10
4.28	14.0	14.93	5.20	Clay	CL/CH	stiff	125	12		100			0.84	9.59
4.43	14.5	15.49	4.86	Clay	CL/CH	stiff	125	12		100			0.87	>10
4.58	15.0	18.22	4.65	Clay	CL/CH	very stiff	125	15		100			1.03	>10
4.73	15.5	22.11	4.64	Clay	CL/CH	very stiff	125	18		90			1.26	>10
4.88	16.0	19.85	4.92	Clay	CL/CH	very stiff	125	16		100			1.13	>10
5.03	16.5	19.77	4.96	Clay	CL/CH	very stiff	125	16		100			1.12	>10
5.18	17.0	18.38	5.96	Clay	CL/CH	very stiff	125	15		100			1.04	>10
5.33	17.5	17.64	5.69	Clay	CL/CH	stiff	125	14		100			0.99	9.79
5.48	18.0	25.50	4.80	Clay	CL/CH	very stiff	125	20		90			1.45	>10
5.65	18.5	32.47	3.36	Clayey Silt to Silty Clay	ML/CL	very stiff	120	13		75			1.86	>10
5.80	19.0	13.48	4.36	Clay	CL/CH	stiff	125	11		100			0.75	5.53
5.95	19.5	18.41	4.55	Clay	CL/CH	very stiff	125	15		100			1.03	9.00
6.10	20.0	22.07	5.36	Clay	CL/CH	very stiff	125	18		100			1.25	>10
6.25	20.5	24.57	5.40	Clay	CL/CH	very stiff	125	20		100			1.40	>10
6.40	21.0	26.18	6.13	Clay	CL/CH	very stiff	125	21		100			1.49	>10
6.55	21.5	23.24	6.19	Clay	CL/CH	very stiff	125	19		100			1.31	>10
6.70	22.0	22.66	5.55	Clay	CL/CH	very stiff	125	18		100			1.28	>10
6.85	22.5	26.25	6.97	Clay	CL/CH	very stiff	125	21		100			1.49	>10
7.00	23.0	25.11	6.17	Clay	CL/CH	very stiff	125	20		100			1.42	>10
7.18	23.5	22.18	6.48	Clay	CL/CH	very stiff	125	18		100			1.25	>10
7.33	24.0	21.09	6.24	Clay	CL/CH	very stiff	125	17		100			1.18	8.70
7.48	24.5	23.54	7.51	Clay	CL/CH	very stiff	125	19		100			1.33	>10
7.63	25.0	21.31	6.90	Clay	CL/CH	very stiff	125	17		100			1.19	8.41
7.78	25.5	18.21	6.87	Clay	CL/CH	very stiff	125	15		100			1.01	6.21
7.93	26.0	15.91	6.78	Clay	CL/CH	stiff	125	13		100			0.88	4.89
8.08	26.5	13.54	5.59	Clay	CL/CH	stiff	125	11		100			0.74	3.66
8.23	27.0	11.78	5.53	Clay	CL/CH	stiff	125	9		100			0.63	3.00
8.38	27.5	14.49	5.56	Clay	CL/CH	stiff	125	12		100			0.79	3.91
8.53	28.0	16.02	5.84	Clay	CL/CH	stiff	125	13		100			0.88	4.47
8.68	28.5	15.04	5.37	Clay	CL/CH	stiff	125	12		100			0.82	3.91
8.85	29.0	20.59	6.98	Clay	CL/CH	very stiff	125	16		100			1.15	6.43
9.00	29.5	16.05	6.66	Clay	CL/CH	stiff	125	13		100			0.88	4.18
9.15	30.0	44.48	3.37	Clayey Silt to Silty Clay	ML/CL	hard	120	18		75			2.55	>10
9.30	30.5	27.03	5.86	Clay	CL/CH	very stiff	125	22		100			1.52	9.79
9.45	31.0	24.88	4.56	Clay	CL/CH	very stiff	125	20		100			1.39	8.14
9.60	31.5	17.85	4.68	Clay	CL/CH	stiff	125	14		100			0.98	4.57
9.75	32.0	21.43	4.98	Clay	CL/CH	very stiff	125	17		100			1.19	6.00
9.90	32.5	19.94	5.01	Clay	CL/CH	very stiff	125	16		100			1.10	5.21
10.05	33.0	21.67	6.03	Clay	CL/CH	very stiff	125	17		100			1.20	5.88
10.20	33.5	17.09	5.96	Clay	CL/CH	stiff	125	14		100			0.93	3.91
10.38	34.0	13.75	5.92	Clay	CL/CH	stiff	125	11		100			0.73	2.91
10.53	34.5	14.75	5.27	Clay	CL/CH	stiff	125	12		100			0.79	3.14
10.68	35.0	17.80	4.91	Clay	CL/CH	stiff	125	14		100			0.97	3.91
10.83	35.5	19.50	4.45	Clay	CL/CH	very stiff	125	16		100			1.07	4.47
10.98	36.0	20.06	4.23	Silty Clay to Clay	CL	very stiff	125	11		100			1.10	6.00
11.13	36.5	23.73	5.01	Clay	CL/CH	very stiff	125	19		100			1.32	6.00
11.28	37.0	26.37	5.33	Clay	CL/CH	very stiff	125	21		100			1.47	6.88
11.43	37.5	29.22	5.23	Clay	CL/CH	very stiff	125	23		100			1.64	8.14
11.58	38.0	28.26	4.00	Silty Clay to Clay	CL	very stiff	125	16		100			1.58	>10
11.73	38.5	26.29	3.66	Clayey Silt to Silty Clay	ML/CL	very stiff	120	11		100			1.46	>10

LANDMARK CONSULTANTS, INC.

CONE PENETROMETER INTERPRETATION (based on Robertson & Campanella, 1989, refer to Key to CPT logs)

Project: Heber 2 Repower Project - Heber, CA **Project No:** LE19075 **Date:** 5/2/2007

CONE SOUNDING: CPT-4

Est. GWT (ft): 8

Phi Correlation: 0 0-Schm(78),1-R&C(83),2-PHT(74)

Base Depth (m)	Base Depth (ft)	Avg Tip Qc, tsf	Avg Friction Ratio, %	Soil Classification	USCS	Density or Consistency	Est. Density (pcf)	SPT N(60)	Norm. Qc1n	Est. % Fines	Rel. Dens. Dr (%)	Nk: Phi (deg.)	17 Su (tsf)	OCR
11.88	39.0	24.98	3.19	Clayey Silt to Silty Clay	ML/CL	very stiff	120	10		100			1.39	>10
12.05	39.5	23.62	3.00	Clayey Silt to Silty Clay	ML/CL	very stiff	120	9		100			1.30	>10
12.20	40.0	21.78	2.80	Clayey Silt to Silty Clay	ML/CL	very stiff	120	9		100			1.20	8.27
12.35	40.5	17.57	2.75	Clayey Silt to Silty Clay	ML/CL	stiff	120	7		100			0.95	5.53
12.50	41.0	19.10	2.36	Clayey Silt to Silty Clay	ML/CL	very stiff	120	8		100			1.04	6.32
12.65	41.5	22.54	2.42	Clayey Silt to Silty Clay	ML/CL	very stiff	120	9		100			1.24	8.27
12.80	42.0	23.41	3.23	Clayey Silt to Silty Clay	ML/CL	very stiff	120	9		100			1.29	8.70
12.95	42.5	22.05	3.08	Clayey Silt to Silty Clay	ML/CL	very stiff	120	9		100			1.21	7.70
13.10	43.0	21.46	2.78	Clayey Silt to Silty Clay	ML/CL	very stiff	120	9		100			1.17	7.13
13.25	43.5	22.21	3.76	Silty Clay to Clay	CL	very stiff	125	13		100			1.21	5.42
13.40	44.0	22.69	3.76	Silty Clay to Clay	CL	very stiff	125	13		100			1.24	5.53
13.58	44.5	25.69	2.81	Clayey Silt to Silty Clay	ML/CL	very stiff	120	10		100			1.42	9.59
13.73	45.0	26.50	2.66	Clayey Silt to Silty Clay	ML/CL	very stiff	120	11		100			1.46	>10
13.88	45.5	25.22	2.66	Clayey Silt to Silty Clay	ML/CL	very stiff	120	10		100			1.39	8.85
14.03	46.0	24.83	3.10	Clayey Silt to Silty Clay	ML/CL	very stiff	120	10		100			1.36	8.41
14.18	46.5	18.88	2.93	Clayey Silt to Silty Clay	ML/CL	very stiff	120	8		100			1.01	5.21
14.33	47.0	19.43	2.64	Clayey Silt to Silty Clay	ML/CL	very stiff	120	8		100			1.05	5.31
14.48	47.5	22.40	3.03	Clayey Silt to Silty Clay	ML/CL	very stiff	120	9		100			1.22	6.65
14.63	48.0	23.12	2.75	Clayey Silt to Silty Clay	ML/CL	very stiff	120	9		100			1.26	7.00
14.78	48.5	18.94	1.38	Sandy Silt to Clayey Silt	ML	very loose	115	5	14.1	100	15	30		
14.93	49.0	18.77	1.78	Sandy Silt to Clayey Silt	ML	very loose	115	5	13.9	100	14	30		
15.10	49.5	21.59	2.73	Clayey Silt to Silty Clay	ML/CL	very stiff	120	9		100			1.17	6.00
15.25	50.0	23.82	3.12	Clayey Silt to Silty Clay	ML/CL	very stiff	120	10		100			1.30	6.88

CLIENT: Ormat Nevada Inc
PROJECT: Heber 2 Repower Project - Heber, CA

CONE PENETROMETER: Middle Earth Geotesting Truck Mounted Electric Cone with 23 ton reaction weight

LOCATION: See Site and Boring Location Plan

DATE: 5/2/2007

CONE SOUNDING DATA CPT-5

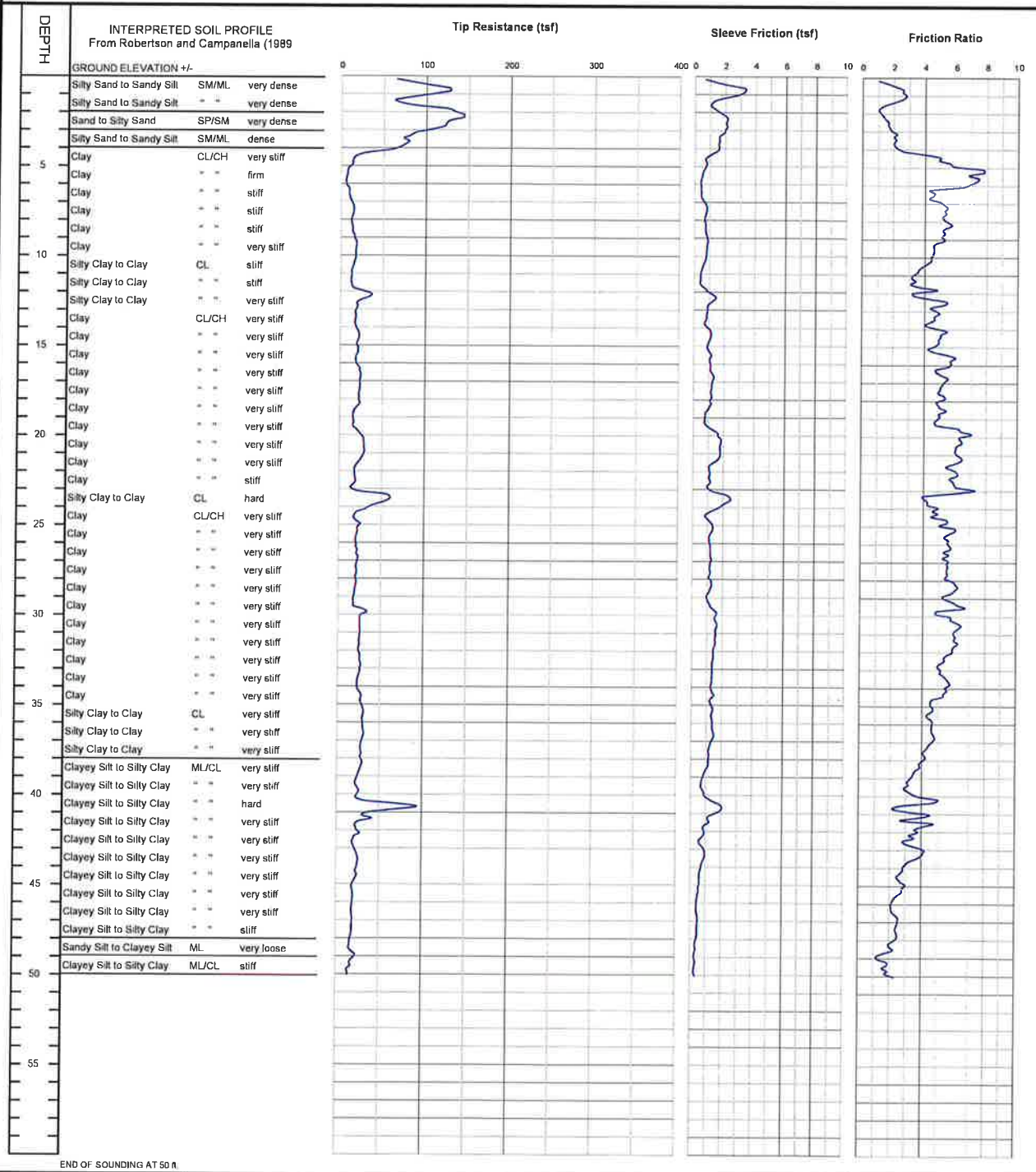

Project No.		PLATE
LE19075	LANDMARK Geo-Engineers and Geologists	B-5

LANDMARK CONSULTANTS, INC.

CONE PENETROMETER INTERPRETATION (based on Robertson & Campanella, 1989, refer to Key to CPT logs)

Project: Heber 2 Repower Project - Heber, CA **Project No:** LE19075 **Date:** 5/2/2007

CONE SOUNDING: CPT-5
Est. GWT (ft): 8
Phi Correlation: 0 0-Schm(78),1-R&C(83),2-PHT(74)

Base Depth (m)	Base Depth (ft)	Avg Tip Qc, tsf	Avg Friction Ratio, %	Soil Classification	USCS	Density or Consistency	Est. Density (pcf)	SPT N(60)	Norm. Qc1n	Est. % Fines	Rel. Dens. Dr (%)	Nk: Phi (deg.)	17 Su (tsf)	OCR
0.15	0.5	85.14	1.61	Silty Sand to Sandy Silt	SM/ML	very dense	115	19	161.0	25	130	46		
0.30	1.0	120.36	2.66	Silty Sand to Sandy Silt	SM/ML	very dense	115	27	227.5	30	124	45		
0.45	1.5	72.28	2.13	Silty Sand to Sandy Silt	SM/ML	very dense	115	16	136.6	30	101	42		
0.60	2.0	116.67	1.12	Sand to Silty Sand	SP/SM	very dense	115	21	220.6	15	110	43		
0.75	2.5	138.05	1.48	Sand to Silty Sand	SP/SM	very dense	115	25	261.0	15	111	44		
0.93	3.0	117.13	1.76	Silty Sand to Sandy Silt	SM/ML	very dense	115	26	221.4	20	104	42		
1.08	3.5	81.23	2.12	Silty Sand to Sandy Silt	SM/ML	very dense	115	18	153.5	30	90	41		
1.23	4.0	74.63	2.12	Silty Sand to Sandy Silt	SM/ML	dense	115	17	141.1	30	86	40		
1.38	4.5	34.90	3.90	Clayey Silt to Silty Clay	ML/CL	hard	120	14		60			2.04	>10
1.53	5.0	13.76	5.45	Clay	CL/CH	stiff	125	11		100			0.79	>10
1.68	5.5	7.57	7.44	Clay	CL/CH	firm	125	6		100			0.43	>10
1.83	6.0	5.99	6.88	Clay	CL/CH	firm	125	5		100			0.33	6.10
1.98	6.5	9.47	4.51	Clay	CL/CH	stiff	125	8		100			0.54	>10
2.13	7.0	11.69	4.84	Clay	CL/CH	stiff	125	9		100			0.66	>10
2.28	7.5	14.81	5.37	Clay	CL/CH	stiff	125	12		95			0.85	>10
2.45	8.0	13.05	5.28	Clay	CL/CH	stiff	125	10		100			0.74	>10
2.60	8.5	13.41	5.40	Clay	CL/CH	stiff	125	11		100			0.76	>10
2.75	9.0	15.40	5.21	Clay	CL/CH	stiff	125	12		95			0.88	>10
2.90	9.5	18.24	4.66	Clay	CL/CH	very stiff	125	15		85			1.04	>10
3.05	10.0	17.49	4.50	Clay	CL/CH	stiff	125	14		90			1.00	>10
3.20	10.5	16.07	4.15	Clay	CL/CH	stiff	125	13		90			0.91	>10
3.35	11.0	13.34	3.48	Silty Clay to Clay	CL	stiff	125	8		95			0.75	>10
3.50	11.5	12.52	3.24	Silty Clay to Clay	CL	stiff	125	7		95			0.70	>10
3.65	12.0	18.93	3.91	Silty Clay to Clay	CL	very stiff	125	11		85			1.08	>10
3.80	12.5	31.15	4.38	Silty Clay to Clay	CL	very stiff	125	18		75			1.80	>10
3.95	13.0	19.46	4.78	Clay	CL/CH	very stiff	125	16		95			1.11	>10
4.13	13.5	17.74	4.74	Clay	CL/CH	very stiff	125	14		100			1.01	>10
4.28	14.0	17.58	4.34	Clay	CL/CH	stiff	125	14		95			1.00	>10
4.43	14.5	21.21	5.18	Clay	CL/CH	very stiff	125	17		95			1.21	>10
4.58	15.0	20.43	4.83	Clay	CL/CH	very stiff	125	16		95			1.16	>10
4.73	15.5	20.79	4.75	Clay	CL/CH	very stiff	125	17		95			1.18	>10
4.88	16.0	18.89	5.75	Clay	CL/CH	very stiff	125	15		100			1.07	>10
5.03	16.5	23.41	4.88	Clay	CL/CH	very stiff	125	19		95			1.33	>10
5.18	17.0	23.59	5.34	Clay	CL/CH	very stiff	125	19		95			1.34	>10
5.33	17.5	23.27	4.98	Clay	CL/CH	very stiff	125	19		95			1.32	>10
5.48	18.0	22.19	5.13	Clay	CL/CH	very stiff	125	18		100			1.26	>10
5.65	18.5	20.81	5.10	Clay	CL/CH	very stiff	125	17		100			1.18	>10
5.80	19.0	15.78	4.92	Clay	CL/CH	stiff	125	13		100			0.88	7.13
5.95	19.5	16.06	5.23	Clay	CL/CH	stiff	125	13		100			0.90	7.00
6.10	20.0	22.81	6.58	Clay	CL/CH	very stiff	125	18		100			1.29	>10
6.25	20.5	28.53	6.30	Clay	CL/CH	very stiff	125	23		100			1.63	>10
6.40	21.0	28.99	6.06	Clay	CL/CH	very stiff	125	23		100			1.65	>10
6.55	21.5	24.82	6.26	Clay	CL/CH	very stiff	125	20		100			1.41	>10
6.70	22.0	18.48	5.79	Clay	CL/CH	very stiff	125	15		100			1.03	7.70
6.85	22.5	18.41	5.89	Clay	CL/CH	very stiff	125	15		100			1.03	7.41
7.00	23.0	15.96	6.46	Clay	CL/CH	stiff	125	13		100			0.88	5.76
7.18	23.5	46.63	4.62	Silty Clay to Clay	CL	hard	125	27		75			2.69	>10
7.33	24.0	47.09	4.48	Silty Clay to Clay	CL	hard	125	27		75			2.71	>10
7.48	24.5	23.27	4.67	Clay	CL/CH	very stiff	125	19		100			1.31	>10
7.63	25.0	21.09	5.34	Clay	CL/CH	very stiff	125	17		100			1.18	8.27
7.78	25.5	21.71	5.85	Clay	CL/CH	very stiff	125	17		100			1.22	8.41
7.93	26.0	19.90	5.47	Clay	CL/CH	very stiff	125	16		100			1.11	7.00
8.08	26.5	20.78	5.59	Clay	CL/CH	very stiff	125	17		100			1.16	7.41
8.23	27.0	21.98	5.44	Clay	CL/CH	very stiff	125	18		100			1.23	8.00
8.38	27.5	20.73	5.53	Clay	CL/CH	very stiff	125	17		100			1.16	6.88
8.53	28.0	20.36	5.62	Clay	CL/CH	very stiff	125	16		100			1.13	6.54
8.68	28.5	19.99	6.11	Clay	CL/CH	very stiff	125	16		100			1.11	6.21
8.85	29.0	18.33	5.49	Clay	CL/CH	very stiff	125	15		100			1.01	5.31
9.00	29.5	17.78	6.27	Clay	CL/CH	stiff	125	14		100			0.98	4.89
9.15	30.0	29.76	5.16	Clay	CL/CH	very stiff	125	24		100			1.68	>10
9.30	30.5	25.36	6.14	Clay	CL/CH	very stiff	125	20		100			1.42	8.56
9.45	31.0	25.65	6.08	Clay	CL/CH	very stiff	125	21		100			1.44	8.56
9.60	31.5	24.99	6.11	Clay	CL/CH	very stiff	125	20		100			1.40	8.00
9.75	32.0	24.42	5.93	Clay	CL/CH	very stiff	125	20		100			1.37	7.41
9.90	32.5	25.69	5.42	Clay	CL/CH	very stiff	125	21		100			1.44	8.00
10.05	33.0	26.43	5.06	Clay	CL/CH	very stiff	125	21		100			1.48	8.27
10.20	33.5	24.95	5.31	Clay	CL/CH	very stiff	125	20		100			1.39	7.27
10.38	34.0	22.88	5.62	Clay	CL/CH	very stiff	125	18		100			1.27	6.21
10.53	34.5	25.51	5.40	Clay	CL/CH	very stiff	125	20		100			1.42	7.27
10.68	35.0	27.31	4.56	Silty Clay to Clay	CL	very stiff	125	16		100			1.53	>10
10.83	35.5	30.04	4.55	Silty Clay to Clay	CL	very stiff	125	17		100			1.69	>10
10.98	36.0	29.52	4.52	Silty Clay to Clay	CL	very stiff	125	17		100			1.66	>10
11.13	36.5	30.25	4.64	Silty Clay to Clay	CL	very stiff	125	17		100			1.70	>10
11.28	37.0	29.39	4.68	Silty Clay to Clay	CL	very stiff	125	17		100			1.65	>10
11.43	37.5	27.60	4.22	Silty Clay to Clay	CL	very stiff	125	16		100			1.54	>10
11.58	38.0	27.92	4.11	Silty Clay to Clay	CL	very stiff	125	16		100			1.56	>10
11.73	38.5	28.57	3.77	Clayey Silt to Silty Clay	ML/CL	very stiff	120	11		100			1.60	>10

LANDMARK CONSULTANTS, INC.

CONE PENETROMETER INTERPRETATION (based on Robertson & Campanella, 1989, refer to Key to CPT logs)

Project: Heber 2 Repower Project - Heber, CA **Project No:** LE19075 **Date:** 5/2/2007

CONE SOUNDING: CPT-5
Est. GWT (ft): 8
Phi Correlation: 0 0-Schm(78),1-R&C(83),2-PHT(74)

Base Depth (m)	Base Depth (ft)	Avg Tip Qc, tsf	Avg Friction Ratio, %	Soil Classification	USCS	Density or Consistency	Est. Density (pcf)	SPT N(60)	Norm. Qc1n	Est. % Fines	Rel. Dens. Dr (%)	Nk: Phi (deg.)	17 Su (tsf)	OCR
11.88	39.0	24.62	3.37	Clayey Silt to Silty Clay	ML/CL	very stiff	120	10		100			1.36	>10
12.05	39.5	22.28	3.04	Clayey Silt to Silty Clay	ML/CL	very stiff	120	9		100			1.23	8.70
12.20	40.0	24.64	3.45	Clayey Silt to Silty Clay	ML/CL	very stiff	120	10		100			1.36	>10
12.35	40.5	41.78	4.14	Clayey Silt to Silty Clay	ML/CL	hard	120	17		95			2.37	>10
12.50	41.0	64.96	3.22	Sandy Silt to Clayey Silt	ML	medium dense	115	19	51.8	70	53	35		
12.65	41.5	32.37	3.75	Clayey Silt to Silty Clay	ML/CL	very stiff	120	13		100			1.82	>10
12.80	42.0	22.75	3.82	Silty Clay to Clay	CL	very stiff	125	13		100			1.25	6.00
12.95	42.5	22.78	3.20	Clayey Silt to Silty Clay	ML/CL	very stiff	120	9		100			1.25	8.14
13.10	43.0	19.79	3.62	Silty Clay to Clay	CL	very stiff	125	11		100			1.07	4.57
13.25	43.5	23.86	3.91	Silty Clay to Clay	CL	very stiff	125	14		100			1.31	6.10
13.40	44.0	24.93	3.00	Clayey Silt to Silty Clay	ML/CL	very stiff	120	10		100			1.37	9.19
13.58	44.5	23.46	2.65	Clayey Silt to Silty Clay	ML/CL	very stiff	120	9		100			1.29	8.00
13.73	45.0	21.13	2.78	Clayey Silt to Silty Clay	ML/CL	very stiff	120	8		100			1.15	6.54
13.88	45.5	19.10	2.73	Clayey Silt to Silty Clay	ML/CL	very stiff	120	8		100			1.03	5.42
14.03	46.0	19.63	2.23	Clayey Silt to Silty Clay	ML/CL	very stiff	120	8		100			1.06	5.65
14.18	46.5	18.74	2.12	Clayey Silt to Silty Clay	ML/CL	very stiff	120	7		100			1.01	5.10
14.33	47.0	18.93	2.49	Clayey Silt to Silty Clay	ML/CL	very stiff	120	8		100			1.02	5.10
14.48	47.5	18.85	2.42	Clayey Silt to Silty Clay	ML/CL	very stiff	120	8		100			1.01	5.00
14.63	48.0	17.53	2.38	Clayey Silt to Silty Clay	ML/CL	stiff	120	7		100			0.93	4.37
14.78	48.5	16.01	2.08	Clayey Silt to Silty Clay	ML/CL	stiff	120	6		100			0.84	3.74
14.93	49.0	20.91	1.36	Sandy Silt to Clayey Silt	ML	very loose	115	6	15.5	100	17	30		
15.10	49.5	17.29	1.76	Sandy Silt to Clayey Silt	ML	very loose	115	5	12.8	100	12	30		
15.25	50.0	13.85	1.98	Clayey Silt to Silty Clay	ML/CL	stiff	120	6		100			0.71	3.00

Simplified Soil Classification Chart

After Robertson & Campanella (1989)

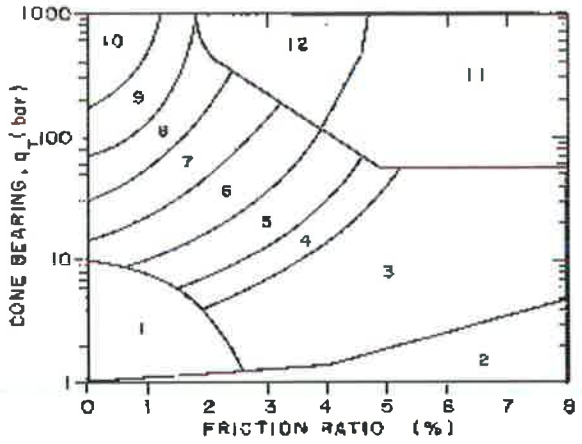

Geotechnical Parameters from CPT Data:

Equivalent SPT N(60) blow count = Qc/(Qc/N Ratio)
N1(60) = Cn*N(60) Normalized SPT blow count
Cn = 1/(p'o)^0.5 < 1.6 max. from Liao & Whitman (1986)
p'o = effective overburden pressure (tsf) using unit densities given below and estimated groundwater table.
Dr = Relative density (%) from Jamiolkowski et. al. (1986) relationship
= -98 +68*log(Qc/p'o^0.5) where Qc, p'o in tonne/sqm
Note: 1 tonne/sqm = 0.1024 tsf, 1 bar =1.0443 tsf
Phi = Friction Angle estimated from either:
1. Roberton & Campanella (1983) chart:
Phi = 5.3 + 24*(log(Qc/p'o))+3(log(Qc/p'o))^2
2. Peck, Hansen & Thornburn (1974) N-Phi Correlation
3. Schmertman (1978) chart [Phi = 28+0.14*Dr for fine uniform sands]
Su = undrained shear strength (tsf)
= (Qc-p'o)/Nk where Nk varies from 10 to 22, 17 for OC clays
OCR = Overconsolidation Ratio estimated from Schmertman (1978) chart using Su/p'o ratio and estimated normal consolidated Su/p'o

Variation of Qc/N Ratio with Grain Size

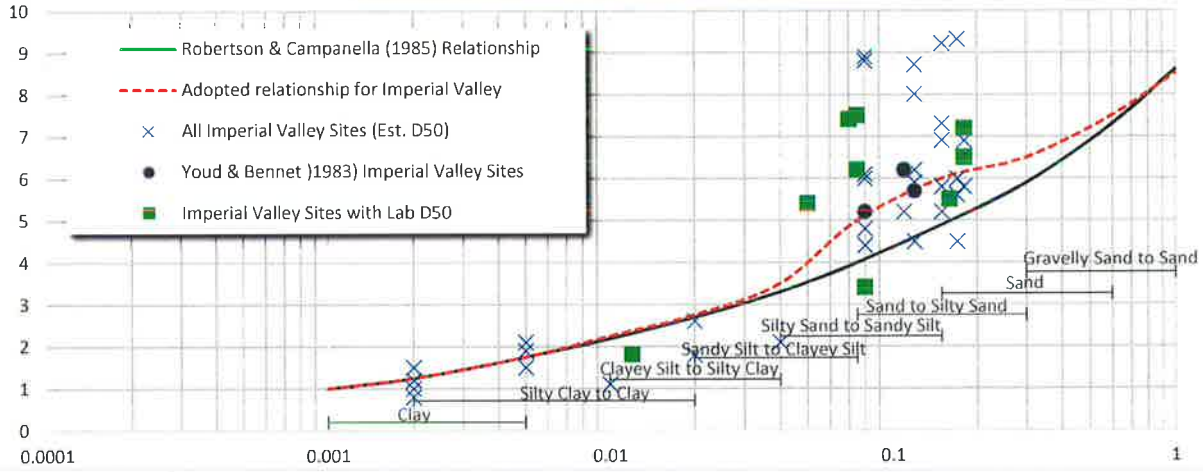

Note: Assumed Properties and Adopted Qc/N Ratio based on correlations from Imperial Valley, California soils

Table of Soil Types and Assumed Properties

Zone	Soil Classification	UCS	Density (pcf)	R&C Qc/N	Adopted Qc/N	Est. PI	Fines (%)	D50 (mm)
1	Sensitive fine grained	ML	120	2	2	NP-15	65-100	0.02
2	Organic Material	OL/OH	120	1	1	--	--	--
3	Clay	CL/CH	125	1	1.25	25-40+	90-100	0.002
4	Silty Clay to Clay	CL	125	1.5	2	15-40	90-100	0.01
5	Clayey Silt to Silty Clay	ML/CL	120	2	2.75	25-May	90-100	0.02
6	Sandy Silt to Clayey Silt	ML	115	2.5	3.5	NP-10	65-100	0.04
7	Silty Sand to Sandy Silt	SM/ML	115	3	5	NP	35-75	0.075
8	Sand to Silty Sand	SP/SM	115	4	6	NP	May-35	0.15
9	Sand	SP	110	5	6.5	NP	0-5	0.3
10	Gravelly Sand to Sand	SW	115	6	7.5	NP	0-5	0.6
11	Overconsolidated Soil	--	120	1	1	NP	90-100	0.01
12	Sand to Clayey Sand	SP/SC	115	2	2	NP-5	--	---

Su (tsf)	Consistency
0-0.13	very soft
0.13-.25	soft
0.25-0.5	firm
0.5-1.0	stiff
1.0-2.0	very stiff
>2.0	hard
Dr (%)	**Relative Density**
0-15	very loose
15-35	loose
35-65	medium dense
65-85	dense
>85	very dense

LANDMARK
Geo-Engineers and Geologists

Project No: LE19075

Key to CPT Interpretation of Logs

Plate B-6

APPENDIX C

Landmark Consultants, Inc.
780 N. 4th Street
El Centro, CA 92243

LIQUEFACTION ANALYSIS REPORT

Project title : Heber 2 Repower Project **Location : Heber, CA**

CPT file : CPT-1

Input parameters and analysis data

Analysis method:	NCEER (1998)	G.W.T. (in-situ):	8.00 ft	Use fill:	No	Clay like behavior applied:	Sands only
Fines correction method:	NCEER (1998)	G.W.T. (earthq.):	8.00 ft	Fill height:	N/A	Limit depth applied:	No
Points to test:	Based on Ic value	Average results interval:	3	Fill weight:	N/A	Limit depth:	N/A
Earthquake magnitude M_w:	7.00	Ic cut-off value:	2.60	Trans. detect. applied:	Yes	MSF method:	Method based
Peak ground acceleration:	0.50	Unit weight calculation:	Based on SBT	K_σ applied:	Yes		

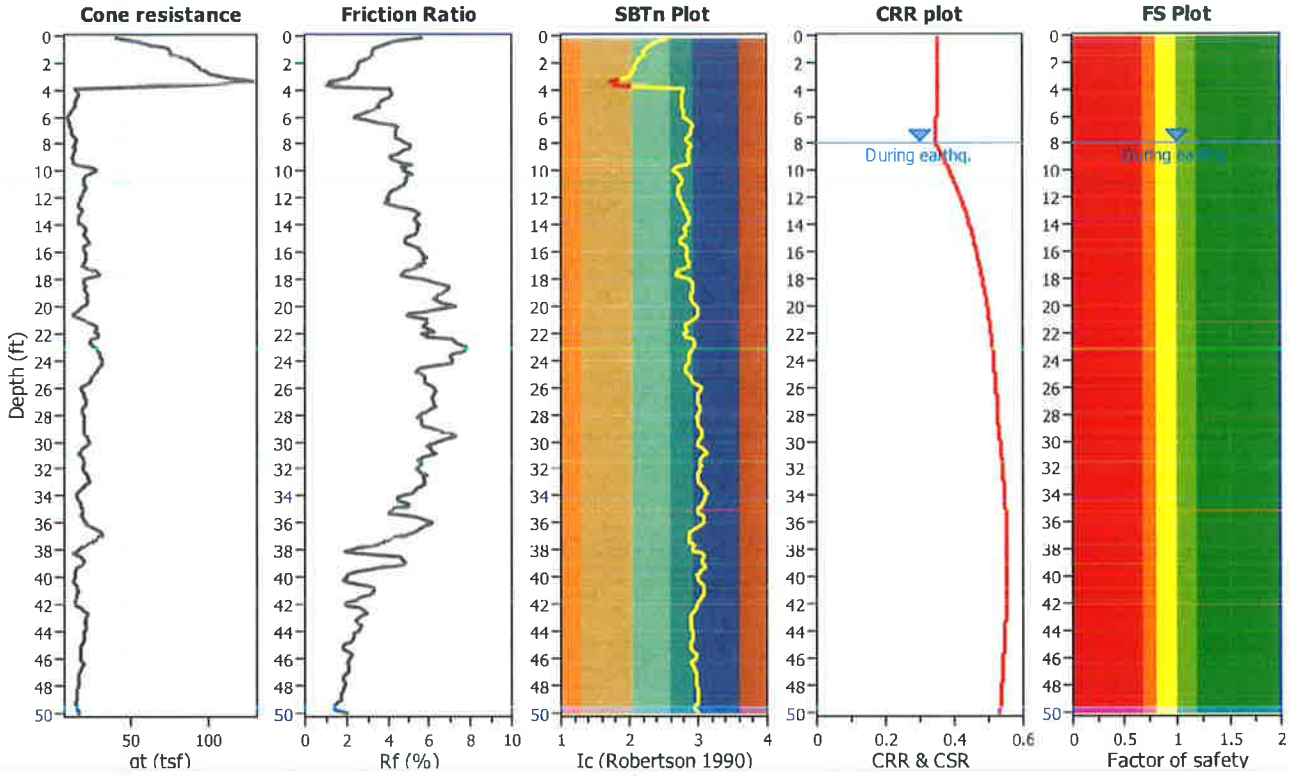

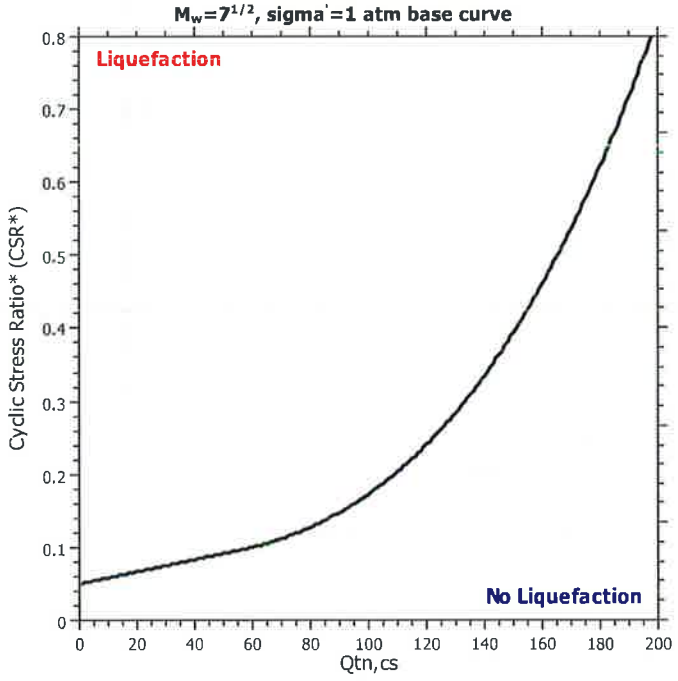

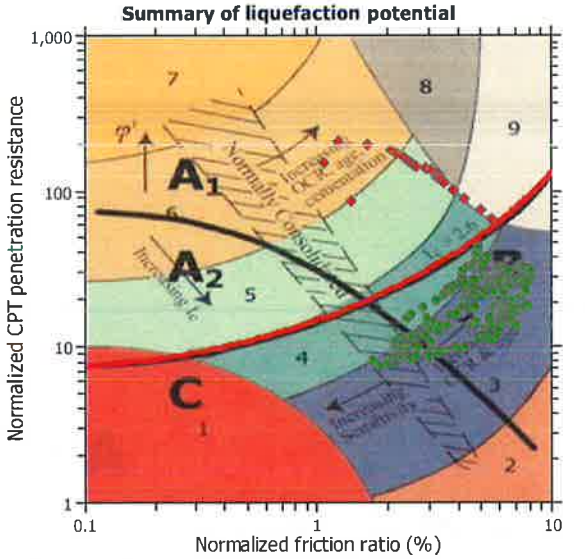

Zone A_1: Cyclic liquefaction likely depending on size and duration of cyclic loading
Zone A_2: Cyclic liquefaction and strength loss likely depending on loading and ground geometry
Zone B: Liquefaction and post-earthquake strength loss unlikely, check cyclic softening
Zone C: Cyclic liquefaction and strength loss possible depending on soil plasticity, brittleness/sensitivity, strain to peak undrained strength and ground geometry

CPT basic interpretation plots

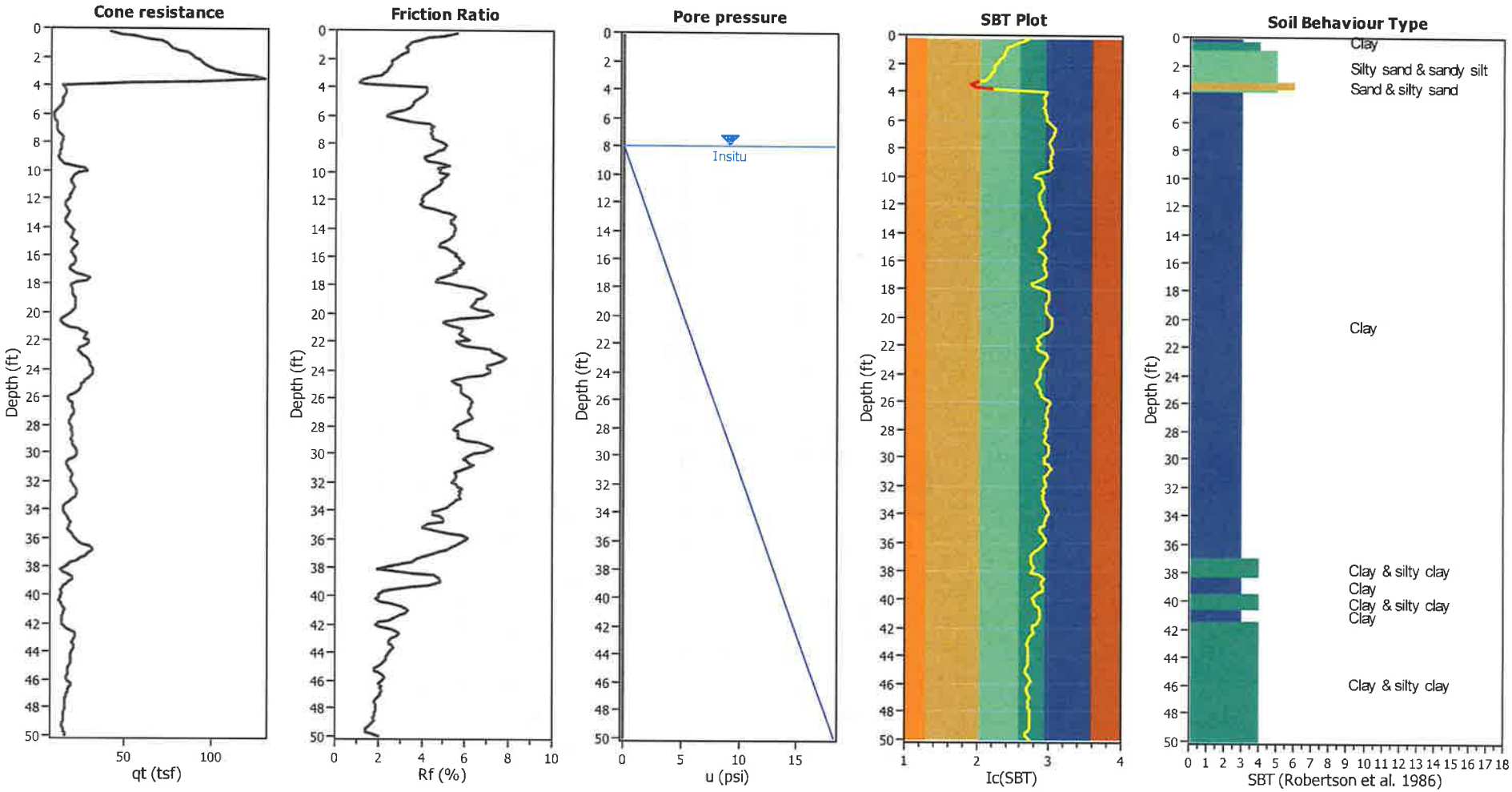

Input parameters and analysis data

Analysis method:	NCEER (1998)	Depth to water table (erthq.):	8.00 ft	Fill weight:	N/A
Fines correction method:	NCEER (1998)	Average results interval:	3	Transition detect. applied:	Yes
Points to test:	Based on Ic value	Ic cut-off value:	2.60	K_σ applied:	Yes
Earthquake magnitude M_w:	7.00	Unit weight calculation:	Based on SBT	Clay like behavior applied:	Sands only
Peak ground acceleration:	0.50	Use fill:	No	Limit depth applied:	No
Depth to water table (insitu):	8.00 ft	Fill height:	N/A	Limit depth:	N/A

SBT legend

1. Sensitive fine grained
2. Organic material
3. Clay to silty clay
4. Clayey silt to silty
5. Silty sand to sandy silt
6. Clean sand to silty sand
7. Gravely sand to sand
8. Very stiff sand to
9. Very stiff fine grained

Estimation of post-earthquake settlements

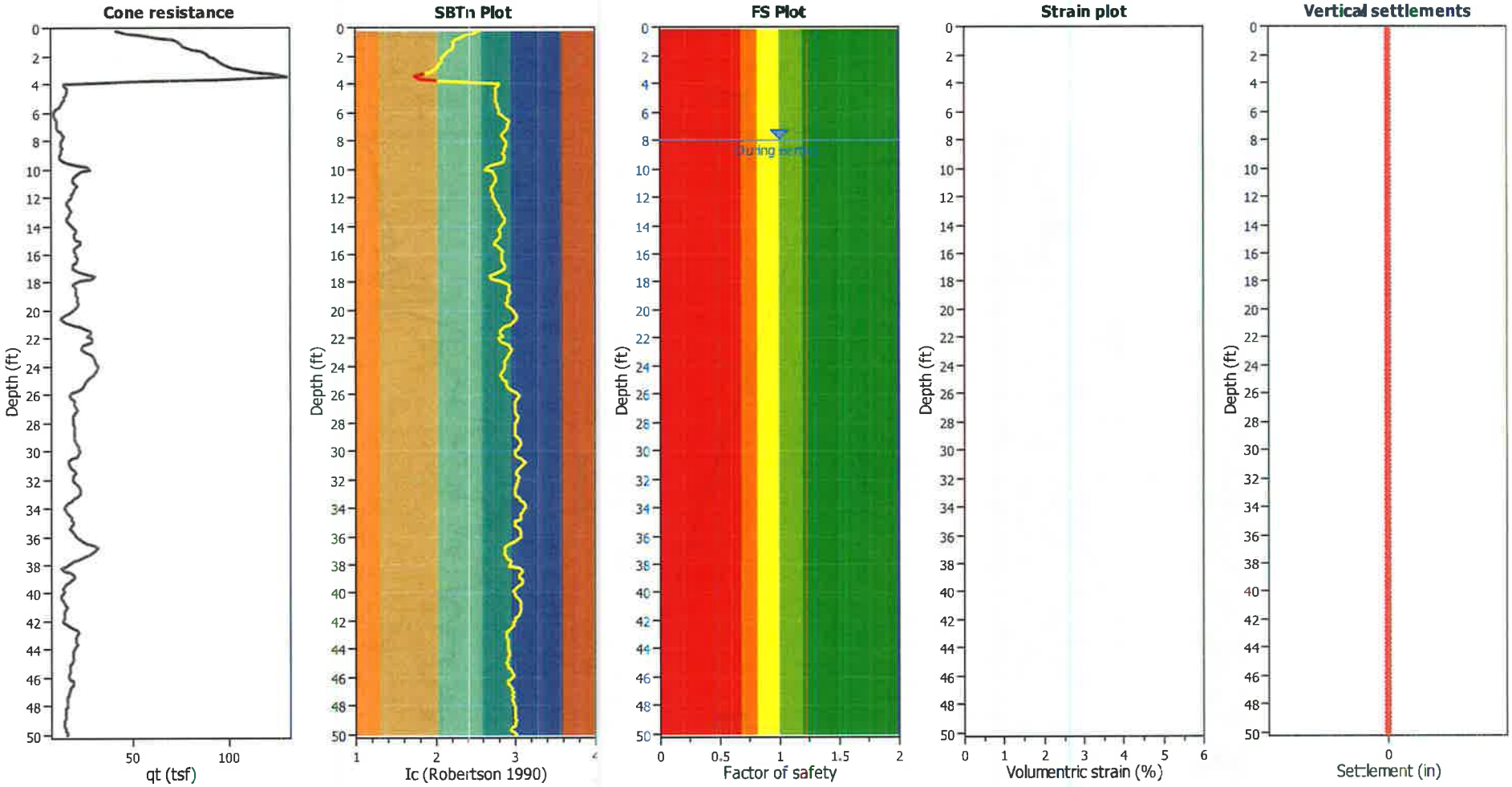

Abbreviations

q_t:	Total cone resistance (cone resistance q_c corrected for pore water effects)
I_c:	Soil Behaviour Type Index
FS:	Calculated Factor of Safety against liquefaction
Volumentric strain:	Post-liquefaction volumentric strain

:: Post-earthquake settlement due to soil liquefaction ::

Depth (ft)	$Q_{tn,cs}$	FS	e_v (%)	DF	Settlement (in)	Depth (ft)	$Q_{tn,cs}$	FS	e_v (%)	DF	Settlement (in)
8.04	119.97	2.00	0.00	0.86	0.00	8.20	118.98	2.00	0.00	0.86	0.00
8.37	118.57	2.00	0.00	0.86	0.00	8.53	116.33	2.00	0.00	0.86	0.00
8.69	111.11	2.00	0.00	0.85	0.00	8.86	105.42	2.00	0.00	0.85	0.00
9.02	103.12	2.00	0.00	0.85	0.00	9.19	106.12	2.00	0.00	0.84	0.00
9.35	114.80	2.00	0.00	0.84	0.00	9.51	129.15	2.00	0.00	0.84	0.00
9.68	142.81	2.00	0.00	0.84	0.00	9.84	155.83	2.00	0.00	0.83	0.00
10.01	158.63	2.00	0.00	0.83	0.00	10.17	154.96	2.00	0.00	0.83	0.00
10.33	145.30	2.00	0.00	0.82	0.00	10.50	138.73	2.00	0.00	0.82	0.00
10.66	137.47	2.00	0.00	0.82	0.00	10.83	136.96	2.00	0.00	0.82	0.00
10.99	137.99	2.00	0.00	0.81	0.00	11.15	137.59	2.00	0.00	0.81	0.00
11.32	134.89	2.00	0.00	0.81	0.00	11.48	129.13	2.00	0.00	0.81	0.00
11.65	123.50	2.00	0.00	0.80	0.00	11.81	121.19	2.00	0.00	0.80	0.00
11.98	119.62	2.00	0.00	0.80	0.00	12.14	117.79	2.00	0.00	0.79	0.00
12.30	113.63	2.00	0.00	0.79	0.00	12.47	115.50	2.00	0.00	0.79	0.00
12.63	123.82	2.00	0.00	0.79	0.00	12.80	132.97	2.00	0.00	0.78	0.00
12.96	139.15	2.00	0.00	0.78	0.00	13.12	139.59	2.00	0.00	0.78	0.00
13.29	136.63	2.00	0.00	0.77	0.00	13.45	131.74	2.00	0.00	0.77	0.00
13.62	130.26	2.00	0.00	0.77	0.00	13.78	134.95	2.00	0.00	0.77	0.00
13.94	140.91	2.00	0.00	0.76	0.00	14.11	145.02	2.00	0.00	0.76	0.00
14.27	146.42	2.00	0.00	0.76	0.00	14.44	144.79	2.00	0.00	0.76	0.00
14.60	141.29	2.00	0.00	0.75	0.00	14.76	138.10	2.00	0.00	0.75	0.00
14.93	137.24	2.00	0.00	0.75	0.00	15.09	138.96	2.00	0.00	0.74	0.00
15.26	139.60	2.00	0.00	0.74	0.00	15.42	140.43	2.00	0.00	0.74	0.00
15.58	139.21	2.00	0.00	0.74	0.00	15.75	140.96	2.00	0.00	0.73	0.00
15.91	141.85	2.00	0.00	0.73	0.00	16.08	145.91	2.00	0.00	0.73	0.00
16.24	147.66	2.00	0.00	0.72	0.00	16.40	149.68	2.00	0.00	0.72	0.00
16.57	145.56	2.00	0.00	0.72	0.00	16.73	140.89	2.00	0.00	0.72	0.00
16.90	134.62	2.00	0.00	0.71	0.00	17.06	136.61	2.00	0.00	0.71	0.00
17.22	140.20	2.00	0.00	0.71	0.00	17.39	146.14	2.00	0.00	0.71	0.00
17.55	148.16	2.00	0.00	0.70	0.00	17.72	144.49	2.00	0.00	0.70	0.00
17.88	139.25	2.00	0.00	0.70	0.00	18.04	138.26	2.00	0.00	0.69	0.00
18.21	144.57	2.00	0.00	0.69	0.00	18.37	151.78	2.00	0.00	0.69	0.00
18.54	154.52	2.00	0.00	0.69	0.00	18.70	153.95	2.00	0.00	0.68	0.00
18.86	153.12	2.00	0.00	0.68	0.00	19.03	151.55	2.00	0.00	0.68	0.00
19.19	150.73	2.00	0.00	0.67	0.00	19.36	148.04	2.00	0.00	0.67	0.00
19.52	147.69	2.00	0.00	0.67	0.00	19.69	151.40	2.00	0.00	0.67	0.00
19.85	154.31	2.00	0.00	0.66	0.00	20.01	150.07	2.00	0.00	0.66	0.00
20.18	135.86	2.00	0.00	0.66	0.00	20.34	119.17	2.00	0.00	0.66	0.00
20.51	104.85	2.00	0.00	0.65	0.00	20.67	104.13	2.00	0.00	0.65	0.00
20.83	114.48	2.00	0.00	0.65	0.00	21.00	131.00	2.00	0.00	0.64	0.00
21.16	142.62	2.00	0.00	0.64	0.00	21.33	149.15	2.00	0.00	0.64	0.00
21.49	153.07	2.00	0.00	0.64	0.00	21.65	154.99	2.00	0.00	0.63	0.00
21.82	156.00	2.00	0.00	0.63	0.00	21.98	152.30	2.00	0.00	0.63	0.00
22.15	154.57	2.00	0.00	0.62	0.00	22.31	156.68	2.00	0.00	0.62	0.00
22.47	159.95	2.00	0.00	0.62	0.00	22.64	157.92	2.00	0.00	0.62	0.00
22.80	160.98	2.00	0.00	0.61	0.00	22.97	169.52	2.00	0.00	0.61	0.00
23.13	176.91	2.00	0.00	0.61	0.00	23.29	178.34	2.00	0.00	0.61	0.00
23.46	174.45	2.00	0.00	0.60	0.00	23.62	171.54	2.00	0.00	0.60	0.00

:: Post-earthquake settlement due to soil liquefaction :: (continued)

Depth (ft)	$Q_{tn,cs}$	FS	e_v (%)	DF	Settlement (in)	Depth (ft)	$Q_{tn,cs}$	FS	e_v (%)	DF	Settlement (in)
23.79	172.69	2.00	0.00	0.60	0.00	23.95	175.54	2.00	0.00	0.59	0.00
24.11	175.55	2.00	0.00	0.59	0.00	24.28	168.97	2.00	0.00	0.59	0.00
24.44	157.41	2.00	0.00	0.59	0.00	24.61	146.69	2.00	0.00	0.58	0.00
24.77	140.58	2.00	0.00	0.58	0.00	24.93	139.79	2.00	0.00	0.58	0.00
25.10	139.62	2.00	0.00	0.57	0.00	25.26	138.81	2.00	0.00	0.57	0.00
25.43	136.75	2.00	0.00	0.57	0.00	25.59	133.88	2.00	0.00	0.57	0.00
25.75	129.01	2.00	0.00	0.56	0.00	25.92	123.09	2.00	0.00	0.56	0.00
26.08	121.15	2.00	0.00	0.56	0.00	26.25	124.71	2.00	0.00	0.56	0.00
26.41	127.90	2.00	0.00	0.55	0.00	26.57	128.10	2.00	0.00	0.55	0.00
26.74	126.91	2.00	0.00	0.55	0.00	26.90	128.06	2.00	0.00	0.54	0.00
27.07	129.48	2.00	0.00	0.54	0.00	27.23	128.59	2.00	0.00	0.54	0.00
27.40	126.11	2.00	0.00	0.54	0.00	27.56	122.56	2.00	0.00	0.53	0.00
27.72	119.14	2.00	0.00	0.53	0.00	27.89	116.40	2.00	0.00	0.53	0.00
28.05	117.08	2.00	0.00	0.52	0.00	28.22	116.67	2.00	0.00	0.52	0.00
28.38	118.11	2.00	0.00	0.52	0.00	28.54	118.18	2.00	0.00	0.52	0.00
28.71	118.83	2.00	0.00	0.51	0.00	28.87	118.78	2.00	0.00	0.51	0.00
29.04	120.47	2.00	0.00	0.51	0.00	29.20	126.00	2.00	0.00	0.51	0.00
29.36	131.40	2.00	0.00	0.50	0.00	29.53	135.95	2.00	0.00	0.50	0.00
29.69	136.80	2.00	0.00	0.50	0.00	29.86	135.40	2.00	0.00	0.49	0.00
30.02	131.15	2.00	0.00	0.49	0.00	30.18	127.34	2.00	0.00	0.49	0.00
30.35	121.69	2.00	0.00	0.49	0.00	30.51	115.70	2.00	0.00	0.48	0.00
30.68	111.80	2.00	0.00	0.48	0.00	30.84	112.22	2.00	0.00	0.48	0.00
31.00	112.33	2.00	0.00	0.47	0.00	31.17	111.25	2.00	0.00	0.47	0.00
31.33	112.16	2.00	0.00	0.47	0.00	31.50	114.87	2.00	0.00	0.47	0.00
31.66	114.02	2.00	0.00	0.46	0.00	31.82	110.25	2.00	0.00	0.46	0.00
31.99	108.73	2.00	0.00	0.46	0.00	32.15	112.92	2.00	0.00	0.46	0.00
32.32	116.75	2.00	0.00	0.45	0.00	32.48	119.82	2.00	0.00	0.45	0.00
32.64	120.23	2.00	0.00	0.45	0.00	32.81	121.28	2.00	0.00	0.44	0.00
32.97	120.46	2.00	0.00	0.44	0.00	33.14	117.67	2.00	0.00	0.44	0.00
33.30	111.47	2.00	0.00	0.44	0.00	33.46	105.37	2.00	0.00	0.43	0.00
33.63	100.20	2.00	0.00	0.43	0.00	33.79	95.08	2.00	0.00	0.43	0.00
33.96	90.37	2.00	0.00	0.42	0.00	34.12	87.91	2.00	0.00	0.42	0.00
34.28	90.52	2.00	0.00	0.42	0.00	34.45	96.32	2.00	0.00	0.42	0.00
34.61	99.51	2.00	0.00	0.41	0.00	34.78	99.39	2.00	0.00	0.41	0.00
34.94	95.45	2.00	0.00	0.41	0.00	35.10	92.69	2.00	0.00	0.41	0.00
35.27	91.26	2.00	0.00	0.40	0.00	35.43	95.67	2.00	0.00	0.40	0.00
35.60	104.11	2.00	0.00	0.40	0.00	35.76	111.84	2.00	0.00	0.39	0.00
35.93	115.82	2.00	0.00	0.39	0.00	36.09	116.17	2.00	0.00	0.39	0.00
36.25	118.60	2.00	0.00	0.39	0.00	36.42	122.19	2.00	0.00	0.38	0.00
36.58	126.65	2.00	0.00	0.38	0.00	36.75	127.95	2.00	0.00	0.38	0.00
36.91	123.10	2.00	0.00	0.37	0.00	37.07	114.03	2.00	0.00	0.37	0.00
37.24	104.72	2.00	0.00	0.37	0.00	37.40	98.46	2.00	0.00	0.37	0.00
37.57	91.59	2.00	0.00	0.36	0.00	37.73	82.25	2.00	0.00	0.36	0.00
37.89	70.62	2.00	0.00	0.36	0.00	38.06	60.48	2.00	0.00	0.35	0.00
38.22	63.21	2.00	0.00	0.35	0.00	38.39	76.34	2.00	0.00	0.35	0.00
38.55	91.11	2.00	0.00	0.35	0.00	38.71	98.86	2.00	0.00	0.34	0.00
38.88	99.34	2.00	0.00	0.34	0.00	39.04	95.61	2.00	0.00	0.34	0.00
39.21	86.80	2.00	0.00	0.34	0.00	39.37	76.19	2.00	0.00	0.33	0.00

:: Post-earthquake settlement due to soil liquefaction :: (continued)

Depth (ft)	$Q_{tn,cs}$	FS	e_v (%)	DF	Settlement (in)	Depth (ft)	$Q_{tn,cs}$	FS	e_v (%)	DF	Settlement (in)
39.53	64.64	2.00	0.00	0.33	0.00	39.70	60.43	2.00	0.00	0.33	0.00
39.86	58.79	2.00	0.00	0.32	0.00	40.03	58.19	2.00	0.00	0.32	0.00
40.19	55.59	2.00	0.00	0.32	0.00	40.35	57.57	2.00	0.00	0.32	0.00
40.52	62.98	2.00	0.00	0.31	0.00	40.68	69.67	2.00	0.00	0.31	0.00
40.85	73.76	2.00	0.00	0.31	0.00	41.01	74.59	2.00	0.00	0.30	0.00
41.17	72.68	2.00	0.00	0.30	0.00	41.34	69.91	2.00	0.00	0.30	0.00
41.50	66.62	2.00	0.00	0.30	0.00	41.67	63.67	2.00	0.00	0.29	0.00
41.83	58.22	2.00	0.00	0.29	0.00	41.99	56.51	2.00	0.00	0.29	0.00
42.16	59.31	2.00	0.00	0.29	0.00	42.32	68.96	2.00	0.00	0.28	0.00
42.49	76.21	2.00	0.00	0.28	0.00	42.65	79.83	2.00	0.00	0.28	0.00
42.81	78.47	2.00	0.00	0.27	0.00	42.98	75.37	2.00	0.00	0.27	0.00
43.14	72.19	2.00	0.00	0.27	0.00	43.31	72.07	2.00	0.00	0.27	0.00
43.47	73.96	2.00	0.00	0.26	0.00	43.64	75.40	2.00	0.00	0.26	0.00
43.80	74.08	2.00	0.00	0.26	0.00	43.96	71.55	2.00	0.00	0.25	0.00
44.13	69.30	2.00	0.00	0.25	0.00	44.29	68.40	2.00	0.00	0.25	0.00
44.46	68.25	2.00	0.00	0.25	0.00	44.62	67.81	2.00	0.00	0.24	0.00
44.78	65.86	2.00	0.00	0.24	0.00	44.95	62.49	2.00	0.00	0.24	0.00
45.11	59.84	2.00	0.00	0.24	0.00	45.28	59.58	2.00	0.00	0.23	0.00
45.44	61.66	2.00	0.00	0.23	0.00	45.60	63.62	2.00	0.00	0.23	0.00
45.77	63.78	2.00	0.00	0.22	0.00	45.93	62.47	2.00	0.00	0.22	0.00
46.10	62.45	2.00	0.00	0.22	0.00	46.26	63.43	2.00	0.00	0.22	0.00
46.42	64.80	2.00	0.00	0.21	0.00	46.59	63.69	2.00	0.00	0.21	0.00
46.75	62.33	2.00	0.00	0.21	0.00	46.92	61.14	2.00	0.00	0.20	0.00
47.08	60.30	2.00	0.00	0.20	0.00	47.24	58.40	2.00	0.00	0.20	0.00
47.41	57.02	2.00	0.00	0.20	0.00	47.57	56.85	2.00	0.00	0.19	0.00
47.74	57.68	2.00	0.00	0.19	0.00	47.90	57.58	2.00	0.00	0.19	0.00
48.06	57.06	2.00	0.00	0.19	0.00	48.23	56.18	2.00	0.00	0.18	0.00
48.39	55.57	2.00	0.00	0.18	0.00	48.56	54.87	2.00	0.00	0.18	0.00
48.72	54.42	2.00	0.00	0.17	0.00	48.88	54.29	2.00	0.00	0.17	0.00
49.05	53.61	2.00	0.00	0.17	0.00	49.21	51.61	2.00	0.00	0.17	0.00
49.38	49.82	2.00	0.00	0.16	0.00	49.54	49.51	2.00	0.00	0.16	0.00
49.70	49.89	2.00	0.00	0.16	0.00	49.87	54.16	2.00	0.00	0.15	0.00
50.03	57.29	2.00	0.00	0.15	0.00						

Total estimated settlement: 0.00

Abbreviations

$Q_{tn,cs}$:	Equivalent clean sand normalized cone resistance
FS:	Factor of safety against liquefaction
e_v (%):	Post-liquefaction volumentric strain
DF:	e_v depth weighting factor
Settlement:	Calculated settlement

Landmark Consultants, Inc.
780 N. 4th Street
El Centro, CA 92243

LIQUEFACTION ANALYSIS REPORT

Project title : Heber 2 Repower Project **Location : Heber, CA**

CPT file : CPT-2

Input parameters and analysis data

Analysis method:	NCEER (1998)	G.W.T. (in-situ):	8.00 ft	Use fill:	No	Clay like behavior applied:	Sands only
Fines correction method:	NCEER (1998)	G.W.T. (earthq.):	8.00 ft	Fill height:	N/A	Limit depth applied:	No
Points to test:	Based on Ic value	Average results interval:	3	Fill weight:	N/A	Limit depth:	N/A
Earthquake magnitude M_w:	7.00	Ic cut-off value:	2.60	Trans. detect. applied:	Yes	MSF method:	Method based
Peak ground acceleration:	0.50	Unit weight calculation:	Based on SBT	K_σ applied:	Yes		

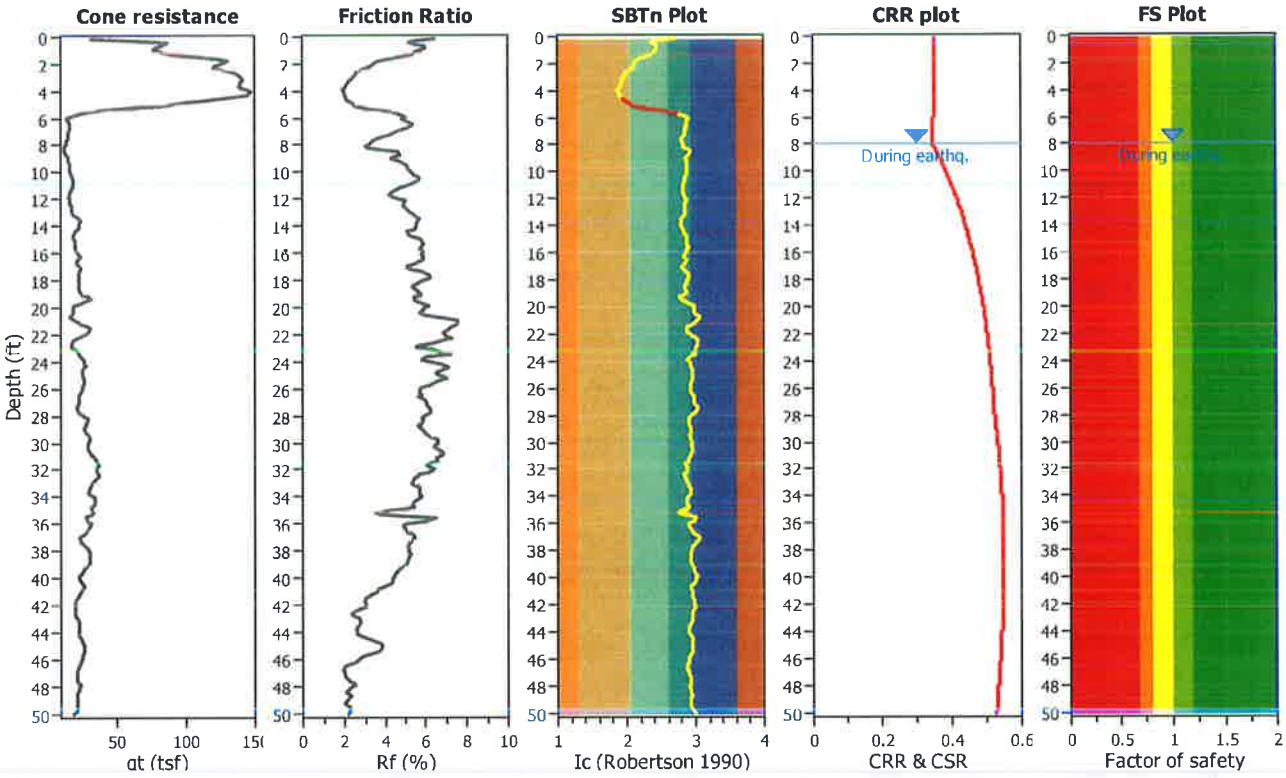

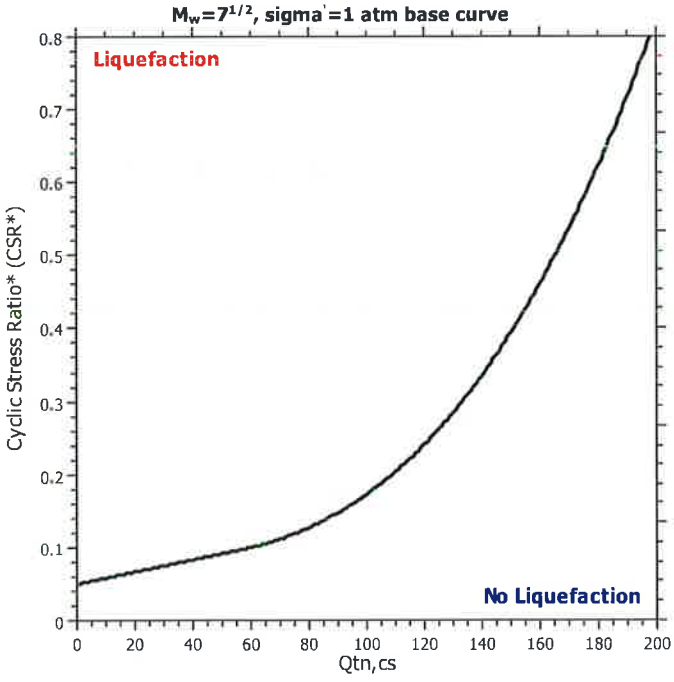

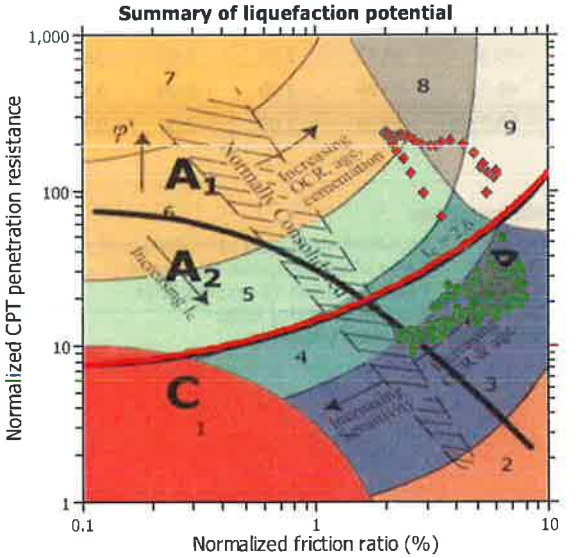

Zone A_1: Cyclic liquefaction likely depending on size and duration of cyclic loading
Zone A_2: Cyclic liquefaction and strength loss likely depending on loading and ground geometry
Zone B: Liquefaction and post-earthquake strength loss unlikely, check cyclic softening
Zone C: Cyclic liquefaction and strength loss possible depending on soil plasticity, brittleness/sensitivity, strain to peak undrained strength and ground geometry

CPT basic interpretation plots

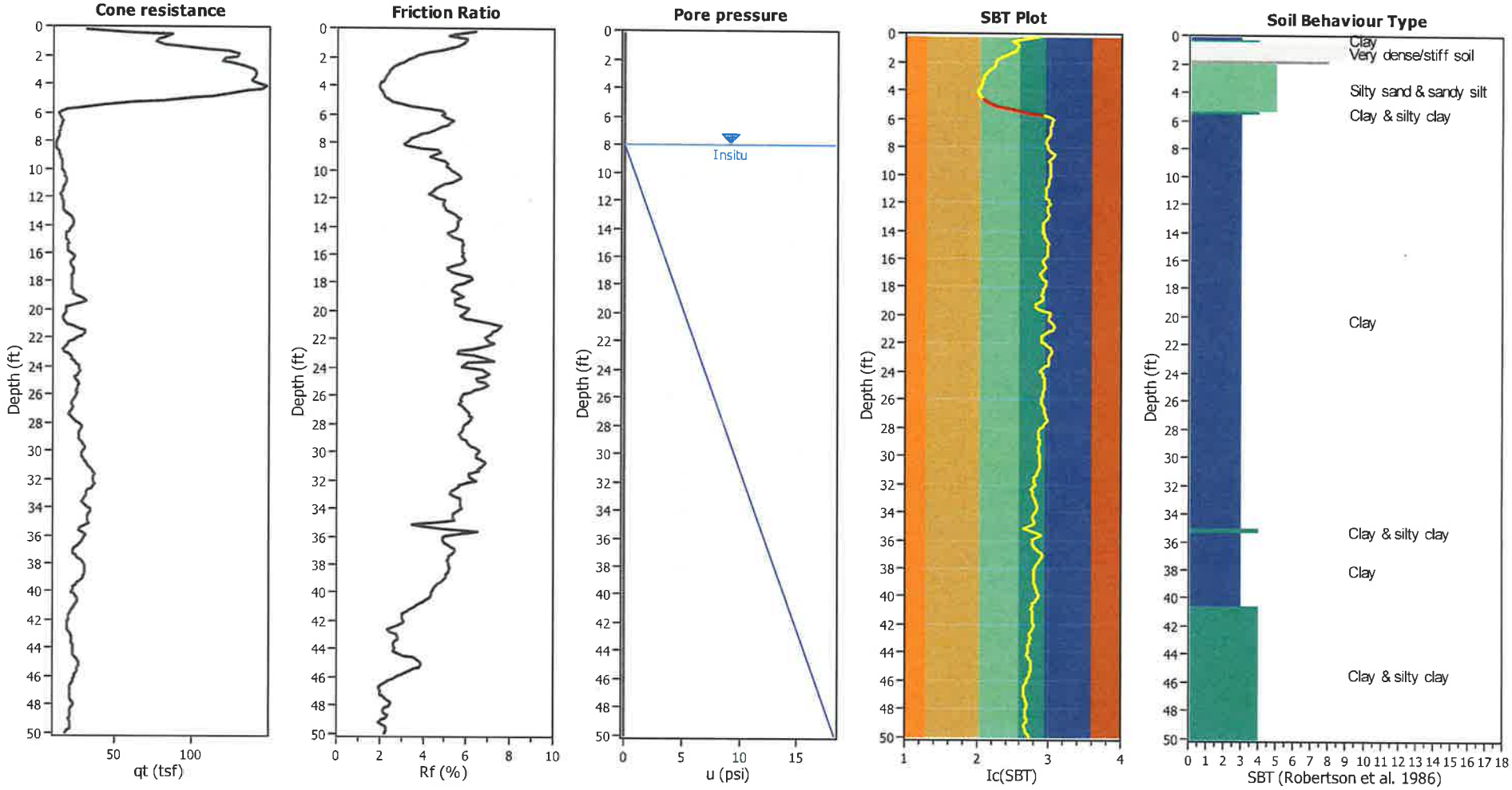

Input parameters and analysis data

Analysis method:	NCEER (1998)	Depth to water table (erthq.):	8.00 ft	Fill weight:	N/A
Fines correction method:	NCEER (1998)	Average results interval:	3	Transition detect. applied:	Yes
Points to test:	Based on Ic value	Ic cut-off value:	2.60	K_σ applied:	Yes
Earthquake magnitude M_w:	7.00	Unit weight calculation:	Based on SBT	Clay like behavior applied:	Sands only
Peak ground acceleration:	0.50	Use fill:	No	Limit depth applied:	No
Depth to water table (insitu):	8.00 ft	Fill height:	N/A	Limit depth:	N/A

SBT legend

1. Sensitive fine grained
2. Organic material
3. Clay to silty clay
4. Clayey silt to silty
5. Silty sand to sandy silt
6. Clean sand to silty sand
7. Gravely sand to sand
8. Very stiff sand to
9. Very stiff fine grained

Estimation of post-earthquake settlements

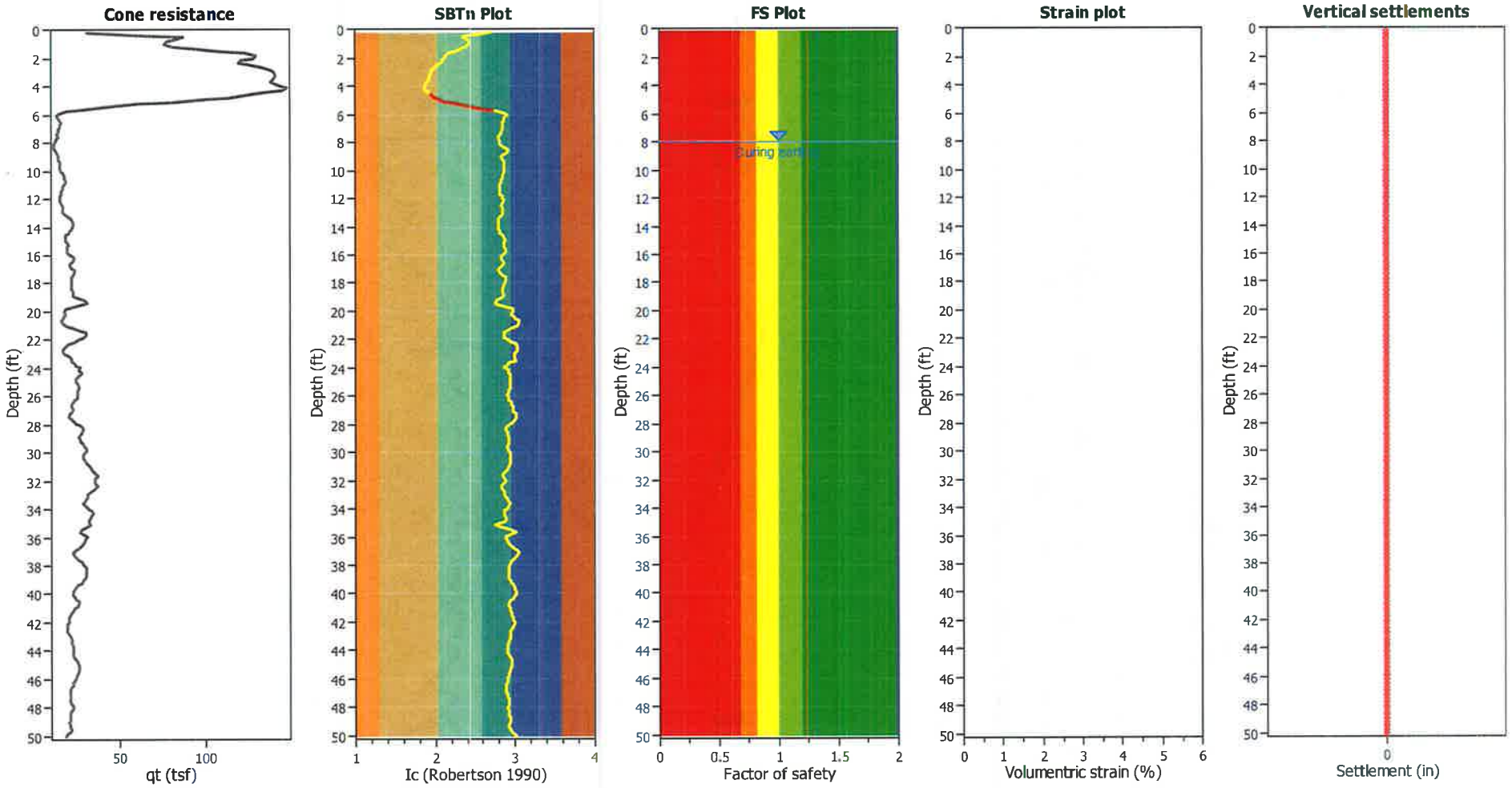

Abbreviations

q_t:	Total cone resistance (cone resistance q_c corrected for pore water effects)
I_c:	Soil Behaviour Type Index
FS:	Calculated Factor of Safety against liquefaction
Volumentric strain:	Post-liquefaction volumentric strain

:: Post-earthquake settlement due to soil liquefaction ::

Depth (ft)	$Q_{tn,cs}$	FS	e_v (%)	DF	Settlement (in)	Depth (ft)	$Q_{tn,cs}$	FS	e_v (%)	DF	Settlement (in)
8.04	87.36	2.00	0.00	0.86	0.00	8.20	87.19	2.00	0.00	0.86	0.00
8.37	96.18	2.00	0.00	0.86	0.00	8.53	106.38	2.00	0.00	0.86	0.00
8.69	112.48	2.00	0.00	0.85	0.00	8.86	110.89	2.00	0.00	0.85	0.00
9.02	111.02	2.00	0.00	0.85	0.00	9.19	116.47	2.00	0.00	0.84	0.00
9.35	122.07	2.00	0.00	0.84	0.00	9.51	124.70	2.00	0.00	0.84	0.00
9.68	124.57	2.00	0.00	0.84	0.00	9.84	125.67	2.00	0.00	0.83	0.00
10.01	128.65	2.00	0.00	0.83	0.00	10.17	133.81	2.00	0.00	0.83	0.00
10.33	139.27	2.00	0.00	0.82	0.00	10.50	141.24	2.00	0.00	0.82	0.00
10.66	140.53	2.00	0.00	0.82	0.00	10.83	137.12	2.00	0.00	0.82	0.00
10.99	132.08	2.00	0.00	0.81	0.00	11.15	125.69	2.00	0.00	0.81	0.00
11.32	121.22	2.00	0.00	0.81	0.00	11.48	118.55	2.00	0.00	0.81	0.00
11.65	114.78	2.00	0.00	0.80	0.00	11.81	114.47	2.00	0.00	0.80	0.00
11.98	117.86	2.00	0.00	0.80	0.00	12.14	123.32	2.00	0.00	0.79	0.00
12.30	124.95	2.00	0.00	0.79	0.00	12.47	126.35	2.00	0.00	0.79	0.00
12.63	127.12	2.00	0.00	0.79	0.00	12.80	126.75	2.00	0.00	0.78	0.00
12.96	128.67	2.00	0.00	0.78	0.00	13.12	137.01	2.00	0.00	0.78	0.00
13.29	146.43	2.00	0.00	0.77	0.00	13.45	152.65	2.00	0.00	0.77	0.00
13.62	152.23	2.00	0.00	0.77	0.00	13.78	150.77	2.00	0.00	0.77	0.00
13.94	149.69	2.00	0.00	0.76	0.00	14.11	147.77	2.00	0.00	0.76	0.00
14.27	143.23	2.00	0.00	0.76	0.00	14.44	134.40	2.00	0.00	0.76	0.00
14.60	130.85	2.00	0.00	0.75	0.00	14.76	131.78	2.00	0.00	0.75	0.00
14.93	137.68	2.00	0.00	0.75	0.00	15.09	141.06	2.00	0.00	0.74	0.00
15.26	142.59	2.00	0.00	0.74	0.00	15.42	140.26	2.00	0.00	0.74	0.00
15.58	137.71	2.00	0.00	0.74	0.00	15.75	138.11	2.00	0.00	0.73	0.00
15.91	142.76	2.00	0.00	0.73	0.00	16.08	148.65	2.00	0.00	0.73	0.00
16.24	151.42	2.00	0.00	0.72	0.00	16.40	149.65	2.00	0.00	0.72	0.00
16.57	142.62	2.00	0.00	0.72	0.00	16.73	137.02	2.00	0.00	0.72	0.00
16.90	134.47	2.00	0.00	0.71	0.00	17.06	136.99	2.00	0.00	0.71	0.00
17.22	140.40	2.00	0.00	0.71	0.00	17.39	144.16	2.00	0.00	0.71	0.00
17.55	147.16	2.00	0.00	0.70	0.00	17.72	147.34	2.00	0.00	0.70	0.00
17.88	145.63	2.00	0.00	0.70	0.00	18.04	142.20	2.00	0.00	0.69	0.00
18.21	137.49	2.00	0.00	0.69	0.00	18.37	134.79	2.00	0.00	0.69	0.00
18.54	135.52	2.00	0.00	0.69	0.00	18.70	138.83	2.00	0.00	0.68	0.00
18.86	142.10	2.00	0.00	0.68	0.00	19.03	147.42	2.00	0.00	0.68	0.00
19.19	153.72	2.00	0.00	0.67	0.00	19.36	155.93	2.00	0.00	0.67	0.00
19.52	149.47	2.00	0.00	0.67	0.00	19.69	138.34	2.00	0.00	0.67	0.00
19.85	130.61	2.00	0.00	0.66	0.00	20.01	127.39	2.00	0.00	0.66	0.00
20.18	126.45	2.00	0.00	0.66	0.00	20.34	122.79	2.00	0.00	0.66	0.00
20.51	120.62	2.00	0.00	0.65	0.00	20.67	123.16	2.00	0.00	0.65	0.00
20.83	132.56	2.00	0.00	0.65	0.00	21.00	144.81	2.00	0.00	0.64	0.00
21.16	158.42	2.00	0.00	0.64	0.00	21.33	169.86	2.00	0.00	0.64	0.00
21.49	175.02	2.00	0.00	0.64	0.00	21.65	173.22	2.00	0.00	0.63	0.00
21.82	164.99	2.00	0.00	0.63	0.00	21.98	158.59	2.00	0.00	0.63	0.00
22.15	151.83	2.00	0.00	0.62	0.00	22.31	144.28	2.00	0.00	0.62	0.00
22.47	133.91	2.00	0.00	0.62	0.00	22.64	122.50	2.00	0.00	0.62	0.00
22.80	113.97	2.00	0.00	0.61	0.00	22.97	115.77	2.00	0.00	0.61	0.00
23.13	130.82	2.00	0.00	0.61	0.00	23.29	142.43	2.00	0.00	0.61	0.00
23.46	145.56	2.00	0.00	0.60	0.00	23.62	138.07	2.00	0.00	0.60	0.00

:: Post-earthquake settlement due to soil liquefaction :: (continued)

Depth (ft)	$Q_{tn,cs}$	FS	e_v (%)	DF	Settlement (in)	Depth (ft)	$Q_{tn,cs}$	FS	e_v (%)	DF	Settlement (in)
23.79	137.78	2.00	0.00	0.60	0.00	23.95	142.26	2.00	0.00	0.59	0.00
24.11	152.61	2.00	0.00	0.59	0.00	24.28	157.26	2.00	0.00	0.59	0.00
24.44	157.24	2.00	0.00	0.59	0.00	24.61	149.93	2.00	0.00	0.58	0.00
24.77	142.55	2.00	0.00	0.58	0.00	24.93	143.51	2.00	0.00	0.58	0.00
25.10	149.66	2.00	0.00	0.57	0.00	25.26	152.78	2.00	0.00	0.57	0.00
25.43	148.83	2.00	0.00	0.57	0.00	25.59	143.18	2.00	0.00	0.57	0.00
25.75	139.46	2.00	0.00	0.56	0.00	25.92	135.62	2.00	0.00	0.56	0.00
26.08	133.19	2.00	0.00	0.56	0.00	26.25	130.04	2.00	0.00	0.56	0.00
26.41	126.80	2.00	0.00	0.55	0.00	26.57	123.29	2.00	0.00	0.55	0.00
26.74	124.77	2.00	0.00	0.55	0.00	26.90	128.04	2.00	0.00	0.54	0.00
27.07	127.87	2.00	0.00	0.54	0.00	27.23	124.65	2.00	0.00	0.54	0.00
27.40	123.42	2.00	0.00	0.54	0.00	27.56	125.82	2.00	0.00	0.53	0.00
27.72	129.41	2.00	0.00	0.53	0.00	27.89	132.22	2.00	0.00	0.53	0.00
28.05	136.18	2.00	0.00	0.52	0.00	28.22	139.19	2.00	0.00	0.52	0.00
28.38	139.58	2.00	0.00	0.52	0.00	28.54	136.40	2.00	0.00	0.52	0.00
28.71	132.41	2.00	0.00	0.51	0.00	28.87	131.90	2.00	0.00	0.51	0.00
29.04	133.41	2.00	0.00	0.51	0.00	29.20	135.88	2.00	0.00	0.51	0.00
29.36	139.24	2.00	0.00	0.50	0.00	29.53	144.11	2.00	0.00	0.50	0.00
29.69	147.91	2.00	0.00	0.50	0.00	29.86	148.75	2.00	0.00	0.49	0.00
30.02	146.27	2.00	0.00	0.49	0.00	30.18	143.95	2.00	0.00	0.49	0.00
30.35	143.23	2.00	0.00	0.49	0.00	30.51	146.19	2.00	0.00	0.48	0.00
30.68	150.88	2.00	0.00	0.48	0.00	30.84	153.31	2.00	0.00	0.48	0.00
31.00	153.80	2.00	0.00	0.47	0.00	31.17	154.28	2.00	0.00	0.47	0.00
31.33	157.57	2.00	0.00	0.47	0.00	31.50	153.01	2.00	0.00	0.47	0.00
31.66	154.59	2.00	0.00	0.46	0.00	31.82	152.70	2.00	0.00	0.46	0.00
31.99	155.75	2.00	0.00	0.46	0.00	32.15	151.09	2.00	0.00	0.46	0.00
32.32	147.83	2.00	0.00	0.45	0.00	32.48	145.76	2.00	0.00	0.45	0.00
32.64	140.14	2.00	0.00	0.45	0.00	32.81	133.97	2.00	0.00	0.44	0.00
32.97	130.32	2.00	0.00	0.44	0.00	33.14	132.24	2.00	0.00	0.44	0.00
33.30	133.70	2.00	0.00	0.44	0.00	33.46	131.98	2.00	0.00	0.43	0.00
33.63	130.38	2.00	0.00	0.43	0.00	33.79	132.66	2.00	0.00	0.43	0.00
33.96	137.36	2.00	0.00	0.42	0.00	34.12	139.02	2.00	0.00	0.42	0.00
34.28	136.49	2.00	0.00	0.42	0.00	34.45	134.01	2.00	0.00	0.42	0.00
34.61	131.99	2.00	0.00	0.41	0.00	34.78	130.99	2.00	0.00	0.41	0.00
34.94	124.05	2.00	0.00	0.41	0.00	35.10	106.18	2.00	0.00	0.41	0.00
35.27	108.32	2.00	0.00	0.40	0.00	35.43	116.24	2.00	0.00	0.40	0.00
35.60	131.29	2.00	0.00	0.40	0.00	35.76	128.43	2.00	0.00	0.39	0.00
35.93	124.20	2.00	0.00	0.39	0.00	36.09	120.99	2.00	0.00	0.39	0.00
36.25	118.67	2.00	0.00	0.39	0.00	36.42	117.46	2.00	0.00	0.38	0.00
36.58	116.41	2.00	0.00	0.38	0.00	36.75	114.96	2.00	0.00	0.38	0.00
36.91	112.18	2.00	0.00	0.37	0.00	37.07	109.16	2.00	0.00	0.37	0.00
37.24	108.67	2.00	0.00	0.37	0.00	37.40	109.91	2.00	0.00	0.37	0.00
37.57	113.02	2.00	0.00	0.36	0.00	37.73	115.42	2.00	0.00	0.36	0.00
37.89	118.48	2.00	0.00	0.36	0.00	38.06	120.42	2.00	0.00	0.35	0.00
38.22	120.97	2.00	0.00	0.35	0.00	38.39	120.42	2.00	0.00	0.35	0.00
38.55	119.67	2.00	0.00	0.35	0.00	38.71	118.51	2.00	0.00	0.34	0.00
38.88	117.61	2.00	0.00	0.34	0.00	39.04	115.20	2.00	0.00	0.34	0.00
39.21	110.80	2.00	0.00	0.34	0.00	39.37	105.70	2.00	0.00	0.33	0.00

:: Post-earthquake settlement due to soil liquefaction :: (continued)

Depth (ft)	$Q_{tn,cs}$	FS	e_v (%)	DF	Settlement (in)	Depth (ft)	$Q_{tn,cs}$	FS	e_v (%)	DF	Settlement (in)
39.53	101.48	2.00	0.00	0.33	0.00	39.70	98.49	2.00	0.00	0.33	0.00
39.86	96.59	2.00	0.00	0.32	0.00	40.03	95.67	2.00	0.00	0.32	0.00
40.19	97.13	2.00	0.00	0.32	0.00	40.35	98.64	2.00	0.00	0.32	0.00
40.52	98.88	2.00	0.00	0.31	0.00	40.68	96.83	2.00	0.00	0.31	0.00
40.85	92.14	2.00	0.00	0.31	0.00	41.01	88.77	2.00	0.00	0.30	0.00
41.17	84.35	2.00	0.00	0.30	0.00	41.34	81.40	2.00	0.00	0.30	0.00
41.50	77.39	2.00	0.00	0.30	0.00	41.67	76.16	2.00	0.00	0.29	0.00
41.83	76.40	2.00	0.00	0.29	0.00	41.99	76.66	2.00	0.00	0.29	0.00
42.16	75.61	2.00	0.00	0.29	0.00	42.32	71.98	2.00	0.00	0.28	0.00
42.49	68.05	2.00	0.00	0.28	0.00	42.65	66.80	2.00	0.00	0.28	0.00
42.81	69.47	2.00	0.00	0.27	0.00	42.98	73.47	2.00	0.00	0.27	0.00
43.14	75.84	2.00	0.00	0.27	0.00	43.31	76.24	2.00	0.00	0.27	0.00
43.47	75.02	2.00	0.00	0.26	0.00	43.64	74.38	2.00	0.00	0.26	0.00
43.80	74.31	2.00	0.00	0.26	0.00	43.96	74.98	2.00	0.00	0.25	0.00
44.13	74.60	2.00	0.00	0.25	0.00	44.29	76.20	2.00	0.00	0.25	0.00
44.46	80.54	2.00	0.00	0.25	0.00	44.62	86.78	2.00	0.00	0.24	0.00
44.78	90.93	2.00	0.00	0.24	0.00	44.95	93.24	2.00	0.00	0.24	0.00
45.11	93.73	2.00	0.00	0.24	0.00	45.28	92.65	2.00	0.00	0.23	0.00
45.44	89.03	2.00	0.00	0.23	0.00	45.60	84.92	2.00	0.00	0.23	0.00
45.77	80.93	2.00	0.00	0.22	0.00	45.93	77.69	2.00	0.00	0.22	0.00
46.10	74.24	2.00	0.00	0.22	0.00	46.26	71.34	2.00	0.00	0.22	0.00
46.42	68.07	2.00	0.00	0.21	0.00	46.59	65.10	2.00	0.00	0.21	0.00
46.75	63.06	2.00	0.00	0.21	0.00	46.92	62.80	2.00	0.00	0.20	0.00
47.08	63.25	2.00	0.00	0.20	0.00	47.24	63.50	2.00	0.00	0.20	0.00
47.41	64.30	2.00	0.00	0.20	0.00	47.57	66.85	2.00	0.00	0.19	0.00
47.74	69.90	2.00	0.00	0.19	0.00	47.90	71.36	2.00	0.00	0.19	0.00
48.06	69.62	2.00	0.00	0.19	0.00	48.23	66.49	2.00	0.00	0.18	0.00
48.39	64.48	2.00	0.00	0.18	0.00	48.56	65.33	2.00	0.00	0.18	0.00
48.72	67.11	2.00	0.00	0.17	0.00	48.88	66.06	2.00	0.00	0.17	0.00
49.05	63.01	2.00	0.00	0.17	0.00	49.21	61.74	2.00	0.00	0.17	0.00
49.38	63.70	2.00	0.00	0.16	0.00	49.54	65.97	2.00	0.00	0.16	0.00
49.70	65.40	2.00	0.00	0.16	0.00	49.87	62.98	2.00	0.00	0.15	0.00
50.03	60.76	2.00	0.00	0.15	0.00						

Total estimated settlement: 0.00

Abbreviations

$Q_{tn,cs}$:	Equivalent clean sand normalized cone resistance
FS:	Factor of safety against liquefaction
e_v (%):	Post-liquefaction volumentric strain
DF:	e_v depth weighting factor
Settlement:	Calculated settlement

LANDMARK
Geo-Engineers and Geologists

Landmark Consultants, Inc.
780 N. 4th Street
El Centro, CA 92243

LIQUEFACTION ANALYSIS REPORT

Project title : Heber 2 Repower Project **Location : Heber, CA**

CPT file : CPT-3

Input parameters and analysis data

Analysis method:	NCEER (1998)	G.W.T. (in-situ):	8.00 ft	Use fill:	No	Clay like behavior applied:	Sands only
Fines correction method:	NCEER (1998)	G.W.T. (earthq.):	8.00 ft	Fill height:	N/A	Limit depth applied:	No
Points to test:	Based on Ic value	Average results interval:	3	Fill weight:	N/A	Limit depth:	N/A
Earthquake magnitude M_w:	7.00	Ic cut-off value:	2.60	Trans. detect. applied:	Yes	MSF method:	Method based
Peak ground acceleration:	0.50	Unit weight calculation:	Based on SBT	K_o applied:	Yes		

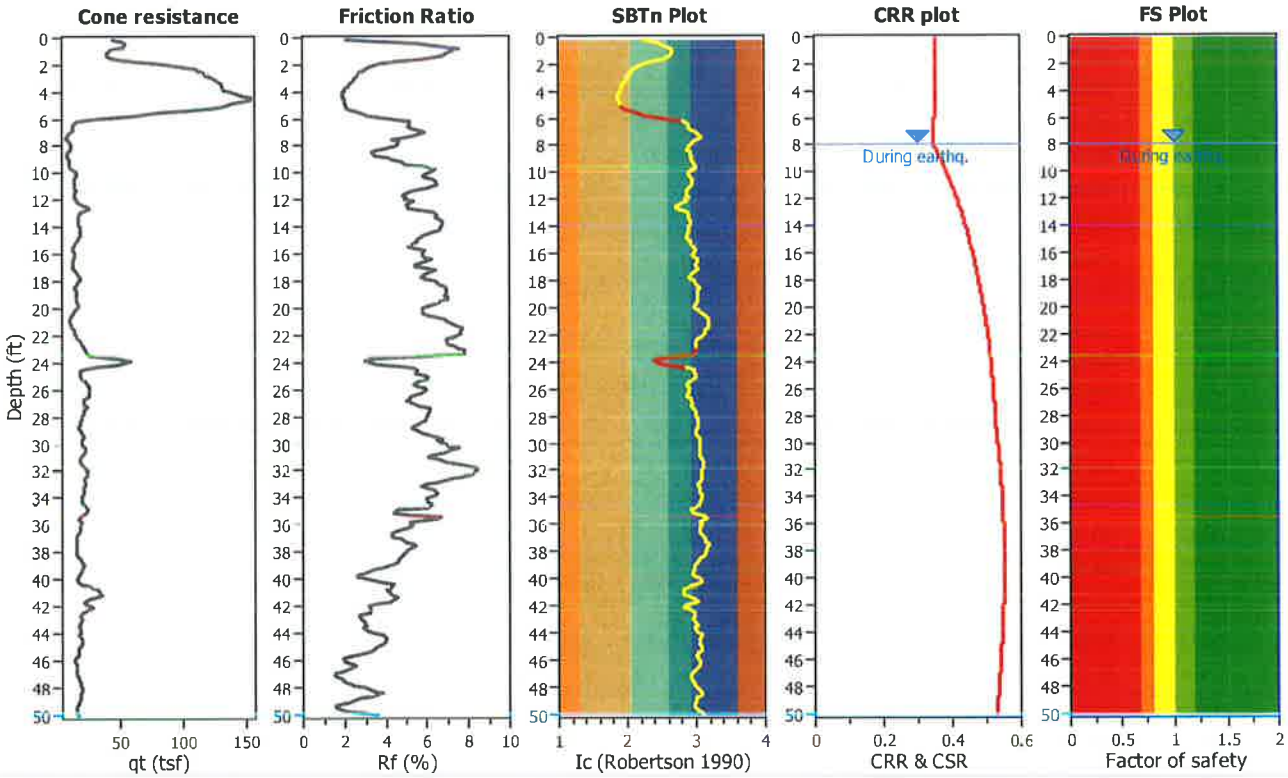

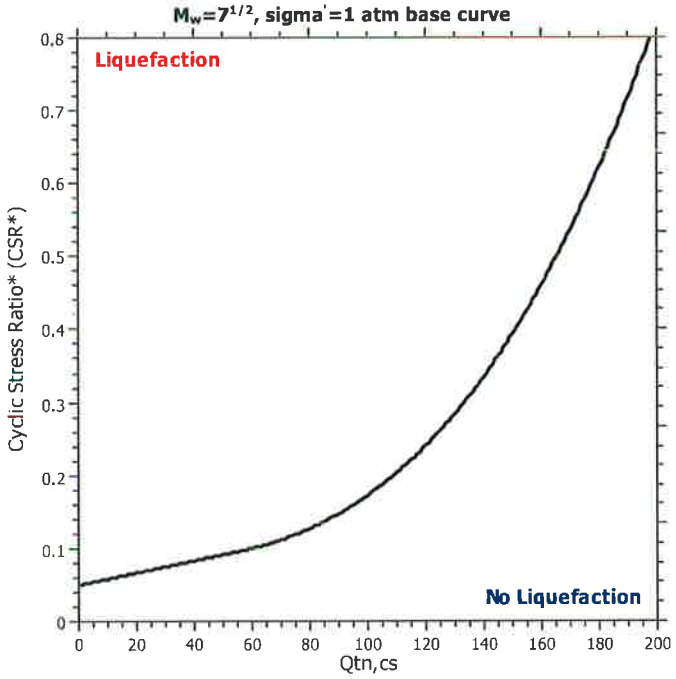

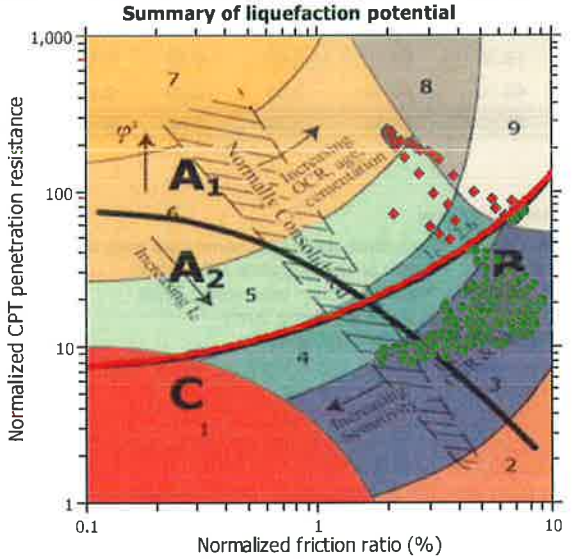

Zone A_1: Cyclic liquefaction likely depending on size and duration of cyclic loading
Zone A_2: Cyclic liquefaction and strength loss likely depending on loading and ground geometry
Zone B: Liquefaction and post-earthquake strength loss unlikely, check cyclic softening
Zone C: Cyclic liquefaction and strength loss possible depending on soil plasticity, brittleness/sensitivity, strain to peak undrained strength and ground geometry

CPT basic interpretation plots

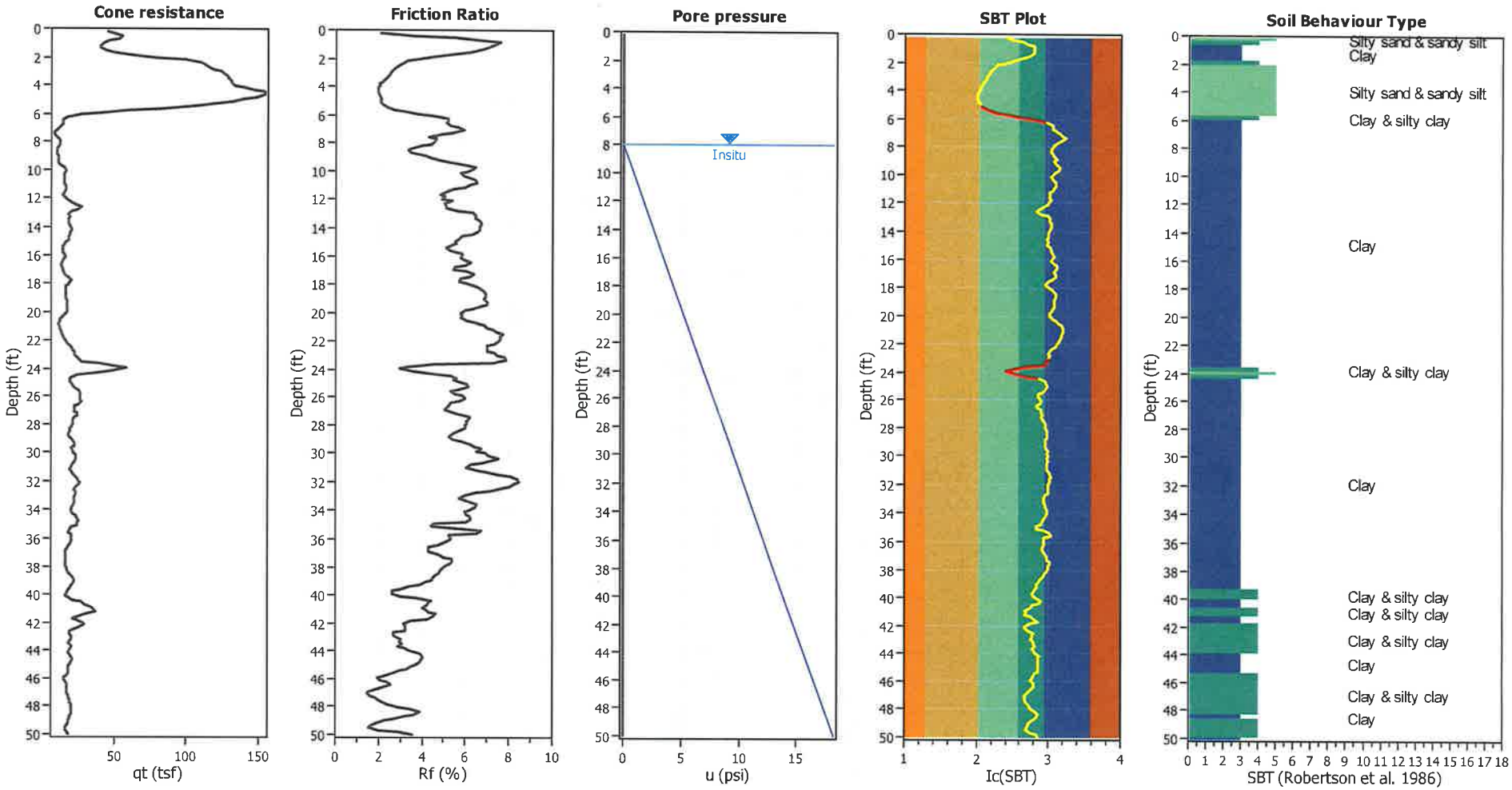

Input parameters and analysis data

Analysis method:	NCEER (1998)	Depth to water table (erthq.):	8.00 ft	Fill weight:	N/A
Fines correction method:	NCEER (1998)	Average results interval:	3	Transition detect. applied:	Yes
Points to test:	Based on Ic value	Ic cut-off value:	2.60	K_σ applied:	Yes
Earthquake magnitude M_w:	7.00	Unit weight calculation:	Based on SBT	Clay like behavior applied:	Sands only
Peak ground acceleration:	0.50	Use fill:	No	Limit depth applied:	No
Depth to water table (insitu):	8.00 ft	Fill height:	N/A	Limit depth:	N/A

SBT legend

1. Sensitive fine grained
2. Organic material
3. Clay to silty clay
4. Clayey silt to silty
5. Silty sand to sandy silt
6. Clean sand to silty sand
7. Gravely sand to sand
8. Very stiff sand to
9. Very stiff fine grained

Estimation of post-earthquake settlements

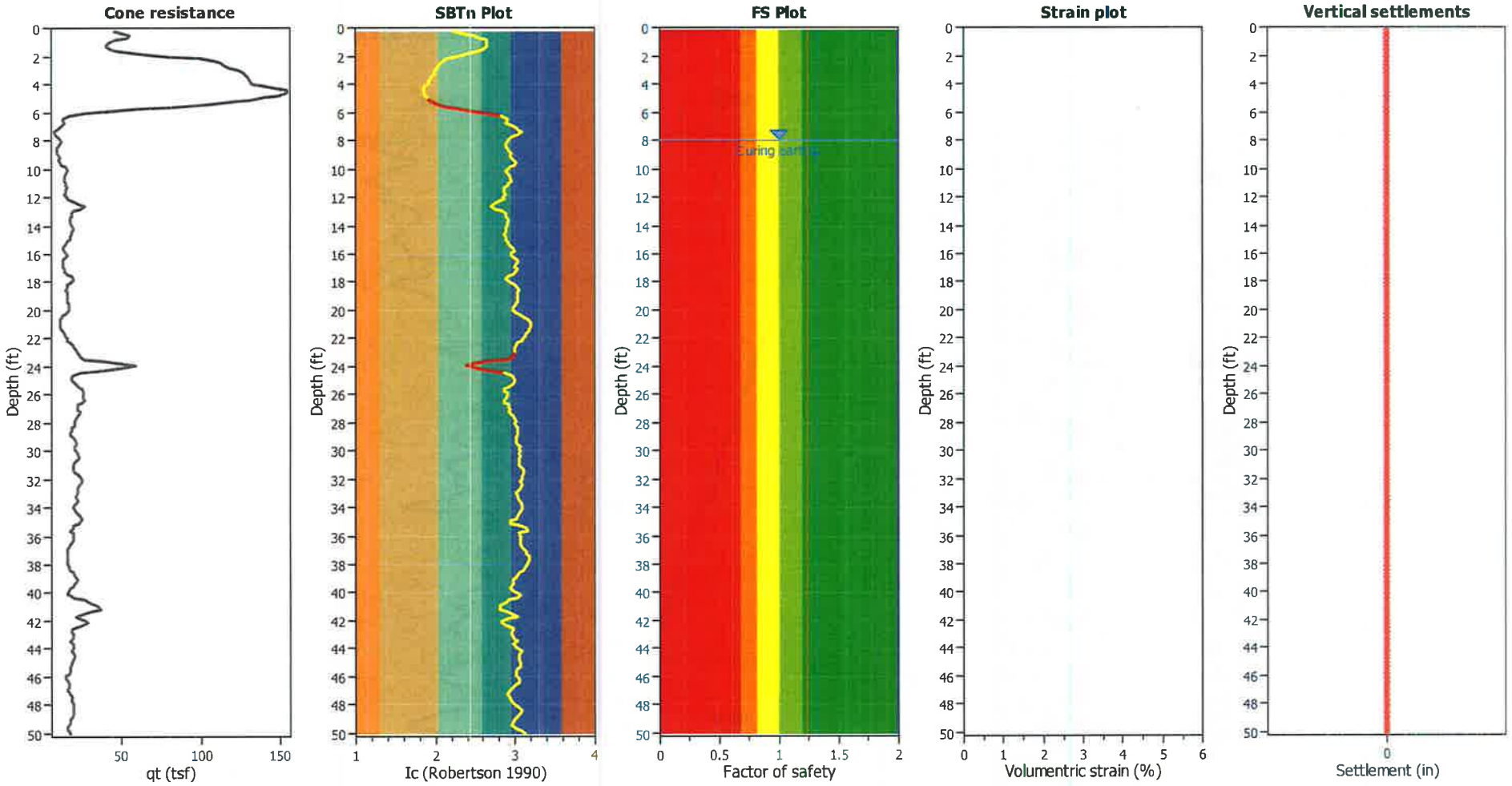

Abbreviations

q_t:	Total cone resistance (cone resistance q_c corrected for pore water effects)
I_c:	Soil Behaviour Type Index
FS:	Calculated Factor of Safety against liquefaction
Volumentric strain:	Post-liquefaction volumentric strain

:: Post-earthquake settlement due to soil liquefaction ::

Depth (ft)	$Q_{tn,cs}$	FS	e_v (%)	DF	Settlement (in)	Depth (ft)	$Q_{tn,cs}$	FS	e_v (%)	DF	Settlement (in)
8.04	105.22	2.00	0.00	0.86	0.00	8.20	98.09	2.00	0.00	0.86	0.00
8.37	89.48	2.00	0.00	0.86	0.00	8.53	84.06	2.00	0.00	0.86	0.00
8.69	85.12	2.00	0.00	0.85	0.00	8.86	93.40	2.00	0.00	0.85	0.00
9.02	99.67	2.00	0.00	0.85	0.00	9.19	104.91	2.00	0.00	0.84	0.00
9.35	106.95	2.00	0.00	0.84	0.00	9.51	115.87	2.00	0.00	0.84	0.00
9.68	128.34	2.00	0.00	0.84	0.00	9.84	137.59	2.00	0.00	0.83	0.00
10.01	139.16	2.00	0.00	0.83	0.00	10.17	135.75	2.00	0.00	0.83	0.00
10.33	134.00	2.00	0.00	0.82	0.00	10.50	136.19	2.00	0.00	0.82	0.00
10.66	138.03	2.00	0.00	0.82	0.00	10.83	138.95	2.00	0.00	0.82	0.00
10.99	137.77	2.00	0.00	0.81	0.00	11.15	136.64	2.00	0.00	0.81	0.00
11.32	132.10	2.00	0.00	0.81	0.00	11.48	125.76	2.00	0.00	0.81	0.00
11.65	120.13	2.00	0.00	0.80	0.00	11.81	120.19	2.00	0.00	0.80	0.00
11.98	125.19	2.00	0.00	0.80	0.00	12.14	132.55	2.00	0.00	0.79	0.00
12.30	140.53	2.00	0.00	0.79	0.00	12.47	151.43	2.00	0.00	0.79	0.00
12.63	157.43	2.00	0.00	0.79	0.00	12.80	158.94	2.00	0.00	0.78	0.00
12.96	155.22	2.00	0.00	0.78	0.00	13.12	152.28	2.00	0.00	0.78	0.00
13.29	151.52	2.00	0.00	0.77	0.00	13.45	152.54	2.00	0.00	0.77	0.00
13.62	152.19	2.00	0.00	0.77	0.00	13.78	153.09	2.00	0.00	0.77	0.00
13.94	154.64	2.00	0.00	0.76	0.00	14.11	156.69	2.00	0.00	0.76	0.00
14.27	155.45	2.00	0.00	0.76	0.00	14.44	149.53	2.00	0.00	0.76	0.00
14.60	141.82	2.00	0.00	0.75	0.00	14.76	137.16	2.00	0.00	0.75	0.00
14.93	132.83	2.00	0.00	0.75	0.00	15.09	128.46	2.00	0.00	0.74	0.00
15.26	120.02	2.00	0.00	0.74	0.00	15.42	114.98	2.00	0.00	0.74	0.00
15.58	115.12	2.00	0.00	0.74	0.00	15.75	121.64	2.00	0.00	0.73	0.00
15.91	125.61	2.00	0.00	0.73	0.00	16.08	126.76	2.00	0.00	0.73	0.00
16.24	125.34	2.00	0.00	0.72	0.00	16.40	122.47	2.00	0.00	0.72	0.00
16.57	116.72	2.00	0.00	0.72	0.00	16.73	112.12	2.00	0.00	0.72	0.00
16.90	113.22	2.00	0.00	0.71	0.00	17.06	120.49	2.00	0.00	0.71	0.00
17.22	126.45	2.00	0.00	0.71	0.00	17.39	130.53	2.00	0.00	0.71	0.00
17.55	132.64	2.00	0.00	0.70	0.00	17.72	135.99	2.00	0.00	0.70	0.00
17.88	137.42	2.00	0.00	0.70	0.00	18.04	136.58	2.00	0.00	0.69	0.00
18.21	132.83	2.00	0.00	0.69	0.00	18.37	131.91	2.00	0.00	0.69	0.00
18.54	132.44	2.00	0.00	0.69	0.00	18.70	132.83	2.00	0.00	0.68	0.00
18.86	132.94	2.00	0.00	0.68	0.00	19.03	132.94	2.00	0.00	0.68	0.00
19.19	135.47	2.00	0.00	0.67	0.00	19.36	134.98	2.00	0.00	0.67	0.00
19.52	132.82	2.00	0.00	0.67	0.00	19.69	129.87	2.00	0.00	0.67	0.00
19.85	126.97	2.00	0.00	0.66	0.00	20.01	123.39	2.00	0.00	0.66	0.00
20.18	116.87	2.00	0.00	0.66	0.00	20.34	109.55	2.00	0.00	0.66	0.00
20.51	105.52	2.00	0.00	0.65	0.00	20.67	105.35	2.00	0.00	0.65	0.00
20.83	107.65	2.00	0.00	0.65	0.00	21.00	108.62	2.00	0.00	0.64	0.00
21.16	112.61	2.00	0.00	0.64	0.00	21.33	117.42	2.00	0.00	0.64	0.00
21.49	121.92	2.00	0.00	0.64	0.00	21.65	125.67	2.00	0.00	0.63	0.00
21.82	129.09	2.00	0.00	0.63	0.00	21.98	130.92	2.00	0.00	0.63	0.00
22.15	132.02	2.00	0.00	0.62	0.00	22.31	133.84	2.00	0.00	0.62	0.00
22.47	140.34	2.00	0.00	0.62	0.00	22.64	144.51	2.00	0.00	0.62	0.00
22.80	149.71	2.00	0.00	0.61	0.00	22.97	152.21	2.00	0.00	0.61	0.00
23.13	158.62	2.00	0.00	0.61	0.00	23.29	164.29	2.00	0.00	0.61	0.00
23.46	163.34	2.00	0.00	0.60	0.00	23.62	149.57	2.00	0.00	0.60	0.00

:: Post-earthquake settlement due to soil liquefaction :: (continued)

Depth (ft)	$Q_{tn,cs}$	FS	e_v (%)	DF	Settlement (in)	Depth (ft)	$Q_{tn,cs}$	FS	e_v (%)	DF	Settlement (in)
23.79	137.21	2.00	0.00	0.60	0.00	23.95	138.01	2.00	0.00	0.59	0.00
24.11	142.14	2.00	0.00	0.59	0.00	24.28	141.20	2.00	0.00	0.59	0.00
24.44	130.89	2.00	0.00	0.59	0.00	24.61	121.03	2.00	0.00	0.58	0.00
24.77	117.62	2.00	0.00	0.58	0.00	24.93	121.38	2.00	0.00	0.58	0.00
25.10	126.27	2.00	0.00	0.57	0.00	25.26	130.22	2.00	0.00	0.57	0.00
25.43	129.59	2.00	0.00	0.57	0.00	25.59	131.09	2.00	0.00	0.57	0.00
25.75	135.18	2.00	0.00	0.56	0.00	25.92	139.49	2.00	0.00	0.56	0.00
26.08	139.40	2.00	0.00	0.56	0.00	26.25	137.13	2.00	0.00	0.56	0.00
26.41	133.24	2.00	0.00	0.55	0.00	26.57	128.22	2.00	0.00	0.55	0.00
26.74	120.94	2.00	0.00	0.55	0.00	26.90	117.65	2.00	0.00	0.54	0.00
27.07	123.39	2.00	0.00	0.54	0.00	27.23	130.15	2.00	0.00	0.54	0.00
27.40	134.00	2.00	0.00	0.54	0.00	27.56	130.29	2.00	0.00	0.53	0.00
27.72	125.72	2.00	0.00	0.53	0.00	27.89	123.53	2.00	0.00	0.53	0.00
28.05	123.09	2.00	0.00	0.52	0.00	28.22	121.41	2.00	0.00	0.52	0.00
28.38	117.09	2.00	0.00	0.52	0.00	28.54	111.50	2.00	0.00	0.52	0.00
28.71	108.31	2.00	0.00	0.51	0.00	28.87	107.69	2.00	0.00	0.51	0.00
29.04	112.56	2.00	0.00	0.51	0.00	29.20	119.74	2.00	0.00	0.51	0.00
29.36	125.93	2.00	0.00	0.50	0.00	29.53	127.06	2.00	0.00	0.50	0.00
29.69	126.51	2.00	0.00	0.50	0.00	29.86	125.39	2.00	0.00	0.49	0.00
30.02	129.92	2.00	0.00	0.49	0.00	30.18	135.27	2.00	0.00	0.49	0.00
30.35	140.32	2.00	0.00	0.49	0.00	30.51	137.30	2.00	0.00	0.48	0.00
30.68	129.14	2.00	0.00	0.48	0.00	30.84	120.95	2.00	0.00	0.48	0.00
31.00	116.56	2.00	0.00	0.47	0.00	31.17	119.19	2.00	0.00	0.47	0.00
31.33	123.11	2.00	0.00	0.47	0.00	31.50	131.51	2.00	0.00	0.47	0.00
31.66	140.19	2.00	0.00	0.46	0.00	31.82	148.00	2.00	0.00	0.46	0.00
31.99	151.97	2.00	0.00	0.46	0.00	32.15	151.52	2.00	0.00	0.46	0.00
32.32	145.89	2.00	0.00	0.45	0.00	32.48	138.22	2.00	0.00	0.45	0.00
32.64	131.44	2.00	0.00	0.45	0.00	32.81	126.66	2.00	0.00	0.44	0.00
32.97	120.92	2.00	0.00	0.44	0.00	33.14	115.82	2.00	0.00	0.44	0.00
33.30	117.32	2.00	0.00	0.44	0.00	33.46	122.10	2.00	0.00	0.43	0.00
33.63	123.45	2.00	0.00	0.43	0.00	33.79	118.97	2.00	0.00	0.43	0.00
33.96	114.29	2.00	0.00	0.42	0.00	34.12	113.26	2.00	0.00	0.42	0.00
34.28	116.07	2.00	0.00	0.42	0.00	34.45	120.77	2.00	0.00	0.42	0.00
34.61	124.37	2.00	0.00	0.41	0.00	34.78	124.30	2.00	0.00	0.41	0.00
34.94	107.22	2.00	0.00	0.41	0.00	35.10	104.14	2.00	0.00	0.41	0.00
35.27	103.90	2.00	0.00	0.40	0.00	35.43	114.48	2.00	0.00	0.40	0.00
35.60	108.91	2.00	0.00	0.40	0.00	35.76	103.69	2.00	0.00	0.39	0.00
35.93	103.19	2.00	0.00	0.39	0.00	36.09	102.94	2.00	0.00	0.39	0.00
36.25	100.79	2.00	0.00	0.39	0.00	36.42	95.16	2.00	0.00	0.38	0.00
36.58	89.61	2.00	0.00	0.38	0.00	36.75	86.08	2.00	0.00	0.38	0.00
36.91	85.66	2.00	0.00	0.37	0.00	37.07	88.52	2.00	0.00	0.37	0.00
37.24	90.83	2.00	0.00	0.37	0.00	37.40	92.89	2.00	0.00	0.37	0.00
37.57	92.98	2.00	0.00	0.36	0.00	37.73	92.32	2.00	0.00	0.36	0.00
37.89	90.55	2.00	0.00	0.36	0.00	38.06	89.64	2.00	0.00	0.35	0.00
38.22	90.25	2.00	0.00	0.35	0.00	38.39	91.89	2.00	0.00	0.35	0.00
38.55	94.23	2.00	0.00	0.35	0.00	38.71	96.50	2.00	0.00	0.34	0.00
38.88	96.89	2.00	0.00	0.34	0.00	39.04	94.80	2.00	0.00	0.34	0.00
39.21	90.16	2.00	0.00	0.34	0.00	39.37	83.66	2.00	0.00	0.33	0.00

:: Post-earthquake settlement due to soil liquefaction :: (continued)

Depth (ft)	$Q_{tn,cs}$	FS	e_v (%)	DF	Settlement (in)	Depth (ft)	$Q_{tn,cs}$	FS	e_v (%)	DF	Settlement (in)
39.53	76.97	2.00	0.00	0.33	0.00	39.70	70.89	2.00	0.00	0.33	0.00
39.86	68.91	2.00	0.00	0.32	0.00	40.03	71.76	2.00	0.00	0.32	0.00
40.19	81.13	2.00	0.00	0.32	0.00	40.35	93.57	2.00	0.00	0.32	0.00
40.52	103.75	2.00	0.00	0.31	0.00	40.68	107.44	2.00	0.00	0.31	0.00
40.85	110.91	2.00	0.00	0.31	0.00	41.01	115.14	2.00	0.00	0.30	0.00
41.17	118.91	2.00	0.00	0.30	0.00	41.34	114.80	2.00	0.00	0.30	0.00
41.50	103.67	2.00	0.00	0.30	0.00	41.67	91.95	2.00	0.00	0.29	0.00
41.83	88.04	2.00	0.00	0.29	0.00	41.99	90.47	2.00	0.00	0.29	0.00
42.16	92.83	2.00	0.00	0.29	0.00	42.32	87.29	2.00	0.00	0.28	0.00
42.49	78.72	2.00	0.00	0.28	0.00	42.65	71.54	2.00	0.00	0.28	0.00
42.81	71.84	2.00	0.00	0.27	0.00	42.98	73.65	2.00	0.00	0.27	0.00
43.14	75.58	2.00	0.00	0.27	0.00	43.31	74.00	2.00	0.00	0.27	0.00
43.47	73.64	2.00	0.00	0.26	0.00	43.64	73.86	2.00	0.00	0.26	0.00
43.80	76.92	2.00	0.00	0.26	0.00	43.96	78.92	2.00	0.00	0.25	0.00
44.13	81.06	2.00	0.00	0.25	0.00	44.29	83.91	2.00	0.00	0.25	0.00
44.46	85.95	2.00	0.00	0.25	0.00	44.62	85.68	2.00	0.00	0.24	0.00
44.78	83.55	2.00	0.00	0.24	0.00	44.95	80.58	2.00	0.00	0.24	0.00
45.11	77.10	2.00	0.00	0.24	0.00	45.28	74.16	2.00	0.00	0.23	0.00
45.44	71.31	2.00	0.00	0.23	0.00	45.60	66.96	2.00	0.00	0.23	0.00
45.77	60.99	2.00	0.00	0.22	0.00	45.93	55.97	2.00	0.00	0.22	0.00
46.10	56.91	2.00	0.00	0.22	0.00	46.26	61.03	2.00	0.00	0.22	0.00
46.42	64.41	2.00	0.00	0.21	0.00	46.59	62.81	2.00	0.00	0.21	0.00
46.75	58.05	2.00	0.00	0.21	0.00	46.92	53.06	2.00	0.00	0.20	0.00
47.08	52.59	2.00	0.00	0.20	0.00	47.24	54.97	2.00	0.00	0.20	0.00
47.41	58.19	2.00	0.00	0.20	0.00	47.57	61.05	2.00	0.00	0.19	0.00
47.74	64.16	2.00	0.00	0.19	0.00	47.90	66.86	2.00	0.00	0.19	0.00
48.06	73.10	2.00	0.00	0.19	0.00	48.23	77.76	2.00	0.00	0.18	0.00
48.39	80.72	2.00	0.00	0.18	0.00	48.56	78.24	2.00	0.00	0.18	0.00
48.72	74.42	2.00	0.00	0.17	0.00	48.88	68.90	2.00	0.00	0.17	0.00
49.05	63.15	2.00	0.00	0.17	0.00	49.21	57.14	2.00	0.00	0.17	0.00
49.38	52.74	2.00	0.00	0.16	0.00	49.54	51.53	2.00	0.00	0.16	0.00
49.70	56.86	2.00	0.00	0.16	0.00	49.87	66.86	2.00	0.00	0.15	0.00
50.03	74.65	2.00	0.00	0.15	0.00						

Total estimated settlement: 0.00

Abbreviations

$Q_{tn,cs}$:	Equivalent clean sand normalized cone resistance
FS:	Factor of safety against liquefaction
e_v (%):	Post-liquefaction volumentric strain
DF:	e_v depth weighting factor
Settlement:	Calculated settlement

LANDMARK
Geo-Engineers and Geologists

Landmark Consultants, Inc.
780 N. 4th Street
El Centro, CA 92243

LIQUEFACTION ANALYSIS REPORT

Project title : Heber 2 Repower Project **Location : Heber, CA**

CPT file : CPT-4

Input parameters and analysis data

Analysis method:	NCEER (1998)	G.W.T. (in-situ):	8.00 ft	Use fill:	No	Clay like behavior applied:	Sands only
Fines correction method:	NCEER (1998)	G.W.T. (earthq.):	8.00 ft	Fill height:	N/A	Limit depth applied:	No
Points to test:	Based on Ic value	Average results interval:	3	Fill weight:	N/A	Limit depth:	N/A
Earthquake magnitude M_w:	7.00	Ic cut-off value:	2.60	Trans. detect. applied:	Yes	MSF method:	Method based
Peak ground acceleration:	0.50	Unit weight calculation:	Based on SBT	K_σ applied:	Yes		

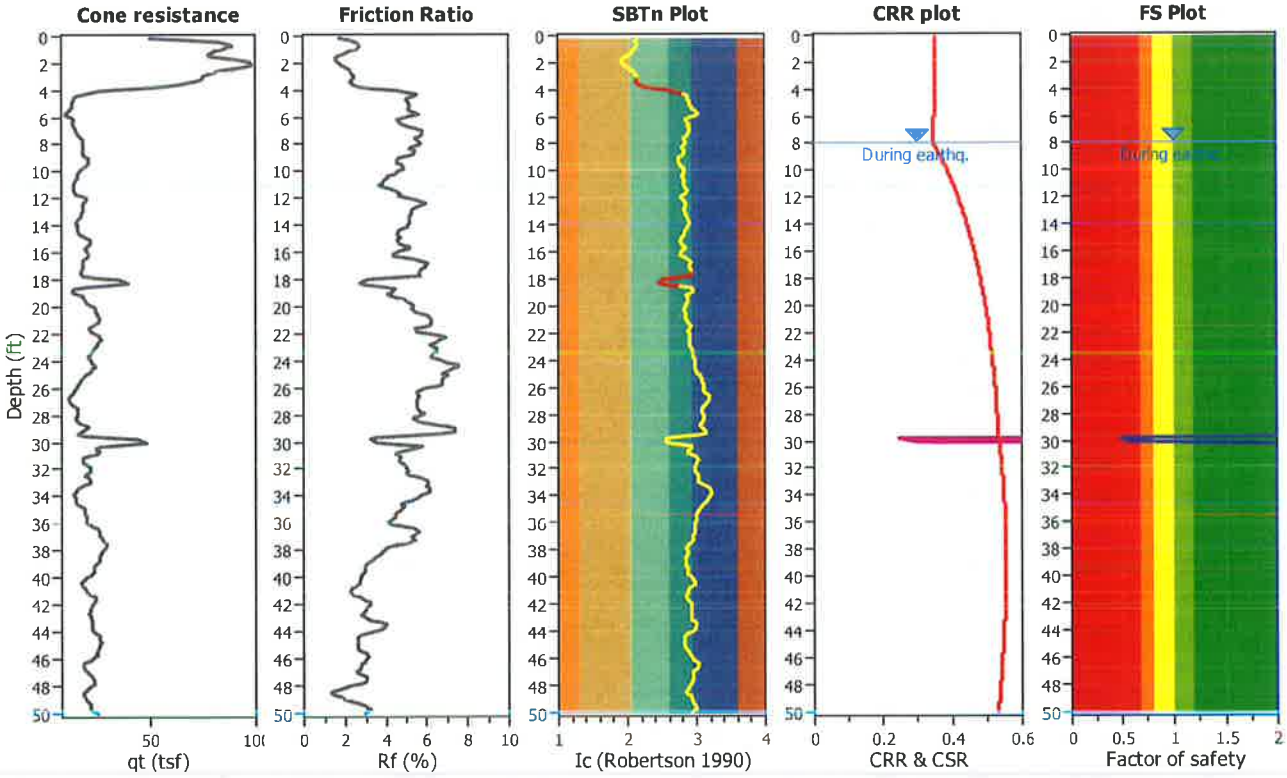

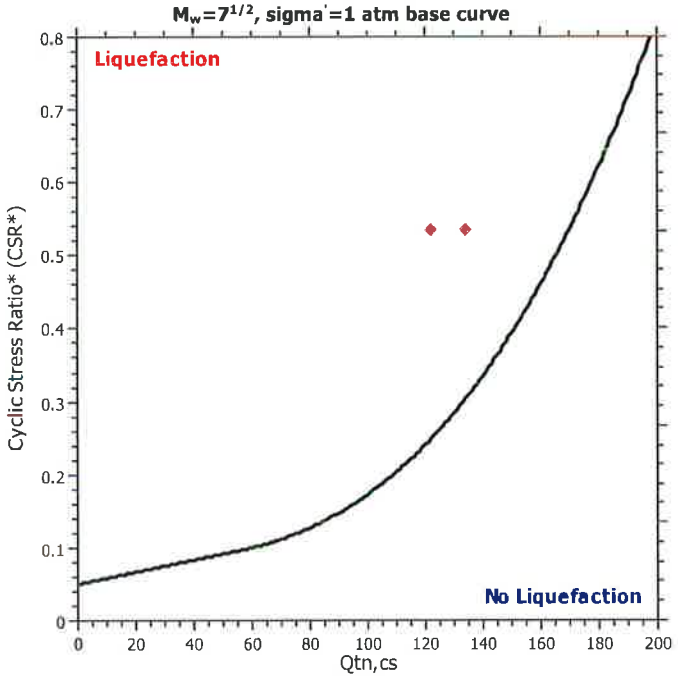

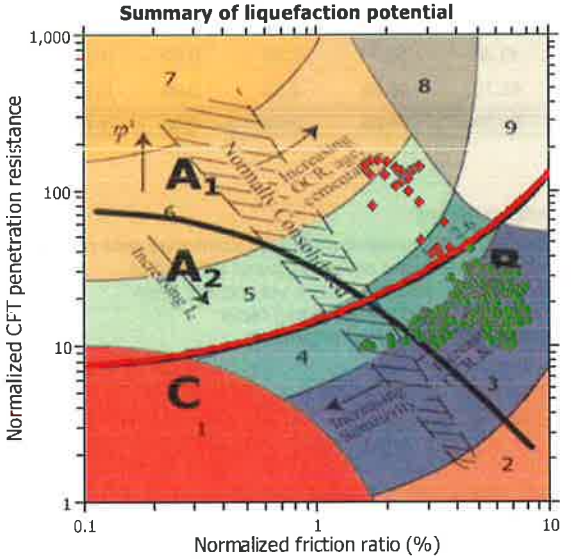

Zone A_1: Cyclic liquefaction likely depending on size and duration of cyclic loading
Zone A_2: Cyclic liquefaction and strength loss likely depending on loading and ground geometry
Zone B: Liquefaction and post-earthquake strength loss unlikely, check cyclic softening
Zone C: Cyclic liquefaction and strength loss possible depending on soil plasticity, brittleness/sensitivity, strain to peak undrained strength and ground geometry

CPT basic interpretation plots

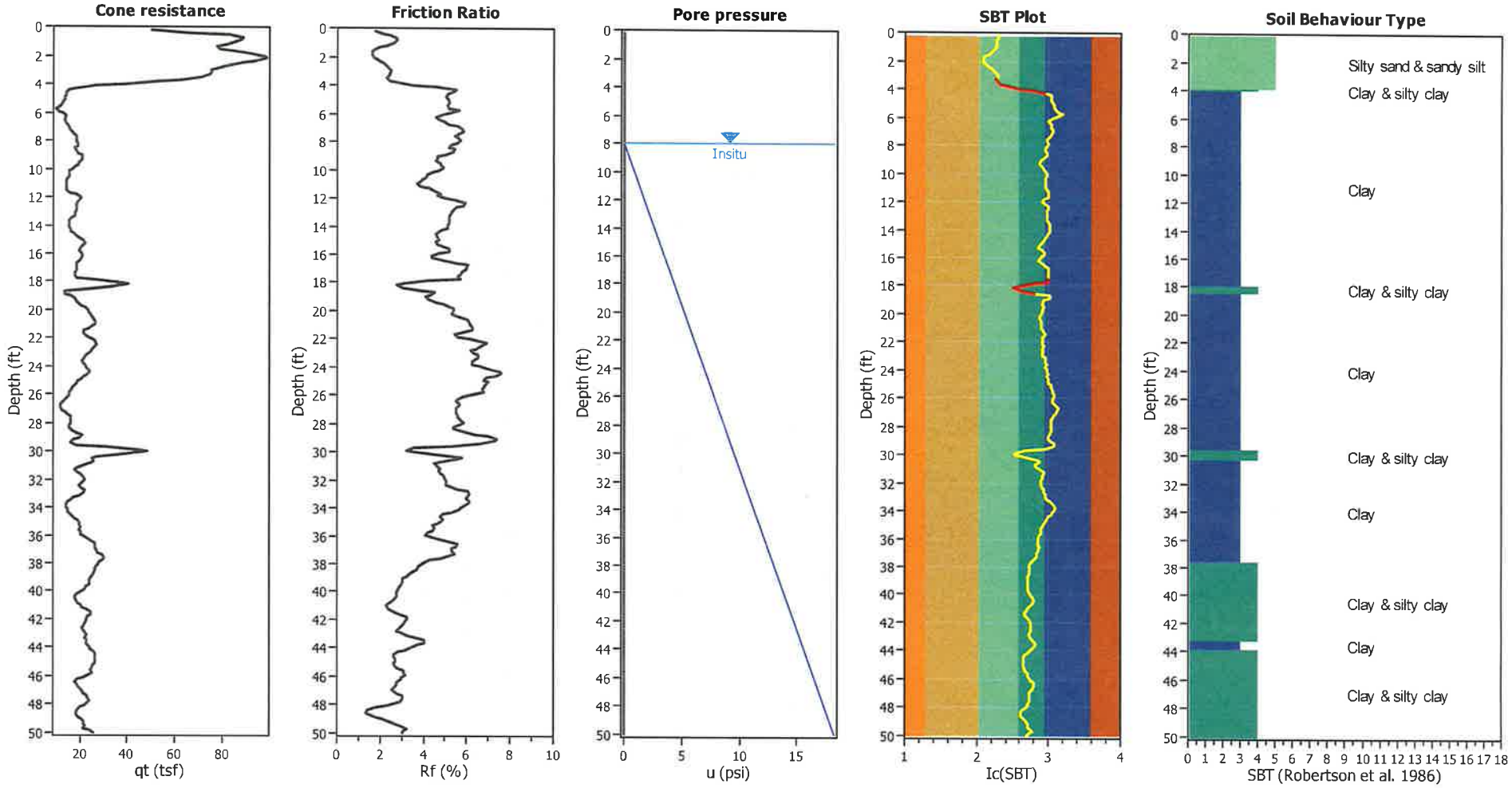

Input parameters and analysis data

Analysis method:	NCEER (1998)	Depth to water table (erthq.):	8.00 ft	Fill weight:	N/A
Fines correction method:	NCEER (1998)	Average results interval:	3	Transition detect. applied:	Yes
Points to test:	Based on Ic value	Ic cut-off value:	2.60	K_σ applied:	Yes
Earthquake magnitude M_w:	7.00	Unit weight calculation:	Based on SBT	Clay like behavior applied:	Sands only
Peak ground acceleration:	0.50	Use fill:	No	Limit depth applied:	No
Depth to water table (insitu):	8.00 ft	Fill height:	N/A	Limit depth:	N/A

SBT legend

1. Sensitive fine grained
2. Organic material
3. Clay to silty clay
4. Clayey silt to silty
5. Silty sand to sandy silt
6. Clean sand to silty sand
7. Gravely sand to sand
8. Very stiff sand to
9. Very stiff fine grained

Estimation of post-earthquake settlements

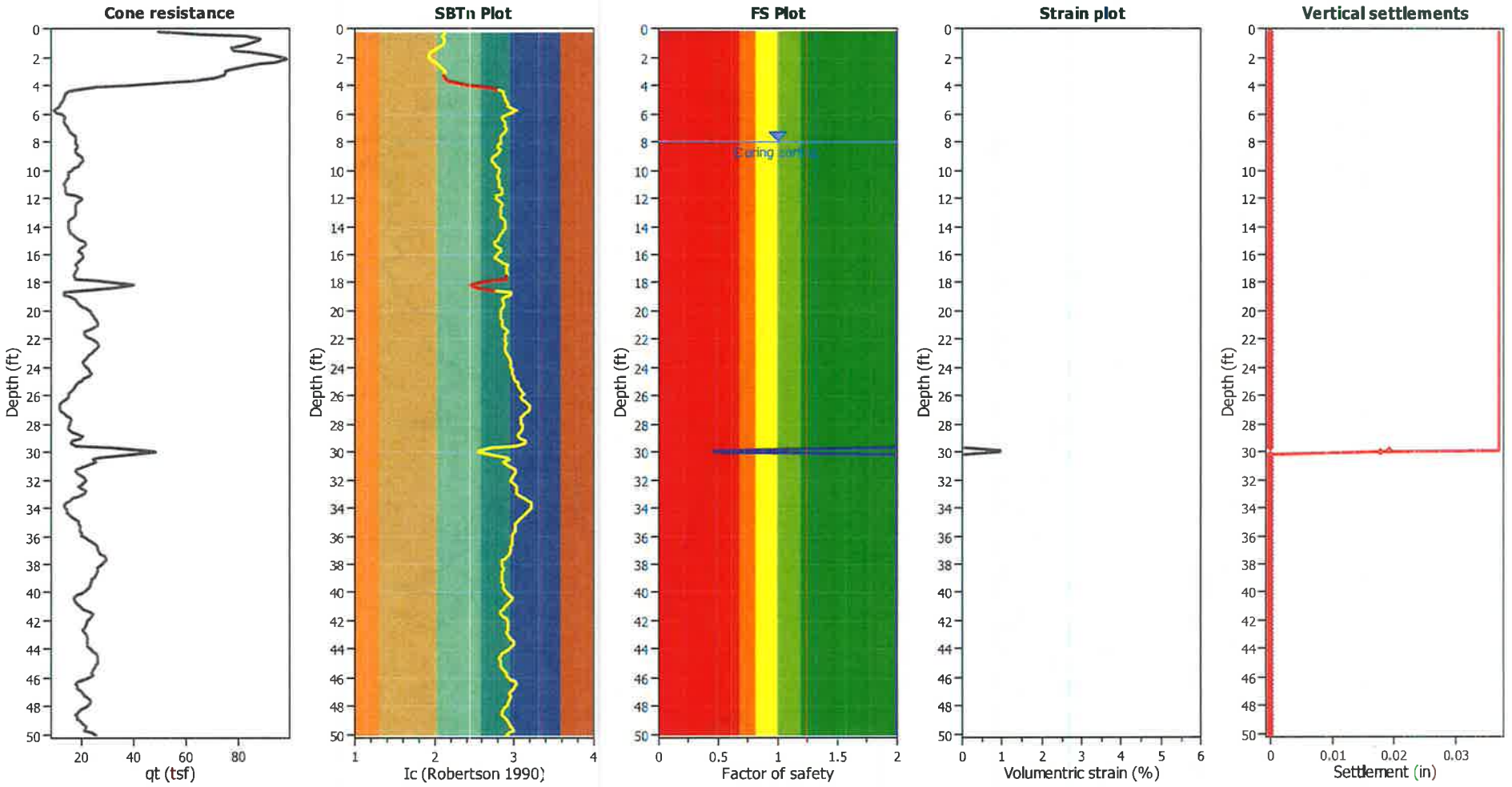

Abbreviations

q_t:	Total cone resistance (cone resistance q_c corrected for pore water effects)
I_c:	Soil Behaviour Type Index
FS:	Calculated Factor of Safety against liquefaction
Volumentric strain:	Post-liquefaction volumentric strain

:: Post-earthquake settlement due to soil liquefaction ::

Depth (ft)	$Q_{tn,cs}$	FS	e_v (%)	DF	Settlement (in)	Depth (ft)	$Q_{tn,cs}$	FS	e_v (%)	DF	Settlement (in)
8.04	142.33	2.00	0.00	0.86	0.00	8.20	139.48	2.00	0.00	0.86	0.00
8.37	138.37	2.00	0.00	0.86	0.00	8.53	139.38	2.00	0.00	0.86	0.00
8.69	139.25	2.00	0.00	0.85	0.00	8.86	137.40	2.00	0.00	0.85	0.00
9.02	135.29	2.00	0.00	0.85	0.00	9.19	135.08	2.00	0.00	0.84	0.00
9.35	134.94	2.00	0.00	0.84	0.00	9.51	135.74	2.00	0.00	0.84	0.00
9.68	134.20	2.00	0.00	0.84	0.00	9.84	130.53	2.00	0.00	0.83	0.00
10.01	123.17	2.00	0.00	0.83	0.00	10.17	117.24	2.00	0.00	0.83	0.00
10.33	113.17	2.00	0.00	0.82	0.00	10.50	112.17	2.00	0.00	0.82	0.00
10.66	108.77	2.00	0.00	0.82	0.00	10.83	104.41	2.00	0.00	0.82	0.00
10.99	101.82	2.00	0.00	0.81	0.00	11.15	104.52	2.00	0.00	0.81	0.00
11.32	109.26	2.00	0.00	0.81	0.00	11.48	112.95	2.00	0.00	0.81	0.00
11.65	119.67	2.00	0.00	0.80	0.00	11.81	128.35	2.00	0.00	0.80	0.00
11.98	140.47	2.00	0.00	0.80	0.00	12.14	147.20	2.00	0.00	0.79	0.00
12.30	148.82	2.00	0.00	0.79	0.00	12.47	144.70	2.00	0.00	0.79	0.00
12.63	140.44	2.00	0.00	0.79	0.00	12.80	138.49	2.00	0.00	0.78	0.00
12.96	137.16	2.00	0.00	0.78	0.00	13.12	135.57	2.00	0.00	0.78	0.00
13.29	132.50	2.00	0.00	0.77	0.00	13.45	129.05	2.00	0.00	0.77	0.00
13.62	125.64	2.00	0.00	0.77	0.00	13.78	124.00	2.00	0.00	0.77	0.00
13.94	123.55	2.00	0.00	0.76	0.00	14.11	123.41	2.00	0.00	0.76	0.00
14.27	120.42	2.00	0.00	0.76	0.00	14.44	118.59	2.00	0.00	0.76	0.00
14.60	119.72	2.00	0.00	0.75	0.00	14.76	124.75	2.00	0.00	0.75	0.00
14.93	129.68	2.00	0.00	0.75	0.00	15.09	132.02	2.00	0.00	0.74	0.00
15.26	133.55	2.00	0.00	0.74	0.00	15.42	134.74	2.00	0.00	0.74	0.00
15.58	134.99	2.00	0.00	0.74	0.00	15.75	133.14	2.00	0.00	0.73	0.00
15.91	128.53	2.00	0.00	0.73	0.00	16.08	125.13	2.00	0.00	0.73	0.00
16.24	124.40	2.00	0.00	0.72	0.00	16.40	129.52	2.00	0.00	0.72	0.00
16.57	133.92	2.00	0.00	0.72	0.00	16.73	138.54	2.00	0.00	0.72	0.00
16.90	138.35	2.00	0.00	0.71	0.00	17.06	138.11	2.00	0.00	0.71	0.00
17.22	135.17	2.00	0.00	0.71	0.00	17.39	131.59	2.00	0.00	0.71	0.00
17.55	129.88	2.00	0.00	0.70	0.00	17.72	132.65	2.00	0.00	0.70	0.00
17.88	129.80	2.00	0.00	0.70	0.00	18.04	125.42	2.00	0.00	0.69	0.00
18.21	120.72	2.00	0.00	0.69	0.00	18.37	117.18	2.00	0.00	0.69	0.00
18.54	111.78	2.00	0.00	0.69	0.00	18.70	102.14	2.00	0.00	0.68	0.00
18.86	99.81	2.00	0.00	0.68	0.00	19.03	103.57	2.00	0.00	0.68	0.00
19.19	110.46	2.00	0.00	0.67	0.00	19.36	115.60	2.00	0.00	0.67	0.00
19.52	121.21	2.00	0.00	0.67	0.00	19.69	128.63	2.00	0.00	0.67	0.00
19.85	135.46	2.00	0.00	0.66	0.00	20.01	137.97	2.00	0.00	0.66	0.00
20.18	138.68	2.00	0.00	0.66	0.00	20.34	141.42	2.00	0.00	0.66	0.00
20.51	148.20	2.00	0.00	0.65	0.00	20.67	152.28	2.00	0.00	0.65	0.00
20.83	154.70	2.00	0.00	0.65	0.00	21.00	155.14	2.00	0.00	0.64	0.00
21.16	153.33	2.00	0.00	0.64	0.00	21.33	146.51	2.00	0.00	0.64	0.00
21.49	137.48	2.00	0.00	0.64	0.00	21.65	130.46	2.00	0.00	0.63	0.00
21.82	135.64	2.00	0.00	0.63	0.00	21.98	146.28	2.00	0.00	0.63	0.00
22.15	157.92	2.00	0.00	0.62	0.00	22.31	162.22	2.00	0.00	0.62	0.00
22.47	158.98	2.00	0.00	0.62	0.00	22.64	153.08	2.00	0.00	0.62	0.00
22.80	147.97	2.00	0.00	0.61	0.00	22.97	147.24	2.00	0.00	0.61	0.00
23.13	146.00	2.00	0.00	0.61	0.00	23.29	142.46	2.00	0.00	0.61	0.00
23.46	137.35	2.00	0.00	0.60	0.00	23.62	134.72	2.00	0.00	0.60	0.00

:: Post-earthquake settlement due to soil liquefaction :: (continued)

Depth (ft)	$Q_{tn,cs}$	FS	e_v (%)	DF	Settlement (in)	Depth (ft)	$Q_{tn,cs}$	FS	e_v (%)	DF	Settlement (in)
23.79	135.51	2.00	0.00	0.60	0.00	23.95	140.30	2.00	0.00	0.59	0.00
24.11	148.28	2.00	0.00	0.59	0.00	24.28	155.88	2.00	0.00	0.59	0.00
24.44	157.27	2.00	0.00	0.59	0.00	24.61	150.21	2.00	0.00	0.58	0.00
24.77	141.21	2.00	0.00	0.58	0.00	24.93	135.75	2.00	0.00	0.58	0.00
25.10	133.99	2.00	0.00	0.57	0.00	25.26	129.44	2.00	0.00	0.57	0.00
25.43	124.86	2.00	0.00	0.57	0.00	25.59	121.99	2.00	0.00	0.57	0.00
25.75	119.46	2.00	0.00	0.56	0.00	25.92	114.39	2.00	0.00	0.56	0.00
26.08	108.01	2.00	0.00	0.56	0.00	26.25	102.56	2.00	0.00	0.56	0.00
26.41	98.09	2.00	0.00	0.55	0.00	26.57	94.88	2.00	0.00	0.55	0.00
26.74	93.00	2.00	0.00	0.55	0.00	26.90	92.55	2.00	0.00	0.54	0.00
27.07	94.48	2.00	0.00	0.54	0.00	27.23	98.16	2.00	0.00	0.54	0.00
27.40	102.11	2.00	0.00	0.54	0.00	27.56	105.58	2.00	0.00	0.53	0.00
27.72	108.32	2.00	0.00	0.53	0.00	27.89	108.90	2.00	0.00	0.53	0.00
28.05	105.70	2.00	0.00	0.52	0.00	28.22	101.01	2.00	0.00	0.52	0.00
28.38	101.21	2.00	0.00	0.52	0.00	28.54	109.35	2.00	0.00	0.52	0.00
28.71	122.45	2.00	0.00	0.51	0.00	28.87	132.20	2.00	0.00	0.51	0.00
29.04	132.26	2.00	0.00	0.51	0.00	29.20	122.61	2.00	0.00	0.51	0.00
29.36	113.45	2.00	0.00	0.50	0.00	29.53	108.45	2.00	0.00	0.50	0.00
29.69	112.51	2.00	0.00	0.50	0.00	29.86	122.10	0.47	0.98	0.49	0.02
30.02	134.00	0.57	0.90	0.49	0.02	30.18	139.79	2.00	0.00	0.49	0.00
30.35	134.38	2.00	0.00	0.49	0.00	30.51	125.58	2.00	0.00	0.48	0.00
30.68	118.58	2.00	0.00	0.48	0.00	30.84	113.67	2.00	0.00	0.48	0.00
31.00	107.11	2.00	0.00	0.47	0.00	31.17	101.29	2.00	0.00	0.47	0.00
31.33	99.19	2.00	0.00	0.47	0.00	31.50	101.98	2.00	0.00	0.47	0.00
31.66	105.65	2.00	0.00	0.46	0.00	31.82	110.41	2.00	0.00	0.46	0.00
31.99	112.05	2.00	0.00	0.46	0.00	32.15	110.51	2.00	0.00	0.46	0.00
32.32	106.64	2.00	0.00	0.45	0.00	32.48	106.90	2.00	0.00	0.45	0.00
32.64	113.40	2.00	0.00	0.45	0.00	32.81	120.33	2.00	0.00	0.44	0.00
32.97	120.02	2.00	0.00	0.44	0.00	33.14	113.57	2.00	0.00	0.44	0.00
33.30	105.91	2.00	0.00	0.44	0.00	33.46	102.21	2.00	0.00	0.43	0.00
33.63	98.16	2.00	0.00	0.43	0.00	33.79	94.29	2.00	0.00	0.43	0.00
33.96	92.81	2.00	0.00	0.42	0.00	34.12	94.31	2.00	0.00	0.42	0.00
34.28	92.55	2.00	0.00	0.42	0.00	34.45	90.14	2.00	0.00	0.42	0.00
34.61	91.88	2.00	0.00	0.41	0.00	34.78	97.81	2.00	0.00	0.41	0.00
34.94	99.81	2.00	0.00	0.41	0.00	35.10	98.30	2.00	0.00	0.41	0.00
35.27	96.86	2.00	0.00	0.40	0.00	35.43	97.74	2.00	0.00	0.40	0.00
35.60	97.15	2.00	0.00	0.40	0.00	35.76	95.38	2.00	0.00	0.39	0.00
35.93	94.33	2.00	0.00	0.39	0.00	36.09	98.44	2.00	0.00	0.39	0.00
36.25	106.57	2.00	0.00	0.39	0.00	36.42	116.11	2.00	0.00	0.38	0.00
36.58	121.17	2.00	0.00	0.38	0.00	36.75	121.27	2.00	0.00	0.38	0.00
36.91	118.99	2.00	0.00	0.37	0.00	37.07	118.97	2.00	0.00	0.37	0.00
37.24	121.97	2.00	0.00	0.37	0.00	37.40	122.80	2.00	0.00	0.37	0.00
37.57	119.74	2.00	0.00	0.36	0.00	37.73	112.21	2.00	0.00	0.36	0.00
37.89	105.81	2.00	0.00	0.36	0.00	38.06	101.75	2.00	0.00	0.35	0.00
38.22	99.67	2.00	0.00	0.35	0.00	38.39	97.89	2.00	0.00	0.35	0.00
38.55	95.90	2.00	0.00	0.35	0.00	38.71	93.10	2.00	0.00	0.34	0.00
38.88	89.59	2.00	0.00	0.34	0.00	39.04	86.60	2.00	0.00	0.34	0.00
39.21	85.25	2.00	0.00	0.34	0.00	39.37	84.76	2.00	0.00	0.33	0.00

:: Post-earthquake settlement due to soil liquefaction :: (continued)

Depth (ft)	$Q_{tn,cs}$	FS	e_v (%)	DF	Settlement (in)	Depth (ft)	$Q_{tn,cs}$	FS	e_v (%)	DF	Settlement (in)
39.53	83.85	2.00	0.00	0.33	0.00	39.70	81.80	2.00	0.00	0.33	0.00
39.86	79.22	2.00	0.00	0.32	0.00	40.03	76.47	2.00	0.00	0.32	0.00
40.19	73.46	2.00	0.00	0.32	0.00	40.35	71.67	2.00	0.00	0.32	0.00
40.52	70.72	2.00	0.00	0.31	0.00	40.68	69.95	2.00	0.00	0.31	0.00
40.85	69.28	2.00	0.00	0.31	0.00	41.01	69.53	2.00	0.00	0.30	0.00
41.17	71.27	2.00	0.00	0.30	0.00	41.34	74.52	2.00	0.00	0.30	0.00
41.50	80.79	2.00	0.00	0.30	0.00	41.67	83.97	2.00	0.00	0.29	0.00
41.83	85.73	2.00	0.00	0.29	0.00	41.99	83.77	2.00	0.00	0.29	0.00
42.16	83.35	2.00	0.00	0.29	0.00	42.32	81.51	2.00	0.00	0.28	0.00
42.49	78.90	2.00	0.00	0.28	0.00	42.65	77.04	2.00	0.00	0.28	0.00
42.81	76.77	2.00	0.00	0.27	0.00	42.98	78.97	2.00	0.00	0.27	0.00
43.14	83.16	2.00	0.00	0.27	0.00	43.31	88.56	2.00	0.00	0.27	0.00
43.47	91.55	2.00	0.00	0.26	0.00	43.64	91.06	2.00	0.00	0.26	0.00
43.80	88.91	2.00	0.00	0.26	0.00	43.96	86.77	2.00	0.00	0.25	0.00
44.13	84.65	2.00	0.00	0.25	0.00	44.29	82.07	2.00	0.00	0.25	0.00
44.46	80.48	2.00	0.00	0.25	0.00	44.62	80.38	2.00	0.00	0.24	0.00
44.78	80.96	2.00	0.00	0.24	0.00	44.95	80.56	2.00	0.00	0.24	0.00
45.11	79.49	2.00	0.00	0.24	0.00	45.28	79.02	2.00	0.00	0.23	0.00
45.44	79.84	2.00	0.00	0.23	0.00	45.60	82.76	2.00	0.00	0.23	0.00
45.77	83.63	2.00	0.00	0.22	0.00	45.93	82.78	2.00	0.00	0.22	0.00
46.10	77.11	2.00	0.00	0.22	0.00	46.26	72.76	2.00	0.00	0.22	0.00
46.42	69.37	2.00	0.00	0.21	0.00	46.59	69.74	2.00	0.00	0.21	0.00
46.75	69.62	2.00	0.00	0.21	0.00	46.92	69.91	2.00	0.00	0.20	0.00
47.08	72.01	2.00	0.00	0.20	0.00	47.24	75.02	2.00	0.00	0.20	0.00
47.41	78.40	2.00	0.00	0.20	0.00	47.57	79.97	2.00	0.00	0.19	0.00
47.74	79.74	2.00	0.00	0.19	0.00	47.90	76.12	2.00	0.00	0.19	0.00
48.06	69.32	2.00	0.00	0.19	0.00	48.23	60.53	2.00	0.00	0.18	0.00
48.39	53.50	2.00	0.00	0.18	0.00	48.56	51.55	2.00	0.00	0.18	0.00
48.72	53.74	2.00	0.00	0.17	0.00	48.88	58.38	2.00	0.00	0.17	0.00
49.05	63.34	2.00	0.00	0.17	0.00	49.21	68.92	2.00	0.00	0.17	0.00
49.38	72.80	2.00	0.00	0.16	0.00	49.54	76.03	2.00	0.00	0.16	0.00
49.70	77.80	2.00	0.00	0.16	0.00	49.87	79.94	2.00	0.00	0.15	0.00
50.03	81.33	2.00	0.00	0.15	0.00						

Total estimated settlement: 0.04

Abbreviations

$Q_{tn,cs}$: Equivalent clean sand normalized cone resistance
FS: Factor of safety against liquefaction
e_v (%): Post-liquefaction volumentric strain
DF: e_v depth weighting factor
Settlement: Calculated settlement

Landmark Consultants, Inc.
780 N. 4th Street
El Centro, CA 92243

LIQUEFACTION ANALYSIS REPORT

Project title : Heber 2 Repower Project **Location : Heber, CA**

CPT file : CPT-5

Input parameters and analysis data

Analysis method:	NCEER (1998)	G.W.T. (in-situ):	8.00 ft	Use fill:	No	Clay like behavior applied:	Sands only
Fines correction method:	NCEER (1998)	G.W.T. (earthq.):	8.00 ft	Fill height:	N/A	Limit depth applied:	No
Points to test:	Based on Ic value	Average results interval:	3	Fill weight:	N/A	Limit depth:	N/A
Earthquake magnitude M_w:	7.00	Ic cut-off value:	2.60	Trans. detect. applied:	Yes	MSF method:	Method based
Peak ground acceleration:	0.50	Unit weight calculation:	Based on SBT	K_σ applied:	Yes		

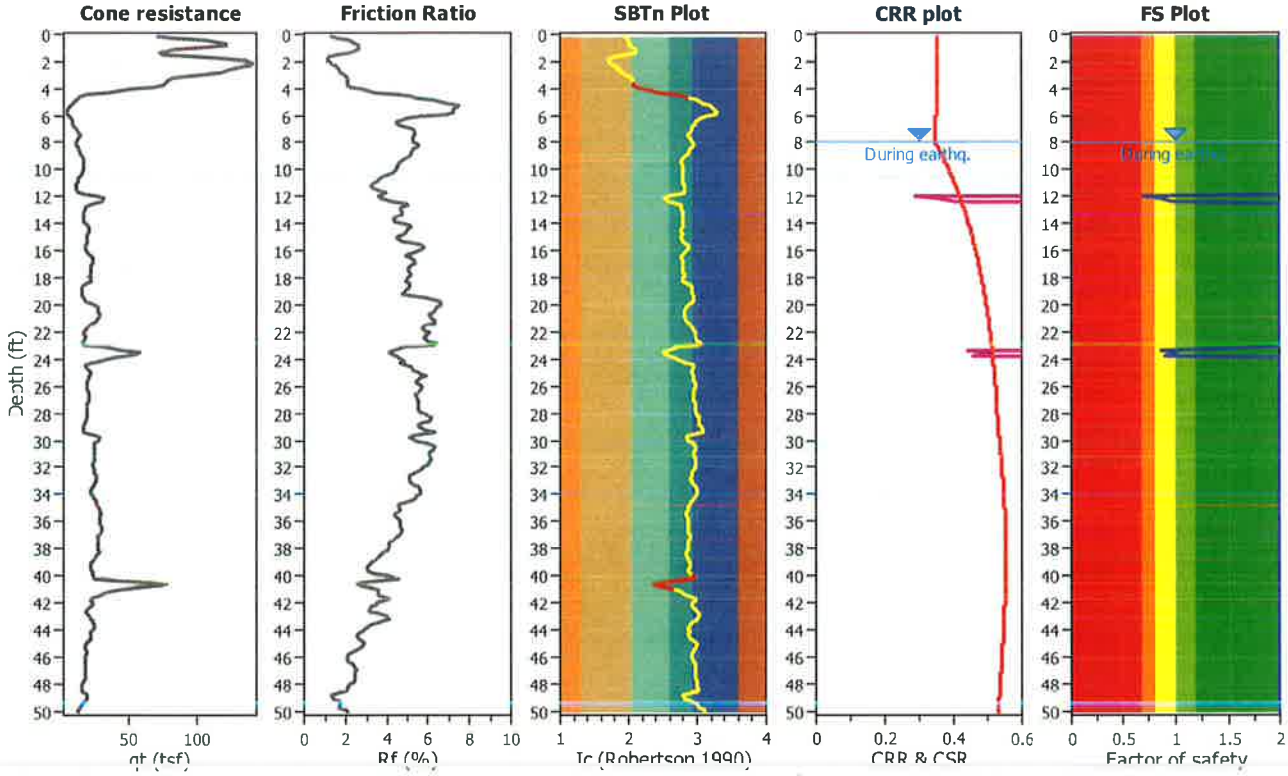

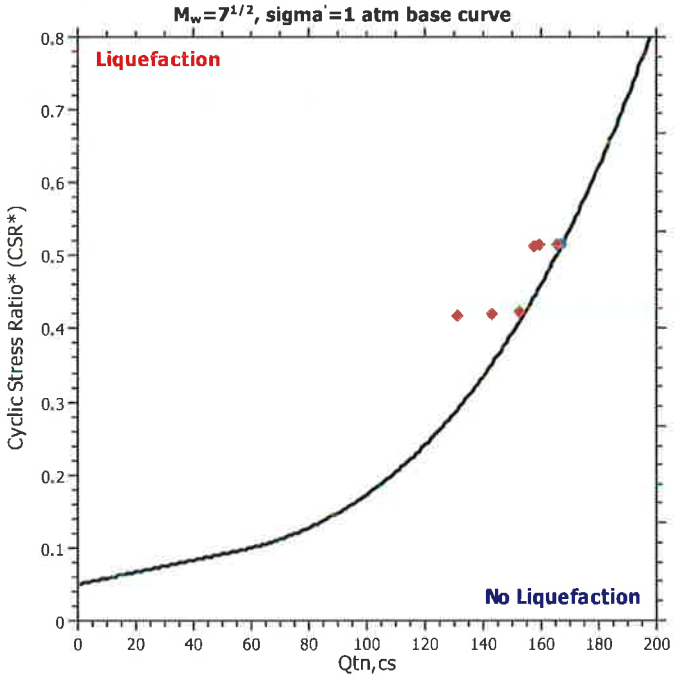

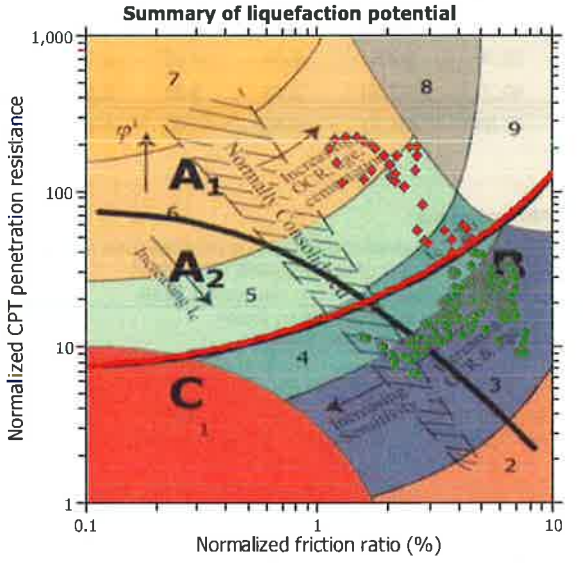

Zone A_1: Cyclic liquefaction likely depending on size and duration of cyclic loading
Zone A_2: Cyclic liquefaction and strength loss likely depending on loading and ground geometry
Zone B: Liquefaction and post-earthquake strength loss unlikely, check cyclic softening
Zone C: Cyclic liquefaction and strength loss possible depending on soil plasticity, brittleness/sensitivity, strain to peak undrained strength and ground geometry

CPT basic interpretation plots

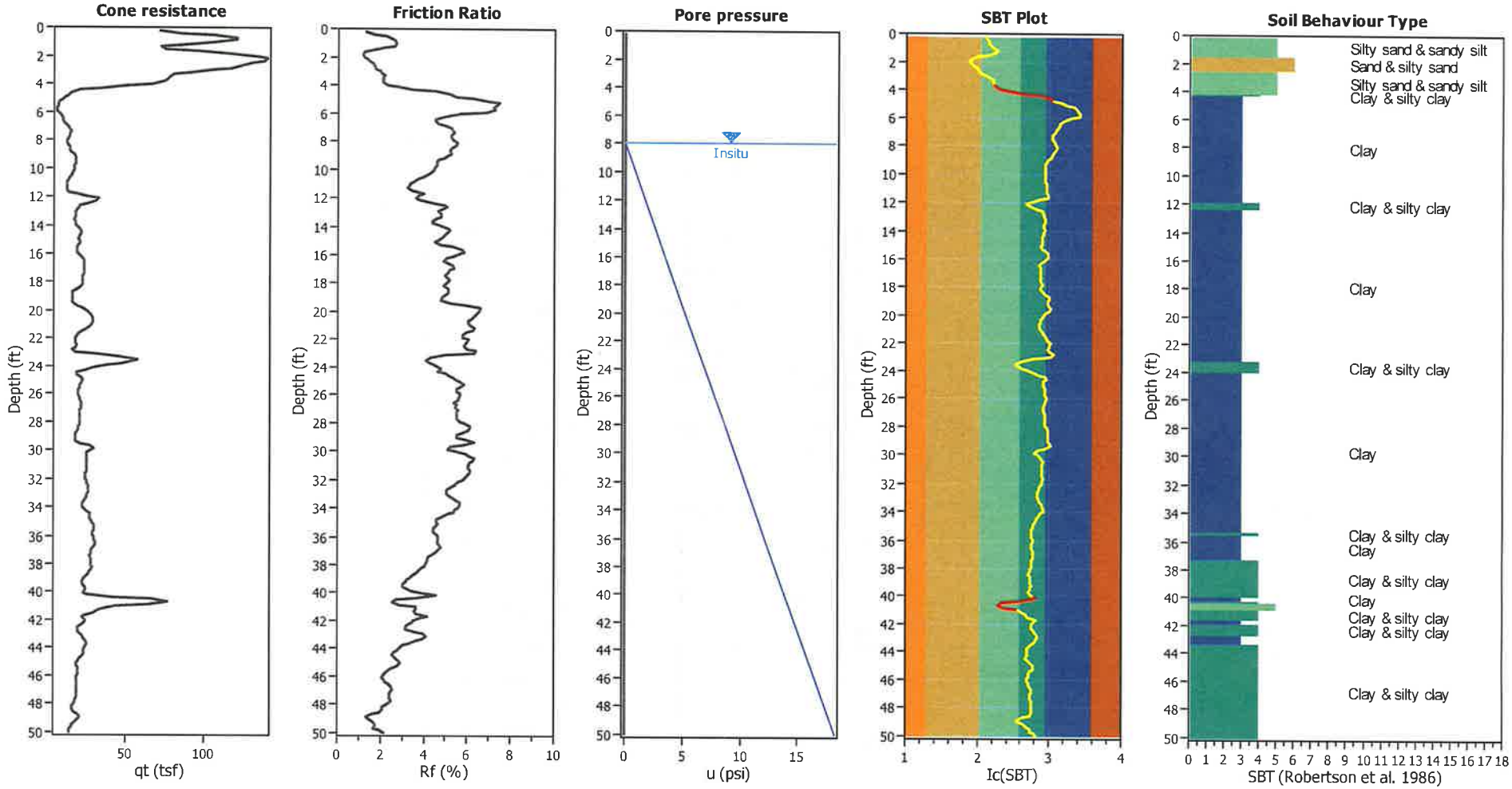

Input parameters and analysis data

Analysis method:	NCEER (1998)	Depth to water table (erthq.):	8.00 ft	Fill weight:	N/A
Fines correction method:	NCEER (1998)	Average results interval:	3	Transition detect. applied:	Yes
Points to test:	Based on Ic value	Ic cut-off value:	2.60	K_σ applied:	Yes
Earthquake magnitude M_w:	7.00	Unit weight calculation:	Based on SBT	Clay like behavior applied:	Sands only
Peak ground acceleration:	0.50	Use fill:	No	Limit depth applied:	No
Depth to water table (insitu):	8.00 ft	Fill height:	N/A	Limit depth:	N/A

SBT legend

1. Sensitive fine grained
2. Organic material
3. Clay to silty clay
4. Clayey silt to silty
5. Silty sand to sandy silt
6. Clean sand to silty sand
7. Gravely sand to sand
8. Very stiff sand to
9. Very stiff fine grained

Estimation of post-earthquake settlements

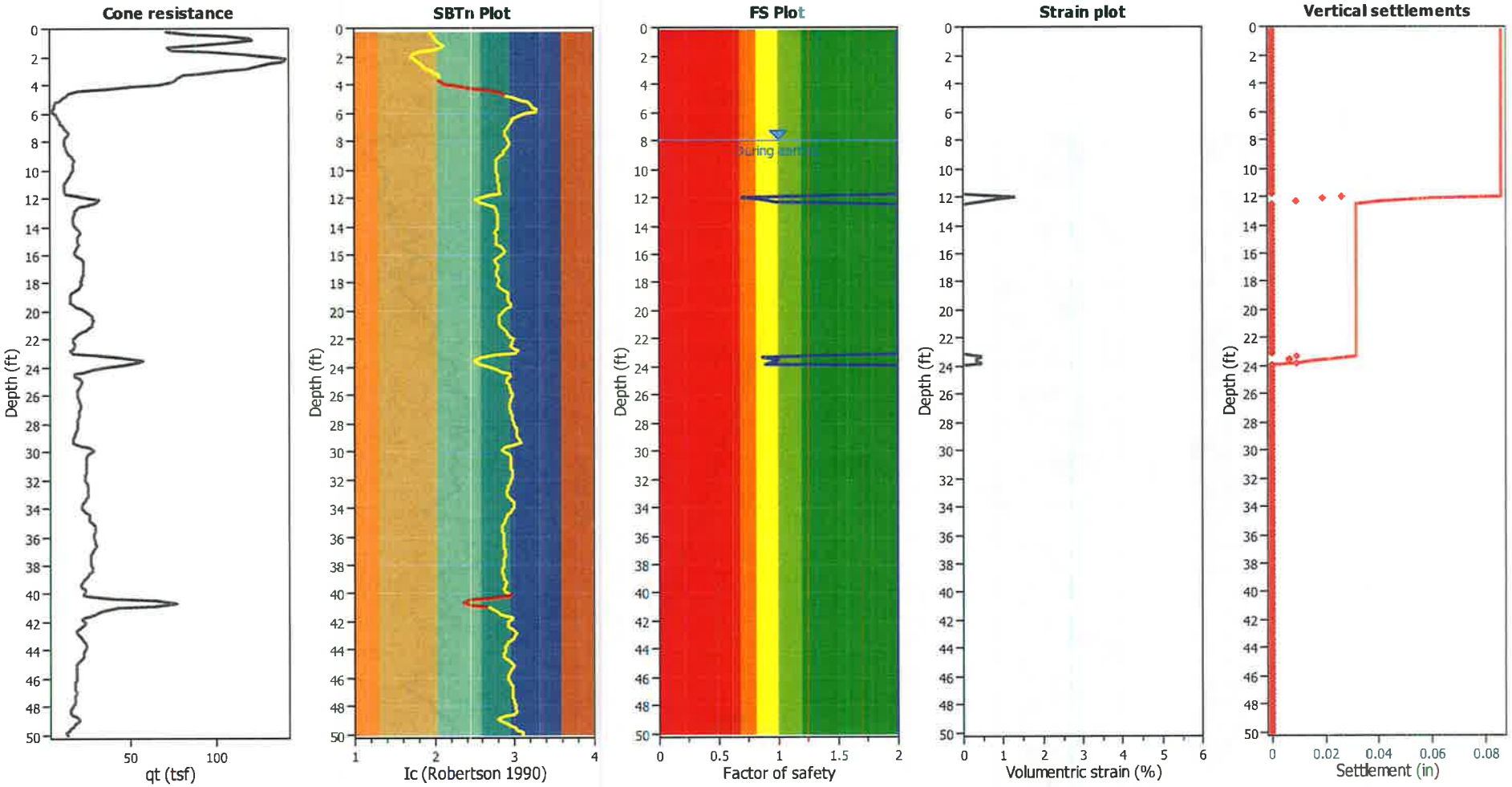

Abbreviations

q_t:	Total cone resistance (cone resistance q_c corrected for pore water effects)
I_c:	Soil Behaviour Type Index
FS:	Calculated Factor of Safety against liquefaction
Volumentric strain:	Post-liquefaction volumentric strain

:: Post-earthquake settlement due to soil liquefaction ::

Depth (ft)	$Q_{tn,cs}$	FS	e_v (%)	DF	Settlement (in)	Depth (ft)	$Q_{tn,cs}$	FS	e_v (%)	DF	Settlement (in)
8.04	119.22	2.00	0.00	0.86	0.00	8.20	120.85	2.00	0.00	0.86	0.00
8.37	121.77	2.00	0.00	0.86	0.00	8.53	121.74	2.00	0.00	0.86	0.00
8.69	123.66	2.00	0.00	0.85	0.00	8.86	127.30	2.00	0.00	0.85	0.00
9.02	130.40	2.00	0.00	0.85	0.00	9.19	130.61	2.00	0.00	0.84	0.00
9.35	129.25	2.00	0.00	0.84	0.00	9.51	127.22	2.00	0.00	0.84	0.00
9.68	125.93	2.00	0.00	0.84	0.00	9.84	124.71	2.00	0.00	0.83	0.00
10.01	123.50	2.00	0.00	0.83	0.00	10.17	120.59	2.00	0.00	0.83	0.00
10.33	115.49	2.00	0.00	0.82	0.00	10.50	108.81	2.00	0.00	0.82	0.00
10.66	102.72	2.00	0.00	0.82	0.00	10.83	97.88	2.00	0.00	0.82	0.00
10.99	94.40	2.00	0.00	0.81	0.00	11.15	93.33	2.00	0.00	0.81	0.00
11.32	92.09	2.00	0.00	0.81	0.00	11.48	95.09	2.00	0.00	0.81	0.00
11.65	105.48	2.00	0.00	0.80	0.00	11.81	117.60	2.00	0.00	0.80	0.00
11.98	131.26	0.69	1.33	0.80	0.03	12.14	143.05	0.84	0.96	0.79	0.02
12.30	152.70	0.97	0.47	0.79	0.01	12.47	152.80	2.00	0.00	0.79	0.00
12.63	143.18	2.00	0.00	0.79	0.00	12.80	134.31	2.00	0.00	0.78	0.00
12.96	130.65	2.00	0.00	0.78	0.00	13.12	129.65	2.00	0.00	0.78	0.00
13.29	127.91	2.00	0.00	0.77	0.00	13.45	124.35	2.00	0.00	0.77	0.00
13.62	120.29	2.00	0.00	0.77	0.00	13.78	120.60	2.00	0.00	0.77	0.00
13.94	128.55	2.00	0.00	0.76	0.00	14.11	137.42	2.00	0.00	0.76	0.00
14.27	142.24	2.00	0.00	0.76	0.00	14.44	141.06	2.00	0.00	0.76	0.00
14.60	138.35	2.00	0.00	0.75	0.00	14.76	133.75	2.00	0.00	0.75	0.00
14.93	129.06	2.00	0.00	0.75	0.00	15.09	127.77	2.00	0.00	0.74	0.00
15.26	132.22	2.00	0.00	0.74	0.00	15.42	138.42	2.00	0.00	0.74	0.00
15.58	140.75	2.00	0.00	0.74	0.00	15.75	139.78	2.00	0.00	0.73	0.00
15.91	138.74	2.00	0.00	0.73	0.00	16.08	138.05	2.00	0.00	0.73	0.00
16.24	137.36	2.00	0.00	0.72	0.00	16.40	138.60	2.00	0.00	0.72	0.00
16.57	143.48	2.00	0.00	0.72	0.00	16.73	146.06	2.00	0.00	0.72	0.00
16.90	145.22	2.00	0.00	0.71	0.00	17.06	141.94	2.00	0.00	0.71	0.00
17.22	139.81	2.00	0.00	0.71	0.00	17.39	137.72	2.00	0.00	0.71	0.00
17.55	137.02	2.00	0.00	0.70	0.00	17.72	137.39	2.00	0.00	0.70	0.00
17.88	136.19	2.00	0.00	0.70	0.00	18.04	135.45	2.00	0.00	0.69	0.00
18.21	132.44	2.00	0.00	0.69	0.00	18.37	130.93	2.00	0.00	0.69	0.00
18.54	124.17	2.00	0.00	0.69	0.00	18.70	118.78	2.00	0.00	0.68	0.00
18.86	113.72	2.00	0.00	0.68	0.00	19.03	112.47	2.00	0.00	0.68	0.00
19.19	112.04	2.00	0.00	0.67	0.00	19.36	117.35	2.00	0.00	0.67	0.00
19.52	128.21	2.00	0.00	0.67	0.00	19.69	143.57	2.00	0.00	0.67	0.00
19.85	153.43	2.00	0.00	0.66	0.00	20.01	160.71	2.00	0.00	0.66	0.00
20.18	163.07	2.00	0.00	0.66	0.00	20.34	164.44	2.00	0.00	0.66	0.00
20.51	162.92	2.00	0.00	0.65	0.00	20.67	161.17	2.00	0.00	0.65	0.00
20.83	160.88	2.00	0.00	0.65	0.00	21.00	160.69	2.00	0.00	0.64	0.00
21.16	158.54	2.00	0.00	0.64	0.00	21.33	151.78	2.00	0.00	0.64	0.00
21.49	140.81	2.00	0.00	0.64	0.00	21.65	130.93	2.00	0.00	0.63	0.00
21.82	126.27	2.00	0.00	0.63	0.00	21.98	126.66	2.00	0.00	0.63	0.00
22.15	126.16	2.00	0.00	0.62	0.00	22.31	126.33	2.00	0.00	0.62	0.00
22.47	126.09	2.00	0.00	0.62	0.00	22.64	123.91	2.00	0.00	0.62	0.00
22.80	121.99	2.00	0.00	0.61	0.00	22.97	126.99	2.00	0.00	0.61	0.00
23.13	143.39	2.00	0.00	0.61	0.00	23.29	157.57	0.86	0.48	0.61	0.01
23.46	167.32	1.00	0.33	0.60	0.01	23.62	165.76	0.98	0.33	0.60	0.01

:: Post-earthquake settlement due to soil liquefaction :: (continued)

Depth (ft)	$Q_{tn,cs}$	FS	e_v (%)	DF	Settlement (in)	Depth (ft)	$Q_{tn,cs}$	FS	e_v (%)	DF	Settlement (in)
23.79	159.66	0.89	0.47	0.60	0.01	23.95	148.21	2.00	0.00	0.59	0.00
24.11	135.94	2.00	0.00	0.59	0.00	24.28	120.89	2.00	0.00	0.59	0.00
24.44	113.50	2.00	0.00	0.59	0.00	24.61	115.23	2.00	0.00	0.58	0.00
24.77	123.04	2.00	0.00	0.58	0.00	24.93	128.87	2.00	0.00	0.58	0.00
25.10	131.54	2.00	0.00	0.57	0.00	25.26	130.14	2.00	0.00	0.57	0.00
25.43	125.79	2.00	0.00	0.57	0.00	25.59	121.98	2.00	0.00	0.57	0.00
25.75	120.15	2.00	0.00	0.56	0.00	25.92	121.20	2.00	0.00	0.56	0.00
26.08	122.21	2.00	0.00	0.56	0.00	26.25	122.93	2.00	0.00	0.56	0.00
26.41	122.83	2.00	0.00	0.55	0.00	26.57	122.65	2.00	0.00	0.55	0.00
26.74	123.77	2.00	0.00	0.55	0.00	26.90	123.52	2.00	0.00	0.54	0.00
27.07	122.85	2.00	0.00	0.54	0.00	27.23	120.78	2.00	0.00	0.54	0.00
27.40	120.44	2.00	0.00	0.54	0.00	27.56	120.16	2.00	0.00	0.53	0.00
27.72	118.94	2.00	0.00	0.53	0.00	27.89	119.67	2.00	0.00	0.53	0.00
28.05	121.33	2.00	0.00	0.52	0.00	28.22	123.92	2.00	0.00	0.52	0.00
28.38	122.71	2.00	0.00	0.52	0.00	28.54	119.82	2.00	0.00	0.52	0.00
28.71	115.02	2.00	0.00	0.51	0.00	28.87	111.29	2.00	0.00	0.51	0.00
29.04	109.61	2.00	0.00	0.51	0.00	29.20	112.15	2.00	0.00	0.51	0.00
29.36	116.02	2.00	0.00	0.50	0.00	29.53	122.43	2.00	0.00	0.50	0.00
29.69	128.66	2.00	0.00	0.50	0.00	29.86	132.51	2.00	0.00	0.49	0.00
30.02	133.32	2.00	0.00	0.49	0.00	30.18	133.01	2.00	0.00	0.49	0.00
30.35	134.24	2.00	0.00	0.49	0.00	30.51	135.73	2.00	0.00	0.48	0.00
30.68	134.98	2.00	0.00	0.48	0.00	30.84	133.52	2.00	0.00	0.48	0.00
31.00	132.42	2.00	0.00	0.47	0.00	31.17	131.76	2.00	0.00	0.47	0.00
31.33	131.41	2.00	0.00	0.47	0.00	31.50	130.79	2.00	0.00	0.47	0.00
31.66	129.46	2.00	0.00	0.46	0.00	31.82	127.40	2.00	0.00	0.46	0.00
31.99	125.47	2.00	0.00	0.46	0.00	32.15	124.76	2.00	0.00	0.46	0.00
32.32	123.94	2.00	0.00	0.45	0.00	32.48	122.71	2.00	0.00	0.45	0.00
32.64	121.40	2.00	0.00	0.45	0.00	32.81	120.70	2.00	0.00	0.44	0.00
32.97	120.37	2.00	0.00	0.44	0.00	33.14	120.33	2.00	0.00	0.44	0.00
33.30	119.72	2.00	0.00	0.44	0.00	33.46	119.43	2.00	0.00	0.43	0.00
33.63	118.76	2.00	0.00	0.43	0.00	33.79	117.66	2.00	0.00	0.43	0.00
33.96	117.16	2.00	0.00	0.42	0.00	34.12	117.75	2.00	0.00	0.42	0.00
34.28	120.54	2.00	0.00	0.42	0.00	34.45	119.94	2.00	0.00	0.42	0.00
34.61	117.36	2.00	0.00	0.41	0.00	34.78	114.03	2.00	0.00	0.41	0.00
34.94	115.06	2.00	0.00	0.41	0.00	35.10	117.56	2.00	0.00	0.41	0.00
35.27	118.09	2.00	0.00	0.40	0.00	35.43	116.84	2.00	0.00	0.40	0.00
35.60	115.80	2.00	0.00	0.40	0.00	35.76	116.35	2.00	0.00	0.39	0.00
35.93	117.12	2.00	0.00	0.39	0.00	36.09	117.39	2.00	0.00	0.39	0.00
36.25	117.58	2.00	0.00	0.39	0.00	36.42	118.84	2.00	0.00	0.38	0.00
36.58	119.93	2.00	0.00	0.38	0.00	36.75	119.47	2.00	0.00	0.38	0.00
36.91	116.76	2.00	0.00	0.37	0.00	37.07	113.06	2.00	0.00	0.37	0.00
37.24	109.88	2.00	0.00	0.37	0.00	37.40	107.43	2.00	0.00	0.37	0.00
37.57	106.75	2.00	0.00	0.36	0.00	37.73	106.32	2.00	0.00	0.36	0.00
37.89	106.17	2.00	0.00	0.36	0.00	38.06	105.28	2.00	0.00	0.35	0.00
38.22	104.58	2.00	0.00	0.35	0.00	38.39	102.50	2.00	0.00	0.35	0.00
38.55	98.98	2.00	0.00	0.35	0.00	38.71	94.70	2.00	0.00	0.34	0.00
38.88	90.90	2.00	0.00	0.34	0.00	39.04	87.39	2.00	0.00	0.34	0.00
39.21	84.59	2.00	0.00	0.34	0.00	39.37	82.78	2.00	0.00	0.33	0.00

:: Post-earthquake settlement due to soil liquefaction :: (continued)

Depth (ft)	$Q_{tn,cs}$	FS	e_v (%)	DF	Settlement (in)	Depth (ft)	$Q_{tn,cs}$	FS	e_v (%)	DF	Settlement (in)
39.53	84.00	2.00	0.00	0.33	0.00	39.70	87.03	2.00	0.00	0.33	0.00
39.86	90.97	2.00	0.00	0.32	0.00	40.03	96.73	2.00	0.00	0.32	0.00
40.19	105.29	2.00	0.00	0.32	0.00	40.35	115.76	2.00	0.00	0.32	0.00
40.52	121.29	2.00	0.00	0.31	0.00	40.68	125.41	2.00	0.00	0.31	0.00
40.85	123.12	2.00	0.00	0.31	0.00	41.01	117.19	2.00	0.00	0.30	0.00
41.17	107.63	2.00	0.00	0.30	0.00	41.34	102.80	2.00	0.00	0.30	0.00
41.50	99.33	2.00	0.00	0.30	0.00	41.67	95.42	2.00	0.00	0.29	0.00
41.83	90.50	2.00	0.00	0.29	0.00	41.99	89.98	2.00	0.00	0.29	0.00
42.16	88.92	2.00	0.00	0.29	0.00	42.32	83.52	2.00	0.00	0.28	0.00
42.49	78.18	2.00	0.00	0.28	0.00	42.65	77.51	2.00	0.00	0.28	0.00
42.81	82.85	2.00	0.00	0.27	0.00	42.98	88.58	2.00	0.00	0.27	0.00
43.14	92.04	2.00	0.00	0.27	0.00	43.31	92.24	2.00	0.00	0.27	0.00
43.47	90.25	2.00	0.00	0.26	0.00	43.64	86.84	2.00	0.00	0.26	0.00
43.80	83.41	2.00	0.00	0.26	0.00	43.96	80.95	2.00	0.00	0.25	0.00
44.13	78.49	2.00	0.00	0.25	0.00	44.29	76.67	2.00	0.00	0.25	0.00
44.46	75.23	2.00	0.00	0.25	0.00	44.62	74.90	2.00	0.00	0.24	0.00
44.78	74.57	2.00	0.00	0.24	0.00	44.95	73.31	2.00	0.00	0.24	0.00
45.11	72.32	2.00	0.00	0.24	0.00	45.28	70.79	2.00	0.00	0.23	0.00
45.44	69.68	2.00	0.00	0.23	0.00	45.60	67.68	2.00	0.00	0.23	0.00
45.77	65.78	2.00	0.00	0.22	0.00	45.93	64.39	2.00	0.00	0.22	0.00
46.10	63.45	2.00	0.00	0.22	0.00	46.26	63.10	2.00	0.00	0.22	0.00
46.42	63.80	2.00	0.00	0.21	0.00	46.59	65.52	2.00	0.00	0.21	0.00
46.75	67.21	2.00	0.00	0.21	0.00	46.92	67.86	2.00	0.00	0.20	0.00
47.08	67.38	2.00	0.00	0.20	0.00	47.24	66.55	2.00	0.00	0.20	0.00
47.41	66.19	2.00	0.00	0.20	0.00	47.57	66.07	2.00	0.00	0.19	0.00
47.74	65.63	2.00	0.00	0.19	0.00	47.90	63.67	2.00	0.00	0.19	0.00
48.06	60.77	2.00	0.00	0.19	0.00	48.23	58.45	2.00	0.00	0.18	0.00
48.39	57.99	2.00	0.00	0.18	0.00	48.56	57.54	2.00	0.00	0.18	0.00
48.72	56.34	2.00	0.00	0.17	0.00	48.88	54.30	2.00	0.00	0.17	0.00
49.05	55.00	2.00	0.00	0.17	0.00	49.21	55.85	2.00	0.00	0.17	0.00
49.38	55.75	2.00	0.00	0.16	0.00	49.54	53.84	2.00	0.00	0.16	0.00
49.70	52.12	2.00	0.00	0.16	0.00	49.87	53.14	2.00	0.00	0.15	0.00
50.03	54.80	2.00	0.00	0.15	0.00						

Total estimated settlement: 0.09

Abbreviations

$Q_{tn,cs}$:	Equivalent clean sand normalized cone resistance
FS:	Factor of safety against liquefaction
e_v (%):	Post-liquefaction volumentric strain
DF:	e_v depth weighting factor
Settlement:	Calculated settlement

APPENDIX D

Geotechnical Report

New Turbine Generator and Cooling Tower
Heber 2 Geothermal Plant
Heber, CA

Prepared for:

ORMAT
947 Dogwood Road
Heber, CA 92249

LANDMARK
Geo-Engineers and Geologists
a DBE/MBE/SBE Company

Prepared by:

Landmark Consultants, Inc.
780 N. 4th Street
El Centro, CA 92243
(760) 370-3000

January 2005

LANDMARK
Geo-Engineers and Geologists
a DBE/MBE/SBE Company

780 N. 4th Street
El Centro, CA 92243
(760) 370-3000
(760) 337-8900 fax

77-948 Wildcat Drive
Palm Desert, CA 92211
(760) 360-0665
(760) 360-0521 fax

January 10, 2005

Mr. Mike Collins
ORMAT
947 Dogwood Road
Heber, CA 92249

Geotechnical Investigation
New Turbine Generator and Cooling Tower
Heber 2 Geothermal Plant
Dogwood Road
Heber, California
LCI Report No. LE04354 (2)

Dear Mr. Collins:

This geotechnical report is provided for design and construction of the new turbine generator and cooling tower additions to the Ormat Heber 2 geothermal power plant located on Dogwood Road southwest of Heber, California. Our geotechnical investigation was conducted in response to your request for our services. The enclosed report describes our soil engineering investigation and presents our professional opinions regarding geotechnical conditions at the site to be considered in the design and construction of the project.

This executive summary presents ***selected*** elements of our findings and recommendations only. It ***does not*** present crucial details needed for the proper application of our findings and recommendations. Our findings, recommendations, and application options are related ***only through reading the full report***, and are best evaluated with the active participation of the engineer of record who developed them.

The findings of this study indicate that the site is predominantly underlain by clays of moderate expansion.

The soil are highly corrosive to metals and contain sufficient sulfates and chlorides to require special concrete mixes (4,500 psi with a 0.45 maximum water cement ratio) and protection of embedded steel building components when concrete is placed in contact with native soil. If the native soils are replaced with imported granular soils with low sulfate and chloride content, no special concrete mixes are required.

Evaluation of liquefaction potential at the site indicates that it is unlikely that the subsurface soil will liquefy under seismically induced groundshaking due to the nature of the soil (clays soils predominate). No mitigation is required for liquefaction effects at this site.

Foundation settlements are indicated on figures 2 thru 5. Differential settlement is estimated to be about of two-thirds of total settlement.

We did not encounter soil conditions that would preclude development of the site for its intended use provided the recommendations contained in this report are implemented in the design and construction of this project.

We appreciate the opportunity to provide our findings and professional opinions regarding geotechnical conditions at the site. If you have any questions or comments regarding our findings, please call our office at (760) 370-3000.

Respectfully Submitted,
Landmark Consultants, Inc.

REGISTERED GEOLOGIST
STEVEN K. WILLIAMS
CERTIFIED ENGINEERING GEOLOGIST
CEG 2261
STATE OF CALIFORNIA

Steven K. Williams, CEG
Senior Engineering Geologist

Julian R. Avalos
Staff Engineer

REGISTERED PROFESSIONAL ENGINEER
JEFFREY O. LYON
No. 31921
EXPIRES 12-31-06
CIVIL
STATE OF CALIFORNIA

Jeffrey O. Lyon, PE
President

Distribution:
Client (4)

TABLE OF CONTENTS

Section 1
INTRODUCTION

1.1 Project Description

This report presents the findings of our geotechnical investigation for the proposed additions to the Ormat Heber 2 geothermal power plant located on Dogwood Road southwest of Heber, California (See Vicinity Map, Plate A-1). The proposed development will consist of the addition of one (1) turbine/generator set and one (1) cooling tower. A site plan for the proposed power plant improvements was not made available to us at the time that this report was prepared.

Small structures may be are planned for electrical control panels, consisting of masonry or panelized concrete construction. Expected footing loads are estimated at 1 to 2 kips per lineal foot for the small structures. Expected plant components, cooling tower and turbine/generator columns loads range from 5 to 400 kips. If structural loads exceed those stated above, we should be notified so we may evaluate their impact on foundation settlement and bearing capacity. Site development will include foundation support pad preparation and underground utility installation.

1.2 Purpose and Scope of Work

The purpose of this geotechnical study was to investigate the upper 50 feet of subsurface soil at selected locations within the site for physical/engineering properties. From the subsequent field and laboratory data, professional opinions were developed and are provided in this report regarding geotechnical conditions at this site and the effect on design and construction. The scope of our services consisted of the following:

- Field exploration and in-situ testing of the site soils at selected locations and depths.
- Laboratory testing for physical properties of selected samples.
- A review of the available literature and publications pertaining to local geology, faulting, and seismicity.
- Engineering analysis and evaluation of the data collected.
- Preparation of this report presenting our findings, professional opinions, and recommendations for the geotechnical aspects of project design and construction.

This report addresses the following geotechnical issues:

- Subsurface soil and groundwater conditions
- Site geology, regional faulting and seismicity, near source factors, and site seismic accelerations
- Liquefaction potential and its mitigation
- Expansive soil and methods of mitigation
- Aggressive soil conditions to metals and concrete

Professional opinions with regard to the above issues are presented for the following:

- Site grading and earthwork
- Foundation subgrade preparation
- Allowable soil bearing pressures and expected settlements
- Concrete slabs-on-grade
- Mitigation of the potential effects of salt concentrations in native soil to concrete mixes and steel reinforcement
- Seismic design parameters

Our scope of work for this report did not include an evaluation of the site for the presence of environmentally hazardous materials or conditions.

1.3 Authorization

Mr. Mike Collins, Project Manager of Ormat for Power Generation Construction provided authorization by written agreement to proceed with our work on December 14, 2004. We conducted our work according to our written proposal dated December 13, 2004.

Section 2
METHODS OF INVESTIGATION

2.1 Field Exploration

Subsurface exploration was performed on December 20, 2004 using Holguin, Fahan, & Associates, Inc. of Cypress, California to advance three (3) electric cone penetrometer (CPT) soundings to an approximate depth of 50 feet below existing ground surface. The soundings were made at the locations shown on the Site and Exploration Plan (Plate A-2). The approximate sounding locations were established in the field and plotted on the site map by sighting to discernable site features.

CPT soundings provide a continuous profile of the soil stratigraphy with readings every 2.5cm (1 inch) in depth. Direct sampling for visual and physical confirmation of soil properties has been used by our firm to establish direct correlations with CPT exploration in this geographical region.

The CPT exploration was conducted by hydraulically advancing an instrumented Hogentogler 10cm^2 conical probe into the ground at a rate of 2cm per second using a 23-ton truck as a reaction mass. An electronic data acquisition system recorded a nearly continuous log of the resistance of the soil against the cone tip (Qc) and soil friction against the cone sleeve (Fs) as the probe was advanced. Empirical relationships (Robertson and Campanella, 1989) were then applied to the data to give a continuous profile of the soil stratigraphy. Interpretation of CPT data provides correlations for SPT blow count, phi (ϕ) angle (soil friction angle), undrained shear strength (S_u) of clays and over-consolidation ratio (OCR). These correlations may then be used to evaluate vertical and lateral soil bearing capacities and consolidation characteristics of the subsurface soil.

Interpretive logs of the CPT soundings were produced and presented in final form after review of field and laboratory data and are presented on Plates B-1 through B-3 in Appendix B. A key to the interpretation of CPT soundings is presented on Plate B-4. The stratification lines shown on the subsurface logs represent the approximate boundaries between the various strata. However, the transition from one stratum to another may be gradual over some range of depth.

2.2 Laboratory Testing

Laboratory tests were conducted on selected bulk soil samples obtained from hand auger borings made adjacent to the CPT locations to aid in classification and evaluation of selected engineering properties of the near surface soils. The tests were conducted in general conformance to the procedures of the American Society for Testing and Materials (ASTM) or other standardized methods as referenced below. The laboratory testing program consisted of the following tests:

- Plasticity Index (ASTM D4318) – used for soil classification and expansive soil design criteria.
- Chemical Analyses (soluble sulfates & chlorides, pH, and resistivity) (Caltrans Methods) – used for concrete mix evaluations and corrosion protection requirements.

The laboratory test results are presented on the subsurface logs (Appendix B) and on Plates C-1, C-2 and C-3 in Appendix C.

Engineering parameters of soil strength, compressibility and relative density utilized for developing design criteria provided within this report were either extrapolated from correlations with the subsurface CPT data or from data obtained from the field and laboratory testing program.

Section 3
DISCUSSION

3.1 Site Conditions

The plant additions are located in the northwest corner of the Heber 2 geothermal plant on the west side of the existing turbine generators and cooling tower. The area is relatively vacant and approximately has the same elevation as the existing plant facilities. An overhead pipe rack is located to the south side of the proposed location.

Adjacent properties outside of the fenced operations yard consist of agricultural land to the north and west. The site is bounded on the east by Dogwood Road and headquarters facilities of a general engineering construction company lie to the south side. Dogwood Road is slated to be a 6-lane north-south arterial from Calexico to Brawley in Imperial County. Adjacent properties are flat-lying and are approximately at the same elevation with this site.

The project site lies at an elevation of approximately 15 feet below mean sea level (MSL) (El. 985 local datum) in the Imperial Valley region of the California low desert. The surrounding properties lie on terrain which is flat (planar), part of a large agricultural valley, which was previously an ancient lake bed covered with fresh water to an elevation of 43± feet above MSL. Annual rainfall in this arid region is less than 4 inches per year with four months of average summertime temperatures above 100 °F. Winter temperatures are mild, seldom reaching freezing.

3.2 Geologic Setting

The project site is located in the Imperial Valley portion of the Salton Trough physiographic province. The Salton Trough is a geologic structural depression resulting from large scale regional faulting. The trough is bounded on the northeast by the San Andreas Fault and Chocolate Mountains and the southwest by the Peninsular Range and faults of the San Jacinto Fault Zone. The Salton Trough represents the northward extension of the Gulf of California, containing both marine and non-marine sediments since the Miocene Epoch. Tectonic activity that formed the trough continues at a high rate as evidenced by deformed young sedimentary deposits and high levels of seismicity. Figure 1 shows the location of the site in relation to regional faults and physiographic features.

The Imperial Valley is directly underlain by lacustrine deposits, which consist of interbedded lenticular and tabular silt, sand, and clay. The Late Pleistocene to Holocene lake deposits are probably less than 100 feet thick and derived from periodic flooding of the Colorado River which intermittently formed a fresh water lake (Lake Cahuilla). Older deposits consist of Miocene to Pleistocene non-marine and marine sediments deposited during intrusions of the Gulf of California. Basement rock consisting of Mesozoic granite and Paleozoic metamorphic rocks are estimated to exist at depths between 15,000 - 20,000 feet.

3.3 Seismicity and Faulting

Faulting and Seismic Sources: We have performed a computer-aided search of known faults or seismic zones that lie within a 62 mile (100 kilometers) radius of the project site as shown on Figure 1 and Table 1. The search identifies known faults within this distance and computes deterministic ground accelerations at the site based on the maximum credible earthquake expected on each of the faults and the distance from the fault to the site. The Maximum Magnitude Earthquake (Mmax) listed was taken from published geologic information available for each fault (CDMG OFR 96-08 and Jennings, 1994).

Seismic Risk: The project site is located in the seismically active Imperial Valley of southern California and is considered likely to be subjected to moderate to strong ground motion from earthquakes in the region. The proposed site structures should be designed in accordance with the California Building Code (CBC) for near source factors derived from a "Design Basis Earthquake" (DBE). The DBE is defined as the motion having a 10 percent probability of being exceeded in 50 years. The DBE generally corresponds to the Mmax magnitude discussed here.

Seismic Hazards.

- **Groundshaking.** The primary seismic hazard at the project site is the potential for strong groundshaking during earthquakes along the Imperial, Brawley, and Superstition Hills Faults. A further discussion of groundshaking follows in Section 3.4.
- **Surface Rupture.** The project site does not lie within a State of California, Alquist-Priolo Earthquake Fault Zone. Surface fault rupture is considered to be unlikely at the project site because of the well-delineated fault lines through the Imperial Valley as shown on USGS and CGS maps. However, because of the high tectonic activity and deep alluvium of the region, we cannot preclude the potential for surface rupture on undiscovered or new faults that may underlie the site.

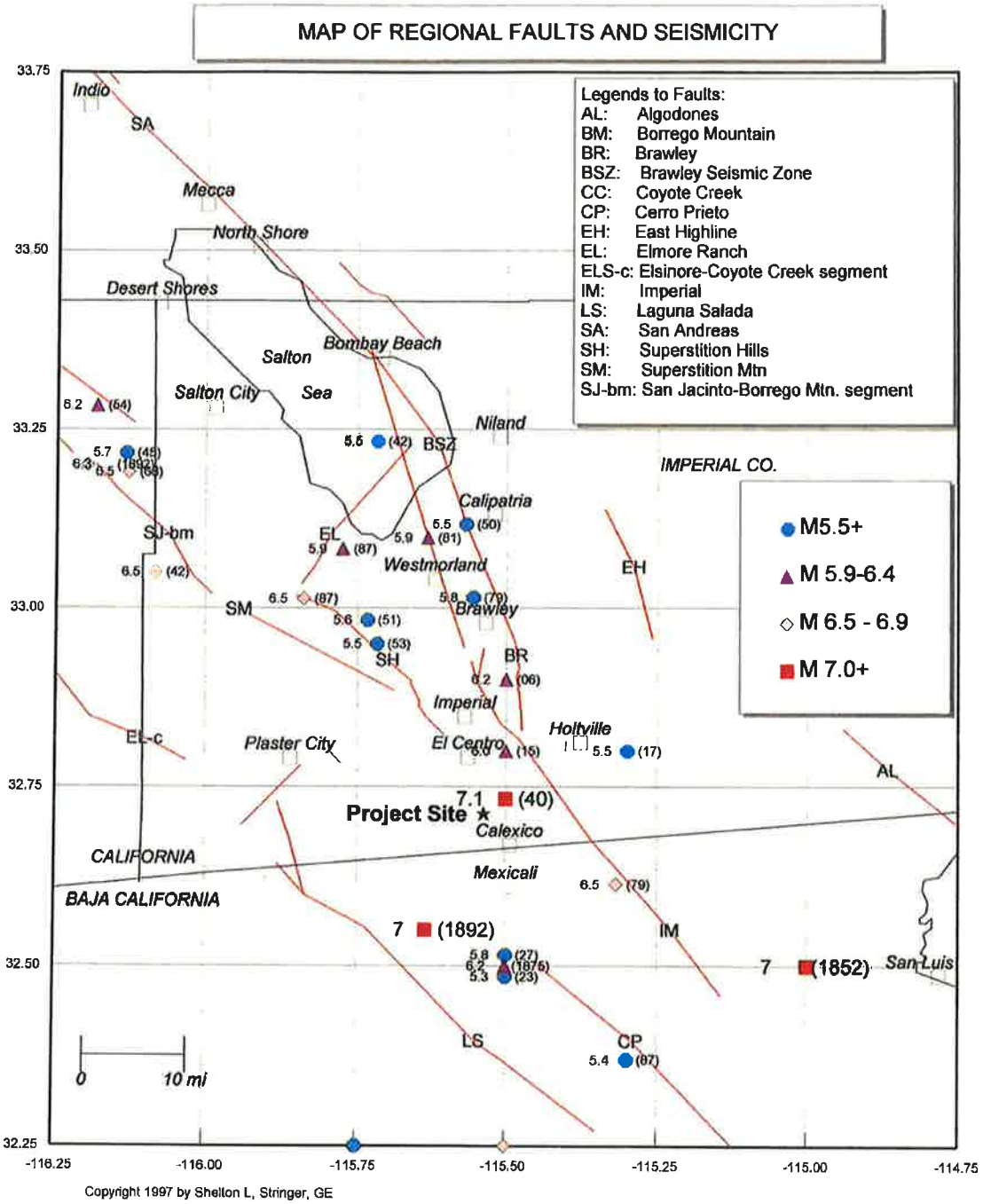

Faults and Seismic Zones from Jennings (1994), Earthquakes modified from Ellsworth (1990) catalog.

Figure 1. Map of Regional Faults and Seismicity

Table 1
FAULT PARAMETERS & DETERMINISTIC
ESTIMATES OF PEAK GROUND ACCELERATION (PGA)

Fault Name or Seismic Zone	Distance (mi) & Direction from Site	Fault Type		Fault Length (km)	Maximum Magnitude Mmax (Mw)	Avg Slip Rate (mm/yr)	Avg Return Period (yrs)	Date of Last Rupture (year)	Largest Historic Event >5.5M	(year)	Est. Site PGA (g)
Reference Notes: (1)		(2)	(3)	(2)	(4)	(3)	(3)	(3)	(5)		(6)
Imperial Valley Faults											
Imperial	7.0 NE	A	B	62	**7.0**	20	79	1979	7.0	1940	**0.33**
Brawley	8.8 NNE	B	B	14	**7.0**	20	---	1979	5.8	1979	**0.28**
Cerro Prieto	15 SSE	A	B	116	**7.2**	34	50	1980	7.1	1934	**0.21**
Brawley Seismic Zone	16 N	B	B	42	**6.4**	25	24		5.9	1981	**0.13**
East Highline Canal	23 NE	C	C	22	**6.3**	1	774				**0.09**
San Jacinto Fault System											
- Superstition Hills	8.5 NNW	B	A	22	**6.6**	4	250	1987	6.5	1987	**0.23**
- Superstition Mtn.	15 NW	B	A	23	**6.6**	5	500	1440 +/-			**0.16**
- Elmore Ranch	28 NW	B	A	29	**6.6**	1	225	1987	5.9	1987	**0.10**
- Borrego Mtn	34 NW	B	A	29	**6.6**	4	175		6.5	1942	**0.08**
- Anza Segment	51 NW	A	A	90	**7.2**	12	250	1918	6.8	1918	**0.08**
- Coyote Creek	53 NW	B	A	40	**6.8**	4	175	1968	6.5	1968	**0.07**
- Whole Zone	15 NW	A	A	245	**7.5**	---	---				**0.25**
Elsinore Fault System											
- Laguna Salada	16 SW	B	B	67	**7.0**	3.5	336		7.0	1891	**0.18**
- Coyote Segment	29 W	B	A	38	**6.8**	4	625				**0.11**
- Julian Segment	55 WNW	A	A	75	**7.1**	5	340				**0.08**
- Earthquake Valley	57 WNW	B	A	20	**6.5**	2	351				**0.05**
- Whole Zone	29 W	A	A	250	**7.5**	---	---				**0.15**
San Andreas Fault System											
Coachella Valley	45 NNW	A	A	95	**7.4**	25	220	1690 +/-	6.5	1948	**0.10**
- Whole S. Calif. Zone	45 NNW	A	A	458	**7.9**	---	---	1857	7.8	1857	**0.13**
Algodones	36 E	C	C	74	**7.0**	0.1	20,000				**0.10**

Notes:

1. Jennings (1994) and CDMG (1996)
2. CDMG (1996), where Type A faults -- slip rate >5 mm/yr and well constrained paleoseismic data
   Type B faults -- all other faults.
3. WGCEP (1995)
4. CDMG (1996) based on Wells & Coppersmith (1994)
5. Ellsworth Catalog in USGS PP 1515 (1990) and USBR (1976), Mw = moment magnitude,
6. The deterministic estimates of the Site PGA are based on the attenuation relationship of:
   Boore, Joyner, Fumal (1997)

▸ **Liquefaction.** Liquefaction is unlikely to be a potential hazard at the site due to the lack of saturated granular soil (clay soils predominate).

Other Secondary Hazards.

▸ **Landsliding.** The hazard of landsliding is unlikely due to the regional planar topography. No ancient landslides are shown on geologic maps of the region and no indications of landslides were observed during our site investigation.

▸ **Volcanic hazards.** The site is not located in proximity to any known volcanically active area and the risk of volcanic hazards is considered very low.

▸ **Tsunamis, sieches, and flooding.** The site does not lie near any large bodies of water, so the threat of tsunami, sieches, or other seismically-induced flooding is unlikely.

▸ **Expansive soil.** In general, much of the near surface soils in the Imperial Valley consist of silty clays and clays which are moderate to highly expansive. The expansive soil conditions are discussed in more detail in Section 3.5.

3.4 Site Acceleration and UBC Seismic Coefficients

Deterministic horizontal peak ground accelerations (PGA) from maximum probable earthquakes on regional faults have been estimated and are included in Table 1. Ground motions are dependent primarily on the earthquake magnitude and distance to the seismogenic (rupture) zone. Accelerations also are dependent upon attenuation by rock and soil deposits, direction of rupture and type of fault; therefore, ground motions may vary considerably in the same general area.

We have used the computer program FRISKSP (Blake, 2000) to provide a probabilistic estimate of the site PGA using the attenuation relationship of Boore, Joyner, and Fumal (1997) Soil (250). The PGA estimate for the project site having a 10% probability of being exceeded in 50 years (return period of 475 years) is **0.60g**.

CBC Seismic Coefficients: The CBC seismic coefficients are roughly based on an earthquake ground motion that has a 10% probability of being exceeded in 50 years. The following table lists seismic and site coefficients (near source factors) determined by Chapter 16 of the 2001 CBC. ***This site lies within 11.3 km of a Type A fault overlying S_D (stiff) soil.***

CBC Seismic Coefficients for Chapter 16 Seismic Provisions

CBC Code Edition	Soil Profile Type	Seismic Source Type	Distance to Critical Source	Near Source Factors		Seismic Coefficients	
				Na	Nv	Ca	Cv
2001	S_D (stiff soil)	A	< 11.3 km	1.00	1.15	0.44	0.74
Ref. Table	16-J	16-U	---	16-S	16-T	16-Q	16-R

3.5 Subsurface Soil

Subsurface soils encountered during the field exploration conducted on December 20, 2004 indicates that 1.0 to 1.5 feet of stiff clay are at ground surface. Dense to very dense silty sands lie below the clays and extend to a depth of 4 to 5 feet. Stiff to very stiff clays extend a depth of 50 feet, the maximum depth of exploration. The subsurface logs (Plates B-1 through B-3) depict the stratigraphic relationships of the various soil types.

The native surface clays exhibit moderate swell potential (Expansion Index, EI = 51 - 90) when correlated to Plasticity index tests (ASTM D4318) performed on the native clays. The clay is expansive when wetted and can shrink with moisture loss (drying). Development of building foundations, concrete flatwork, and asphaltic concrete pavements should include provisions for mitigating potential swelling forces and reduction in soil strength, which can occur from saturation of the soil. Causes for soil saturation include landscape irrigation, broken utility lines, or capillary rise in moisture upon sealing the ground surface to evaporation. Moisture losses can occur with lack of landscape watering, close proximity of structures to downslopes and root system moisture extraction from deep rooted shrubs and trees placed near the foundations. Typical measures used for industrial projects to remediate expansive soil include:

- replacement of silt/clay with non-expansive granular fill,
- moisture conditioning subgrade soils to a minimum of 5% above optimum moisture (ASTM D1557) for the full range in depth of surface soils.
- design of foundations that are resistant to shrink/swell forces of silt/clay soil.

3.6 Groundwater

Groundwater was not noted on the CPT sounding at the time of exploration, but is typically encountered at approximately 10 to 15 feet below ground surface in the vicinity of the site. There is uncertainty in the accuracy of short-term water level measurements, particularly in fine-grained soil. Groundwater levels may fluctuate with precipitation, irrigation of adjacent properties, drainage, and site grading. The referenced groundwater level should not be interpreted to represent an accurate or permanent condition.

3.7 Liquefaction

Liquefaction occurs when granular soil below the water table is subjected to vibratory motions, such as produced by earthquakes. With strong ground shaking, an increase in pore water pressure develops as the soil tends to reduce in volume. If the increase in pore water pressure is sufficient to reduce the vertical effective stress (suspending the soil particles in water), the soil strength decreases and the soil behaves as a liquid (similar to quicksand). Liquefaction can produce excessive settlement, ground rupture, lateral spreading, or failure of shallow bearing foundations.

Four conditions are generally required for liquefaction to occur:

(1) the soil must be saturated (relatively shallow groundwater);
(2) the soil must be loosely packed (low to medium relative density);
(3) the soil must be relatively cohesionless (not clayey); and
(4) groundshaking of sufficient intensity must occur to function as a trigger mechanism.

All of these conditions exist to some degree at this site.

Methods of Analysis: Liquefaction potential at the project site was evaluated using the 1997 NCEER Liquefaction Workshop methods that are based on the Seed, et. al. 1985 and Robertson and Campanella (1985) methods. The 1997 NCEER methods utilize direct SPT blow counts or CPT cone readings from site exploration and earthquake magnitude/PGA estimates from the seismic hazard analysis. The resistance to liquefaction is plotted on a chart of cyclic shear stress ratio (CSR) versus a corrected blow count $N_{1(60)}$ or Qc_{1N}. A ground acceleration of 0.60g was used in the analysis with a 12 foot groundwater depth.

Liquefaction induced settlements have been estimated using the 1987 Tokimatsu and Seed method. Fines content of liquefiable sands and silt increase the liquefaction resistance in that more cycles of ground motions are required to fully develop pore pressures. The SPT blow counts were adjusted to an equivalent clean sand blow count, $N_{1(60)}$ prior to calculating settlements using Robertson and Wride (1997) adjustments. A computed factor of safety less than 1.0 indicates a liquefiable condition.

Liquefaction Effects: Based on empirical relationships, liquefaction is not expected to occur at the project site.

Section 4
RECOMMENDATIONS

4.1 Site Preparation

Clearing and Grubbing: All surface improvements, debris or vegetation including grass and weeds on the site at the time of construction should be removed from the construction area. Organic strippings should be hauled from the site and not used as fill. Any trash, construction debris, concrete slabs, old pavement, landfill, and buried obstructions such as old foundations and utility lines exposed during rough grading should be traced to the limits of the foreign material by the grading contractor and removed under our supervision. Any excavations resulting from site clearing should be dish-shaped to the lowest depth of disturbance and backfilled under observation by the geotechnical engineer's representative with compacted fill as described below.

Structure Subgrade Preparation: The exposed surface soil within the foundation areas should be removed to 12 inches below the foundation elevation or existing grade (whichever is lower). Exposed subgrade should be scarified to a depth of 8 inches, uniformly moisture conditioned to 3 to 8% above optimum moisture content (clays) or 0 to 4% above optimum (silts), and recompacted to at least 90% of the maximum density determined in accordance with ASTM D1557 methods.

The native soil is suitable for use as engineered fill provided it is free from concentrations of organic matter or other deleterious material. The fill soil should be uniformly moisture conditioned by discing and watering to the limits specified above, placed in maximum 8-inch lifts (loose), and compacted to the limits specified above.

Imported fill soil (if required) should have a Plasticity Index less than 15 and sulfates (SO_4) less than 1,000 ppm or non-expansive, granular soil meeting the USCS classifications of SM, SP-SM, or SW-SM with a maximum rock size of 3 inches and 5 to 35% passing the No. 200 sieve. The geotechnical engineer should approve imported fill soil sources before hauling material to the site. Imported granular fill should be placed in lifts no greater than 8 inches in loose thickness and compacted to at least 90% of ASTM D1557 maximum dry density at optimum moisture ±2%.

In areas other than the structures pad which are to receive area concrete slabs, the ground surface should be presaturated to a minimum depth of 18 inches and then scarified to 6 inches, moisture conditioned to a minimum of 5% over optimum, and recompacted to 83-87% of ASTM D1 557 maximum density just prior to concrete placement.

Trench Backfill: On-site soil free of debris, vegetation, and other deleterious matter may be suitable for use as utility trench backfill, but may be difficult to uniformly maintain at specified moistures and compact to the specified densities. Granular material is often more cost effective for backfill of utility trenches.

Backfill soil within roadways or traffic areas should be placed in layers not more that 6 inches in thickness and mechanically compacted to a minimum of 87% of the ASTM D1557 maximum dry density except for the top 12 inches of the trench which shall be compacted to at least 90%. Native backfill should only be placed and compacted after encapsulating buried pipes with suitable bedding and pipe envelope material. Pipe envelope/bedding should either be clean sand (Sand Equivalent SE>30) or crushed rock when encountering groundwater. A geotextile filter fabric (Mirafi 140N or equivalent) should be used to encapsulate the crushed rock when placed below groundwater to reduce the potential for in-washing of fines into the gravel void space. Precautions should be taken in the compaction of the backfill to avoid damage to the pipes and structures.

Observation and Density Testing: All site preparation and fill placement should be continuously observed and tested by a representative of a qualified geotechnical engineering firm. Full-time observation services during the excavation and scarification process is necessary to detect undesirable materials or conditions and soft areas that may be encountered in the construction area. The geotechnical firm that provides observation and testing during construction shall assume the responsibility of "*geotechnical engineer of record*" and, as such, shall perform additional tests and investigation as necessary to satisfy themselves as to the site conditions and the recommendations for site development.

Auxiliary Structures Foundation Preparation: Auxiliary structures such as free standing or retaining walls should have the existing soil beneath the structure foundation prepared in the manner recommended for the building pad except the preparation needed only to extend 12 inches below and beyond the footing.

4.2 Foundations and Settlements

Shallow spread footings and continuous wall footings are suitable to support the structures associated with the turbine generator and cooling tower. Footings shall be founded on a layer of properly prepared and compacted soil as described in Section 4.1. The foundations may be designed using an allowable soil bearing pressure of 1,500 psf for compacted native clay soil and 2,000 psf when foundations are supported on imported sands (extending a minimum of 1.0 feet below footings). The allowable soil pressure may be increased by 20% for each foot of embedment depth in excess of 18 inches and by one-third for short term loads induced by winds or seismic events. The maximum allowable soil pressure at increased embedment depths shall not exceed 3,000 psf (clays). Settlements associated with variable loadings and structure/footing sizes are shown on figures 2 thru 5. As an alternative to shallow spread foundations, flat plate structural mats or grade-beam reinforced foundations may be used to mitigate expansive soil heave.

Flat Plate Structural Mats: Structural mats may be designed for a modulus of subgrade reaction (Ks) of 100 pci when placed on compacted clay or a subgrade modulus of 250 pci when placed on 2.5 feet of granular fill. Mats shall overlay 2 inches of sand and a 10-mil polyethylene vapor retarder. The structure support pad shall be moisture conditioned and recompacted as specified in Section 4.1 of this report.

All exterior and interior foundations should be embedded a minimum of 18 inches below the structure support pad or lowest adjacent final grade, whichever is deeper. Continuous wall footings should have a minimum width of 12 inches. Spread footings should have a minimum width of 24 inches. Recommended concrete reinforcement and sizing for all footings should be provided by the structural engineer.

Resistance to horizontal loads will be developed by passive earth pressure on the sides of footings or grade beams and frictional resistance developed along the bases of footings or grade beams and concrete slabs. Passive resistance to lateral earth pressure may be calculated using an equivalent fluid pressure of 250 pcf (300 pcf for sands) to resist lateral loadings. The top one foot of embedment should not be considered in computing passive resistance unless the adjacent area is confined by a slab or pavement. An allowable friction coefficient of 0.25 (0.35 for sands) may also be used at the base of the footings or grade beams to resist lateral loading.

Total foundation movements under estimated loadings are shown on the load/settlement curves (Figures 2 thru 5). Differential movement is estimated to be about two-thirds of total movement

4.3 Slabs-On-Grade

Thin concrete slabs and flatwork (6 inches or less in thickness) placed over native clay soil should be designed in accordance with Chapter 18, Division III of the 2001 CBC (using an Effective Plasticity Index of 17) and shall be a minimum of 5 inches thick due to expansive soil conditions. Concrete floor slabs shall be monolithically placed with the foundations unless placed on 2.5 feet of granular fill or lime treated soil.

The concrete slabs should be underlain by a minimum of 4 inches of clean sand (Sand Equivalent SE>30) or aggregate base or may be placed directly on a 2.5-foot thick granular fill pad (if used) that has been moistened to approximately optimum moisture just before the concrete placement. A 10-mil visqueen vapor retarder, properly lapped and sealed with a 2-inch sand cover and extended a minimum of 12 inches into the footing, should be placed as a capillary break to prevent moisture migration into the slab section. Concrete slabs may be placed directly over a 15-mil vapor retarder if desired (Stego-Wrap or equivalent).

Concrete slab and flatwork reinforcement should consist of chaired rebar slab reinforcement (minimum of No. 4 bars at 18-inch centers, both horizontal directions) placed at slab mid-height to resist potential swell forces and cracking. Slab thickness and steel reinforcement are minimums only and should be verified by the structural engineer/designer knowing the actual project loadings. All steel components of the foundation system should be protected from corrosion by maintaining a 4-inch minimum concrete cover of densely consolidated concrete at footings (by use of a vibrator). The construction joint between the foundation and any mowstrips/sidewalks placed adjacent to foundations should be sealed with a polyurethane based non-hardening sealant to prevent moisture migration between the joint. Epoxy coated embedded steel components or permanent waterproofing membranes placed at the exterior footing sidewall may also be used to mitigate the corrosion potential of concrete placed in contact with native soil.

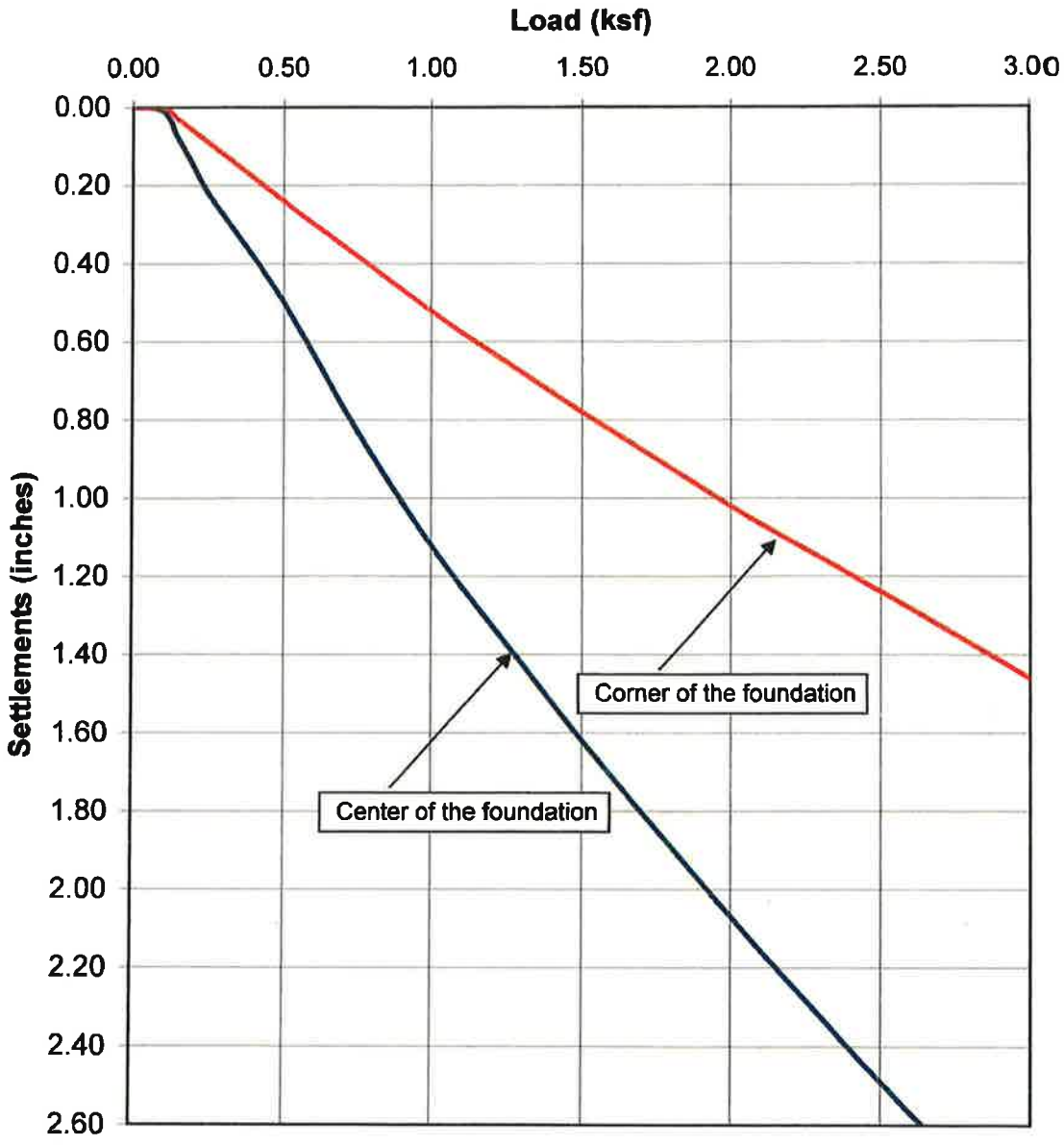

Notes:

1. A 15' x 15' foundation was used for settlement analysis

LANDMARK
Geo-Engineers and Geologists
a DBE/MBE/SBE Company
Project No.: LE04354

Total Settlements for a Turbine Generator Foundation at Heber 2 Geothermal Plant

Figure 2

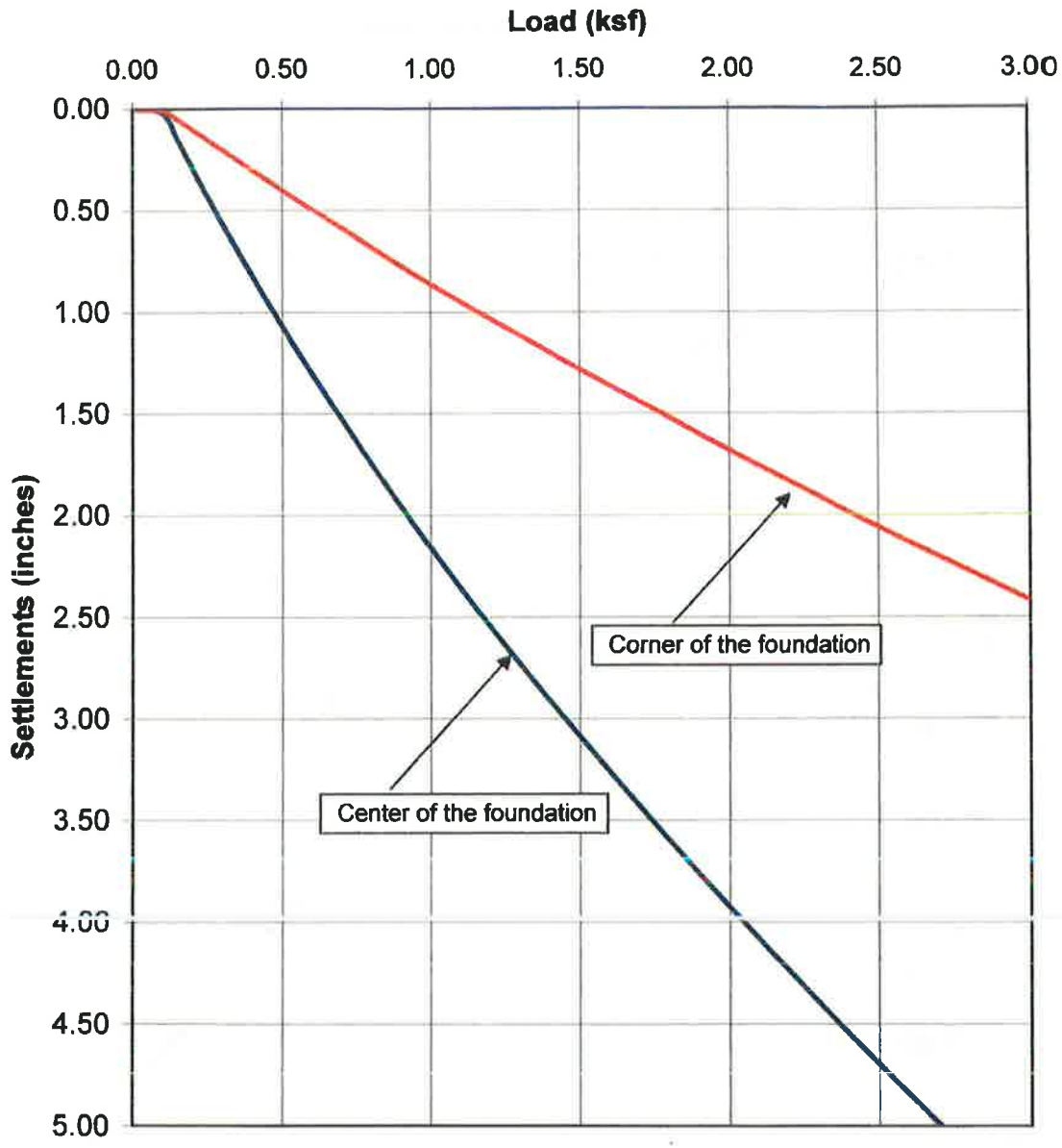

Notes:

1. A 30' x 60' foundation was used for settlement analysis

LANDMARK
Geo-Engineers and Geologists
a DBE/MBE/SBE Company
Project No.: LE04354

Total Settlements for a Turbine Generator Foundation at Heber 2 Geothermal Plant

Figure 3

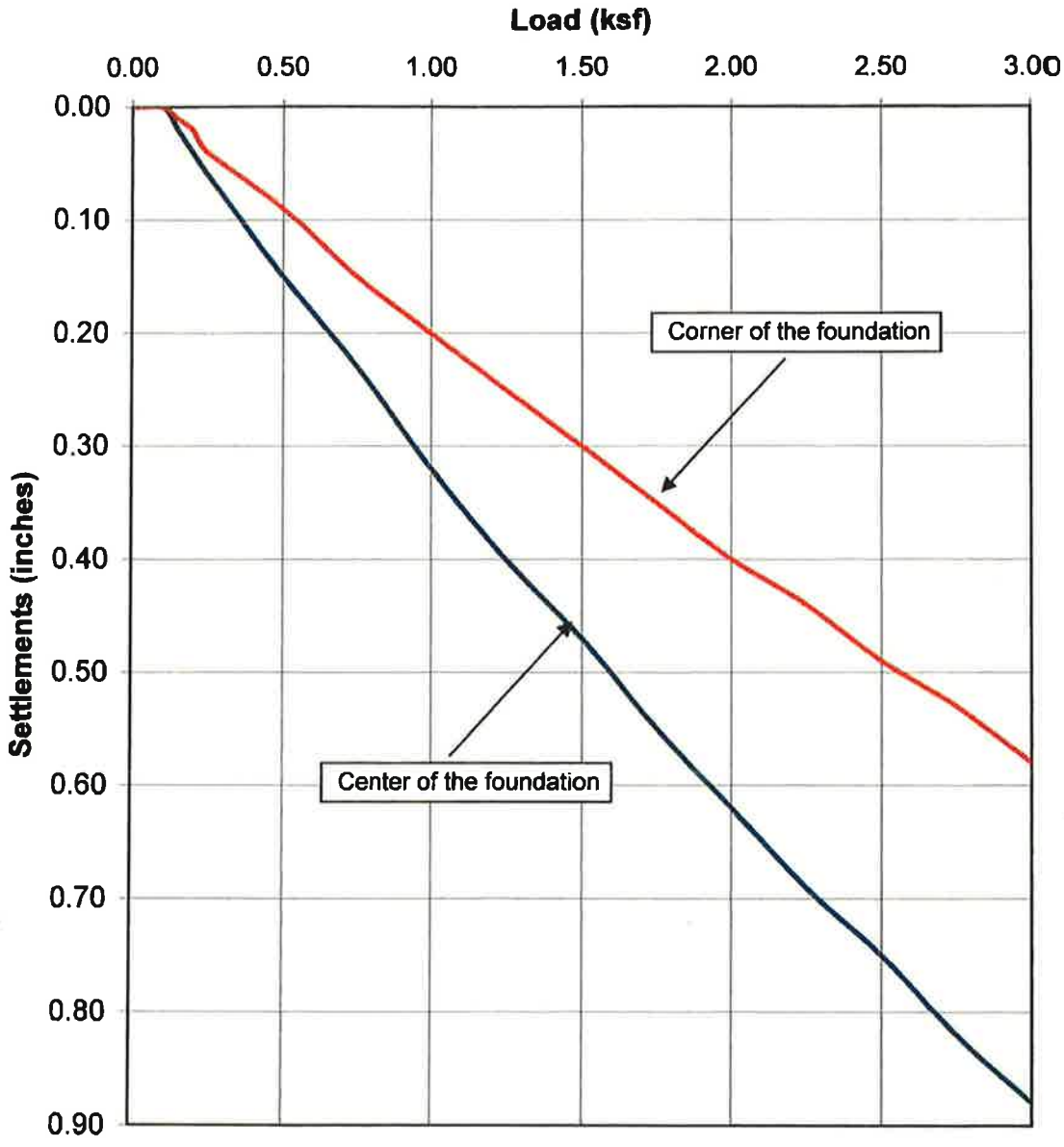

Notes:

1. A 5' x 5' foundation was used for settlement analysis

LANDMARK
Geo-Engineers and Geologists
a DBE/MBE/SBE Company
Project No.: LE04354

Total Settlements for a Cooling Tower Foundation at Heber 2 Geothermal Plant

Figure 4

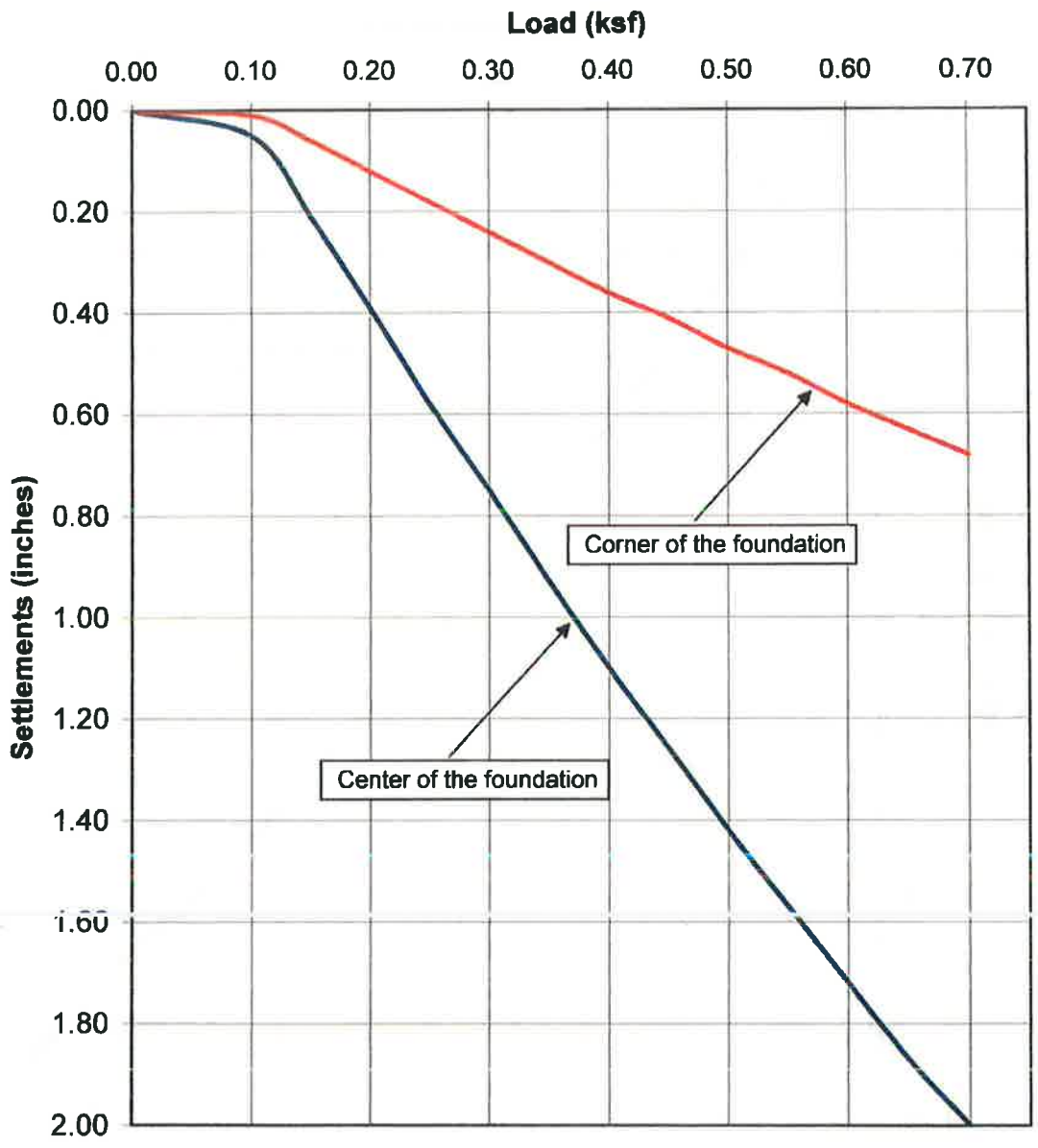

Notes:

1. A 60' x 180' foundation was used for settlement analysis

LANDMARK
Geo-Engineers and Geologists
a DBE/MBE/SBE Company
Project No.: LE04354

Total Settlements for a Cooling Tower Foundation at Heber 2 Geothermal Plant

Figure 5

Control joints should be provided in all concrete slabs-on-grade at a maximum spacing (in feet) of 2 to 3 times the slab thickness (in inches) as recommended by American Concrete Institute (ACI) guidelines. All joints should form approximately square patterns to reduce randomly oriented contraction cracks. Contraction joints in the slabs should be tooled at the time of the pour or sawcut (¼ of slab depth) within 6 to 8 hours of concrete placement. Construction (cold) joints in foundations and area flatwork should either be thickened butt-joints with dowels or a thickened keyed-joint designed to resist vertical deflection at the joint. All joints in flatwork should be sealed to prevent moisture, vermin, or foreign material intrusion. Precautions should be taken to prevent curling of slabs in this arid desert region (refer to ACI guidelines).

All independent flatwork (sidewalks, housekeeping slabs) should be placed on a minimum of 2 inches of concrete sand or aggregate base, dowelled to the perimeter foundations where adjacent to the structures and sloped 1% or more away from the structure. A minimum of 18 inches of moisture conditioned (3% minimum above optimum) and 8 inches of compacted subgrade (83 to 87%) and a 10-mil (minimum) polyethylene separation sheet should underlie the flatwork. All flatwork should be jointed in square patterns and at irregularities in shape at a maximum spacing of 10 feet or the least width of the sidewalk.

4.4 Concrete Mixes and Corrosivity

Selected chemical analyses for corrosivity were conducted on bulk samples of the near surface soil from the project site (Plates C-2 and C-3). The native soils were found to have moderate to severe levels of sulfate ion concentration (1,052 to 3,006 ppm). Sulfate ions in high concentrations can attack the cementitious material in concrete, causing weakening of the cement matrix and eventual deterioration by raveling. The California Building Code recommends that increased quantities of Type II Portland Cement be used at a low water/cement ratio when concrete is subjected to moderate sulfate concentrations. Type V Portland Cement and/or Type II/V cement with 25% flyash replacement is recommended when the concrete is subjected to soil with severe sulfate concentration.

A minimum of 6.25 sacks per cubic yard of concrete (4,500 psi) of Type V Portland Cement with a maximum water/cement ratio of 0.45 (by weight) should be used for concrete placed in contact with native soil on this project. Admixtures may be required to allow placement of this low water/cement ratio concrete.

There are no special requirements for concrete mixes when foundations are placed on 2.5 feet of low sulfate content granular fill.

The native soil has moderate to very severe level of chloride ion concentration (210 to 3,040 ppm). Chloride ions can cause corrosion of reinforcing steel, anchor bolts and other buried metallic conduits. Resistivity determinations on the soil indicate very severe potential for metal loss because of electrochemical corrosion processes. Mitigation of the corrosion of steel can be achieved by using steel pipes coated with epoxy corrosion inhibitors, asphaltic and epoxy coatings, cathodic protection or by encapsulating the portion of the pipe lying above groundwater with a minimum of 4 inches of densely consolidated concrete. ***No metallic pipes or conduits should be placed below foundations.***

Foundation designs shall provide a minimum concrete cover of four (4 inches around steel reinforcing or embedded components (anchor bolts, hold-downs, etc.) exposed to native soil or landscape water (to 18 inches above grade). If the 4-inch concrete edge distance cannot be achieved, all embedded steel components (anchor bolts, hold-downs, etc.) shall be epoxy dipped for corrosion protection or a corrosion inhibitor and a permanent waterproofing membrane shall be placed along the exterior face of the exterior footings. Additionally, the concrete should be thoroughly vibrated at footings during placement to decrease the permeability of the concrete.

4.5 Excavations

All site excavations should conform to CalOSHA requirements for Type B soil. The contractor is solely responsible for the safety of workers entering trenches. Temporary excavations with depths of 4 feet or less may be cut nearly vertical for short duration. Excavations deeper than 4 feet will require shoring or slope inclinations in conformance to CAL/OSHA regulations for Type B soil. Surcharge loads of stockpiled soil or construction materials should be set back from the top of the slope a minimum distance equal to the height of the slope. All permanent slopes should not be steeper than 3:1 to reduce wind and rain erosion. Protected slopes with ground cover may be as steep as 2:1. However, maintenance with motorized equipment may not be possible at this inclination.

4.6 Seismic Design

This site is located in the seismically active southern California area and the site structures are subject to strong ground shaking due to potential fault movements along the Brawley, Superstition Hills, and Imperial Faults. Engineered design and earthquake-resistant construction are the common solutions to increase safety and development of seismic areas. Designs should comply with the latest edition of the CBC for Seismic Zone 4 using the seismic coefficients given in Section 3.4 of this report. ***This site lies within 11.3 km of a Type A fault overlying S_D (stiff) soil.***

Section 5
LIMITATIONS AND ADDITIONAL SERVICES

5.1 Limitations

The recommendations and conclusions within this report are based on current information regarding the proposed additions to the Ormat Heber 2 geothermal power plant located on Dogwood Road southwest of Heber, California. The conclusions and recommendations of this report are invalid if:

- Structural loads change from those stated or the structures are relocated.
- The Additional Services section of this report is not followed.
- This report is used for adjacent or other property.
- Changes of grade or groundwater occur between the issuance of this report and construction other than those anticipated in this report.
- Any other change that materially alters the project from that proposed at the time this report was prepared.

Findings and recommendations in this report are based on selected points of field exploration, geologic literature, laboratory testing, and our understanding of the proposed project. Our analysis of data and recommendations presented herein are based on the assumption that soil conditions do not vary significantly from those found at specific exploratory locations. Variations in soil conditions can exist between and beyond the exploration points or groundwater elevations may change. If detected, these conditions may require additional studies, consultation, and possible design revisions.

This report contains information that may be useful in the preparation of contract specifications. However, the report is not worded is such a manner that we recommend its use as a construction specification document without proper modification. The use of information contained in this report for bidding purposes should be done at the contractor's option and risk.

This report was prepared according to the generally accepted *geotechnical engineering standards of practice* that existed in Imperial County at the time the report was prepared. No express or implied warranties are made in connection with our services. This report should be considered invalid for periods after two years from the report date without a review of the validity of the findings and recommendations by our firm, because of potential changes in the Geotechnical Engineering Standards of Practice.

APPENDIX A

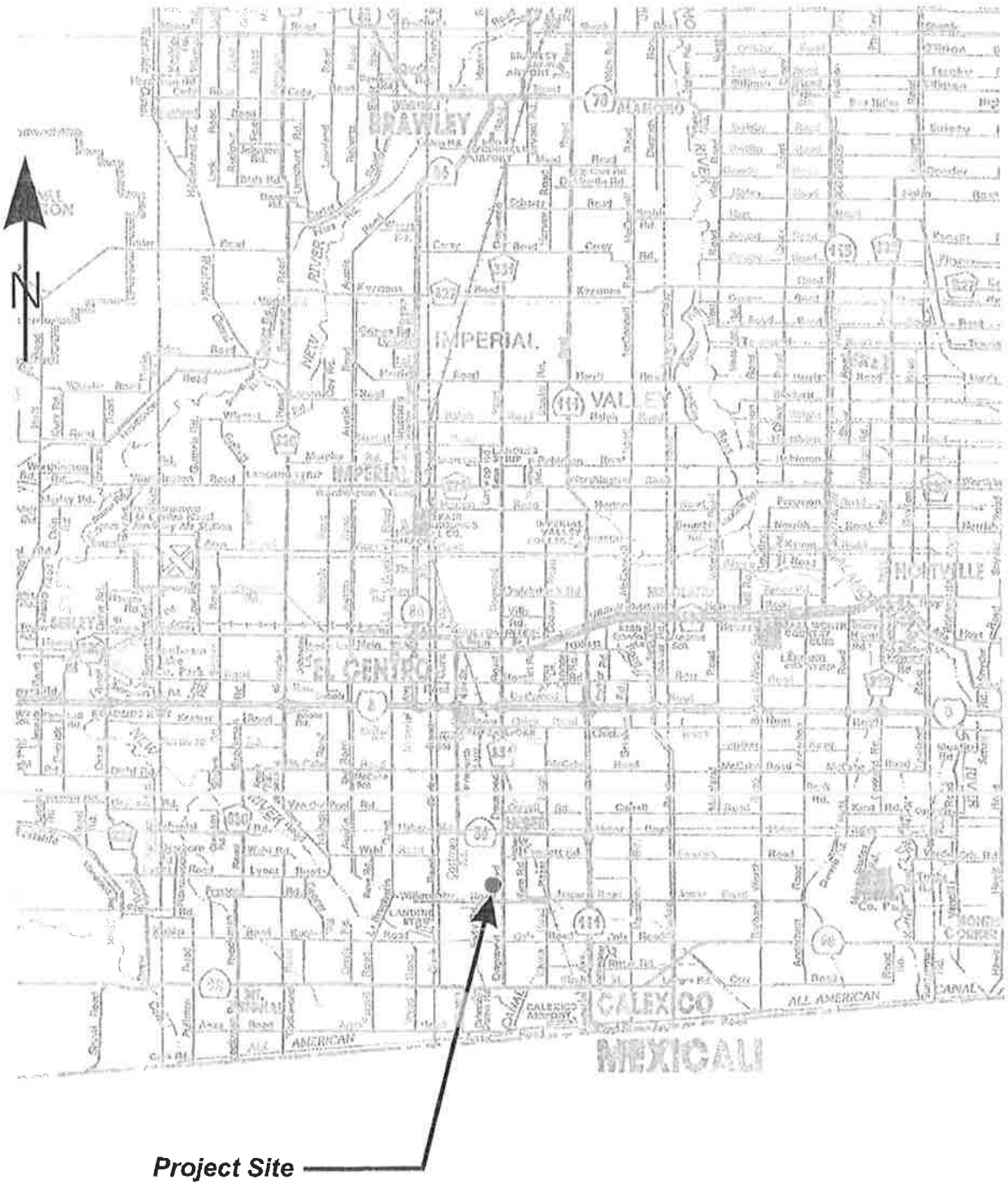

LANDMARK Geo-Engineers and Geologists, a DIE/MBE/SBE Company Project No.: LE04354	Vicinity Map	Plate A-1

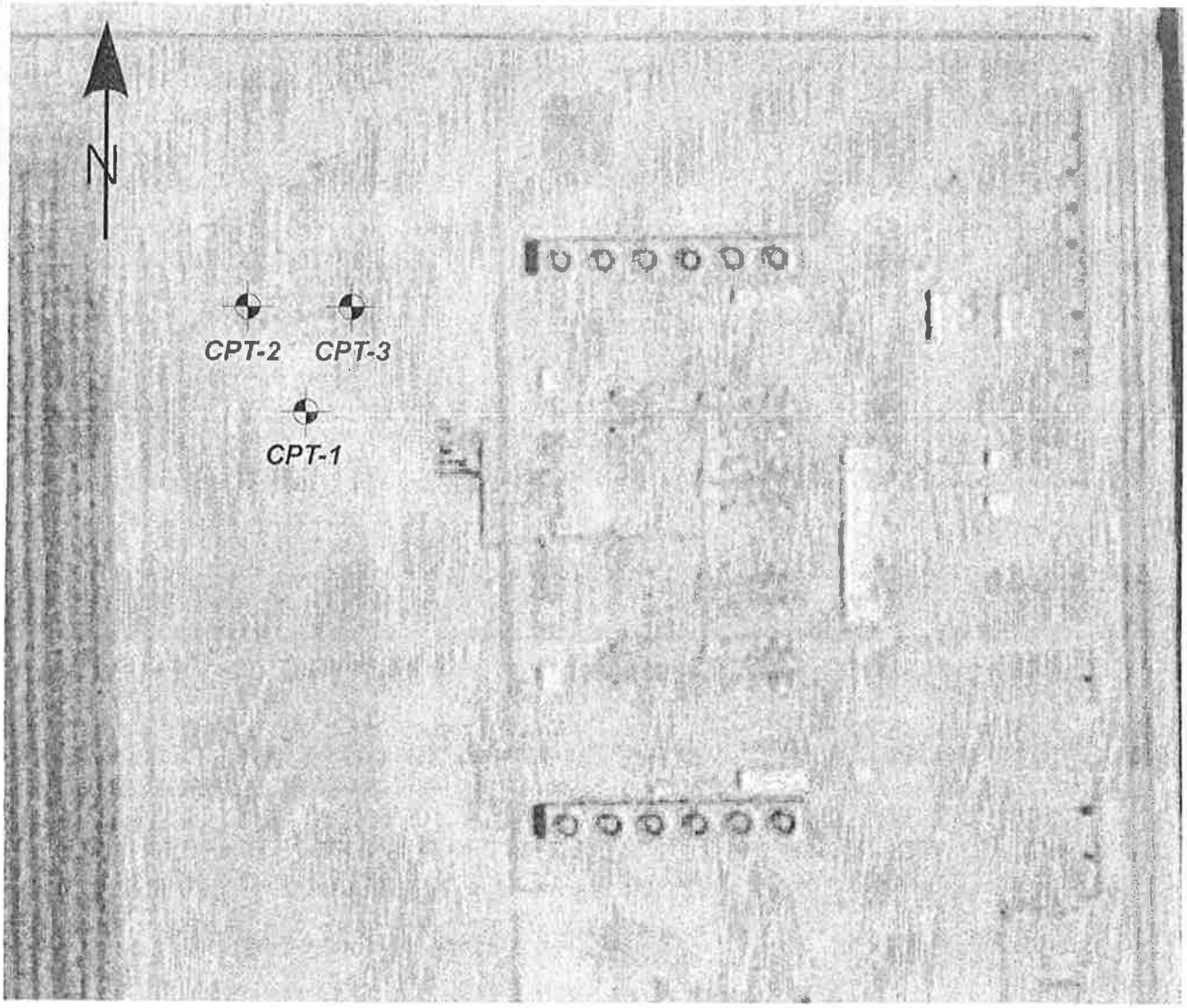

LANDMARK Geo-Engineers and Geologists, a DBE/MBE/SBE Company Project No.: LE04354	Site and Exploration Map	Plate A-2

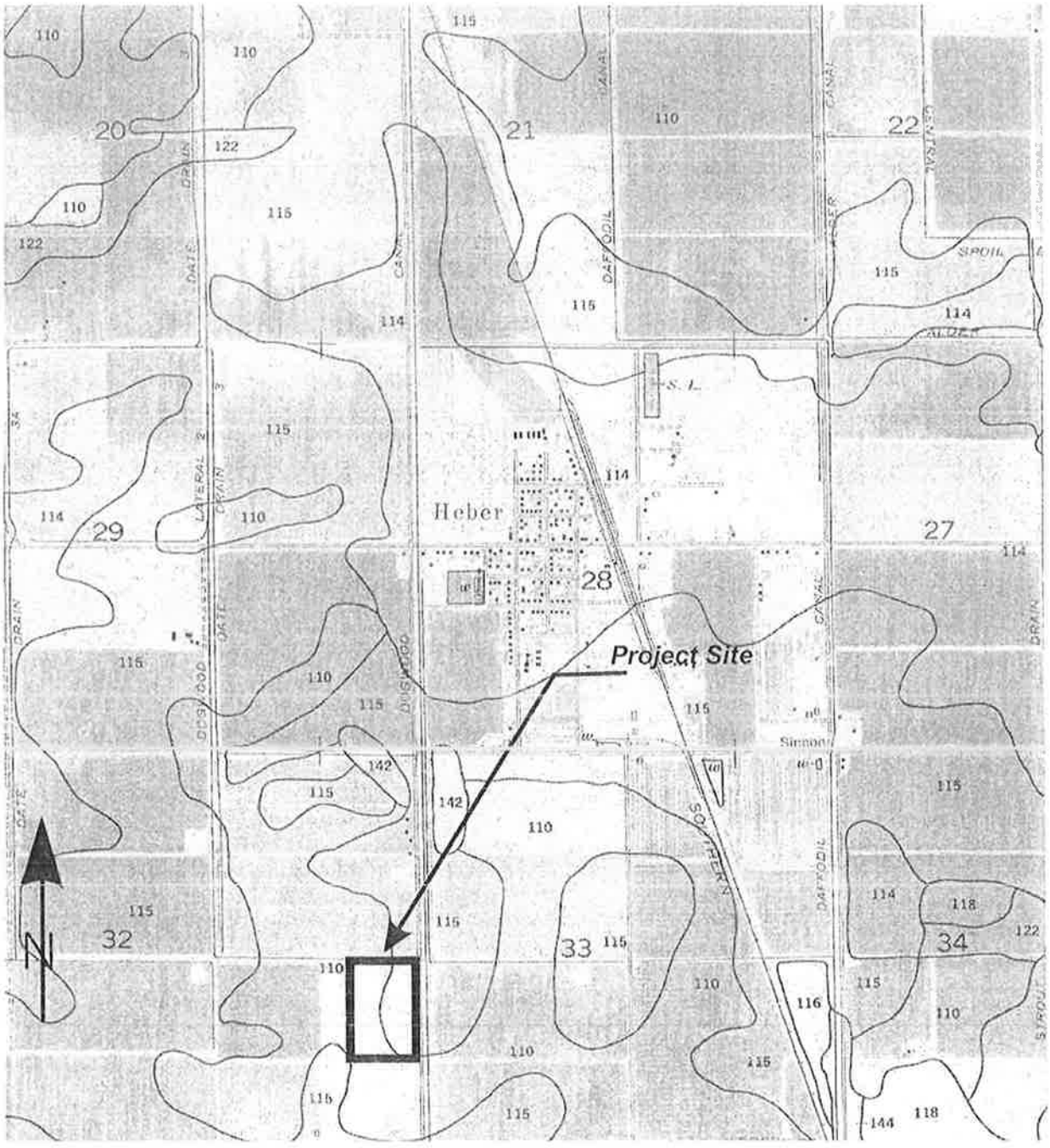

LANDMARK Geo-Engineers and Geologists a DBE/MBE/SBE Company **Project No.: LE04354**	**Soil Survey Map**	**Plate A-3**

Soil Survey of

IMPERIAL COUNTY CALIFORNIA IMPERIAL VALLEY AREA

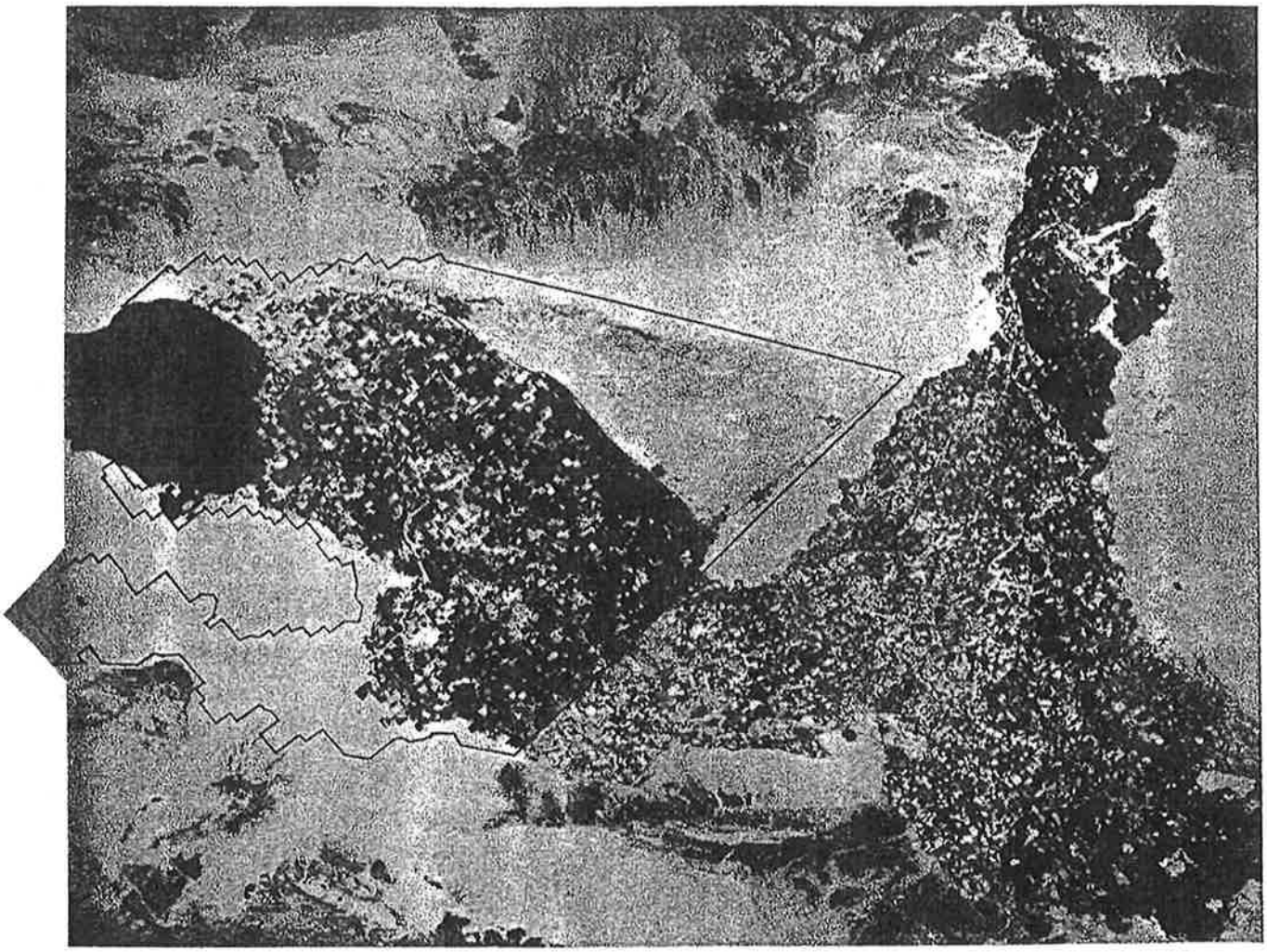

United States Department of Agriculture Soil Conservation Service
in cooperation with
University of California Agricultural Experiment Station
and
Imperial Irrigation District

TABLE 11.--ENGINEERING INDEX PROPERTIES

[The symbol > means more than. Absence of an entry indicates that data were not estimated]

Soil name and map symbol	Depth	USDA texture	Classification		Frag-ments > 3 inches	Percentage passing sieve number--				Liquid limit	Plas-ticity index
			Unified	AASHTO		4	10	40	200		
	In				Pct					Pct	
100----------	0-13	Loamy fine sand	SM	A-2	0	100	100	75-85	10-30	---	NP
Antho	13-60	Sandy loam, fine sandy loam.	SM	A-2, A-4	0	90-100	75-95	50-60	15-40	---	NP
101*:											
Antho----------	0-8	Loamy fine sand	SM	A-2	0	100	100	75-85	10-30	---	NP
	8-60	Sandy loam, fine sandy loam.	SM	A-2, A-4	0	90-100	75-95	50-60	15-40	---	NP
Superstition------	0-6	Fine sand-------	SM	A-2	0	100	95-100	70-85	15-25	---	NP
	6-60	Loamy fine sand, fine sand, sand.	SM	A-2	0	100	95-100	70-85	15-25	---	NP
102*. Badland											
103----------	0-10	Gravelly sand---	SP, SP-SM	A-1, A-2	0-5	60-90	50-85	30-55	0-10	---	NP
Carsitas	10-60	Gravelly sand, gravelly coarse sand, sand.	SP, SP-SM	A-1	0-5	60-90	50-85	25-50	0-10	---	NP
104* Fluvaquents											
105----------	0-13	Clay loam-------	CL	A-6	0	100	100	90-100	70-95	35-45	15-30
Glenbar	13-60	Clay loam, silty clay loam.	CL	A-6	0	100	100	90-100	70-95	35-45	15-30
106----------	0-13	Clay loam-------	CL	A-6, A-7	0	100	100	90-100	70-95	35-45	15-25
Glenbar	13-60	Clay loam, silty clay loam.	CL	A-6, A-7	0	100	100	90-100	70-95	35-45	15-25
107*----------	0-13	Loam----------	ML, CL-ML, CL	A-4	0	100	100	100	70-80	20-30	NP-10
Glenbar	13-60	Clay loam, silty clay loam.	CL	A-6, A-7	0	100	100	95-100	70-95	35-45	15-30
108----------	0-14	Loam----------	ML	A-4	0	100	100	85-100	55-95	25-35	NP-10
Holtville	14-22	Clay, silty clay	CL, CH	A-7	0	100	100	95-100	85-95	40-65	20-35
	22-60	Silt loam, very fine sandy loam.	ML	A-4	0	100	100	95-100	65-85	25-35	NP-10
109----------	0-17	Silty clay------	CL, CH	A-7	0	100	100	95-100	85-95	40-65	20-35
Holtville	17-24	Clay, silty clay	CL, CH	A-7	0	100	100	95-100	85-95	40-65	20-35
	24-35	Silt loam, very fine sandy loam.	ML	A-4	0	100	100	95-100	65-85	25-35	NP-10
	35-60	Loamy very fine sand, loamy fine sand.	SM, ML	A-2, A-4	0	100	100	75-100	20-55	---	NP
110----------	0-17	Silty clay------	CH, CL	A-7	0	100	100	95-100	85-95	40-65	20-35
Holtville	17-24	Clay, silty clay	CH, CL	A-7	0	100	100	95-100	85-95	40-65	20-35
	24-35	Silt loam, very fine sandy loam.	ML	A-4	0	100	100	95-100	55-85	25-35	NP-10
	35-60	Loamy very fine sand, loamy fine sand.	SM, ML	A-2, A-4	0	100	100	75-100	20-55	---	NP

See footnote at end of table.

TABLE 11.--ENGINEERING INDEX PROPERTIES--Continued

Soil name and map symbol	Depth	USDA texture	Classification		Fragments > 3 inches	Percentage passing sieve number--				Liquid limit	Plasticity index
			Unified	AASHTO		4	10	40	200		
	In				Pct					Pct	
111*:											
Holtville	0-10	Silty clay loam	CL, CH	A-7	0	100	100	95-100	85-95	40-65	20-35
	10-22	Clay, silty clay	CL, CH	A-7	0	100	100	95-100	85-95	40-65	20-35
	22-60	Silt loam, very fine sandy loam.	ML	A-4	0	100	100	95-100	65-85	25-35	NP-10
Imperial	0-12	Silty clay loam	CL	A-7	0	100	100	100	85-95	40-50	10-20
	12-60	Silty clay loam, silty clay, clay.	CH	A-7	0	100	100	100	85-95	50-70	25-45
112	0-12	Silty clay	CH	A-7	0	100	100	100	85-95	50-70	25-45
Imperial	12-60	Silty clay loam, silty clay, clay.	CH	A-7	0	100	100	100	85-95	50-70	25-45
113	0-12	Silty clay	CH	A-7	0	100	100	100	85-95	50-70	25-45
Imperial	12-60	Silty clay, clay, silty clay loam.	CH	A-7	0	100	100	100	85-95	50-70	25-45
114	0-12	Silty clay	CH	A-7	0	100	100	100	85-95	50-70	25-45
Imperial	12-60	Silty clay loam, silty clay, clay.	CH	A-7	0	100	100	100	85-95	50-70	25-45
115*:											
Imperial	0-12	Silty clay loam	CL	A-7	0	100	100	100	85-95	40-50	10-20
	12-60	Silty clay loam, silty clay, clay.	CH	A-7	0	100	100	100	85-95	50-70	25-45
Glenbar	0-13	Silty clay loam	CL	A-6, A-7	0	100	100	90-100	70-95	35-45	15-25
	13-60	Clay loam, silty clay loam.	CL	A-6, A-7	0	100	100	90-100	70-95	35-45	15-25
116*:											
Imperial	0-13	Silty clay loam	CL	A-7	0	100	100	100	85-95	40-50	10-20
	13-60	Silty clay loam, silty clay, clay.	CH	A-7	0	100	100	100	85-95	50-70	25-45
Glenbar	0-13	Silty clay loam	CL	A-6, A-7	0	100	100	90-100	70-95	35-45	15-25
	13-60	Clay loam, silty clay loam.	CL	A-6	0	100	100	90-100	70-95	35-45	15-30
117, 118	0-12	Loam	ML	A-4	0	95-100	95-100	85-100	75-90	20-30	NP-5
Indio	12-72	Stratified loamy very fine sand to silt loam.	ML	A-4	0	95-100	95-100	85-100	75-90	20-30	NP-5
119*:											
Indio	0-12	Loam	ML	A-4	0	95-100	95-100	85-100	75-90	20-30	NP-5
	12-72	Stratified loamy very fine sand to silt loam.	ML	A-4	0	95-100	95-100	85-100	75-90	20-30	NP-5
Vint	0-10	Loamy fine sand	SM	A-2	0	95-100	95-100	70-80	25-35	---	NP
	10-60	Loamy sand, loamy fine sand.	SM	A-2	0	95-100	95-100	70-80	20-30	---	NP
120*	0-12	Loam	ML, CL-ML	A-4	0	100	95-100	75-85	55-65	20-30	NP-10
Laveen	12-60	Loam, very fine sandy loam.	ML, CL-ML	A-4	0	95-100	85-95	70-80	55-65	15-25	NP-10

See footnote at end of table.

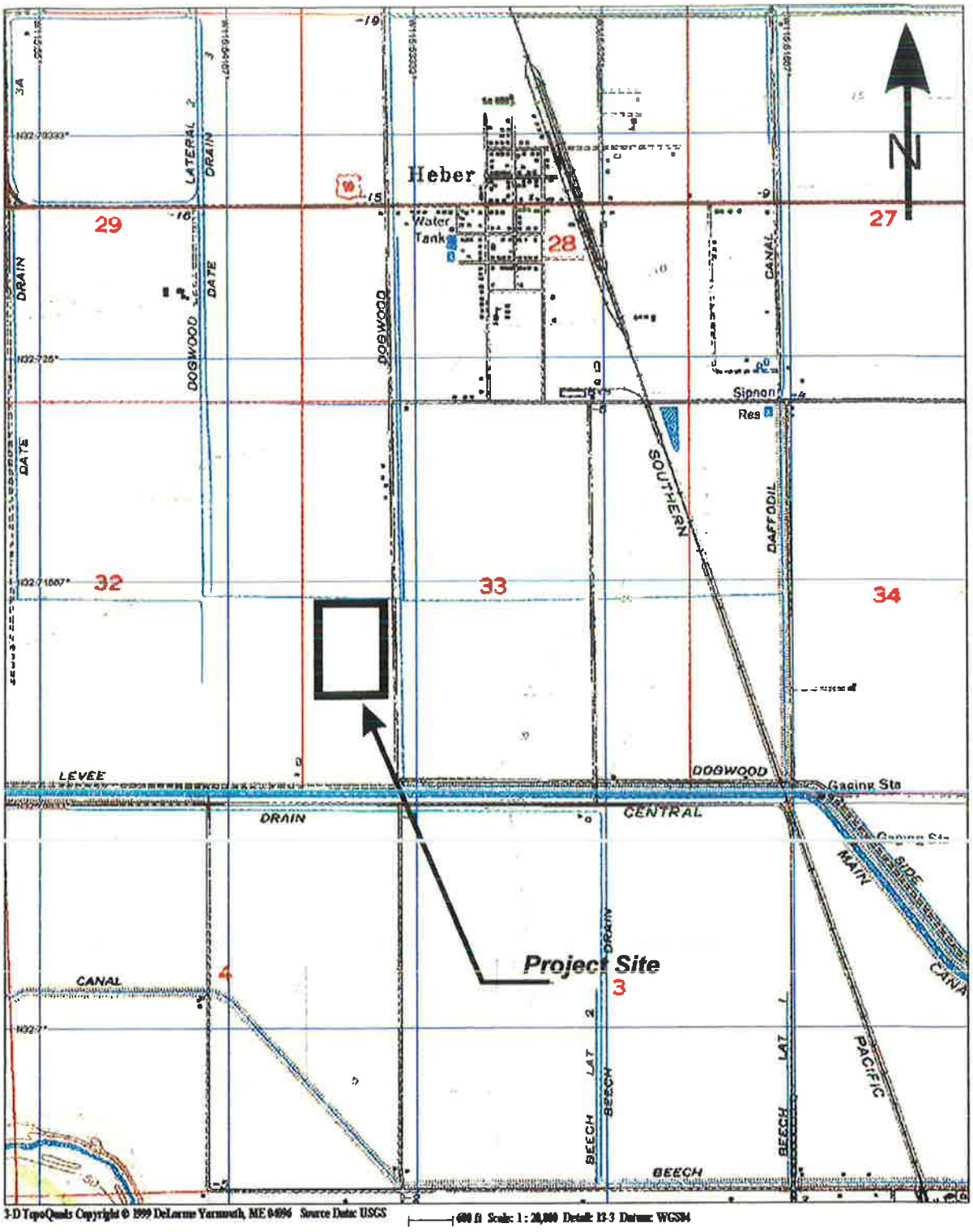

LANDMARK
Geo-Engineers and Geologists
a OBE/MBE/SBE Company

Project No.: LE04354

Topographic Map

Plate A-4

APPENDIX B

CLIENT: ORMAT

PROJECT: ORMAT Heber 2 Facilities, Heber, CA

LOCATION: See Site and Boring Location Plan

CONE PENETROMETER: HOLGUIN, FAHAN & ASSC. Truck Mounted Electric Cone with 23 ton reaction weight

DATE: 12/20/04

LOG OF CONE SOUNDING DATA CPT-1

DEPTH (FEET)	INTERPRETED SOIL PROFILE From Robertson & Campanella (1989)		
	GROUND El. +/-		
	Clay	CL/CH	hard
	Sandy Silt to Clayey Silt	ML	very dense
	Silty Sand to Sandy Silt	SM/ML	very dense
	Silty Sand to Sandy Silt	" "	very dense
	Silty Clay to Clay	CL	stiff
	Silty Clay to Clay	" "	stiff
	Clay	CL/CH	stiff
	Clay	" "	stiff
	Clay	" "	stiff
10	Clay	" "	very stiff
	Clay	" "	very stiff
	Silty Clay to Clay	CL	very stiff
	Clay	CL/CH	stiff
	Clay	" "	stiff
	Clay	" "	very stiff
	Clay	" "	very stiff
	Clay	" "	very stiff
	Clay	" "	very stiff
	Clay	" "	very stiff
20	Clay	" "	very stiff
	Clay	" "	stiff
	Clay	" "	very stiff
	Clay	" "	very stiff
	Clay	" "	very stiff
	Clay	" "	very stiff
	Clay	" "	very stiff
	Clay	" "	very stiff
	Clay	" "	very stiff
30	Clay	" "	very stiff
	Clay	" "	very stiff
	Clay	" "	very stiff
	Clay	" "	stiff
	Clay	" "	stiff
	Clay	" "	very stiff
	Clay	" "	very stiff
	Clayey Silt to Silty Clay	ML/CL	very stiff
	Silty Clay to Clay	CL	stiff
40	Clayey Silt to Silty Clay	ML/CL	stiff
	Clayey Silt to Silty Clay	" "	stiff
	Clayey Silt to Silty Clay	" "	stiff
	Clayey Silt to Silty Clay	" "	very stiff
	Clayey Silt to Silty Clay	" "	very stiff
	Clayey Silt to Silty Clay	" "	very stiff
	Clayey Silt to Silty Clay	" "	stiff
	Sandy Silt to Clayey Silt	ML	very loose
	Sandy Silt to Clayey Silt	" "	very loose
	Clayey Silt to Silty Clay	ML/CL	stiff
50			

End of Sounding @ 49.5 ft.

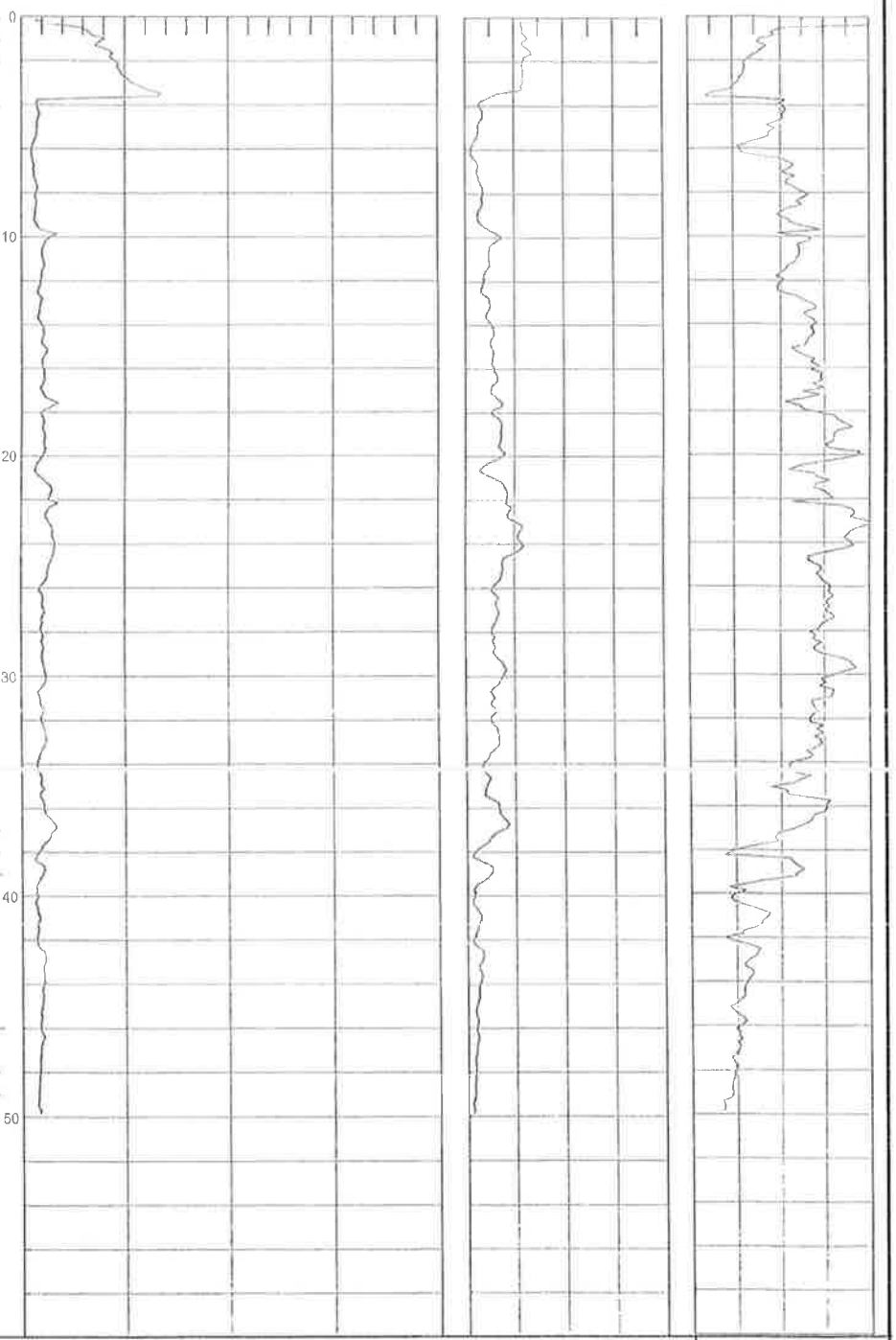

Project No: LE04354

LANDMARK
Geo-Engineers and Geologists
a DBE/MBE/SBE Company

Plate B-1

LANDMARK CONSULTANTS, INC.

CONE PENETROMETER INTERPRETATION (based on Robertson & Campanella, 1989, refer to Key to CPT logs)

Project: ORMAT Heber 2 Facilities, Heber, CA Project No: LE04354 Date: 12/20/04

CONE SOUNDING: CPT-1

Est. GWT (ft): 12.0

Phi Correlation: 0 0-Schm(78),1-R&C(83),2-PHT(74)

Base Depth meters	Base Depth feet	Avg Tip Qc, tsf	Avg Friction Ratio, %	1 Soil Type	Soil Classification	USC	Density or Consistency	Est. Density (pcf)	Qc to N	SPT N(60)	Cn or Cq	Norm. Qc1n	Est. % Fines	Rel. Dens. Dr (%)	Nk; Phi (deg.)	17.0 Su (tsf)	OCR
0.15	0.5	31.82	10.13	3	Clay	CL/CH	very stiff	125	1.3	25	2.00		95			1.87	>10
0.30	1.0	71.19	3.50	6	Sandy Silt to Clayey Silt	ML	very dense	115	3.5	20	2.00	134.6	45	107	43		
0.45	1.5	76.38	3.27	6	Sandy Silt to Clayey Silt	ML	very dense	115	3.5	22	2.00	144.4	40	102	42		
0.60	2.0	88.21	2.88	6	Sandy Silt to Clayey Silt	ML	very dense	115	3.5	25	2.00	166.8	35	101	42		
0.75	2.5	94.19	2.53	7	Silty Sand to Sandy Silt	SM/ML	very dense	115	4.5	21	2.00	178.0	30	100	42		
0.93	3.0	101.94	2.35	7	Silty Sand to Sandy Silt	SM/ML	very dense	115	4.5	23	2.00	192.7	30	99	42		
1.08	3.5	123.24	1.66	8	Sand to Silty Sand	SP/SM	very dense	115	5.5	22	2.00	233.0	20	102	42		
1.23	4.0	53.93	2.99	6	Sandy Silt to Clayey Silt	ML	dense	115	3.5	15	2.00	101.9	45	76	39		
1.38	4.5	16.43	4.19	3	Clay	CL/CH	stiff	125	1.3	13	2.00		85			0.95	>10
1.53	5.0	15.53	3.80	4	Silty Clay to Clay	CL	stiff	125	1.8	9	1.95		85			0.90	>10
1.68	5.5	13.99	3.48	4	Silty Clay to Clay	CL	stiff	125	1.8	8	1.85		85			0.80	>10
1.83	6.0	10.16	2.42	5	Clayey Silt to Silty Clay	ML/CL	stiff	120	2.5	4	1.76		85			0.58	>10
1.98	6.5	10.41	3.55	4	Silty Clay to Clay	CL	stiff	125	1.8	6	1.69		95			0.59	>10
2.13	7.0	11.62	4.38	3	Clay	CL/CH	stiff	125	1.3	9	1.62		100			0.66	>10
2.28	7.5	13.29	4.44	3	Clay	CL/CH	stiff	125	1.3	11	1.56		95			0.76	>10
2.45	8.0	14.55	4.93	3	Clay	CL/CH	stiff	125	1.3	12	1.51		95			0.83	>10
2.60	8.5	13.90	4.96	3	Clay	CL/CH	stiff	125	1.3	11	1.46		100			0.79	>10
2.75	9.0	13.23	4.08	3	Clay	CL/CH	stiff	125	1.3	11	1.42		95			0.75	>10
2.90	9.5	13.66	4.68	3	Clay	CL/CH	stiff	125	1.3	11	1.38		100			0.77	>10
3.05	10.0	26.88	5.00	3	Clay	CL/CH	very stiff	125	1.3	22	1.34		80			1.55	>10
3.20	10.5	21.69	5.01	3	Clay	CL/CH	very stiff	125	1.3	17	1.32		90			1.24	>10
3.35	11.0	19.84	4.85	3	Clay	CL/CH	very stiff	125	1.3	16	1.30		95			1.13	>10
3.50	11.5	21.31	4.45	4	Silty Clay to Clay	CL	very stiff	125	1.8	12	1.29		90			1.22	>10
3.65	12.0	18.97	4.00	4	Silty Clay to Clay	CL	very stiff	125	1.8	11	1.27		90			1.08	>10
3.80	12.5	16.82	3.88	4	Silty Clay to Clay	CL	stiff	125	1.8	10	1.26		95			0.95	>10
3.95	13.0	18.18	4.91	3	Clay	CL/CH	very stiff	125	1.3	15	1.24		100			1.03	>10
4.13	13.5	17.33	5.43	3	Clay	CL/CH	stiff	125	1.3	14	1.23		100			0.98	>10
4.28	14.0	17.04	5.46	3	Clay	CL/CH	stiff	125	1.3	14	1.22		100			0.96	>10
4.43	14.5	21.21	5.45	3	Clay	CL/CH	very stiff	125	1.3	17	1.20		100			1.20	>10
4.58	15.0	19.96	5.21	3	Clay	CL/CH	very stiff	125	1.3	16	1.19		100			1.13	>10
4.73	15.5	23.41	4.80	3	Clay	CL/CH	very stiff	125	1.3	19	1.18		95			1.33	>10
4.88	16.0	20.50	5.51	3	Clay	CL/CH	very stiff	125	1.3	16	1.17		100			1.16	>10
5.03	16.5	21.94	5.88	3	Clay	CL/CH	very stiff	125	1.3	18	1.15		100			1.24	>10
5.18	17.0	19.22	5.48	3	Clay	CL/CH	very stiff	125	1.3	15	1.14		100			1.08	>10
5.33	17.5	27.57	5.03	3	Clay	CL/CH	very stiff	125	1.3	22	1.13		95			1.57	>10
5.48	18.0	23.29	5.22	3	Clay	CL/CH	very stiff	125	1.3	19	1.12		100			1.32	>10
5.65	18.5	20.85	6.67	3	Clay	CL/CH	very stiff	125	1.3	17	1.11		100			1.18	>10
5.80	19.0	21.33	6.77	3	Clay	CL/CH	very stiff	125	1.3	17	1.10		100			1.20	>10
5.95	19.5	21.97	6.29	3	Clay	CL/CH	very stiff	125	1.3	18	1.09		100			1.24	>10
6.10	20.0	21.34	7.09	3	Clay	CL/CH	very stiff	125	1.3	17	1.08		100			1.20	>10
6.25	20.5	15.48	5.72	3	Clay	CL/CH	stiff	125	1.3	12	1.07		100			0.86	5.53
6.40	21.0	15.87	5.20	3	Clay	CL/CH	stiff	125	1.3	13	1.06		100			0.88	5.65
6.55	21.5	26.53	5.79	3	Clay	CL/CH	very stiff	125	1.3	21	1.05		100			1.50	>10
6.70	22.0	27.19	6.21	3	Clay	CL/CH	very stiff	125	1.3	22	1.05		100			1.54	>10
6.85	22.5	29.12	6.18	3	Clay	CL/CH	very stiff	125	1.3	23	1.04		100			1.65	>10
7.00	23.0	24.40	7.41	3	Clay	CL/CH	very stiff	125	1.3	20	1.03		100			1.38	>10
7.18	23.5	29.74	7.65	3	Clay	CL/CH	very stiff	125	1.3	24	1.02		100			1.69	>10
7.33	24.0	31.24	7.01	3	Clay	CL/CH	very stiff	125	1.3	25	1.01		100			1.78	>10
7.48	24.5	31.71	6.74	3	Clay	CL/CH	very stiff	125	1.3	25	1.01		100			1.80	>10
7.63	25.0	28.38	5.36	3	Clay	CL/CH	very stiff	125	1.3	23	1.00		100			1.61	>10
7.78	25.5	25.50	5.79	3	Clay	CL/CH	very stiff	125	1.3	20	0.99		100			1.44	>10
7.93	26.0	21.23	6.01	3	Clay	CL/CH	very stiff	125	1.3	17	0.98		100			1.18	7.00
8.08	26.5	19.41	6.26	3	Clay	CL/CH	very stiff	125	1.3	16	0.98		100			1.08	6.00
8.23	27.0	21.10	6.12	3	Clay	CL/CH	very stiff	125	1.3	17	0.97		100			1.17	6.65
8.38	27.5	20.13	6.30	3	Clay	CL/CH	very stiff	125	1.3	16	0.96		100			1.12	6.00
8.53	28.0	19.23	5.66	3	Clay	CL/CH	very stiff	125	1.3	15	0.96		100			1.06	5.42
8.68	28.5	20.08	5.65	3	Clay	CL/CH	very stiff	125	1.3	16	0.95		100			1.11	5.76
8.85	29.0	20.55	5.67	3	Clay	CL/CH	very stiff	125	1.3	16	0.94		100			1.14	5.88
9.00	29.5	20.76	7.00	3	Clay	CL/CH	very stiff	125	1.3	17	0.94		100			1.15	5.88
9.15	30.0	22.80	6.88	3	Clay	CL/CH	very stiff	125	1.3	18	0.93		100			1.27	6.65

LANDMARK CONSULTANTS, INC.

CONE PENETROMETER INTERPRETATION (based on Robertson & Campanella, 1989, refer to Key to CPT logs)

Project: ORMAT Heber 2 Facilities, Heber, CA Project No: LE04354 Date: 12/20/04

CONE SOUNDING: CPT-1

Est. GWT (ft): 12.0

Phi Correlation: 0 0-Schm(78),1-R&C(83),2-PH(74)

Base Depth meters	Base Depth feet	Avg Tip Qc, tsf	Avg Friction Ratio, %		Soil Type	Soil Classification	USC	Density or Consistency	Est. Density (pcf)	Qc to N	SPT N(60)	Cn or Cq	Norm. Qc1n	Est. % Fines	Rel. Dens. Dr (%)	Nk Phi (deg.)	17.0 Su (tsf)	OCR
9.30	30.5	21.00	5.00	3	3	Clay	CL/CH	very stiff	125	1.3	17	0.93		100			1.20	6.00
9.45	31.0	17.19	6.36	3	3	Clay	CL/CH	stiff	125	1.3	14	0.92		100			0.94	4.00
9.60	31.5	20.05	5.47	3	3	Clay	CL/CH	very stiff	125	1.3	16	0.92		100			1.10	5.10
9.75	32.0	19.47	5.50	3	3	Clay	CL/CH	very stiff	125	1.3	16	0.91		100			1.07	4.68
9.90	32.5	21.74	5.63	3	3	Clay	CL/CH	very stiff	125	1.3	17	0.90		100			1.20	5.53
10.05	33.0	23.37	5.76	3	3	Clay	CL/CH	very stiff	125	1.3	19	0.90		100			1.30	6.10
10.20	33.5	20.39	5.56	3	3	Clay	CL/CH	very stiff	125	1.3	16	0.89		100			1.12	4.78
10.38	34.0	15.97	5.12	3	3	Clay	CL/CH	stiff	125	1.3	13	0.89		100			0.86	3.28
10.53	34.5	16.45	4.48	3	3	Clay	CL/CH	stiff	125	1.3	13	0.88		100			0.89	3.35
10.68	35.0	16.50	4.96	3	3	Clay	CL/CH	very stiff	125	1.3	15	0.88		100			1.01	3.91
10.83	35.5	19.11	4.05	4	4	Silty Clay to Clay	CL	very stiff	125	1.8	11	0.87		100			1.04	5.21
10.98	36.0	20.64	5.86	3	3	Clay	CL/CH	very stiff	125	1.3	17	0.87		100			1.13	4.47
11.13	36.5	25.44	5.72	3	3	Clay	CL/CH	very stiff	125	1.3	20	0.86		100			1.41	6.21
11.28	37.0	31.72	4.84	4	4	Silty Clay to Clay	CL	very stiff	125	1.8	18	0.86		100			1.78	>10
11.43	37.5	25.49	3.77	5	5	Clayey Silt to Silty Clay	ML/CL	very stiff	120	2.5	10	0.85		100			1.41	>10
11.58	38.0	17.68	2.48	5	5	Clayey Silt to Silty Clay	ML/CL	stiff	120	2.5	7	0.85		100			0.95	5.65
11.73	38.5	15.25	3.47	4	4	Silty Clay to Clay	CL	stiff	125	1.8	9	0.85		100			0.81	3.35
11.88	39.0	20.64	4.84	3	3	Clay	CL/CH	very stiff	125	1.3	17	0.84		100			1.13	4.00
12.05	39.5	15.50	3.51	4	4	Silty Clay to Clay	CL	stiff	125	1.8	9	0.84		100			0.82	3.28
12.20	40.0	14.77	2.00	5	5	Clayey Silt to Silty Clay	ML/CL	stiff	120	2.5	6	0.83		100			0.78	3.91
12.35	40.5	13.50	2.07	5	5	Clayey Silt to Silty Clay	ML/CL	stiff	120	2.5	5	0.83		100			0.70	3.43
12.50	41.0	15.96	3.29	4	4	Silty Clay to Clay	CL	stiff	125	1.8	9	0.82		100			0.85	3.28
12.65	41.5	15.32	3.05	5	5	Clayey Silt to Silty Clay	ML/CL	stiff	120	2.5	6	0.82		100			0.81	4.00
12.80	42.0	14.74	2.01	5	5	Clayey Silt to Silty Clay	ML/CL	stiff	120	2.5	6	0.82		100			0.77	3.66
12.95	42.5	17.48	2.54	5	5	Clayey Silt to Silty Clay	ML/CL	stiff	120	2.5	7	0.81		100			0.93	4.78
13.10	43.0	22.47	2.80	5	5	Clayey Silt to Silty Clay	ML/CL	very stiff	120	2.5	9	0.81		100			1.23	7.13
13.25	43.5	20.78	2.49	5	5	Clayey Silt to Silty Clay	ML/CL	very stiff	120	2.5	8	0.81		100			1.13	6.21
13.40	44.0	21.29	2.62	5	5	Clayey Silt to Silty Clay	ML/CL	very stiff	120	2.5	9	0.80		100			1.16	6.43
13.58	44.5	19.71	2.35	5	5	Clayey Silt to Silty Clay	ML/CL	very stiff	120	2.5	8	0.80		100			1.06	5.53
13.73	45.0	19.60	2.17	5	5	Clayey Silt to Silty Clay	ML/CL	very stiff	120	2.5	8	0.80		100			1.05	5.42
13.88	45.5	18.05	1.84	6	6	Sandy Silt to Clayey Silt	ML	very loose	115	3.5	5	0.79	13.5	100	13	30		
14.03	46.0	17.42	2.29	5	5	Clayey Silt to Silty Clay	ML/CL	stiff	120	2.5	7	0.79		100			0.92	4.26
14.18	46.5	19.49	2.03	6	6	Sandy Silt to Clayey Silt	ML	very loose	115	3.5	6	0.79	14.5	100	15	30		
14.33	47.0	17.99	2.10	5	5	Clayey Silt to Silty Clay	ML/CL	stiff	120	2.5	7	0.78		100			0.88	3.83
14.48	47.5	16.62	1.85	5	5	Clayey Silt to Silty Clay	ML/CL	stiff	120	2.5	7	0.78		100			0.88	3.83
14.63	48.0	16.66	1.91	5	5	Clayey Silt to Silty Clay	ML/CL	stiff	120	2.5	7	0.78		100			0.88	3.83
14.78	48.5	15.96	1.83	5	5	Clayey Silt to Silty Clay	ML/CL	stiff	120	2.5	6	0.77		100			0.83	3.58
14.93	49.0	15.56	1.78	5	5	Clayey Silt to Silty Clay	ML/CL	stiff	120	2.5	6	0.77		100			0.81	3.35
15.10	49.5	14.89	1.48	6	6	Sandy Silt to Clayey Silt	ML	very loose	115	3.5	4	0.77	10.8	100	7	29		

CLIENT: ORMAT

PROJECT: ORMAT Heber 2 Facilities, Heber, CA

LOCATION: See Site and Boring Location Plan

CONE PENETROMETER: HOLGUIN, FAHAN & ASSC. Truck Mounted Electric Cone with 23 ton reaction weight

DATE: 12/20/04

LOG OF CONE SOUNDING DATA CPT-2

DEPTH (FEET)	INTERPRETED SOIL PROFILE From Robertson & Campanella (1989)		
	GROUND EL. +/-		
	Overconsolidated Soil	??	very dense
	Overconsolidated Soil	" "	very dense
	Silty Sand to Sandy Silt	SM/ML	very dense
	Silty Sand to Sandy Silt	" "	very dense
	Silty Sand to Sandy Silt	" "	very dense
	Clayey Silt to Silty Clay	ML/CL	hard
	Clay	CL/CH	stiff
	Silty Clay to Clay	CL	stiff
	Clay	CL/CH	stiff
10	Clay	" "	stiff
	Clay	" "	stiff
	Clay	" "	stiff
	Clay	" "	stiff
	Clay	" "	very stiff
	Clay	" "	very stiff
	Clay	" "	very stiff
	Clay	" "	very stiff
	Clay	" "	very stiff
	Clay	" "	very stiff
20	Clay	" "	very stiff
	Clay	" "	stiff
	Clay	" "	very stiff
	Clay	" "	very stiff
	Clay	" "	very stiff
	Clay	" "	very stiff
	Clay	" "	very stiff
	Clay	" "	very stiff
	Clay	" "	very stiff
30	Clay	" "	very stiff
	Clay	" "	very stiff
	Clay	" "	very stiff
	Clay	" "	very stiff
	Clay	" "	very stiff
	Clay	" "	very stiff
	Clay	" "	very stiff
	Clay	" "	very stiff
	Clay	" "	very stiff
40	Silty Clay to Clay	CL	very stiff
	Silty Clay to Clay	" "	very stiff
	Clayey Silt to Silty Clay	ML/CL	very stiff
	Clayey Silt to Silty Clay	" "	very stiff
	Clayey Silt to Silty Clay	" "	very stiff
	Clayey Silt to Silty Clay	" "	very stiff
	Clayey Silt to Silty Clay	" "	very stiff
	Sandy Silt to Clayey Silt	ML	very loose
	Clayey Silt to Silty Clay	ML/CL	very stiff
	Sandy Silt to Clayey Silt	ML	very loose
50	Sandy Silt to Clayey Silt	" "	very loose

End of Sounding @ 50.0 ft.

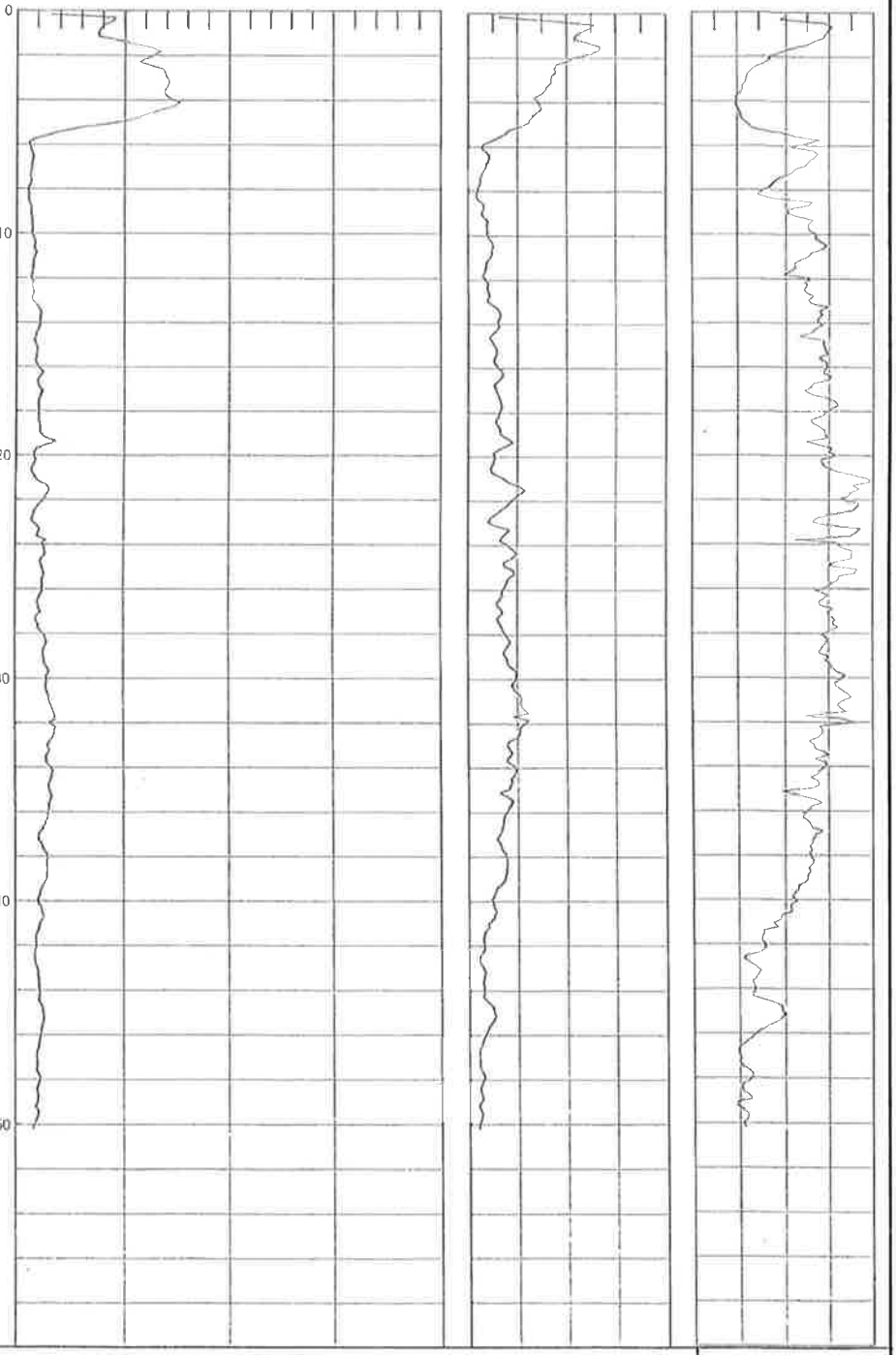

Project No: LE04354

LANDMARK
Geo-Engineers and Geologists
a DBE/MBE/SBE Company

Plate B-2

LANDMARK CONSULTANTS, INC.

CONE PENETROMETER INTERPRETATION (based on Robertson & Campanella, 1989, refer to Key to CPT logs)

Project: ORMAT Heber 2 Facilities, Heber, CA Project No: LE04354 Date: 12/20/04

CONE SOUNDING: CPT-2

Est. GWT (ft): 12.0 Phi Correlation: 0 0:Schm(78),1-R&C(83),2-PHT(74)

Base Depth meters	Base Depth feet	Avg Tip Qc, tsf	Avg Friction Ratio, %	I Soil Type	Soil Classification	USC	Density or Consistency	Est. Density (pcf)	Qc to N	SPT N(60)	Cn or Cq	Norm. Qc1n	Est. % Fines	Rel. Dens. Dr (%)	Nk: 17.0 Phi (deg.)	Su (tsf)	OCR
0.15	0.5	70.28	4.52	5 5	Clayey Silt to Silty Clay	ML/CL	hard	120	2.5	28	2.00		50			4.13	>10
0.30	1.0	77.82	5.97	11 11	Overconsolidated Soil	??	very dense	120	1.0	78	2.00	147.1	55	110	43		
0.45	1.5	91.98	5.31	11 11	Overconsolidated Soil	??	very dense	120	1.0	92	2.00	173.9	50	107	43		
0.60	2.0	129.94	3.78	6 6	Sandy Silt to Clayey Silt	ML	very dense	115	3.5	37	2.00	245.6	35	113	44		
0.75	2.5	119.62	3.11	6 6	Sandy Silt to Clayey Silt	ML	very dense	115	3.5	34	2.00	226.1	30	107	43		
0.93	3.0	137.68	2.51	7 7	Silty Sand to Sandy Silt	SM/ML	very dense	115	4.5	31	2.00	260.3	25	108	43		
1.08	3.5	140.87	2.30	7 7	Silty Sand to Sandy Silt	SM/ML	very dense	115	4.5	31	2.00	266.3	25	106	43		
1.23	4.0	139.35	2.04	7 7	Silty Sand to Sandy Silt	SM/ML	very dense	115	4.5	31	2.00	263.4	20	104	43		
1.38	4.5	144.85	2.01	7 7	Silty Sand to Sandy Silt	SM/ML	very dense	115	4.5	32	2.00	273.8	20	103	42		
1.53	5.0	113.08	2.24	7 7	Silty Sand to Sandy Silt	SM/ML	very dense	115	4.5	25	1.95	208.9	25	94	41		
1.68	5.5	52.70	3.38	5 5	Clayey Silt to Silty Clay	ML/CL	hard	120	2.5	21	1.86		50			3.08	>10
1.83	6.0	13.87	4.91	3 3	Clay	CL/CH	stiff	125	1.3	11	1.77		95			0.80	>10
1.98	6.5	15.08	5.36	3 3	Clay	CL/CH	stiff	125	1.3	12	1.70		95			0.87	>10
2.13	7.0	14.77	4.81	3 3	Clay	CL/CH	stiff	125	1.3	12	1.63		95			0.85	>10
2.28	7.5	13.38	3.90	3 3	Clay	CL/CH	stiff	125	1.3	11	1.57		90			0.76	>10
2.45	8.0	12.25	3.27	4 4	Silty Clay to Clay	CL	stiff	125	1.8	7	1.51		90			0.69	>10
2.60	8.5	11.34	3.86	3 3	Clay	CL/CH	stiff	125	1.3	9	1.46		100			0.64	9.79
2.75	9.0	13.62	4.43	3 3	Clay	CL/CH	stiff	125	1.3	11	1.42		95			0.77	>10
2.90	9.5	14.76	4.97	3 3	Clay	CL/CH	stiff	125	1.3	12	1.38		100			0.84	>10
3.05	10.0	15.04	5.19	3 3	Clay	CL/CH	stiff	125	1.3	12	1.34		100			0.85	>10
3.20	10.5	17.24	5.61	3 3	Clay	CL/CH	stiff	125	1.3	14	1.33		100			0.98	>10
3.35	11.0	17.82	5.31	3 3	Clay	CL/CH	very stiff	125	1.3	14	1.31		100			1.01	>10
3.50	11.5	16.22	4.53	3 3	Clay	CL/CH	stiff	125	1.3	13	1.29		100			0.92	>10
3.65	12.0	14.59	4.45	3 3	Clay	CL/CH	stiff	125	1.3	12	1.28		100			0.82	9.19
3.80	12.5	15.95	4.89	3 3	Clay	CL/CH	stiff	125	1.3	13	1.26		100			0.90	>10
3.95	13.0	16.10	5.07	3 3	Clay	CL/CH	stiff	125	1.3	13	1.25		100			0.91	>10
4.13	13.5	20.52	5.55	3 3	Clay	CL/CH	very stiff	125	1.3	16	1.23		100			1.17	>10
4.28	14.0	22.48	5.55	3 3	Clay	CL/CH	very stiff	125	1.3	18	1.22		100			1.28	>10
4.43	14.5	20.89	5.42	3 3	Clay	CL/CH	very stiff	125	1.3	17	1.21		100			1.19	>10
4.58	15.0	17.79	5.37	3 3	Clay	CL/CH	very stiff	125	1.3	14	1.19		100			1.00	>10
4.73	15.5	19.47	5.86	3 3	Clay	CL/CH	very stiff	125	1.3	16	1.18		100			1.10	>10
4.88	16.0	19.76	5.77	3 3	Clay	CL/CH	very stiff	125	1.3	16	1.17		100			1.12	>10
5.03	16.5	22.50	5.91	3 3	Clay	CL/CH	very stiff	125	1.3	18	1.16		100			1.28	>10
5.18	17.0	21.67	5.09	3 3	Clay	CL/CH	very stiff	125	1.3	17	1.15		100			1.23	>10
5.33	17.5	22.15	5.77	3 3	Clay	CL/CH	very stiff	125	1.3	18	1.13		100			1.25	>10
5.48	18.0	21.43	6.10	3 3	Clay	CL/CH	very stiff	125	1.3	17	1.12		100			1.21	>10
5.65	18.5	21.56	5.34	3 3	Clay	CL/CH	very stiff	125	1.3	17	1.11		100			1.22	>10
5.80	19.0	22.73	5.72	3 3	Clay	CL/CH	very stiff	125	1.3	18	1.10		100			1.29	>10
5.95	19.5	30.63	5.48	3 3	Clay	CL/CH	very stiff	125	1.3	25	1.09		95			1.75	>10
6.10	20.0	17.95	6.14	3 3	Clay	CL/CH	very stiff	125	1.3	14	1.08		100			1.00	7.41
6.25	20.5	17.30	5.70	3 3	Clay	CL/CH	stiff	125	1.3	14	1.07		100			0.96	6.65
6.40	21.0	16.60	6.99	3 3	Clay	CL/CH	stiff	125	1.3	13	1.07		100			0.92	6.10
6.55	21.5	26.75	7.44	3 3	Clay	CL/CH	very stiff	125	1.3	21	1.06		100			1.52	>10
6.70	22.0	28.17	6.81	3 3	Clay	CL/CH	very stiff	125	1.3	23	1.05		100			1.60	>10
6.85	22.5	20.17	7.24	3 3	Clay	CL/CH	very stiff	125	1.3	16	1.04		100			1.13	7.85
7.00	23.0	16.15	5.62	3 3	Clay	CL/CH	stiff	125	1.3	13	1.03		100			0.89	5.21
7.18	23.5	21.37	6.84	3 3	Clay	CL/CH	very stiff	125	1.3	17	1.02		100			1.20	8.27
7.33	24.0	24.23	5.98	3 3	Clay	CL/CH	very stiff	125	1.3	19	1.02		100			1.36	>10
7.48	24.5	27.09	6.88	3 3	Clay	CL/CH	very stiff	125	1.3	22	1.01		100			1.53	>10
7.63	25.0	23.97	6.46	3 3	Clay	CL/CH	very stiff	125	1.3	19	1.00		100			1.35	9.39
7.78	25.5	25.90	6.98	3 3	Clay	CL/CH	very stiff	125	1.3	21	0.99		100			1.46	>10
7.93	26.0	24.80	6.17	3 3	Clay	CL/CH	very stiff	125	1.3	20	0.99		100			1.39	9.59
8.08	26.5	22.94	5.66	3 3	Clay	CL/CH	very stiff	125	1.3	18	0.98		100			1.28	8.00
8.23	27.0	22.28	5.92	3 3	Clay	CL/CH	very stiff	125	1.3	18	0.97		100			1.24	7.27
8.38	27.5	20.15	6.14	3 3	Clay	CL/CH	very stiff	125	1.3	16	0.97		100			1.12	6.10
8.53	28.0	24.13	6.05	3 3	Clay	CL/CH	very stiff	125	1.3	19	0.96		100			1.35	8.14
8.68	28.5	28.28	5.86	3 3	Clay	CL/CH	very stiff	125	1.3	23	0.95		100			1.59	>10
8.85	29.0	26.02	5.73	3 3	Clay	CL/CH	very stiff	125	1.3	21	0.95		100			1.46	8.85
9.00	29.5	28.06	6.01	3 3	Clay	CL/CH	very stiff	125	1.3	22	0.94		100			1.58	>10
9.15	30.0	29.72	6.57	3 3	Clay	CL/CH	very stiff	125	1.3	24	0.93		100			1.68	>10

LANDMARK CONSULTANTS, INC.

CONE PENETROMETER INTERPRETATION (based on Robertson & Campanella, 1989, refer to Key to CPT logs)

Project: ORMAT Heber 2 Facilities, Heber, CA Project No: LE04354 Date: 12/20/04

CONE SOUNDING: CPT-2

Est. GWT (ft): 12.0

Phi Correlation: 0 0-Schm(78),1-R&C(83),2-PHT(74)

Base Depth meters	Base Depth feet	Avg Tip Qc, tsf	Avg Friction Ratio, %	1 Soil Type		Soil Classification	USC	Density or Consistency	Est. Density (pcf)	Qc to N	SPT N(60)	Cn or Cq	Norm. Qc1n	Est. % Fines	Rel. Dens. Dr (%)	Nk: Phi (deg.)	17.0 Su (tsf)	OCR
9.30	30.5	28.55	6.41	3	3	Clay	CL/CH	very stiff	125	1.3	23	0.93		100			1.61	>10
9.45	31.0	31.07	6.84	3	3	Clay	CL/CH	very stiff	125	1.3	25	0.92		100			1.75	>10
9.60	31.5	34.71	6.59	3	3	Clay	CL/CH	very stiff	125	1.3	28	0.92		100			1.97	>10
9.75	32.0	35.27	6.25	3	3	Clay	CL/CH	very stiff	125	1.3	28	0.91		100			2.00	>10
9.90	32.5	37.01	5.65	3	3	Clay	CL/CH	hard	125	1.3	30	0.91		100			2.10	>10
10.05	33.0	32.37	5.31	3	3	Clay	CL/CH	very stiff	125	1.3	26	0.90		100			1.83	>10
10.20	33.5	30.28	5.70	3	3	Clay	CL/CH	very stiff	125	1.3	24	0.89		100			1.70	9.59
10.38	34.0	29.97	5.71	3	3	Clay	CL/CH	very stiff	125	1.3	24	0.89		100			1.68	9.19
10.53	34.5	34.16	5.42	3	3	Clay	CL/CH	very stiff	125	1.3	27	0.88		100			1.93	>10
10.68	35.0	31.53	5.44	3	3	Clay	CL/CH	very stiff	125	1.3	25	0.88		100			1.77	9.79
10.83	35.5	33.18	4.62	4	4	Silty Clay to Clay	CL	very stiff	125	1.8	19	0.87		100			1.87	>10
10.98	36.0	31.41	5.32	3	3	Clay	CL/CH	very stiff	125	1.3	25	0.87		100			1.77	9.19
11.13	36.5	28.95	4.94	3	3	Clay	CL/CH	very stiff	125	1.3	23	0.86		100			1.62	7.70
11.28	37.0	23.74	5.43	3	3	Clay	CL/CH	very stiff	125	1.3	19	0.86		100			1.31	5.42
11.43	37.5	24.03	5.19	3	3	Clay	CL/CH	very stiff	125	1.3	19	0.85		100			1.33	5.42
11.58	38.0	28.73	5.16	3	3	Clay	CL/CH	very stiff	125	1.3	23	0.85		100			1.60	7.13
11.73	38.5	29.89	5.19	3	3	Clay	CL/CH	very stiff	125	1.3	24	0.85		100			1.67	7.56
11.88	39.0	29.55	5.05	3	3	Clay	CL/CH	very stiff	125	1.3	24	0.84		100			1.65	7.27
12.05	39.5	25.32	4.72	3	3	Clay	CL/CH	very stiff	125	1.3	20	0.84		100			1.40	5.53
12.20	40.0	22.19	4.46	3	3	Clay	CL/CH	very stiff	125	1.3	18	0.83		100			1.22	4.37
12.35	40.5	24.43	4.30	4	4	Silty Clay to Clay	CL	very stiff	125	1.8	14	0.83		100			1.35	6.54
12.50	41.0	24.85	3.66	5	5	Clayey Silt to Silty Clay	ML/CL	very stiff	120	2.5	10	0.82		100			1.37	9.39
12.65	41.5	21.29	3.25	5	5	Clayey Silt to Silty Clay	ML/CL	very stiff	120	2.5	9	0.82		100			1.16	6.88
12.80	42.0	19.81	3.04	5	5	Clayey Silt to Silty Clay	ML/CL	very stiff	120	2.5	8	0.82		100			1.07	6.00
12.95	42.5	18.87	2.79	5	5	Clayey Silt to Silty Clay	ML/CL	very stiff	120	2.5	8	0.81		100			1.02	5.42
13.10	43.0	19.60	2.48	5	5	Clayey Silt to Silty Clay	ML/CL	very stiff	120	2.5	8	0.81		100			1.06	5.76
13.25	43.5	21.70	2.84	5	5	Clayey Silt to Silty Clay	ML/CL	very stiff	120	2.5	9	0.81		100			1.18	6.65
13.40	44.0	22.24	2.62	5	5	Clayey Silt to Silty Clay	ML/CL	very stiff	120	2.5	9	0.80		100			1.21	6.88
13.58	44.5	22.52	2.78	5	5	Clayey Silt to Silty Clay	ML/CL	very stiff	120	2.5	9	0.80		100			1.23	6.88
13.73	45.0	25.15	3.77	5	5	Clayey Silt to Silty Clay	ML/CL	very stiff	120	2.5	10	0.80		100			1.38	8.27
13.88	45.5	26.20	3.80	5	5	Clayey Silt to Silty Clay	ML/CL	very stiff	120	2.5	10	0.79		100			1.44	8.85
14.03	46.0	24.44	3.02	5	5	Clayey Silt to Silty Clay	ML/CL	very stiff	120	2.5	10	0.79		100			1.34	7.70
14.18	46.5	22.65	2.43	5	5	Clayey Silt to Silty Clay	ML/CL	very stiff	120	2.5	9	0.79		100			1.23	6.54
14.33	47.0	20.81	1.98	6	6	Sandy Silt to Clayey Silt	ML	very loose	115	3.5	6	0.78	15.4	100	17	30		
14.48	47.5	20.51	2.12	6	6	Sandy Silt to Clayey Silt	ML	very loose	115	3.5	6	0.78	15.1	100	17	30		
14.63	48.0	22.61	2.50	5	5	Clayey Silt to Silty Clay	ML/CL	very stiff	120	2.5	9	0.78		100			1.23	6.32
14.78	48.5	20.83	2.13	6	6	Sandy Silt to Clayey Silt	ML	very loose	115	3.5	6	0.77	15.2	100	17	30		
14.93	49.0	20.93	2.27	5	5	Clayey Silt to Silty Clay	ML/CL	very stiff	120	2.5	8	0.77		100			1.13	5.42
15.10	49.5	20.67	2.11	6	6	Sandy Silt to Clayey Silt	ML	very loose	115	3.5	6	0.77	15.0	100	16	30		
15.25	50.0	19.06	2.25	5	5	Clayey Silt to Silty Clay	ML/CL	very stiff	120	2.5	8	0.76		100			1.01	4.47

CLIENT: ORMAT

PROJECT: ORMAT Heber 2 Facilities, Heber, CA

LOCATION: See Site and Boring Location Plan

CONE PENETROMETER: HOLGUIN, FAHAN & ASSC. Truck Mounted Electric Cone with 23 ton reaction weight

DATE: 12/20/04

LOG OF CONE SOUNDING DATA CPT-3

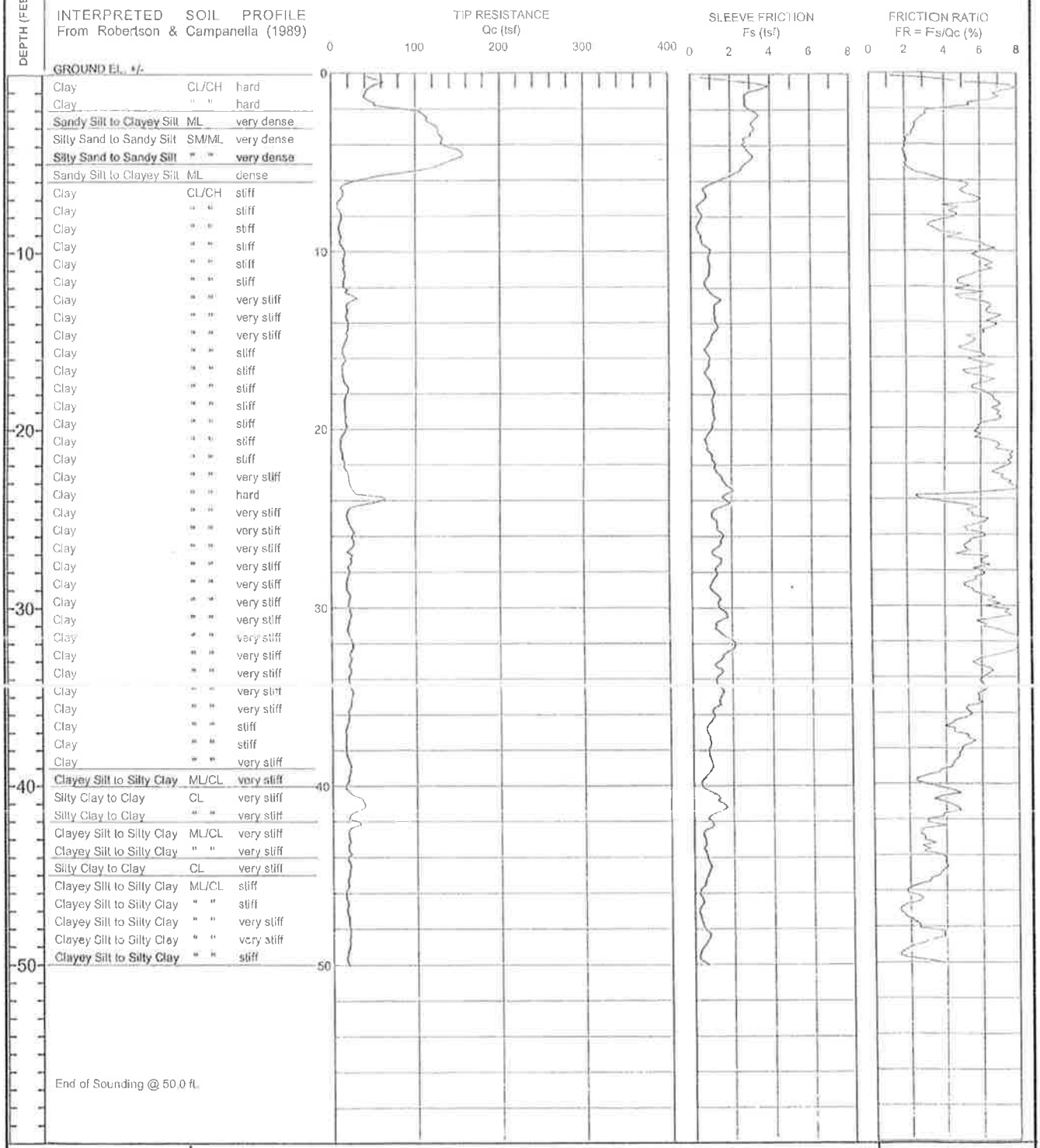

Project No: LE04354	LANDMARK Geo-Engineers and Geologists a DBE/MBE/SBE Company	Plate B-3

LANDMARK CONSULTANTS, INC.

CONE PENETROMETER INTERPRETATION (based on Robertson & Campanella, 1989, refer to Key to CPT logs)

Project: ORMAT Heber 2 Facilities, Heber, CA Project No: LE04354 Date: 12/20/04

CONE SOUNDING: CPT-3

Est. GWT (ft): 12.0

Phi Correlation: 0 0-Schm(78),1-R&C(83),2-PHT(74)

Base Depth meters	Base Depth feet	Avg Tip Qc, tsf	Avg Friction Ratio, %	I Soil Type	Soil Classification	USC	Density or Consistency	Est. Density (pcf)	Qc to N	SPT N(60)	Cn or Cq	Norm. Qc1n	Est. % Fines	Rel. Dens. Dr (%)	Nk: 17.0 Phi (deg.)	Su (tsf)	OCR
0.15	0.5	51.76	3.36	5 5	Clayey Silt to Silty Clay	ML/CL	hard	120	2.5	21	2.00		50			3.04	>10
0.30	1.0	46.42	7.56	3 3	Clay	CL/CH	hard	125	1.3	37	2.00		75			2.73	>10
0.45	1.5	40.35	6.79	3 3	Clay	CL/CH	hard	125	1.3	32	2.00		75			2.37	>10
0.60	2.0	61.72	4.80	4 4	Silty Clay to Clay	CL	hard	125	1.8	35	2.00		55			3.62	>10
0.75	2.5	109.67	3.07	6 6	Sandy Silt to Clayey Silt	ML	very dense	115	3.5	31	2.00	207.3	35	104	43		
0.93	3.0	118.60	2.64	7 7	Silty Sand to Sandy Silt	SM/ML	very dense	115	4.5	26	2.00	224.2	30	103	42		
1.08	3.5	127.70	2.43	7 7	Silty Sand to Sandy Silt	SM/ML	very dense	115	4.5	28	2.00	241.4	25	103	42		
1.23	4.0	131.15	2.02	7 7	Silty Sand to Sandy Silt	SM/ML	very dense	115	4.5	29	2.00	247.9	25	102	42		
1.38	4.5	147.55	1.96	7 7	Silty Sand to Sandy Silt	SM/ML	very dense	115	4.5	33	2.00	278.9	20	103	42		
1.53	5.0	148.38	2.05	7 7	Silty Sand to Sandy Silt	SM/ML	very dense	115	4.5	33	1.94	271.7	20	102	42		
1.68	5.5	111.44	2.28	7 7	Silty Sand to Sandy Silt	SM/ML	very dense	115	4.5	25	1.85	194.4	25	92	41		
1.83	6.0	40.17	4.02	5 5	Clayey Silt to Silty Clay	ML/CL	hard	120	2.5	16	1.76		60			2.34	>10
1.98	6.5	13.36	5.18	3 3	Clay	CL/CH	stiff	125	1.3	11	1.69		100			0.76	>10
2.13	7.0	13.22	5.65	3 3	Clay	CL/CH	stiff	125	1.3	11	1.62		100			0.75	>10
2.28	7.5	7.68	4.85	3 3	Clay	CL/CH	firm	125	1.3	6	1.56		100			0.43	6.10
2.45	8.0	11.50	4.55	3 3	Clay	CL/CH	stiff	125	1.3	9	1.51		100			0.65	>10
2.60	8.5	10.61	3.49	4 4	Silty Clay to Clay	CL	stiff	125	1.8	6	1.46		95			0.60	>10
2.75	9.0	9.81	4.10	3 3	Clay	CL/CH	stiff	125	1.3	8	1.42		100			0.55	6.54
2.90	9.5	10.85	5.09	3 3	Clay	CL/CH	stiff	125	1.3	9	1.38		100			0.61	7.00
3.05	10.0	14.61	6.36	3 3	Clay	CL/CH	stiff	125	1.3	12	1.34		100			0.82	>10
3.20	10.5	14.97	5.91	3 3	Clay	CL/CH	stiff	125	1.3	12	1.32		100			0.85	>10
3.35	11.0	14.49	6.53	3 3	Clay	CL/CH	stiff	125	1.3	12	1.31		100			0.82	>10
3.50	11.5	15.94	5.42	3 3	Clay	CL/CH	stiff	125	1.3	13	1.29		100			0.90	>10
3.65	12.0	14.15	5.01	3 3	Clay	CL/CH	stiff	125	1.3	11	1.27		100			0.79	8.56
3.80	12.5	20.31	5.15	3 3	Clay	CL/CH	very stiff	125	1.3	16	1.26		95			1.16	>10
3.95	13.0	23.81	5.79	3 3	Clay	CL/CH	very stiff	125	1.3	19	1.24		95			1.36	>10
4.13	13.5	18.35	6.42	3 3	Clay	CL/CH	very stiff	125	1.3	15	1.23		100			1.04	>10
4.28	14.0	18.13	6.73	3 3	Clay	CL/CH	very stiff	125	1.3	15	1.22		100			1.02	>10
4.43	14.5	19.70	6.56	3 3	Clay	CL/CH	very stiff	125	1.3	16	1.20		100			1.12	>10
4.58	15.0	18.07	5.71	3 3	Clay	CL/CH	very stiff	125	1.3	14	1.19		100			1.02	>10
4.73	15.5	14.86	5.24	3 3	Clay	CL/CH	stiff	125	1.3	12	1.18		100			0.83	7.00
4.88	16.0	14.60	5.69	3 3	Clay	CL/CH	stiff	125	1.3	12	1.17		100			0.81	6.65
5.03	16.5	13.49	6.25	3 3	Clay	CL/CH	stiff	125	1.3	11	1.16		100			0.75	5.65
5.18	17.0	13.31	5.44	3 3	Clay	CL/CH	stiff	125	1.3	11	1.14		100			0.74	5.31
5.33	17.5	16.20	6.21	3 3	Clay	CL/CH	stiff	125	1.3	13	1.13		100			0.90	7.13
5.48	18.0	19.16	5.98	3 3	Clay	CL/CH	very stiff	125	1.3	15	1.12		100			1.08	9.59
5.65	18.5	15.49	6.80	3 3	Clay	CL/CH	stiff	125	1.3	12	1.11		100			0.86	6.32
5.80	19.0	15.81	6.89	3 3	Clay	CL/CH	stiff	125	1.3	13	1.10		100			0.88	6.32
5.95	19.5	16.32	7.00	3 3	Clay	CL/CH	stiff	125	1.3	13	1.09		100			0.91	6.43
6.10	20.0	17.26	5.95	3 3	Clay	CL/CH	stiff	125	1.3	14	1.08		100			0.96	6.88
6.25	20.5	13.28	5.76	3 3	Clay	CL/CH	stiff	125	1.3	11	1.07		100			0.73	4.37
6.40	21.0	11.14	6.84	3 3	Clay	CL/CH	stiff	125	1.3	9	1.06		100			0.60	3.28
6.55	21.5	12.48	7.40	3 3	Clay	CL/CH	stiff	125	1.3	10	1.06		100			0.68	3.74
6.70	22.0	14.92	7.62	3 3	Clay	CL/CH	stiff	125	1.3	12	1.05		100			0.82	4.89
6.85	22.5	17.77	6.98	3 3	Clay	CL/CH	stiff	125	1.3	14	1.04		100			0.99	6.32
7.00	23.0	21.45	7.34	3 3	Clay	CL/CH	very stiff	125	1.3	17	1.03		100			1.20	8.41
7.18	23.5	24.58	7.84	3 3	Clay	CL/CH	very stiff	125	1.3	20	1.02		100			1.39	>10
7.33	24.0	51.65	3.68	5 5	Clayey Silt to Silty Clay	ML/CL	hard	120	2.5	21	1.02		70			2.98	>10
7.48	24.5	34.37	4.91	3 3	Clay	CL/CH	very stiff	125	1.3	27	1.01		95			1.96	>10
7.63	25.0	18.84	5.44	3 3	Clay	CL/CH	very stiff	125	1.3	15	1.00		100			1.05	6.10
7.78	25.5	21.09	6.11	3 3	Clay	CL/CH	very stiff	125	1.3	17	0.99		100			1.18	7.13
7.93	26.0	26.12	5.49	3 3	Clay	CL/CH	very stiff	125	1.3	21	0.99		100			1.47	>10
8.08	26.5	26.28	5.55	3 3	Clay	CL/CH	very stiff	125	1.3	21	0.98		100			1.48	>10
8.23	27.0	21.92	5.06	3 3	Clay	CL/CH	very stiff	125	1.3	18	0.97		100			1.22	7.13
8.38	27.5	23.63	6.15	3 3	Clay	CL/CH	very stiff	125	1.3	19	0.97		100			1.32	8.00
8.53	28.0	20.49	6.07	3 3	Clay	CL/CH	very stiff	125	1.3	16	0.96		100			1.14	6.10
8.68	28.5	19.11	5.87	3 3	Clay	CL/CH	very stiff	125	1.3	15	0.95		100			1.06	5.31
8.85	29.0	18.15	5.24	3 3	Clay	CL/CH	stiff	125	1.3	15	0.95		100			1.00	4.78
9.00	29.5	21.72	6.18	3 3	Clay	CL/CH	very stiff	125	1.3	17	0.94		100			1.21	6.32
9.15	30.0	20.63	6.55	3 3	Clay	CL/CH	very stiff	125	1.3	17	0.93		100			1.14	5.65

LANDMARK CONSULTANTS, INC.

CONE PENETROMETER INTERPRETATION (based on Robertson & Campanella, 1989, refer to Key to CPT logs)

Project: ORMAT Heber 2 Facilities, Heber, CA Project No: LE04354 Date: 12/20/04

CONE SOUNDING: CPT-3

Est. GWT (ft): 12.0 Phi Correlation: 0 0-Schm(78),1-R&C(83),2-PHT(74)

Base Depth meters	Base Depth feet	Avg Tip Qc, tsf	Avg Friction Ratio, %	1 Soil Type		Soil Classification	USC	Density or Consistency	Est. Density (pcf)	Qc to N	SPT N(60)	Cn or Cq	Norm. Qc1n	Est. % Fines	Rel. Dens. Dr (%)	Nk; Phi (deg.)	17.0 Su (tsf)	OCR
9.30	30.5	22.90	7.51	3	3	Clay	CL/CH	very stiff	125	1.3	18	0.93		100			1.27	6.54
9.45	31.0	20.57	6.23	3	3	Clay	CL/CH	very stiff	125	1.3	16	0.92		100			1.14	5.42
9.60	31.5	19.55	6.90	3	3	Clay	CL/CH	very stiff	125	1.3	16	0.92		100			1.08	4.89
9.75	32.0	23.76	8.37	3	3	Clay	CL/CH	very stiff	125	1.3	19	0.91		100			1.32	6.54
9.90	32.5	24.30	8.05	3	3	Clay	CL/CH	very stiff	125	1.3	19	0.90		100			1.35	6.65
10.05	33.0	22.78	6.54	3	3	Clay	CL/CH	very stiff	125	1.3	18	0.90		100			1.26	5.88
10.20	33.5	21.56	5.91	3	3	Clay	CL/CH	very stiff	125	1.3	17	0.89		100			1.19	5.31
10.38	34.0	20.82	6.40	3	3	Clay	CL/CH	very stiff	125	1.3	17	0.89		100			1.15	4.89
10.53	34.5	21.17	6.04	3	3	Clay	CL/CH	very stiff	125	1.3	17	0.88		100			1.17	4.89
10.68	35.0	24.71	6.05	3	3	Clay	CL/CH	very stiff	125	1.3	20	0.88		100			1.37	6.21
10.83	35.5	23.14	5.91	3	3	Clay	CL/CH	very stiff	125	1.3	19	0.87		100			1.28	5.53
10.98	36.0	19.96	5.21	3	3	Clay	CL/CH	very stiff	125	1.3	16	0.87		100			1.09	4.28
11.13	36.5	19.03	4.88	3	3	Clay	CL/CH	very stiff	125	1.3	15	0.86		100			1.04	3.91
11.28	37.0	16.19	4.33	3	3	Clay	CL/CH	stiff	125	1.3	13	0.86		100			0.87	3.07
11.43	37.5	16.02	5.36	3	3	Clay	CL/CH	stiff	125	1.3	13	0.85		100			0.86	3.00
11.58	38.0	16.15	5.06	3	3	Clay	CL/CH	stiff	125	1.3	13	0.85		100			0.86	3.00
11.73	38.5	17.81	4.75	3	3	Clay	CL/CH	stiff	125	1.3	14	0.85		100			0.96	3.35
11.88	39.0	21.66	4.41	4	4	Silty Clay to Clay	CL	very stiff	125	1.8	12	0.84		100			1.19	5.65
12.05	39.5	20.18	3.42	5	5	Clayey Silt to Silty Clay	ML/CL	very stiff	120	2.5	8	0.84		100			1.10	6.65
12.20	40.0	17.00	2.62	5	5	Clayey Silt to Silty Clay	ML/CL	stiff	120	2.5	7	0.83		100			0.91	5.00
12.35	40.5	20.64	4.32	4	4	Silty Clay to Clay	CL	very stiff	125	1.8	12	0.83		100			1.12	5.00
12.50	41.0	36.57	3.70	5	5	Clayey Silt to Silty Clay	ML/CL	hard	120	2.5	15	0.82		95			2.06	>10
12.65	41.5	31.64	4.64	4	4	Silty Clay to Clay	CL	very stiff	125	1.8	18	0.82		100			1.77	>10
12.80	42.0	23.58	3.56	5	5	Clayey Silt to Silty Clay	ML/CL	very stiff	120	2.5	9	0.82		100			1.29	8.14
12.95	42.5	24.97	3.28	5	5	Clayey Silt to Silty Clay	ML/CL	very stiff	120	2.5	10	0.81		100			1.37	8.85
13.10	43.0	19.07	2.71	5	5	Clayey Silt to Silty Clay	ML/CL	very stiff	120	2.5	8	0.81		100			1.03	5.42
13.25	43.5	18.86	2.98	5	5	Clayey Silt to Silty Clay	ML/CL	very stiff	120	2.5	8	0.81		100			1.01	5.31
13.40	44.0	19.54	3.20	5	5	Clayey Silt to Silty Clay	ML/CL	very stiff	120	2.5	8	0.80		100			1.05	5.53
13.58	44.5	19.29	3.97	4	4	Silty Clay to Clay	CL	very stiff	125	1.8	11	0.80		100			1.04	3.91
13.73	45.0	19.79	3.86	4	4	Silty Clay to Clay	CL	very stiff	125	1.8	11	0.80		100			1.07	4.00
13.88	45.5	17.66	3.31	5	5	Clayey Silt to Silty Clay	ML/CL	stiff	120	2.5	7	0.79		100			0.94	4.47
14.03	46.0	16.42	2.18	5	5	Clayey Silt to Silty Clay	ML/CL	stiff	120	2.5	7	0.79		100			0.87	3.91
14.18	46.5	15.61	2.35	5	5	Clayey Silt to Silty Clay	ML/CL	stiff	120	2.5	6	0.78		100			0.82	3.58
14.33	47.0	10.00	1.00	6	6	Sandy Silt to Clayey Silt	ML	very loose	115	3.5	5	0.78	12.3	100	11	29		
14.48	47.5	18.25	1.80	6	6	Sandy Silt to Clayey Silt	ML	very loose	115	3.5	5	0.78	13.4	100	13	30		
14.63	48.0	19.39	2.43	5	5	Clayey Silt to Silty Clay	ML/CL	very stiff	120	2.5	8	0.78		100			1.04	4.89
14.78	48.5	19.39	3.87	4	4	Silty Clay to Clay	CL	very stiff	125	1.8	11	0.77		100			1.04	3.58
14.93	49.0	19.13	2.69	5	5	Clayey Silt to Silty Clay	ML/CL	very stiff	120	2.5	8	0.77		100			1.02	4.57
15.10	49.5	16.46	1.59	6	6	Sandy Silt to Clayey Silt	ML	very loose	115	3.5	5	0.77	11.9	100	10	29		
15.25	50.0	16.91	2.83	5	5	Clayey Silt to Silty Clay	ML/CL	stiff	120	2.5	7	0.76		100			0.89	3.74

APPENDIX C

LANDMARK CONSULTANTS, INC.

CLIENT: ORMAT
PROJECT: ORMAT Heber 2 Facilities, Heber, CA
JOB NO: LE04354
DATE: 12/28/04

ATTERBERG LIMITS (ASTM D4318)

Sample Location	Sample Depth (ft)	Liquid Limit (LL)	Plastic Limit (PL)	Plasticity Index (PI)	USCS Classif-ation
CPT-1	0-1.5	35	18	17	CL
CPT-2	0-2	35	17	18	CL
CPT-3	0-1.5	36	15	21	CL

PLASTICITY CHART

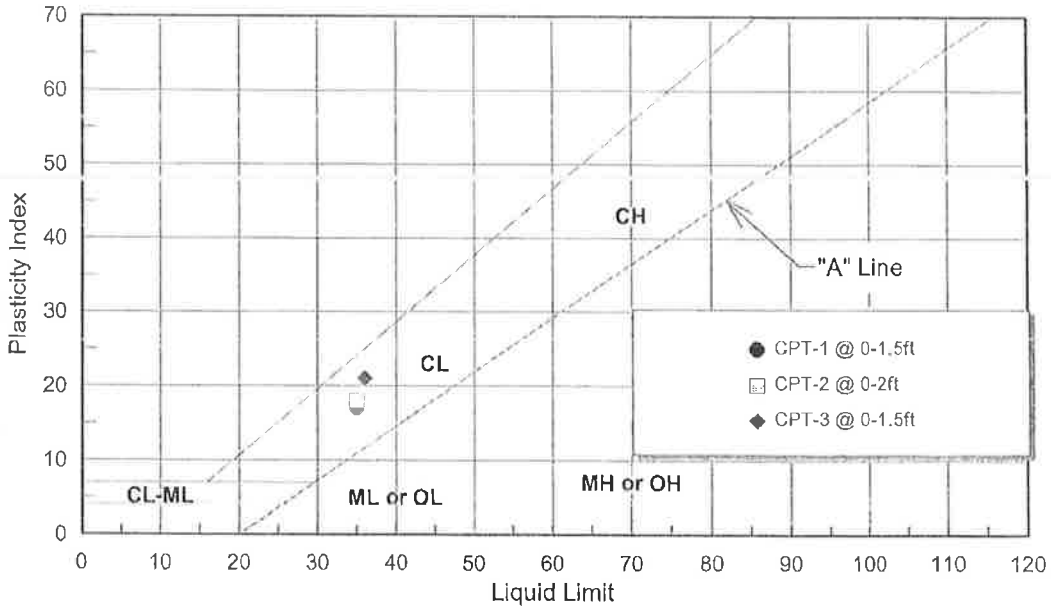

LANDMARK
Geo-Engineers and Geologists
a DBE/MBE/SBE Company

Project No: LE04354

Atterberg Limits Test Results

Plate C-1

LANDMARK CONSULTANTS, INC.

CLIENT: ORMAT
PROJECT: ORMAT Heber 2 Facilities, Heber, CA
JOB NO: LE04354
DATE: 12/28/04

CHEMICAL ANALYSES

Boring:	CPT-1	CPT-1	CPT-2	CPT-2	CalTrans
Sample Depth, ft:	0-1.5	1.5-3	0-2	2-3	Method
pH:	7.9	7.9	7.8	7.9	643
Electrical Conductivity (mmhos):	2.5	1.7	1.8	0.9	424
Resistivity (ohm-cm):	260	1000	300	1000	643
Chloride (Cl), ppm:	3,040	230	1,490	220	422
Sulfate (SO4), ppm:	2,812	3,006	1,500	1,106	417

General Guidelines for Soil Corrosivity

Material Affected	Chemical Agent	Amount in Soil (ppm)	Degree of Corrosivity
Concrete	Soluble Sulfates	0 -1000	Low
		1000 - 2000	Moderate
		2000 - 20,000	Severe
		> 20,000	Very Severe
Normal Grade Steel	Soluble Chlorides	0 - 200	Low
		200 - 700	Moderate
		700 - 1500	Severe
		> 1500	Very Severe
Normal Grade Steel	Resistivity	1-1000	Very Severe
		1000-2000	Severe
		2000-10,000	Moderate
		10,000+	Low

LANDMARK Geo-Engineers and Geologists
a DBE/MBE/SBE Company

Project No: LE04354

Selected Chemical Analyses Results

Plate C-2

LANDMARK CONSULTANTS, INC.

CLIENT: ORMAT
PROJECT: ORMAT Heber 2 Facilities, Heber, CA
JOB NO: LE04354
DATE: 12/28/04

CHEMICAL ANALYSES

Boring:	CPT-3	CPT-3	CalTrans
Sample Depth, ft:	0-1.5	1.5-3	Method
pH:	7.9	7.8	643
Electrical Conductivity (mmhos):	1.5	1.3	424
Resistivity (ohm-cm):	450	1000	643
Chloride (Cl), ppm:	570	210	422
Sulfate (SO4), ppm:	1,785	1,052	417

General Guidelines for Soil Corrosivity

Material Affected	Chemical Agent	Amount in Soil (ppm)	Degree of Corrosivity
Concrete	Soluble Sulfates	0 -1000	Low
		1000 - 2000	Moderate
		2000 - 20,000	Severe
		> 20,000	Very Severe
Normal Grade Steel	Soluble Chlorides	0 - 200	Low
		200 - 700	Moderate
		700 - 1500	Severe
		> 1500	Very Severe
Normal Grade Steel	Resistivity	1-1000	Very Severe
		1000-2000	Severe
		2000-10,000	Moderate
		10,000+	Low

LANDMARK
Geo-Engineers and Geologists
a DBE/MBE/SBE Company

Project No: LE04354

Selected Chemical Analyses Results

Plate C-3

APPENDIX D

REFERENCES

Arango I., 1996, Magnitude Scaling Factors for Soil Liquefaction Evaluations: ASCE Geotechnical Journal, Vol. 122, No. 11.

Bartlett, Steven F. and Youd, T. Leslie, 1995, Empirical Prediction of Liquefaction-Induced Lateral Spread: ASCE Geotechnical Journal, Vol. 121, No. 4.

Blake, T. F., 2000, FRISKSP - A computer program for the probabilistic estimation of seismic hazard using faults as earthquake sources.

Boore, D. M., Joyner, W. B., and Fumal, T. E., 1997, Empirical Near-Source Attenuation Relationships for Horizontal and Vertical Components of Peak Ground Acceleration, Peak Ground Velocity, and Pseudo-Absolute Acceleration Response Spectra: Seismological Research Letters, Vol. 68, No. 1, p. 154-179.

Building Seismic Safety Council (BSSC), 1991, NEHRP recommended provisions for the development of seismic regulations of new buildings, Parts 1, 2 and Maps: FEMA 222, January 1992

California Division of Mines and Geology (CDMG), 1996, California Fault Parameters: available at http://www.consrv.ca.gov/dmg/shezp/fltindex.html.

California Division of Mines and Geology (CDMG), 1962, Geologic Map of California – San Diego-El Centro Sheet: California Division of Mines and Geology, Scale 1:250,000.

Ellsworth, W. L., 1990, Earthquake History, 1769-1989 in: The San Andreas Fault System, California: U.S. Geological Survey Professional Paper 1515, 283 p.

International Conference of Building Officials (ICBO), 1997, Uniform Building Code, 1997 Edition.

Ishihara, K. (1985), Stability of natural deposits during earthquakes, Proc. 11th Int. Conf. On Soil Mech. And Found. Engrg., Vol. 1, A. A. Balkema, Rotterdam, The Netherlands, 321-376.

Jennings, C. W., 1994, Fault activity map of California and Adjacent Areas: California Division of Mines and Geology, DMG Geologic Map No. 6.

Jones, L. and Hauksson, E., 1994, Review of potential earthquake sources in Southern California: Applied Technology Council, Proceedings of ATC 35-1.

Maley, R. P. and Etheredge, E. C., 1981, Strong motion data from the Westmorland, California earthquake of April 26, 1981: U.S. Geological Survey Open File Report 81-1149, 18 p.

Morton, P. K., 1977, Geology and mineral resources of Imperial County, California: California Division of Mines and Geology, County Report No. 7, 104 p.

Mualchin, L. and Jones, A. L., 1992, Peak acceleration from maximum credible earthquakes in California (Rock and Stiff Soil Sites): California Division of Mines and Geology, DMG Open File Report 92-01.

Naeim, F. and Anderson, J. C., 1993, Classification and evaluation of earthquake records for design: Earthquake Engineering Research Institute, NEHRP Report.

National Research Council, Committee of Earthquake Engineering, 1985, Liquefaction of Soils during Earthquakes: National Academy Press, Washington, D.C.

Porcella, R., Etheredge, E., Maley, R., and Switzer, J., 1987, Strong motion data from the Superstition Hills earthquake of November 24, 1987: U.S. Geological Survey Open File Report 87-672, 56 p.

Robertson, P. K. and Wride, C. E., 1996, Cyclic Liquefaction and its Evaluation based on the SPT and CPT, Proceeding of the NCEER Workshop on Evaluation of Liquefaction Resistance of Soils, NCEER Technical Report 97-0022, p. 41-88.

Seed, Harry B., Idriss, I. M., and Arango I., 1983, Evaluation of liquefaction potential using field performance data: ASCE Geotechnical Journal, Vol. 109, No. 3.

Seed, Harry B., et al, 1985, Influence of SPT Procedures in Soil Liquefaction Resistance Evaluations: ASCE Geotechnical Journal, Vol. 113, No. 8.

Sharp, R. V., 1982, Tectonic setting of the Imperial Valley region: U.S. Geological Survey Professional Paper 1254, p. 5-14.

Sylvester, A. G., 1979, Earthquake damage in Imperial Valley, California May 18, 1940, as reported by T. A. Clark: Bulletin of the Seismological Society of America, v. 69, no. 2, p. 547-568.

Tokimatsu, K. and Seed H. B., 1987, Evaluation of settlements in sands due to earthquake shaking: ASCE Geotechnical Journal, v. 113, no. 8.

U.S. Geological Survey (USGS), 1982, The Imperial Valley California Earthquake of October 15, 1979: Professional Paper 1254, 451 p.

U.S. Geological Survey (USGS), 1990, The San Andreas Fault System, California, Professional Paper 1515.

U.S. Geological Survey (USGS), 1996, National Seismic Hazard Maps: available at http://gldage.cr.usgs.gov

Working Group on California Earthquake Probabilities (WGCEP), 1992, Future seismic hazards in southern California, Phase I Report: California Division of Mines and Geology.

Working Group on California Earthquake Probabilities (WGCEP), 1995, Seismic hazards in southern California, Probable Earthquakes, 1994-2014, Phase II Report: Southern California Earthquake Center.

Youd, T. Leslie and Garris, C. T., 1995, Liquefaction induced ground surface disruption: ASCE Geotechnical Journal, Vol. 121, No. 11.

Youd, T. L. et. al., 2001, Liquefaction Resistance of Soils: Summary Report from the 1996 NCEER and 1998 NCEER/NSF Workshops on Evaluation of Liquefaction Resistance of Soils: Journal of Geotechnical and Geoenvironmental Engineering, Vol. 127, No. 10, p. 817-833.

Zimmerman, R. P., 1981, Soil survey of Imperial County, California, Imperial Valley Area: U.S. Dept. of Agriculture Soil Conservation Service, 112 p.

APPENDIX E

LANDMARK
Geo-Engineers and Geologists

780 N. 4th Street
El Centro, CA 92243
(760) 370-3000
(760) 337-8900 fax

77-948 Wildcat Drive
Palm Desert, CA 92211
(760) 360-0665
(760) 360-0521 fax

May 9, 2007

Mr. Yuri Gal
ORMAT Nevada, Inc.
947 Dogwood Road
Heber, CA 92249

Geotechnical Investigation
Proposed Heber South Geothermal Plant
Dogwood Road
Heber, California
LCI Project No. L07178

Dear Mr. Gal:

Landmark Consultants, Inc. is pleased to present this geotechnical report update for design and construction of the Heber South Geothermal Plant facility located on Dogwood Road south of Heber, California. The project site is located in the southwest corner of the existing Heber geothermal plant site. The proposed plant will consist of one OEC unit, one cooling tower, and various ancillary structures including pumps, filters, and shelter.

This update report presents selected elements of our findings and recommendations only. For the proper application of our findings and recommendations, reading of the full geotechnical report (LCI Report No. LE04354, dated January 5, 2005) is required, and are best evaluated with the active participation of the engineer of record who developed them.

The scope of work consisted of conducting two (2) electronic CPT soundings within the OEC and cooling tower footprints and review of the existing geotechnical report for the Heber 2 plant expansion (Landmark, 2005) to determine suitability of the prior geotechnical report for use with the design and construction of the proposed Heber South plant.

Small structures are planned for electrical control panels, consisting of masonry or panelized concrete construction. Expected footing loads are estimated at 1 to 2 kips per lineal foot for the small structures. Expected plant components, cooling tower and turbine/generator columns loads range from 5 to 400 kips. If structural loads exceed those stated above, we should be notified so we may evaluate their impact on foundation settlement and bearing capacity. Site development will include foundation support pad preparation and underground utility installation.

Subsurface Exploration

Subsurface exploration was performed on May 2, 2007 using Holguin, Fahan, & Associates, Inc. of Cypress, California to advance three (3) electric cone penetrometer (CPT) soundings to an approximate depth of 50 feet below existing ground surface. The soundings were made at the locations shown on the Site and Exploration Plan (Plate A-2). The approximate sounding locations were established in the field and plotted on the site map by sighting to discernable site features.

Interpretive logs of the CPT soundings were produced and presented in final form after review of field and laboratory data and are presented on Plates B-1 and B-2 in Appendix B. A key to the interpretation of CPT soundings is presented on Plate B-3. The stratification lines shown on the subsurface logs represent the approximate boundaries between the various strata. However, the transition from one stratum to another may be gradual over some range of depth.

Subsurface soils encountered during the field exploration conducted on May 2, 2007 consist of medium dense to dense silty sands extend to a depth of 4 to 5 feet below ground surface. Stiff to very stiff clays extend from 4 feet to a depth of 50 feet, the maximum depth of exploration. The subsurface logs (Plates B-1 and B-2) depict the stratigraphic relationships of the various soil types.

Groundwater Elevation

Groundwater was not noted in the CPT soundings at the time of exploration, but is typically encountered at approximately 10 to 15 feet below ground surface in the vicinity of the site. There is uncertainty in the accuracy of short-term water level measurements, particularly in fine-grained soil. Groundwater levels may fluctuate with precipitation, irrigation of adjacent properties, drainage, and site grading. The referenced groundwater level should not be interpreted to represent an accurate or permanent condition.

Seismic Parameters

The project site is located in the seismically active Imperial Valley in Southern California, and is considered likely to be subjected to moderate to strong ground shaking from earthquakes in the region. The project site lies approximately 11.3 km southwest of the Imperial Fault. Strong ground shaking can be expected for magnitudes of 6.0 to 7.2 events on the Imperial Fault with a recurrence interval for 6.0 magnitude events at about 29 years. We have used the computer program FRISKSP (Blake, 2000) to provide a probabilistic estimate of the site Peak Ground Acceleration (PGA) using the attenuation relationship of Boore, Joyner, and Fumal (1997) NEHRP D (250). The PGA estimate for the project site having a 10% probability of being exceeded in 50 years (return period of 475 years) is **0.60g**.

CBC Seismic Coefficients: The California Building Code (CBC) seismic response coefficients are calculated from the near-source factors for Seismic Zone 4. The near-source factors are based on the distance from the fault and the seismic source type. The following table lists seismic and site coefficients (near source factors) determined by Chapter 16 of the 2001 CBC. ***This site lies within 11.3 km of a Type A fault overlying S_D (stiff) soil.***

CBC Seismic Coefficients for Chapter 16 Seismic Provisions

CBC Code Edition	Soil Profile Type	Seismic Source Type	Distance to Critical Source	Near Source Factors		Seismic Coefficients	
				Na	Nv	Ca	Cv
2001	S_D (stiff soil)	A	< 11.3 km	1.00	1.15	0.44	0.74
Ref. Table	16-J	16-U	---	16-S	16-T	16-Q	16-R

Liquefaction Potential

Evaluation of liquefaction potential at the site indicates that it is unlikely that the subsurface soil will liquefy under seismically induced groundshaking due to the predominance of cohesive clay (non-liquefiable) subsurface soil below the groundwater depth. No mitigation is required for liquefaction effects at this site.

Lateral Earth Pressures

Earth retaining structures, such as retaining walls, should be designed to resist the soil pressure imposed by the retained soil mass. Walls with granular drained backfill may be designed for an assumed static earth pressure equivalent to that exerted by a fluid weighing 55 pcf for unrestrained (active) conditions (able to rotate 0.1% of wall height), and 70 pcf for restrained (at-rest) conditions.

Surcharge loads should be considered if loads are applied within a zone between the face of the wall and a plane projected behind the wall 45 degrees upward from the base of the wall. The increase in lateral earth pressure acting uniformly against the back of the wall should be taken as 50% of the surcharge load within this zone. Areas of the retaining wall subjected to traffic loads should be designed for a uniform surcharge load equivalent to two feet of native soil.

Walls should be provided with backdrains to reduce the potential for the buildup of hydrostatic pressure. The drainage system should consist of a composite HDPE drainage panel or a 2-foot wide zone of free draining crushed rock placed adjacent to the wall and extending 2/3 the height of the wall. The gravel should be completely enclosed in an approved filter fabric to separate the gravel and backfill soil. A perforated pipe should be placed perforations down at the base of the permeable material at least six inches below finished floor elevations. The pipe should be sloped to drain to an appropriate outlet that is protected against erosion. Walls should be properly waterproofed. The project geotechnical engineer should approve any alternative drain system.

Structure Support Pads/Foundation

The subsurface exploration conducted in May 2007 identified engineering properties of the soil nearly identical to the Landmark, 2005 geotechnical report. The findings and recommendations within the 2005 geotechnical report may be used for the Heber South project. A copy of the Landmark 2005 geotechnical report is provide in Appendix C.

Closure

We appreciate the opportunity to provide our findings and professional opinions regarding geotechnical conditions at the site. If you have any questions or comments regarding our findings, please call our office at (760) 370-3000.

Respectfully Submitted,
Landmark Consultants, Inc.

PROFESSIONAL GEOLOGIST
STEVEN K. WILLIAMS
CERTIFIED ENGINEERING GEOLOGIST
CEG 2261
STATE OF CALIFORNIA

Steven K. Williams, CEG
Senior Engineering Geologist

Julian R. Avalos, EIT
Staff Engineer

REGISTERED PROFESSIONAL ENGINEER
JEFFREY O. LYON
No. 31921
EXPIRES 12-31-08
CIVIL
STATE OF CALIFORNIA

Jeffrey O. Lyon, PE
President

APPENDIX A

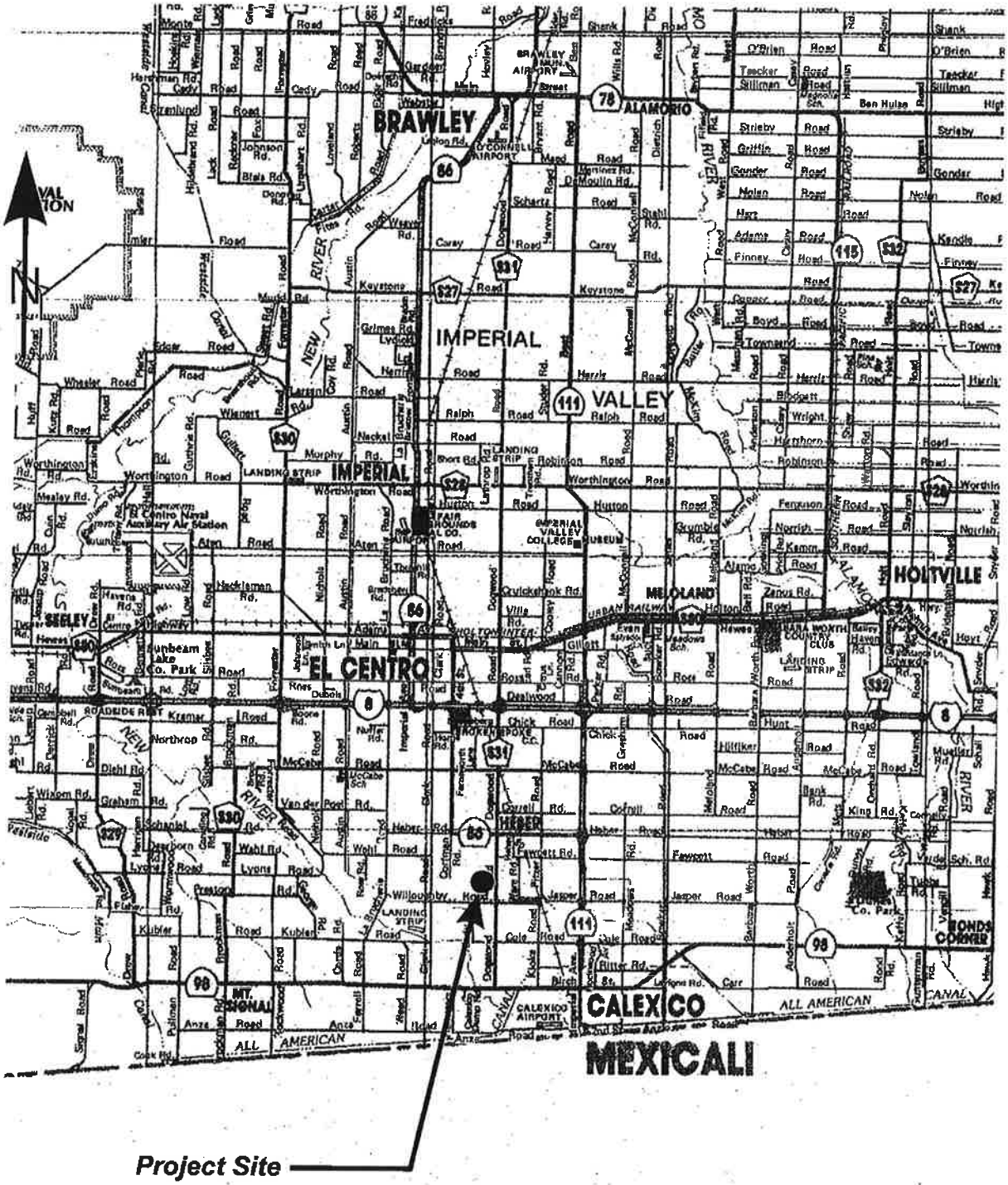

LANDMARK
Geo-Engineers and Geologists

Project No.: LE07178

Vicinity Map

Plate
A-1

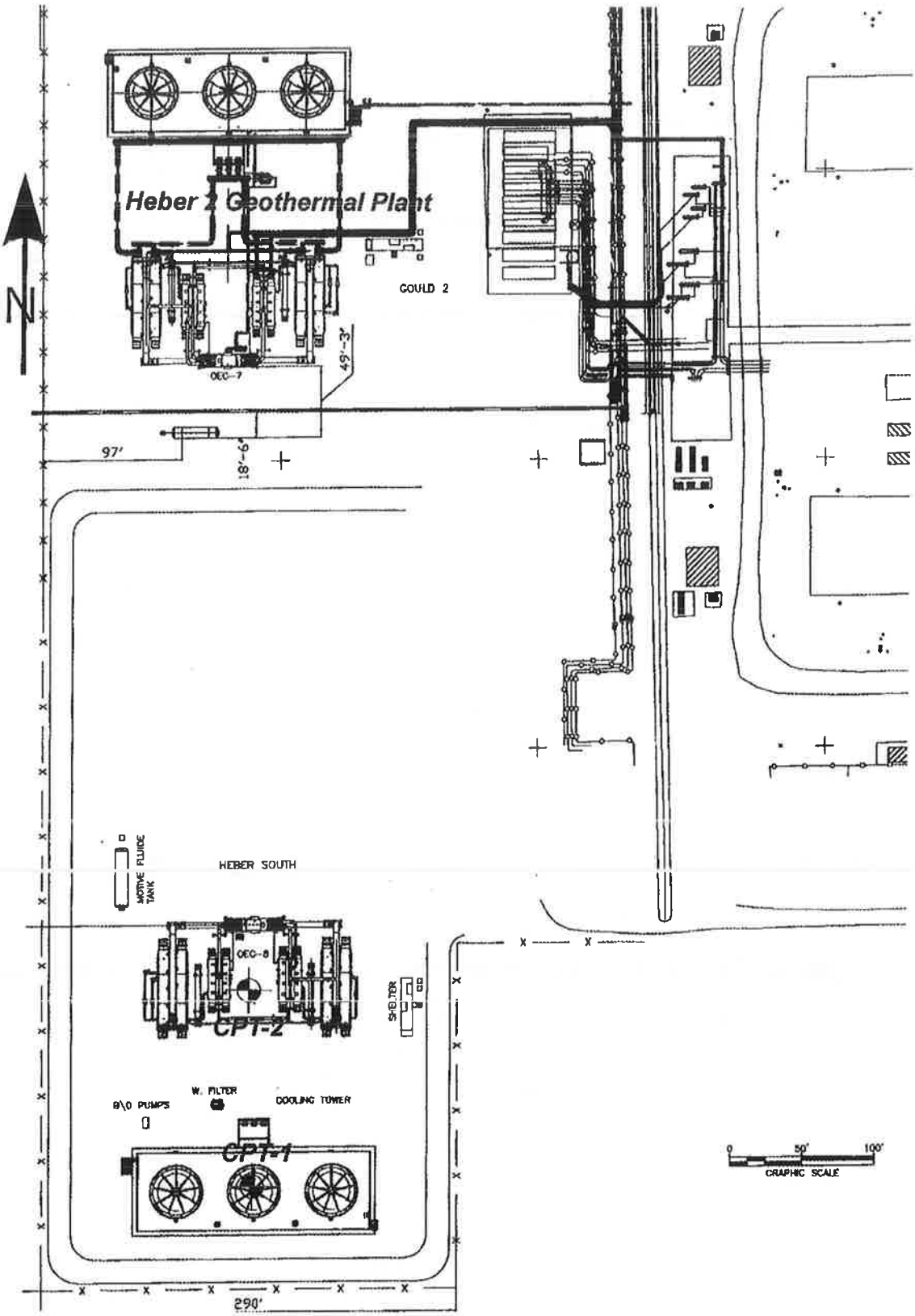

LANDMARK
Geo-Engineers and Geologists

Project No.: LE07178

Site and Exploration Map

Plate
A-2

APPENDIX B

CLIENT: Ormat Nevada

CONE PENETROMETER: HOLGUIN, FAHAN & ASSC. Truck Mounted Electric Cone with 23 ton reaction weight

PROJECT: Heber South Geothermal Plant -- Heber, CA

LOCATION: See Site and Boring Location Plan

DATE: 05/02/07

LOG OF CONE SOUNDING DATA CPT-1

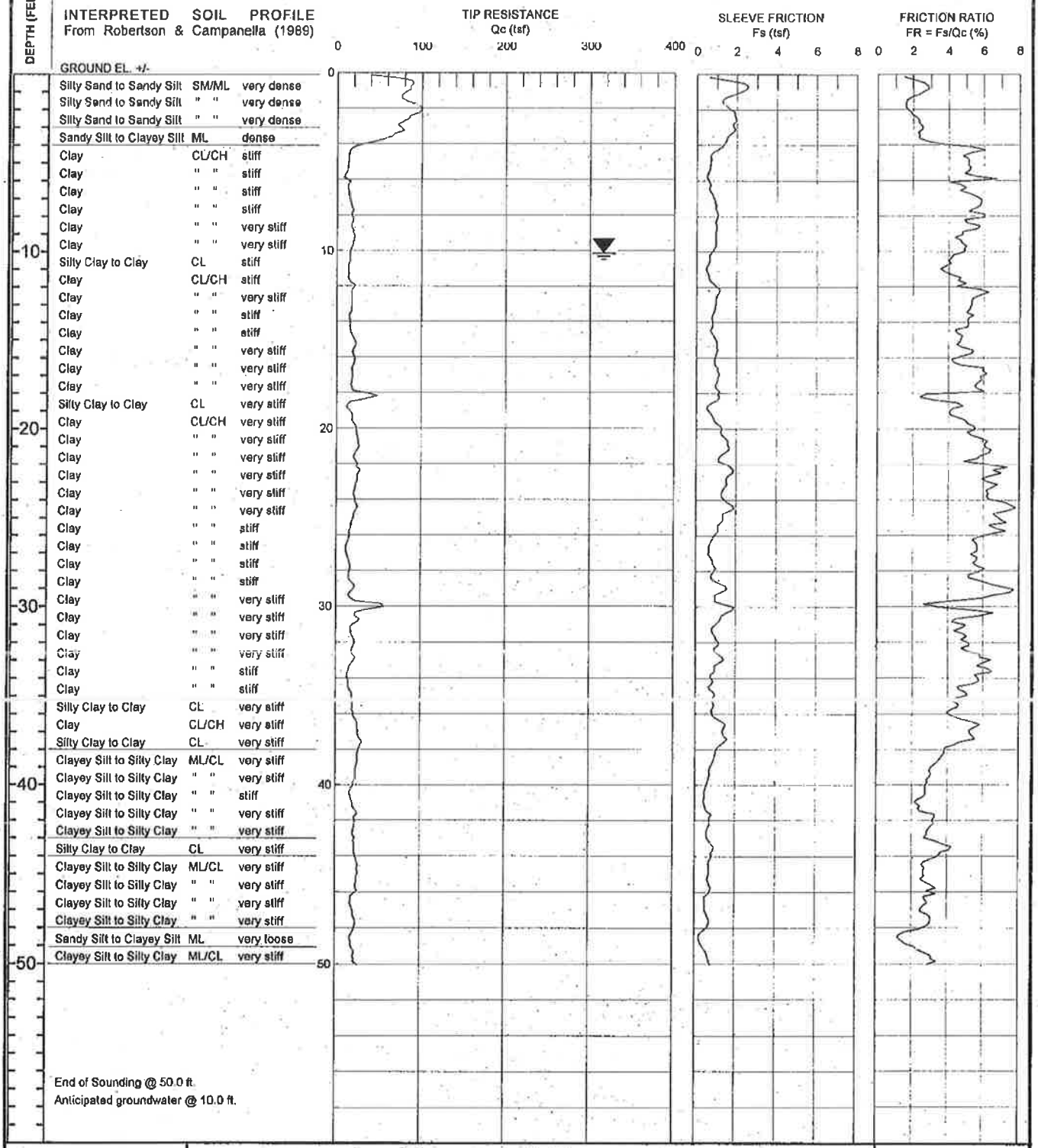

Project No: LE07178	LANDMARK Geo-Engineers and Geologists	Plate B-1

LANDMARK CONSULTANTS, INC.

CONE PENETROMETER INTERPRETATION (based on Robertson & Campanella, 1989, refer to Key to CPT logs)

Project: Heber South Plant -- Heber, CA Project No: LE07178 Date: 05/02/07

CONE SOUNDING: CPT-1

Est. GWT (ft): 10.0

Phi Correlation: 0 (0-Schm(78),1-R&C(83),2-PHT(74))

Base Depth meters	Base Depth feet	Avg Tip Qc, tsf	Avg Friction Ratio, %	I Soil Type	Soil Classification	USC	Density or Consistency	Est. Density (pcf)	Qc to N	SPT N(60)	Cn or Cq	Norm. Qc1n	Est. % Fines	Rel. Dens. Dr (%)	Nk: Phi (deg.)	17.0 Su (tsf)	OCR
0.15	0.5	66.25	2.04	7	Silty Sand to Sandy Silt	SM/ML	very dense	115	4.5	15	2.00	125.2	35	122	45		
0.30	1.0	88.18	2.75	6	Sandy Silt to Clayey Silt	ML	very dense	115	3.5	25	2.00	166.7	35	114	44		
0.45	1.5	77.73	1.95	7	Silty Sand to Sandy Silt	SM/ML	very dense	115	4.5	17	2.00	146.9	30	103	42		
0.60	2.0	92.53	1.60	7	Silty Sand to Sandy Silt	SM/ML	very dense	115	4.5	21	2.00	174.9	25	103	42		
0.75	2.5	93.95	2.02	7	Silty Sand to Sandy Silt	SM/ML	very dense	115	4.5	21	2.00	177.6	25	100	42		
0.93	3.0	77.68	2.40	7	Silty Sand to Sandy Silt	SM/ML	very dense	115	4.5	17	2.00	146.8	35	91	41		
1.08	3.5	74.47	2.39	6	Sandy Silt to Clayey Silt	ML	dense	115	3.5	21	2.00	140.8	35	88	40		
1.23	4.0	52.73	2.83	6	Sandy Silt to Clayey Silt	ML	dense	115	3.5	15	2.00	99.7	45	75	39		
1.38	4.5	18.49	5.55	3	Clay	CL/CH	very stiff	125	1.3	15	2.00		90			1.07	>10
1.53	5.0	13.75	5.02	3	Clay	CL/CH	stiff	125	1.3	11	1.95		100			0.79	>10
1.68	5.5	12.39	5.11	3	Clay	CL/CH	stiff	125	1.3	10	1.85		100			0.71	>10
1.83	6.0	10.98	5.45	3	Clay	CL/CH	stiff	125	1.3	9	1.77		100			0.63	>10
1.98	6.5	13.51	4.77	3	Clay	CL/CH	stiff	125	1.3	11	1.69		95			0.77	>10
2.13	7.0	14.72	5.56	3	Clay	CL/CH	stiff	125	1.3	12	1.62		100			0.84	>10
2.28	7.5	16.58	5.71	3	Clay	CL/CH	stiff	125	1.3	13	1.56		95			0.95	>10
2.45	8.0	17.99	5.72	3	Clay	CL/CH	very stiff	125	1.3	14	1.51		95			1.03	>10
2.60	8.5	18.67	5.21	3	Clay	CL/CH	very stiff	125	1.3	15	1.46		90			1.07	>10
2.75	9.0	19.02	5.07	3	Clay	CL/CH	very stiff	125	1.3	15	1.42		90			1.09	>10
2.90	9.5	20.56	4.59	3	Clay	CL/CH	very stiff	125	1.3	16	1.38		85			1.18	>10
3.05	10.0	17.46	4.91	3	Clay	CL/CH	stiff	125	1.3	14	1.34		95			0.99	>10
3.20	10.5	15.45	4.14	3	Clay	CL/CH	stiff	125	1.3	12	1.32		95			0.87	>10
3.35	11.0	13.93	3.83	4	Silty Clay to Clay	CL	stiff	125	1.8	8	1.31		100			0.78	>10
3.50	11.5	13.83	4.23	3	Clay	CL/CH	stiff	125	1.3	11	1.29		100			0.78	8.56
3.65	12.0	18.01	4.65	3	Clay	CL/CH	very stiff	125	1.3	14	1.27		95			1.02	>10
3.80	12.5	18.70	5.93	3	Clay	CL/CH	very stiff	125	1.3	15	1.26		100			1.06	>10
3.95	13.0	18.01	5.35	3	Clay	CL/CH	very stiff	125	1.3	14	1.24		100			1.02	>10
4.13	13.5	17.39	5.15	3	Clay	CL/CH	stiff	125	1.3	14	1.23		100			0.98	>10
4.28	14.0	14.93	5.20	3	Clay	CL/CH	stiff	125	1.3	12	1.22		100			0.84	8.00
4.43	14.5	15.49	4.86	3	Clay	CL/CH	stiff	125	1.3	12	1.20		100			0.87	8.27
4.58	15.0	18.22	4.65	3	Clay	CL/CH	very stiff	125	1.3	15	1.19		100			1.03	>10
4.73	15.5	22.11	4.64	3	Clay	CL/CH	very stiff	125	1.3	18	1.18		95			1.26	>10
4.88	16.0	19.85	4.92	3	Clay	CL/CH	very stiff	125	1.3	16	1.17		100			1.12	>10
5.03	16.5	19.77	4.96	3	Clay	CL/CH	very stiff	125	1.3	16	1.16		100			1.12	>10
5.18	17.0	18.38	5.96	3	Clay	CL/CH	very stiff	125	1.3	15	1.14		100			1.03	9.39
5.33	17.5	17.64	5.69	3	Clay	CL/CH	stiff	125	1.3	14	1.13		100			0.99	8.41
5.48	18.0	25.50	4.80	3	Clay	CL/CH	very stiff	125	1.3	20	1.12		95			1.45	>10
5.65	18.5	32.47	3.36	5	Clayey Silt to Silty Clay	ML/CL	very stiff	120	2.5	13	1.11		75			1.86	>10
5.80	19.0	13.48	4.36	3	Clay	CL/CH	stiff	125	1.3	11	1.10		100			0.74	4.89
5.95	19.5	18.41	4.55	3	Clay	CL/CH	very stiff	125	1.3	15	1.09		100			1.03	8.00
6.10	20.0	22.07	5.36	3	Clay	CL/CH	very stiff	125	1.3	18	1.08		100			1.25	>10
6.25	20.5	24.57	5.40	3	Clay	CL/CH	very stiff	125	1.3	20	1.07		100			1.39	>10
6.40	21.0	26.16	6.13	3	Clay	CL/CH	very stiff	125	1.3	21	1.07		100			1.49	>10
6.55	21.5	23.24	6.19	3	Clay	CL/CH	very stiff	125	1.3	19	1.06		100			1.31	>10
6.70	22.0	22.66	5.55	3	Clay	CL/CH	very stiff	125	1.3	18	1.05		100			1.28	>10
6.85	22.5	26.25	6.97	3	Clay	CL/CH	very stiff	125	1.3	21	1.04		100			1.49	>10
7.00	23.0	25.11	6.17	3	Clay	CL/CH	very stiff	125	1.3	20	1.03		100			1.42	>10
7.18	23.5	22.18	6.48	3	Clay	CL/CH	very stiff	125	1.3	18	1.02		100			1.25	8.70
7.33	24.0	21.09	6.24	3	Clay	CL/CH	very stiff	125	1.3	17	1.02		100			1.18	7.85
7.48	24.5	23.54	7.51	3	Clay	CL/CH	very stiff	125	1.3	19	1.01		100			1.32	9.39
7.63	25.0	21.31	6.90	3	Clay	CL/CH	very stiff	125	1.3	17	1.00		100			1.19	7.56
7.78	25.5	18.21	6.67	3	Clay	CL/CH	very stiff	125	1.3	15	0.99		100			1.01	5.65
7.93	26.0	15.91	6.78	3	Clay	CL/CH	stiff	125	1.3	13	0.99		100			0.87	4.37
8.08	26.5	13.54	5.59	3	Clay	CL/CH	stiff	125	1.3	11	0.98		100			0.73	3.43
8.23	27.0	11.78	5.53	3	Clay	CL/CH	stiff	125	1.3	9	0.97		100			0.63	2.73
8.38	27.5	14.49	5.56	3	Clay	CL/CH	stiff	125	1.3	12	0.97		100			0.79	3.58
8.53	28.0	16.02	5.84	3	Clay	CL/CH	stiff	125	1.3	13	0.96		100			0.87	4.09
8.68	28.5	15.04	5.37	3	Clay	CL/CH	stiff	125	1.3	12	0.95		100			0.82	3.66
8.85	29.0	20.59	6.98	3	Clay	CL/CH	very stiff	125	1.3	16	0.95		100			1.14	5.88
9.00	29.5	16.05	6.66	3	Clay	CL/CH	stiff	125	1.3	13	0.94		100			0.87	3.83
9.15	30.0	44.48	3.37	5	Clayey Silt to Silty Clay	ML/CL	hard	120	2.5	18	0.93		80			2.54	>10
9.30	30.5	27.03	5.86	3	Clay	CL/CH	very stiff	125	1.3	22	0.93		100			1.52	8.85

LANDMARK CONSULTANTS, INC.

CONE PENETROMETER INTERPRETATION (based on Robertson & Campanella, 1989, refer to Key to CPT logs)

Project: Heber South Plant -- Heber, CA Project No: LE07178 Date: 05/02/07

CONE SOUNDING: CPT-1

Est. GWT (ft): 10.0 Phi Correlation: 0 0-Schm(78),1-R&C(83),2-PHT(74)

Base Depth meters	Base Depth feet	Avg Tip Qc, tsf	Avg Friction Ratio, %	1 Soil Type	Soil Classification	USC	Density or Consistency	Est. Density (pcf)	Qc to N	SPT N(60)	Cn or Cq	Norm. Qc1n	Est. % Fines	Rel. Dens. Dr (%)	Nk: Phi (deg.)	17.0 Su (tsf)	OCR
9.45	31.0	24.88	4.56	3	Clay	CL/CH	very stiff	125	1.3	20	0.92		100			1.39	7.41
9.60	31.5	17.85	4.68	3	Clay	CL/CH	stiff	125	1.3	14	0.92		100			0.98	4.18
9.75	32.0	21.43	4.98	3	Clay	CL/CH	very stiff	125	1.3	17	0.91		100			1.19	5.53
9.90	32.5	19.94	5.01	3	Clay	CL/CH	very stiff	125	1.3	16	0.91		100			1.10	4.78
10.05	33.0	21.67	6.03	3	Clay	CL/CH	very stiff	125	1.3	17	0.90		100			1.20	5.42
10.20	33.5	17.09	5.96	3	Clay	CL/CH	stiff	125	1.3	14	0.89		100			0.93	3.66
10.38	34.0	13.75	5.92	3	Clay	CL/CH	stiff	125	1.3	11	0.89		100			0.73	2.65
10.53	34.5	14.75	5.27	3	Clay	CL/CH	stiff	125	1.3	12	0.88		100			0.79	2.91
10.68	35.0	17.80	4.91	3	Clay	CL/CH	stiff	125	1.3	14	0.88		100			0.97	3.66
10.83	35.5	19.50	4.45	3	Clay	CL/CH	very stiff	125	1.3	16	0.87		100			1.07	4.18
10.98	36.0	20.06	4.23	4	Silty Clay to Clay	CL	very stiff	125	1.8	11	0.87		100			1.10	5.53
11.13	36.5	23.73	5.01	3	Clay	CL/CH	very stiff	125	1.3	19	0.86		100			1.31	5.53
11.28	37.0	26.37	5.33	3	Clay	CL/CH	very stiff	125	1.3	21	0.86		100			1.47	6.43
11.43	37.5	29.22	5.23	3	Clay	CL/CH	very stiff	125	1.3	23	0.85		100			1.63	7.56
11.58	38.0	28.26	4.00	4	Silty Clay to Clay	CL	very stiff	125	1.8	16	0.85		100			1.58	9.39
11.73	38.5	26.29	3.66	5	Clayey Silt to Silty Clay	ML/CL	very stiff	120	2.5	11	0.85		100			1.46	>10
11.88	39.0	24.98	3.19	5	Clayey Silt to Silty Clay	ML/CL	very stiff	120	2.5	10	0.84		100			1.38	>10
12.05	39.5	23.62	3.00	5	Clayey Silt to Silty Clay	ML/CL	very stiff	120	2.5	9	0.84		100			1.30	9.00
12.20	40.0	21.78	2.80	5	Clayey Silt to Silty Clay	ML/CL	very stiff	120	2.5	9	0.83		100			1.19	7.56
12.35	40.5	17.57	2.75	5	Clayey Silt to Silty Clay	ML/CL	stiff	120	2.5	7	0.83		100			0.94	5.21
12.50	41.0	19.10	2.36	5	Clayey Silt to Silty Clay	ML/CL	very stiff	120	2.5	8	0.83		100			1.03	5.88
12.65	41.5	22.54	2.42	5	Clayey Silt to Silty Clay	ML/CL	very stiff	120	2.5	9	0.82		100			1.23	7.70
12.80	42.0	23.41	3.23	5	Clayey Silt to Silty Clay	ML/CL	very stiff	120	2.5	9	0.82		100			1.28	8.14
12.95	42.5	22.05	3.08	5	Clayey Silt to Silty Clay	ML/CL	very stiff	120	2.5	9	0.81		100			1.20	7.13
13.10	43.0	21.46	2.78	5	Clayey Silt to Silty Clay	ML/CL	very stiff	120	2.5	9	0.81		100			1.17	6.65
13.25	43.5	22.21	3.76	4	Silty Clay to Clay	CL	very stiff	125	1.8	13	0.81		100			1.21	5.10
13.40	44.0	22.69	3.76	4	Silty Clay to Clay	CL	very stiff	125	1.8	13	0.80		100			1.24	5.21
13.58	44.5	25.69	2.81	5	Clayey Silt to Silty Clay	ML/CL	very stiff	120	2.5	10	0.80		100			1.41	8.85
13.73	45.0	26.50	2.66	5	Clayey Silt to Silty Clay	ML/CL	very stiff	120	2.5	11	0.80		100			1.46	9.19
13.88	45.5	25.22	2.66	5	Clayey Silt to Silty Clay	ML/CL	very stiff	120	2.5	10	0.79		100			1.38	8.27
14.03	46.0	24.63	3.10	5	Clayey Silt to Silty Clay	ML/CL	very stiff	120	2.5	10	0.79		100			1.36	7.85
14.18	46.5	18.88	2.93	5	Clayey Silt to Silty Clay	ML/CL	very stiff	120	2.5	8	0.79		100			1.01	4.89
14.33	47.0	19.43	2.84	5	Clayey Silt to Silty Clay	ML/CL	very stiff	120	2.5	8	0.78		100			1.04	5.00
14.48	47.5	22.40	3.03	5	Clayey Silt to Silty Clay	ML/CL	very stiff	120	2.5	9	0.78		100			1.22	6.32
14.63	48.0	23.12	2.75	5	Clayey Silt to Silty Clay	ML/CL	very stiff	120	2.5	9	0.78		100			1.26	6.54
14.78	48.5	18.94	1.38	6	Sandy Silt to Clayey Silt	ML	very loose	115	3.5	5	0.77	13.8	100	14	30		
14.93	49.0	18.77	1.78	6	Sandy Silt to Clayey Silt	ML	very loose	115	3.5	5	0.77	13.7	100	14	30		
15.09	49.5	21.59	2.73	5	Clayey Silt to Silty Clay	ML/CL	very stiff	120	2.5	9	0.77		100			1.16	5.65
15.25	50.0	23.82	3.12	5	Clayey Silt to Silty Clay	ML/CL	very stiff	120	2.5	10	0.76		100			1.29	6.54

CLIENT: Ormat Nevada

PROJECT: Heber South Plant -- Heber, CA

LOCATION: See Site and Boring Location Plan

CONE PENETROMETER: HOLGUIN, FAHAN & ASSC. Truck Mounted Electric Cone with 23 ton reaction weight

DATE: 05/02/07

LOG OF CONE SOUNDING DATA CPT-2

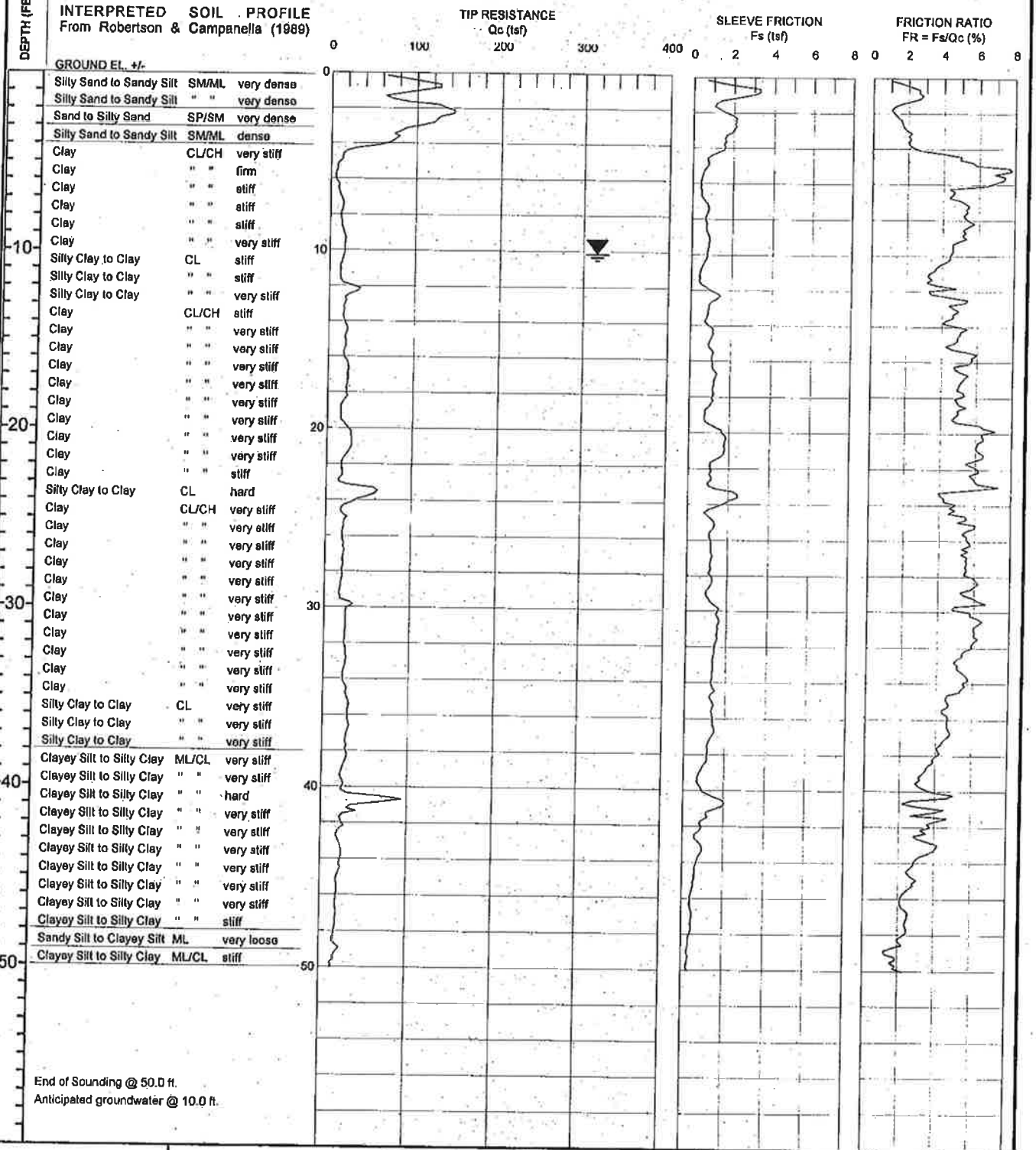

Project No: LE07178

LANDMARK Geo-Engineers and Geologists

Plate B-2

LANDMARK CONSULTANTS, INC.

CONE PENETROMETER INTERPRETATION (based on Robertson & Campanella, 1989, refer to Key to CPT logs)

Project: Heber South Plant – Heber, CA Project No: LE07178 Date: 05/02/07

CONE SOUNDING: CPT-2

Est. GWT (ft): 10.0 Phi Correlation: 0 0-Schm(78),1-R&C(83),2-PHT(74)

Base Depth meters	Base Depth feet	Avg Tip Qc, tsf	Avg Friction Ratio, %	1 Soil Type	Soil Classification	USC	Density or Consistency	Est. Density (pcf)	Qc to N	SPT N(60)	Cn or Cq	Norm. Qc1n	Est. % Fines	Rel. Dens. Dr (%)	Nk Phi (deg.)	17.0 Su (tsf)	OCR
0.15	0.5	85.14	1.61	7	Silty Sand to Sandy Silt	SM/ML	very dense	115	4.5	19	2.00	161.0	25	130	46		
0.30	1.0	120.36	2.66	7	Silty Sand to Sandy Silt	SM/ML	very dense	115	4.5	27	2.00	227.5	30	124	45		
0.45	1.5	72.28	2.13	7	Silty Sand to Sandy Silt	SM/ML	very dense	115	4.5	16	2.00	136.6	30	101	42		
0.60	2.0	116.67	1.12	6	Sand to Silty Sand	SP/SM	very dense	115	5.5	21	2.00	220.6	15	110	43		
0.75	2.5	138.05	1.48	6	Sand to Silty Sand	SP/SM	very dense	115	5.5	25	2.00	261.0	15	111	44		
0.93	3.0	117.13	1.76	7	Silty Sand to Sandy Silt	SM/ML	very dense	115	4.5	26	2.00	221.4	20	104	42		
1.08	3.5	81.23	2.12	7	Silty Sand to Sandy Silt	SM/ML	very dense	115	4.5	18	2.00	153.5	30	90	41		
1.23	4.0	74.63	2.12	7	Silty Sand to Sandy Silt	SM/ML	dense	115	4.5	17	2.00	141.1	30	86	40		
1.38	4.5	34.90	3.90	5	Clayey Silt to Silty Clay	ML/CL	hard	120	2.5	14	2.00		60			2.04	>10
1.53	5.0	13.76	5.45	3	Clay	CL/CH	stiff	125	1.3	11	1.96		100			0.79	>10
1.68	5.5	7.57	7.44	3	Clay	CL/CH	firm	125	1.3	6	1.86		100			0.43	>10
1.83	6.0	5.99	6.88	3	Clay	CL/CH	firm	125	1.3	5	1.77		100			0.33	6.10
1.98	6.5	9.47	4.51	3	Clay	CL/CH	stiff	125	1.3	8	1.69		100			0.54	>10
2.13	7.0	11.69	4.84	3	Clay	CL/CH	stiff	125	1.3	9	1.63		100			0.66	>10
2.28	7.5	14.81	5.37	3	Clay	CL/CH	stiff	125	1.3	12	1.57		95			0.85	>10
2.45	8.0	13.05	5.26	3	Clay	CL/CH	stiff	125	1.3	10	1.51		100			0.74	>10
2.60	8.5	13.41	5.40	3	Clay	CL/CH	stiff	125	1.3	11	1.46		100			0.76	>10
2.75	9.0	15.40	5.21	3	Clay	CL/CH	stiff	125	1.3	12	1.42		100			0.88	>10
2.90	9.5	18.24	4.66	3	Clay	CL/CH	very stiff	125	1.3	15	1.38		90			1.04	>10
3.05	10.0	17.49	4.50	3	Clay	CL/CH	stiff	125	1.3	14	1.34		95			0.99	>10
3.20	10.5	16.07	4.15	3	Clay	CL/CH	stiff	125	1.3	13	1.32		95			0.91	>10
3.35	11.0	13.34	3.48	4	Silty Clay to Clay	CL	stiff	125	1.8	8	1.31		95			0.75	>10
3.50	11.5	12.52	3.24	4	Silty Clay to Clay	CL	stiff	125	1.8	7	1.29		100			0.70	9.79
3.65	12.0	18.93	3.91	4	Silty Clay to Clay	CL	very stiff	125	1.8	11	1.28		90			1.08	>10
3.80	12.5	31.15	4.38	4	Silty Clay to Clay	CL	very stiff	125	1.8	18	1.26		75			1.79	>10
3.95	13.0	19.46	4.78	3	Clay	CL/CH	very stiff	125	1.3	16	1.25		95			1.10	>10
4.13	13.5	17.74	4.74	3	Clay	CL/CH	very stiff	125	1.3	14	1.23		100			1.00	>10
4.28	14.0	17.58	4.34	3	Clay	CL/CH	stiff	125	1.3	14	1.22		100			0.99	>10
4.43	14.5	21.21	5.18	3	Clay	CL/CH	very stiff	125	1.3	17	1.20		100			1.20	>10
4.58	15.0	20.43	4.83	3	Clay	CL/CH	very stiff	125	1.3	16	1.19		100			1.16	>10
4.73	15.5	20.79	4.75	3	Clay	CL/CH	very stiff	125	1.3	17	1.18		100			1.18	>10
4.88	16.0	18.89	5.75	3	Clay	CL/CH	very stiff	125	1.3	15	1.17		100			1.07	>10
5.03	16.5	23.41	4.88	3	Clay	CL/CH	very stiff	125	1.3	19	1.16		95			1.33	>10
5.18	17.0	23.59	5.34	3	Clay	CL/CH	very stiff	125	1.3	19	1.14		100			1.34	>10
5.33	17.5	23.27	4.98	3	Clay	CL/CH	very stiff	125	1.3	19	1.13		100			1.32	>10
5.48	18.0	22.19	5.13	3	Clay	CL/CH	very stiff	125	1.3	18	1.12		100			1.26	>10
5.65	18.5	20.81	5.10	3	Clay	CL/CH	very stiff	125	1.3	17	1.11		100			1.17	>10
5.80	19.0	15.76	4.92	3	Clay	CL/CH	stiff	125	1.3	13	1.10		100			0.88	6.32
5.95	19.5	16.06	5.23	3	Clay	CL/CH	stiff	125	1.3	13	1.09		100			0.89	6.32
6.10	20.0	22.81	6.58	3	Clay	CL/CH	very stiff	125	1.3	18	1.08		100			1.29	>10
6.25	20.5	28.53	6.30	3	Clay	CL/CH	very stiff	125	1.3	23	1.07		100			1.62	>10
6.40	21.0	28.99	6.06	3	Clay	CL/CH	very stiff	125	1.3	23	1.07		100			1.65	>10
6.55	21.5	24.82	6.28	3	Clay	CL/CH	very stiff	125	1.3	20	1.06		100			1.40	>10
6.70	22.0	18.48	5.79	3	Clay	CL/CH	very stiff	125	1.3	15	1.05		100			1.03	6.88
6.85	22.5	18.41	5.89	3	Clay	CL/CH	very stiff	125	1.3	15	1.04		100			1.03	6.65
7.00	23.0	15.96	6.46	3	Clay	CL/CH	stiff	125	1.3	13	1.03		100			0.88	5.10
7.18	23.5	46.63	4.62	4	Silty Clay to Clay	CL	hard	125	1.8	27	1.02		80			2.68	>10
7.33	24.0	47.09	4.48	4	Silty Clay to Clay	CL	hard	125	1.8	27	1.02		80			2.71	>10
7.48	24.5	23.27	4.67	3	Clay	CL/CH	very stiff	125	1.3	19	1.01		100			1.31	9.00
7.63	25.0	21.09	5.34	3	Clay	CL/CH	very stiff	125	1.3	17	1.00		100			1.18	7.41
7.78	25.5	21.71	5.85	3	Clay	CL/CH	very stiff	125	1.3	17	0.99		100			1.21	7.56
7.93	26.0	19.90	5.47	3	Clay	CL/CH	very stiff	125	1.3	16	0.99		100			1.11	6.32
8.08	26.5	20.78	5.59	3	Clay	CL/CH	very stiff	125	1.3	17	0.98		100			1.16	6.65
8.23	27.0	21.98	5.44	3	Clay	CL/CH	very stiff	125	1.3	18	0.97		100			1.23	7.13
8.38	27.5	20.73	5.53	3	Clay	CL/CH	very stiff	125	1.3	17	0.97		100			1.15	6.32
8.53	28.0	20.36	5.62	3	Clay	CL/CH	very stiff	125	1.3	16	0.96		100			1.13	6.00
8.68	28.5	19.99	6.11	3	Clay	CL/CH	very stiff	125	1.3	16	0.95		100			1.11	5.76
8.85	29.0	18.33	5.49	3	Clay	CL/CH	very stiff	125	1.3	15	0.95		100			1.01	4.89
9.00	29.5	17.78	6.27	3	Clay	CL/CH	stiff	125	1.3	14	0.94		100			0.98	4.47
9.15	30.0	29.76	5.16	3	Clay	CL/CH	very stiff	125	1.3	24	0.93		100			1.68	>10
9.30	30.5	25.36	6.14	3	Clay	CL/CH	very stiff	125	1.3	20	0.93		100			1.42	7.85

LANDMARK CONSULTANTS, INC.

CONE PENETROMETER INTERPRETATION (based on Robertson & Campanella, 1989, refer to Key to CPT logs)

Project: Heber South Plant – Heber, CA Project No: LE07178 Date: 05/02/07

CONE SOUNDING: CPT-2

Est. GWT (ft): 10.0 Phi Correlation: 0 (0-Schm(78),1-R&C(83),2-PHT(74))

Base Depth meters	Base Depth feet	Avg Tip Qc, tsf	Avg Friction Ratio, %	1 Soil Type	Soil Classification	USC	Density or Consistency	Est. Density (pcf)	Qc to N	SPT N(60)	Cn or Cq	Norm. Qc1n	Est. % Fines	Rel. Dens. Dr (%)	Nk: Phi (deg.)	17.0 Su (tsf)	OCR
9.45	31.0	25.65	6.08	3	Clay	CL/CH	very stiff	125	1.3	21	0.92		100			1.44	7.85
9.60	31.5	24.99	6.11	3	Clay	CL/CH	very stiff	125	1.3	20	0.92		100			1.40	7.27
9.75	32.0	24.42	5.93	3	Clay	CL/CH	very stiff	125	1.3	20	0.91		100			1.36	6.88
9.90	32.5	25.69	5.42	3	Clay	CL/CH	very stiff	125	1.3	21	0.90		100			1.43	7.27
10.05	33.0	26.43	5.06	3	Clay	CL/CH	very stiff	125	1.3	21	0.90		100			1.48	7.56
10.20	33.5	24.95	5.31	3	Clay	CL/CH	very stiff	125	1.3	20	0.89		100			1.39	6.65
10.36	34.0	22.88	5.62	3	Clay	CL/CH	very stiff	125	1.3	18	0.89		100			1.27	5.65
10.53	34.5	25.51	5.40	3	Clay	CL/CH	very stiff	125	1.3	20	0.88		100			1.42	6.65
10.68	35.0	27.31	4.56	4	Silty Clay to Clay	CL	very stiff	125	1.8	16	0.88		100			1.53	>10
10.83	35.5	30.04	4.55	4	Silty Clay to Clay	CL	very stiff	125	1.8	17	0.87		100			1.69	>10
10.98	36.0	29.52	4.52	4	Silty Clay to Clay	CL	very stiff	125	1.8	17	0.87		100			1.65	>10
11.13	36.5	30.25	4.64	4	Silty Clay to Clay	CL	very stiff	125	1.8	17	0.86		100			1.70	>10
11.28	37.0	29.39	4.68	4	Silty Clay to Clay	CL	very stiff	125	1.8	17	0.86		100			1.64	>10
11.43	37.5	27.60	4.22	4	Silty Clay to Clay	CL	very stiff	125	1.8	16	0.85		100			1.54	9.00
11.58	38.0	27.92	4.11	4	Silty Clay to Clay	CL	very stiff	125	1.8	16	0.85		100			1.56	9.00
11.73	38.5	28.57	3.77	5	Clayey Silt to Silty Clay	ML/CL	very stiff	120	2.5	11	0.85		100			1.59	>10
11.88	39.0	24.62	3.37	5	Clayey Silt to Silty Clay	ML/CL	very stiff	120	2.5	10	0.84		100			1.36	>10
12.05	39.5	22.28	3.04	5	Clayey Silt to Silty Clay	ML/CL	very stiff	120	2.5	9	0.84		100			1.22	8.00
12.20	40.0	24.64	3.45	5	Clayey Silt to Silty Clay	ML/CL	very stiff	120	2.5	10	0.83		100			1.36	9.59
12.35	40.5	41.78	4.14	5	Clayey Silt to Silty Clay	ML/CL	hard	120	2.5	17	0.83		95			2.37	>10
12.50	41.0	64.96	3.22	6	Sandy Silt to Clayey Silt	ML	medium dense	115	3.5	19	0.83	50.7	70	52	35		
12.65	41.5	32.37	3.75	5	Clayey Silt to Silty Clay	ML/CL	very stiff	120	2.5	13	0.82		100			1.81	>10
12.80	42.0	22.75	3.82	4	Silty Clay to Clay	CL	very stiff	125	1.8	13	0.82		100			1.25	5.53
12.95	42.5	22.78	3.20	5	Clayey Silt to Silty Clay	ML/CL	very stiff	120	2.5	9	0.81		100			1.25	7.56
13.10	43.0	19.79	3.62	4	Silty Clay to Clay	CL	very stiff	125	1.8	11	0.81		100			1.07	4.28
13.25	43.5	23.86	3.91	4	Silty Clay to Clay	CL	very stiff	125	1.8	14	0.81		100			1.31	5.76
13.40	44.0	24.93	3.00	5	Clayey Silt to Silty Clay	ML/CL	very stiff	120	2.5	10	0.80		100			1.37	8.41
13.58	44.5	23.46	2.65	5	Clayey Silt to Silty Clay	ML/CL	very stiff	120	2.5	9	0.80		100			1.28	7.41
13.73	45.0	21.13	2.78	5	Clayey Silt to Silty Clay	ML/CL	very stiff	120	2.5	8	0.80		100			1.14	6.10
13.88	45.5	19.10	2.73	5	Clayey Silt to Silty Clay	ML/CL	very stiff	120	2.5	8	0.79		100			1.02	5.10
14.03	46.0	19.63	2.23	5	Clayey Silt to Silty Clay	ML/CL	very stiff	120	2.5	8	0.79		100			1.06	5.31
14.18	46.5	18.74	2.12	5	Clayey Silt to Silty Clay	ML/CL	very stiff	120	2.5	7	0.79		100			1.00	4.78
14.33	47.0	18.93	2.49	5	Clayey Silt to Silty Clay	ML/CL	very stiff	120	2.5	8	0.78		100			1.01	4.78
14.48	47.5	18.85	2.42	5	Clayey Silt to Silty Clay	ML/CL	very stiff	120	2.5	8	0.78		100			1.01	4.68
14.63	48.0	17.53	2.38	5	Clayey Silt to Silty Clay	ML/CL	stiff	120	2.5	7	0.78		100			0.93	4.09
14.78	48.5	16.01	2.08	5	Clayey Silt to Silty Clay	ML/CL	stiff	120	2.5	6	0.77		100			0.84	3.58
14.93	49.0	20.91	1.36	6	Sandy Silt to Clayey Silt	ML	very loose	115	3.5	6	0.77	15.2	100	17	30		
15.09	49.5	17.29	1.76	6	Sandy Silt to Clayey Silt	ML	very loose	115	3.5	5	0.77	12.5	100	11	30		
15.25	50.0	13.85	1.98	5	Clayey Silt to Silty Clay	ML/CL	stiff	120	2.5	6	0.76		100			0.71	2.82

Simplified Soil Classification Chart

After Robertson & Campanella (1989)

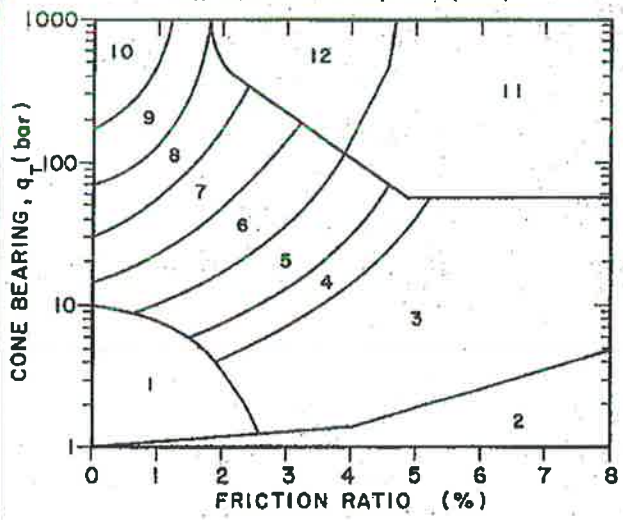

Geotechnical Parameters from CPT Data:

Equivalent SPT N(60) blow count = Qc/(Qc/N Ratio)

N1(60) = Cn*N(60) Normalized SPT blow count

Cn = 1/(p'o)^0.5 < 1.6 max. from Liao & Whitman (1986)

p'o = effective overburden pressure (tsf) using unit densities given below and estimated groundwater table.

Dr = Relative density (%) from Jamiolkowski et. al. (1986) relationship

= -98 +68*log(Qc/p'o^0.5) where Qc, p'o in tonne/sqm

Note: 1 tonne/sqm = 0.1024 tsf, 1 bar =1.0443 tsf

Phi = Friction Angle estimated from either:

1. Roberton & Campanella (1983) chart:
   Phi = 5.3 + 24*(log(Qc/p'o))+3(log(Qc/p'o))^2
2. Peck, Hansen & Thornburn (1974) N-Phi Correlation
3. Schmertman (1978) chart [Phi = 28+0.14*Dr for fine uniform sands]

Su = undrained shear strength (tsf)

= (Qc-p'o)/Nk where Nk varies from 10 to 22, 17 for OC clays

OCR = Overconsolidation Ratio estimated from Schmertman (1978) chart using Su/p'o ratio and estimated normal consolidated Su/p'o

Variation of Qc/N Ratio with Grain Size

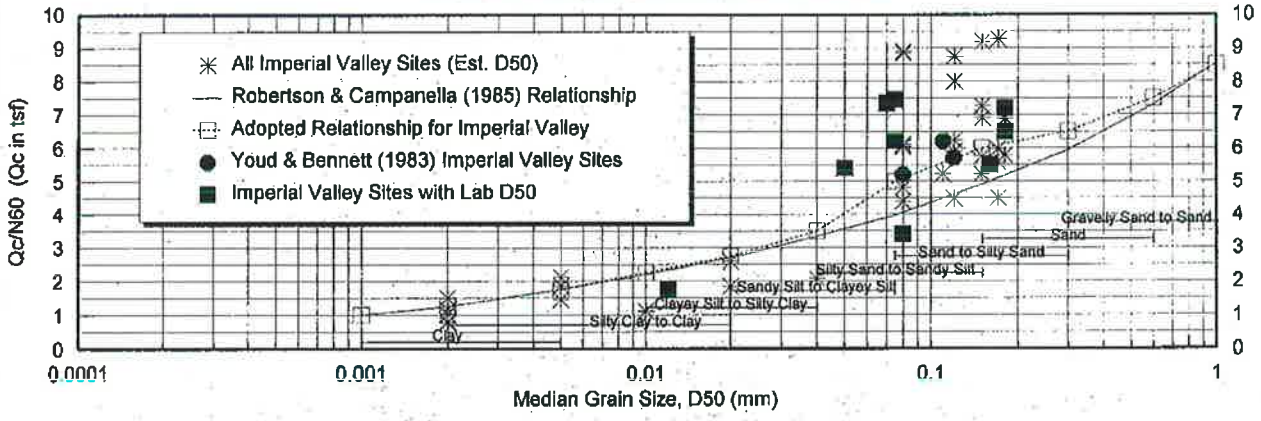

Note: Assumed Properties and Adopted Qc/N Ratio based on correlations from Imperial Valley, California soils

Table of Soil Types and Assumed Properties

Zone	Soil Classification	UCS	Density (pcf)	R&C Qc/N	Adopted Qc/N	Est. PI	Fines (%)	D50 (mm)	Su (tsf)	Consistency
1	Sensitive fine grained	ML	120	2	2	NP-15	65-100	0.020	0-0.13	very soft
2	Organic Material	OL/OH	120	1	1	--	--	--	0.13-.25	soft
3	Clay	CL/CH	125	1	1.25	25-40+	90-100	0.002	0.25-0.5	firm
4	Silty Clay to Clay	CL	125	1.5	2	15-40	90-100	0.010	0.5-1.0	stiff
5	Clayey Silt to Silty Clay	ML/CL	120	2	2.75	5-25	90-100	0.020	1.0-2.0	very stiff
6	Sandy Silt to Clayey Silt	ML	115	2.5	3.5	NP-10	65-100	0.040	>2.0	hard
7	Silty Sand to Sandy Silt	SM/ML	115	3	5	NP	35-75	0.075	Dr (%)	Relative Density
8	Sand to Silty Sand	SP/SM	115	4	6	NP	5-35	0.150	0-15	very loose
9	Sand	SP	110	5	6.5	NP	0-5	0.300	15-35	loose
10	Gravelly Sand to Sand	SW	115	6	7.5	NP	0-5	0.600	35-65	medium dense
11	Overconsolidated Soil	--	120	1	1	NP	90-100	0.010	65-85	dense
12	Sand to Clayey Sand	SP/SC	115	2	2	NP-5	--	---	>85	very dense

LANDMARK
Geo-Engineers and Geologists

Project No: LE07178

Key to CPT Interpretation of Logs

Plate B-3

APPENDIX C

Geotechnical Report

New Turbine Generator and Cooling Tower
Heber 2 Geothermal Plant
Heber, CA

Prepared for:

ORMAT
947 Dogwood Road
Heber, CA 92249

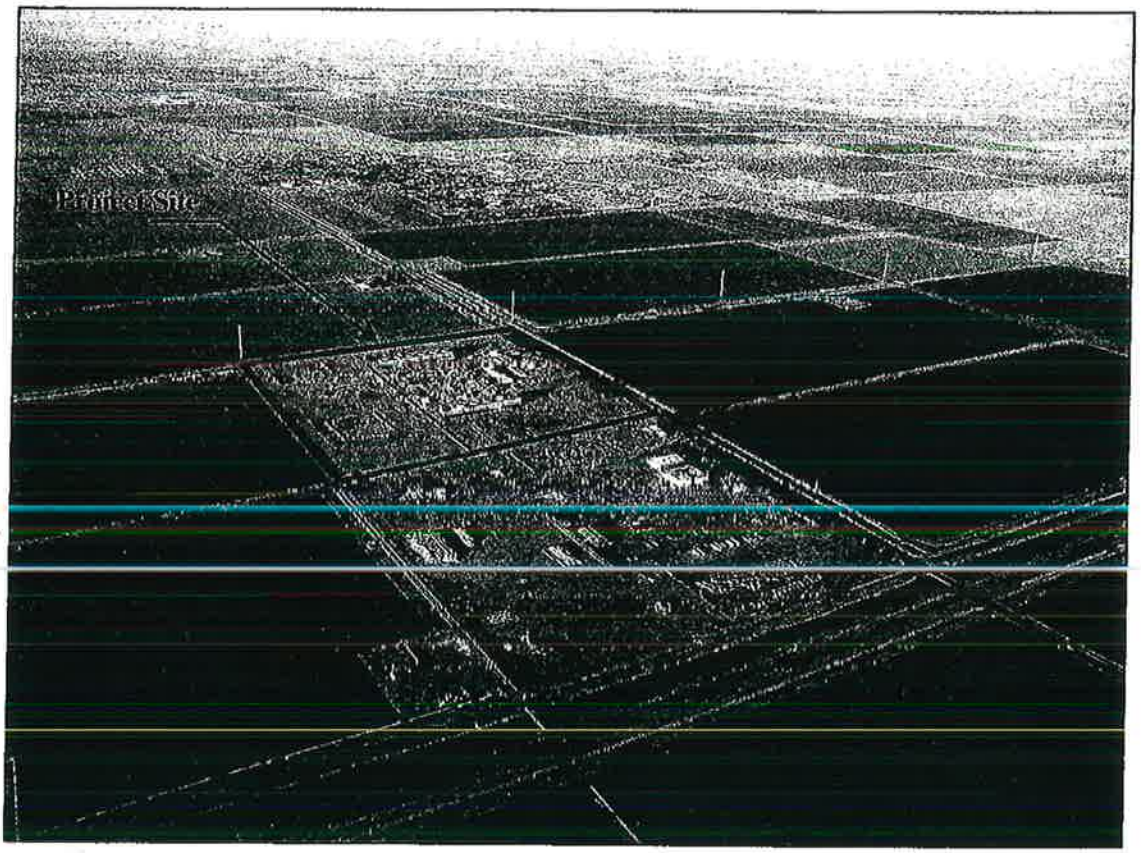

LANDMARK
Geo-Engineers and Geologists
a DBE/MBE/SBE Company

Prepared by:

Landmark Consultants, Inc.
780 N. 4th Street
El Centro, CA 92243
(760) 370-3000

January 2005

LANDMARK
Geo-Engineers and Geologists
a DBE/MBE/SBE Company

January 10, 2005

780 N. 4th Street
El Centro, CA 92243
(760) 370-3000
(760) 337-8900 fax

77-948 Wildcat Drive
Palm Desert, CA 92211
(760) 360-0665
(760) 360-0521 fax

Mr. Mike Collins
ORMAT
947 Dogwood Road
Heber, CA 92249

Geotechnical Investigation
New Turbine Generator and Cooling Tower
Heber 2 Geothermal Plant
Dogwood Road
Heber, California
LCI Report No. LE04354 (2)

Dear Mr. Collins:

This geotechnical report is provided for design and construction of the new turbine generator and cooling tower additions to the Ormat Heber 2 geothermal power plant located on Dogwood Road southwest of Heber, California. Our geotechnical investigation was conducted in response to your request for our services. The enclosed report describes our soil engineering investigation and presents our professional opinions regarding geotechnical conditions at the site to be considered in the design and construction of the project.

This executive summary presents ***selected*** elements of our findings and recommendations only. It ***does not*** present crucial details needed for the proper application of our findings and recommendations. Our findings, recommendations, and application options are related ***only through reading the full report***, and are best evaluated with the active participation of the engineer of record who developed them.

The findings of this study indicate that the site is predominantly underlain by clays of moderate expansion.

The soil are highly corrosive to metals and contain sufficient sulfates and chlorides to require special concrete mixes (4,500 psi with a 0.45 maximum water cement ratio) and protection of embedded steel building components when concrete is placed in contact with native soil. If the native soils are replaced with imported granular soils with low sulfate and chloride content, no special concrete mixes are required.

Evaluation of liquefaction potential at the site indicates that it is unlikely that the subsurface soil will liquefy under seismically induced groundshaking due to the nature of the soil (clays soils predominate). No mitigation is required for liquefaction effects at this site.

Foundation settlements are indicated on figures 2 thru 5. Differential settlement is estimated to be about of two-thirds of total settlement.

We did not encounter soil conditions that would preclude development of the site for its intended use provided the recommendations contained in this report are implemented in the design and construction of this project.

We appreciate the opportunity to provide our findings and professional opinions regarding geotechnical conditions at the site. If you have any questions or comments regarding our findings, please call our office at (760) 370-3000.

Respectfully Submitted,
Landmark Consultants, Inc.

REGISTERED GEOLOGIST
STEVEN K. WILLIAMS
CERTIFIED ENGINEERING GEOLOGIST
CEG 2261
STATE OF CALIFORNIA

Steven K. Williams, CEG
Senior Engineering Geologist

Julian R. Avalos
Staff Engineer

REGISTERED PROFESSIONAL ENGINEER
JEFFREY O. LYON
No. 31921
EXPIRES 12-31-04
CIVIL
STATE OF CALIFORNIA

Jeffrey O. Lyon, PE
President

Distribution:
Client (4)

TABLE OF CONTENTS

Section 1
INTRODUCTION

1.1 Project Description

This report presents the findings of our geotechnical investigation for the proposed additions to the Ormat Heber 2 geothermal power plant located on Dogwood Road southwest of Heber, California (See Vicinity Map, Plate A-1). The proposed development will consist of the addition of one (1) turbine/generator set and one (1) cooling tower. A site plan for the proposed power plant improvements was not made available to us at the time that this report was prepared.

Small structures may be are planned for electrical control panels, consisting of masonry or panelized concrete construction. Expected footing loads are estimated at 1 to 2 kips per lineal foot for the small structures. Expected plant components, cooling tower and turbine/generator columns loads range from 5 to 400 kips. If structural loads exceed those stated above, we should be notified so we may evaluate their impact on foundation settlement and bearing capacity. Site development will include foundation support pad preparation and underground utility installation.

1.2 Purpose and Scope of Work

The purpose of this geotechnical study was to investigate the upper 50 feet of subsurface soil at selected locations within the site for physical/engineering properties. From the subsequent field and laboratory data, professional opinions were developed and are provided in this report regarding geotechnical conditions at this site and the effect on design and construction. The scope of our services consisted of the following:

- Field exploration and in-situ testing of the site soils at selected locations and depths.
- Laboratory testing for physical properties of selected samples.
- A review of the available literature and publications pertaining to local geology, faulting, and seismicity.
- Engineering analysis and evaluation of the data collected.
- Preparation of this report presenting our findings, professional opinions, and recommendations for the geotechnical aspects of project design and construction.

This report addresses the following geotechnical issues:

- Subsurface soil and groundwater conditions
- Site geology, regional faulting and seismicity, near source factors, and site seismic accelerations
- Liquefaction potential and its mitigation
- Expansive soil and methods of mitigation
- Aggressive soil conditions to metals and concrete

Professional opinions with regard to the above issues are presented for the following:

- Site grading and earthwork
- Foundation subgrade preparation
- Allowable soil bearing pressures and expected settlements
- Concrete slabs-on-grade
- Mitigation of the potential effects of salt concentrations in native soil to concrete mixes and steel reinforcement
- Seismic design parameters

Our scope of work for this report did not include an evaluation of the site for the presence of environmentally hazardous materials or conditions.

1.3 Authorization

Mr. Mike Collins, Project Manager of Ormat for Power Generation Construction provided authorization by written agreement to proceed with our work on December 14, 2004. We conducted our work according to our written proposal dated December 13, 2004.

Section 2
METHODS OF INVESTIGATION

2.1 Field Exploration

Subsurface exploration was performed on December 20, 2004 using Holguin, Fahan, & Associates, Inc. of Cypress, California to advance three (3) electric cone penetrometer (CPT) soundings to an approximate depth of 50 feet below existing ground surface. The soundings were made at the locations shown on the Site and Exploration Plan (Plate A-2). The approximate sounding locations were established in the field and plotted on the site map by sighting to discernable site features.

CPT soundings provide a continuous profile of the soil stratigraphy with readings every 2.5cm (1 inch) in depth. Direct sampling for visual and physical confirmation of soil properties has been used by our firm to establish direct correlations with CPT exploration in this geographical region.

The CPT exploration was conducted by hydraulically advancing an instrumented Hogentogler 10cm^2 conical probe into the ground at a rate of 2cm per second using a 23-ton truck as a reaction mass. An electronic data acquisition system recorded a nearly continuous log of the resistance of the soil against the cone tip (Qc) and soil friction against the cone sleeve (Fs) as the probe was advanced. Empirical relationships (Robertson and Campanella, 1989) were then applied to the data to give a continuous profile of the soil stratigraphy. Interpretation of CPT data provides correlations for SPT blow count, phi (ϕ) angle (soil friction angle), undrained shear strength (S_u) of clays and over-consolidation ratio (OCR). These correlations may then be used to evaluate vertical and lateral soil bearing capacities and consolidation characteristics of the subsurface soil.

Interpretive logs of the CPT soundings were produced and presented in final form after review of field and laboratory data and are presented on Plates B-1 through B-3 in Appendix B. A key to the interpretation of CPT soundings is presented on Plate B-4. The stratification lines shown on the subsurface logs represent the approximate boundaries between the various strata. However, the transition from one stratum to another may be gradual over some range of depth.

2.2 Laboratory Testing

Laboratory tests were conducted on selected bulk soil samples obtained from hand auger borings made adjacent to the CPT locations to aid in classification and evaluation of selected engineering properties of the near surface soils. The tests were conducted in general conformance to the procedures of the American Society for Testing and Materials (ASTM) or other standardized methods as referenced below. The laboratory testing program consisted of the following tests:

- Plasticity Index (ASTM D4318) – used for soil classification and expansive soil design criteria.

- Chemical Analyses (soluble sulfates & chlorides, pH, and resistivity) (Caltrans Methods) – used for concrete mix evaluations and corrosion protection requirements.

The laboratory test results are presented on the subsurface logs (Appendix B) and on Plates C-1, C-2 and C-3 in Appendix C.

Engineering parameters of soil strength, compressibility and relative density utilized for developing design criteria provided within this report were either extrapolated from correlations with the subsurface CPT data or from data obtained from the field and laboratory testing program.

Section 3
DISCUSSION

3.1 Site Conditions

The plant additions are located in the northwest corner of the Heber 2 geothermal plant on the west side of the existing turbine generators and cooling tower. The area is relatively vacant and approximately has the same elevation as the existing plant facilities. An overhead pipe rack is located to the south side of the proposed location.

Adjacent properties outside of the fenced operations yard consist of agricultural land to the north and west. The site is bounded on the east by Dogwood Road and headquarters facilities of a general engineering construction company lie to the south side. Dogwood Road is slated to be a 6-lane north-south arterial from Calexico to Brawley in Imperial County. Adjacent properties are flat-lying and are approximately at the same elevation with this site.

The project site lies at an elevation of approximately 15 feet below mean sea level (MSL) (El. 985 local datum) in the Imperial Valley region of the California low desert. The surrounding properties lie on terrain which is flat (planar), part of a large agricultural valley, which was previously an ancient lake bed covered with fresh water to an elevation of 43± feet above MSL. Annual rainfall in this arid region is less than 4 inches per year with four months of average summertime temperatures above 100 °F. Winter temperatures are mild, seldom reaching freezing.

3.2 Geologic Setting

The project site is located in the Imperial Valley portion of the Salton Trough physiographic province. The Salton Trough is a geologic structural depression resulting from large scale regional faulting. The trough is bounded on the northeast by the San Andreas Fault and Chocolate Mountains and the southwest by the Peninsular Range and faults of the San Jacinto Fault Zone. The Salton Trough represents the northward extension of the Gulf of California, containing both marine and non-marine sediments since the Miocene Epoch. Tectonic activity that formed the trough continues at a high rate as evidenced by deformed young sedimentary deposits and high levels of seismicity. Figure 1 shows the location of the site in relation to regional faults and physiographic features.

The Imperial Valley is directly underlain by lacustrine deposits, which consist of interbedded lenticular and tabular silt, sand, and clay. The Late Pleistocene to Holocene lake deposits are probably less than 100 feet thick and derived from periodic flooding of the Colorado River which intermittently formed a fresh water lake (Lake Cahuilla). Older deposits consist of Miocene to Pleistocene non-marine and marine sediments deposited during intrusions of the Gulf of California. Basement rock consisting of Mesozoic granite and Paleozoic metamorphic rocks are estimated to exist at depths between 15,000 - 20,000 feet.

3.3 Seismicity and Faulting

Faulting and Seismic Sources: We have performed a computer-aided search of known faults or seismic zones that lie within a 62 mile (100 kilometers) radius of the project site as shown on Figure 1 and Table 1. The search identifies known faults within this distance and computes deterministic ground accelerations at the site based on the maximum credible earthquake expected on each of the faults and the distance from the fault to the site. The Maximum Magnitude Earthquake (Mmax) listed was taken from published geologic information available for each fault (CDMG OFR 96-08 and Jennings, 1994).

Seismic Risk: The project site is located in the seismically active Imperial Valley of southern California and is considered likely to be subjected to moderate to strong ground motion from earthquakes in the region. The proposed site structures should be designed in accordance with the California Building Code (CBC) for near source factors derived from a "Design Basis Earthquake" (DBE). The DBE is defined as the motion having a 10 percent probability of being exceeded in 50 years. The DBE generally corresponds to the Mmax magnitude discussed here.

Seismic Hazards.

- **Groundshaking.** The primary seismic hazard at the project site is the potential for strong groundshaking during earthquakes along the Imperial, Brawley, and Superstition Hills Faults. A further discussion of groundshaking follows in Section 3.4.
- **Surface Rupture.** The project site does not lie within a State of California, Alquist-Priolo Earthquake Fault Zone. Surface fault rupture is considered to be unlikely at the project site because of the well-delineated fault lines through the Imperial Valley as shown on USGS and CGS maps. However, because of the high tectonic activity and deep alluvium of the region, we cannot preclude the potential for surface rupture on undiscovered or new faults that may underlie the site.

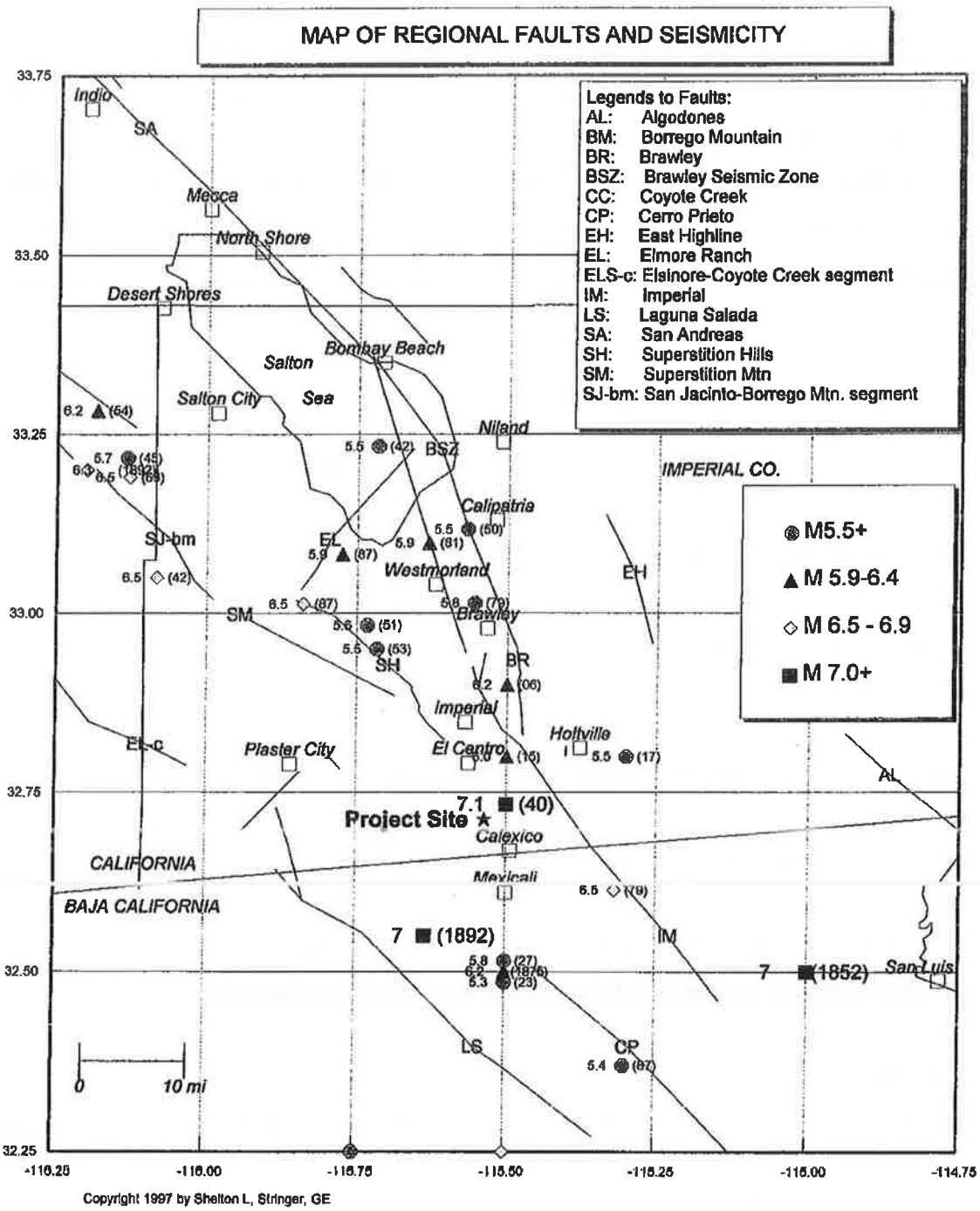

Faults and Seismic Zones from Jennings (1994), Earthquakes modified from Ellsworth (1990) catalog.

Figure 1. Map of Regional Faults and Seismicity

Table 1
FAULT PARAMETERS & DETERMINISTIC
ESTIMATES OF PEAK GROUND ACCELERATION (PGA)

Fault Name or Seismic Zone	Distance (mi) & Direction from Site	Fault Type		Fault Length (km)	Maximum Magnitude Mmax (Mw)	Avg Slip Rate (mm/yr)	Avg Return Period (yrs)	Date of Last Rupture (year)	Largest Historic Event >5.5M (year)	Est. Site PGA (g)
Reference Notes: (1)		(2)	(3)	(2)	(4)	(3)	(3)	(3)	(5)	(6)
Imperial Valley Faults										
Imperial	7.0 NE	A	B	62	**7.0**	20	79	1979	7.0 1940	**0.33**
Brawley	8.8 NNE	B	B	14	**7.0**	20	—	1979	5.8 1979	**0.28**
Cerro Prieto	15 SSE	A	B	116	**7.2**	34	50	1980	7.1 1934	**0.21**
Brawley Seismic Zone	16 N	B	B	42	**6.4**	25	24		5.9 1981	**0.13**
East Highline Canal	23 NE	C	C	22	**6.3**	1	774			**0.09**
San Jacinto Fault System										
- Superstition Hills	8.5 NNW	B	A	22	**6.6**	4	250	1987	6.5 1987	**0.23**
- Superstition Mtn.	15 NW	B	A	23	**6.6**	5	500	1440 +/-		**0.16**
- Elmore Ranch	28 NW	B	A	29	**6.6**	1	225	1987	5.9 1987	**0.10**
- Borrego Mtn	34 NW	B	A	29	**6.6**	4	175		6.5 1942	**0.08**
- Anza Segment	51 NW	A	A	90	**7.2**	12	250	1918	6.8 1918	**0.08**
- Coyote Creek	53 NW	B	A	40	**6.8**	4	175	1968	6.5 1968	**0.07**
- Whole Zone	15 NW	A	A	245	**7.5**	—	—			**0.25**
Elsinore Fault System										
- Laguna Salada	16 SW	B	B	67	**7.0**	3.5	336		7.0 1891	**0.18**
- Coyote Segment	29 W	B	A	38	**6.8**	4	625			**0.11**
- Julian Segment	55 WNW	A	A	75	**7.1**	5	340			**0.08**
- Earthquake Valley	57 WNW	B	A	20	**6.5**	2	351			**0.05**
- Whole Zone	29 W	A	A	250	**7.5**	—	—			**0.15**
San Andreas Fault System										
- Coachella Valley	45 NNW	A	A	95	**7.4**	25	220	1690+/-	6.5 1948	**0.10**
- Whole S. Calif. Zone	45 NNW	A	A	458	**7.9**	—	—	1857	7.8 1857	**0.13**
Algodones	36 E	C	C	74	**7.0**	0.1	20,000			**0.10**

Notes:

1. Jennings (1994) and CDMG (1996)
2. CDMG (1996), where Type A faults -- slip rate >5 mm/yr and well constrained paleoseismic data
   Type B faults -- all other faults.
3. WGCEP (1995)
4. CDMG (1996) based on Wells & Coppersmith (1994)
5. Ellsworth Catalog in USGS PP 1515 (1990) and USBR (1976), Mw = moment magnitude,
6. The deterministic estimates of the Site PGA are based on the attenuation relationship of:
   Boore, Joyner, Fumal (1997)

▸ **Liquefaction.** Liquefaction is unlikely to be a potential hazard at the site due to the lack of saturated granular soil (clay soils predominate).

Other Secondary Hazards.

▸ **Landsliding.** The hazard of landsliding is unlikely due to the regional planar topography. No ancient landslides are shown on geologic maps of the region and no indications of landslides were observed during our site investigation.

▸ **Volcanic hazards.** The site is not located in proximity to any known volcanically active area and the risk of volcanic hazards is considered very low.

▸ **Tsunamis, sieches, and flooding.** The site does not lie near any large bodies of water, so the threat of tsunami, sieches, or other seismically-induced flooding is unlikely.

▸ **Expansive soil.** In general, much of the near surface soils in the Imperial Valley consist of silty clays and clays which are moderate to highly expansive. The expansive soil conditions are discussed in more detail in Section 3.5.

3.4 Site Acceleration and UBC Seismic Coefficients

Deterministic horizontal peak ground accelerations (PGA) from maximum probable earthquakes on regional faults have been estimated and are included in Table 1. Ground motions are dependent primarily on the earthquake magnitude and distance to the seismogenic (rupture) zone. Accelerations also are dependent upon attenuation by rock and soil deposits, direction of rupture and type of fault; therefore, ground motions may vary considerably in the same general area.

We have used the computer program FRISKSP (Blake, 2000) to provide a probabilistic estimate of the site PGA using the attenuation relationship of Boore, Joyner, and Fumal (1997) Soil (250). The PGA estimate for the project site having a 10% probability of being exceeded in 50 years (return period of 475 years) is **0.60g**.

CBC Seismic Coefficients: The CBC seismic coefficients are roughly based on an earthquake ground motion that has a 10% probability of being exceeded in 50 years. The following table lists seismic and site coefficients (near source factors) determined by Chapter 16 of the 2001 CBC. ***This site lies within 11.3 km of a Type A fault overlying S_D (stiff) soil.***

CBC Seismic Coefficients for Chapter 16 Seismic Provisions

CBC Code Edition	Soil Profile Type	Seismic Source Type	Distance to Critical Source	Near Source Factors		Seismic Coefficients	
				Na	Nv	Ca	Cv
2001	S_D (stiff soil)	A	< 11.3 km	1.00	1.15	0.44	0.74
Ref. Table	16-J	16-U	---	16-S	16-T	16-Q	16-R

3.5 Subsurface Soil

Subsurface soils encountered during the field exploration conducted on December 20, 2004 indicates that 1.0 to 1.5 feet of stiff clay are at ground surface. Dense to very dense silty sands lie below the clays and extend to a depth of 4 to 5 feet. Stiff to very stiff clays extend a depth of 50 feet, the maximum depth of exploration. The subsurface logs (Plates B-1 through B-3) depict the stratigraphic relationships of the various soil types.

The native surface clays exhibit moderate swell potential (Expansion Index, EI = 51 - 90) when correlated to Plasticity index tests (ASTM D4318) performed on the native clays. The clay is expansive when wetted and can shrink with moisture loss (drying). Development of building foundations, concrete flatwork, and asphaltic concrete pavements should include provisions for mitigating potential swelling forces and reduction in soil strength, which can occur from saturation of the soil. Causes for soil saturation include landscape irrigation, broken utility lines, or capillary rise in moisture upon sealing the ground surface to evaporation. Moisture losses can occur with lack of landscape watering, close proximity of structures to downslopes and root system moisture extraction from deep rooted shrubs and trees placed near the foundations. Typical measures used for industrial projects to remediate expansive soil include:

- replacement of silt/clay with non-expansive granular fill,
- moisture conditioning subgrade soils to a minimum of 5% above optimum moisture (ASTM D1557) for the full range in depth of surface soils.
- design of foundations that are resistant to shrink/swell forces of silt/clay soil.

3.6 Groundwater

Groundwater was not noted on the CPT sounding at the time of exploration, but is typically encountered at approximately 10 to 15 feet below ground surface in the vicinity of the site. There is uncertainty in the accuracy of short-term water level measurements, particularly in fine-grained soil. Groundwater levels may fluctuate with precipitation, irrigation of adjacent properties, drainage, and site grading. The referenced groundwater level should not be interpreted to represent an accurate or permanent condition.

3.7 Liquefaction

Liquefaction occurs when granular soil below the water table is subjected to vibratory motions, such as produced by earthquakes. With strong ground shaking, an increase in pore water pressure develops as the soil tends to reduce in volume. If the increase in pore water pressure is sufficient to reduce the vertical effective stress (suspending the soil particles in water), the soil strength decreases and the soil behaves as a liquid (similar to quicksand). Liquefaction can produce excessive settlement, ground rupture, lateral spreading, or failure of shallow bearing foundations.

Four conditions are generally required for liquefaction to occur:

(1) the soil must be saturated (relatively shallow groundwater);
(2) the soil must be loosely packed (low to medium relative density);
(3) the soil must be relatively cohesionless (not clayey); and
(4) groundshaking of sufficient intensity must occur to function as a trigger mechanism.

All of these conditions exist to some degree at this site.

Methods of Analysis: Liquefaction potential at the project site was evaluated using the 1997 NCEER Liquefaction Workshop methods that are based on the Seed, et. al. 1985 and Robertson and Campanella (1985) methods. The 1997 NCEER methods utilize direct SPT blow counts or CPT cone readings from site exploration and earthquake magnitude/PGA estimates from the seismic hazard analysis. The resistance to liquefaction is plotted on a chart of cyclic shear stress ratio (CSR) versus a corrected blow count $N_{1(60)}$ or Qc_{IN}. A ground acceleration of 0.60g was used in the analysis with a 12 foot groundwater depth.

Liquefaction induced settlements have been estimated using the 1987 Tokimatsu and Seed method. Fines content of liquefiable sands and silt increase the liquefaction resistance in that more cycles of ground motions are required to fully develop pore pressures. The SPT blow counts were adjusted to an equivalent clean sand blow count, $N_{1(60)}$ prior to calculating settlements using Robertson and Wride (1997) adjustments. A computed factor of safety less than 1.0 indicates a liquefiable condition.

Liquefaction Effects: Based on empirical relationships, liquefaction is not expected to occur at the project site.

Section 4
RECOMMENDATIONS

4.1 Site Preparation

Clearing and Grubbing: All surface improvements, debris or vegetation including grass and weeds on the site at the time of construction should be removed from the construction area. Organic strippings should be hauled from the site and not used as fill. Any trash, construction debris, concrete slabs, old pavement, landfill, and buried obstructions such as old foundations and utility lines exposed during rough grading should be traced to the limits of the foreign material by the grading contractor and removed under our supervision. Any excavations resulting from site clearing should be dish-shaped to the lowest depth of disturbance and backfilled under observation by the geotechnical engineer's representative with compacted fill as described below.

Structure Subgrade Preparation: The exposed surface soil within the foundation areas should be removed to 12 inches below the foundation elevation or existing grade (whichever is lower). Exposed subgrade should be scarified to a depth of 8 inches, uniformly moisture conditioned to 3 to 8% above optimum moisture content (clays) or 0 to 4% above optimum (silts), and recompacted to at least 90% of the maximum density determined in accordance with ASTM D1557 methods.

The native soil is suitable for use as engineered fill provided it is free from concentrations of organic matter or other deleterious material. The fill soil should be uniformly moisture conditioned by discing and watering to the limits specified above, placed in maximum 8-inch lifts (loose), and compacted to the limits specified above.

Imported fill soil (if required) should have a Plasticity Index less than 15 and sulfates (SO_4) less than 1,000 ppm or non-expansive, granular soil meeting the USCS classifications of SM, SP-SM, or SW-SM with a maximum rock size of 3 inches and 5 to 35% passing the No. 200 sieve. The geotechnical engineer should approve imported fill soil sources before hauling material to the site. Imported granular fill should be placed in lifts no greater than 8 inches in loose thickness and compacted to at least 90% of ASTM D1557 maximum dry density at optimum moisture ±2%.

In areas other than the structures pad which are to receive area concrete slabs, the ground surface should be presaturated to a minimum depth of 18 inches and then scarified to 6 inches, moisture conditioned to a minimum of 5% over optimum, and recompacted to 83-87% of ASTM D1557 maximum density just prior to concrete placement.

Trench Backfill: On-site soil free of debris, vegetation, and other deleterious matter may be suitable for use as utility trench backfill, but may be difficult to uniformly maintain at specified moistures and compact to the specified densities. Granular material is often more cost effective for backfill of utility trenches.

Backfill soil within roadways or traffic areas should be placed in layers not more that 6 inches in thickness and mechanically compacted to a minimum of 87% of the ASTM D1557 maximum dry density except for the top 12 inches of the trench which shall be compacted to at least 90%. Native backfill should only be placed and compacted after encapsulating buried pipes with suitable bedding and pipe envelope material. Pipe envelope/bedding should either be clean sand (Sand Equivalent SE>30) or crushed rock when encountering groundwater. A geotextile filter fabric (Mirafi 140N or equivalent) should be used to encapsulate the crushed rock when placed below groundwater to reduce the potential for in-washing of fines into the gravel void space. Precautions should be taken in the compaction of the backfill to avoid damage to the pipes and structures.

Observation and Density Testing: All site preparation and fill placement should be continuously observed and tested by a representative of a qualified geotechnical engineering firm. Full-time observation services during the excavation and scarification process is necessary to detect undesirable materials or conditions and soft areas that may be encountered in the construction area. The geotechnical firm that provides observation and testing during construction shall assume the responsibility of "*geotechnical engineer of record*" and, as such, shall perform additional tests and investigation as necessary to satisfy themselves as to the site conditions and the recommendations for site development.

Auxiliary Structures Foundation Preparation: Auxiliary structures such as free standing or retaining walls should have the existing soil beneath the structure foundation prepared in the manner recommended for the building pad except the preparation needed only to extend 12 inches below and beyond the footing.

4.2 Foundations and Settlements

Shallow spread footings and continuous wall footings are suitable to support the structures associated with the turbine generator and cooling tower. Footings shall be founded on a layer of properly prepared and compacted soil as described in Section 4.1. The foundations may be designed using an allowable soil bearing pressure of 1,500 psf for compacted native clay soil and 2,000 psf when foundations are supported on imported sands (extending a minimum of 1.0 feet below footings). The allowable soil pressure may be increased by 20% for each foot of embedment depth in excess of 18 inches and by one-third for short term loads induced by winds or seismic events. The maximum allowable soil pressure at increased embedment depths shall not exceed 3,000 psf (clays). Settlements associated with variable loadings and structure/footing sizes are shown on figures 2 thru 5. As an alternative to shallow spread foundations, flat plate structural mats or grade-beam reinforced foundations may be used to mitigate expansive soil heave.

Flat Plate Structural Mats: Structural mats may be designed for a modulus of subgrade reaction (Ks) of 100 pci when placed on compacted clay or a subgrade modulus of 250 pci when placed on 2.5 feet of granular fill. Mats shall overlay 2 inches of sand and a 10-mil polyethylene vapor retarder. The structure support pad shall be moisture conditioned and recompacted as specified in Section 4.1 of this report.

All exterior and interior foundations should be embedded a minimum of 18 inches below the structure support pad or lowest adjacent final grade, whichever is deeper. Continuous wall footings should have a minimum width of 12 inches. Spread footings should have a minimum width of 24 inches. Recommended concrete reinforcement and sizing for all footings should be provided by the structural engineer.

Resistance to horizontal loads will be developed by passive earth pressure on the sides of footings or grade beams and frictional resistance developed along the bases of footings or grade beams and concrete slabs. Passive resistance to lateral earth pressure may be calculated using an equivalent fluid pressure of 250 pcf (300 pcf for sands) to resist lateral loadings. The top one foot of embedment should not be considered in computing passive resistance unless the adjacent area is confined by a slab or pavement. An allowable friction coefficient of 0.25 (0.35 for sands) may also be used at the base of the footings or grade beams to resist lateral loading.

Total foundation movements under estimated loadings are shown on the load/settlement curves (Figures 2 thru 5). Differential movement is estimated to be about two-thirds of total movement

4.3 Slabs-On-Grade

Thin concrete slabs and flatwork (6 inches or less in thickness) placed over native clay soil should be designed in accordance with Chapter 18, Division III of the 2001 CBC (using an Effective Plasticity Index of 17) and shall be a minimum of 5 inches thick due to expansive soil conditions. Concrete floor slabs shall be monolithically placed with the foundations unless placed on 2.5 feet of granular fill or lime treated soil.

The concrete slabs should be underlain by a minimum of 4 inches of clean sand (Sand Equivalent SE>30) or aggregate base or may be placed directly on a 2.5-foot thick granular fill pad (if used) that has been moistened to approximately optimum moisture just before the concrete placement. A 10-mil visqueen vapor retarder, properly lapped and sealed with a 2-inch sand cover and extended a minimum of 12 inches into the footing, should be placed as a capillary break to prevent moisture migration into the slab section. Concrete slabs may be placed directly over a 15-mil vapor retarder if desired (Stego-Wrap or equivalent).

Concrete slab and flatwork reinforcement should consist of chaired rebar slab reinforcement (minimum of No. 4 bars at 18-inch centers, both horizontal directions) placed at slab mid-height to resist potential swell forces and cracking. Slab thickness and steel reinforcement are minimums only and should be verified by the structural engineer/designer knowing the actual project loadings. All steel components of the foundation system should be protected from corrosion by maintaining a 4-inch minimum concrete cover of densely consolidated concrete at footings (by use of a vibrator). The construction joint between the foundation and any mowstrips/sidewalks placed adjacent to foundations should be sealed with a polyurethane based non-hardening sealant to prevent moisture migration between the joint. Epoxy coated embedded steel components or permanent waterproofing membranes placed at the exterior footing sidewall may also be used to mitigate the corrosion potential of concrete placed in contact with native soil.

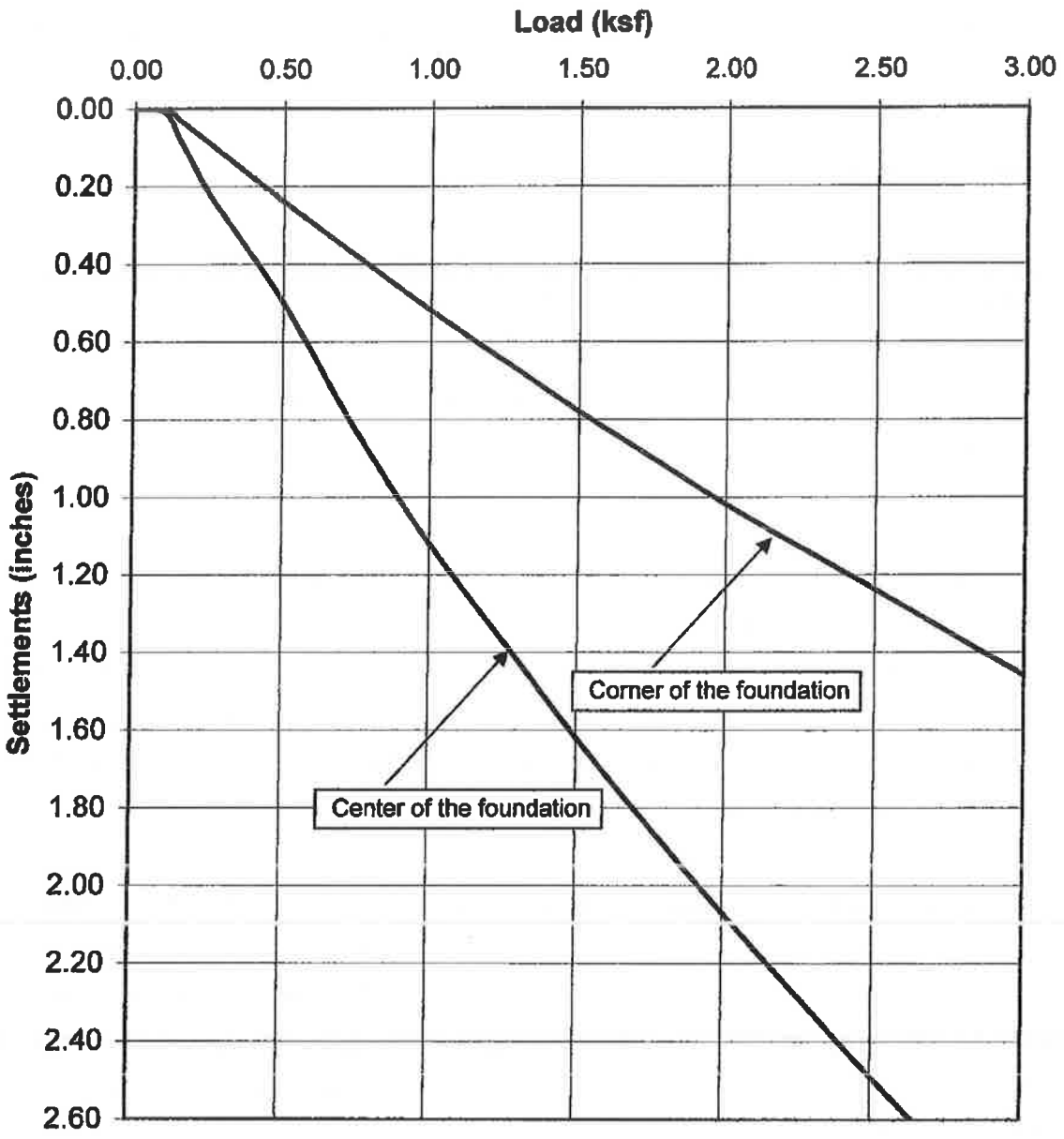

Notes:

1. A 15' x 15' foundation was used for settlement analysis

LANDMARK Geo-Engineers and Geologists *a DBE/MBE/SBE Company* **Project No.: LE04354**	**Total Settlements for a Turbine Generator Foundation at Heber 2 Geothermal Plant**	**Figure 2**

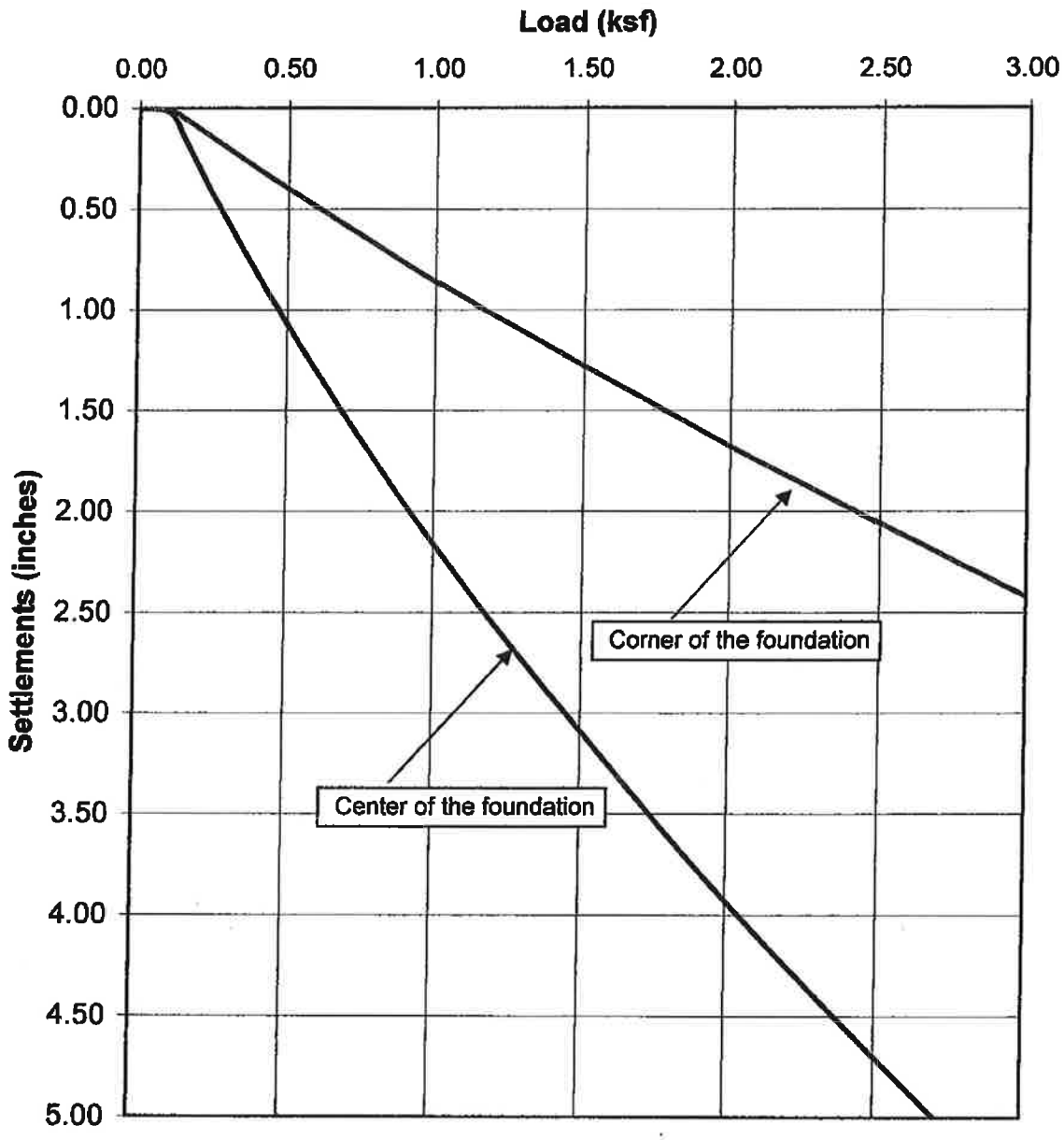

Notes:

1. A 30' x 60' foundation was used for settlement analysis

LANDMARK
Geo-Engineers and Geologists
a DBE/MBE/SBE Company
Project No.: LE04354

Total Settlements for a Turbine Generator Foundation at Heber 2 Geothermal Plant

Figure 3

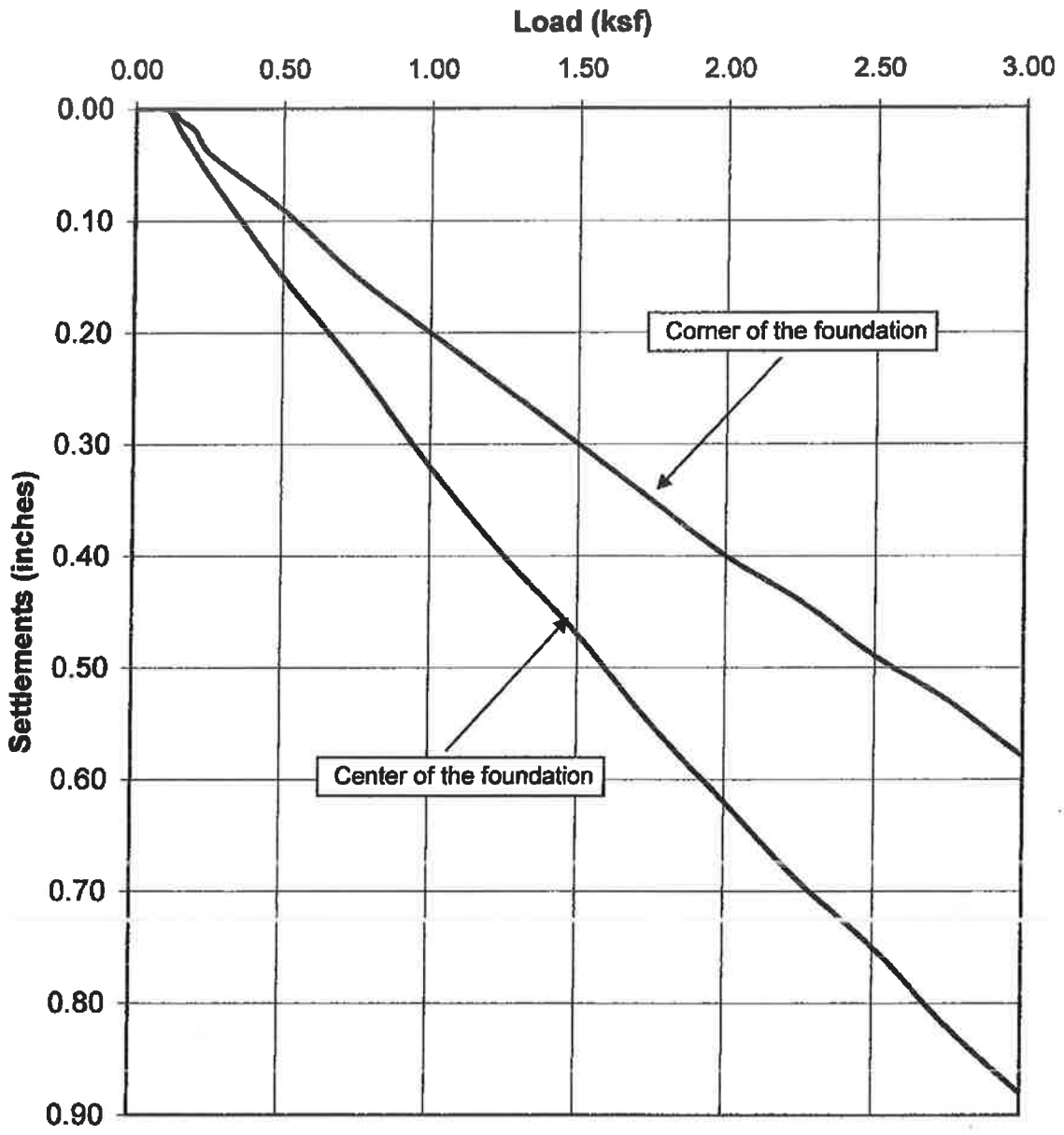

Notes:

1. A 5' x 5' foundation was used for settlement analysis

LANDMARK
Geo-Engineers and Geologists
a DBE/MBE/SBE Company
Project No.: LE04354

Total Settlements for a Cooling Tower Foundation at Heber 2 Geothermal Plant

Figure 4

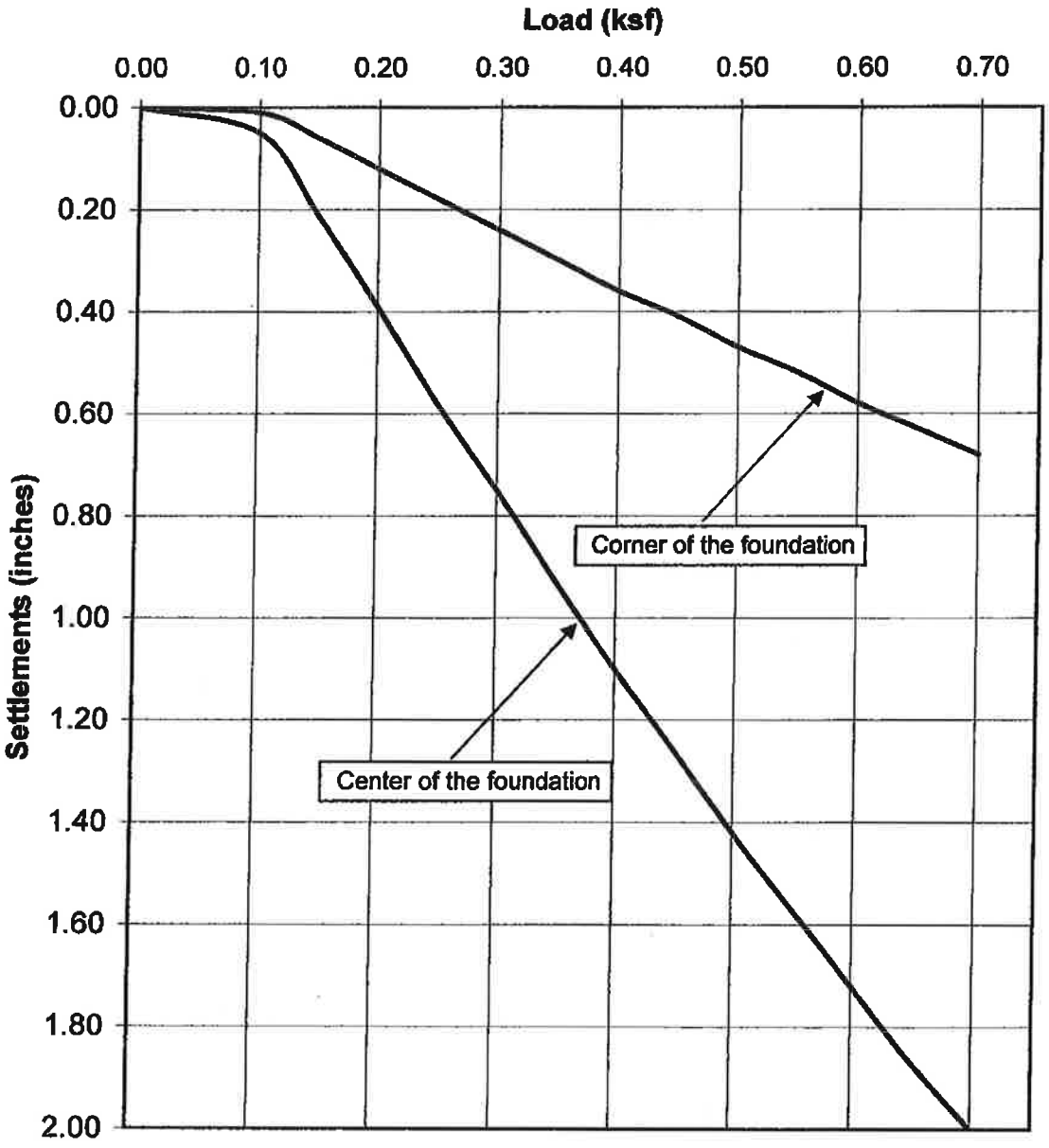

Notes:

1. A 60' x 180' foundation was used for settlement analysis

LANDMARK
Geo-Engineers and Geologists
a DBE/MBE/SBE Company
Project No.: LE04354

Total Settlements for a Cooling Tower Foundation at Heber 2 Geothermal Plant

Figure 5

Control joints should be provided in all concrete slabs-on-grade at a maximum spacing (in feet) of 2 to 3 times the slab thickness (in inches) as recommended by American Concrete Institute (ACI) guidelines. All joints should form approximately square patterns to reduce randomly oriented contraction cracks. Contraction joints in the slabs should be tooled at the time of the pour or sawcut (¼ of slab depth) within 6 to 8 hours of concrete placement. Construction (cold) joints in foundations and area flatwork should either be thickened butt-joints with dowels or a thickened keyed-joint designed to resist vertical deflection at the joint. All joints in flatwork should be sealed to prevent moisture, vermin, or foreign material intrusion. Precautions should be taken to prevent curling of slabs in this arid desert region (refer to ACI guidelines).

All independent flatwork (sidewalks, housekeeping slabs) should be placed on a minimum of 2 inches of concrete sand or aggregate base, dowelled to the perimeter foundations where adjacent to the structures and sloped 1% or more away from the structure. A minimum of 18 inches of moisture conditioned (3% minimum above optimum) and 8 inches of compacted subgrade (83 to 87%) and a 10-mil (minimum) polyethylene separation sheet should underlie the flatwork. All flatwork should be jointed in square patterns and at irregularities in shape at a maximum spacing of 10 feet or the least width of the sidewalk.

4.4 Concrete Mixes and Corrosivity

Selected chemical analyses for corrosivity were conducted on bulk samples of the near surface soil from the project site (Plates C-2 and C-3). The native soils were found to have moderate to severe levels of sulfate ion concentration (1,052 to 3,006 ppm). Sulfate ions in high concentrations can attack the cementitious material in concrete, causing weakening of the cement matrix and eventual deterioration by raveling. The California Building Code recommends that increased quantities of Type II Portland Cement be used at a low water/cement ratio when concrete is subjected to moderate sulfate concentrations. Type V Portland Cement and/or Type II/V cement with 25% flyash replacement is recommended when the concrete is subjected to soil with severe sulfate concentration.

A minimum of 6.25 sacks per cubic yard of concrete (4,500 psi) of Type V Portland Cement with a maximum water/cement ratio of 0.45 (by weight) should be used for concrete placed in contact with native soil on this project. Admixtures may be required to allow placement of this low water/cement ratio concrete.

There are no special requirements for concrete mixes when foundations are placed on 2.5 feet of low sulfate content granular fill.

The native soil has moderate to very severe level of chloride ion concentration (210 to 3,040 ppm). Chloride ions can cause corrosion of reinforcing steel, anchor bolts and other buried metallic conduits. Resistivity determinations on the soil indicate very severe potential for metal loss because of electrochemical corrosion processes. Mitigation of the corrosion of steel can be achieved by using steel pipes coated with epoxy corrosion inhibitors, asphaltic and epoxy coatings, cathodic protection or by encapsulating the portion of the pipe lying above groundwater with a minimum of 4 inches of densely consolidated concrete. ***No metallic pipes or conduits should be placed below foundations.***

Foundation designs shall provide a minimum concrete cover of four (4 inches around steel reinforcing or embedded components (anchor bolts, hold-downs, etc.) exposed to native soil or landscape water (to 18 inches above grade). If the 4-inch concrete edge distance cannot be achieved, all embedded steel components (anchor bolts, hold-downs, etc.) shall be epoxy dipped for corrosion protection or a corrosion inhibitor and a permanent waterproofing membrane shall be placed along the exterior face of the exterior footings. Additionally, the concrete should be thoroughly vibrated at footings during placement to decrease the permeability of the concrete.

4.5 Excavations

All site excavations should conform to CalOSHA requirements for Type B soil. The contractor is solely responsible for the safety of workers entering trenches. Temporary excavations with depths of 4 feet or less may be cut nearly vertical for short duration. Excavations deeper than 4 feet will require shoring or slope inclinations in conformance to CAL/OSHA regulations for Type B soil. Surcharge loads of stockpiled soil or construction materials should be set back from the top of the slope a minimum distance equal to the height of the slope. All permanent slopes should not be steeper than 3:1 to reduce wind and rain erosion. Protected slopes with ground cover may be as steep as 2:1. However, maintenance with motorized equipment may not be possible at this inclination.

4.6 Seismic Design

This site is located in the seismically active southern California area and the site structures are subject to strong ground shaking due to potential fault movements along the Brawley, Superstition Hills, and Imperial Faults. Engineered design and earthquake-resistant construction are the common solutions to increase safety and development of seismic areas. Designs should comply with the latest edition of the CBC for Seismic Zone 4 using the seismic coefficients given in Section 3.4 of this report. ***This site lies within 11.3 km of a Type A fault overlying S_D (stiff) soil.***

Section 5
LIMITATIONS AND ADDITIONAL SERVICES

5.1 Limitations

The recommendations and conclusions within this report are based on current information regarding the proposed additions to the Ormat Heber 2 geothermal power plant located on Dogwood Road southwest of Heber, California. The conclusions and recommendations of this report are invalid if:

- Structural loads change from those stated or the structures are relocated.
- The Additional Services section of this report is not followed.
- This report is used for adjacent or other property.
- Changes of grade or groundwater occur between the issuance of this report and construction other than those anticipated in this report.
- Any other change that materially alters the project from that proposed at the time this report was prepared.

Findings and recommendations in this report are based on selected points of field exploration, geologic literature, laboratory testing, and our understanding of the proposed project. Our analysis of data and recommendations presented herein are based on the assumption that soil conditions do not vary significantly from those found at specific exploratory locations. Variations in soil conditions can exist between and beyond the exploration points or groundwater elevations may change. If detected, these conditions may require additional studies, consultation, and possible design revisions.

This report contains information that may be useful in the preparation of contract specifications. However, the report is not worded is such a manner that we recommend its use as a construction specification document without proper modification. The use of information contained in this report for bidding purposes should be done at the contractor's option and risk.

This report was prepared according to the generally accepted *geotechnical engineering standards of practice* that existed in Imperial County at the time the report was prepared. No express or implied warranties are made in connection with our services. This report should be considered invalid for periods after two years from the report date without a review of the validity of the findings and recommendations by our firm, because of potential changes in the Geotechnical Engineering Standards of Practice.

The client has responsibility to see that all parties to the project including, designer, contractor, and subcontractor are made aware of this entire report. The use of information contained in this report for bidding purposes should be done at the contractor's option and risk.

5.2 Additional Services

We recommend that Landmark Consultants, Inc. be retained as the geotechnical consultant to provide the tests and observations services during construction. If Landmark Consultants does not provide such services then *the geotechnical engineering firm providing such tests and observations shall become the geotechnical engineer of record and assume responsibility for the project.*

The recommendations presented in this report are based on the assumption that:

- Consultation during development of design and construction documents to check that the geotechnical recommendations are appropriate for the proposed project and that the geotechnical recommendations are properly interpreted and incorporated into the documents.
- Landmark Consultants will have the opportunity to review and comment on the plans and specifications for the project prior to the issuance of such for bidding.
- Continuous observation, inspection, and testing by the geotechnical consultant of record during site clearing, grading, excavation, placement of fills, building pad and subgrade preparation, and backfilling of utility trenches.
- Observation of foundation excavations and reinforcing steel before concrete placement.
- Other consultation as necessary during design and construction.

We emphasize our review of the project plans and specifications to check for compatibility with our recommendations and conclusions. Additional information concerning the scope and cost of these services can be obtained from our office.

APPENDIX A

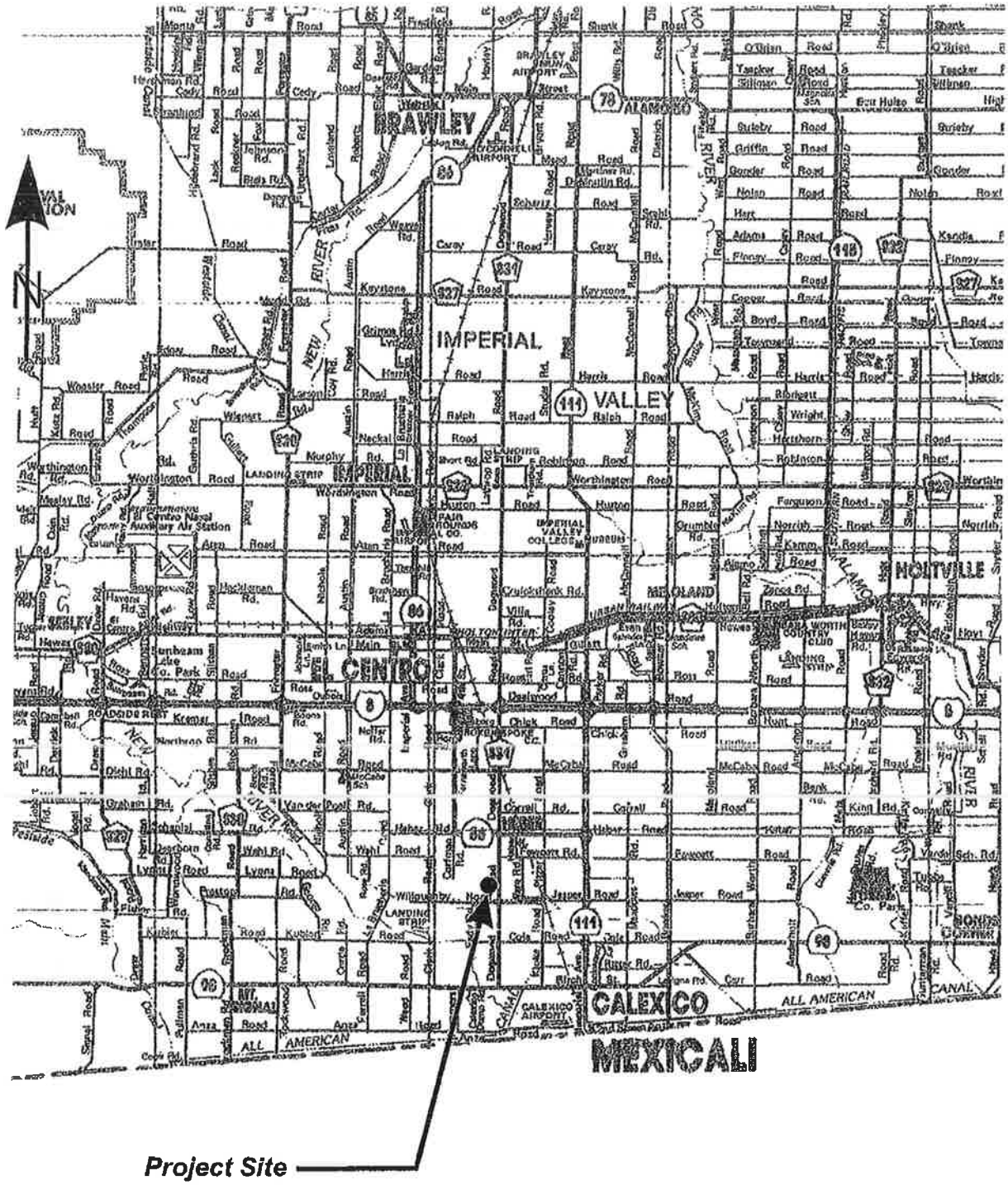

LANDMARK
Geo-Engineers and Geologists
a DBE/MBE/SBE Company

Project No.: LE04354

Vicinity Map

Plate
A-1

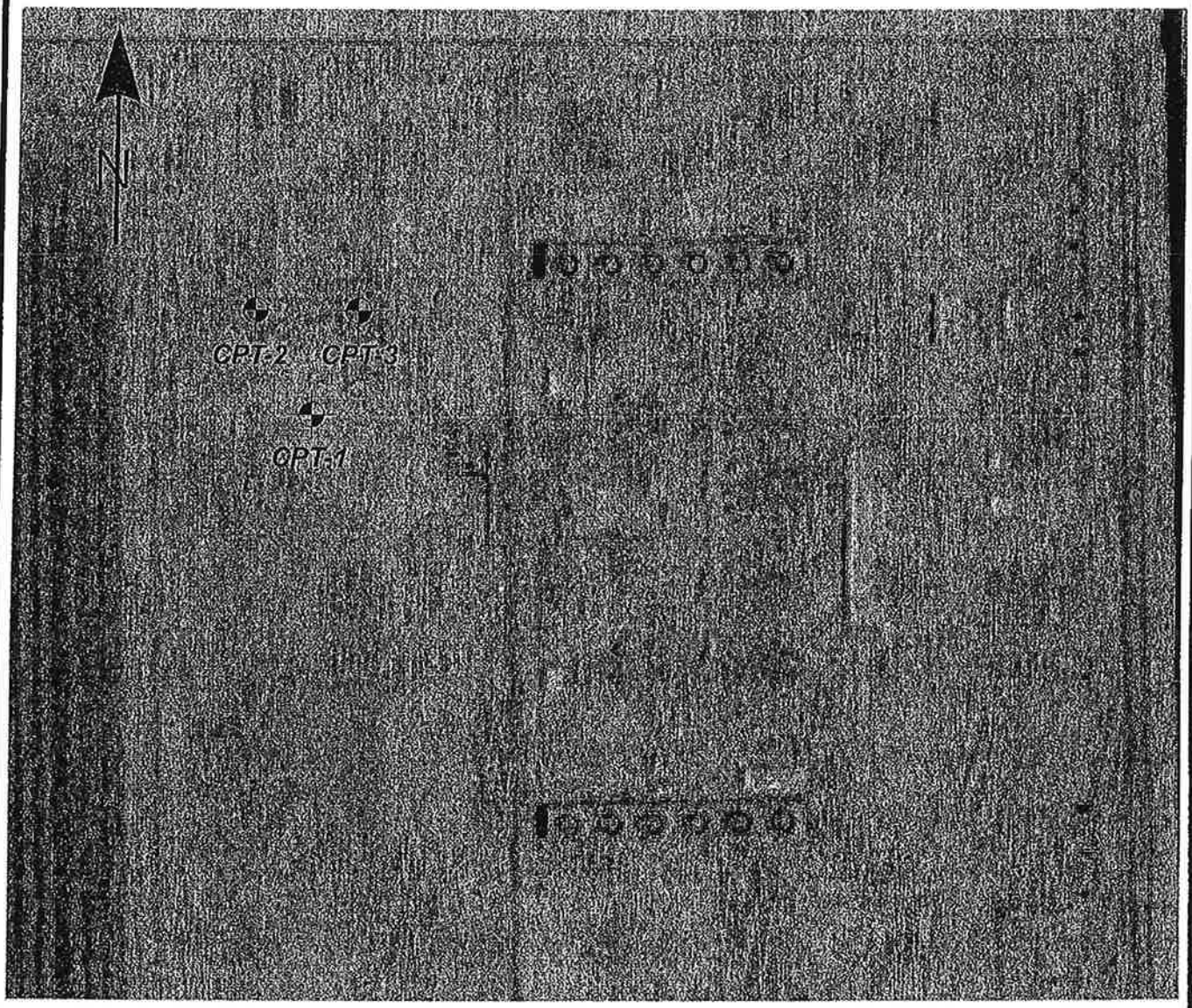

LANDMARK
Geo-Engineers and Geologists
a DBE/MBE/SBE Company

Project No.: LE04354

Site and Exploration Map

Plate
A-2

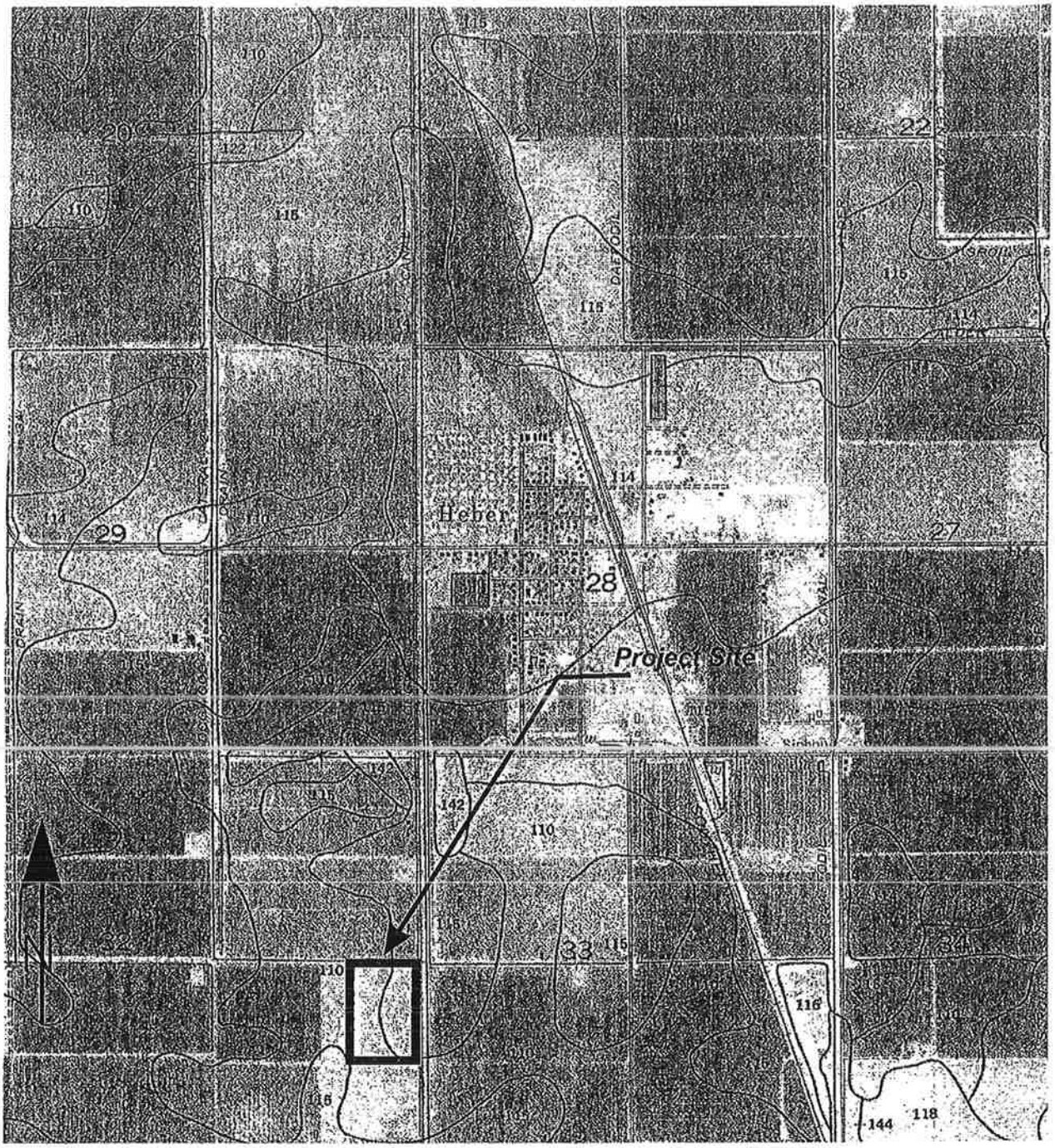

LANDMARK Geo-Engineers and Geologists a DBE/MSE/SBE Company Project No.: LE04354	Soil Survey Map	Plate A-3

Soil Survey of

IMPERIAL COUNTY CALIFORNIA IMPERIAL VALLEY AREA

United States Department of Agriculture Soil Conservation Service
in cooperation with
University of California Agricultural Experiment Station
and
Imperial Irrigation District

TABLE 11.--ENGINEERING INDEX PROPERTIES

[The symbol > means more than. Absence of an entry indicates that data were not estimated]

Soil name and map symbol	Depth	USDA texture	Classification		Fragments > 3 inches	Percentage passing sieve number--				Liquid limit	Plasticity index
			Unified	AASHTO		4	10	40	200		
	In				Pct					Pct	
100----------	0-13	Loamy fine sand	SM	A-2	0	100	100	75-85	10-30	---	NP
Antho	13-60	Sandy loam, fine sandy loam.	SM	A-2, A-4	0	90-100	75-95	50-60	15-40	---	NP
101*:											
Antho----------	0-8	Loamy fine sand	SM	A-2	0	100	100	75-85	10-30	---	NP
	8-60	Sandy loam, fine sandy loam.	SM	A-2, A-4	0	90-100	75-95	50-60	15-40	---	NP
Superstition------	0-6	Fine sand-------	SM	A-2	0	100	95-100	70-85	15-25	---	NP
	6-60	Loamy fine sand, fine sand, sand.	SM	A-2	0	100	95-100	70-85	15-25	---	NP
102*. Badland											
103----------	0-10	Gravelly sand---	SP, SP-SM	A-1, A-2	0-5	60-90	50-85	30-55	0-10	---	NP
Carsitas	10-60	Gravelly sand, gravelly coarse sand, sand.	SP, SP-SM	A-1	0-5	60-90	50-85	25-50	0-10	---	NP
104* Fluvaquents											
105----------	0-13	Clay loam-------	CL	A-6	0	100	100	90-100	70-95	35-45	15-30
Glenbar	13-60	Clay loam, silty clay loam.	CL	A-6	0	100	100	90-100	70-95	35-45	15-30
106----------	0-13	Clay loam-------	CL	A-6, A-7	0	100	100	90-100	70-95	35-45	15-25
Glenbar	13-60	Clay loam, silty clay loam.	CL	A-6, A-7	0	100	100	90-100	70-95	35-45	15-25
107*----------	0-13	Loam----------	ML, CL-ML, CL	A-4	0	100	100	100	70-80	20-30	NP-10
Glenbar	13-60	Clay loam, silty clay loam.	CL	A-6, A-7	0	100	100	95-100	75-95	35-45	15-30
108----------	0-14	Loam----------	ML	A-4	0	100	100	85-100	55-95	25-35	NP-10
Holtville	14-22	Clay, silty clay	CL, CH	A-7	0	100	100	95-100	85-95	40-65	20-35
	22-60	Silt loam, very fine sandy loam.	ML	A-4	0	100	100	95-100	65-85	25-35	NP-10
109----------	0-17	Silty clay------	CL, CH	A-7	0	100	100	95-100	85-95	40-65	20-35
Holtville	17-24	Clay, silty clay	CL, CH	A-7	0	100	100	95-100	85-95	40-65	20-35
	24-35	Silt loam, very fine sandy loam.	ML	A-4	0	100	100	95-100	65-85	25-35	NP-10
	35-60	Loamy very fine sand, loamy fine sand.	SM, ML	A-2, A-4	0	100	100	75-100	20-55	---	NP
110----------	0-17	Silty clay------	CH, CL	A-7	0	100	100	95-100	85-95	40-65	20-35
Holtville	17-24	Clay, silty clay	CH, CL	A-7	0	100	100	95-100	85-95	40-65	20-35
	24-35	Silt loam, very fine sandy loam.	ML	A-4	0	100	100	95-100	55-85	25-35	NP-10
	35-60	Loamy very fine sand, loamy fine sand.	SM, ML	A-2, A-4	0	100	100	75-100	20-55	---	NP

See footnote at end of table.

TABLE 11.--ENGINEERING INDEX PROPERTIES--Continued

Soil name and map symbol	Depth	USDA texture	Classification		Frag-ments > 3 inches	Percentage passing sieve number--				Liquid limit	Plas-ticity index
			Unified	AASHTO		4	10	40	200		
	In				Pct					Pct	
111*:											
Holtville	0-10	Silty clay loam	CL, CH	A-7	0	100	100	95-100	85-95	40-65	20-35
	10-22	Clay, silty clay	CL, CH	A-7	0	100	100	95-100	85-95	40-65	20-35
	22-60	Silt loam, very fine sandy loam.	ML	A-4	0	100	100	95-100	65-85	25-35	NP-10
Imperial	0-12	Silty clay loam	CL	A-7	0	100	100	100	85-95	40-50	10-20
	12-60	Silty clay loam, silty clay, clay.	CH	A-7	0	100	100	100	85-95	50-70	25-45
112	0-12	Silty clay	CH	A-7	0	100	100	100	85-95	50-70	25-45
Imperial	12-60	Silty clay loam, silty clay, clay.	CH	A-7	0	100	100	100	85-95	50-70	25-45
113	0-12	Silty clay	CH	A-7	0	100	100	100	85-95	50-70	25-45
Imperial	12-60	Silty clay, clay, silty clay loam.	CH	A-7	0	100	100	100	85-95	50-70	25-45
114	0-12	Silty clay	CH	A-7	0	100	100	100	85-95	50-70	25-45
Imperial	12-60	Silty clay loam, silty clay, clay.	CH	A-7	0	100	100	100	85-95	50-70	25-45
115*:											
Imperial	0-12	Silty clay loam	CL	A-7	0	100	100	100	85-95	40-50	10-20
	12-60	Silty clay loam, silty clay, clay.	CH	A-7	0	100	100	100	85-95	50-70	25-45
Glenbar	0-13	Silty clay loam	CL	A-6, A-7	0	100	100	90-100	70-95	35-45	15-25
	13-60	Clay loam, silty clay loam.	CL	A-6, A-7	0	100	100	90-100	70-95	35-45	15-25
116*:											
Imperial	0-13	Silty clay loam	CL	A-7	0	100	100	100	85-95	40-50	10-20
	13-60	Silty clay loam, silty clay, clay.	CH	A-7	0	100	100	100	85-95	50-70	25-45
Glenbar	0-13	Silty clay loam	CL	A-6, A-7	0	100	100	90-100	70-95	35-45	15-25
	13-60	Clay loam, silty clay loam.	CL	A-6	0	100	100	90-100	70-95	35-45	15-30
117, 118	0-12	Loam	ML	A-4	0	95-100	95-100	85-100	75-90	20-30	NP-5
Indio	12-72	Stratified loamy very fine sand to silt loam.	ML	A-4	0	95-100	95-100	85-100	75-90	20-30	NP-5
119*:											
Indio	0-12	Loam	ML	A-4	0	95-100	95-100	85-100	75-90	20-30	NP-5
	12-72	Stratified loamy very fine sand to silt loam.	ML	A-4	0	95-100	95-100	85-100	75-90	20-30	NP-5
Vint	0-10	Loamy fine sand	SM	A-2	0	95-100	95-100	70-80	25-35	---	NP
	10-60	Loamy sand, loamy fine sand.	SM	A-2	0	95-100	95-100	70-80	20-30	---	NP
120*	0-12	Loam	ML, CL-ML	A-4	0	100	95-100	75-85	55-65	20-30	NP-10
Laveen	12-60	Loam, very fine sandy loam.	ML, CL-ML	A-4	0	95-100	85-95	70-80	55-65	15-25	NP-10

See footnote at end of table.

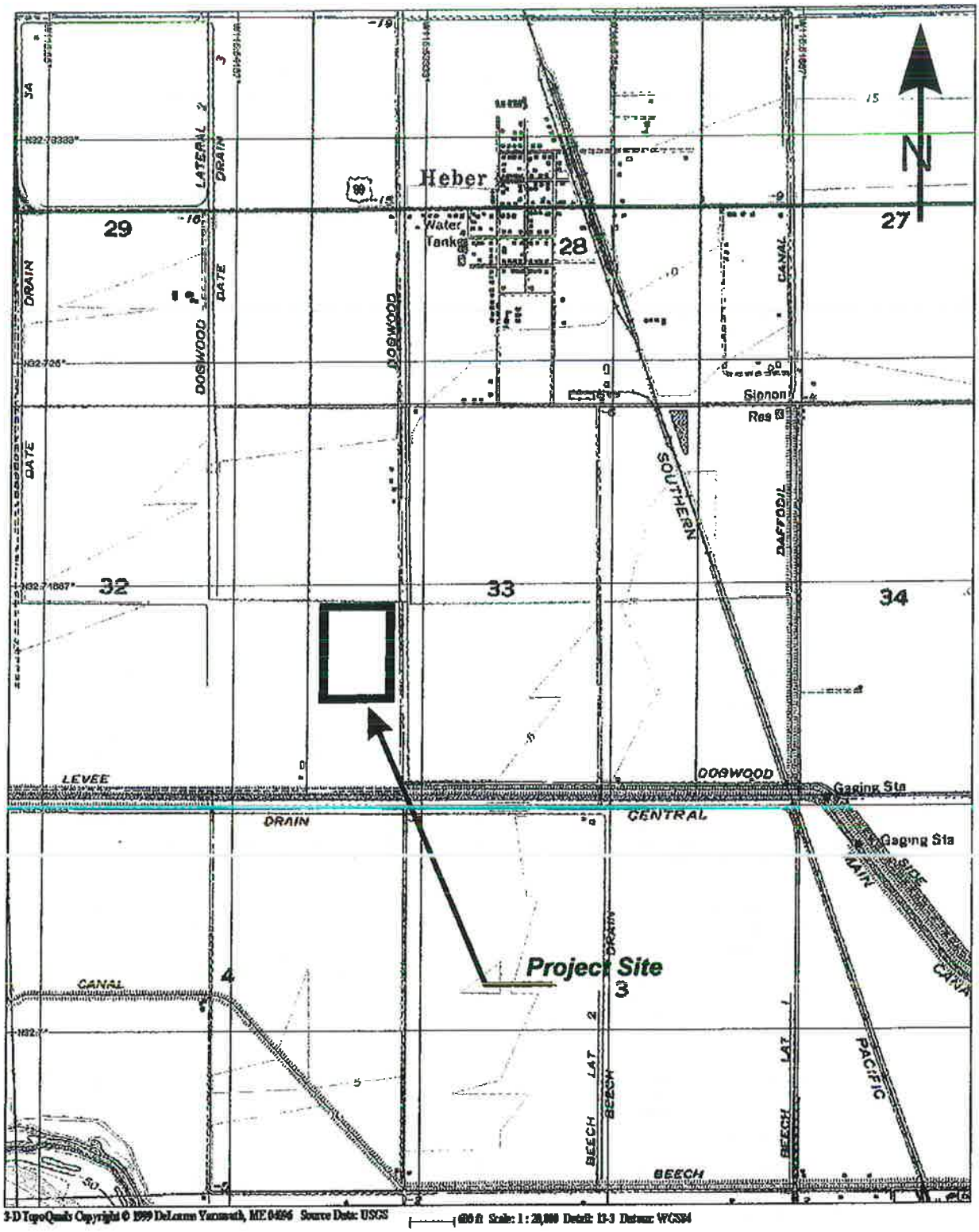

LANDMARK Geo-Engineers and Geologists a DBE/MBE/SBE Company **Project No.: LE04354**	**Topographic Map**	**Plate A-4**

APPENDIX B

CLIENT: ORMAT

PROJECT: ORMAT Heber 2 Facilities, Heber, CA

LOCATION: See Site and Boring Location Plan

CONE PENETROMETER: HOLGUIN, FAHAN & ASSC. Truck Mounted Electric Cone with 23 ton reaction weight

DATE: 12/20/04

LOG OF CONE SOUNDING DATA CPT-1

DEPTH (FEET)	INTERPRETED SOIL PROFILE From Robertson & Campanella (1989)		
	GROUND EL. +/-		
	Clay	CL/CH	hard
	Sandy Silt to Clayey Silt	ML	very dense
	Silty Sand to Sandy Silt	SM/ML	very dense
	Silty Sand to Sandy Silt	" "	very dense
	Silty Clay to Clay	CL	stiff
	Silty Clay to Clay	" "	stiff
	Clay	CL/CH	stiff
	Clay	" "	stiff
	Clay	" "	stiff
10	Clay	" "	very stiff
	Clay	" "	very stiff
	Silty Clay to Clay	CL	very stiff
	Clay	CL/CH	stiff
	Clay	" "	stiff
	Clay	" "	very stiff
	Clay	" "	very stiff
	Clay	" "	very stiff
	Clay	" "	very stiff
	Clay	" "	very stiff
20	Clay	" "	very stiff
	Clay	" "	stiff
	Clay	" "	very stiff
	Clay	" "	very stiff
	Clay	" "	very stiff
	Clay	" "	very stiff
	Clay	" "	very stiff
	Clay	" "	very stiff
	Clay	" "	very stiff
	Clay	" "	very stiff
30	Clay	" "	very stiff
	Clay	" "	very stiff
	Clay	" "	very stiff
	Clay	" "	very stiff
	Clay	" "	stiff
	Clay	" "	stiff
	Clay	" "	very stiff
	Clay	" "	very stiff
	Clayey Silt to Silty Clay	ML/CL	very stiff
	Silty Clay to Clay	CL	stiff
40	Clayey Silt to Silty Clay	ML/CL	stiff
	Clayey Silt to Silty Clay	" "	stiff
	Clayey Silt to Silty Clay	" "	stiff
	Clayey Silt to Silty Clay	" "	very stiff
	Clayey Silt to Silty Clay	" "	very stiff
	Clayey Silt to Silty Clay	" "	very stiff
	Clayey Silt to Silty Clay	" "	stiff
	Sandy Silt to Clayey Silt	ML	very loose
	Sandy Silt to Clayey Silt	" "	very loose
50	Clayey Silt to Silty Clay	ML/CL	stiff

End of Sounding @ 49.5 ft.

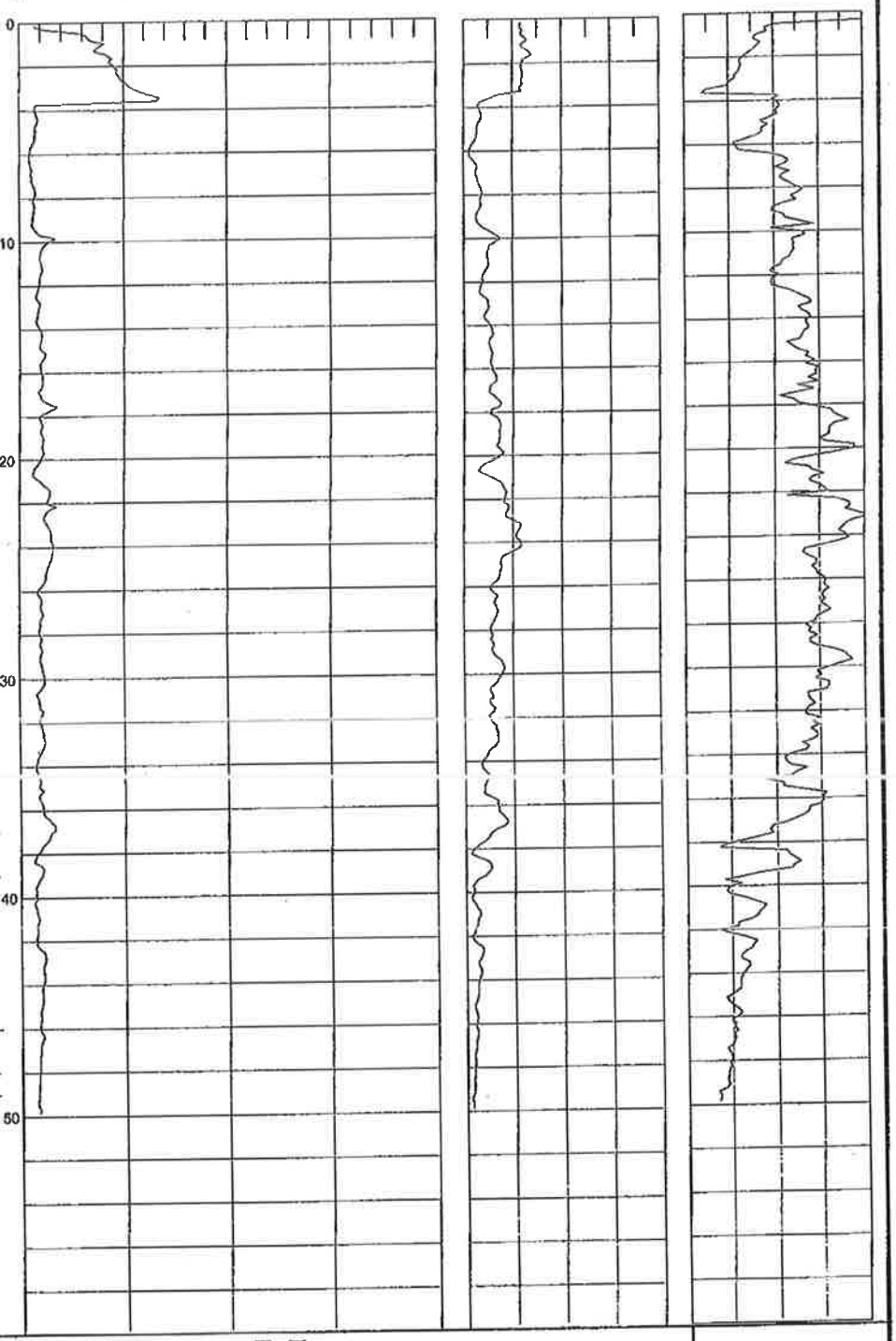

Project No: LE04354

LANDMARK Geo-Engineers and Geologists
a DBE/MBE/SBE Company

Plate B-1

LANDMARK CONSULTANTS, INC.

CONE PENETROMETER INTERPRETATION (based on Robertson & Campanella, 1989, refer to Key to CPT logs)

Project: ORMAT Heber 2 Facilities, Heber, CA Project No: LE04354 Date: 12/20/04

CONE SOUNDING: CPT-1

Est. GWT (ft): 12.0 Phi Correlation: 0 (0-Schm(78),1-R&C(83),2-PHT(74))

Base Depth meters	Base Depth feet	Avg Tip Qc, tsf	Avg Friction Ratio, %	1 Soil Type	Soil Classification	USC	Density or Consistency	Est. Density (pcf)	Qc to N	SPT N(60)	Cn or Cq	Norm. Qc1n	Est. % Fines	Rel. Dens. Dr (%)	Nk: Phi (deg.)	17.0 Su (tsf)	OCR
0.15	0.5	31.82	10.13	3	Clay	CL/CH	very stiff	125	1.3	25	2.00		95			1.87	>10
0.30	1.0	71.19	3.50	6	Sandy Silt to Clayey Silt	ML	very dense	115	3.5	20	2.00	134.6	45	107	43		
0.45	1.5	76.38	3.27	6	Sandy Silt to Clayey Silt	ML	very dense	115	3.5	22	2.00	144.4	40	102	42		
0.60	2.0	88.21	2.88	6	Sandy Silt to Clayey Silt	ML	very dense	115	3.5	25	2.00	166.8	35	101	42		
0.75	2.5	94.19	2.53	7	Silty Sand to Sandy Silt	SM/ML	very dense	115	4.5	21	2.00	178.0	30	100	42		
0.93	3.0	101.94	2.35	7	Silty Sand to Sandy Silt	SM/ML	very dense	115	4.5	23	2.00	192.7	30	99	42		
1.08	3.5	123.24	1.66	8	Sand to Silty Sand	SP/SM	very dense	115	5.5	22	2.00	233.0	20	102	42		
1.23	4.0	53.93	2.99	6	Sandy Silt to Clayey Silt	ML	dense	115	3.5	15	2.00	101.9	45	76	39		
1.38	4.5	16.43	4.19	3	Clay	CL/CH	stiff	125	1.3	13	2.00		85			0.95	>10
1.53	5.0	15.53	3.80	4	Silty Clay to Clay	CL	stiff	125	1.8	9	1.95		85			0.90	>10
1.68	5.5	13.99	3.48	4	Silty Clay to Clay	CL	stiff	125	1.8	8	1.85		85			0.80	>10
1.83	6.0	10.16	2.42	5	Clayey Silt to Silty Clay	ML/CL	stiff	120	2.5	4	1.76		85			0.58	>10
1.98	6.5	10.41	3.55	4	Silty Clay to Clay	CL	stiff	125	1.8	6	1.69		95			0.59	>10
2.13	7.0	11.62	4.38	3	Clay	CL/CH	stiff	125	1.3	9	1.62		100			0.66	>10
2.28	7.5	13.29	4.44	3	Clay	CL/CH	stiff	125	1.3	11	1.56		95			0.76	>10
2.45	8.0	14.55	4.93	3	Clay	CL/CH	stiff	125	1.3	12	1.51		95			0.83	>10
2.60	8.5	13.90	4.96	3	Clay	CL/CH	stiff	125	1.3	11	1.46		100			0.79	>10
2.75	9.0	13.23	4.08	3	Clay	CL/CH	stiff	125	1.3	11	1.42		95			0.75	>10
2.90	9.5	13.66	4.68	3	Clay	CL/CH	stiff	125	1.3	11	1.38		100			0.77	>10
3.05	10.0	26.88	5.00	3	Clay	CL/CH	very stiff	125	1.3	22	1.34		80			1.55	>10
3.20	10.5	21.69	5.01	3	Clay	CL/CH	very stiff	125	1.3	17	1.32		90			1.24	>10
3.35	11.0	19.84	4.85	3	Clay	CL/CH	very stiff	125	1.3	16	1.30		95			1.13	>10
3.50	11.5	21.31	4.45	4	Silty Clay to Clay	CL	very stiff	125	1.8	12	1.29		90			1.22	>10
3.65	12.0	18.97	4.00	4	Silty Clay to Clay	CL	very stiff	125	1.8	11	1.27		90			1.08	>10
3.80	12.5	16.82	3.86	4	Silty Clay to Clay	CL	stiff	125	1.8	10	1.26		95			0.95	>10
3.95	13.0	18.18	4.91	3	Clay	CL/CH	very stiff	125	1.3	15	1.24		100			1.03	>10
4.13	13.5	17.33	5.43	3	Clay	CL/CH	stiff	125	1.3	14	1.23		100			0.98	>10
4.28	14.0	17.04	5.46	3	Clay	CL/CH	stiff	125	1.3	14	1.22		100			0.96	>10
4.43	14.5	21.21	5.45	3	Clay	CL/CH	very stiff	125	1.3	17	1.20		100			1.20	>10
4.58	15.0	19.96	5.21	3	Clay	CL/CH	very stiff	125	1.3	16	1.19		100			1.13	>10
4.73	15.5	23.41	4.80	3	Clay	CL/CH	very stiff	125	1.3	19	1.18		95			1.33	>10
4.88	16.0	20.50	5.51	3	Clay	CL/CH	very stiff	125	1.3	16	1.17		100			1.16	>10
5.03	16.5	21.94	5.88	3	Clay	CL/CH	very stiff	125	1.3	18	1.15		100			1.24	>10
5.18	17.0	19.22	5.48	3	Clay	CL/CH	very stiff	125	1.3	15	1.14		100			1.08	>10
5.33	17.5	27.57	5.03	3	Clay	CL/CH	very stiff	125	1.3	22	1.13		95			1.57	>10
5.48	18.0	23.29	5.22	3	Clay	CL/CH	very stiff	125	1.3	19	1.12		100			1.32	>10
5.65	18.5	20.85	6.67	3	Clay	CL/CH	very stiff	125	1.3	17	1.11		100			1.18	>10
5.80	19.0	21.33	6.77	3	Clay	CL/CH	very stiff	125	1.3	17	1.10		100			1.20	>10
5.95	19.5	21.97	6.29	3	Clay	CL/CH	very stiff	125	1.3	18	1.09		100			1.24	>10
6.10	20.0	21.34	7.09	3	Clay	CL/CH	very stiff	125	1.3	17	1.08		100			1.20	>10
6.25	20.5	15.48	5.72	3	Clay	CL/CH	stiff	125	1.3	12	1.07		100			0.86	5.53
6.40	21.0	15.87	5.20	3	Clay	CL/CH	stiff	125	1.3	13	1.06		100			0.88	5.65
6.55	21.5	26.53	5.79	3	Clay	CL/CH	very stiff	125	1.3	21	1.05		100			1.50	>10
6.70	22.0	27.19	6.21	3	Clay	CL/CH	very stiff	125	1.3	22	1.05		100			1.54	>10
6.85	22.5	29.12	6.18	3	Clay	CL/CH	very stiff	125	1.3	23	1.04		100			1.65	>10
7.00	23.0	24.40	7.41	3	Clay	CL/CH	very stiff	125	1.3	20	1.03		100			1.38	>10
7.18	23.5	29.74	7.65	3	Clay	CL/CH	very stiff	125	1.3	24	1.02		100			1.69	>10
7.33	24.0	31.24	7.01	3	Clay	CL/CH	very stiff	125	1.3	25	1.01		100			1.78	>10
7.48	24.5	31.71	6.74	3	Clay	CL/CH	very stiff	125	1.3	25	1.01		100			1.80	>10
7.63	25.0	28.38	5.36	3	Clay	CL/CH	very stiff	125	1.3	23	1.00		100			1.61	>10
7.78	25.5	25.50	5.79	3	Clay	CL/CH	very stiff	125	1.3	20	0.99		100			1.44	>10
7.93	26.0	21.23	6.01	3	Clay	CL/CH	very stiff	125	1.3	17	0.98		100			1.18	7.00
8.08	26.5	19.41	6.26	3	Clay	CL/CH	very stiff	125	1.3	16	0.98		100			1.08	6.00
8.23	27.0	21.10	6.12	3	Clay	CL/CH	very stiff	125	1.3	17	0.97		100			1.17	6.65
8.38	27.5	20.13	6.30	3	Clay	CL/CH	very stiff	125	1.3	16	0.96		100			1.12	6.00
8.53	28.0	19.23	5.66	3	Clay	CL/CH	very stiff	125	1.3	15	0.96		100			1.06	5.42
8.68	28.5	20.08	5.65	3	Clay	CL/CH	very stiff	125	1.3	16	0.95		100			1.11	5.76
8.85	29.0	20.55	5.67	3	Clay	CL/CH	very stiff	125	1.3	16	0.94		100			1.14	5.88
9.00	29.5	20.76	7.00	3	Clay	CL/CH	very stiff	125	1.3	17	0.94		100			1.15	5.88
9.15	30.0	22.80	6.88	3	Clay	CL/CH	very stiff	125	1.3	18	0.93		100			1.27	6.65

LANDMARK CONSULTANTS, INC.

CONE PENETROMETER INTERPRETATION (based on Robertson & Campanella, 1989, refer to Key to CPT logs)

Project: ORMAT Heber 2 Facilities, Heber, CA Project No: LE04354 Date: 12/20/04

CONE SOUNDING: CPT-1

Est. GWT (ft): 12.0 Phi Correlation: 0 0-Schm(78),1-R&C(83),2-PHT(74)

Base Depth meters	Base Depth feet	Avg Tip Qc, tsf	Avg Friction Ratio, %	1 Soil Type	Soil Classification	USC	Density or Consistency	Est. Density (pcf)	Qc to N	SPT N(60)	Cn or Cq	Norm. Qc1n	Est. % Fines	Rel. Dens. Dr (%)	Nk: Phi (deg.)	17.0 Su (tsf)	OCR
9.30	30.5	21.60	5.89	3 3	Clay	CL/CH	very stiff	125	1.3	17	0.93		100			1.20	6.00
9.45	31.0	17.19	6.36	3 3	Clay	CL/CH	stiff	125	1.3	14	0.92		100			0.94	4.00
9.60	31.5	20.05	5.47	3 3	Clay	CL/CH	very stiff	125	1.3	16	0.92		100			1.10	5.10
9.75	32.0	19.47	5.50	3 3	Clay	CL/CH	very stiff	125	1.3	16	0.91		100			1.07	4.88
9.90	32.5	21.74	5.63	3 3	Clay	CL/CH	very stiff	125	1.3	17	0.90		100			1.20	5.53
10.05	33.0	23.37	5.76	3 3	Clay	CL/CH	very stiff	125	1.3	19	0.90		100			1.30	6.10
10.20	33.5	20.39	5.56	3 3	Clay	CL/CH	very stiff	125	1.3	16	0.89		100			1.12	4.78
10.36	34.0	15.97	5.12	3 3	Clay	CL/CH	stiff	125	1.3	13	0.89		100			0.86	3.28
10.53	34.5	16.45	4.48	3 3	Clay	CL/CH	stiff	125	1.3	13	0.88		100			0.89	3.35
10.68	35.0	18.50	4.96	3 3	Clay	CL/CH	very stiff	125	1.3	15	0.88		100			1.01	3.91
10.83	35.5	19.11	4.05	4 4	Silty Clay to Clay	CL	very stiff	125	1.8	11	0.87		100			1.04	5.21
10.98	36.0	20.64	5.86	3 3	Clay	CL/CH	very stiff	125	1.3	17	0.87		100			1.13	4.47
11.13	36.5	25.44	5.72	3 3	Clay	CL/CH	very stiff	125	1.3	20	0.86		100			1.41	6.21
11.28	37.0	31.72	4.84	4 4	Silty Clay to Clay	CL	very stiff	125	1.8	18	0.86		100			1.78	>10
11.43	37.5	25.49	3.77	5 5	Clayey Silt to Silty Clay	ML/CL	very stiff	120	2.5	10	0.85		100			1.41	>10
11.58	38.0	17.68	2.48	5 5	Clayey Silt to Silty Clay	ML/CL	stiff	120	2.5	7	0.85		100			0.95	5.65
11.73	38.5	15.25	3.47	4 4	Silty Clay to Clay	CL	stiff	125	1.8	9	0.85		100			0.81	3.35
11.88	39.0	20.64	4.84	3 3	Clay	CL/CH	very stiff	125	1.3	17	0.84		100			1.13	4.00
12.05	39.5	15.50	3.51	4 4	Silty Clay to Clay	CL	stiff	125	1.8	9	0.84		100			0.82	3.28
12.20	40.0	14.77	2.00	5 5	Clayey Silt to Silty Clay	ML/CL	stiff	120	2.5	6	0.83		100			0.78	3.91
12.35	40.5	13.50	2.07	5 5	Clayey Silt to Silty Clay	ML/CL	stiff	120	2.5	5	0.83		100			0.70	3.43
12.50	41.0	15.96	3.29	4 4	Silty Clay to Clay	CL	stiff	125	1.8	9	0.82		100			0.85	3.28
12.65	41.5	15.32	3.05	5 5	Clayey Silt to Silty Clay	ML/CL	stiff	120	2.5	6	0.82		100			0.81	4.00
12.80	42.0	14.74	2.01	5 5	Clayey Silt to Silty Clay	ML/CL	stiff	120	2.5	6	0.82		100			0.77	3.66
12.95	42.5	17.48	2.54	5 5	Clayey Silt to Silty Clay	ML/CL	stiff	120	2.5	7	0.81		100			0.93	4.78
13.10	43.0	22.47	2.80	5 5	Clayey Silt to Silty Clay	ML/CL	very stiff	120	2.5	9	0.81		100			1.23	7.13
13.25	43.5	20.78	2.49	5 5	Clayey Silt to Silty Clay	ML/CL	very stiff	120	2.5	8	0.81		100			1.13	6.21
13.40	44.0	21.29	2.62	5 5	Clayey Silt to Silty Clay	ML/CL	very stiff	120	2.5	9	0.80		100			1.16	6.43
13.56	44.5	19.71	2.35	5 5	Clayey Silt to Silty Clay	ML/CL	very stiff	120	2.5	8	0.80		100			1.06	5.53
13.73	45.0	19.60	2.17	5 5	Clayey Silt to Silty Clay	ML/CL	very stiff	120	2.5	8	0.80		100			1.05	5.42
13.88	45.5	18.05	1.84	6 6	Sandy Silt to Clayey Silt	ML	very loose	115	3.5	5	0.79	13.5	100	13	30		
14.03	46.0	17.42	2.29	5 5	Clayey Silt to Silty Clay	ML/CL	stiff	120	2.5	7	0.79		100			0.92	4.28
14.18	46.5	19.49	2.03	6 6	Sandy Silt to Clayey Silt	ML	very loose	115	3.5	6	0.79	14.5	100	15	30		
14.33	47.0	17.99	2.10	5 5	Clayey Silt to Silty Clay	ML/CL	stiff	120	2.5	7	0.78		100			0.96	4.37
14.48	47.5	16.62	1.85	5 5	Clayey Silt to Silty Clay	ML/CL	stiff	120	2.5	7	0.78		100			0.88	3.83
14.63	48.0	16.66	1.91	5 5	Clayey Silt to Silty Clay	ML/CL	stiff	120	2.5	7	0.78		100			0.88	3.83
14.78	48.5	15.96	1.83	5 5	Clayey Silt to Silty Clay	ML/CL	stiff	120	2.5	6	0.77		100			0.83	3.58
14.93	49.0	15.56	1.78	5 5	Clayey Silt to Silty Clay	ML/CL	stiff	120	2.5	6	0.77		100			0.81	3.35
15.10	49.5	14.89	1.48	6 6	Sandy Silt to Clayey Silt	ML	very loose	115	3.5	4	0.77	10.8	100	7	29		

CLIENT: ORMAT

PROJECT: ORMAT Heber 2 Facilities, Heber, CA

LOCATION: See Site and Boring Location Plan

CONE PENETROMETER: HOLGUIN, FAHAN & ASSC. Truck Mounted Electric Cone with 23 ton reaction weight

DATE: 12/20/04

LOG OF CONE SOUNDING DATA CPT-2

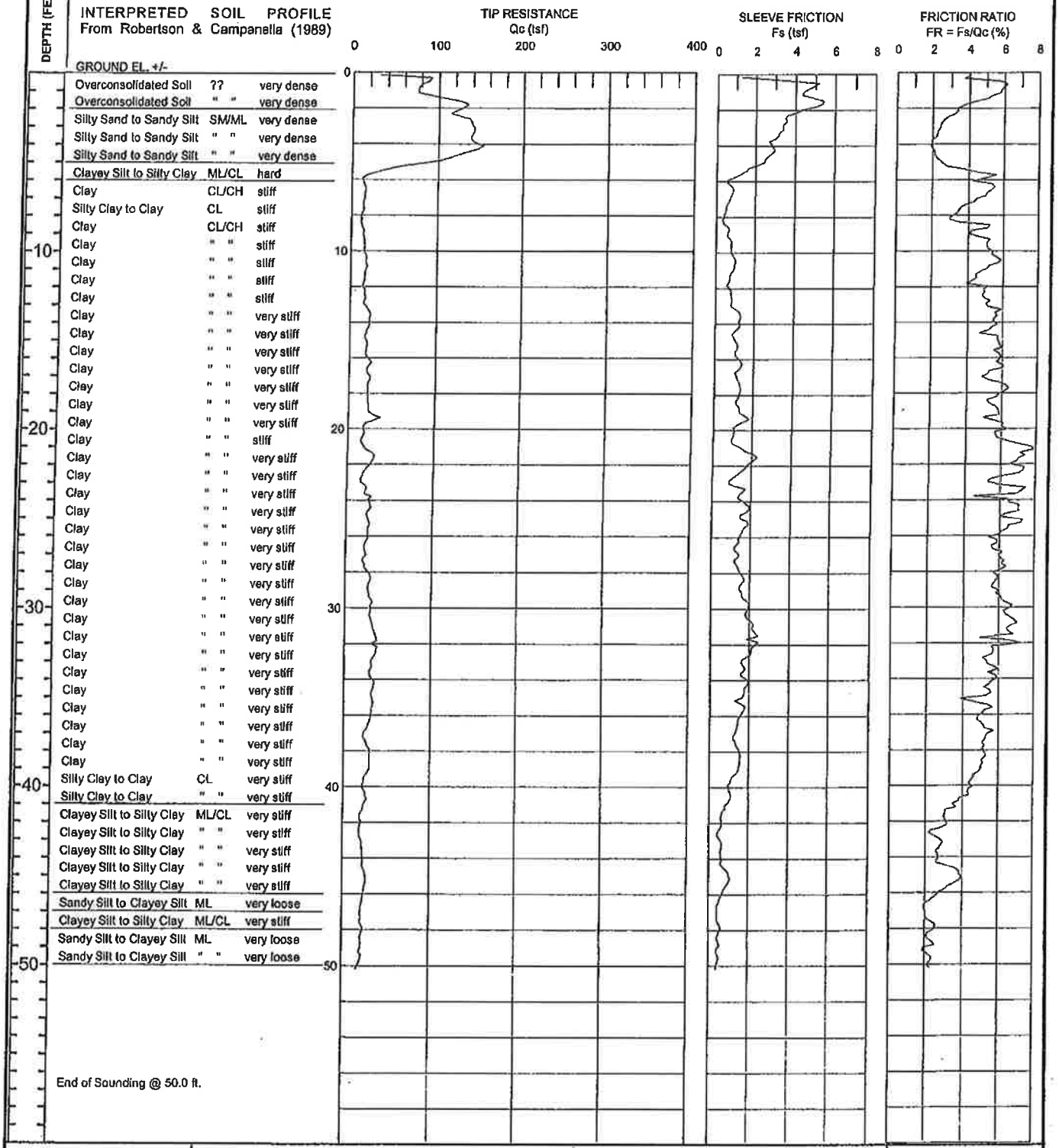

Project No: LE04354	LANDMARK Geo-Engineers and Geologists a DBE/MBE/SBE Company	Plate B-2

LANDMARK CONSULTANTS, INC.

CONE PENETROMETER INTERPRETATION (based on Robertson & Campanella, 1989, refer to Key to CPT logs)

Project: ORMAT Heber 2 Facilities, Heber, CA Project No: LE04354 Date: 12/20/04

CONE SOUNDING: CPT-2

Est. GWT (ft): 12.0 Phi Correlation: 0 0-Schm(78),1-R&C(83),2-PHT(74)

Base Depth meters	Base Depth feet	Avg Tip Qc, tsf	Avg Friction Ratio, %	1	Soil Type	Soil Classification	USC	Density or Consistency	Est. Density (pcf)	Qc to N	SPT N(60)	Cn or Cq	Norm. Qc1n	Est. % Fines	Rel. Dens. Dr (%)	Nk: Phi (deg.)	17.0 Su (tsf)	OCR
0.15	0.5	70.28	4.52	5	5	Clayey Silt to Silty Clay	ML/CL	hard	120	2.5	28	2.00		50			4.13	>10
0.30	1.0	77.82	5.97	11	11	Overconsolidated Soil	??	very dense	120	1.0	78	2.00	147.1	55	110	43		
0.45	1.5	91.98	5.31	11	11	Overconsolidated Soil	??	very dense	120	1.0	92	2.00	173.9	50	107	43		
0.60	2.0	129.94	3.78	6	6	Sandy Silt to Clayey Silt	ML	very dense	115	3.5	37	2.00	245.6	35	113	44		
0.76	2.5	119.62	3.11	6	6	Sandy Silt to Clayey Silt	ML	very dense	115	3.5	34	2.00	226.1	30	107	43		
0.93	3.0	137.68	2.51	7	7	Silty Sand to Sandy Silt	SM/ML	very dense	115	4.5	31	2.00	260.3	25	108	43		
1.08	3.5	140.87	2.30	7	7	Silty Sand to Sandy Silt	SM/ML	very dense	115	4.5	31	2.00	266.3	25	106	43		
1.23	4.0	139.35	2.04	7	7	Silty Sand to Sandy Silt	SM/ML	very dense	115	4.5	31	2.00	263.4	20	104	43		
1.38	4.5	144.85	2.01	7	7	Silty Sand to Sandy Silt	SM/ML	very dense	115	4.5	32	2.00	273.8	20	103	42		
1.53	5.0	113.08	2.24	7	7	Silty Sand to Sandy Silt	SM/ML	very dense	115	4.5	25	1.95	208.9	25	94	41		
1.68	5.5	52.70	3.38	5	5	Clayey Silt to Silty Clay	ML/CL	hard	120	2.5	21	1.86		50			3.08	>10
1.83	6.0	13.87	4.91	3	3	Clay	CL/CH	stiff	125	1.3	11	1.77		95			0.80	>10
1.98	6.5	15.08	5.36	3	3	Clay	CL/CH	stiff	125	1.3	12	1.70		95			0.87	>10
2.13	7.0	14.77	4.81	3	3	Clay	CL/CH	stiff	125	1.3	12	1.63		95			0.85	>10
2.28	7.5	13.38	3.90	3	3	Clay	CL/CH	stiff	125	1.3	11	1.57		90			0.76	>10
2.45	8.0	12.25	3.27	4	4	Silty Clay to Clay	CL	stiff	125	1.8	7	1.51		90			0.69	>10
2.60	8.5	11.34	3.86	3	3	Clay	CL/CH	stiff	125	1.3	9	1.46		100			0.64	9.79
2.75	9.0	13.62	4.43	3	3	Clay	CL/CH	stiff	125	1.3	11	1.42		95			0.77	>10
2.90	9.5	14.76	4.97	3	3	Clay	CL/CH	stiff	125	1.3	12	1.38		100			0.84	>10
3.05	10.0	15.04	5.19	3	3	Clay	CL/CH	stiff	125	1.3	12	1.34		100			0.85	>10
3.20	10.5	17.24	5.61	3	3	Clay	CL/CH	stiff	125	1.3	14	1.33		100			0.98	>10
3.35	11.0	17.82	5.31	3	3	Clay	CL/CH	very stiff	125	1.3	14	1.31		100			1.01	>10
3.50	11.5	16.22	4.53	3	3	Clay	CL/CH	stiff	125	1.3	13	1.29		100			0.92	>10
3.65	12.0	14.59	4.45	3	3	Clay	CL/CH	stiff	125	1.3	12	1.28		100			0.82	9.19
3.80	12.5	15.95	4.89	3	3	Clay	CL/CH	stiff	125	1.3	13	1.26		100			0.90	>10
3.95	13.0	16.10	5.07	3	3	Clay	CL/CH	stiff	125	1.3	13	1.25		100			0.91	>10
4.13	13.5	20.52	5.55	3	3	Clay	CL/CH	very stiff	125	1.3	16	1.23		100			1.17	>10
4.28	14.0	22.48	5.55	3	3	Clay	CL/CH	very stiff	125	1.3	18	1.22		100			1.28	>10
4.43	14.5	20.89	5.42	3	3	Clay	CL/CH	very stiff	125	1.3	17	1.21		100			1.19	>10
4.58	15.0	17.79	5.37	3	3	Clay	CL/CH	very stiff	125	1.3	14	1.19		100			1.00	>10
4.73	15.5	19.47	5.86	3	3	Clay	CL/CH	very stiff	125	1.3	16	1.18		100			1.10	>10
4.88	16.0	19.76	5.77	3	3	Clay	CL/CH	very stiff	125	1.3	16	1.17		100			1.12	>10
5.03	16.5	22.53	5.91	3	3	Clay	CL/CH	very stiff	125	1.3	18	1.16		100			1.28	>10
5.18	17.0	21.67	5.09	3	3	Clay	CL/CH	very stiff	125	1.3	17	1.15		100			1.23	>10
5.33	17.5	22.15	5.77	3	3	Clay	CL/CH	very stiff	125	1.3	18	1.13		100			1.25	>10
5.48	18.0	21.43	6.10	3	3	Clay	CL/CH	very stiff	125	1.3	17	1.12		100			1.21	>10
5.65	18.5	21.56	5.34	3	3	Clay	CL/CH	very stiff	125	1.3	17	1.11		100			1.22	>10
5.80	19.0	22.73	5.72	3	3	Clay	CL/CH	very stiff	125	1.3	18	1.10		100			1.29	>10
5.95	19.5	30.63	5.48	3	3	Clay	CL/CH	very stiff	125	1.3	25	1.09		95			1.75	>10
6.10	20.0	17.95	6.14	3	3	Clay	CL/CH	very stiff	125	1.3	14	1.08		100			1.00	7.41
6.25	20.5	17.30	5.70	3	3	Clay	CL/CH	stiff	125	1.3	14	1.07		100			0.96	6.65
6.40	21.0	16.60	6.99	3	3	Clay	CL/CH	stiff	125	1.3	13	1.07		100			0.92	6.10
6.55	21.5	26.75	7.44	3	3	Clay	CL/CH	very stiff	125	1.3	21	1.06		100			1.52	>10
6.70	22.0	28.17	6.81	3	3	Clay	CL/CH	very stiff	125	1.3	23	1.05		100			1.60	>10
6.85	22.5	20.17	7.24	3	3	Clay	CL/CH	very stiff	125	1.3	16	1.04		100			1.13	7.85
7.00	23.0	16.15	5.62	3	3	Clay	CL/CH	stiff	125	1.3	13	1.03		100			0.89	5.21
7.18	23.5	21.37	6.84	3	3	Clay	CL/CH	very stiff	125	1.3	17	1.02		100			1.20	8.27
7.33	24.0	24.23	5.98	3	3	Clay	CL/CH	very stiff	125	1.3	19	1.02		100			1.36	>10
7.48	24.5	27.09	6.88	3	3	Clay	CL/CH	very stiff	125	1.3	22	1.01		100			1.53	>10
7.63	25.0	23.97	6.46	3	3	Clay	CL/CH	very stiff	125	1.3	19	1.00		100			1.35	9.39
7.78	25.5	25.90	6.98	3	3	Clay	CL/CH	very stiff	125	1.3	21	0.99		100			1.46	>10
7.93	26.0	24.80	6.17	3	3	Clay	CL/CH	very stiff	125	1.3	20	0.99		100			1.39	9.59
8.08	26.5	22.94	5.66	3	3	Clay	CL/CH	very stiff	125	1.3	18	0.98		100			1.28	8.00
8.23	27.0	22.28	5.92	3	3	Clay	CL/CH	very stiff	125	1.3	18	0.97		100			1.24	7.27
8.38	27.5	20.15	6.14	3	3	Clay	CL/CH	very stiff	125	1.3	16	0.97		100			1.12	6.10
8.53	28.0	24.13	6.05	3	3	Clay	CL/CH	very stiff	125	1.3	19	0.96		100			1.35	8.14
8.68	28.5	28.28	5.86	3	3	Clay	CL/CH	very stiff	125	1.3	23	0.95		100			1.59	>10
8.85	29.0	26.02	5.73	3	3	Clay	CL/CH	very stiff	125	1.3	21	0.95		100			1.46	8.85
9.00	29.5	28.06	6.01	3	3	Clay	CL/CH	very stiff	125	1.3	22	0.94		100			1.56	>10
9.15	30.0	29.72	6.57	3	3	Clay	CL/CH	very stiff	125	1.3	24	0.93		100			1.68	>10

LANDMARK CONSULTANTS, INC.

CONE PENETROMETER INTERPRETATION (based on Robertson & Campanella, 1989, refer to Key to CPT logs)

Project: ORMAT Heber 2 Facilities, Heber, CA Project No: LE04354 Date: 12/20/04

CONE SOUNDING: CPT-2

Est. GWT (ft): 12.0 Phi Correlation: 0 0-Schm(78),1-R&C(83),2-PHT(74)

Base Depth meters	Base Depth feet	Avg Tip Qc, tsf	Avg Friction Ratio, %	1 Soil Type	Soil Classification	USC	Density or Consistency	Est. Density (pcf)	Qc to N	SPT N(60)	Cn or Cq	Norm. Qc1n	Est. % Fines	Rel. Dens. Dr (%)	Nk: Phi (deg.)	17.0 Su (tsf)	OCR
9.30	30.5	28.55	6.41	3	Clay	CL/CH	very stiff	125	1.3	23	0.93		100			1.61	>10
9.45	31.0	31.07	6.84	3	Clay	CL/CH	very stiff	125	1.3	25	0.92		100			1.75	>10
9.60	31.5	34.71	6.59	3	Clay	CL/CH	very stiff	125	1.3	28	0.92		100			1.97	>10
9.75	32.0	35.27	6.25	3	Clay	CL/CH	very stiff	125	1.3	28	0.91		100			2.00	>10
9.90	32.5	37.01	5.65	3	Clay	CL/CH	hard	125	1.3	30	0.91		100			2.10	>10
10.05	33.0	32.37	5.31	3	Clay	CL/CH	very stiff	125	1.3	26	0.90		100			1.83	>10
10.20	33.5	30.28	5.70	3	Clay	CL/CH	very stiff	125	1.3	24	0.89		100			1.70	9.59
10.38	34.0	29.97	5.71	3	Clay	CL/CH	very stiff	125	1.3	24	0.89		100			1.68	9.19
10.53	34.5	34.16	5.42	3	Clay	CL/CH	very stiff	125	1.3	27	0.88		100			1.93	>10
10.68	35.0	31.53	5.44	3	Clay	CL/CH	very stiff	125	1.3	25	0.88		100			1.77	9.79
10.83	35.5	33.18	4.62	4	Silty Clay to Clay	CL	very stiff	125	1.8	19	0.87		100			1.87	>10
10.98	36.0	31.41	5.32	3	Clay	CL/CH	very stiff	125	1.3	25	0.87		100			1.77	9.19
11.13	36.5	28.95	4.94	3	Clay	CL/CH	very stiff	125	1.3	23	0.86		100			1.62	7.70
11.28	37.0	23.74	5.43	3	Clay	CL/CH	very stiff	125	1.3	19	0.86		100			1.31	5.42
11.43	37.5	24.03	5.19	3	Clay	CL/CH	very stiff	125	1.3	19	0.85		100			1.33	5.42
11.58	38.0	28.73	5.16	3	Clay	CL/CH	very stiff	125	1.3	23	0.85		100			1.60	7.13
11.73	38.5	29.89	5.19	3	Clay	CL/CH	very stiff	125	1.3	24	0.85		100			1.67	7.56
11.88	39.0	29.55	5.05	3	Clay	CL/CH	very stiff	125	1.3	24	0.84		100			1.65	7.27
12.05	39.5	25.32	4.72	3	Clay	CL/CH	very stiff	125	1.3	20	0.84		100			1.40	5.53
12.20	40.0	22.19	4.46	3	Clay	CL/CH	very stiff	125	1.3	18	0.83		100			1.22	4.37
12.35	40.5	24.43	4.30	4	Silty Clay to Clay	CL	very stiff	125	1.8	14	0.83		100			1.35	6.54
12.50	41.0	24.85	3.66	5	Clayey Silt to Silty Clay	ML/CL	very stiff	120	2.5	10	0.82		100			1.37	9.39
12.65	41.5	21.29	3.25	5	Clayey Silt to Silty Clay	ML/CL	very stiff	120	2.5	9	0.82		100			1.16	6.88
12.80	42.0	19.81	3.04	5	Clayey Silt to Silty Clay	ML/CL	very stiff	120	2.5	8	0.82		100			1.07	6.00
12.95	42.5	18.87	2.79	5	Clayey Silt to Silty Clay	ML/CL	very stiff	120	2.5	8	0.81		100			1.02	5.42
13.10	43.0	19.60	2.48	5	Clayey Silt to Silty Clay	ML/CL	very stiff	120	2.5	8	0.81		100			1.06	5.76
13.25	43.5	21.70	2.84	5	Clayey Silt to Silty Clay	ML/CL	very stiff	120	2.5	9	0.81		100			1.18	6.65
13.40	44.0	22.24	2.62	5	Clayey Silt to Silty Clay	ML/CL	very stiff	120	2.5	9	0.80		100			1.21	6.88
13.58	44.5	22.52	2.78	5	Clayey Silt to Silty Clay	ML/CL	very stiff	120	2.5	9	0.80		100			1.23	6.88
13.73	45.0	25.15	3.77	5	Clayey Silt to Silty Clay	ML/CL	very stiff	120	2.5	10	0.80		100			1.38	8.27
13.88	45.5	26.20	3.80	5	Clayey Silt to Silty Clay	ML/CL	very stiff	120	2.5	10	0.79		100			1.44	8.85
14.03	46.0	24.44	3.02	5	Clayey Silt to Silty Clay	ML/CL	very stiff	120	2.5	10	0.79		100			1.34	7.70
14.18	46.5	22.65	2.43	5	Clayey Silt to Silty Clay	ML/CL	very stiff	120	2.5	9	0.79		100			1.23	6.54
14.33	47.0	20.81	1.98	6	Sandy Silt to Clayey Silt	ML	very loose	115	3.5	6	0.78	15.4	100	17	30		
14.48	47.5	20.51	2.12	6	Sandy Silt to Clayey Silt	ML	very loose	115	3.5	6	0.78	15.1	100	17	30		
14.63	48.0	22.61	2.50	5	Clayey Silt to Silty Clay	ML/CL	very stiff	120	2.5	9	0.78		100			1.23	8.32
14.78	48.5	20.83	2.13	6	Sandy Silt to Clayey Silt	ML	very loose	115	3.5	6	0.77	15.2	100	17	30		
14.93	49.0	20.93	2.27	5	Clayey Silt to Silty Clay	ML/CL	very stiff	120	2.5	8	0.77		100			1.13	5.42
15.10	49.5	20.67	2.11	6	Sandy Silt to Clayey Silt	ML	very loose	115	3.5	6	0.77	15.0	100	16	30		
15.25	50.0	19.06	2.25	5	Clayey Silt to Silty Clay	ML/CL	very stiff	120	2.5	8	0.76		100			1.01	4.47

CLIENT: ORMAT

PROJECT: ORMAT Heber 2 Facilities, Heber, CA

LOCATION: See Site and Boring Location Plan

CONE PENETROMETER: HOLGUIN, FAHAN & ASSC. Truck Mounted Electric Cone with 23 ton reaction weight

DATE: 12/20/04

LOG OF CONE SOUNDING DATA CPT-3

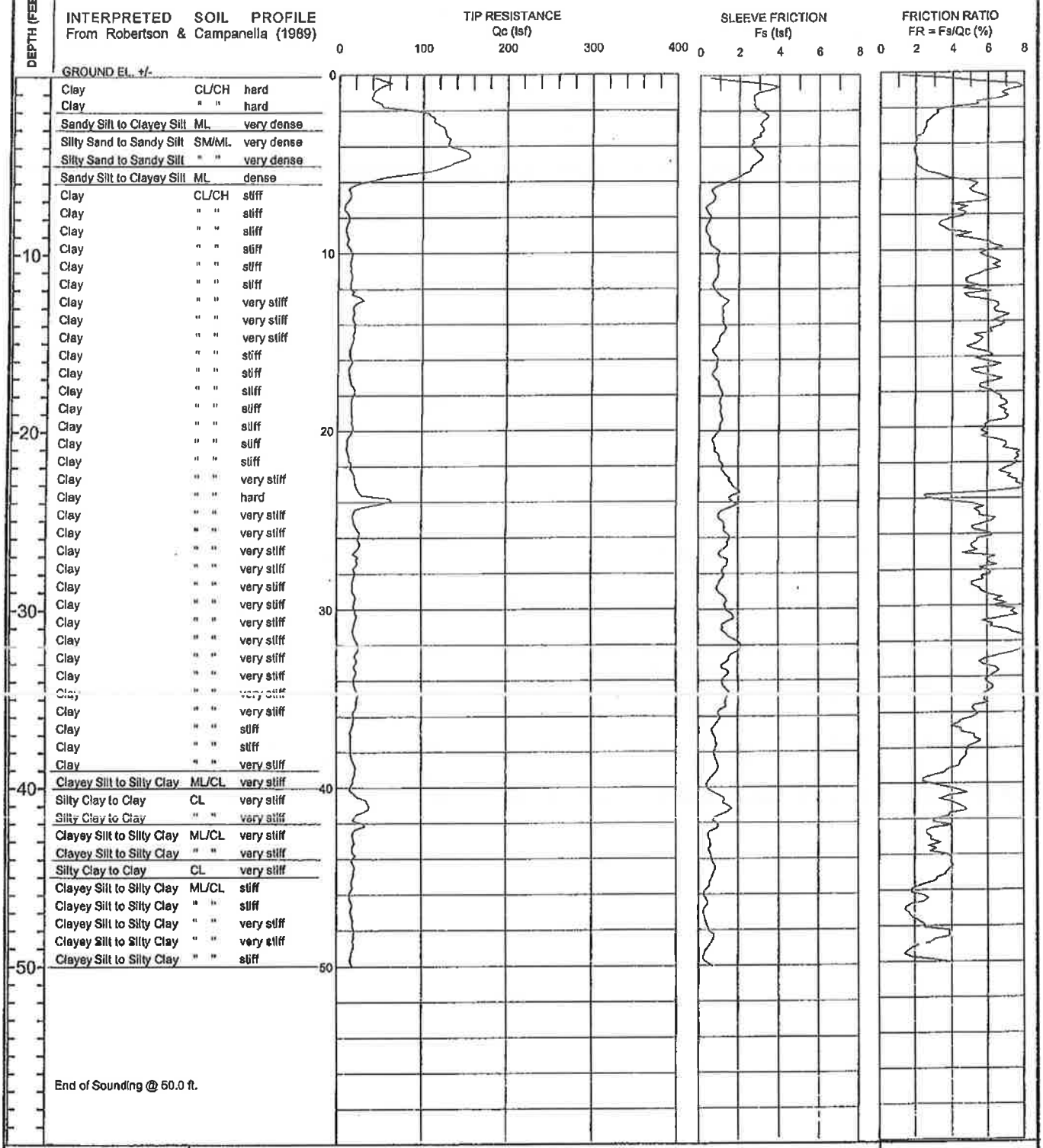

Project No: LE04354

LANDMARK
Geo-Engineers and Geologists
a DBE/MBE/SBE Company

Plate B-3

LANDMARK CONSULTANTS, INC.

CONE PENETROMETER INTERPRETATION (based on Robertson & Campanella, 1989, refer to Key to CPT logs)

Project: ORMAT Heber 2 Facilities, Heber, CA Project No: LE04354 Date: 12/20/04

CONE SOUNDING: CPT-3

Est. GWT (ft): 12.0 Phi Correlation: 0 (0-Schm(78),1-R&C(83),2-PHT(74))

Base Depth meters	Base Depth feet	Avg Tip Qc, tsf	Avg Friction Ratio, %		1 Soil Type	Soil Classification	USC	Density or Consistency	Est. Density (pcf)	Qc to N	SPT N(60)	Cn or Cq	Norm. Qc1n	Est. % Fines	Rel. Dens. Dr (%)	Nk: Phi (deg.)	17.0 Su (tsf)	OCR
0.15	0.5	51.76	3.36	5	5	Clayey Silt to Silty Clay	ML/CL	hard	120	2.5	21	2.00		50			3.04	>10
0.30	1.0	46.42	7.56	3	3	Clay	CL/CH	hard	125	1.3	37	2.00		75			2.73	>10
0.45	1.5	40.35	6.79	3	3	Clay	CL/CH	hard	125	1.3	32	2.00		75			2.37	>10
0.60	2.0	61.72	4.80	4	4	Silty Clay to Clay	CL	hard	125	1.8	35	2.00		55			3.62	>10
0.75	2.5	109.67	3.07	6	6	Sandy Silt to Clayey Silt	ML	very dense	115	3.5	31	2.00	207.3	35	104	43		
0.93	3.0	116.60	2.64	7	7	Silty Sand to Sandy Silt	SM/ML	very dense	115	4.5	26	2.00	224.2	30	103	42		
1.08	3.5	127.70	2.43	7	7	Silty Sand to Sandy Silt	SM/ML	very dense	115	4.5	28	2.00	241.4	25	103	42		
1.23	4.0	131.15	2.02	7	7	Silty Sand to Sandy Silt	SM/ML	very dense	115	4.5	29	2.00	247.9	25	102	42		
1.38	4.5	147.55	1.96	7	7	Silty Sand to Sandy Silt	SM/ML	very dense	115	4.5	33	2.00	278.9	20	103	42		
1.53	5.0	148.38	2.05	7	7	Silty Sand to Sandy Silt	SM/ML	very dense	115	4.5	33	1.94	271.7	20	102	42		
1.68	5.5	111.44	2.28	7	7	Silty Sand to Sandy Silt	SM/ML	very dense	115	4.5	25	1.85	194.4	25	92	41		
1.83	6.0	40.17	4.02	5	5	Clayey Silt to Silty Clay	ML/CL	hard	120	2.5	16	1.76		60			2.34	>10
1.98	6.5	13.36	5.18	3	3	Clay	CL/CH	stiff	125	1.3	11	1.69		100			0.76	>10
2.13	7.0	13.22	5.65	3	3	Clay	CL/CH	stiff	125	1.3	11	1.62		100			0.75	>10
2.28	7.5	7.68	4.85	3	3	Clay	CL/CH	firm	125	1.3	6	1.56		100			0.43	6.10
2.45	8.0	11.50	4.55	3	3	Clay	CL/CH	stiff	125	1.3	9	1.51		100			0.65	>10
2.60	8.5	10.61	3.49	4	4	Silty Clay to Clay	CL	stiff	125	1.8	6	1.46		95			0.60	>10
2.75	9.0	9.81	4.10	3	3	Clay	CL/CH	stiff	125	1.3	8	1.42		100			0.55	6.54
2.90	9.5	10.85	5.09	3	3	Clay	CL/CH	stiff	125	1.3	9	1.38		100			0.61	7.00
3.05	10.0	14.61	6.36	3	3	Clay	CL/CH	stiff	125	1.3	12	1.34		100			0.82	>10
3.20	10.5	14.97	5.91	3	3	Clay	CL/CH	stiff	125	1.3	12	1.32		100			0.85	>10
3.35	11.0	14.49	6.53	3	3	Clay	CL/CH	stiff	125	1.3	12	1.31		100			0.82	>10
3.50	11.5	15.94	5.42	3	3	Clay	CL/CH	stiff	125	1.3	13	1.29		100			0.90	>10
3.65	12.0	14.15	5.01	3	3	Clay	CL/CH	stiff	125	1.3	11	1.27		100			0.79	8.56
3.80	12.5	20.31	5.15	3	3	Clay	CL/CH	very stiff	125	1.3	16	1.26		95			1.16	>10
3.95	13.0	23.81	5.79	3	3	Clay	CL/CH	very stiff	125	1.3	19	1.24		95			1.36	>10
4.13	13.5	18.35	6.42	3	3	Clay	CL/CH	very stiff	125	1.3	15	1.23		100			1.04	>10
4.28	14.0	18.13	6.73	3	3	Clay	CL/CH	very stiff	125	1.3	15	1.22		100			1.02	>10
4.43	14.5	19.70	6.56	3	3	Clay	CL/CH	very stiff	125	1.3	16	1.20		100			1.12	>10
4.58	15.0	18.07	5.71	3	3	Clay	CL/CH	very stiff	125	1.3	14	1.19		100			1.02	>10
4.73	15.5	14.86	5.24	3	3	Clay	CL/CH	stiff	125	1.3	12	1.18		100			0.83	7.00
4.88	16.0	14.60	5.69	3	3	Clay	CL/CH	stiff	125	1.3	12	1.17		100			0.81	6.85
5.03	16.5	13.49	6.25	3	3	Clay	CL/CH	stiff	125	1.3	11	1.16		100			0.75	5.65
5.18	17.0	13.31	5.44	3	3	Clay	CL/CH	stiff	125	1.3	11	1.14		100			0.74	5.31
5.33	17.5	16.20	6.21	3	3	Clay	CL/CH	stiff	125	1.3	13	1.13		100			0.90	7.13
5.48	18.0	19.16	5.98	3	3	Clay	CL/CH	very stiff	125	1.3	15	1.12		100			1.08	9.59
5.65	18.5	15.49	6.80	3	3	Clay	CL/CH	stiff	125	1.3	12	1.11		100			0.86	6.32
5.80	19.0	15.81	6.89	3	3	Clay	CL/CH	stiff	125	1.3	13	1.10		100			0.88	6.32
5.95	19.5	16.32	7.00	3	3	Clay	CL/CH	stiff	125	1.3	13	1.09		100			0.91	6.43
6.10	20.0	17.26	5.95	3	3	Clay	CL/CH	stiff	125	1.3	14	1.08		100			0.96	6.88
6.25	20.5	13.28	5.76	3	3	Clay	CL/CH	stiff	125	1.3	11	1.07		100			0.73	4.37
6.40	21.0	11.14	6.84	3	3	Clay	CL/CH	stiff	125	1.3	9	1.06		100			0.60	3.28
6.55	21.5	12.48	7.40	3	3	Clay	CL/CH	stiff	125	1.3	10	1.06		100			0.68	3.74
6.70	22.0	14.92	7.62	3	3	Clay	CL/CH	stiff	125	1.3	12	1.05		100			0.82	4.89
6.85	22.5	17.77	6.98	3	3	Clay	CL/CH	stiff	125	1.3	14	1.04		100			0.99	6.32
7.00	23.0	21.45	7.34	3	3	Clay	CL/CH	very stiff	125	1.3	17	1.03		100			1.20	8.41
7.18	23.5	24.58	7.84	3	3	Clay	CL/CH	very stiff	125	1.3	20	1.02		100			1.39	>10
7.33	24.0	51.65	3.68	5	5	Clayey Silt to Silty Clay	ML/CL	hard	120	2.5	21	1.02		70			2.98	>10
7.48	24.5	34.37	4.91	3	3	Clay	CL/CH	very stiff	125	1.3	27	1.01		95			1.98	>10
7.63	25.0	18.84	5.44	3	3	Clay	CL/CH	very stiff	125	1.3	15	1.00		100			1.05	6.10
7.78	25.5	21.09	6.11	3	3	Clay	CL/CH	very stiff	125	1.3	17	0.99		100			1.18	7.13
7.93	26.0	26.12	5.49	3	3	Clay	CL/CH	very stiff	125	1.3	21	0.99		100			1.47	>10
8.08	26.5	26.28	5.55	3	3	Clay	CL/CH	very stiff	125	1.3	21	0.98		100			1.48	>10
8.23	27.0	21.92	5.06	3	3	Clay	CL/CH	very stiff	125	1.3	18	0.97		100			1.22	7.13
8.38	27.5	23.63	6.15	3	3	Clay	CL/CH	very stiff	125	1.3	19	0.97		100			1.32	8.00
8.53	28.0	20.49	6.07	3	3	Clay	CL/CH	very stiff	125	1.3	16	0.96		100			1.14	6.10
8.68	28.5	19.11	5.87	3	3	Clay	CL/CH	very stiff	125	1.3	15	0.95		100			1.06	5.31
8.85	29.0	18.15	5.24	3	3	Clay	CL/CH	stiff	125	1.3	15	0.95		100			1.00	4.78
9.00	29.5	21.72	6.18	3	3	Clay	CL/CH	very stiff	125	1.3	17	0.94		100			1.21	6.32
9.15	30.0	20.63	6.55	3	3	Clay	CL/CH	very stiff	125	1.3	17	0.93		100			1.14	5.65

LANDMARK CONSULTANTS, INC.

CONE PENETROMETER INTERPRETATION (based on Robertson & Campanella, 1989, refer to Key to CPT logs)

Project: ORMAT Heber 2 Facilities, Heber, CA Project No: LE04354 Date: 12/20/04

CONE SOUNDING: CPT-3

Est. GWT (ft): 12.0 Phi Correlation: 0 0-Schm(78),1-R&C(83),2-PHT(74)

Base Depth meters	Base Depth feet	Avg Tip Qc, tsf	Avg Friction Ratio, %	1 Soil Type	Soil Classification	USC	Density or Consistency	Est. Density (pcf)	Qc to N	SPT N(60)	Cn or Cq	Norm. Qc1n	Est. % Fines	Rel.. Dens. Dr (%)	Nk: Phi (deg.)	17.0 Su (tsf)	OCR
9.30	30.5	22.90	7.51	3	Clay	CL/CH	very stiff	125	1.3	18	0.93		100			1.27	6.54
9.45	31.0	20.57	6.23	3	Clay	CL/CH	very stiff	125	1.3	16	0.92		100			1.14	5.42
9.60	31.5	19.55	6.90	3	Clay	CL/CH	very stiff	125	1.3	16	0.92		100			1.08	4.89
9.75	32.0	23.76	8.37	3	Clay	CL/CH	very stiff	125	1.3	19	0.91		100			1.32	6.54
9.90	32.5	24.30	8.05	3	Clay	CL/CH	very stiff	125	1.3	19	0.90		100			1.35	6.65
10.05	33.0	22.78	6.54	3	Clay	CL/CH	very stiff	125	1.3	18	0.90		100			1.26	5.88
10.20	33.5	21.56	5.91	3	Clay	CL/CH	very stiff	125	1.3	17	0.89		100			1.19	5.31
10.38	34.0	20.82	6.40	3	Clay	CL/CH	very stiff	125	1.3	17	0.89		100			1.15	4.89
10.53	34.5	21.17	6.04	3	Clay	CL/CH	very stiff	125	1.3	17	0.88		100			1.17	4.89
10.68	35.0	24.71	6.05	3	Clay	CL/CH	very stiff	125	1.3	20	0.88		100			1.37	6.21
10.83	35.5	23.14	5.91	3	Clay	CL/CH	very stiff	125	1.3	19	0.87		100			1.28	5.53
10.98	36.0	19.96	5.21	3	Clay	CL/CH	very stiff	125	1.3	16	0.87		100			1.09	4.28
11.13	36.5	19.03	4.88	3	Clay	CL/CH	very stiff	125	1.3	15	0.86		100			1.04	3.91
11.28	37.0	16.19	4.33	3	Clay	CL/CH	stiff	125	1.3	13	0.86		100			0.87	3.07
11.43	37.5	16.02	5.36	3	Clay	CL/CH	stiff	125	1.3	13	0.85		100			0.86	3.00
11.58	38.0	16.15	5.06	3	Clay	CL/CH	stiff	125	1.3	13	0.85		100			0.86	3.00
11.73	38.5	17.81	4.75	3	Clay	CL/CH	stiff	125	1.3	14	0.85		100			0.96	3.35
11.88	39.0	21.66	4.41	4	Silty Clay to Clay	CL	very stiff	125	1.8	12	0.84		100			1.19	5.65
12.05	39.5	20.18	3.42	5	Clayey Silt to Silty Clay	ML/CL	very stiff	120	2.5	8	0.84		100			1.10	6.65
12.20	40.0	17.00	2.62	5	Clayey Silt to Silty Clay	ML/CL	stiff	120	2.5	7	0.83		100			0.91	5.00
12.35	40.5	20.64	4.32	4	Silty Clay to Clay	CL	very stiff	125	1.8	12	0.83		100			1.12	5.00
12.50	41.0	36.57	3.70	5	Clayey Silt to Silty Clay	ML/CL	hard	120	2.5	15	0.82		95			2.06	>10
12.65	41.5	31.64	4.64	4	Silty Clay to Clay	CL	very stiff	125	1.8	18	0.82		100			1.77	>10
12.80	42.0	23.58	3.56	5	Clayey Silt to Silty Clay	ML/CL	very stiff	120	2.5	9	0.82		100			1.29	8.14
12.95	42.5	24.97	3.28	5	Clayey Silt to Silty Clay	ML/CL	very stiff	120	2.5	10	0.81		100			1.37	8.85
13.10	43.0	19.07	2.71	5	Clayey Silt to Silty Clay	ML/CL	very stiff	120	2.5	8	0.81		100			1.03	5.42
13.25	43.5	18.86	2.98	5	Clayey Silt to Silty Clay	ML/CL	very stiff	120	2.5	8	0.81		100			1.01	5.31
13.40	44.0	19.54	3.20	5	Clayey Silt to Silty Clay	ML/CL	very stiff	120	2.5	8	0.80		100			1.05	5.53
13.58	44.5	19.29	3.97	4	Silty Clay to Clay	CL	very stiff	125	1.8	11	0.80		100			1.04	3.91
13.73	45.0	19.79	3.86	4	Silty Clay to Clay	CL	very stiff	125	1.8	11	0.80		100			1.07	4.00
13.88	45.5	17.66	3.31	5	Clayey Silt to Silty Clay	ML/CL	stiff	120	2.5	7	0.79		100			0.94	4.47
14.03	46.0	16.42	2.18	5	Clayey Silt to Silty Clay	ML/CL	stiff	120	2.5	7	0.79		100			0.87	3.91
14.18	46.5	15.61	2.35	5	Clayey Silt to Silty Clay	ML/CL	stiff	120	2.5	6	0.78		100			0.82	3.58
14.33	47.0	16.68	1.80	6	Sandy Silt to Clayey Silt	ML	very loose	115	3.5	5	0.78	12.3	100	11	29		
14.48	47.5	18.25	1.80	6	Sandy Silt to Clayey Silt	ML	very loose	115	3.5	5	0.78	13.4	100	13	30		
14.63	48.0	19.39	2.43	5	Clayey Silt to Silty Clay	ML/CL	very stiff	120	2.5	8	0.78		100			1.04	4.89
14.78	48.5	19.39	3.87	4	Silty Clay to Clay	CL	very stiff	125	1.8	11	0.77		100			1.04	3.58
14.93	49.0	19.13	2.69	5	Clayey Silt to Silty Clay	ML/CL	very stiff	120	2.5	8	0.77		100			1.02	4.57
15.10	49.5	16.46	1.59	6	Sandy Silt to Clayey Silt	ML	very loose	115	3.5	5	0.77	11.9	100	10	29		
15.25	50.0	16.91	2.83	5	Clayey Silt to Silty Clay	ML/CL	stiff	120	2.5	7	0.76		100			0.89	3.74

APPENDIX C

LANDMARK CONSULTANTS, INC.

CLIENT: ORMAT
PROJECT: ORMAT Heber 2 Facilities, Heber, CA
JOB NO: LE04354
DATE: 12/28/04

ATTERBERG LIMITS (ASTM D4318)

Sample Location	Sample Depth (ft)	Liquid Limit (LL)	Plastic Limit (PL)	Plasticity Index (PI)	USCS Classif-ation
CPT-1	0-1.5	35	18	17	CL
CPT-2	0-2	35	17	18	CL
CPT-3	0-1.5	36	15	21	CL

PLASTICITY CHART

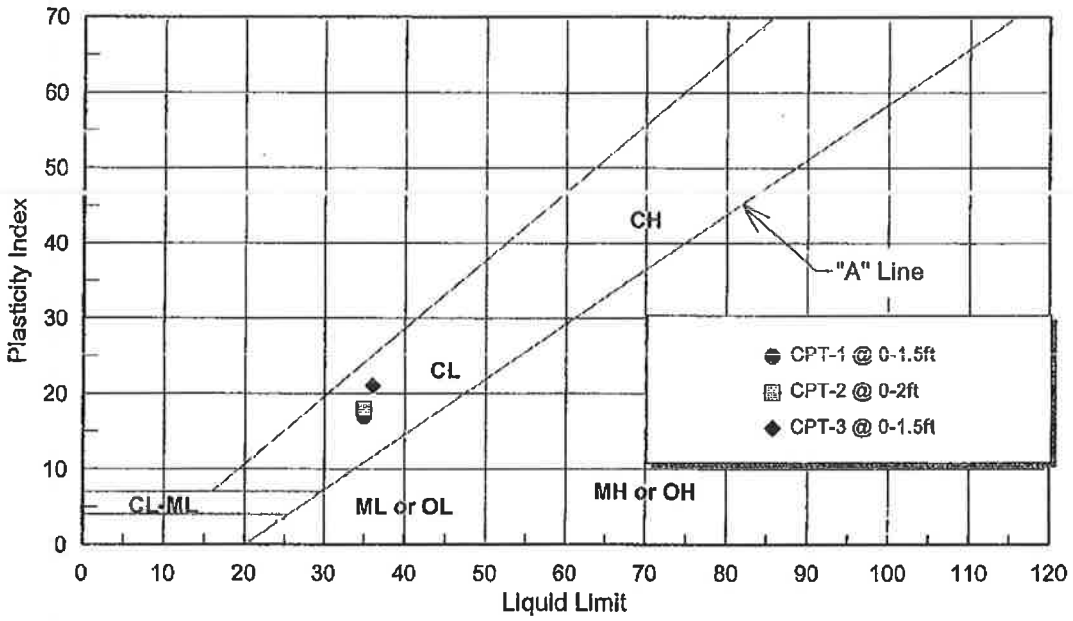

LANDMARK
Geo-Engineers and Geologists
a DBE/MBE/SBE Company

Project No: LE04354

Atterberg Limits Test Results

Plate C-1

LANDMARK CONSULTANTS, INC.

CLIENT: ORMAT
PROJECT: ORMAT Heber 2 Facilities, Heber, CA
JOB NO: LE04354
DATE: 12/28/04

CHEMICAL ANALYSES

Boring:	CPT-1	CPT-1	CPT-2	CPT-2	CalTrans
Sample Depth, ft:	0-1.5	1.5-3	0-2	2-3	Method
pH:	7.9	7.9	7.8	7.9	643
Electrical Conductivity (mmhos):	2.5	1.7	1.8	0.9	424
Resistivity (ohm-cm):	260	1000	300	1000	643
Chloride (Cl), ppm:	3,040	230	1,490	220	422
Sulfate (SO4), ppm:	2,812	3,006	1,500	1,106	417

General Guidelines for Soil Corrosivity

Material Affected	Chemical Agent	Amount in Soil (ppm)	Degree of Corrosivity
Concrete	Soluble Sulfates	0 -1000	Low
		1000 - 2000	Moderate
		2000 - 20,000	Severe
		> 20,000	Very Severe
Normal Grade Steel	Soluble Chlorides	0 - 200	Low
		200 - 700	Moderate
		700 - 1500	Severe
		> 1500	Very Severe
Normal Grade Steel	Resistivity	1-1000	Very Severe
		1000-2000	Severe
		2000-10,000	Moderate
		10,000+	Low

LANDMARK
Géo-Engineers and Geologists
a DBE/MBE/SBE Company

Project No: LE04354

Selected Chemical Analyses Results

Plate C-2

LANDMARK CONSULTANTS, INC.

CLIENT: ORMAT
PROJECT: ORMAT Heber 2 Facilities, Heber, CA
JOB NO: LE04354
DATE: 12/28/04

CHEMICAL ANALYSES

Boring:	CPT-3	CPT-3	CalTrans Method
Sample Depth, ft:	0-1.5	1.5-3	
pH:	7.9	7.8	643
Electrical Conductivity (mmhos):	1.5	1.3	424
Resistivity (ohm-cm):	450	1000	643
Chloride (Cl), ppm:	570	210	422
Sulfate (SO4), ppm:	1,785	1,052	417

General Guidelines for Soil Corrosivity

Material Affected	Chemical Agent	Amount in Soil (ppm)	Degree of Corrosivity
Concrete	Soluble Sulfates	0 -1000	Low
		1000 - 2000	Moderate
		2000 - 20,000	Severe
		> 20,000	Very Severe
Normal Grade Steel	Soluble Chlorides	0 - 200	Low
		200 - 700	Moderate
		700 - 1500	Severe
		> 1500	Very Severe
Normal Grade Steel	Resistivity	1-1000	Very Severe
		1000-2000	Severe
		2000-10,000	Moderate
		10,000+	Low

LANDMARK Geo-Engineers and Geologists
a DBE/MBE/SBE Company

Project No: LE04354

Selected Chemical Analyses Results

Plate C-3

APPENDIX D

REFERENCES

Arango I., 1996, Magnitude Scaling Factors for Soil Liquefaction Evaluations: ASCE Geotechnical Journal, Vol. 122, No. 11.

Bartlett, Steven F. and Youd, T. Leslie, 1995, Empirical Prediction of Liquefaction-Induced Lateral Spread: ASCE Geotechnical Journal, Vol. 121, No. 4.

Blake, T. F., 2000, FRISKSP - A computer program for the probabilistic estimation of seismic hazard using faults as earthquake sources.

Boore, D. M., Joyner, W. B., and Fumal, T. E., 1997, Empirical Near-Source Attenuation Relationships for Horizontal and Vertical Components of Peak Ground Acceleration, Peak Ground Velocity, and Pseudo-Absolute Acceleration Response Spectra: Seismological Research Letters, Vol. 68, No. 1, p. 154-179.

Building Seismic Safety Council (BSSC), 1991, NEHRP recommended provisions for the development of seismic regulations of new buildings, Parts 1, 2 and Maps: FEMA 222, January 1992

California Division of Mines and Geology (CDMG), 1996, California Fault Parameters: available at http://www.consrv.ca.gov/dmg/shezp/fltindex.html.

California Division of Mines and Geology (CDMG), 1962, Geologic Map of California – San Diego-El Centro Sheet: California Division of Mines and Geology, Scale 1:250,000.

Ellsworth, W. L., 1990, Earthquake History, 1769-1989 in: The San Andreas Fault System, California: U.S. Geological Survey Professional Paper 1515, 283 p.

International Conference of Building Officials (ICBO), 1997, Uniform Building Code, 1997 Edition.

Ishihara, K. (1985), Stability of natural deposits during earthquakes, Proc. 11th Int. Conf. On Soil Mech. And Found. Engrg., Vol. 1, A. A. Balkema, Rotterdam, The Netherlands, 321-376.

Jennings, C. W., 1994, Fault activity map of California and Adjacent Areas: California Division of Mines and Geology, DMG Geologic Map No. 6.

Jones, L. and Hauksson, E., 1994, Review of potential earthquake sources in Southern California: Applied Technology Council, Proceedings of ATC 35-1.

Maley, R. P. and Etheredge, E. C., 1981, Strong motion data from the Westmorland, California earthquake of April 26, 1981: U.S. Geological Survey Open File Report 81-1149, 18 p.

Morton, P. K., 1977, Geology and mineral resources of Imperial County, California: California Division of Mines and Geology, County Report No. 7, 104 p.

Mualchin, L. and Jones, A. L., 1992, Peak acceleration from maximum credible earthquakes in California (Rock and Stiff Soil Sites): California Division of Mines and Geology, DMG Open File Report 92-01.

Naeim, F. and Anderson, J. C., 1993, Classification and evaluation of earthquake records for design: Earthquake Engineering Research Institute, NEHRP Report.

National Research Council, Committee of Earthquake Engineering, 1985, Liquefaction of Soils during Earthquakes: National Academy Press, Washington, D.C.

Porcella, R., Etheredge, E., Maley, R., and Switzer, J., 1987, Strong motion data from the Superstition Hills earthquake of November 24, 1987: U.S. Geological Survey Open File Report 87-672, 56 p.

Robertson, P. K. and Wride, C. E., 1996, Cyclic Liquefaction and its Evaluation based on the SPT and CPT, Proceeding of the NCEER Workshop on Evaluation of Liquefaction Resistance of Soils, NCEER Technical Report 97-0022, p. 41-88.

Seed, Harry B., Idriss, I. M., and Arango I., 1983, Evaluation of liquefaction potential using field performance data: ASCE Geotechnical Journal, Vol. 109, No. 3.

Seed, Harry B., et al, 1985, Influence of SPT Procedures in Soil Liquefaction Resistance Evaluations: ASCE Geotechnical Journal, Vol. 113, No. 8.

Sharp, R. V., 1982, Tectonic setting of the Imperial Valley region: U.S. Geological Survey Professional Paper 1254, p. 5-14.

Sylvester, A. G., 1979, Earthquake damage in Imperial Valley, California May 18, 1940, as reported by T. A. Clark: Bulletin of the Seismological Society of America, v. 69, no. 2, p. 547-568.

Tokimatsu, K. and Seed H. B., 1987, Evaluation of settlements in sands due to earthquake shaking: ASCE Geotechnical Journal, v. 113, no. 8.

U.S. Geological Survey (USGS), 1982, The Imperial Valley California Earthquake of October 15, 1979: Professional Paper 1254, 451 p.

U.S. Geological Survey (USGS), 1990, The San Andreas Fault System, California, Professional Paper 1515.

U.S. Geological Survey (USGS), 1996, National Seismic Hazard Maps: available at http://gldage.cr.usgs.gov

Working Group on California Earthquake Probabilities (WGCEP), 1992, Future seismic hazards in southern California, Phase I Report: California Division of Mines and Geology.

Working Group on California Earthquake Probabilities (WGCEP), 1995, Seismic hazards in southern California, Probable Earthquakes, 1994-2014, Phase II Report: Southern California Earthquake Center.

Youd, T. Leslie and Garris, C. T., 1995, Liquefaction induced ground surface disruption: ASCE Geotechnical Journal, Vol. 121, No. 11.

Youd, T. L. et. al., 2001, Liquefaction Resistance of Soils: Summary Report from the 1996 NCEER and 1998 NCEER/NSF Workshops on Evaluation of Liquefaction Resistance of Soils: Journal of Geotechnical and Geoenvironmental Engineering, Vol. 127, No. 10, p. 817-833.

Zimmerman, R. P., 1981, Soil survey of Imperial County, California, Imperial Valley Area: U.S. Dept. of Agriculture Soil Conservation Service, 112 p.

AIR QUALITY ANALYSIS SUMMARY FOR THE ORMAT HEBER 2 GEOTHERMAL REPOWER PROJECT

PREPARED FOR:	Ben Pogue, Catalyst Environmental Solutions
PREPARED BY:	Joel Firebaugh, Air Sciences Inc.
PROJECT NO.:	246-2-1
COPIES:	Melissa Wendt, ORMAT Nevada Inc.
DATE:	August 12, 2019

The Second Imperial Geothermal Company (SIGC), a wholly owned subsidiary of ORMAT Nevada Inc. (ORMAT), proposes to replace six existing water-cooled ORMAT Energy Converters (OECs) with two new water-cooled OECs at the Heber 2 Geothermal Energy Complex in Imperial County, CA. The project also entails installing three new 10,000 gallon above ground storage tanks to accommodate additional isopentane. The project will affect volatile organic compound (VOC) air emissions at the facility. The proposed changes are not expected to affect emission rates of other regulated pollutant emissions.

1.0 Project Description

The Heber 2 Complex is a geothermal power generation facility located on private lands owned by SIGC/ORMAT in southern Imperial County. The facility operates under Imperial County Air Pollution Control District (ICAPCD) Permit to Operate (PTO) #2217A-4. Heber 2 currently consists of six Integrated Two-Level Units (ITLU) which have a gross combined power output rating of 36 megawatts. PTO #2217A-4 also covers two adjacent, connected facilities to Heber 2: Goulds 2 and Heber South. These two facilities each consist of one ORMAT Energy Converter (OEC) with gross outputs of 10 and 12 megawatts, respectively. Ancillary equipment for the combined facilities includes cooling towers, an evacuation skid/vapor recovery maintenance unit (VRMU), motive fluid (MF) storage tanks, and diesel engines for emergency use.

The proposed development would occur entirely on Assessor's Parcel Number (APN) 054-250-031, which is a 39.99-acre property. The address for Heber 2 is 855 Dogwood Road, Heber, CA 92249.

1.1 Proposed Development

Development of the proposed project includes the installation of two new OEC units, manufactured by ORMAT, to replace the six existing ITLUs which were also manufactured by ORMAT in 1992. The total disturbance would be approximately 4 acres, entirely within the

existing Heber 2 site. The existing ITLUs will either be demolished or abandoned in place. The development site is completely devoid of any vegetation and is actively disturbed as part of ongoing energy generation operations at the Heber 2 Complex. Considering its current condition, site preparation for the installation of the proposed facilities would be limited to light excavation and soil compaction.

ORMAT Energy Converter-1 (OEC-1)

The proposed OEC-1 unit is a two-turbine combined cycle binary unit, operating on a subcritical Rankine cycle, with isopentane as the motive fluid for the system. This system also consists of a generator, vaporizer, water cooled condensers, preheaters and recuperators, with the OEC served by the existing evacuation skid/vapor recovery maintenance unit for purging and maintenance events. The design capacity for the unit is 25.43 MW gross.

ORMAT Energy Converter-2 (OEC-2)

The proposed OEC-2 unit is a two-cycle binary unit, operating on a subcritical Rankine cycle, with isopentane as the motive fluid for the system. This system also consists of a generator, turbines, vaporizers, water cooled condensers and preheaters, with the OEC served by the existing evacuation skid/vapor recovery maintenance unit (VRMU) for purging and maintenance events. The design capacity for the unit is 14.01 MW gross.

Three Additional Isopentane Above Ground Storage Tanks

To support the new OEC units, three new storage tanks for additional isopentane supply would be installed. There are two existing storage tanks at Heber 2 and one at Goulds 2. The new tanks would be sited adjacent to the existing Heber 2 tanks. Each of the new and existing tanks has a capacity of 10,000 gallons.

2.0 Existing Air Emissions

The Heber 2 facility is a minor source of air pollution and operates in compliance with all applicable air quality requirements and its permit to operate (PTO #2217A-4). Air emission sources currently at the facility include the geothermal power generating units, cooling towers, VRMU, and emergency diesel equipment.

The existing power generating units (6 ITLUs and 2 OECs) have a combined gross power generating capacity of 58 megawatts. These units generate power by taking geothermal energy (e.g. heat) to vaporize liquid isopentane, which is the motive fluid that powers the turbines to create electricity.

The primary air pollutant from the facility is isopentane, which is a VOC. Isopentane emissions occur due to maintenance, purging, and fugitive leaks. During maintenance, the unit is shut

down and the isopentane is evacuated before the system is opened for the necessary work to be performed. To evacuate the system, the liquid isopentane is transferred to storage tanks, and the remaining vapors are passed through the VRMU. The overall recovery rate of isopentane during evacuation is greater than 99.9%. However, trace quantities of vapors as well as liquid collected at low points in the system where the liquid cannot be completely drained result in VOC emissions when the unit is opened to the atmosphere.

Purging is the process by which impurities are removed from the isopentane closed circuit. Contamination of the isopentane causes operating efficiency losses, so purging is performed on a regular basis. Vapors are passed through the VRMU and the isopentane is collected and returned to the system while other gases are removed.

Fugitive losses of isopentane can occur due to failing seals, valves, flanges, etc.

Current permitted emission limits for the facility are provided in Table 1. In addition to isopentane emissions, there are particulate emissions from the cooling towers as well as particulates, NO_X, CO, SO_2, and VOC emissions from the emergency diesel engines. Potential emissions of PM_{10}, $PM_{2.5}$, NO_X, CO, SO_2 and VOCs from the cooling towers and diesel engines, combined, are less than 2 tons per year for each pollutant.

Table 1. Facility-wide Isopentane Emission Limits

Emission Source	Isopentane Emission Limit
1st Quarter (Jan – Mar)	185 lbs/day
2nd Quarter (Apr – Jun)	137 lbs/day
3rd Quarter (Jul – Sep)	137 lbs/day
4th Quarter (Oct – Dec)	218 lbs/day

Emissions are calculated on a quarterly average basis.

3.0 Method for Predicting Emissions for Proposed Development

The proposed changes to the facility do not include changes to the cooling towers or emergency diesel equipment. The only expected change to emissions from the proposed development is the isopentane emissions from the geothermal power generating units (OECs and ITLUs).

Future potential isopentane emissions were estimated based on actual emissions from the facility for the previous two years. Isopentane emissions are related to the size of the system, so emissions were estimated by scaling the previous actual emissions according to the change in MF volume at the facility. The existing six ITLUs and two OECs have a combined volume of 120,000 gallons, and the three MF storage tanks have a total capacity of 30,000 gallons. After the

proposed development, the combined volume of the existing and new OECs will be 111,000 gallons, and the MF tanks will have 60,000 gallons total capacity.

Maintenance and fugitive emissions were also adjusted for the decreased complexity of the new units. By replacing six smaller units with two larger units, the number of seals, flanges, pumps valves, etc. is reduced significantly. A 50% emission reduction factor was applied to account for the approximately 50% fewer potential sites for leaks and equipment failure.

Isopentane emissions were estimated as follows:

- Maintenance and purging emissions were estimated based on the worst-case quarterly emissions for maintenance and purging from the previous two years. These emission rates were scaled based on the ratio of the future OEC volume (111,000 gallons) to the existing ITLU plus OEC volume (120,000 gallons). Maintenance emissions were then scaled using the 50% reduction factor described above.

- Fugitive emissions were estimated based on the worst-case quarterly emission rate over the last two years, scaled based on the total system capacity of the system including MF tanks (171,000 gallons proposed versus 150,000 existing). Emissions were then scaled with the 50% reduction factor described above.

This emission estimation method is a reasonably conservative estimate (e.g. an overestimation) of future emissions. The new units benefit from improvements in the design and technology that have occurred during the decades since the existing units were constructed. These improvements reduce fugitive leaks as well as emissions during MF evacuation for maintenance but are not accounted for in the emission estimate. Additionally, these new units are expected to have lower emissions because the units they are replacing have higher maintenance requirements due to their age.

4.0 Potential Emissions Summary for Proposed Development

Previous actual isopentane emissions, estimated potential emissions, as well as emission limits in PTO #2217A-4 for the Heber 2 Complex are given below in Table 2. Note that the estimated emissions for the facility after the proposed development remain below the current permitted emission limits. The estimated emissions are reasonably conservative for the reasons described above.

Table 2. Actual and Potential Emissions for Heber 2 Facility

	Facility Total Emissions	
Isopentane Emissions	**lbs / day**	**tons / year**
Actual Emissions (2017 – 2018)	117.5	14.9
Estimated Potential Emissions	64.5	11.8
Emissions Increase	-52.9	-3.1
Current Permit Limit (varies)	137 - 218	
Proposed Permit Limit (varies)	137 - 202	

The currently permitted isopentane emission limits vary by calendar quarter. In quarters two and three, the limit is 137 pounds per day. In quarters one and four, additional facility maintenance is typically performed, which potentially increase emissions. The current limit for the first quarter is 185 pounds per day and the fourth quarter limit is 218 pounds per day. The proposed reduction in OEC total size from 130,000 to 121,000 will reduce the volume of isopentane that needs to be evacuated for maintenance operations. SIGC is requesting to reduce the isopentane emission limits by an amount equivalent to the reduction in OEC volume (7.5%) for the two quarter with higher maintenance emissions. The proposed limits are 171 and 202 pounds per day for the first and fourth quarters, respectively.

The proposed changes are not expected to affect emissions of other regulated pollutants.

5.0 Air Quality Protection Measures

ORMAT has implemented measures to limit air emissions at Heber 2. These measures include but are not limited to the following:

- A water truck is used on site to control fugitive dust emissions.
- A five mile per hour speed limit at the site further reduces fugitive dust emissions.
- During windy conditions, additional watering is conducted to minimize wind-blown fugitive dust.
- Equipment is operated according to best practices and maintained according to design specifications.
- The OECs and ITLUs are inspected for leaks using specialized leak detection equipment during every shift, and leaks are repaired quickly.

- Any breakdown resulting in air emissions is reported to ICAPCD and corrected promptly (within 24 hours when possible).

- The VRMU is tested annually to confirm proper function and high isopentane recovery rates.

ORMAT, HEBER 2
GEOTHERMAL POWER GENERATION FACILITY
HEBER, CALIFORNIA

Hazard Assessment for Heber 2 Expansion Project

Revision	Date	Description
0.0	July 10, 2019	Initial Issue

Risk Management Professionals, Inc.
Two Venture Plaza, Suite 500, Irvine, California 92618
Phone: 949-282-0123 – E-mail: Client.Services@RMPCorp.com